

UNIVERSITÀ DEGLI STUDI DI NAPOLI  
FEDERICO II



Dottorato di Ricerca in

INGEGNERIA STRUTTURALE, GEOTECNICA e  
RISCHIO SISMICO

30° CICLO

*TESI DI DOTTORATO*

**LONG SPAN BRIDGES: THE EVOLUTION OF  
DECK STIFFENED SYSTEM AND A CASE STUDY  
ON THE SEISMIC BEHAVIOUR OF A MAILLART-  
ARCH- TYPE BRIDGE:VIADOTTO OLIVIERI (SA)**

**TUTOR**

**PhD**

**Ch.mo Prof. Antonello De Luca**

**Guidi Laura Giovanna**

**COORDINATORE DEL  
DOTTORATO**

**Ch.mo Prof Luciano Rosati**

**LONG SPAN BRIDGES: THE EVOLUTION OF DECK STIFFENED SYSTEMS AND A CASE STUDY ON THE SEISMIC BEHAVIOUR OF A MAILLART- ARCH- TYPE BRIDGE, VIADOTTO OLIVIERI (SA)**

- 1. Deck stiffened systems as a mean for evaluating and designing different long span bridge types – Introduction to chapters....pag. 1**
- 2. Suspension bridges..... pag. 17**
  - 2.1** Deck stiffened system: a common mean to read suspension bridge evolution
  - 2.2** Historical development: changing role of stiffened girder
    - 2.2.1** From the precursor to the birth of modern suspension bridges
    - 2.2.2** Earliest failures of deck unstiffened system and new design proposals
    - 2.2.3** Roebling's revolution
    - 2.2.4** Early applications of deflection theory (1883 - 1940), till Tacoma Narrows collapse
    - 2.2.5** New generation of deck stiffened suspension bridges(1940 – 1964)
    - 2.2.6** Aerofoil revolution for record suspension bridges ((1964 till nowadays)
  - 2.3** Critical evaluation of existing suspension bridges: design parameters improvement

**Appendix (A):** Suspension bridges drawings.....**pag.56**
- 3. Steel arch bridges.....pag.69**
  - 3.1** Deck stiffened system: a common mean to read arch bridge evolution
  - 3.2** Historical evolution of deck arch bridges: masonry precursors
  - 3.3** 18th century revolution: steel deck arch bridges
  - 3.4** The spreading of bowstring arch bridges and the innovative solution of strutted arch by Arenas
  - 3.5** Steel arch bridge evolution: parametric analysis

**Appendix (B):** Case study n.1: static behaviour of Ponte di Rialto.**pag.104**
- 4. The role of deck stiffened system in long span bridge design: the original contribution of Santiago Calatrava.....pag.115**
  - 4.1** Calatrava's innovative design approach



4.2	Arch bridges structural optimization: the evolution of Calatrava's design approach from earliest bowstring arch bridges to the "pure arch" system of Ponte della Costituzione	
4.3	Calatrava's experience in rigid tension arm suspension system	
4.4	Parametric evolution	
4.5	<b>Appendix (C) - Case study: n.2: the innovative system of Ponte della Costituzione .....</b>	<b>pag.153</b>
5.	<b>Cable-stayed bridges.....</b>	<b>pag.173</b>
5.1	Deck stiffened system: a common way to read cable stayed bridge design	
5.2	Historical development	
5.2.1	First generation (1955- 1966)	
5.2.2	Second generation (1967 – 1988)	
5.2.3	Third generation ((1991 till nowadays)	
5.2.4	New frontier for cable-stayed bridge design: hybrid suspension system	
	<b>Appendix (D): Cable stayed bridges drawings.....</b>	<b>pag.218</b>
6.	<b>Deck stiffened system in concrete arch bridges: Maillart's innovation.....</b>	<b>pag.227</b>
6.1.1	The evolution of concrete arch bridges	
6.1.2	The revolutionary bridges by Robert Maillart	
6.1.3	Advantages of arch- to –beam transferring system by Maillart	
6.1.4	The spreading of Maillart-type arch bridges	
6.1.5	Italian examples: works financed by Cassa del Mezzogiorno in 1950s	

<b>7. Case study: seismic behavior and retrofit proposal for Viadotto Olivieri (SA).....</b>	<b>pag.263</b>
<b>7.1 Structural characterization</b>	
7.1.1 Report of the current state and critical aspects	
7.1.2 Loads analysis	
<b>7.2 FEM analysis: a way to understand bridge static behaviour under horizontal forces</b>	
7.2.1 Deck constraints influence modelling fixed arch:	
4.2.1.1 Three- deformable - decks model with fixed joints	
4.2.1.2 Single – undeformable- deck model with fixed joints	
4.2.1.3 Single – deformable- deck model with fixed joints	
7.2.2 Deck constraints influence modelling two-hinged arch	
4.2.2.1 Three- deformable - decks model with hinged joints	
4.2.2.2 Single – undeformable- deck model with hinged joints	
4.2.2.3 Single – deformable- deck model with hinged joints	
<b>7.3 Bridge dynamic characterization through modal analysis: variability of participation factor</b>	
7.3.1 Deck constraints influence modeling fixed arch:	
4.3.1.1 Three- deformable - decks model with fixed joints	
4.3.1.2 Single – undeformable- deck model with fixed joints	
4.3.1.3 Single – deformable- deck model with fixed joints	
7.3.2 Deck constraints influence modelling two-hinged arch	
4.3.2.1 Three- deformable - decks model with hinged joints	
4.3.2.2 Single – undeformable- deck model with hinged joints	
4.3.2.3 Single – deformable- deck model with hinged joints	
<b>7.4 Seismic retrof proposal for Viadotto Olivieri</b>	
 <b>Appendix (E) Seismic behaviour of Viadotto Olivieri - modal deformed shape.....</b>	 <b>pag.372</b>

## Figure caption list

**Fig. 2.1.a:** Linear theory [black line: dead loads funicular curve; red line: applied live loads funicular curve]

**Fig. 2.1.b:** Deflection theory [black line: dead loads funicular curve; red line: applied live loads funicular curve; dashed line: cable deformed shape]

**Fig. 2.2** Suspension bridge scheme: main design parameters

**Fig. 2.3. (a), (b), (c)** suspension bridge (Perù: Africa), V-shaped and U-shaped parameters \_ **(d)** d Kazura Vine Suspension Bridge, Japan

**Fig. 2.4** Jacob's Creek Bridge, Finley (1810) (A description of the patent Chain Bridge, in The Port Folio, Vol. III, No. 6, p. 440)

**Fig. 2.5** Dryburgh Abbey Bridge (1817), Smith, collapsed

**Fig. 2.6** Union Bridge (1820). Brown. River Tweed, Scotland. L=140m

**Fig. 2.7\_** (a), (b) Menai Bridge, completed in 1826. From The Life of T.Telford(1838).\_ (c) 1826. Photo of original transverse struts between cables.

**Fig. 2.8** Menai Strait Bridge (after rehabilitations of 1938-39)

**Fig.2.9** Real Ferdinando Bridge on Garigliano River. (1828-32). Luigi Giura

**Fig.2.10 \_**(a) (Original) Britannia Tubular Bridge- Menai Strait. (1850)\_ (b) (Rebuilt) Britannia Bridge- Menai Strait. (1972)

**Fig.2.11** Niagara Falls Bridge, J.Roebling, 1855

**Fig.2.12** Wheeling Suspension Bridge, 1872, Washington Roebling and Hildenbrand

**Fig.2.13** Brooklyn Bridge. Manhattan/Brooklyn, New York, USA, 1883, John A. Roebling

**Fig.2.14** Brooklyn Bridge\_ **(a)** deck detail\_ **(b)** cable system detail

**Fig.2.15** Williamsburg Bridge. Manhattan/ Brooklyn, New York, USA, 1903, Leffert L. Buck\_ **(a)** longitudinal view\_ **(b)** tower detail\_ **(c)** railroad detail\_ **(d)** deck bottom view\_ **(e)** cast iron stairway on the Manhattan side

**Fig.2.16** Williamsburg Bridge. New York, USA, 1903\_ **(a)** deck bottom view\_ **(b)** cast iron stairway on the Manhattan side

**Fig.2.17** Manhattan Bridge. Manhattan/ Brooklyn, New York, USA, 1912, Leon Solomon Moisseiff

**Fig.2.19** George Washington Bridge. Fort Lee/Manhattan, New Jersey/New York, Othmar Ammann\_ **(a)** (1931) original configuration: single unstiffened deck\_ **(b)** (1962) final configuration: double deck stiffened system

**Fig.2.19** George Washington Bridge. **(a)** (1931) original configuration: unstiffened deck construction\_ **(b)** (1962) final configuration: double truss deck

**Fig.2.20** George Washington Bridge\_ steel tower\_ **(a)** (1931)version; **(b)** Hypothesis of covering tower with concrete and granite plates (Cass Gilbert)\_ **(c)** final configuration

**Fig.2.21** George Washington Bridge\_ deck\_ **(a)** (1931) Six lanes for vehicular traffic (single deck); **(b)** (2017) Eight lanes for traffic (upper level of double deck)

**Fig.2.22** Golden Gate Bridge. San Francisco, California, USA, 1937, Joseph Straus, Amman, Moisseiff

**Fig.2.23** Golden Gate Bridge. San Francisco\_ **(a)** lateral view of deck cross section\_ **(b)** bottom view of adding bracings

**Fig.2.24** First Tacoma Narrows Bridge. Tacoma, Washington, USA, 1940, Leon Solomon Moisseiff

**Fig.2.25** First Tacoma Narrows Bridge (1940)\_ **(a)** deck bottom view\_ **(b)** **(c)** bridge collapse (November 7,1940)

**Fig.2.26** Second Tacoma Narrows Bridge. Tacoma, Washington, USA, 1950, Charles E. Andrew, Dexter R. Smith

**Fig.2.27** Mackinac Bridge. Mackinaw City, Michigan, USA, 1957, David B. Steinman

**Fig.2.28** Verrazano Narrows Bridge. Staten Island/Bay Ridge, New York, USA, 1964, Othmar Ammann

**Fig.2.30** Severn Bridge. (1966)\_ **(a)** construction phases\_ **(b)** tower view

**Fig.2.31** First Bosphorus Bridge. Istanbul, Turkey, 1973, W. Brown, G. Roberts, Freeman Fox & Partners

**Fig.2.32** Humber Bridge. Kingston upon Hull, England, 1981, C. Douglas Strachan, Freeman Fox & Partners

**Fig.2.33** Akashi Kaikyo Bridge. Kobe/Awaji, Japan, 1998, Honshu Shikoku Bridge Authority

**Fig.2.34** Akashi Kaikyo Bridge\_ (a) truss deck, global view\_(b) lower deck detail

**Fig.2.35** Great Belt East Bridge. Korsør, Denmark, 1998, COWI Consulting Engineers and Planners AS

**Fig.2.36** Great Belt East Bridge (1998)\_ (a) deck construction\_ (b) upper deck view

**Fig.2.37** Messina Strait Bridge (2009)\_ rendering

**Fig.2.38** Messina Strait Bridge (2009)\_ deck cross section

**Fig. 3.1\_ (a)** Corbelled arch\_ scheme\_ **(b)** Arkadiko Corbelled Bridge (1335-1190 B.C.), Peloponnese, Greece. Mycenaean stone corbel bridge.  $L= 22\text{m}$ ;  $w= 2.50\text{m}$ .\_ **(c)** Eleutherna Bridge (400 - 300 B.C.), Crete, Greece. Stone corbel bridge.  $L= 9.35\text{m}$ ;  $w= 5.05 - 5.20\text{m}$ .

**Fig. 3.2** Alcántara Bridge (104-106.), Alcántara, Spain. Semi- circular masonry arch bridge,  $L(\text{main span}) = 28.8\text{m}$ ;  $w= 8.0\text{m}$ .

**Fig. 3.3** Pont du Gard (1st century.), Nîmes, France. Three-story semi-circular masonry arch bridge,  $L(\text{arch}) = 24.4\text{m}$ ;  $h=47.5\text{m}$ .

**Fig. 3.4\_ (a)** Ponte Milvio (109 BC), Rome, Italy. - vaulted arch bridge,  $L(\text{main span}) = 18.70\text{m}$ ;  $w= 8.75\text{m}$ \_ **(b)** Ponte Fabricio (64 BC.), Rome, Italy- masonry arch bridge,  $L(\text{main span}) = 2 \times 24.5\text{m}$ ;  $w= 5.50\text{m}$ .

**Fig. 3.5** Bridge of Tiberio, (20 AD), Rimini.  $L_{\text{tot}}= 70\text{m}$ \_ semi-circular Istrian stone arch bridge

**Fig. 3.6\_ (a)** Devil's Bridge (1283), Martorell, Spain. Stone arch bridge.  $L(\text{main span})= 37.3\text{m}$ ;  $L(\text{side span})= 19.1\text{m}$ \_ **(b)** San Martin Bridge (14th century). Toledo, Spain.  $L(\text{main span})= 40\text{m}$

**Fig. 3.7** Ponte Vecchio (1335-1345), Florence\_ Taddeo Gaddi, Neri di Fioravante. Segmental masonry arch bridge.  $L(\text{main span})= 30\text{m}$ ;  $l(\text{side span}) = 27\text{m}$ ; deck width=  $32\text{m}$

**Fig. 3.8** Scaliger Bridge (1354 - 1356), Verona, Guglielmo Bevilacqua. Vaulted stone arch bridge.  $L$  (main span)= 48.70m, deck width= 6m

**Fig. 3.9** Ponte Santa Trinità (1566-69), Florence\_ Bartolomeo di Antonio Ammannati. Elliptical masonry arch bridge.  $L$  (main span)= 32m;

**Fig. 3.10** Pont- Neuf (1578- 1607), Paris \_ Jacques Ier Androuët du Cerceau. Vaulted masonry arch bridge.  $L_{tot}$ = 232m; n of spans=5; span length= 9 – 16.40m; deck width= 22m

**Fig. 3.11** Pulteney Bridge (1769- 1774), Bath\_ Robert Adam. Masonry arch bridge.  $L_{tot}$ = 45m;  $L$  (main span)=28m; deck width= 18m

**Fig. 3.12** Rialto Bridge, Antonio Da Ponte (1591).  $L$ =28.83m, rise=7.5 ( $r/L$ = 1/4),  $h$ (keystone) = 1.25m ( $h/L$ = 1/23)

**Fig. 3.13** Ponte di Rialto-1588, Antonio da Ponte – bridge section: detail of foundation system; plan (deck width: 22.90m)

**Fig. 3.14** Rialto Bridge, Antonio Da Ponte (1591).  $L$ =28.83m, rise=7.5 ( $r/L$ = 1/4),  $h$ (keystone) = 1.25m ( $h/L$ = 1/23)

**Fig. 3.15** Coalbrookdale Bridge (1775-79), England  $L_{tot}$ =60m;  $L_{main\ span}$ = 30.5m. Weight of iron= 378.5tons

**Fig. 3.16** Bonar Bridge (1802), Telford. Scotland.  $L_{tot}$ = 45m, rise=6.2.  $r/L$ = 1/7.3

**Fig. 3.17** Newcastle High Level bridge (1846-49), Stephenson, England.  $L_{tot}$ =408m; Clearance=25.92m; Span lengths=6x38.1m

**Fig. 3.18** Saint Louis Bridge (1867-74). Bouscaren.Missouri (USA)  $L_{tot}$ = 1964m;  $L_{main\ span}$ = 158.5m; Clearance= 16.8m. Total weight= 3510m

**Fig. 3.19** Maria Pia Bridge (1876-77). Eiffel, Porto (Portugal).  $L_{tot}$ = 563m;  $L_{arch}$ = 160m; Clearance= 61.20m

**Fig. 3.20** Garabit Viaduct, Loubaresse (France) (1881-84)  $L_{tot}$ = 565m;  $L_{arch}$ = 165m; rise=57m ( $r/L$ =1/2.8),height=122m; Weight= 3249t

**Fig. 3.21** San Michele Bridge. Paderno d'Adda (Italy). Röthlisberger (1887- 89).  $L_{tot}$ = 226m;  $L_{arch}$ = 150m; height= 85m

**Fig. 3.22(a)** Vaur Viaduct (1895-1902)France. Bodin.  $L_{tot}$ = 410m;  $L_{arch}$ = 220m; rise= 53.73m ( $r/L$ =1/4) height above ground= 116m

**Fig. 3.22(b)** Alexandre III Bridge by Amédée Alby and Jean Résal (Paris, 1896-1900)  $L_{tot}= 160\text{m}$ ;  $L_{arch}= 107.5\text{m}$ ;  $\text{rise}= 6\text{m}$  ( $r/L=1/17$ )

**Fig. 3.23** Hell's Gate Bridge (1912-16). Lindenthal, Steinman, Ammann. New York.  $L_{tot}= 5200\text{m}$ ;  $L_{arch}= 298\text{m}$ ,  $\text{rise}=93\text{m}$  ( $r/L= 1/3.2$ ).  $h_{arch}/L = 1/24$   $h_{girder}/L = 1/67$

**Fig. 3.24** Bayonne Bridge (1928-31). Moisseiff. New York.  $L_{tot}= 1762\text{m}$ ;  $L_{arch}= 510\text{m}$ ,  $\text{rise}=98.53\text{m}$  ( $r/L= 1/5$ ).  $h_{arch}/L = 1/25$   $h_{girder}/L = 1/102$

**Fig. 3.25** Sidney Harbour Bridge (1923-32). Sir Ralph Freeman. Australia.  $L_{tot}= 1150\text{m}$ ;  $L_{arch}= 503\text{m}$ ,  $\text{rise}=55\text{m}$  ( $r/L= 1/3.7$ ).  $h_{arch}/L = 1/25$   $h_{girder}/L = 1/100$

**Fig. 3.26** Fremont Bridge (1973) Portland. Parsons Brinckerhoff Quade & Douglas.  $L_{tot}= 656\text{m}$ ;  $L_{arch}= 382.5$ ,  $\text{rise}=45.5\text{m}$  ( $r/L= 1/8$ ).  $h_{arch}/L = 1/109$   $h_{girder}/L = 1/32$

**Fig. 3.27** Fehmansund Bridge (1958-63). Lohmer (Germany).  $L_{tot}= 963\text{m}$ ;  $L_{arch}= 248$ ,  $\text{rise}=45$  ( $r/L= 1/5$ ).  $h_{arch}/L = 1/82$   $h_{girder}/L = 1/100$

**Fig. 3.28** Roosevelt Lake Bridge (1990) . Howard, Needles, Tammen & Bergendoff.  $L_{arch}= 329$ ,  $\text{rise}=65$  ( $r/L= 1/5$ ).  $h_{arch}/L = 1/160$   $h_{girder}/L = 1/150$

**Fig. 3.29** Lupu Bridge (2003), Shanhai (China). Shanghai Municipal Engineering Design Institute.

$L_{tot}=3600\text{m}$ ;  $L_{arch}= 550\text{m}$ ,  $\text{rise}=100\text{m}$  ( $r/L= 1/5$ ).  $h_{arch}/L = 1/40$ ;  $h_{girder}/L = 1/80$

**Fig. 3.30** Chaotianmen Bridge (2008), China,  $L_{tot}=1740$ ;  $L_{arch}= 552\text{m}$ ,  $\text{rise}=128\text{m}$  ( $r/L=1/3.8$ ).  $h_{arch}/L = 1/40$ ;  $h_{girder}/L = 1/45$ .

**Fig. 3.31** Apollo Bridge, Bratislava (2003-2005) Slovakia. Dopravoprojekt a.s.

$L_{tot}=854\text{m}$ ;  $L_{arch}= 231\text{m}$ ,  $\text{rise}=36\text{m}$  ( $r/L=1/6.4$ ).  $h_{arch}/L = 1/46$ ;  $h_{girder}/L = 1/30$

**Fig. 3.33** Vallecrosia Bridge (2011) Malerba  $L_{arch}= 26\text{m}$ ;  $\text{rise}=6\text{m}$  ( $r/L=1/4.3$ ).  $h_{arch}/L = 1/52$ ;  $h_{girder}/L = 1/52$

**Fig. 3.34** Barqueta Bridge (Seville), 1992, Apia XXI (Arenas)  $L_{tot}=198.8\text{m}$ ,  $L_{arch}= 168\text{m}$ ,  $h_{a}/L = 1/70$ ;  $h_{girder}/L = 1/42$

**Fig. 3.35** Barqueta Bridge (Seville) (1992) **(a)** bridge deck\_ **(b)** inclined struts detail

**Fig. 3.36** Ponte della Costituzione, Venice (IT), 2001 - 2007, S. Calatrava.\_  
 $L = 80.80\text{m}$ ;  $r/L = 1/14$ ;  $i.p/L = 1.3\%$ ,  $ha/L = 2.5\%$ .

**Fig. 3.B.1:** Rialto Bridge vault characterization: Istrian stones distribution

**Fig. 3.B2**Rialto Bridge load definition: VAULT DEAD LOADS distribution

**Fig. 3.B3** Rialto Bridge load definition: VAULT DEAD LOADS distribution

**Fig. 4.1** Calatrava's design evolution for flexible suspension system :  $ip./L$

**Fig. 4.2** Calatrava's design evolution for flexible suspension system:  
 $h(\text{arch})=L$

**Fig. 4.3** Calatrava's design evolution for flexible suspension system:  
 $h(\text{girder})=L$

**Fig. 4.4** Bach de Roda, Barcellona (1985-87), Calatrava\_  $L'=129\text{m}$ ;  $L=46\text{m}$ ;  
 $r = 10\text{m}$ ;  $r/L = 1/5$ ;  $ip/L = 5.4\%$ ;  $ha/L = 1/71$ ;  $ht/L = 1/5$ .

**Fig. 4.5** Bach de Roda, Barcellona (1985-87). Double arches system\_ cross section detail, valuing buckling effects

**Fig. 4.6** Bach de Roda, Barcellona (1985-87)\_ **(a)**double arches system: connection details\_ **(b)** abutments

**Fig. 4.7** Bach de Roda, Barcellona (1985-87)\_ plan view: arches effective length

**Fig. 4.8** Oudry- Mesly Bridge, Créteil (1987-88),  $L_{\text{tot}}=120\text{m}$ ;  $L_{\text{arch}}=53.8\text{m}$ ;  
 $\text{rise} = 8\text{m}$ ;  $r/L = 1/7$ ;  $ip/L = 3.45\%$ ;  $ha/L = 0.70\%$ ;  $ht/L = 2.20\%$

**Fig. 4.9** Oudry- Mesly Bridge, Créteil (1987-88), deck detail

**Fig. 4.10** Lusitania Bridge (1988-91),  $L_{\text{tot}}=465\text{m}$ ;  $L_{\text{arch}}=189\text{m}$ ;  $\text{rise} = 32\text{m}$ ;  
 $r/L = 1/6$ ;  $ip/L = 3.7\%$ ;  $ha/L = 1.9\%$ ;  $ht/L = 2.6\%$

**Fig. 4.11** Lusitania Bridge (1988-91)\_ **(a)** longitudinal view\_ **(b)** deck bottom view

**Fig. 4.12** Campo de Volantin Footbridge (1994-97),  $L_{\text{tot}}=L_{\text{arch}} = 75.5\text{m}$ ;  
 $\text{rise} = 14.5\text{m}$ ;  $r/L = 1/5.20$ ;  $ip/L = 3.1\%$ ;  $ha/L = 0.6\%$ ;  $ht/L = 1.3\%$

**Fig. 4.13** Campo de Volantin Footbridge (1994-97), final solution\_ **(a)** **(b)** deck upper view\_ **(c)** deck bottom view



**Fig. 4.14** Caltrava's bridges in Reggio Emilia , A1 Highway (Autostrada del Sole) (2002-2007)

**Fig. 4.15** Ponte Centrale (Reggio Emilia) (2002-2007) Larch=221m; rise=46m;  $r/L = 1/4.8$ ;  $ip/L = 1.6\%$ ;  $ha/L = 0.7\%$ ,  $hgirder/L = 1.2\%$

**Fig. 4.16** Ponte della Costituzione, Venice (IT), 2001 - 2007, S. Calatrava.\_  
 $L = 80.80\text{m}$ ;  $r/L = 1/14$ ;  $i.p/L = 1.3\%$ ,  $ha/L = 2.5\%$ .

**Fig. 4.17** Ponte della Costituzione, Venice (IT), 2001 - 2007)\_ (a) longitudinal view\_ (b) abutment detail

**Fig. 4.18** Puerto Bridge (1988-95), Larch=71.5m; rise= 15m;  $r/L = 1/5$ ;  $ip/L = 4.1\%$ ;  $ha/L = 0.9\%$ ;  $ht/L = 5.1\%$

**Fig. 4.19** Comparison between suspension systems

**Fig. 4.20** La Devesa Footbridge,(1989-91),  $L_{tot}=65\text{m}$ ; Larch=42.8m; rise= 6.5m;  $r/L = 1/6.5$ ;  $ip/L = 61\%$ ;  $ha/L = 0.6\%$ ;  $ht/L = 1.4\%$

**Fig. 4.21** La Devesa Footbridge,(1989-91)\_ (a) Inclined arch\_ (b) wooden deck bottom view

**Fig. 4.22** Alameda Bridge (1991-95),  $L_{tot}=163\text{m}$ ; Larch=130.8m; rise= 14m;  $r/L = 1/6.5$ ;  $ip/L = 4.4\%$ ;  $ha/L = 0.6\%$ ;  $ht/L = 1.4\%$

**Fig. 4.23** Alameda Bridge (1991-95)\_arch detail

**Fig. 4.24** Parametric synthesis of Calatrava's bowstring arch bridges\_  $ip/L$

**Fig. 4.25** Parametric synthesis of Calatrava's bowstring arch bridges\_  
 $h(\text{arch})/L$

**Fig. 4.26** Parametric synthesis of Calatrava's bowstring arch bridges\_  
 $h(\text{girder})/L$

**Fig. 4.27** Alamillo Bridge (Seville,1987-92)  $ip/L = 6.75\%$ ;  $h/L = 1/44$  (2.25%),  
 $L(\text{main span}) = 200\text{m}$

**Fig. 4.28** Alamillo Bridge (Seville,1987-92)\_ bending effects upon deck cross section

**Fig. 4.29** Alamillo Bridge (Seville,1987-92)\_ (a) bridge deck bottom view\_  
(b) deck upper view

**Fig. 4.30** Trinity Footbridge (Manchester, 1993-95)\_  $L(\text{main span}) = 54,00\text{m}$ ;  
 $ip/L = 4.20\%$ ;  $h/L = 1/78$

**Fig. 4.31** Trinity Footbridge (Manchester, 1993-95)\_ (a) deck bottom view\_  
(b) longitudinal view

**Fig. 4.32** Bridge of Strings (light rail train) Jerusalem (2002-2008)\_  $L(\text{main span}) = 160\text{m}$ ;  $i_p/L = 1,85\%$ ;  $h/L = 1/75$

**Fig. 4.33** Bridge of Strings (light rail train) Jerusalem (2002-2008) bridge deck detail

**Fig. 4.34** Bridge of Strings (light rail train) Jerusalem (2002-2008) \_ force resultants upon the pylon

**Fig. 4.B1** Venice aerial map: focus in Gran Canal

**Fig. 4.B2** Venetian subsoil: sedimentary interbeddings coming from lithostratigraphical analysis of Late Pleistocene- Holocene Era deposits in the historical center of Venice (Giudecca – Canal Grande- San Marco e Sant'Elena) . Taken from: ZEZZA, F., Geologia, proprietà e deformazione dei terreni del centro storico di Venezia, “Geologia e progettazione nel centro storico di Venezia – La riqualificazione della città e dei territori”, Padova, 2007, pag.21

**Fig. 4.B3** Ponte della Costituzione, Venice (IT), 2001 - 2007, S. Calatrava.\_  $L = 80.80\text{m}$ ;  $r/L = 1/14$ ;  $i_p/L = 1.3\%$ ,  $h_a/L = 2,5\%$ .

**Fig. 4.B4** Ponte della Costituzione, Venice (IT), 2001 - 2007,\_ design steps

**Fig. 4.B5** Ponte della Costituzione, Venice (IT), 2001 - 2007, S. Calatrava.\_ Bridge deck (glass and Istrian stones flooring)

**Fig. 4.B6** (1) Lateral segment transported by barge passing under Rialto Bridge (2) Assembly of central portion (3) Construction end

**Fig. 4.B7** Ponte della Costituzione. Bottom view of steel cross sections ( $i_p = 1.36\%$ )

**Fig. 4.B8** Ponte della Costituzione. Radial distribution of deck cross sections

**Fig. 4.B9** Ponte della Costituzione. Deck cross section

**Fig. 4.B10** FEM model: arch and girders discretization

**Fig. 4.B11** FEM model: DEAD and LIVE loads distribution

**Fig. 4.B12** Reference model: two-hinged parabolic arch with (FULL) symmetrical load distribution

**Fig. 4.B13** Moment distribution at arch-crown section

**Fig. 4.B14** Scheme of Ponte della Costituzione: effective length

**Fig. 5.1**\_ Economic main range of long span bridges types.[1]

**Fig. 5.2**\_ Cable stayed bridge basic resistant arrangement and main design parameters.

**Fig. 5.3**\_ Cable stayed bridge evolution: proposal for three different generations

**Fig. 5.4**\_ Strömsund Bridge \_ Strömsund (Sweden), 1955\_ Dishinger\_ Longitudinal view

**Fig. 5.5**\_ Strömsund Bridge \_ Strömsund (Sweden), 1955\_ Dishinger

**Fig. 5.6** Dusseldorf Bridges family, 1958-1969

**Fig. 5.7**\_ North Bridge (o Theodor Heuss Bridge)\_ Düsseldorf (Germany), 1957\_ Grassl , Leonhardt . Longitudinal view

**Fig. 5.8**\_ North Bridge (o Theodor Heuss Bridge)\_ Düsseldorf (Germany), 1957\_ Grassl , Leonhardt .

**Fig. 5.9**\_ North Bridge (1957)\_ deck detail **(a)** upper view\_ **(b)** bottom view

**Fig. 5.10**\_ Knie Bridge\_ Düsseldorf (Germany), 1969\_ Leonhardt

**Fig. 5.11**\_ Knie Bridge (1969)\_ (a) harp cable arrangement\_ (b) cable anchorage detail\_ (c) hybrid deck solution

**Fig. 5.12** Severin Bridge\_ Cologne(Germany), 1955\_ Grassl & Leonhard

**Fig. 5.13** Severin Bridge\_(1955)\_ longitudinal and plan view

**Fig. 5.14** Severin Bridge\_(1955)\_ (a) longitudinal view\_ (b) deck bottom view

**Fig. 5.15** Rhine river bridge at Mannheim Ludwigshafen\_ (Germany), 1969-72 \_ Leonhardt und Andrä

**Fig. 5.16** Rhine river bridge at Mannheim Ludwigshafen\_ (a) lanes distribution\_ (b) cable system

**Fig. 5.17** Friedrich- Erbert Bridge (or Bonn Nord Bridge) \_ Bonn (Germany), 1967\_ Homberg

**Fig. 5.18** Friedrich- Erbert Bridge (or Bonn Nord Bridge) (1967)\_ longitudinal view

**Fig. 5.19** Friedrich- Erbert Bridge (or Bonn Nord Bridge) (1967)\_ (a) fan arrangement\_ (b) deck bottom view longitudinal view

**Fig. 5.19** Friedrich- Erbert Bridge (or Bonn Nord Bridge) (1967)\_ (a) fan arrangement\_ (b) deck bottom view longitudinal view

**Fig. 5.19** Friedrich- Erbert Bridge (or Bonn Nord Bridge) (1967)\_ (a) fan arrangement\_ (b) deck bottom view longitudinal view

**Fig. 5.21** Saint Nazaire Bridge\_ Loire (France), 1975\_ SAEM du pont de Saint-Nazaire

**Fig. 5.22** Saint Nazaire Bridge (1975)\_ (a) deck upper view\_ (b) deck bottom view

**Fig. 5.23** Pasco- Kennewick Bridge\_ Washington (USA), 1978\_ Svensson ,Grant

**Fig. 5.24** Brotonne Bridge \_ Normandie (France), 1977\_ Muller , Mathivat, Combault

**Fig. 5.25** Brotonne Bridge (1977) longitudinal view

**Fig. 5.26** Brotonne Bridge (1977) deck detail

**Fig. 5.27** Rande Brdige\_ Vigo, Spain (1978) \_ De Miranda

**Fig. 5.28** Rhine River Bridge at Flehe \_ Düsseldorf, Germany (1979) \_ Grassl

**Fig. 5.29** Helgeland Bridge \_ Sandnessjoen (Norway), 1991 \_ Svensson

**Fig. 5.30** Normandy Bridge : La Havre\_ Normandie (France), 1995 \_ Virloguex

**Fig. 5.31** Normandy Bridge, deck cross section\_ (a) steel deck at middle span\_ (b) PC concrete deck at side spans

**Fig. 5.32** Millau Bridge\_ (multi- span cable stayed bridge): Millau (France), 2004\_ Foster

**Fig. 5.33** Millau Bridge\_ (2004), deck cross section

**Fig. 5.34** Millau Bridge\_ (2004)\_ (a) (b) towers\_ (c) cable arrangement

**Fig. 5.35** Tatara Bridge: Ikuchi- Ohmishima (Japan), 1999 \_ Komai\_ Kawada, IHI\_ Tagagami\_ Matsuo

**Tab. 5.36** Tatara Bridge(1999)\_ (a) deck view \_ (b) cable arrangement at the tower

**Fig. 5.37** Tatara Bridge(1999\_ tower detail

**Fig. 5.38** Tatara Bridge(1999\_ (a) live loads characterization\_ (b)steel deck cross section\_ (c) PC concrete cross section

**Fig. 5.39** Sutong Bridge\_ Jiangsu, China (China), 2009\_ COWI, longitudinal view

**Fig. 5.40** Sutong Bridge\_ Jiangsu, China (China), 2009\_ COWI

**Fig. 5.41** Sutong Bridge (2009)\_ steel box cross section detail

**Fig. 5.42** Sutong Bridge (2009) steel box cross section, construction step

**Fig. 5.43** Stonecutters Bridge\_ Hong Kong (China), 2009\_ Yokogawa Bridge Corporation

**Fig. 5.44** Stonecutters Bridge (2009, twin box section detail

**Fig. 5.45** Stonecutters Bridge (2009, twin box section\_ (a) detail\_ (b) deck bottom view

**Fig. 5.46** Stonecutters Bridge (2009) construction steps

**Fig. 5.47** Russky Bridge\_ Vladivostok (Russia), 2012 \_ SIC Mostovik

**Fig. 5.48** Russky Bridge (2012\_ construction steps in extreme conditions

**Fig. 5.49** Russky Bridge (2012)\_ (b) deck cross section detail

**Fig. 5.50** New Forth Bridge (Queensferry Crossing). 2011-2017

**Fig. 5.51** New Forth Bridge (Queensferry Crossing). 2011-2017

**Fig. 5.52** Yavuz Sultan Selim Bridge or Third Bosphorus Bridge (2013-2016)

**Fig. 5.53** Third Bosphorus Bridge construction steps

**Fig. 5.54** Third Bosphorus Bridge, suspension system details

**Fig. 5.55** Comparison between cable stayed bridge generations

**Fig. 6.1:** Wanxian Bridge over River Yangtze, China (1997) The longest concrete arch bridge in the world  $L_{tot}=864.12m$   $L(arch)=420m$

**Fig. 6.2:** Chatellerault Bridge (river Vienne, France) François Hennebique (1899)  $L_{tot}=144m$   $L(arch)=40m$  rise=4m ( $r/L=1:10$ )

**Fig. 6.3:** Risorgimento Bridge (Rome), Porcheddu, Hennebique licence (1911),  $L=100m$ , rise =10m,  $r/L= 1:10$

**Fig. 6.4:** Establishing the shape of the funicular arch

**Fig. 6.5:** Stauffacher Bridge, River Sihl, Zurich (1899),  $L=40\text{m}$  – unreinforced concrete

**Fig. 6.6:** Inn River Bridge at Zuoz (1901),  $L=40\text{m}$  – Reinforced concrete spandrel arch

**Fig. 6.7** (a) Zuoz Bridge, Maillart (1901) three hinged hollow-box arch\_ (b) Billington, Robert Maillart's Bridges (1989)

**Fig. 6.8** Comparison between conventional arch bridge and hollow-box arch bridge (Scheme by Billington, "The revolutionary bridges of Robert Maillart" – Scientific America, 2000)

**Fig. 6.9** Tavanasa Bridge, Maillart (1905) three hinged arch (a) deck view\_ (b) Billington, Robert Maillart's Bridges (1989)

**Fig. 6.10** Maillart's design of Rhine Bridge at Tavanasa (1905),  $L=51\text{m}$  Three hinged reinforced concrete arch

**Fig. 6.11** Rhine Bridge at Tavanasa (1905),  $L=51\text{m}$  Three hinged reinforced concrete arch

**Fig. 6.12** Aaburg Bridge (1912),  $L=70\text{m}$ , three hinged arch bridge, rise =  $7\text{m}$ ;  $r/L=1/9.75$

**Fig. 6.13** Construction of Salginatobel Bridge (1930), Graubunden canton, Switzerland  $L(\text{arch})=90\text{m}$

**Fig. 6.14** Salginatobel Bridge (1930), Graubunden canton, Switzerland Three-hinged reinforced concrete arch

**Fig. 6.15** Vessy Bridge (1936), Geneva - Switzerland Three-hinged reinforced concrete arch  $L=56\text{m}$ ,  $r/L=11.7$

**Fig. 6.16** Vessy Bridge Calculation of X-shaped cross walls

**Fig. 6.17** Vessy Bridge (1936), Geneva - Switzerland - Detail of X-shaped cross walls

**Fig. 6.18** Maillart-type no rigid arch - (Scheme by Billington, "The revolutionary bridges of Robert Maillart" – Scientific America, 2000)

**Fig. 6.19** Flienglabach Bridge (1923,  $38.7\text{m}$ -span

**Fig. 6.20** Valtschielbach Bridge (1925)  $L=43.20\text{m}$   $h(\text{arch-midspan})=0.23\text{m}$

**Fig. 6.21** Maillart's calculations for the bending in the parapet of the Valtschielbach

**Fig. 6.22** Schwandbach Bridge (1933)  $L(\text{main span})=37\text{m}$ ,  $L(\text{tot})=55.60\text{m}$

**Fig. 6.23** Reichenau Bridge, C. Menn, Switzerland, 1962.  $L_{\text{arch}}=100\text{m}$ ,;  
 $L_{\text{tot}}=158\text{m}$ ; deck width= 8.40m; arch thickness = 0.80 – 1.25m; deck depth=  
1.00m;  $H_{\text{gider}}/L = 1/100$ ;  $H_{\text{arch}}/L= 1/125$

**Fig. 6.24** Viamala Gorge Bridge, C. Menn, Switzerland, 1967.  $L_{\text{arch}}=96\text{m}$ ,;  
 $L_{\text{tot}}=179.80\text{m}$ ; deck width= 10.70; deck slab thickness= 0.29m; girder  
depth= 1.09m;  $H_{\text{gider}}/L = 1/88$ ;  $H_{\text{arch}}/L=1/331$

**Fig. 6.25** Echelsbach Bridge over the River Ammer in Germany, Heinrich  
Spangenberg, 1929

**Fig. 6.26** Bixby Creek Bridge, Stover, Panhorst & Purcell (1933), California  
(USA).  $L_{\text{arch}}=109.70\text{m}$ ;  $L_{\text{tot}}=218\text{m}$

**Fig. 6.26** Bixby Creek Bridge, Stover, Panhorst & Purcell (1933), California  
(USA).  $L_{\text{arch}}=109.70\text{m}$ ;  $L_{\text{tot}}=218\text{m}$

**Fig. 6.28** Bisantis Bridge, Catanzaro (Italy), Riccardo Morandi (1962)  
 $L=231\text{m}$ , rise to span ratio 1/3.09

**Fig. 6.29** Arrabida Bridge, Porto (1963) Edgar Cardoso,  $L_{\text{tot}}=493.20\text{m}$ ;  
 $L_{\text{arch}}=270\text{m}$

**Fig. 6.30** Infant Dom Henrique Bridge (2002), Cardoso.  $L_{\text{tot}}=412.50\text{m}$ ;  
 $L_{\text{arch}}=280\text{m}$

**Fig. 7.1:** Viadotto Olivieri. A3, SA-NA Highway. Benine schmidt design,  
1954-1958)

**Fig. 7.2:** Viadotto Olivieri. A3, SA-NA Highway. Benine schmidt design,  
1954-1958) – Upper deck longitudinal view

**Fig. 7.3:** Viadotto Olivieri. A3, SA-NA Highway. Benine schmidt design,  
1954-1958) – Bridge longitudinal view

**Fig. 7.4:** Viadotto Olivieri. A3, SA-NA Highway. Benini & chmidt design,  
1954-1958) – Bridge upper view

**Fig. 7.5:** Viadotto Olivieri. A3, SA-NA Highway\_ arch vault detail

**Fig. 7.6:** Viadotto Olivieri. A3, SA-NA Highway\_ deck cross section

**Fig. 7.7:** Viadotto Olivieri. Bridge deck \_ (a) bottom view\_ (b) joint detail

**Fig. 7.8:** Viadotto Olivieri. Cross walls\_ (a) longitudinal view\_ (b)  
connection at foundation



*To my Family*

*To my best supporter, Mick*

*To everyone believes in me*

## **The evolution of long span bridge types read through the changing role of deck stiffened systems**

This doctoral thesis deals with the design evolution of long span bridges and the corresponding technical improvements which have changed the role of deck stiffened system. All typologies (suspension bridges, cable –stayed bridges, deck arch bridges, bowstring arch bridges) usually adopted to cover long distances, have been taken into account, reading in the same perspective the process which allows their structural optimization. The interaction between load-bearing structural elements has been analysed, particularly valuing, for deck - stiffened system, how longitudinal girders have lost their main load bearing function progressively.

Deck - stiffened system has been considered the “*fil rouge*” in reading long span bridges evolution, a common mean to understand different structural types, giving a cognitive background to better approach in long span bridges design. From back analysis, supporting this thesis, it’s deducible that the attempt to cover longer spans with slender structures has been accompanied by the passage from flexural regime of short span structures, acting like simple beam-bridges with rigid deck systems, to extensional regime of lighter aerofoil long span solutions, whose strict succession of deck cross sections guarantees them to carry loads mainly through tensile or compression strength. In this way, deck-bending moments are reduced, while torsional effects are often counteracted by bridge deck box sections. This modern design approach, inevitably having a relevant effect on bridges aesthetic and their relationship with the surrounding contest, leads to an innovative conception of deck – stiffened system, completely modifying bridge design classical approach.

Apart from old masonry arch bridges and earliest examples of segmental metal arches, which make no easily recognizable the separation between upper bending-effected girder and lower compressed arch, for each type, earliest solutions adopted to cover 100m-longer spans were often characterized by rigid truss deck systems, designed to carry especially bending moments due to acting loads. The need to cover longer spans and carry heavier loads, as railway ones, making structure lighter, led designers to take better advantages from load

bearing elements interaction, well “exploiting” structural material properties. To reduce elements size, increasing covered distances, the better way was to prefer the extensional regime to the flexural one in designing bridges, with the primal aim of bringing down deck system wide depth.\*

From this perspective, pioneering Eads’s solution applied for Saint Luis deck arch bridge marked a great step forward in long span bridge evolution. This work firstly proves that, increasing number of transversal load bearing elements, which is to say reducing the effective loaded length of longitudinal main ones, loads are directly transferred (without additional bending effects) to the main load bearing system; this one corresponds to the lower arch for deck- arch bridges, to the upper arch for bowstring arch bridge, to the main cable and hangers system for suspension bridges, to the strain stays anchored at the bottom of compressed pylons in the case of cable-stayed bridges. As lower deep longitudinal girder, as its higher deck slenderness guarantees to reduce greatly bending effects (also for asymmetric loads configuration): the choice for a close succession of deck cross sections makes each element to carry only local effects valued for loads acting upon their corresponding wheelbase. As consequence of valuing inconsiderable bending effects, main structure can size proportionally to the occurring axial forces: in this way, if torsional effects make necessary the use of stiffened box sections, structural slenderness points out the problem of buckling instability in bridge design.

The following excursus wants to emphasize the effects on structural response that deck characterization could have: so, some peculiar cases study have been taken into account, as “pure arch” solution of Ponte della Costituzione by Calatrava, or Viadotto Olivieri, as representative of Maillart arch type bridge. Especially for cable supported bridges, a classification in successive generations has been proposed: the passage from one another represents a change in bridge structural behaviour.

Modern design approach, as later described, seems to put into practice the idea of “dematerializing” longitudinal girder, till completely denied it, as it occurs for Calatrava’s works. Apart from aesthetic reasons, the attempt to cover record spans and the need to contain construction cost, i.e. to reduce dead loads,

ensuring the required stiffness to the resulting slender structures, make necessary the increase of deck cross sections' number, also requiring the use of thick suspension systems and of stream-lined shape deck solution to counteract wind-induced dynamic effects.

The proposed analytical approach leads to synthetize the evolution of deck stiffened system through some particular design factors. Geometrical characteristics usually adopted to describe each typology have been taken into account. However, back analysis of existing bridges (about 100 cases) is described using two main design parameters; these ones better reflect how bridge behaviour changes, rather improves, varying structural elements interaction: (i.p./L), i.e. cable spacing-to-main span length ratio, used to describe both suspension cable distribution and deck cross sections sequence along bridge deck (considering that suspenders often anchorage along deck in a section which is stiffened by transverse element); (h/L), element depth-to main span ratio, to define its corresponding slenderness.

*“Standing on the shoulders of giants”* has been seen as the only way to really understand the process which leads to modern long span bridges design and construction: their extremely slender decks, the impressive span covered, their capacity to improve the surrounding landscape with diaphanous constructions, are the consequence of progressive attempts to optimize structures, till dematerializing longitudinal girder. Modern approach in bridge design has changed the role of longitudinal girder as main load bearing structural element: this “revolution” is a “simple” consequence of discretizing bridge deck in a huge number of cross sections, quite far one from the other, consequently reducing spacing between hangers or cable stays, in order to make longitudinal girder carry only local effect due to live loads. From Amman's George Washington to Great Belt suspension Bridge, from Stromsund to Russky cable-stayed bridge, from San Louis deck arch bridge to Calatrava's Ponte della Costituzione, this evolution in structural behaviour is really clear. It's easy to note that technical improvements occurred over the centuries help to solve some problems due to adverse surrounding conditions in bridge design, giving the possibility to create extraordinary “engineering work of art”, whose record spans ad extreme slenderness were absolutely unpredictable just two centuries before. The

Newtonian metaphor, which leads to “*discover truth by building on previous breakthroughs*”, nowadays justifies the choice for past pioneering technical solutions and design approaches, re-read in a critical and more efficient view, also thanks to the use of the necessary calculation tools, in order to really gain the advantages that designers hoped to obtain in the past. With this mind, it’s interesting to consider the vicissitudes which accompanied the spreading of hybrid suspension system, often adopted for long span slender bridge. Used by Roebling for the Brooklyn Bridge, it has been re-introduced in the longest hybrid cable-stayed/ suspension solution, the extremely elegant Third Bosphorus Bridge. With a main span of 1408m, the so called Yavuz Sultan Selim Bridge combines the hybrid steel-concrete deck solution, typical of modern cable-stay system, to the hybrid suspension cable arrangement which strengthens the stay-cable one with the suspension system at the mid span.

If cable-stayed system was early used (19th century) to stiffen suspension one, above all in the case of more flexible deck bridge, failed on account of insufficient resistance to wind pressure, firstly Roebling understood the huge potential of stay-cable solution: in connection with stiffening truss and efficient lateral bracings, inclined stays proved more effective. However, in Roebling’s proposal, cables of suspension bridges were always “assisted” by stays, as efficient and economic mean for stiffening the floor against the cumulative undulations that may be started by the action of the wind. This radiating stay system had primarily the critical function of adding rigidity to the span, ingeniously taking the advantage of the increasing the loading-carrying capacity which they incidentally supplied. But the earliest hybrid system appeared quite redundant; as Roebling said: “*The floor in connection with the stay, will support itself without the assistance of the cable, the supporting power of the stays alone will be ample to hold up the floor. If the cable were removed, the bridge would sink in the centre but would not all*”. Nowadays, the restatement of the hybrid suspension system, proposed for Third Bosphorus Bridge (2016), has given the possibility to overcome the span record of cable-stayed system, hold by 1104m-long central span of Russky Bridge up until 2012. The economic, constructive and structural advantages of hybrid suspension solution, agree the request for an extremely short period of design and construction (only 36 months, Virlogeux),

creating an iconic and outstanding landmark of Istanbul region, connecting Europe with Asia. In this case, the choice of suspending girder with a parabolic cable in the centre part, in addition to stays on the other part, has been dictated by several reasons: (1) the severe loading scheme (it's the widest and longest hybrid railway bridge, carrying 8 lanes for motorway and 2 lanes of railways on a single level,; live loads are almost 60% of the permanent loads); (2) the need to reduce construction period; (3) the need to better govern slender deck bridge deflection (compared to usual cable stayed bridge, adding the main parabolic cable guarantees to greatly reduce, of about 10%, displacement of the girder, as well as bending moment of the towers, due to live loads.

Previous insert well underlines how progressive technological improvement has marked the evolution of long span bridge, from the earliest 18th century examples, until nowadays. The pleasant “journey” through different typologies and their design approach, traced in this thesis, starts from suspension type, underlining the changing role of deck stiffened system through the earliest collapses, the following split between European and American “design school”, and the resulting choice for slender aerofoil deck despite of stiffed truss girder solution. Then the arch type has been analysed, investigating the role of stiffening deck, both for rigid arch solution, as in the case of Garabit Viaduct by Eiffel, and in the opposite configuration which characterises deck stiffened arch bridges, firstly proposed by Maillart. The historical excursus traced, that starts from the earliest masonry spandrel arches whose upper-vault filling collaborated in load distribution, underlines the arch bridge technological improvements till the innovative solution of “pure arch”, which makes Calatrava's Ponte della Costituzione an “unicum” in bridge design. The role of Valencian artist has been influential also for cable-stayed bridges, a typology which represents an important stage in this journey through deck stiffened system optimization. Considering that no evaluations have been done about dynamic characterization of common long span bridges, it has been interesting to point out the seismic behaviour of a Maillart arch bridges, seen as one of the most common type used along Italian highways.

## **Chapter 2: Suspension bridges**

There is no doubt that suspension bridge constitutes the main solution for long-span structures, covering approximately 90 % of span range between 300m and 2000m. Considering that suspension system configuration have had no many changes since the origin, although a great improvement can be recognised in cable technologies, there is no doubts that the most influential aspect in suspension bridge design has always been the deck system configuration. It's interesting to note how the process towards structural optimization of deck stiffened system has been marked by two main theoretical approaches, firstly the linear theory (1858 - Rankine, Steinman), then the deflection theory (1888 - Ritter, Lévy, Melan). Critically looking at the earliest suspension bridge collapses, it has been noted the importance of rigid deck as the only way to better exploit the potentialities of this structural system; meanwhile, it has been seen how the improving studies concerning aerodynamic stability (subject which lies outside the scope of this thesis) have guaranteed the use of lighter and slender superstructures, greatly reducing bridge weight and construction costs.

Primitive suspension bridges were probably used by people even before the arch bridges in ancient Rome. The common configuration of these catenary-shaped bridges consists of the main cable where people walk, while two or more cables that hung at both sides as the handrails formed a V-section: having no deck, these unstiffened systems allowed only one person to pass. A great step beyond the primitive examples was necessary for the development of modern suspension bridge, both for the increasing loads, and for the excessive deflection of catenary-curve vines suspension bridges, having no stiffening elements. Even if firstly Finley (1810) understood the necessity of stiffening girder in suspension bridges (*Jacob's Creek Bridge*) as a way to ensure an uniform distribution of loads to many hangers, eliminating excessive deformations in the main cable, early attempts to cover long span with suspension bridge technologies showed the unfavourable use of failing unstiffened deck systems (Dryburg Bridge, Union Bridge, Menai Bridge).

Completely revolutionary was the design method introduced by Roebling, the first one who recognised the necessity of providing an adequate stiffening system to suspension bridges. As a consequence of some spectacular collapses of

suspension Bridges, occurred in 1810s, caused by wind oscillations, Roebling voiced his perception that stiffened girder and additional inclined stays would make rigid suspension bridges. In addition, the deflections from heavy live loads would be reduced. Previous accidents revealed the fact that suspension bridges easily oscillated because of their low stiffness, a defect that became critical especially for railroad bridges. His success in the construction of suspended aqueducts demonstrated the truth of his thesis that cable spans could be built as stiff as desired. But it was in the Niagara Bridge that his new concept received its first full expression: the first use of stiffening trusses in all the history of bridge building. Following Niagara bridge design, his masterpiece, Brooklyn Bridge, marked the beginning of a new generation of stiffened truss-deck suspension bridges. Except for Williamsburg Bridge, designed according to linear theory, from 1930s years the application of deflection theory led to build more slender structure. George Washington Bridge (by Amman) has been, surely, an emblematic case in the evolution of modern suspension bridge design. This pioneer work reveals a completely new approach in bridge design. With this masterpiece, Amman theorized that heavy stiffening trusses were no necessary for long span suspension bridges : high dead loads, both for cables and for deck, allow to stiffen and stabilize bridge. Being main cables really heavy (cables weight-to deck weight ratio: 41%), being dimensioned to carry a double deck system, the effect due to any accidental loads are practically nihil. Apart from the stabilizing effect of dead loads, the choice of a thickening hangers system, linked to the main cable, as well as the increasing number of transverse load-bearing elements ( $i.p/L = 1.72\%$ ), gave the possibility to greatly reduce girder sizing: it resulted in an elegant slender structure. Deflection theory application led Moisseiff to an unconventional depth-to span ratio of 1/356 for its (first) Tacoma Narrows Bridge. This bridge was greatly capable to carry both traffic loads, and static effects of wind load; however, wind dynamic effect were not foreseen. The primary cause of the collapse lies in the general proportions of the bridge and the type of stiffening girders and floor. The ratio of the width of the bridge to the length of the main span was so much smaller and the vertical stiffness was so much less than those of previously constructed bridges . After Tacoma Narrows Bridge collapse (1940), American engineers realised the problem of aerodynamic stability and further extended span lengths. Two main



approaches were used to improve bridge deck stability: against aerodynamic effects (1) adopting a stiffening truss and open grating deck, in order to eliminate the generation of wind vortices; (2) increasing stiffness, adding mass (or weight) to the bridge. A completely different approach was used by European engineers: they adopted streamline-shaped box cross sections, whose aerofoil profile could reduce wind pressure effects, suppressing the emergence of vortices.

Looking at technical improvements occurred, as consequence of deflection theory application, as well as of aerodynamic studies, tracing historical evolution of suspension bridges, three different generations, as many different way to conceive stiffened girder, have been proposed in this thesis. If the earliest examples of the first generation (1883-1940) were characterized by stiffen truss girder, as consequence of linear theory application, Melan's deflection theory gave the possibility to take greater advantages from main cable-to-girder interaction. When taking into account the nonlinear elastic effect related to the displacement of the cable, the bending moments in the deck is reduced, often to less than half of that found by a linear elastic theory, so that deck depth can be greatly contained (till  $h/L = 1/200-1/300$ ). Considering this theoretical background, the pioneer Amman firstly understood the possibility to make slender deck simply increasing hangers and deck cross section number: this makes George Washington Bridge the precursors of modern suspended bridges. If in 40-60s years, no much rigid deck system allowed to cover 1100m longer spans with slender structures, in the last five decades, after Tacoma Narrows disaster and its failed attempt to reduce deck depth, studies concerning aerodynamic stability led to use streamline-shaped cross sections, less vulnerable to dynamic effects: resulting in a great reduction of bridge dead loads, modern orthotropic box cross sections, made rigid by closely deep-spaced transverse diaphragms, guarantee the necessary bending and torsional stiffness to cover record spans.

### **Chapter 3: Steel arch bridges**

Considering the aforementioned case of S. Louis Bridges by Eads, deck arch bridge solution firstly revealed the efficiency of modern design approach in long span bridge design. The principle of “unpacking” main longitudinal girder,

increasing number of transverse load bearing elements, supports the choice to cover longer spans using structures working only in extensional regime, without any additive bending effects. This system makes no necessary the use of complex stiffer deck system to guarantee bridge stability, and completely transforms the role of stiffened deck system, in particular the load bearing capacity required to longitudinal girders. The same principle that leads to govern arch bridge static behaviour simply through a thrust regime has marked the spreading of bowstring arch bridges, as the most efficient way to cover 150m-longer span with arch solution.

Modern steel bridges could be considered a result of technological development of ancient masonry arch bridges. As structural type, the arch is a system that transports the applied loads to supports primarily through compression stresses in the arch, eliminating the possibility of tensile ones occurring within the chosen materials. This is achieved through design of the arch shape above all if it's to match as closely as possible to the line of thrust within the arch, especially in the case of arch bridge with very slender piers and extremely surbased segmental arches. Robustness of existing bridge, which were all designed to carry above all permanent loads, being live ones a little percentage of total vertical loads, shows how the structural behaviour of masonry arch bridges has had no change through centuries: for this typology, dead loads prevailed over live ones, almost until the birth of railroad. In 18th century, increasing live loads due to rail traffic, led designer to consider other aspects in bridge design, as no-negligible dynamic effects or vibrations, as well as valuing the possibility to use new material or different static schemes. The earliest metal arches proposed massive structures, similar to masonry ones, till Eads's solution for his Saint Louis truss arch bridge revealed the possibility to make bridge deck structure slender, increasing number of transversal elements. It's interesting to note that the contemporary Eiffel's Garabit Viaduct, covering a quiet similar span (about 160m) used a completely different solutions, whose arch. – to- deck load transferring system is guarantee by a longitudinal girder slender than the main two-hinged arch, having a very marked rib depth variation, maximum at the crown and minimum at the springing sections.

The introduction of bowstring arch bridge type has guaranteed to cover longer spans: also in this case sizing optimization both for arch and girder has been strictly linked to the use of a thick suspension system, combined with a huge number of transverse deck cross sections. The term “bowstring” is the outcome of the actual behaviour for this kind of balanced structures. The upper arch “bow”, always strongly compressed, is internally balanced by the tensioned deck, which works as a “string”. From this conjugation bowstring arch bridge results. Vertical or inclined ties (or hangers) connected to the arch support deck from above. The arch and the deck are, thus, locked into each other and the deck acts as a stay for the arch, resisting horizontal forces (thrust) through tension.. A great contribution to bowstring arch bridge evolution was given by strutted arch (or split bowstring arch bridge) introduced by Arenas’ system proposed for Barqueta Bridge. This split arch form is one of the first of its kind, and is an innovative way of increasing the main span of the bridge without decreasing the buckling load of the arch. The triangular frames not only extend the lateral length of the arch bridge as they receive the axial force of the arch, but also allow for an increase in the width of the bridge because of the transverse bracing they provide.

#### **Chapter 4: Development of deck stiffened system through the experience of Calatrava**

Tracing the evolution of long span bridges, it emerged that starting from massive deck truss arrangements and open section deck solutions without bracings, the aim of covering longer spans using lighter and slender structures, has led to prefer (aerofoil) box sections; this solution guarantees high torsional stiffness, necessary in the case of structural asymmetrical layout or eccentric load condition. At the same time, the choice of a thickening suspension system, corresponding to an equivalent distribution of deck cross sections, allows to reduce the effective loaded length for structural elements, giving the possibility to reduce their size greatly: their dimension strictly depend on acting axial force, while bending effects, estimated for shorter loaded lengths, can be neglected easily.

In this route through structural types, investigating the occurred changes in deck stiffened system, the contribution of Santiago Calatrava cannot be neglected,

above all in the way this polyhedral artist has been able to combine the role of architect, engineer and urban designer in one person, creating unprecedented works of art. It must give credit to him especially for his capability to make the deck discretization the way to advance his free forms design: deck cross sections become as “vertebrae of spine”, guaranteeing to minimize girder size, till the extraordinary solution of the “pure” arch for Ponte della Costituzione.

Calatrava’s major innovation consists in completely upsetting the traditional role of deck stiffened system both in arch bridge and cable stayed bridge design. Particularly in the case of bowstring arch bridges, his attempt to solve exclusively in extensional regime bridge structural behaviour is put into practice by dematerializing deck stiffened system, “simply” thickening cross section numbers. . Passing from earliest short footbridges to longer bridges, Calatrava’s continuous experimentation is carried out in a progressive optimization of design parameters, heretofore used, which describe the suspension system ( $i.p./L$ ), or arch stiffness ( $ha/L$ ), truss stiffness ( $ht/L$ ), or that of the whole structure ( $h^*/L$ ). Their clear reduction (till  $i.p./L$  of 1%), structurally corresponds to daring and unpredictable solutions, as the innovative “pure arch system” resulting from the evolution of Ponte della Costituzione design. In this case, instead of the typical deck arch solution, he uses a pure arch bridge, without any filling materials between the load bearing structure and the pedestrian walkway. Dividing the main arch into 73 closely spaced sections, Calatrava is capable to leave out the longitudinal girder; so that the floor is supported directly by a slightly sloping central steel arch. Conceptually, this works represent the synthesis of a progressive technological evolution, originally started by Eads and Eiffel two centuries before.

In the last 30 years of his career, this versatile artist, who studied at ETH, has always searched for innovative structural technologies, combining previous aspects in the creation of works of art characterized by naturalistic as anthropomorphic forms (aspect which justifies the term “vertebrizzazione” used in this chapter). Claiming the elegance, identity and recognisability of his structures, Calatrava prefers working in extensional regime also in the case of short spans.

He has given an extraordinary contribution also to arch bridge design also in the way he counteracts buckling effects although using extremely slender structures. As creating urban sculptures, each structural component reaches plastic characterization, easily making perceivable bridge load transferring system, especially in the case of rigid tension arm suspension systems. The dramatically sloped arches characterize some of his bowstring arch bridges: they are well designed to better counteract out- of plane buckling effects, being characterized by a deck system with a high bending stiffness as in Langer system, adopting a rigid box cross section as in Haupt's solution. Compared with flexible suspension system, rigid tension arm solution guarantees to make the upper arch slender, at the expense of a rigid deck, with a slenderness ratio no lower than 1/70. In both cases, Calatrava's attempt to deny bending effects, making his structure acting mostly in extensional regime is realized in the choice of a close succession of deck cross sections which decomposed the longitudinal girder, always seen as bridge's main load bearing structural element. The corresponding thickening of suspension hangers allows to immediately transfer loads acting upon slender deck to the upper arch, where the short distance between cable anchorages allows to greatly reduce strengths in the arch. Controlling bending effects, structural element size is defined in relation to load-induced axial forces, as well as torsional effects due to eccentric load conditions or asymmetric bridge layout.

The innovative approach proposed by Calatrava leads to the construction of spectacular cable-stayed bridges, with unconventional asymmetric structures. The evolution of this structural type will reveal an improvement in their extensional regime, as well as an optimization in structural element size: this has been achieved reducing cable spacing and, consequently, increasing deck cross section number (till the lowest  $ip/L$  of 2%). This process will lead to completely change the role of deck-stiffened system: minimizing spacing between cable anchorages along the deck corresponds to reduce the effective loaded length of longitudinal elements, so that lower compression strength requires less deep structural elements, which is to say slender deck.

In line with this modern approach, Calatrava's contribution appear revolutionary. His apparently unbalanced structures, which evoke a sense of

dynamism, are governed thanks to the creation of a preventive stress condition (especially in the pylon), as it happens regularly in pre-stressed concrete structure, not only to carry compression or tensile strengths, but also to counteract bending and torsional effects, making their effect practically inconsiderable. His look like instable cable stayed bridges are extraordinary “self-tensioned” structure, whose no balanced forces or moments are absorbed directly by the structure itself.

## **Chapter 5: Cable stayed bridges**

As announced before in tracing Calatrava experience and his contribution to long span bridge evolution, the same trend through the perfect optimization, both from a structural and from an aesthetic point of view, can be recognised for cable stayed bridges. The principle of supporting a beam with cables goes far back in time. Early examples are bridges from natural materials such as bamboo for the beam and lianas for ties. Cable-stayed bridges are currently in fast development, worldwide. While in 1986 about 150 major cable-stayed bridges were known, there number has increased to more than 1000 today. Their span also increased by leaps. From 1975, when the record span was 404m, it jumped to 856m in 1995 and today reached 1104m. The position of cable-stayed bridges within all bridge system is given in the previous picture. The economic main span range of cable-stayed bridges thus lies between 100 m with one tower and 1100 m with two towers. Many advantages characterize this typology. First of all the bending moments are greatly reduced by the load transfer of the stay cable. By installing the stay cables with their predetermined precise lengths the support conditions for a beam rigidly supported at the cable anchor points can be achieved and thus the moments from permanent loads are minimized. Even for live loads the bending moments of the beam elastically supported by the stay cables remain small. Negative live load moments may occur over the vertical bearings at the towers. For this type, the effect of stiffened deck is strictly linked to the configuration of cable stayed system. Even if for suspension bridge hangers spacing has no changed enough over the centuries (with a mean  $ip/L$  value of 1-2%), being necessary a low distance between suspenders to ensure a quiet uniform distribution of loads, passing from deck to main cable, in the case of

cable stayed bridges, passing from the earliest examples with few cables to the multi-stay suspension system, bridge behaviour, its load bearing capacity, above all to carry bending stress, completely change.

Efficient use of materials and speed of construction made cable-stayed bridges the most economical type of structure to use for replacements: in a relatively short time, from 1955 to 1974, approximately 60 cable-stayed bridges were built, just less than one-third of the total number in Germany. Decisive for the success of steel cable-stayed bridges was the development of the orthogonal anisotropic lightweight steel deck (orthotropic deck) by Wilhelm Cornelius: it reduced the weight of continuous beams considerably and permitted spans and slenderness ratios unknown until then. At first open rib longitudinal stiffeners were used, later the closed stiffeners with a higher torsion stiffness were introduced. Despite using this technological innovation, earliest examples of cable-stayed bridge had a static behaviour quite similar to that of beam bridges. Few number of stays (corresponding to high value of  $i.p./L$  of 20%) make deck working as simple supported beam. At the same open deck cross section made torsional problem due to asymmetrical load condition not negligible. In 1967, Homberg firstly introduced multi-cable stay system in his Bonn Nord Bridge. This solution guarantees a more continuous support of the deck, while cable forces, that are transmitted at each anchor point, are reduced: in this way a local strengthening of the deck at the anchorages can often be avoided. Lower effective length between stays (i.p.) involves smaller deck compression, so that minimizing section dimensions, bridges appear slender, light, diaphanous. The choice of multi-stay suspension with relatively small spacing (7-15m) greatly facilitates bridge erection and permit the design of bridges with ever-increasing spans. With the aim of covering longer span, new technological solution had to be adopted. This justifies the choice for hybrid structures. Hybrid cable-stayed bridges comprise a steel beam in the main span and a concrete beam in the side spans. The heavier concrete beam serves as a counterweight to the lighter steel main span. Still nowadays, multi-cable stay system is used to cover growing lengths, adopting locked coil ropes, parallel wire cables and parallel strands. Their high durability is guarantee through specific corrosion protection, including, for each strand later assembled to form cable, the following processes:

galvanizing of every single wire in the strand; filling the interstices between the single wires with grease; surrounding each strand with a directly extruded PE-sheath. The installation of these stay cables takes place on site by assembling the individual components. The monostrands are pulled into the PE pipe. Each strand is individually stressed in such way that after complete cable assembly all strands have the same stress. It is possible to restress the complete cable with a large jack. Single strands may be exchanged later individually. Technological innovations, jointed to new construction methods, lead to design bridges with record spans, mainly characterized by hybrid deck structures, as Sutong Bridge (2009,  $L=1008\text{m}$ ) and Russky Bridge (2012,  $L_{\text{main span}}=1104\text{m}$ ).

Concerning cable stayed bridge typology, seen as a quit recent structural system, in this thesis three successive generations are proposed. The first one (1955 – 1966) is characterized by short spans (150-250m): having a few number of stays, bridge static behaviour can be assimilated to that of a simply supported beam; full advantages of cable stayed system cannot be taken from these earliest solutions, which needed stiffened longitudinal girder to carry loads ( $h/L= 1/60$ ). The introduction of multi-cable stay system, occurred in 70-80s, gave the possibility to build slender deck for bridges (second generation): leading to a strict deck –cables interaction, reducing cable spacing (till i.p./L of 2%), this system results in lower compression strength transferred to deck; this guarantees to cover longer spans (300-450m) reducing girder depth ( $h/L= 1/80 - 1/50$ ). In the last decades (third generation), a closer succession of cross load bearing elements, corresponding to a discretization of the deck in portions having little effective length, as well the use of modern multi-box cross sections, ensures the required stiffness to deck, making possible the construction of bridge with high slenderness ratio (as  $1/354$ ).

## **Chapter 6 and 7: Deck stiffened system in concrete arch bridges and the case study of a Maillart arch type bridge**

Following considerations about concrete arch bridges can be inserted into the central thread of this dissertation, whose central aim is to underline the passage from flexural regime of structures having shorter span to the extensional regime of slender long span bridges, whose strict succession of deck cross sections



guarantee them to carry loads mainly through tensile or compression strength, quite deny bending moments upon longitudinal elements. In particular, reviewing the evolution of arch bridges, from the earliest masonry ones to the “pure steel arch” solution proposed by Calatrava, it can be said that the relationship between flexural and extensional regime has greatly changed varying structural materials.

For earliest masonry arch bridges with semi-circular shape, upper deck was clearly distinguishable from lower vault, while filling materials help to better transfer acting load from deck to the arch. From the Middle Ages, when segmental arch bridges became to be spread, their lower rise-to span ratio, implying high thrust values, makes more difficult to isolate flexural regime from extensional one. Instead, in the case of metal arch bridges, except from earliest examples with redundant structures, similar to monolithic masonry ones, the distinction between arch and girder load transferring system was somewhat clear. Starting from lowered segmental solutions, as precursor of modern rigid arch system or deck stiffened arch ones, the evolution of concrete arch bridge has often been marked by a progressive attempt to take better advantage from the use of a material that is capable to resist compression and thus, it's ideal for arches, basically working in compression: it's an artificial stone (Le Corbusier) making the concrete bridge the direct heir of the stone ones.

Passing through Hennebique's great innovative patent helpful to build reinforced concrete bridges, the major innovative approach in their design, especially in changing role of deck stiffened system has been Robert Maillart. His innovative use of concrete, especially in the design of thin arch structures, and his introduction of a wide range of new engineering forms, make him a seminal figure in the history of modern engineering. One of his crucial innovations was incorporating the bridge's arch and roadway into a form called the *hollow-box arch*, which would substantially reduce the bridge expense by minimizing the amount of concrete needed. In a conventional arch bridge the weight of the roadway is transferred by columns to the arch, which must be relatively thick to keep the bending stresses low under the loads resulting from bridge traffic. In Maillart's design, though, the roadway deck and arch were connected by three vertical walls, forming two hollow boxes running under the roadway. The big

advantage of this design was that for most of the bridge's span the load would be carried by all three parts of the hollow box: the deck, arch and walls. Maillart created a new type of structure: the arch without rigidity also called Maillart-type arch. This structure consists in reducing the arch thickness so that it has a minimum rigidity to bending and, therefore, support axial stress almost exclusively; the minimum of this rigidity will be that necessary for the arch not to buckle. Concentrated and asymmetrical live loads are distributed through the deck rigidity, which, in this case, must be greater than in normal arch bridges. Its behaviour is the inverse of suspension bridge one, because there are only axial stress in the resistant element while bending stress due to traffic load are distributed through the deck. With this method, Maillart was able to develop a new arch form, where the arch and the roadway are separated: each one was supported by columns or cross walls. (Billington, 1979). When the arch is made thinner than the upper deck, connecting one to the other through thin cross walls as pendulums, arch can be reduced to a slender ribbed vault, having the shape of dead load funicular curve. Considering that this one is not affected by stress due to accidental loads, the usual "adjustments of thrust line within arch walls" are not required: these one should be necessary to deviate real arch axis from the funicular curve, reducing moments due to permanent load - induced strain, both at the crown and at springing sections. The material required to construct the arch is minimized: all sections along the axis of the arch are in direct compression stress, while the stiffened girder carries bending and torsional effects due to live loads

This economic solution has had a great spreading also in Italy, during II Post-War reconstruction: since 60s, Cassa del Mezzogiorno acted a plane of measures, including environmental renewals and construction of new highways in South of Italy, in order to reduce the existing gap with Northern regions. About 40% of the whole budget has been spent to build a new track in one of the most pleasant tourist place Pompei- Salerno. Viaducts built during this period are still in use, requiring maintenance works to ensure users safety. In order to value vulnerability of Maillart arch type bridge, underlining any problems related to dynamic structural response of bridges designed to carry above all static vertical loads, a specific case is considered, Olivieri Bridge in Salerno.

As all the other bridges built in Southern Italy during the World War II reconstructions, also this one was, designed (by Benini and Schmidt) in such a way that made prevailed vertical loads bearing capacity: no specific computational evaluations were done about wind or seismic force effects. However, the analysis concerning this case study remarks structural engineers' mastery in design an extremely elegant viaduct, been excellently capable to counteract dynamic effects over decades.

Considering that in the previous chapters no evaluations have been exposed on dynamic behaviour of long span bridges since now, the last one debates on this peculiar aspect. Through FEM analysis, static and dynamic characterization of Olivieri Viaduct has been defined, considering both linear analysis applying static forces, and modal response spectrum or time history outputs: making different hypotheses on deck characterization and restraint conditions, the effect of horizontal forces has been valued, confirming a great vulnerability of the central arch for out of plane overturning effects.

Looking at modal analysis outputs, Viadotto Olivieri appears a very rigid structure: through a comparison between modal deformed shapes, it seems that few macro elements are involved in each one, underlining a structural behavior that is completely different from that of ordinary structures. This bridge hasn't been designed for seismic loads, even if its configuration as a Maillart arch type bridge makes this viaduct less vulnerable to dynamic effects than it could be supposed. Despite of current bridge structural response, a retrofit hypothesis is considered: even if it completely modifies bridge static scheme, the solution of cutting bridge deck, introducing seismic isolation and damping system, is analyzed to test against the effective efficiency of the existing structure, eventually strengthened.

## 2. Suspension bridges

### 2.1 Deck stiffened system: a common mean to read suspension bridges evolution

Some lines written by Steinman in “*The Builders of the Bridge – The Story of John Roebling and His Son*” (1944) <sup>[20]</sup> well explain the peculiarities of suspension systems; referring to Niagara Bridge design and construction, he said: [...] *From the most primitive swinging spans of twisted vines and fibers, there had of course been successive improvements in materials and in details of construction, but the full potentialities of the suspension type could not be realized as long as it continued to be represented by swaying, undulating structures. As Roebling expressed it: “Suspension bridges have generally been looked upon as loose fabrics hung up in the air, as if for the very purpose of swinging. Repeated failures of such works have strengthened this belief”. Even in his earliest spans, the master builder grasped the fundamental importance of stiffened construction. His success in the construction of suspended aqueducts – as rigid as stone or cast iron aqueducts- demonstrated the truth of his thesis that cable spans could be built as stiff as desired. [...] But it was in the Niagara Bridge that his new concept received its first full expression – the first use of stiffening trusses in all the history of bridge building (1855)”*.

Passing from the earliest vines suspension bridges to the modern aerofoil deck solutions, the following excursus remarks the great improvements in deck stiffened system, till reaching record slenderness nowadays. Critically looking at the earliest suspension bridge collapses, it has been noted the importance of rigid deck as the only way to better exploit the potentialities of this structural system; meanwhile, it has been seen how the improving studies concerning aerodynamic stability (subject which lies outside the scope of this thesis) have guaranteed the use of lighter and slender superstructures, greatly reducing bridge weight and construction costs.

Form past examples to nowadays record span structures, suspension bridges have always been characterized by four main components: (1) the deck (or stiffening girder); (2) the cable system supporting the deck; (3) the pylons (or towers) supporting the cable system; (4) the anchor blocks (or anchor piers) supporting the cable system.

Considering that suspension system configuration have had no many changes since the origin, although a great improvement can be recognised in cable technologies, there is no doubts that the most influential aspect in suspension bridge design has always been the deck system configuration. It's interesting to note how the process towards structural optimization of deck stiffened system has been marked by two main theoretical approaches, firstly the linear theory (1858 - Rankine, Steinman), then the deflection theory (1888 - Ritter, Lévy, Melan). Rankine <sup>[10]</sup> was probably the first to address the problem of the stiffened

suspension bridge. He assumed that the (parabolic) cable contributes a uniformly distributed reaction to bending of the girder, via the suspenders, of intensity given by the total live load divided by the span: this holds true only in the case of uniform live loading. In <sup>[5]</sup> “*Applied Mechanics* (1858)” he underlined the necessity to have a stiffened deck system, as follows: “*Article 340. The suspension bridge is that which requires the least quantity of material to support a given load. But when it consists, as in Article 169 (cord under uniform vertical load), solely of cables or chains, suspending rods, and platform, it alters its figure with every alteration of the distribution of the load; so that a moving load causes it to oscillate in a manner which, if the load is heavy and the speed great, or even if the application of a small load takes place by repeated shocks, may endanger the bridge. To diminish this evil, it has long been the practice partially to stiffen suspension bridges by means of framework at the sides resembling a lattice girder.[..] It was formerly supposed that, to make a suspension bridge as stiff as a girder bridge, we should use lattice girders sufficiently strong to bear the load of themselves, and that, such being the case, there would be no use for the suspending chains.[..] The weight of the chain itself, being always distributed in the same manner, resists alteration of the figure of the bridge. By leaving it out of account, therefore, an error will be made on the safe side as to the stiffness of the bridge, and the calculation will be simplified.*”

To better understand the role of deck stiffened system, as well as effects of linear and deflection theories on suspension bridge design, a particular loading scheme can be considered (Fig. 2.1). It is assumed that upon a cable, suspended between two points, is applied a uniform distributed dead load, so that the bending moment diagram, as the resulting equilibrium curve of the suspended cable, is a parabola. When a uniform distributed live load asymmetrically acts only upon one half of the cable, the corresponding funicular curve doesn't match with the initial parabola, due to uniform distributed dead loads, so that bending moment caused by acting live loads rises. Two different interpretation of this phenomenon follow.

For the earliest applications, in order to restrict the static distortions of the flexible main cable, as consequence of loads transferred by hangers, a stiffening truss was necessary. Steinman's theory was taken into account, adopting a truss which was sufficiently stiff to render the deformations of the cable due to moving loads, practically nihil. Five assumptions characterized this approach: (1) The cable is supposed perfectly flexible, freely assuming the form of equilibrium polygon of the suspender forces; (2) The truss is considered a beam, initially straight and horizontal, with constant moment of inertia; (3) Truss dead load is assumed uniform per linear unit, so that cable shape is a parabola; (4) It's assumed that cable configuration (shape and coordinates) doesn't change after the application of moving loads; (5) Dead load is carried only by the cable, causing no stress in the stiffening truss. With a linear elastic theory based on the

assumption that the change in geometry due to deflections caused by the applied traffic load can be ignored, the moments to be taken by bending in the deck can be expressed by ( $M = Hy$ ), where ( $H$ ) is the horizontal force (related to the funicular curve) and ( $y$ ) is the vertical distance from the cable axis to the funicular curve.

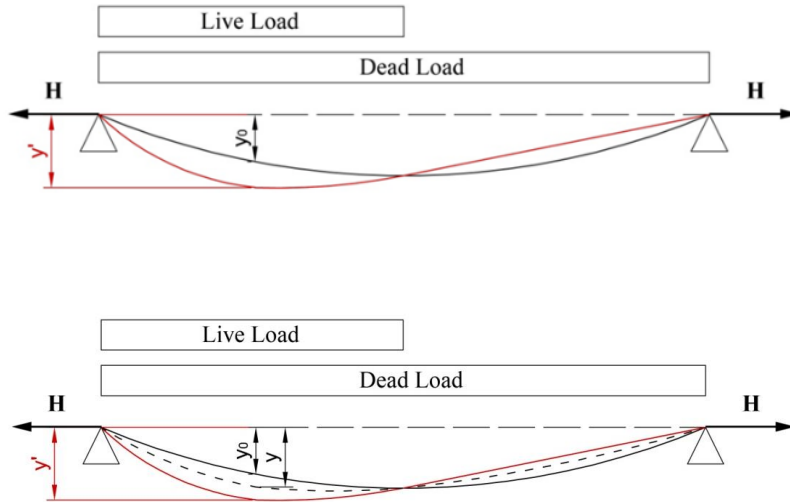


**Fig. 2.1.a:** Linear theory [black line: dead loads funicular curve; red line: applied live loads funicular curve]

**Fig. 2.1.b:** Deflection theory [black line: dead loads funicular curve; red line: applied live loads funicular curve; dashed line: cable deformed shape]

The deflection theory, instead, is a nonlinear elastic theory that takes into account the displacements of the main cable under traffic load when calculating the bending moments in the stiffening truss. Thus, equilibrium is established more correctly for the deflected system than for the system with the initial dead load geometry. Due to the hangers linking the deck to the main cable, the deflection of the deck will cause a change in the geometry of the main cable. It will be seen that the cable moves towards the funicular curve, and as equilibrium must exist in the deflected system, the real moments in the deck will be represented by the horizontal force  $H$  multiplied by the vertical distance ( $y' - y_0$ ) from the funicular curve to the distorted cable. When taking into account the nonlinear elastic effect related to the displacement of the cable, the bending moments in the deck is reduced, often to less than half of that found by a linear elastic theory. Actually, there are no limits to the reduction that can be achieved, as a suspension bridge with a very slender deck and therefore insignificant flexural stiffness deflects under asymmetrical loading until the displaced cable and the funicular curve coincide.

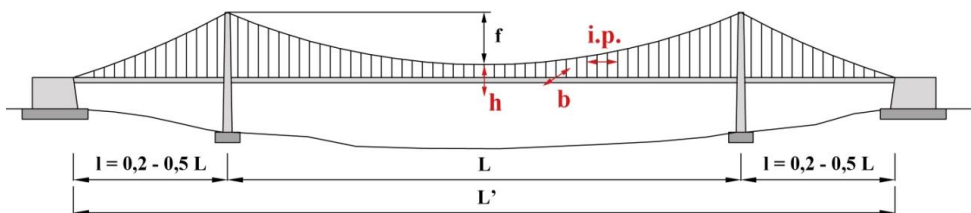


**Fig. 2.2** Suspension bridge scheme: main design parameters




In order to well describe how this typology has changed, underlining its peculiarities and how their variations have had a great influence on bridge behaviour, three main design parameters have been considered.

The following values synthesize how deck-to-cable load-transferring system has been influenced by the choice of increasing hangers number or making the longitudinal girder slender, thanks to the use of deep-close spacing deck cross sections, however preserving the necessary deck width to prevent instability phenomenon; (Fig. 2.2)

- ( $i.p./L$ ), hangers spacing-to-main span length ratio, to describe suspension cable distribution;
- ( $h/L$ ), deck-depth-to span ratio, to define deck slenderness.
- ( $w/L$ ), width deck-to.-span ratio, to define deck torsional stiffness

The structural optimization process towards slender and lighter structures is marked by a change in deck cross section type, passing from the early truss-deck stiffened system to modern slender suspension structures.

Looking at technical improvements occurred, as consequence of deflection theory application, as well as of aerodynamic studies, tracing historical evolution of suspension bridges, three different generations, as many different ways to conceive stiffened girder, have been proposed in this thesis, as follows (Tab. 2.1).

Bridge layout	year	theory	Parameters
 <b>I GENERATION</b> Deck stiffened- suspension system	1883-1940	Linear theory	<b><math>L_{\text{main span}}</math></b> 480- 850m <b><math>i.p./L</math></b> 1 -2% <b><math>h/L</math></b> 1//70
 <b>II GENERATION</b> Slender deck stiffened- suspension system			<b><math>L_{\text{main span}}</math></b> 900-1100m <b><math>i.p./L</math></b> 1% <b><math>h/L</math></b> 1//150
 <b>III GENERATION</b> Aerofoil deck system	1964-2009	Aero-dynamic stability	<b><math>L_{\text{main span}}</math></b> 1200-1400 <b><math>i.p./L</math></b> 1% <b><math>h/L</math></b> 1/400

## 2.1 Historical development: changing role of stiffened girder

### From the precursor to the birth of modern suspension bridges

Even if cable-stayed bridge type has recently demonstrated a significant advancement, there is no doubt that suspension bridge constitutes the main solution for long-span structures. Primitive suspension bridges were probably used by people even before the arch bridges of ancient Rome. Since their origins, Pygmy tribes of Africa, Peru, New Guinea have built bridges entirely of vines. The common configuration of these bridges consists of the main cable where people walk, which coincides with bridge deck, while two or more cables that hang at both sides as the handrails form a V-section. The shortcoming of V-shaped suspension bridges is that the loading point greatly deflects and pulls upper the other cables; in fact, when the load on the main cable is only its weight, it assumes the catenary form: if vertical loads are applied on it (as walking people) the cable assumes a definite polygonal form determined by the reaction between loads. Only one person could cross such suspension bridges, so U-shaped system, with wider deck, became necessary.

Before the suspension bridge was developed to support horse-drawn carriages and, later, cars in modern traffic, a great step beyond the primitive examples was required. (Fig. 2.3) First, the deck should not follow the catenary curve, but it should form a more flat roadway. Second, to avoid excessive deflection due to live loads a certain degree of stiffness was essential. The first suspension bridge which conquered these problems was Jacob's Creek Bridge in Westmoreland County, Pennsylvania in 1801. This bridge was the first to have all the necessary components of a modern suspension bridge and was designed by James Finley who patented a system for suspending a rigid deck from a bridge's cables in 1808. This years is considered as a begging o the era of the modern suspension bridges. In designing his bridge, Finley adhered to a few principles. First, he wanted the bridge to be economically sensible in both construction and maintenance. Additionally, he wanted his bridge to be easy to construct and applicable to any site for implementation throughout the state. Finley conducted several experiments after his final term as state senator in 1793. (Fig. 2.4) Finley would hang weights from cables and observe the results, noting both pressure and movement. After years of testing designs through various experiments, Finley finally found a formula he was pleased with and in 1801, he publicly proposed his design.

**Fig. 2.3.** (a), (b), (c) suspension bridge (Perù: Africa), V-shaped and U-shaped parameters – (d) d Kazura Vine Suspension Bridgez, Japan





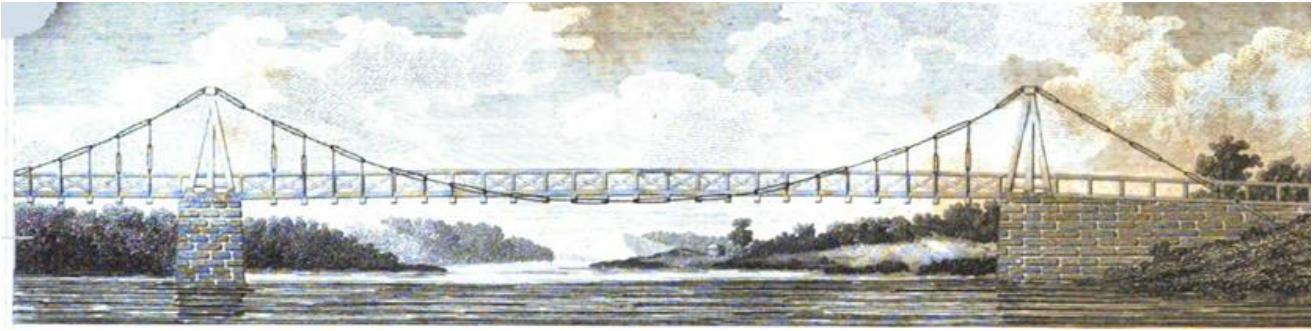


**Fig. 2.4** Jacob's Creek Bridge, Finley (1810) (A description of the patent Chain Bridge, in *The Port Folio*, Vol. III, No. 6, p. 440)

Finley went on to describe the design in 1810 in the political magazine *The Port Folio*<sup>[1]</sup>: *"The bridge is solely supported by two iron chains, one on each side, the ends being well secured in the ground, and the chains raised over piers of a sufficient height erected on the abutments at each side, extended so slack as to describe a curve, so that the two middle joists of the lower tier may rest on the chains"*. What made Finley's bridge stand out most was that it was much stronger than the common wooden truss bridge of the time. In fact, Finley's bridge was able to hold much more than its own weight. The bridge itself would require 140 tons of material, but would ultimately be able to support 540 tons of weight. This would leave 400 tons of weight bearing ability—well over double its own weight. Compared to ancient suspension bridges, one of the most noticeable differences of Finley's bridge was that it had a solid and level horizontal deck. This improvement meant the bridge would be able to handle carts and other wheeled vehicles easily, as opposed to just simple foot traffic. Additionally, Finley's bridge had support points for the cables at both ends of the bridge, not just one. This innovation allowed the weight to be distributed more evenly, resulting in more strength. Most importantly, Finley implemented support joists—beams running horizontally beneath the deck—to aid in bearing weight and to prevent bridge oscillations. Finley stressed the separation of the deck used by people and horse drawn carriages from the main cables that support loads. He claimed that the distribution of loads to many hangers would eliminate excessive deformations in the main cable. Technically, Finley understood the effect of stiffening girder in suspension bridges: *"[...] four or more joints will be necessary for the upper tier to extend from end to end of the bridge. Each will consist of more than one piece; the pieces had best pass each other side by side so that the ends may rest on different joints of the lower tier"* (Finley, 1810). Although many of Finley's bridge had unfortunate endings in North America, his unique concept was introduced by Thomas Pope in *"A Treatise on Bridge Architecture"* (1811) and become widely known in Europe.

**Fig. 2.5** Dryburgh Abbey Bridge (1817), Smith, collapsed



Even in the modern world, Finley's ideas and designs are still appreciated. Historian Emory Kemp has noted, "*In an age when master builders produced designs with little or no engineering sensibilities, Finley overcomes this lacuna in engineering design by producing a method for detailed analysis [...]*". Perhaps one of the greatest acknowledgments to Finley in the modern world is that his designs are still being put to use today. Thousands of bridges today rely on the same suspension technology Finley used. In 1998, a bridge 3911m in length, with a main span of 1991m, was built in Japan (*Akashi Kaikyo Bridge*).

### Early failures of deck unstiffened suspension bridges and new design proposals

Britain was the first European country where Finley-type bridge was built, as *Dryburgh Abbey Bridge* (1817) (Fig. 2.5). This slender deck bridge, built to cross Tweed River, spanned 79.3m with a 1.2m-wide deck. It had a very noticeable vibration when crossed by pedestrian, and the motion of chains appeared to be easily accelerated. In 1818, six months after its completion, the bridge was destroyed by a violent gale. For the reconstruction of *Dryburgh Abbey Bridge*, Brown introduced the design concept of Finley's modern suspension bridge, opening a new era in Britain. After his experience in manufacture and development of chain for ships during his service in the navy, in 1808 Brown invented a bar chain made of round or flat bars with holes at both ends to supplement defects in strength of traditional link. Adopting this technology, Brown built the first modern suspension bridge in Europe, the Union Bridge (Fig. 2.6), which spanned the River Tweed with a 140m-length and 5.5m-width. Despite of its slender deck, wrought iron main cable and vertical hangers dead load have a great effect to stabilize deck. The first large bridge that used the technique invented by Finley was bridge over the *Menai Strait in Wales* (Fig. 2.7) built by Thomas Telford and finished in 1826. Featuring a 168m-main span, with a 4.88m-wide deck, was the first bridge to exceed the record length span of the Union Bridge. The deck was suspended 30.50m above the water and its masonry towers reached a height of 46.60m.

**Fig. 2.6** Union Bridge (1820). Brown. River Tweed, Scotland. L=140m





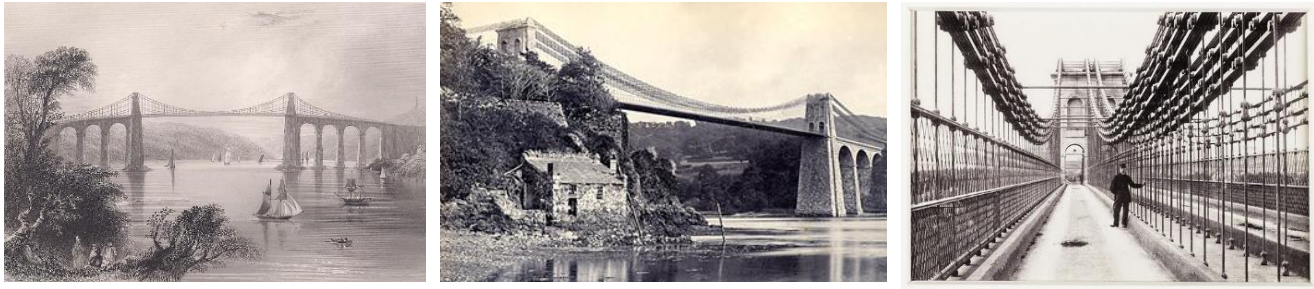


**Fig. 2.7\_ (a), (b)** Menai Bridge, completed in 1826. From *The Life of T. Telford* (1838). \_ (c) 1826. Photo of original transverse struts between cables.

Its 2187 tonnes of iron and its 520m-total length elevated the bridge to an incomparable scale for its era. Telford had not sufficiently understand the necessity of stiffness for his suspension bridge: Menai Bridge had no storm cables and, though it was designed to be relatively heavy with a weight of 435 kg/m<sup>2</sup>, it became “victim” of wind. The suspension bridge frequently oscillated when it was nearly completed: cable of the centre span moved separately and the struts between them as countermeasure proved to be effective (Report, December 12, 1825. Provis). On January 1839, the weakened suspension bridge swayed violently during which torsional vibration was induced: about 444 hangers were damaged; only the central walkway survived. Because strong wind effect, timber deck was replaced with steel structure (1892). During 1938-39 rehabilitations, the wrought iron chains were replaced with steel chains; a steel stiffening truss was installed at this time. (Fig. 2.8)

An extraordinary contemporary example which greatly underline the role of stiffened girder in suspension bridge is the iron chain suspension bridge on Garigliano river, well known as the *Real Ferdinando Bridge* (Fig. 2.9) designed by Luigi Giura (1828-1832). It was the first iron suspension bridge built in Italy, and one of the earliest in continental Europe. This bridge, which was technologically advanced for its age, was built in 1832 by the Bourbon Kingdom of Two Sicilies. The structural scheme of the suspension bridge is characterised by a deck of 5.80 m wide with a span of 85 m. The suspension system consists of two couples of chains, each chain has a rectangular cross-section made of puddled iron, which are connected together by means of cylindrical pins. The vertical suspension ties, 1.36 m spaced, are connected to the pins of the chain.

**Fig. 2.8** Menai Strait Bridge (after rehabilitations of 1938-39)





**Fig.2.9** Real Ferdinando Bridge on Garigliano River. (1828-32). Luigi Giura

The retaining chains are anchored in a massive block of stone masonry at a depth of 6 m and at a distance of 24 m from each pier, where the sphinxes indicate the point of anchorage. From the analysis of the existing original materials (Mazzolani, *Aluminium Structures in Refurbishment: Case of the Real Ferdinando Bridge on Garigliano River*. In: *Structural Engineering International*, v. 16, n. 4 (November 2006), pp. 352-355), it has been possible to value as follows: the total dead load of the bridge structure, including chains, ties and deck, can be evaluated at about 260 kg/m<sup>2</sup> and the structure has been checked for a live load of 240 kg/m<sup>2</sup>; for the total load of 500 kg/m<sup>2</sup> distributed along the span, the value of the axial force in the chains is 500 tons, which corresponds to a stress of about 15 kg/mm<sup>2</sup> in the material (a value too high for the puddled iron).

The structural scheme, proposed by Luigi Giura, has a stable performance under vertical loads, provided that they are symmetrically distributed; the deformability of the bridge is, instead, very high when the live load is not symmetrically distributed; due to the total absence of horizontal bracings, the bridge is not able to resist any kind of lateral forces, like wind and earthquake, so that too large horizontal displacements can arise; the considered live loads are inferior even to the ones which today are requested for a simple foot bridge. These remarks confirm the general consideration that the old structures of the 19th Century were mainly designed to resist vertical and symmetrical loading conditions, but asymmetrical and horizontal loading conditions were ignored.

In contrast to Telford's approach, Robert Stephenson, son of George Stephenson, an inventor of railroad, showed a great interest in the stiffness of suspension bridges, being more cautious in designing a railroad bridge across the Menai Straits, near Telford's bridge. Due to lack of stiffness in traditional suspension bridges, considering excessive deflection due to running trains, an attempt to supplement stiffness was made adopting box section for steel girder. The ever-prudent Stephenson proposed a huge box with 9m-depth and 4m-interior width to span the distance of 146m. Since it was completed in 1850, it has been known as *Britannia Tubular Bridge*: the excessive deck stiffness made suspension system practically unnecessary. (Fig. 2.10)



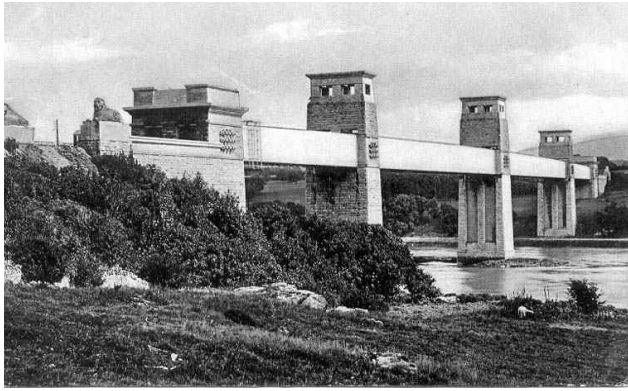


**Fig.2.10** (a) (Original) Britannia Tubular Bridge- Menai Strait. (1850) (b) (Rebuilt) Britannia Bridge- Menai Strait. (1972)

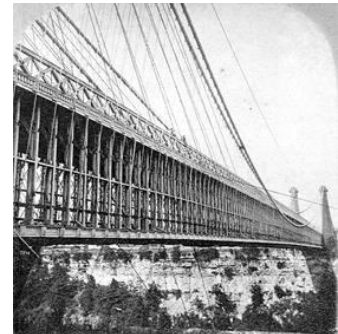
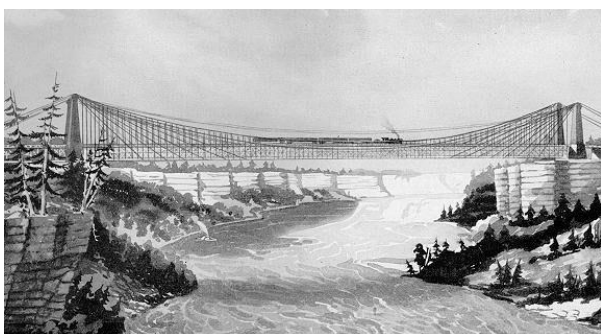
In the decades following the introduction of Finley's approach, several suspension bridges were built, many of them unstiffened. After being dismissed in the design of Britannia Bridge, the concept of stiffened suspension bridge didn't take roots in Europe: the enthusiasm rapidly died because of continuing accidents. Following a disastrous fire in 1970 it was rebuilt, initially as a single-tier steel truss arch bridge, carrying rail traffic. A second tier was added later and opened in 1980 to accommodate road traffic.

### Roebling's revolution

As a consequence of some spectacular collapses of suspension Bridges, occurred in 1810s, caused by wind oscillations, Roebling voiced his perception that stiffened girder and additional inclined stays would make rigid bridges.

After several successful smaller bridges he achieved his breakthrough in 1851 with the *Niagara Falls Bridge*. *"In all the world no place could have been found where the building of suspension bridge would present a more spectacular accomplishment than over the Niagara gorge"* (Fig. 2.11) (Steinmann, 1944). Roebling's bridge had to replace Ellet's temporary suspension bridge, collapsed in a storm in 1854, 5 years following its completion. The collapse was induced by asymmetric torsional vibration. Roebling, *"a practical man as well as a stubborn one"*, was completely different from his rival, as Steinmann (1944) wrote, *"it was the difference between the profound and the superficial, between the enduring and the spectacular. Ellet's performance was a dazzling fireworks display, quickly burning into itself"*.<sup>[20]</sup>

**Fig.2.11** Niagara Falls Bridge, J.Roebling, 1855



In 1851 Roebling began his construction operations on the Niagara bridge, continuing without interruption for four years: in march 1855 the bridge was completed.

The main problem Roebling underlined for this for this suspension bridge with a record span of 251.5 m was to achieve the necessary stiffness for the high railway loads and to stiffen the exposed beam high above water against dangerous wind oscillations. He reached these objectives in two ways. First he used a 6 m deep timber truss in order to stiffen the beam, and second used inclined stays in the outer thirds of the main span. *“Without adding much to the weight of the structure, a surprising degree of stiffness has been obtained by the action of girder and truss”* said Roebling in 1855, about Niagara Falls Bridge. He clearly separated the upper railroad girder from the lower roadway girder; between them, timber post and steel rod tension member were rigidly assembled to make a truss. Combining girder and truss, a more rigid stiffening system was created. The practical experience he was able to gain building canal aqueducts was an important contribution to his significant recognition that simply making a suspension bridge heavier did not improve its bearing capacity and that this could be done more effectively by buttressing of the bearing structure. Roebling recognised that it was possible to optimise the girder’s capacity by dispersing the horizontal bearing diagonal casing in pure support beams and thereby achieved a reduction in the weight of the bearing system. The division into upper and lower decks proved to be particularly effective in improving the bearing capacity and durability of the whole bridge. Roebling recognised that a truss system is lighter than any comparable structure of the same rigidity and bearing capacity. In comparison to simple truss beams, a hung diagonal bridge box has the particular advantage that the danger of sideways movement was avoided by regular attachments. The free spinning procedure that Roebling had already used in building his hanging canal aqueducts provided large scale and compact bearing cables. In his Report to the Directors of the Niagara Falls International and Suspension Bridge Companies from 28 July 1852 Roebling argued that the bearing capacity of a suspension bridge depends essentially on the factors of the resistance of the materials and the rigidity of the construction. In order to achieve a sufficient system resistance for the bridge, as well as the rigidity of the cables from wrapping, Roebling outlined the following three models: (1) *the use of horizontal beams stiffened in mass and bending bearing capacity*. (2) *the use of trusses*; (3) *the stiffening of the system with stays*. Roebling himself believed that the construction of rigid railway bridges made of wood and iron hanging on bearing cables were very economical and predicted possible spans of bridges made only of iron of 600 m and more.

On May 17, 1854, during Niagara Bridge construction, a telegraph announced a great suspension bridge catastrophe: Roebling rival, Ellet’s bridge over the Ohio at Wheeling had collapsed. Completed in 1849 as the longest bridge in the world at the time, the Wheeling Suspension Bridge was destroyed by a wind storm.



**Fig.2.12** Wheeling  
Suspension Bridge, 1872,  
Washington Roebling  
and Wilhelm  
Hildenbrand

Anticipating the emblematic case of Tacoma Narrow collapse in 1940, the complete history of the disaster can be found in the following eyewitness account by a reporter, published in the New York Time, four days later bridge collapse, then reported by Steinmann in his book (1944): “ [...] *The Welling Suspension (Fig. 2.12) Bridge has been swept from its strongholds by the terrific storm and now lies as a mass of ruins. [...] About 3 o'clock yesterday we walked toward the Suspension Bridge and went upon it enjoying the cool breeze and the undulating motion of the bridge, when [...] we saw persons running toward the river bank; we followed just in time to see the whole structure heaving and dashing with tremendous force, [...] lunging like a ship in a storm; at one time it rose to nearly the height of the tower, then fell, and twisted and writhed, and was dashed almost bottom upward. At least there seemed to be a determined twist along the entire span, but one half pf the flooring being nearly reserved, and down went the immense structure from its dizzy height to the stream below. For a mechanical solution of the unexpected fall [...]: the great body of the flooring and the suspenders, forming something like a basket swung between the towers, was swayed to and fro like the motion of a pendulum. Each vibration giving it increased momentum, the cable, which sustained the whole structure, were unable to resist[...].*” According to Steinmann, the dramatic description of Wheeling collapse summarized the “*crux of aerodynamic phenomenon*”, saying that “*Each vibration giving it increased momentum*”.

At that time, Roebling was the only one who grasped the full reason of the disaster: he realized the need of bracing and stiffening suspension spans against “*cumulative undulations that may be started by the action of wind*”. Later in 1874, Washington Roebling and Wilhelm Hildenbrand rebuilt the bridge adding stay cables, thus “*Roeblingizing*” it. Over 166 years after it was built, the bridge still carries traffic over the Ohio River. As in the case of Wheeling Bridge reconstruction, also “*In the Niagara Railway Suspension Bridge Roebling made an outstanding and enduring contribution to the fundamental principle of suspension-bridge design. He taught the profession the importance of stiffening suspension span, and he showed the world the effectiveness of such stiffening. His predecessors and his rivals had failed because they did not realize the importance of this feature and had omitted it in their structures. The necessity of providing an adequate stiffening system was a new concept to the profession*”, Steinman, “*The Builders of the Bridge – The Story of John Roebling and His Son*” (1944).





Roebling's highest achievement as a bridge engineer was the *Brooklyn Bridge* (Fig. 2.13) (Fig. 2.14) (tab. 2.2) in New York with a new record span of 486 m. He started the design in 1865. One of its most distinctive features is the system of inclined stays radiating downward from the towers. Roebling introduced this primarily for the critical function of adding rigidity to the span, and then ingeniously took advantage of the additional load-carrying capacity which they incidentally supplied. The entire bridge floor rises from the towers at an elevation of 42.5 meters above the high water level.

**Fig.2.13** Brooklyn Bridge.  
Manhattan/Brooklyn,  
New York, USA, 1883,  
John A. Roebling

The framework comprises of two systems of girders at right angles to each other. The floor is further united by 25.8m- wide longitudinal trusses together with a system of diagonal braces or stays. The whole combination increases its strength, weight and stiffness. Roebling's design was quite far from the application of linear theory: the principle of use deep-closed spacing transverse elements to carry longitudinal truss girder was similar to that one use in the early examples of suspension bridge, as Telford's Menai: in these cases, using unstiffened deck, main load bearing capability was accomplished above all by transverse elements. In 1944, the elevated trains that ran along the interior of the bridge stopped service. Over the next decade, bridge engineer David Steinman took a reconstruction project which included the strengthening of inner and outer trusses and installation of new horizontal stays between the four main cables. As the railroad and tracks were removed, he widened from two lanes to three lanes in each direction, and constructed new approach ramps.

Roebling firstly introduced the use of steel, which is named as '*the metal of the future*', for the cables. Before the Brooklyn Bridge was constructed, no engineers tried the use of steel wire in bridge construction. Thirty-two drums, 2.9 meters in diameter, were installed in the position of carriage-wheels just clear of the floor. Thousands of coils of wire were delivered on site, dipped in linseed-oil and dried. The cables and suspenders were connected by suspender bands, which were made of wrought iron 127 mm wide and 16mm thick. The bands were cut at one point, two ends turned outward, so that the ends can be placed over the cables. There were holes on the end of the bands for the screw-bolt 44mm in diameter.





**Fig.2.14** Brooklyn Bridge\_ (a) deck detail\_ (b) cable system detail

Although for suspension bridge there are generally one or two stiffening trusses for each suspension system, Brooklyn Bridge is an exception, having six stiffening trusses for four cables; this, however, has proved to be an unsatisfactory and inefficient arrangement (Steinman, 1922)

**Tab 2.2** Brooklyn Bridge\_design parameters

<b>L (main span) [m]</b>	486	<b>width [m]</b>	26
<b>L tot [m]</b>	1053	<b>w/L</b>	1/19
<b>H (girder) [m]</b>	5.60	<b>i.p. (hanger spacing)</b>	2.30
<b>h/L</b>	1/87	<b>i.p./L</b>	1/211 (0.47%)

### Early application of deflection theory (1883 – 1940), till Tacoma Narrow collapse

The precautionary approach of Britannia Tubular Bridge, with its massive stiffened girder, seems to return in designing *Williamsburg Bridge*, a suspension bridge which was greatly criticized by everyone. (tab. 2.3) (Fig. 2.16) (fig. 2.16) Steinman, who at the age of 14 (in 1900) had obtained a pass from the city to walk around on the temporary roadway while the suspender were being worked on, called the design “*ungainly and clumsy*”. Its main suspended span of 488 m was 1.4 m longer than the Brooklyn Bridge, making it the longest in the world for 21 years (until surpassed by the Bear Mountain Bridge). Although a number of engineers were involved with various concepts and designs for the bridge, the design is attributed to Leffert Lefferts Buck.

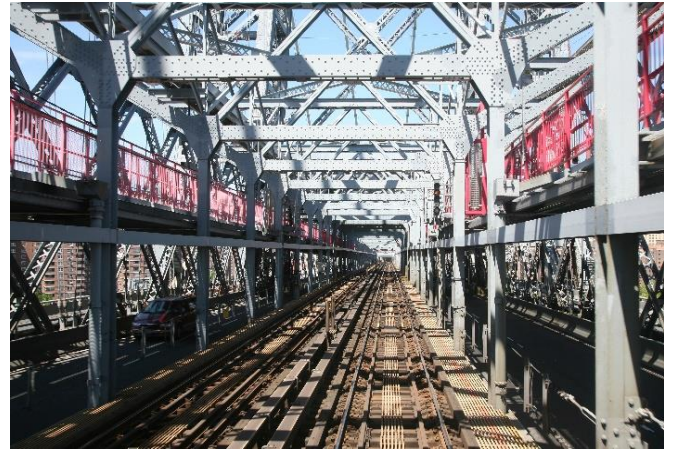
**Tab 2.3** Williamsburg Bridge design parameters

**Fig.2.15** Williamsburg Bridge. Manhattan/Brooklyn, New York, USA, 1903, Leffert L. Buck\_ (a) longitudinal view\_ (b) tower detail\_ (c) railroad detail\_ (d) deck bottom view\_ (e) cast iron stairway on the Manhattan side

<b>L (main span) [m]</b>	488	<b>width [m]</b>	36
<b>L tot [m]</b>	852	<b>w/L</b>	1/14
<b>H (girder) [m]</b>	12	<b>i.p. (hanger spacing)</b>	6.10
<b>h/L</b>	1/41	<b>i.p./L</b>	1/50 (1.25%)







When Gustav Lindenthal was appointed as New York City's bridge commissioner in 1902, he had reservations about the design and appearance of the bridge, but it was too far along in construction to make major changes. The Williamsburg Bridge was the first bridge to use steel instead of masonry towers. Buck recommended the use of steel towers because they would reduce the size of the foundations, could be reinforced if needed at a later date, would be quicker to build, and would cost less than masonry towers. Each tower is 333 feet (101 m) high and contains 3,048 tons (2,765 t) of steel placed on a solid bedrock foundation. Among existing suspension bridges, the design of the Williamsburg Bridge is unique in that no weight is carried by the main cables between the towers and anchorages (similar to Roebling's Niagara Falls Suspension Bridge, which stood from 1855 to 1897). It consists of a no-continuous stiffening truss, having two hinges (no centre-hinged), with free side spans. The bridge deck was supported by truss work in these locations to reduce the overall cost (shortening the distances between anchorages and allowing lighter cables to be used) and to eliminate the bridge deck from being suspended at both of its ends. The stiffening trusses are 12 m deep, designed to support the rail traffic on the deck. The overall width of the bridge is 36 m, over 9 m wider than the Brooklyn Bridge, with double the load carrying capacity. It was the last major suspension bridge to have its stiffening trusses designed by the elastic method first proposed by Rankine.

**Fig.2.16** Williamsburg Bridge. New York, USA, 1903\_ (a) deck bottom view\_ (b) cast iron stairway on the Manhattan side





**Fig.2.17** Manhattan Bridge. Manhattan/Brooklyn, New York, USA, 1912, Leon Solomon Moisseiff

Discussions about the need for a third East River crossing between Manhattan and Brooklyn began as early as 1898, when it became apparent that the completion of the Williamsburg Bridge (then under construction) could not alone satisfy the ever increasing demand in travel between the two boroughs and relieve crowding on the railways across the Brooklyn Bridge. The proposed structure was simply known as "Bridge No. 3" until March 1902 when the Board of Aldermen decided to name it the Manhattan Bridge. The third design for the *Manhattan Bridge*—(Fig. 2.17) (Tab. 2.4) the one eventually approved and constructed—was, instead, the first to use Josef Melan's deflection theory for the stiffening of the deck. Moisseiff's pioneering use of the deflection theory (as opposed to the more conservative elastic theory) resulted in a much lighter and shallower stiffening truss, reducing the amount of materials that were required in construction. As the first suspension bridge to use the deflection theory, it is considered to be the forerunner of modern suspension bridges and served as the model for the major long-span suspension bridges built in the first half of the twentieth century. The bridge was to span 448metres between piers, which was a somewhat shorter distance than the main spans of either the Brooklyn or Williamsburg bridges that neighbour it.

**Tab 2.4** Manhattan Bridge design parameters

<b>L (main span) [m]</b>	448	<b>width [m]</b>	36.60
<b>L tot [m]</b>	890	<b>w/L</b>	1/12
<b>H (girder) [m]</b>	7.30	<b>i.p. (hanger spacing)</b>	5.70
<b>h/L</b>	1/61	<b>i.p./L</b>	1/79 (1.26%)

The entire structure of the Manhattan suspension bridge was to be designed in steel. The Manhattan Bridge contains four parallel stiffening trusses, each below a main cable, and was the first suspension bridge to utilize a Warren truss in its design. The four cables are supported by the two towers and are held down by anchorages 224metres from each side of the main span: nickel steel eyebars were used. The Manhattan Bridge pioneered the use "two-dimensional" slender steel towers, which are 98 m high, and was the earliest bridge to incorporate nickel steel to a large extent in construction. Unlike the Williamsburg Bridge, which had four columns in each of its steel towers, the towers of the Manhattan Bridge were only braced in two directions. This allowed the towers to flex, reducing bending moments and requiring smaller foundations under the towers.





A total of 42,000 tons of nickel steel (which is lighter and stronger than carbon steel) was used in the bridge's superstructure. Nowadays this two-decked suspension bridge carries automobile, truck, subway, bicycle, and pedestrian traffic over the East River. The \$834 million reconstruction program began in 1982; rehabilitation included: reconstruction of the north and south upper roadways; reconstruction of the north and south subway tracks; installation of a truss stiffening system (to reduce twisting).

A crucial example to understand the changing role of stiffened girder for suspension bridges is Amman's *George Washington Bridge*. When the George Washington Bridge first opened to traffic on October 25, 1931, its 1,067 m long main suspended span nearly doubled the length of the Ambassador Bridge, the longest bridge at the time.

While the towers and cables were designed to support the future addition of a lower level to expand capacity, the original bridge had single deck and did not include a stiffening truss (unlike other types of suspension bridges built in that era). A stiffening truss was not necessary because the long roadway and cables provided enough dead weight to provide stability for the bridge deck, and the short side spans acted like cable stays, further reducing its flexibility. One of the busiest bridges in the world, the George Washington Bridge originally carried six lanes of traffic when it opened to traffic on October 25, 1931. (Fig. 2.19)

**Fig.2.19** George Washington Bridge. Fort Lee/Manhattan, New Jersey/New York, Othmar Ammann\_ (a) (1931) original configuration: single unstiffened deck\_ (b) (1962) final configuration: double deck stiffened system





**Fig.2.19** George Washington Bridge.  
(a) (1931) original configuration: unstiffened deck construction\_  
(b) (1962) final configuration: double truss deck

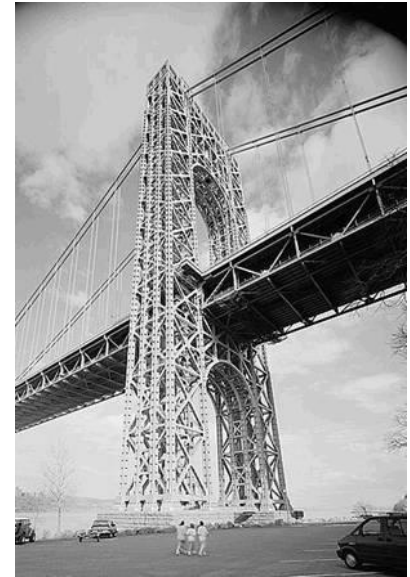
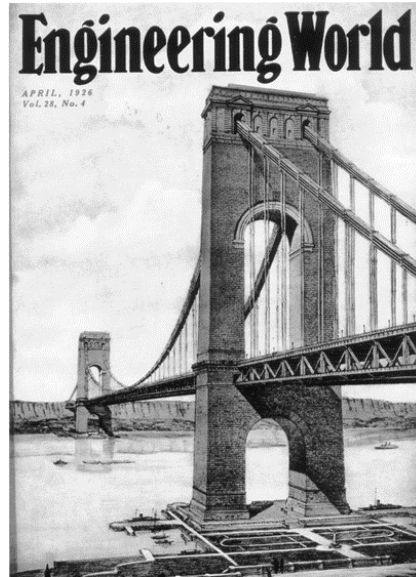
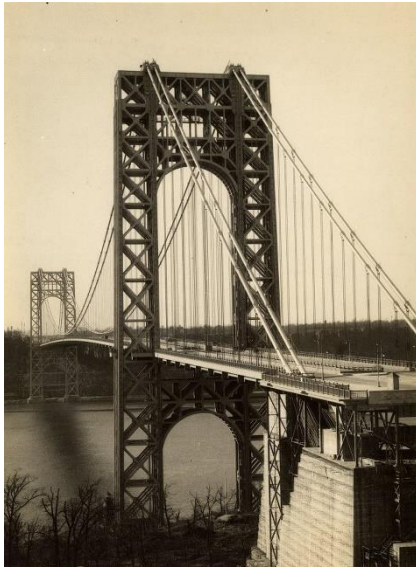
Two more lanes were added to the centre median in 1946. Although Ammann's original design made a provision for the addition of a lower deck to carry four rapid transit tracks, no interest was taken by railroads in operating commuter service across the bridge and the growing volumes of cars, trucks and buses eventually made the addition of more traffic lanes a necessity. The lower level of the George Washington Bridge opened on August 29, 1962. (Tab. 2.5) (Fig. 2.20) (Fig. 2.21) With this masterpiece, Amman theorized that heavy stiffening trusses were no necessary for long span suspension bridges (Amman, *George Washington Bridge: General Conception and Development of Design.1933* )<sup>[18]</sup>

**Tab 2.5** George Washington Bridge design parameters: comparison between different configurations

(1931) original configuration: single unstiffened deck		(1962) final configuration: double deck stiffened system	
<b>L(main span) [m]</b>	1067	<b>L(main span) [m]</b>	1067
<b>Ltot [m]</b>	1450	<b>Ltot [m]</b>	1450
<b>h (girder) [m]</b>	<b>1,70</b>	<b>h (girder) [m]</b>	<b>8.80</b>
<b>h/L</b>	<b>1/630</b>	<b>h/L</b>	<b>1/121</b>
<b>width [m]</b>	36, 10	<b>width [m]</b>	36,10
<b>w/L</b>	1/30	<b>w/L</b>	1/30
<b>i.p.</b>	18.40	<b>i.p.</b>	18.40
<b>i.p./L</b>	1/58 (1.72%)	<b>i.p./L</b>	1/58 (1.72%)

Ammann, Othmar., Transactions of the American Society of Civil Engineers, 1933, Vol. 9): high dead loads, both for cables and for deck, allow to stiffen and stabilize bridge. Being main cables really heavy (cables weight-to deck weight ratio : 41%), being dimensioned to carry a double deck system, the effect due to any accidental loads are practically nihil. This pioneer work reveals a completely new approach in bridge design: apart from the stabilizing effect of dead loads, the choice of a thickening hangers system, linked to the main cable, as well as the increasing number of transverse load-bearing elements ( $i.p./L = 1.72\%$ ), gave the possibility to greatly reduce girder sizing: it resulted in an elegant slender structure.





Never changed since the construction phase, both towers consist of open steel truss structure, height 181m, total transverse width 54,4 m at the top. Between the legs of each tower, there are transverse steel truss cross-beams at the top and under the deck.

Originally, there was a schedule to cover the towers with concrete and granite plates but this was not realized. The sunshine strains the silver coloured paint of the towers, and these are repainted at times. The bridge has 4 main cables  $\varnothing$  91 cm, and these are located as pairs at both edges of the bridge deck. Each main cable consists of 26'474 parallel galvanized steel wires  $\varnothing$  5 mm, tensile strength older units 155 kp/mm<sup>2</sup>. Although Ammann's original design made a provision for the addition of a lower deck to carry four rapid transit tracks, no interest was taken by railroads in operating commuter service across the bridge and the growing volumes of cars, trucks and buses eventually made the addition of more traffic lanes a necessity. The six lanes on the lower level later increased the bridge's capacity by 75 percent, making the George Washington Bridge the only suspension bridge in the world with 14 lanes

**Fig.2.20** George Washington Bridge\_ steel tower\_ (a) (1931)version; (b) Hypothesis of covering tower with concrete and granite plates (Cass Gilbert)\_ (c) final configuration

**Fig.2.21** George Washington Bridge\_ deck\_ (a) (1931) Six lanes for vehicular traffic (single deck); (b) (2017) Eight lanes for traffic (upper level of double deck)



The addition of the lower level (and the stiffening truss connecting it to the upper level) coincided with the opening of a series of approach roads that included the Trans-Manhattan Expressway, ramps to the Henry Hudson Parkway, Riverside Drive, Palisades Parkway, US Routes 1, 9, and 36, and New Jersey Route 46. Today, the George Washington Bridge remains an important link in the New York City regional highway system: opening of the bridge in 1931 also led to a substantial amount of industrial and residential development in Bergen County, New Jersey. About this extraordinary work, Le Corbusier wrote in *“When the Cathedrals Were White”*: *“The George Washington Bridge over the Hudson River is the most beautiful bridge in the world. Made of cables and steel beams, it gleams in the sky like a reversed arch. It is blessed. It is the only seat of grace in the disordered city. It is painted an aluminium colour and, between water and sky, you see nothing but the bent cord supported by two steel towers. When your car moves up the ramp, the two towers rise so high that it brings you happiness; their structure is so pure, so resolute, so regular that here, finally, steel architecture seems to laugh”*.

As in the case of *George Washington Bridge*, also for *Golden Gate Bridge* design deflection theory was applied. The Golden Gate Bridge was the longest and largest Suspension bridge in the world by the time of 1927 when it was completed and started opening to traffic. (Tab. 2.6) (Fig. 2.22) (Fig. 2.23)

There is not another bridge to use as a model: the now familiar art deco design and International Red colour were chosen, becoming an internationally landmark and recognized symbol of both San Francisco. Moisseiff proposed a bridge far more efficient and beautiful than the original design by Strauss and theorized that a long-span suspension bridge could cross the strait. The Golden Gate Bridge's design was very complex which made up of five types of structure not typical of most highway system bridge. In addition to the suspension bridge the approaches include a steel arch bridge, two concrete anchorages, two steel truss viaducts and three concrete pylons. The total bridge weight listed for 1986 includes the reduction in weight due to the redecking in 1986. The weight of the original reinforced concrete deck and its supporting stringers was 150.952t. The weight of the new orthotropic steel plate deck, its two inches of epoxy asphalt surfacing, and its supporting pedestals is now 139.790t. This is a total reduction in weight of the deck of 11.158t. The Golden Gate Bridge has two main cables which pass over the tops of the two 746-ft-tall towers and are secured at either end in giant anchorages. The galvanized carbon steel wire comprising each main cable was laid by spinning the wire, using a loom-type shuttle that moved back and forth as it laid the wire in place to form the cables. The Golden Gate Bridge has 250 pairs of vertical suspender ropes that are spaced 15,20m apart across both sides of the Bridge; all of the ropes were replaced between 1972 and 1976, with the last rope replacement completed on May 4, 1976. Instead of *George Washington Bridge*, it has only two main cables: it has been designed to have a single deck, without any prediction to be extended.





A storm on December 1, 1951, caused the Golden Gate Bridge to twist and vibrate enough to cause some minor damage, so the Bridge was retrofitted from 1953 to 1954.

<b>L (main span) [m]</b>	1280	<b>width [m]</b>	27.40
<b>L tot [m]</b>	1966	<b>w/L</b>	1/47
<b>H (girder) [m]</b>	7.60	<b>i.p. (hanger spacing)</b>	15. 20
<b>h/L</b>	1/168	<b>i.p./L</b>	1/92 (1.1%)

**Fig.2.22** Golden Gate Bridge. San Francisco, California, USA, 1937, Joseph Straus, Amman, Moisseiff

**Tab 2.6** Golden Gate Bridge design parameters

The retrofit added new bracing across the bottom, connecting the two steel trusses that support the roadway deck. This change increased the Bridge's twisting, or torsional, stiffness. Ever since the modern suspension bridge was invented in the early 1800s, one of the biggest challenges engineers have faced is preventing these flexible structures from moving too much in the wind. The choice of closing deck cross section with lower bracings remarks the necessity of stiffened deck system for suspension bridges: Golden Gate represents an important step in the evolution of cross section, above all considering that before 1951 no deck closed sections were used.

The emblematic case, which underlined the necessity to take into account aerodynamic stability in bridge design was (first) *Tacoma Narrows Bridge* (1940). (Fig. 2.24) (Tab. 2.7)The length of the main span (between towers) was 854m, and the width between cables was 14.40m.

**Fig.2.23** Golden Gate Bridge. San Francisco\_ (a) lateral view of deck cross section\_ (b) bottom view of adding bracings







**Fig.2.24** First Tacoma Narrows Bridge. Tacoma, Washington, USA, 1940, Leon Solomon Moisseiff

It was designed by Moisseiff according to deflection theory principals: considering that a great percentage of acting load was carried by main cable, the reduction of bending stress in the flexible deck, made only of two 2,40m-high girders, justified the high deck slenderness as well as the its low torsional stiffness (defined through deck width-to-span length ratio) . The suspension system was made of two main cable, with a diameter of 44cm, having an overall weight of 3817t. From a static point of view, Tacoma Narrows bridge was greatly cable to carry both traffic loads, and static effects of wind load; however, wind dynamic effect were not taken into account.

**Tab 2.7** First Tacoma Narrows Bridge (1940) design parameters

<b>L (main span) [m]</b>	854	<b>width [m]</b>	<b>13.10</b>
<b>L tot [m]</b>	1524	<b>w/L</b>	<b>1/65</b>
<b>H (girder) [m]</b>	<b>2.40</b>	<b>i.p. (hanger spacing)</b>	14.40
<b>h/L</b>	<b>1/356</b>	<b>i.p./L</b>	1/59 (1.7%)

Even during construction, the bridge sometimes developed up-and-down wave motions of extraordinary amplitude. Corrective measures were applied: hydraulic buffers at each end of the main span (which, however, became inoperative soon after installation) and diagonal stays (“ties”) between the stiffening girders and cables at mid-span. After opening to traffic, hold-downs were installed tying the girders in the side spans to massive concrete blocks on land. These reduced the waves in the side spans but not in the main span. The most frequently observed vertical vibration was one with no nodes between the towers (frequency of 8 vibrations/minute); this might well be called the fundamental mode. The maximum recorded double amplitude for this mode was 60cm (*Tacoma Narrows Bridge Collapse*, Franklin Miller, Jr. (1963).

Early on the morning of November 7, 1940, the bridge developed motions of a type previously observed, but with larger-than-usual amplitude. The wind velocity was 40 to 45 miles/hour, larger than any previously encountered by the bridge. Traffic was shut down. The crucial event shortly after 10 a.m. which directly led to the catastrophic torsional vibration, was apparently the loosening of the north cable in its collar which was tied to the deck girder by diagonal stay. The mode was then driven by auto-excitation forces of which the steady wind was the energy source. Soon the vertical oscillations became rotational: this allowed the structure to twist as one of the main cables became longer on one side of the centre and shorter on the other side.



**Fig.2.25** First Tacoma Narrows Bridge (1940)\_ (a) deck bottom view\_ (b) (c) bridge collapse (November 7,1940)

The wind velocity was large enough to cause this mode of torsion to build up, until collapse inevitably took place. The primary cause of the collapse lies in the general proportions of the bridge and the type of stiffening girders and floor. The ratio of the width of the bridge to the length of the main span was so much smaller and the vertical stiffness was so much less than those of previously constructed bridges that forces heretofore not considered became dominant. (Paine, C., et al. “*The Failure of the Suspension Bridge Over Tacoma Narrows.*” Report to the Narrows Bridge Loss Committee , June 26, 1941). (Fig. 2.25)

Once any small undulation of the bridge is started, the resultant effect of a wind tends to cause a building up of vertical undulations. There is a tendency for the undulations to change to a twisting motion, until the torsional oscillations reach destructive proportions (Source: Steinman, David B., and Sara Ruth Watson. *Bridges and Their Builders*. New York: Putnam’s Sons, 1941). The Tacoma Narrows Bridge was not the first suspension bridge to collapse. In fact, a survey of the history of suspension bridges shows that several were destroyed by wind or other oscillating forces. (Tab. 2.8)

**Collapsed Suspension Bridges**

Bridge	Designer	Span Length [m]	Failure date
<b>Dryburg (Scotland)</b>	Smith	79,20	1818
<b>Union (England)</b>	Brown	137	1821
<b>Brighton (England)</b>	Brown	77,70	1836
<b>Montrose (Scotland)</b>	Brown	432	1838
<b>Menai (Wales)</b>	Telford	132	1839
<b>Roche (France)</b>	LeBlanc	195	1852
<b>Wheeling (USA)</b>	Ellet	308	1854
<b>Sully-sur-Loire</b>	Seguin	96	1856
<b>Niagara (USA)</b>	Serrell	317	1864
<b>Niagara (USA)</b>	Keefer	384	1889
<b>Tacoma Narrows (USA)</b>	Moisseiff	854	1940

**Tab 2.8** Synthesis of collapsed suspension bridges

However, the Tacoma Narrows Bridge was by far the longest and most expensive suspension bridge to collapse due to interaction with the wind. The Tacoma Narrows Bridge was unusually long and narrow compared with other suspension bridges previously built. The original design called for stiffening the suspended structure with trusses. However, funds were not available, and a cheaper stiffening was adopted using 2,45 tall girders running the length of the bridge on each side. Unfortunately, the stiffening was inadequate. The bridge was rebuilt using the original anchorages and tower foundations. The new bridge was opened to traffic in the winter of 1950-51, and during that winter it was exposed to some of the highest winds of recent years. The bridge is entirely successful.

A table summarizing the second generation of suspension bridges follows: previous attempt to build slender deck was abandoned, preferring precautionary stiffened systems, above all with rigid trusses. A summary table concerning previous examples is given.

Bridge	L <sup>(1)</sup> [m]	h/L	w/L	ip/L	Dead cables	Dead deck	cable load deck load.
<b>Brooklyn</b> (1883)	486	1/87	1/19	1/211	127 kg/m <sup>2</sup>	223 kg/m <sup>2</sup>	57%
<b>Williamsburg</b> (1903)	488	<b>1/41</b>	1/14	1/80	127 kg/m <sup>2</sup>	401 kg/m <sup>2</sup>	<b>32%</b>
<b>Manhattan</b> (1912)	448	1/61	<b>1/12</b>	1/79	217 kg/m <sup>2</sup>	388 kg/m <sup>2</sup>	64%
<b>George Washington</b> (1931)	<b>1067</b>	1/121	1/30	1/58	<b>460 kg/m<sup>2</sup></b>	1127 kg/m <sup>2</sup>	41%
<b>San Francisco – Oakland Bay</b> (1936)	704	1/78	1/35	1/78	164 kg/m <sup>2</sup>	1110 kg/m <sup>2</sup>	15%
<b>Golden Gate</b> (1937)	<b>1280</b>	1/168	1/47	1/84	362 kg/m <sup>2</sup>	794 kg/m <sup>2</sup>	46%
<b>Tacoma Narrows</b> (1940)	854	<b>1/356</b>	<b>1/65</b>	1/59	191 kg/m <sup>2</sup>	563 kg/m <sup>2</sup>	<b>34%</b>

**Tab 2.9** Synthesis of suspension bridge first generation (1883-1940)

<sup>(1)</sup> L –main span length; <sup>(2)</sup> l –side span length; <sup>(3)</sup> w- deck width

### New generation of deck stiffened suspension bridges (1940- 1964)

After the centre span fell into the Tacoma Narrows, the towers, main cables, side spans, and anchorages remained. The approach spans sustained no damage. The process of dismantling and salvaging the ruined bridge proved as intricate and dangerous as its construction. The proposed design for the new Narrows Bridge needed testing. Issues of aerodynamic stability in the design of suspension bridges had never before been investigated.



Testing the bridge design fell to F. B. Farquharson, professor of engineering at the University of Washington. Engineers faced two major challenges in building the second Narrows Bridge. First, they had to better explain what happened to the 1940 bridge, and to design one that would not meet the same fate. Second, they had to decide how using remnants of the old bridge, especially the piers. In July 1941 Charles E. Andrew, consulting engineer for the Washington State Toll Bridge Authority (WSTBA), appointed Dexter R. Smith as chief design engineer to plan the new structure. The proposed design for the new Narrows Bridge needed testing. Issues of aerodynamic stability in the design of suspension bridges had never before been investigated. Testing the bridge design fell to F. B. Farquharson, professor of engineering at the University of Washington.

**Fig.2.26** Second Tacoma Narrows Bridge. Tacoma, Washington, USA, 1950, Charles E. Andrew, Dexter R. Smith

<b>L (main span) [m]</b>	854	<b>width [m]</b>	<b>18.30</b>
<b>L tot [m]</b>	1524	<b>w/L</b>	<b>1/47</b>
<b>H (girder) [m]</b>	<b>10.10</b>	<b>i.p. (hanger spacing)</b>	8
<b>h/L</b>	<b>1/85</b>	<b>i.p./L</b>	1/107 (0.90%)

**Tab 2.10** Second Tacoma Narrows Bridge. Tacoma, Washington, USA, 1950, design parametres

The new Tacoma Narrows Bridge (Fig. 2.26) (Tab. 2.10) designed to offer the least wind resistance. The solution would be to use deep, open stiffening trusses with trussed floor beams. The truss members would be shallow, to avoid creating any large, solid surfaces like the ones associated with the failure of the 1940 Narrows Bridge. The deck system is made of 10m-high, 18,30m wide Warren stiffening trusses. Three slots of open steel grating 83cm wide separating all four traffic lanes, and a strip 19 inches wide along each curb. Hydraulic shock absorbers at three strategic points in the structure:(1) at mid-span, at the main cable center tie, between the main suspension cables and the top of the stiffening truss; (2) between the top chords of the main span and side span stiffening trusses; and (3) at each tower, where it joins the bottom of the deck truss. A new cable sag ratio of 1:12 was adopted: this required the towers to be higher than the 1940 bridge, which had a sag ratio of 1:10. (Tab. 2.11).

The next generation of large suspension bridges featured deep and rigid stiffening trusses.



**Tab 2.11** Comparison between First Tacoma (1940) and Second Tacoma Narrows Bridge (1950)

	First Tacoma Narrows Bridge (1940)	Second Tacoma Narrows Bridge (1950)
<b>h/L</b>	1/356	1/85
<b>w/L</b>	1/65	1/47
<b>Deal load (cable)</b>	3817 t	5441 t
<b>Dead load (deck)</b>	11250 t	18160 t

Completion of the 1950 Narrows Bridge was soon followed in the United States by the Delaware Memorial Bridge in 1951, the Chesapeake Bay Bridge (Preston Lane Jr. Memorial Bridge) in 1952, David Steinman's great Mackinac Strait Bridge, built from 1954 to 1957, Verrazano Narrow Bridge by Othmar Amman (1964). The *Mackinac Bridge* (Fig. 2.27) (Tab. 2.12) is the one of the world's most beautiful bridges and the longest suspension bridge in the Americas, with a total length of 1158m suspended. It is currently the third longest suspension bridge in the world.

**Fig.2.27** Mackinac Bridge. Mackinaw City, Michigan, USA, 1957, David B. Steinman

Its design was based on requirements for aerodynamic stability. The truss depth was arbitrarily set as (1/100) of man san, even though wind tunnel tests showed this figure to be conservative. The trusses were shop riveted and field bolted, using high strength friction-grip bolts.

**Tab 2.12** Mackinac Bridge (1957) design parameters

<b>L (main span) [m]</b>	1158	<b>width [m]</b>	<b>20.70</b>
<b>L tot [m]</b>	2255	<b>w/L</b>	<b>1/56</b>
<b>H (girder) [m]</b>	<b>11.60</b>	<b>i.p. (hanger spacing)</b>	12
<b>h/L</b>	<b>1/100</b>	<b>i.p./L</b>	1/97 (1%)

The Verrazano-Narrows Bridge (Fig. 2.28) (Tab. 2.13) is a double-decker suspension bridge, having 6 lanes for each level. Each roadway consists of 7.62cm depth concrete slab cast around a steel grid. The proportion of the stiffening truss (7,30m deep) were largely dictated by the clearance require from the double-deck roadway system (4,57m).





The resulting slenderness ratio (1/178) is significantly lower than had been customary for earlier United States Bridges (New Tacoma Narrows –  $h/L$ : 1/85). A relatively shallow depth of suspended structure and high aerodynamic resistance is obtained by a novel rigid framing of the entire steel structure.

<b>L (main span) [m]</b>	1298	<b>width [m]</b>	<b>31.40</b>
<b>L tot [m]</b>	2039	<b>w/L</b>	<b>1/41</b>
<b>H (girder) [m]</b>	<b>7.30</b>	<b>i.p. (hanger spacing)</b>	15.20
<b>h/L</b>	<b>1/178</b>	<b>i.p./L</b>	1/85 (1.2%)

**Fig.2.28** Verrazano Narrows Bridge. Staten Island/Bay Ridge, New York, USA, 1964, Othmar Ammann

**Tab 2.13** Verrazano Narrows Bridge (1964) design parameters

Following table summarizes main design parameters of stiffening truss suspension bridges, which followed Tacoma collapse. (Tab. 2.14)

<b>Bridge</b>	<b>L <sup>(1)</sup> [m]</b>	<b>h/L</b>	<b>w/L</b>	<b>ip/L</b>	<b>Dead cables</b>	<b>Dead deck</b>	<b>cable load deck load.</b>
<b>Second Tacoma (1950)</b>	854	<b>1/85</b>	1/47	1/211	195 kg/m <sup>2</sup>	651 kg/m <sup>2</sup>	30%
<b>Mackinac (1957)</b>	1158	1/100	1/56	1/80	230 kg/m <sup>2</sup>	903 kg/m <sup>2</sup>	26%
<b>Verrazano (1964)</b>	1298	<b>1/178</b>	<b>1/41</b>	1/79	<b>579 kg/m<sup>2</sup></b>	<b>1265 kg/m<sup>2</sup></b>	<b>46%</b>

<sup>(1)</sup> L –main span length; <sup>(2)</sup> l –side span length; <sup>(3)</sup> w- deck width

**Tab 2.14** Synthesis of suspension bridge second generation (1950-1964)

### Aerofoil revolution for record spans suspension bridges (1964 -2009)

After Tacoma Narrows Bridge collapse (1940), American engineers realised the problem of aerodynamic stability and further extended span lengths. Two main approaches were used to improve bridge deck stability: against aerodynamic effects (1) adopting a stiffening truss and open grating deck, in order to eliminate the generation of wind vortices; (2) increasing stiffness, adding mass (or weight) to the bridge. Since Roebling earliest applications, cable stays were sometimes used, only considered as measures of supplementary or emergency nature.



**Fig.2.29** Severn Bridge. Aust/Beachley, England, 1966, Gilbert Roberts, Freeman Fox & Partners

A completely different approach was used by European engineers, adopting streamline-shaped box cross sections, whose aerofoil profile could reduce wind pressure effects, suppressing the emergence of vortices. The first suspension bridge which embodied this revolution was *Severn Bridge*. (Fig. 2.29) (Fig. 2.30) (Tab. 2.15) Its first design was for a truss girder similar to but shallower than the Forth Road Bridge. A model was being tested in a wind tunnel when it broke loose and was destroyed.

**Tab 2.15** Severn Bridge (1966) design parameters

<b>L (main span) [m]</b>	988	<b>width [m]</b>	<b>31.90</b>
<b>L tot [m]</b>	1598	<b>w/L</b>	<b>1/31</b>
<b>H (girder) [m]</b>	3.10	<b>i.p. (hanger spacing)</b>	19.10
<b>h/L</b>	<b>1/324</b>	<b>i.p./L</b>	1/52 (2%)

Its first design was for a truss girder similar to but shallower than the Forth Road Bridge. A model was being tested in a wind tunnel when it broke loose and was destroyed. As it was to take a long time to make a replacement some simple alternatives were tested in the mean time. It was from these that the final aerodynamic box girder design was developed. The streamlined deck shape was the first of its kind and resulted in a bridge that was lighter and easier to paint than the more traditional design of the trussed girder of the Forth Road Bridge. The roadway deck is high strength steel just under 12 mm. thick stiffened by 6 mm. high strength steel troughs 23 mm deep. Main cables cross section is about 0.5 m. consisting of 19 strands of 438 wires of 5 mm. diameter arranged in a hexagon (8322 wires in all). Hangers strands have 178 wires and are inclined to increase the damping of vibrations. The reduction in weight reduced the overall stiffness of the bridge and so the sag to span ratio was reduced to 1/12. Two 7.3m carriageways and one 3.7m cycle track and 3.7m footpath are cantilevered out at the sides. The road surface was then laid on the steel deck: a 38mm layer of hand-laid mastic asphalt has been used. Both towers are 123.2 m. tall from top of piers. Each leg is a simple rectangular tube formed from 4 stiffened plates - the corner joints were arranged so no exterior staging was needed. The tower saddles at the very top were made from mild steel plate and bolted to the tower. The approach spans are two steel box girders 3 m. deep by 2.13 m. wide at 14.3 m centres and with I-section cross girders every 3 m.





The deck is 0.2 m. thick reinforced concrete slab cast in situ. Compared with American suspension bridges, those built in Europe after 1960s reflected significantly reduced steel weights: this trend was most pronounced also in the *Bosphorus* (Fig.2.31) (Tab. 2.16) and *Humber bridges*, which use essentially the same structural concepts as the *Severn Bridge*.

**Fig.2.30** Severn Bridge. (1966)\_ (a) construction phases\_ (b) tower view

Following the opening of the *Humber Bridge*,(Fig.2.32) (Tab. 2.17) its referring prototype *Severn Bridge* began to show some problems, as wind-induced vibration of its hangers.

Dampers were installed soon after erection to reduce oscillations, as suppression measure, eve if the most severe problem concerned bridge slender towers, which were extremely light and fragile. As result, they required extensive reinforcement, inserting steel pips inside each of four corners of towers legs.

<b>L (main span) [m]</b>	1074	<b>width [m]</b>	<b>33.40</b>
<b>L tot [m]</b>	1560	<b>w/L</b>	<b>1/32</b>
<b>H (girder) [m]</b>	3	<b>i.p. (hanger spacing)</b>	16.50
<b>h/L</b>	<b>1/358</b>	<b>i.p./L</b>	1/65 (1.5%)

**Tab 2.16** First Bosphorus Bridge (1973) design parameters

Like its predecessors *Severn* and *Bosporus*, *Humber* has aerodynamic steel box girders and inclined hangers. The spans comprise a total of 124 prefabricated units typically 18.1 m long and 4.5 m deep.

**Fig.2.31** First Bosphorus Bridge. Istanbul, Turkey, 1973, W. Brown, G. Roberts, Freeman Fox & Partners







**Fig.2.32** Humber Bridge. Kingston upon Hull, England, 1981, C. Douglas Strachan, Freeman Fox & Partners

**Tab 2.17** Humber Bridge (1981) design parameters

These are 28.5 m wide and 3 include two 3 m walkways and orthotropic deck plates on which road surfacing is applied.

<b>L (main span) [m]</b>	1410	<b>width [m]</b>	<b>28.50</b>
<b>L tot [m]</b>	2220	<b>w/L</b>	<b>1/49</b>
<b>H (girder) [m]</b>	4.50	<b>i.p. (hanger spacing)</b>	17.20
<b>h/L</b>	<b>1/313</b>	<b>i.p./L</b>	1/82 (1.2%)

The slipformed reinforced concrete towers rise 155.5 m above the caisson foundations and carry the two main cables with nominal sag of 115.5 m. The bridge is exposed to prevailing south-westerly cyclonic winds that can reach hurricane force (exceeding 32.7 m/sec), with atmospheric temperatures ranging from -10° C to 30° C. The deck of the bridge was constructed of 124, 18.1 m long, 140 tonne pre-assembled trapezoidal steel box sections. The main suspension cables contain 14,948 parallel galvanised 5mm wire and total 700mm in diameter. In the design of the Humber Bridge the Deck only acts to spread localised loads over the few nearest hangers and is relatively slender as a to length ratio of the main span is 1/313 which is very shallow compared to 1/170 in the Golden Gate Bridge, which is commonly regarded as the most beautiful bridge in the world.

The same design fundamentals led to exceed the record span length reached untill then: two record suspension bridges were built, the Japanese *Akashi Kaikyo Bridge* and the Danish *Great Belt Bridge*, the first as emblematic of American style, the second representative of European approach to bridge design.

The Akashi Kaikyo Bridge (Fig. 2.33) (Fig. 2.34) (Tab. 2.18) is the perfect symbol of Japan Post War achievement in civil engineering. It's the longest spanning bridge in the world, having three spans, two hinged stiffening girder suspension system: the main span is 1991m long, with a total length of 3911m. The bridge changed the economy of the area it connected: the estimate value of the benefits totalled 250 bilion yen a year. It spans Akashi Strait (Japan), connecting Kobe-Naruto Route with the Keihanshin District.



Typhoon and quake considerations as well as the width of the strait and construction of main towers on deep sea during tidal currents made the construction of this bridge the most difficult in the project.

**Fig.2.33** Akashi Kaikyo Bridge. Kobe/Awaji, Japan, 1998, Honshu Shikoku Bridge Authority

<b>L (main span) [m]</b>	1991	<b>width [m]</b>	<b>35.50</b>
<b>L tot [m]</b>	3911	<b>w/L</b>	<b>1/56</b>
<b>H (girder) [m]</b>	14	<b>i.p. (hanger spacing)</b>	1420
<b>h/L</b>	<b>1/142</b>	<b>i.p./L</b>	1/40 (070%)

**Tab 2.18** Akashi Kaikyo Bridge (1998) design parameters

The main span was designed to be 1,990 meters with two side spans of 960 meters each. The bridge roadway surface is constructed on top of a 14-meter-deep by 35.5-meter-wide truss girder system suspended from main cables passing over two steel towers that rise 298 meters above main sea level. A 65-meter clearance is maintained over the shipping lane. The 1.12-meter-diameter main cables were erected using full-length, prefabricated strands. Approximately 181,400 metric tons of steel were used in the superstructure, and 1.42 million cubic meters of concrete were used in the substructure.

**Fig.2.34** Akashi Kaikyo Bridge\_ (a) truss deck, global view\_(b) lower deck detail



Several unique technologies were developed to support the design and construction of the Akashi Kaikyo suspension bridge. The aerodynamic stability of long suspension bridges poses major challenges to designers. To verify the design of the world's longest suspension bridge, the Honshu-Shikoku Bridge Authority contracted with the Public Works Research Institute to construct the world's largest wind-tunnel facility and to test full-section models in laminar and turbulent wind flow. Other innovations resulting from wind-tunnel testing included installation of vertical plates at the bottom center of the highway deck to increase flutter speed. Several unique technologies were developed to support the design and construction of the Akashi Kaikyo suspension bridge.

The aerodynamic stability of long suspension bridges poses major challenges to designers. To verify the design of the world's longest suspension bridge, the Honshu-Shikoku Bridge Authority contracted with the Public Works Research Institute to construct the world's largest wind-tunnel facility and to test full-section models in laminar and turbulent wind flow. Other innovations resulting from wind-tunnel testing included installation of vertical plates at the bottom center of the highway deck to increase flutter speed. Methods of improved prediction of flutter speed and gust response will be used in future bridge design.

Of particular interest was the performance of the bridge in the Jan. 17, 1995, Hyogo-ken Nanbu Earthquake, which provided a full-scale test of tower response. The complete bridge structure was designed to resist a 150-kilometer-distant, 8.5-Richter-magnitude earthquake. Fortunately, erection of the bridge stiffening truss had not begun.

**Fig.2.35** Great Belt East Bridge. Korsør, Denmark, 1998, COWI Consulting Engineers and Planners AS

The “antagonist” European record proposal is the aerofoil Great Belt East (Fig. 2.35) (Fig. 2.36) (Tab.2.19) Bridge. The East Bridge is the landmark and spans the international navigation route between the Baltic Sea and the North Sea and allows a clearance of 65 m below the bridge girder.







**Fig.2.36** Great Belt East Bridge (1998)\_  
(a) deck construction\_  
(b) upper deck view

The Great Belt is an international shipping route and hence is subject to a large volume of ship traffic, about 20,000 vessels per year. A study was completed involving theoretical ship-collision as well as simulations of actual navigational conditions. These studies indicated that the main span should exceed 1.5 kilometres; this meant that a suspension bridge was the only realistic solution to meet the main span requirements. By optimizing the design, a 1624 metre main span with 535 metre side spans, carrying a four lane motorway plus emergency lanes was finally selected.

The superstructure is an aerodynamically shaped fully welded closed box girder (see Appendix B); it is continuous between the anchor blocks over the whole suspension bridge length of 2700 metres. Hence there are expansion joints located at the anchor blocks but there are no expansion joints at the towers. Vertical elastic support is exclusively provided by the hangers. Compared to a traditional system with joints at the pylons, the continuous system in combination with the hydraulic buffers improves the overall stiffness and stability of the bridge and leads to low maintenance costs.

<b>L (main span) [m]</b>	1624	<b>width [m]</b>	<b>31</b>
<b>L tot [m]</b>	2694	<b>w/L</b>	<b>1/52</b>
<b>H (girder) [m]</b>	4	<b>i.p. (hanger spacing)</b>	24
<b>h/L</b>	<b>1/406</b>	<b>i.p./L</b>	1/68 (1.14%)

**Tab 2.19** Great Belt East Bridge (1998) design parameters

The box girder is suitable for rationalised repetitive fabrication. The interior surfaces, which comprise about 80 percent of the total steel surface, are unpainted and are protected by dehumidification of the inside air volume. The shape of the box girder lends itself well to prefabrication and also helps with the bridges aerodynamic performance. Transverse trusses inside the deck improve the decks fatigue resistance. A cable sag ratio of 1:9 was decided to be optimum to reduce sliding forces in the anchorages. The main cables are 3079 metres long. Each cable consists of 37 strands which in turn are made up of 504 high tensile galvanized wires, which are 5.38 millimetres in diameter. The reinforced concrete pylons reach a height of 254 metres, breaking previous records set by the Humber Bridge.

The anchor blocks are open structures. This was a result of aesthetic input but has practical advantages too such as reducing the amount of concrete needed and also the open shape meant that during cable spinning the anchor blocks could serve as wire handling areas. As a suspension bridge the Great Belt East Bridge gets its strength from the parabolic shape of the main cables. This system has the greatest strength when it is loaded under uniform symmetrical loading. The deck which is in compression is supported by hangers which are then put into tension and thus loading the main cables. The shape of the main cables only allows the steel cables to be under tension forces, which is extremely efficient given the high tensile strength of steel. The anchor blocks stabilise the tensions forces in the cables through gravitational compression through to the foundations. The interaction of the anchor blocks with its foundations also helps it resist the lateral forces from the cables

Comparing Akashi Kaikyo Bridge to Great Belt East Bridge, it can be seen as the difference in depth-to-span ratio greatly influences the weight of the stiffening girder: as a result of the adoption of streamlined box girder, steel deck weight is Great Belt Bridge is 56% of that in Akashi Kaikyo bridge.

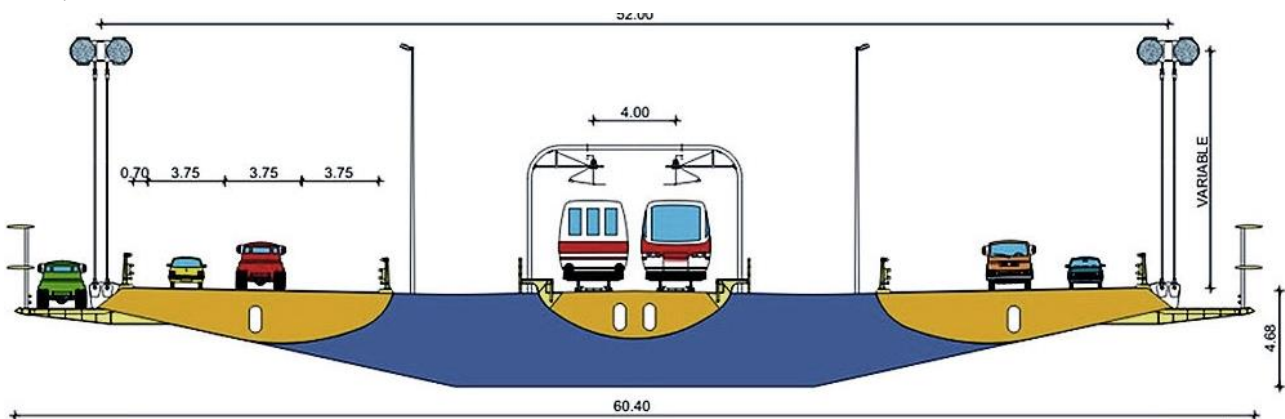
Akashi Kaikyo Bridge			Great Belt East Bridge		
<b>Deck width</b>	[m]	35.50	<b>Deck width</b>	[m]	31.00
<b>h (deck )</b>	[m]	14	<b>h (deck )</b>	[m]	4
<b>Dead (deck)</b>	[kg/m <sup>2</sup> ]	760	<b>Dead (deck)</b>	[kg/m <sup>2</sup> ]	424
<b>Dead (cables)</b>	[kg/m <sup>2</sup> ]	364	<b>Dead (cables)</b>	[kg/m <sup>2</sup> ]	236
<b>Live load (*)</b>	[kg/m <sup>2</sup> ]	125	<b>Live load (2)</b>	[kg/m <sup>2</sup> ]	257
<b>Live /Dead</b>	<b>1:6 (17%)</b>		<b>Live /Dead</b>	<b>1:1,7 (61%)</b>	
<b>h/L</b>	<b>1/142</b>		<b>h/L</b>	<b>1/406</b>	

Tracing suspension bridge historical evolution, Messina Strait Bridge cannot be neglected, even if it has not been built until now. For centuries, a permanent 3km crossing over the Strait of Messina (Fig. 2.37) (Fig. 2.38) (Tab. 2.20) between Calabria in south Italy and Sicily has been considered. Both bored and floating tunnels were considered, but were rejected. Given a tunnel depth of -280m mean sea level (MSL) and link height of about +50m MSL, an impractical 47km of autostrada tunnel links would be Required. Numerous active seismic faults run along the Strait with potential for a repeat of the 1908 Messina earthquake of about magnitude 7.2. Tunnels are commonly perceived to be invulnerable to earthquakes. However, the 1999 collapse of the Turkish Twin Bolu tunnels challenges this view, demonstrating vulnerability to comparable earthquakes. A multi-span bridge involves construction of sea floor founded piers of an unprecedented depth of about 150m, making them hugely difficult to construct.



Such piers must be constructed to withstand the Strait's high design sea flow of 5.1m/s, wave height of 16m, a 200 year design life, and interference during construction and operation with 140,000 vessels through the Strait each year. A single span suspension bridge is able to either avoid or mitigate the aforementioned issues. In March 2009, previously shelved plans for the world's largest single span suspension bridge were resurrected, arguably having overcome countless engineering, political, financial and cultural hurdles. For the design of a crossing structure, the preliminary project definitively opted for a 3,300m-long single-span suspension bridge that will have the world's longest central span. The deck was to be 3,666m long, including the two suspension side spans, and 60m wide. The structure was to be composed of three box sections – two lateral ones for the roadway deck and a central one for the railway tracks. The deck's roadway section was to have three 3.75m-wide lanes in each direction (two driving lanes and one emergency lane). The railway section was to have two tracks and two lateral pedestrian sidewalks. The height of the two towers was set at 382.6m to allow for a navigation clearance with a minimum height of 65m – in the presence of maximum load conditions – and a 600m width; the height of the deck's anchoring on the Sicilian side was lowered by 11m.

**Fig.2.38** Messina Strait Bridge (2009)\_deck cross section



**Tab. 2.20** Messina Strait Bridge (2009)\_ design parameters

<b>L (main span) [m]</b>	3300	<b>width [m]</b>	<b>60.40</b>
<b>L tot [m]</b>	5070	<b>w/L</b>	<b>1/54</b>
<b>H (girder) [m]</b>	4.68	<b>H above water [m]</b>	70
<b>h/L</b>	<b>1/711</b>	<b>Tower height [m]</b>	382.60

The bridge's suspension system was to be secured by two pairs of steel cables, each with a diameter of 1.24m and a total length between the anchor blocks of 5,300m. The bridge was designed to resist, without damage, an earthquake of 7.1 on the Richter scale – much more severe than that which devastated Messina in 1908. Considering that decks of long span bridges have low natural frequencies which may allow wind to subject the deck to cyclic loads, several requirements must be met for aerodynamic stability and structural efficiency of the deck, including high stiffness, low mass and low aerodynamic resistance. So, it could be said that the greatest innovation of the Messina Bridge is the development of the slotted box girder deck design, pioneered by Brown Beech & Associates during the early development (early 1990s) of the current design. Wind tunnel tests showed that such a deck with a slot running between the railway line and each of the road decks had a substantially higher wind flutter velocity than a comparable deck without slots.

Following table summarizes main design parameters of aerofoil bridges, built in the last five decades.

<b>Bridge</b>	<b>L <sup>(1)</sup> [m]</b>	<b>h/L</b>	<b>w/L</b>	<b>ip/L</b>	<b>Dead cables</b>	<b>Dead deck</b>	<b>cable load deck load.</b>
<b>Severn Bridge</b> (1966)	988	1/324	1/31	1/52	125 kg/m <sup>2</sup>	305 kg/m <sup>2</sup>	41%
<b>I Bosphorus</b> (1973)	1074	1/358	1/32	1/65	126 kg/m <sup>2</sup>	289 kg/m <sup>2</sup>	44%
<b>Humber Bridge</b> (1981)	<b>1410</b>	1/313	1/49	1/82	225 kg/m <sup>2</sup>	353 kg/m <sup>2</sup>	<b>64%</b>
<b>II Bosphorus Bridge</b> (1988)	1090	1/363	1/28	1/68	161 kg/m <sup>2</sup>	379 kg/m <sup>2</sup>	42%
<b>Höga Kusten Bridge</b> (1997)	1210	1/303	1/55	1/61	172 kg/m <sup>2</sup>	318 kg/m <sup>2</sup>	54%
<b>Great Belt East Bridge</b> (1998)	1624	<b>1/406</b>	1/52	1/68	236 kg/m <sup>2</sup>	424 kg/m <sup>2</sup>	56%
<b>Akashi Kaikyo Bridge</b> (1998)	<b>1991</b>	1/142	1/56	1/140	<b>364 kg/m<sup>2</sup></b>	<b>760 kg/m<sup>2</sup></b>	48%
<b>Xihoumen Bridge</b> (2009)	1650	<b>1/471</b>	1/46	1/92	266 kg/m <sup>2</sup>	408 kg/m <sup>2</sup>	<b>65%</b>

<sup>(1)</sup> L –main span length; <sup>(2)</sup> l –side span length; <sup>(3)</sup> w- deck width

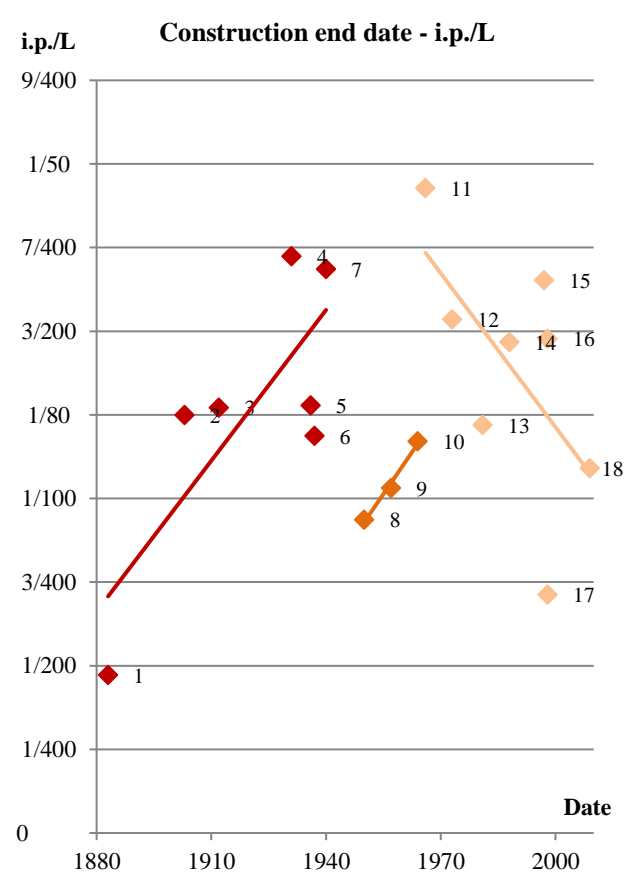
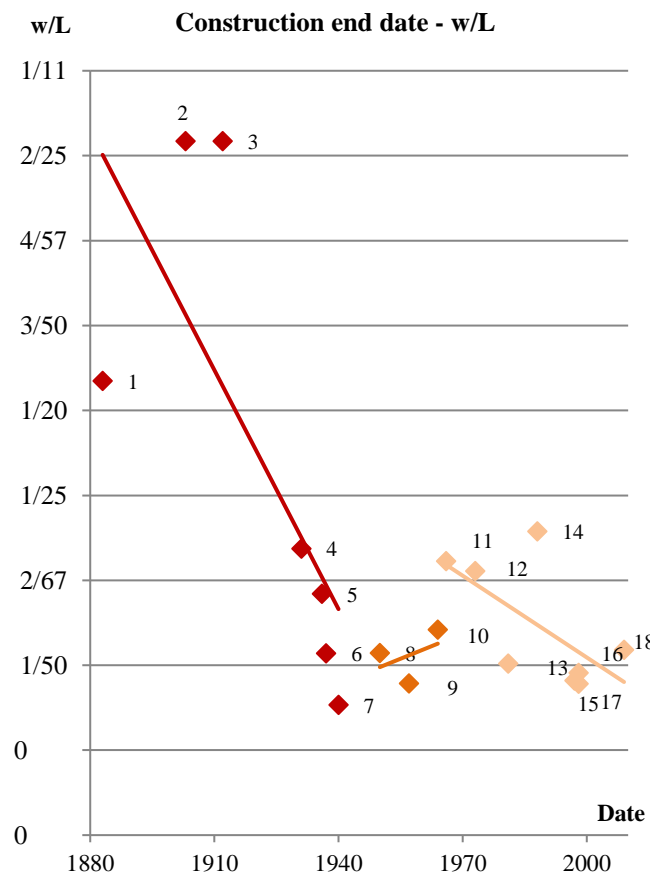
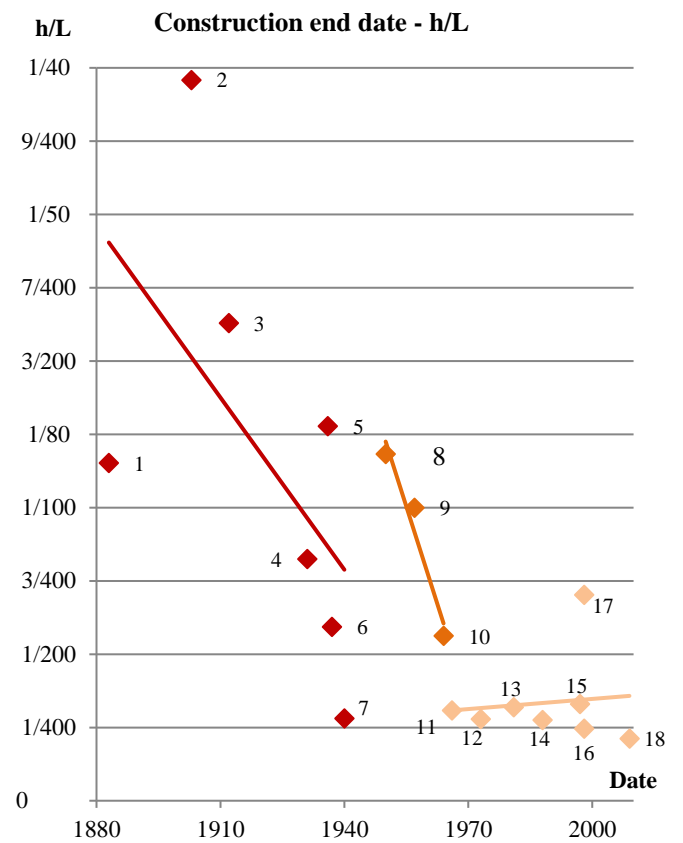
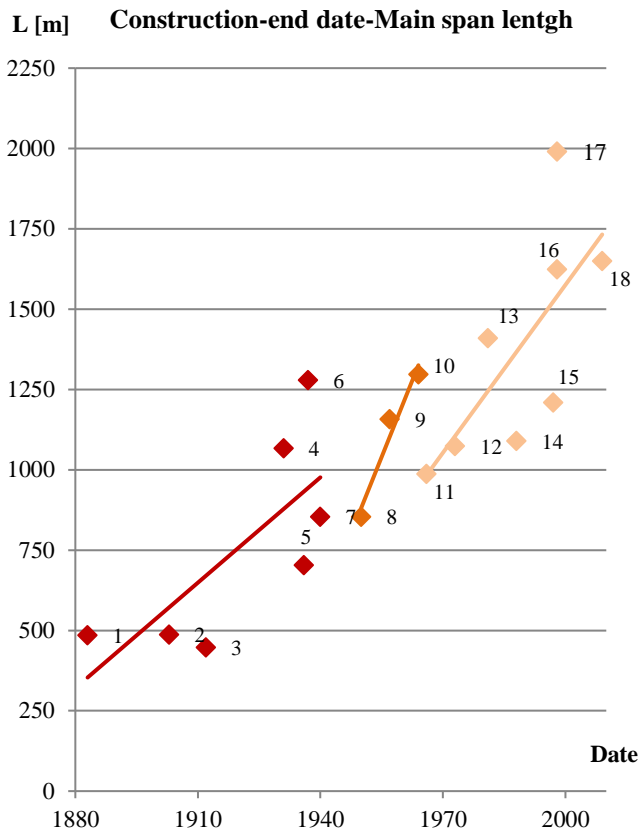
## 2.2 Critical evaluation of existing suspension bridges: design parameters improvement

Previous analysis show how suspension system has guaranteed to cover longer spans, reaching record length of 2000m. Growing span has often been combined to a reduction of bridge deck depth (as consequence of deflection theory application), until using streamlined-shaped box girder, capable to counteract the effect of aerodynamic instability. The evaluation of aerodynamic effects become really resonant after Tacoma Narrow collapse, leading to a double design approach, the American one, inclined to make truss stiffer and heavier to carry dynamic wind effects, and European one, proposing lighter and slender deck, whose aerofoil shape guarantee their resistance against wind effects. Instead of cable –stayed bridge, suspension bridge hanger are always deep-closed spaced ( $ip/L = 1-2\%$ ): in the case of pioneer George Washington bridge, this choice led to an analogue distribution of deck cross section, which guaranteed to greatly reduce truss depth.

The following table summarizes main design parameter, remarking their improvements passing from one generation to the successive.

Gen.	n.	Name	date	L [m]	h/L	ip/L	w/L
I	1	Brooklyn Bridge	1883	486	1/87	1/211 (0.47%)	1/19
I	2	Williamsburg Bridge	1903	488	1/41	1/80 (1.25%)	1/14
I	3	Manhattan Bridge	1912	448	1/61	1/79 (.26%)	1/12
I	4	George Washington Bridge	1931	1067	1/121	1/58 (1.72%)	1/30
I	5	San Francisco-Oakland Bay Bridge	1936	704	1/78	1/78 (1.28%)	1/35
I	6	Golden Gate Bridge	1937	1280	1/168	1/84 (1.19%)	1/47
I	7	Tacoma Narrows Bridge	1940	854	1/356	1/59 (1.69%)	1/65
II	8	Second Tacoma Narrows Bridge	1950	854	1/85	1/107 (0.93%)	1/47
II	9	Mackinac Bridge	1957	1158	1/100	1/97 (1.03%)	1/56
II	10	Verrazano-Narrows Bridge	1964	1298	1/178	1/85 (1.17%)	1/41
III	11	Severn Bridge	1966	988	1/324	1/52 (1.92%)	1/31
III	12	First Bosphorus Bridge	1973	1074	1/358	1/65 (1.53%)	1/32
III	13	Humber Bridge	1981	1410	1/313	1/82 (1.21%)	1/49
III	14	Second Bosphorus Bridge	1988	1090	1/363	1/68 (1.47%)	1/28
III	15	Hoega Kusten Bridge	1997	1210	1/303	1/61 (1.63%)	1/55
III	16	Great Belt East Bridge	1998	1624	1/406	1/68 (1.47%)	1/52
III	17	Akashi Kaikyo Bridge	1998	1991	1/142	1/140 (0.71%)	1/56
III	18	Xihoumen Bridge	2009	1650	1/471	1/92 (1.09%)	1/46



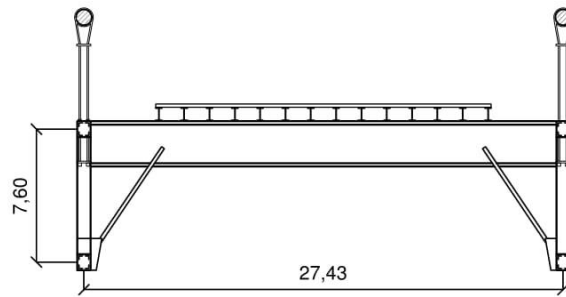


Golden Gate Bridge, 1937

San Francisco, California

L(main span): 1280m;  $ip/L=1.1\%$ ;  $h/L=1/168$

Unstiffened single deck section

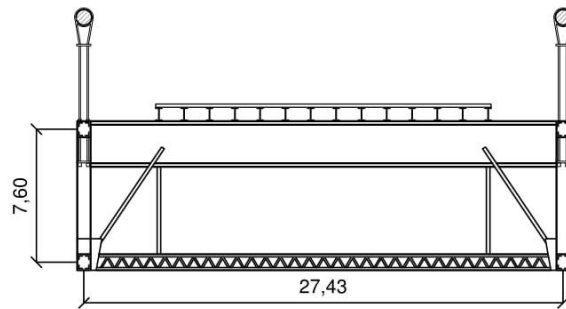


Golden Gate Bridge, 1955

San Francisco, California

L(main span): 1280m;  $ip/L=1.1\%$ ;  $h/L=1/168$

Stiffened double deck system with lower bracings

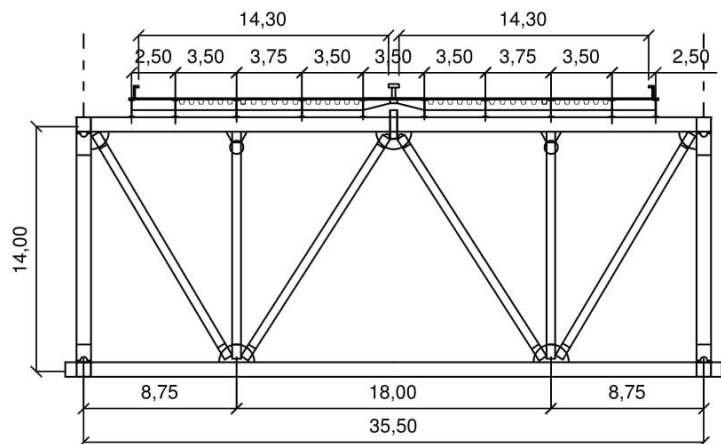


Akashi Kaikyo Bridge, 1998

Kobe/Awaji, Japan

L(main span): 1991m;  $ip/L=0.70\%$ ;  $h/L=1/142$

Stiffened truss deck system

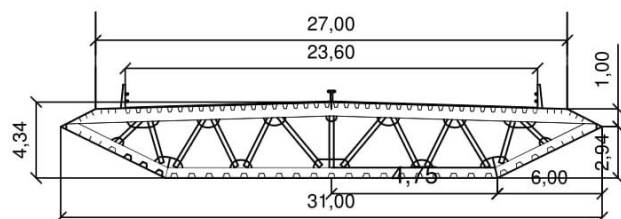


Great Belt East Bridge, 1998

Korsør, Denmark

L(main span): 1624m;  $ip/L=1.47\%$ ;  $h/L=1/406$

Aerofoil deck system

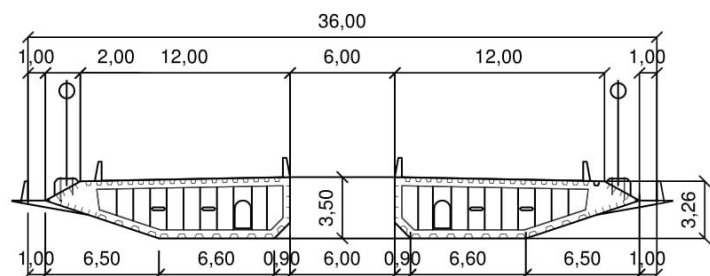


Xihoumen Bridge, 2009

Ningho, Zhejiang, China

L(main span): 1650m;  $ip/L=1.08\%$ ;  $h/L=1/471$

(Advanced) Aerofoil deck system

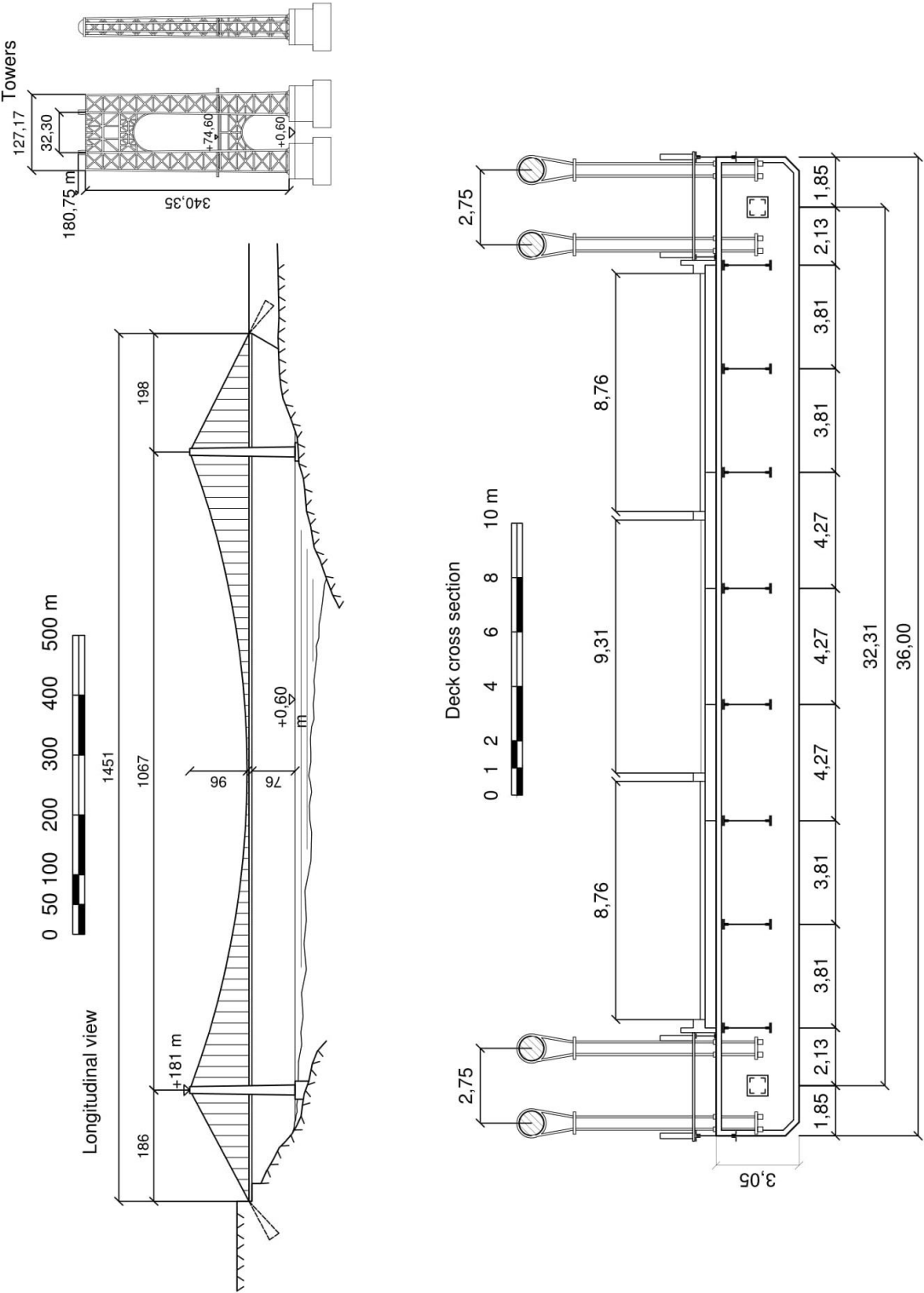


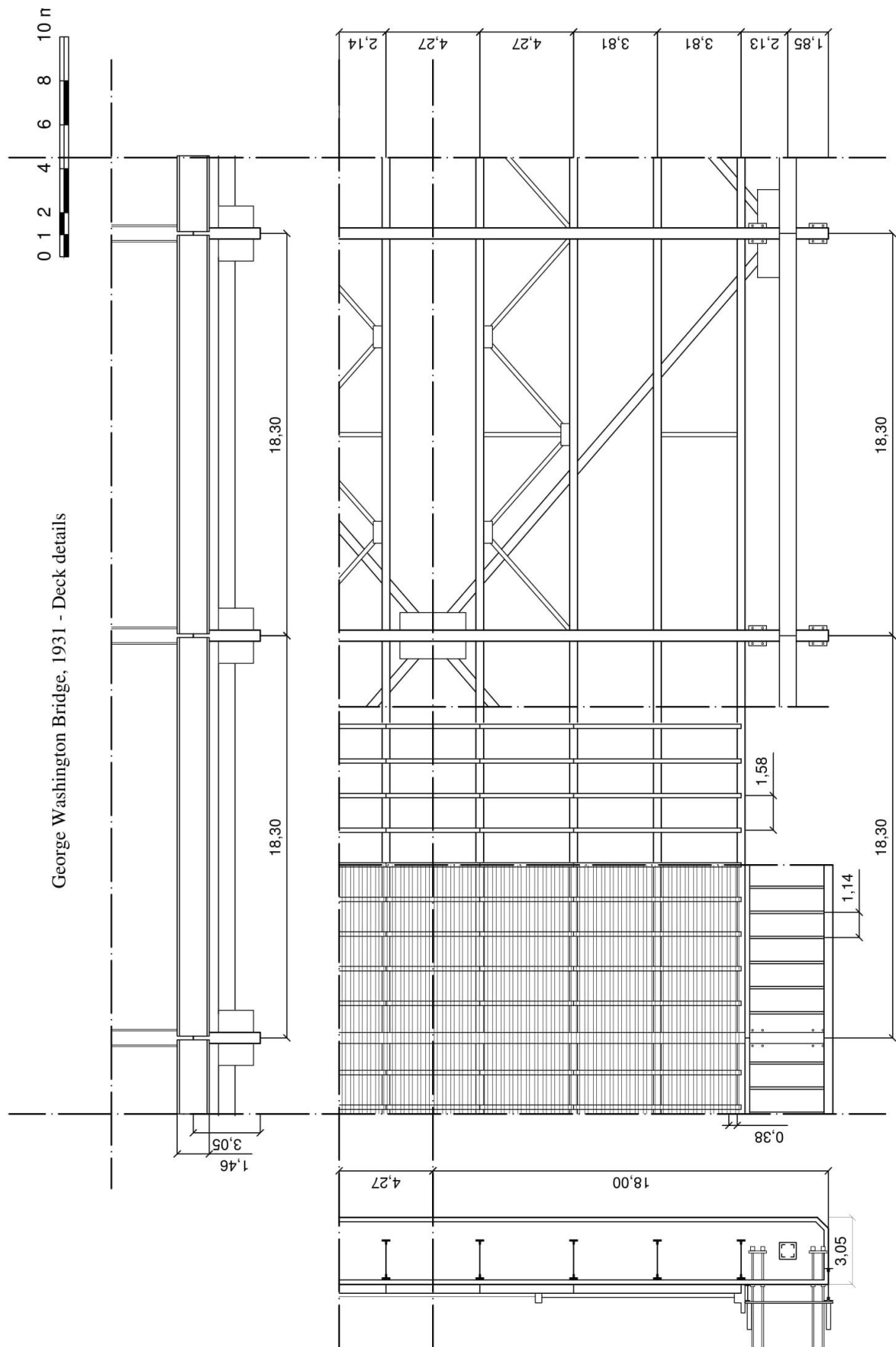
Looking at the following picture, it could be easily understood how deck stiffened system has changed through generations: after Roebling's first attempts to remark the need of stiffened deck system for long span suspension bridges (as in Niagara, Ohio and Brooklyn bridges), earliest unstiffened proposals made the way for rigid double deck solutions, often having lower stiffening bracings. A new generation of stiffened truss deck followed: except for Williamsburg Bridge, designed according to linear theory, from Manhattan to George Washington Bridge design proposals led to more slender structure, as a consequence of deflection theory application. But, Tacoma Narrow collapse underlined the necessity to take into account also dynamic effects due to acting loads (above all wind). If the more precautionary American approach led to heavy and rigid truss system to cover longer span, European designer proposed the first aerofoil decks, whose streamlined-shape prevented them from aerodynamic instability.

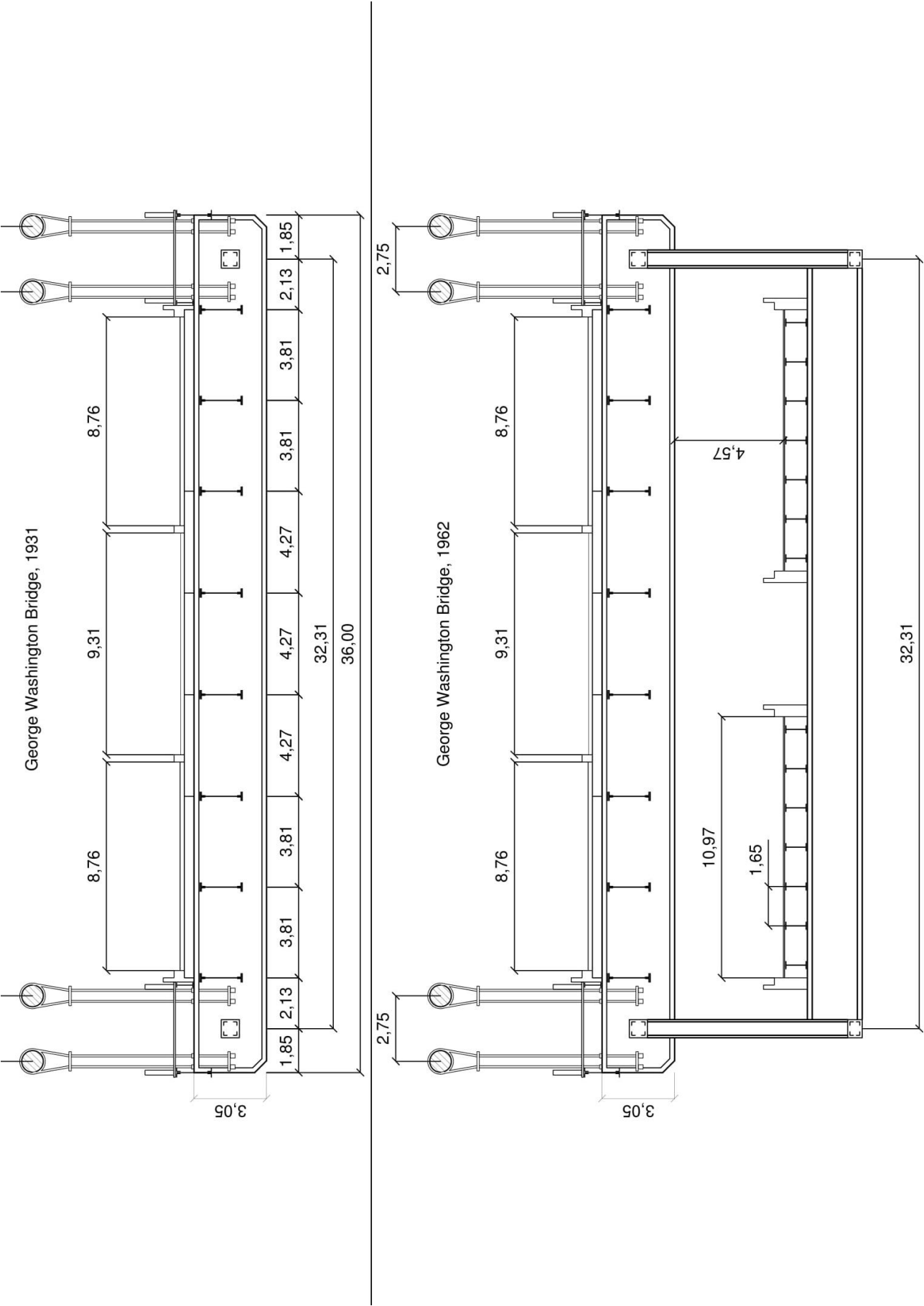
#### **Appendix (A): Suspension bridges drawings**

- 1. George Washington Bridge (1931): longitudinal view and deck cross section**
- 2. George Washington Bridge (1931): deck detail**
- 3. George Washington Bridge (1931): comparison between deck solution of 1931 and 1962**
- 4. Golden Gate bridge: deck cross section (1937) – (1955)**
- 5. Comparison between decks of George Washington Bridge (1931), San Francisco Oakland Bay Bridge (1936) and Golden Gate (1937)**
- 6. Akashi Kaikyo Bridge (1998): longitudinal view, plan, deck cross section, tower detail**
- 7. Great Belt East Bridge (1998): longitudinal view, plan, deck cross section, tower detail**
- 8. Xihoumen Bridge (1998): longitudinal view, plan, deck cross section, tower detail**

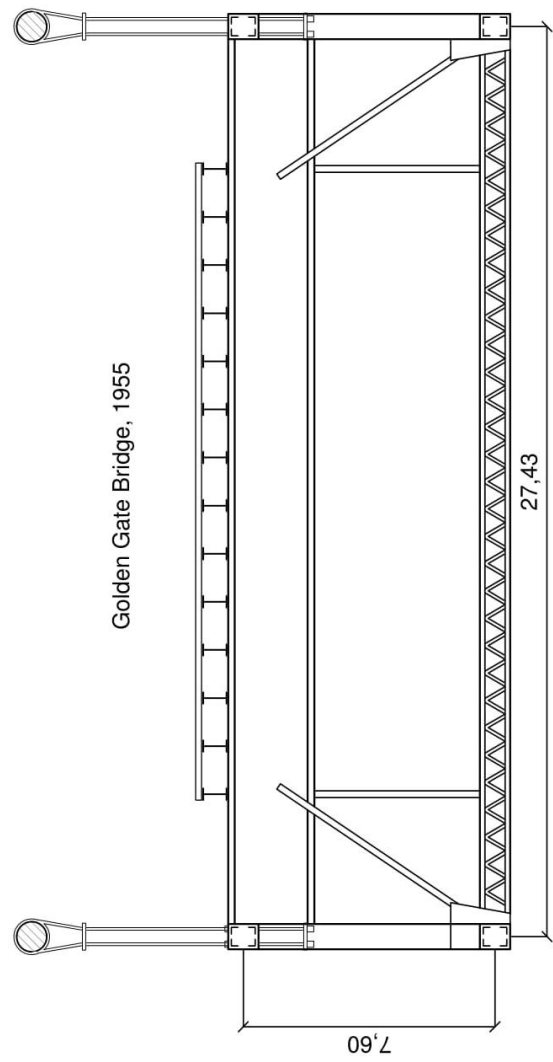
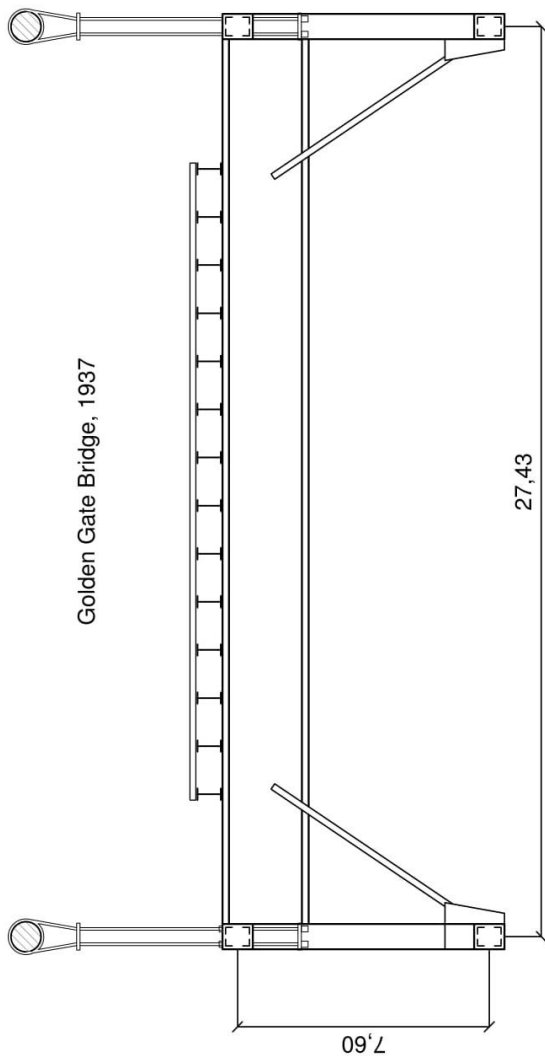
George Washington Bridge, 1931

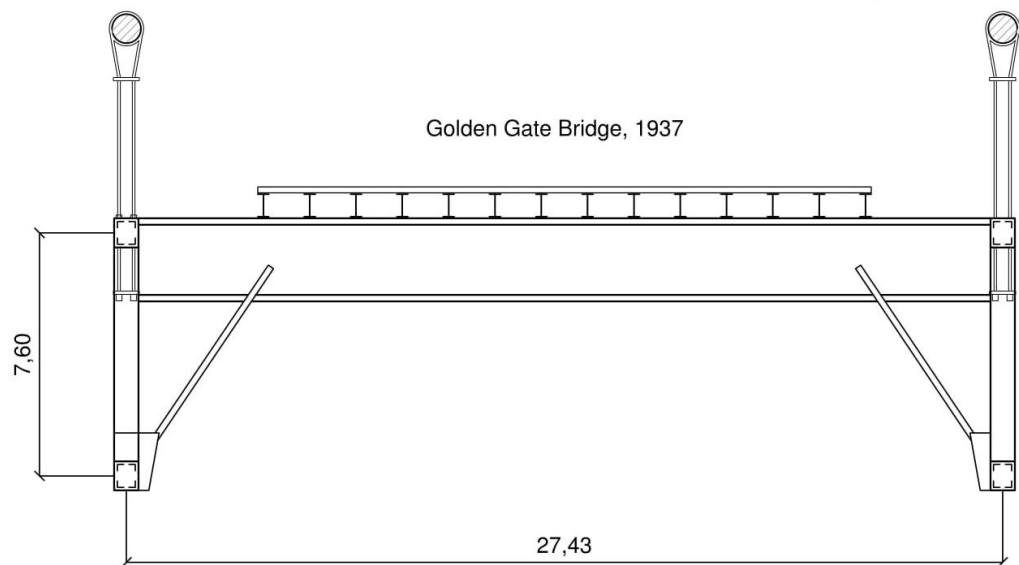
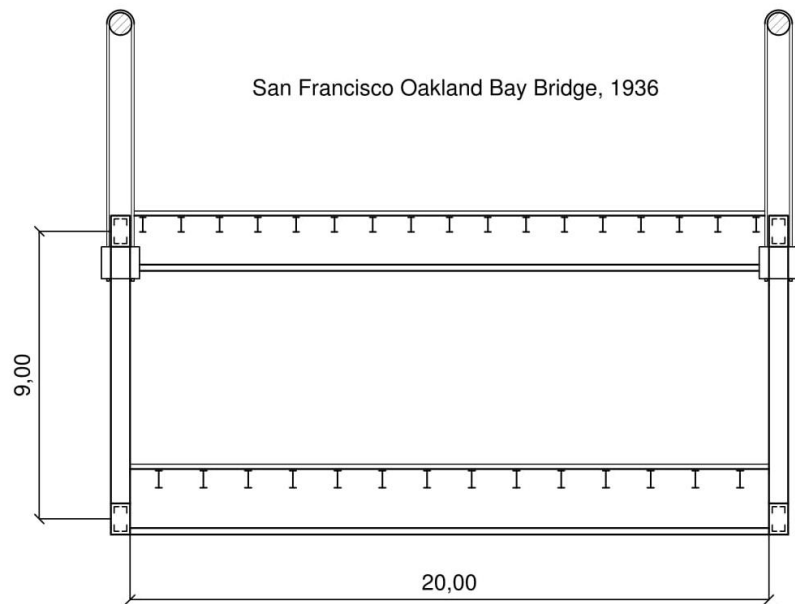
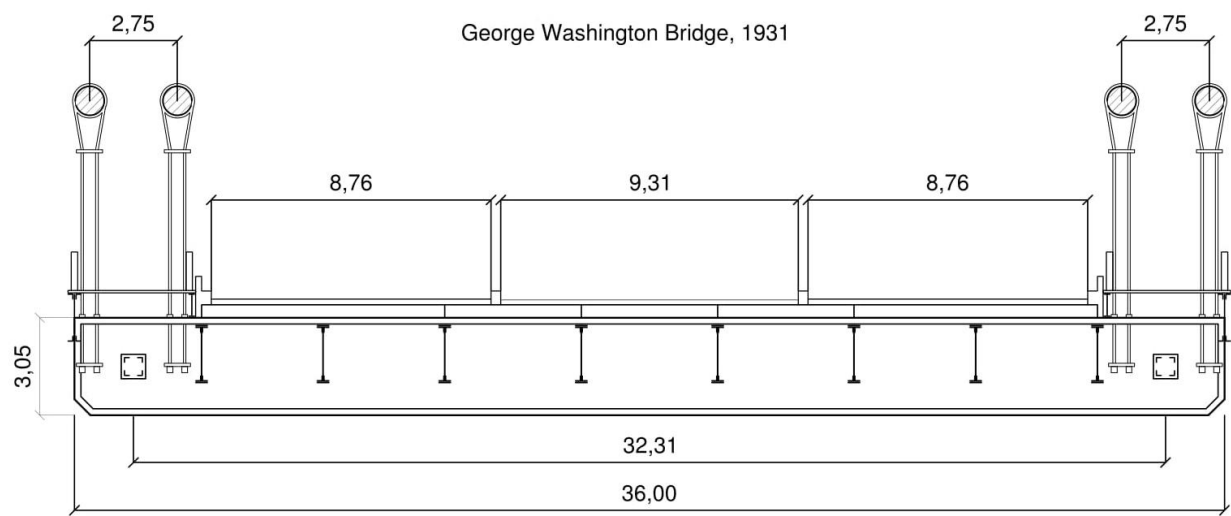




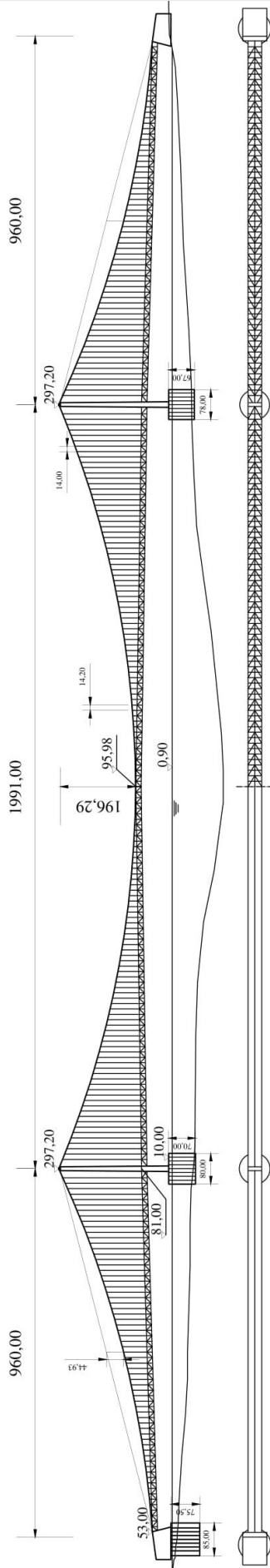




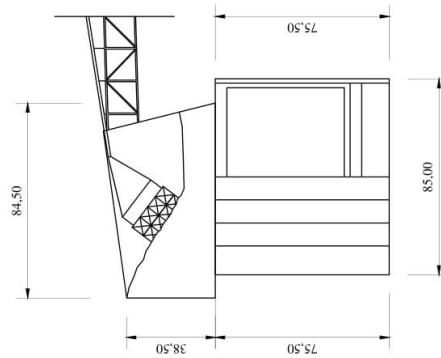




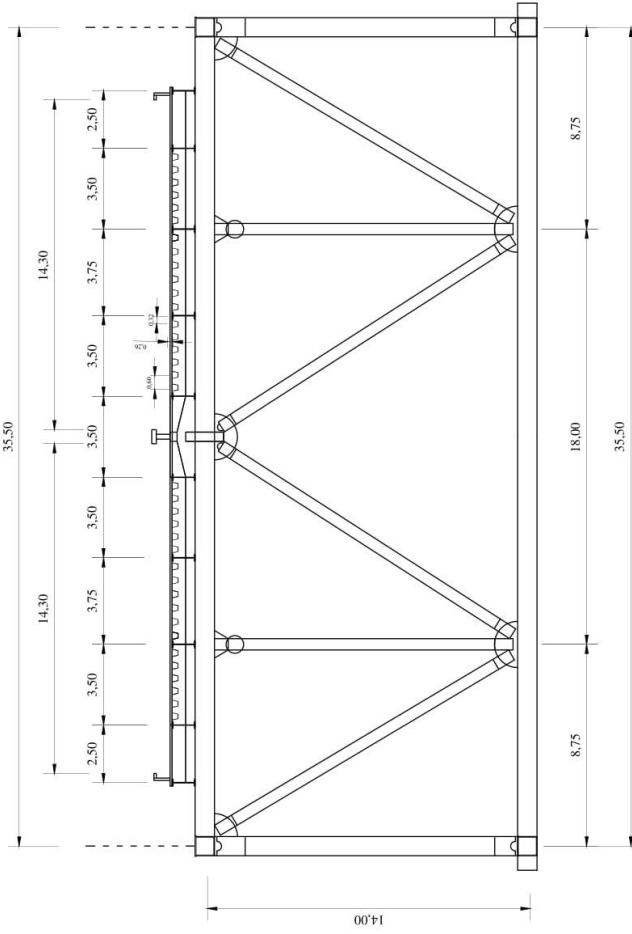
Longitudinal view and plan, 1:10000



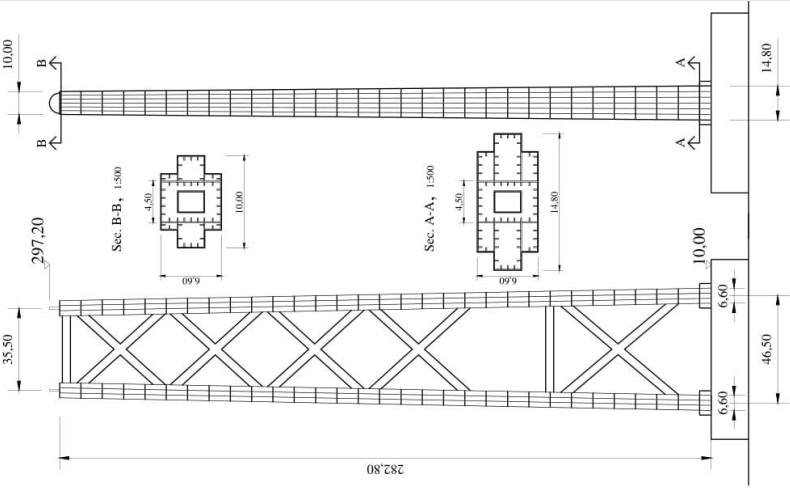
Cable anchorage, 1:2000



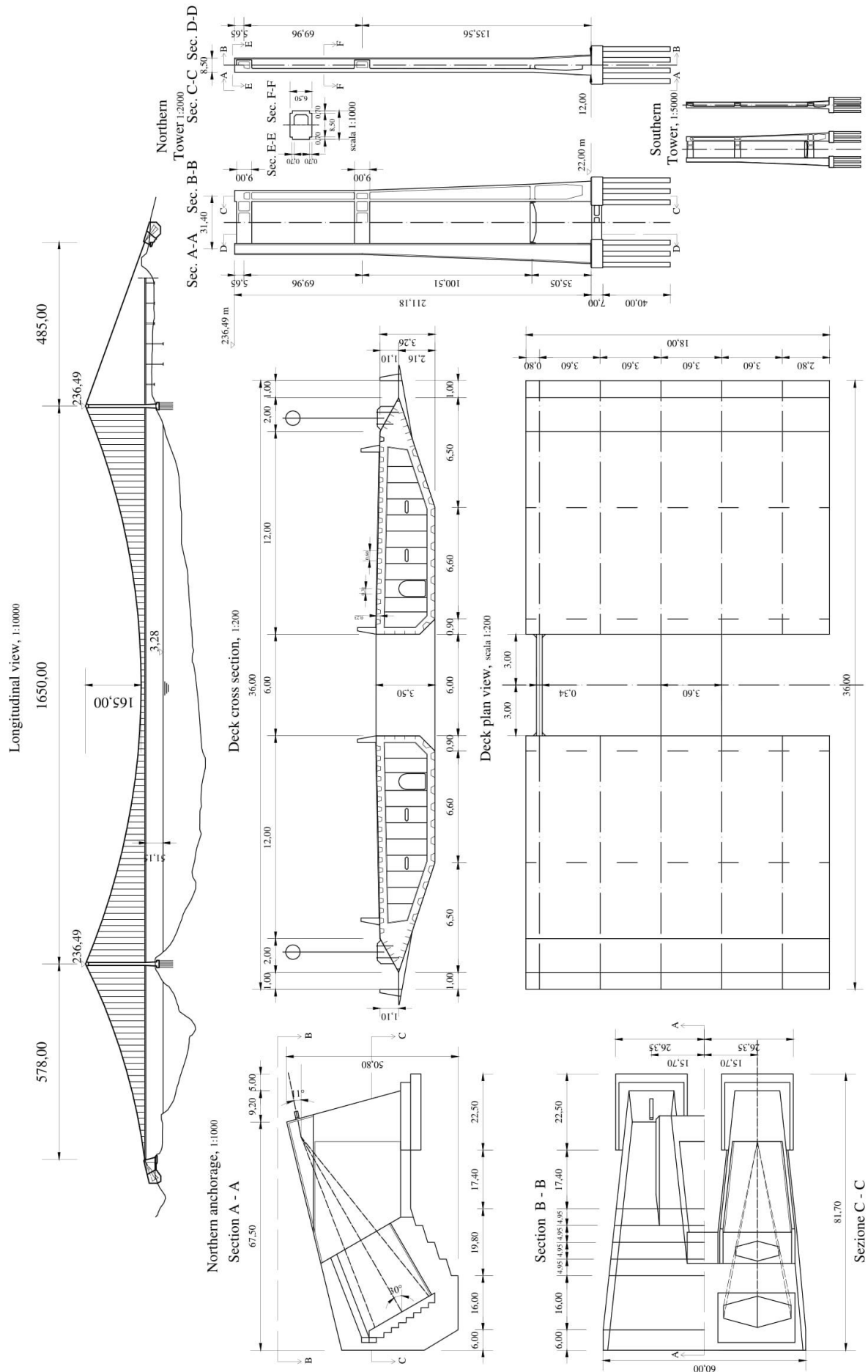
Deck cross section, 1:200



Tower, 1:2000







## Bibliography

- [1] Finley, James. A description of the patent Chain Bridge, in *The Port Folio*, Vol. III, No. 6, Philadelphia, 1810, p. 441
- [2] M.Gauthey, “*Traite de la construction des ponts*”, 1832
- [3] Navier, 1833. *Resumé des Lecons*
- [4] Telford, Thomas. *Life of Thomas Telford*. London : James and Luke G. Hansard and Sons, 1838
- [5] W. J. M. Rankine, *Applied Mechanics*. Griffin, London 1858.
- [6] Anon., Suspension girder bridges for railway traffic. *The Civil Engin. Arch. J.*, 23, 1860, 317-319, 352-356.
- [7] Smiles, Samuel. *The Life of Thomas Telford*. London : John Murray, 1867
- [8] *Description of the Clifton Suspension Bridge*. Barlow, William Henry. London : Institution of Civil Engineers, 1867.
- [9] Roebling, John A. Report of John A. Roebling to the President of Directors of the New York Bridge Company on the proposed East River Bridge. New York : Eagle Book and Job Printing Department, 1870.
- [10] Green, S. W. *A complete history of the New York and Brooklyn Bridge*. New York : S. W. Green's Sons, 1883.
- [11] P. W. BARLOW, On the mechanical effects of combining girder and suspension chains. *The Civil Engin. Arch. J.*, 23, 1860, 225-230. [4] M. LEVY, *Mémoire sur le calcul des ponts suspendus rigides*. *Annales des Ponts et Chaussées*, s. 2, 12, 1886, 179-246
- [12] Hungerford, Edward. *The Williamsburg Bridge*. New York : The Eagle Press, 1903.
- [13] Hungerford, Edward. *The Williamsburg Bridge*. New York : The Eagle Press, 1903.
- [14] Johnson, Alexander. *The Manhattan Bridge*. The Municipal Engineers of the City of New York. 1910, 55.
- [15] Tyrrell, Henry Grattan. *History of bridge engineering*. Chicago, 1911.
- [16] Steinman, 1929. *Suspension Bridges and cantilevers, their economic proportions and limiting spans*.
- [17] The Port of New York Authority. *Fourth Progress Report on Hudson River Bridge*. New York : s.n., 1931.
- [18] *George Washington Bridge: General Conception and Development of Design*. Ammann, Othmar. 1, s.l. : Transactions of the American Society of Civil Engineers, 1933, Vol. 97
- [19] Mensch, E. Cromwell. *The San Francisco Oakland Bay Bridge: A technical description in ordinary language*. San Francisco : s.n., 1936.



- [20] George Washington Bridge: Design of Superstructure. Dana, Allston, Andersen, Aksel, Rapp, George M. 1 : Transactions of the American Society of Civil Engineers, 1933, Vol. 97
- [21] Strauss, Joseph. The Golden Gate Bridge. San Francisco : Golden Gate Bridge and Highway District, 1938.
- [22] Finch, J. K. Wind Failures of suspension bridges or evolution and decay of the stiffening truss. Engineering News Record. 1941, 13.
- [23] Steinman, David B. The Builders of the bridge. The story of John Roeblig and his son. 1944
- [24] Steinman, D. B. e Nevill, J. T. Miracle Bridge at Mackinac. Grand Rapids : Eerdmans Publishing, 1957
- [25] Steinman, David B. The Design of the Mackinac Bridge. [aut. libro] L. A. Rubin. Mighty Mac: The Official Picture History of the Mackinac Bridge. Detroit : Wayne State University Press, 1958
- [26] . Stuessi, Fritz. Sul calcolo dei ponti sospesi di grande luce. Costruzioni Metalliche. 1966, Vol. 3, 35.
- [27] The Severn Bridge Design: a new principle of design. Roberts, Gilbert. Lisbona : Proc., Intl. Symp. on Suspension Bridges, 1966
- [28] Stuessi, Fritz. Sul calcolo dei ponti sospesi di grande luce. Costruzioni Metalliche. 1966, Vol. 3, 35.
- [29] O'Connor, Colin. Design of bridge superstructures. New York : Wiley-Interscience, 1971.
- [30] Aerodynamic aspects of the final design of the 1624 m suspension bridge across the Great Belt. Larsen, Allan. 48, s.l. : Journal of Wind Engineering and Industrial Aerodynamics, Elsevier, 1993.
- [31] Design of the Great Belt East Bridge. Ostenfeld, Klaus H. 4, Zurigo : Structural Engineering International, 1995, Vol. 5
- [32] Comparison between different structural solutions: the Great Belt project. Ostenfeld, Klaus H. Zurigo : IABSE congress report, 1996, Vol. 15.
- [33] . Field measurements of a 1210 m span suspension bridge during erection. Larose, Guy L., Johnson, Rickard e Damsgaard, Aage. Zurigo : IABSE Reports, 1998, Vol. 79.
- [34] Design and Construction of the Akashi Kaikyo bridge's superstructure. Fuchida, Masanobu, Kurino, Sumitaka e Kitagawa, Makoto. Zurigo : IABSE reports, 1998, Vol. 79.
- [35] Il montaggio del ponte sospeso sul Great Belt. de Miranda, Mario. 9 : Le Strade, 1998, Vol. 8

- [36] Okukawa, Atsushi, Suzuki, Shuichi e Harazaki, Ikuo. Suspension Bridges. Wai-Fah Chen e Lian Duan. Bridge Engineering Handbook. Boca Raton : CRC Press LLC, 2000.
- [37] Roberto Parisi. Luigi Giura 1795-1864, Ingegnere e Architetto dell'Ottocento. Electa Napoli (2003)
- [38] The Xihoumen Bridge. Song, Hui, Ding, Dajun e Virola, Juhani. 6, s.l. : RIA, 2005
- [39] Rockland, Michel Aaron. The George Washington Bridge: Poetry in Steel. New York : Rutgers University Press, 2008
- [40] Zhousan Xihoumen Bridge - The world's longest box-girder suspension bridge. Song, Hui e Dong, Wang Xiao. 1, Zurich : IABSE Symposium Report, 2009
- [41] J. Ramsden, A Critical Analysis Of The Proposed Bridge Over The Strait Of Messina. Proceedings of Bridge Engineering 2 Conference 2009 April 2009, University of Bath, Bath,
- [42] Brancaloni, F., Diana, G., Faccioli, E., Fiammenghi, G., Firth, I.P.T., Gimsing, N.J., Jamiolkowski, M., Sluska, P., Solari, G., Valenise, G., Vullo, E. (2009). Messina Strait Bridge - A challenge and a dream, CRC Press, Balkema, ISBN 978-0-415-46814-5.
- [43] Kawada, Tadaki. History of the modern suspension bridge. Reston, Virginia : American Society of Civil Engineers, 2010.
- [44] Jurado, Henrandez, Nieto, Mosquera. Bridge Aeroelasticity: Sensitivity Analysis and Optimal Design. Boston : WIT Press, 2011.
- [45] Gimsing, Niels J. e Georgakis, Christos T. Cable Supported Bridges, Concept and Design, Third Edition. Chichester : John Wiley and Sons, 2012.
- [46] 6. Denison, Edward e Stewart, Ian. Leggere i ponti. Modena : Logos, 2012.

## Web references

- [1] Stretto di Messina S.p.A. [Online] 27 09 2006. [Cited: 30 03 2009.] Accessed via web archives. [www.strettodimessina.it](http://www.strettodimessina.it).
- [2] Nebel, Bernd. Die Clifton Suspension Bridge. 2011. [http:// www.bernd-nebel.de/bruecken/index.html?/bruecken/3\\_bedeutend/clifton/clifton.html](http://www.bernd-nebel.de/bruecken/index.html?/bruecken/3_bedeutend/clifton/clifton.html).
- [3] Menai Suspension Bridge. Sito Web Structurae. [Online] Wilhelm Ernst & Sohn Verlag, 2014. <http://structurae.net/structures/menai-suspension-bridge>.
- [4] Godden, F. T. Clifton Suspension Bridge. 2014 <http://ita.archinform.net/projekte/1589.htm>.
- [5] Historic American Engineering Record. Brooklyn Bridge, Spanning East River between Park Row, Manhattan and Sands Street, Brooklyn, New York, New York County, NY. Library of Congress 1972. <http://loc.gov/pictures/item/NY1234/>. (2015)

- [6] Eastern Roads. Williamsburg Bridge: Historic Overview. New York City Roads. <http://www.nycroads.com/crossings/williamsburg/>. (2015)
- [7] Eastern Roads. Manhattan Bridge: Historic Overview. New York City Roads. <http://www.nycroads.com/crossings/manhattan/> (2015)
- [8] Eastern Roads. George Washington Bridge: Historic Overview. New York City Roads. [www.nycroads.com/crossings/george-washington/](http://www.nycroads.com/crossings/george-washington/). (2015)
- [9] Historic American Engineering Record. Tacoma Narrows Bridge, Spanning Narrows at State Route 16, Tacoma, Pierce County, WA. Library of Congress. (2015) <http://www.loc.gov/pictures/item/wa0453.sheet.00001a/>.
- [10] Eastern Roads. Verrazano - Narrows Bridge: Historic Overview. New York City Roads.(2015) <http://www.nycroads.com/crossings/verrazano-narrows/>.
- [11] Severn River Crossing PLC. Detailed History of the M48 Severn Bridge. Severn River Crossing PLC. 2015. [http://www.severnbridge.co.uk/history\\_sb.html](http://www.severnbridge.co.uk/history_sb.html).
- [12] Technical Information. Humber Bridge Board.] The Humber Bridge Board. [http://www.humberbridge.co.uk/explore\\_the\\_bridge/engineering/technical\\_information.php](http://www.humberbridge.co.uk/explore_the_bridge/engineering/technical_information.php). (2015)
- [13] COWI. The Höga Kusten Bridge, Sweden. (2015) <http://www.cowi.com/menu/project/BridgeTunnelandMarineStructures/Bridges/Suspensionbridges/Pages/h%C3%B6gakustenbridgesweden.aspx>.
- [14] COWI. The Great Belt Link: The East Bridge, Denmark. COWI. [<http://www.cowi.com/menu/project/BridgeTunnelandMarineStructures/Bridges/Suspensionbridges/Pages/thegreatbeltlinktheeastbridgedenmark.aspx>.
- [15] Honshu-Shikoku Bridge Expressway Company Limited. Akashi Kaikyo Bridge. Honshu-Shikoku Bridge Expressway Company Limited. <http://www.jbhonshi.co.jp/english/library/pamphlet.html>.
- [16] International Database and Gallery of Structures, <http://en.structurae.de>

### 3. Steel arch bridges

#### 3.1 Deck stiffened system: a common mean to read arch bridge evolution

In the following chapter the role of deck stiffened system has been assumed as the common denominator in reading the evolution of steel arches: the progressive attempts towards structural optimization, till the “pure arch” solution proposed by Calatrava Ponte della Costituzione, have completely changed the design approach over the centuries, passing from the earliest massive iron arch bridges to the most recent slender solutions.

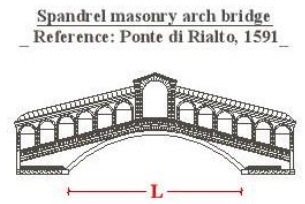
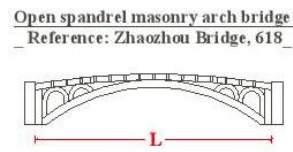
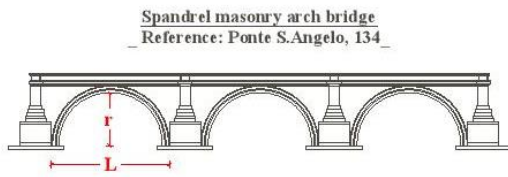
Despite of suspension bridges, for this typology it has been no easy defining successive generations to well synthesize the technological progress which marked the evolution of steel arch bridges; however, it has been noted the paradigmatic contribution of some leading figures, as Telford, Eiffel, Eads, Nielsen, Moisseiff, Arenas, till Calatrava, underlining how the passage from deck-arch solution to tied-arch bridges have given the possibility to increase arch spans, from 150m to 550m.

Modern steel bridges could be considered a result of technological development of ancient masonry arch bridges. As structural type, the arch is a system which transports the applied loads to supports primarily through compression stresses in the arch, eliminating the possibility of tensile ones occurring within the chosen materials. This is achieved through design of the arch shape above all if it's to match as closely as possible to the line of thrust within the arch, especially in the case of arch bridge with very slender piers and extremely surbased segmental arches. Robustness of existing masonry bridge, which were all designed to carry above all permanent loads, being live ones a little percentage of total vertical loads, shows how the structural behaviour of masonry arch bridges has had no changes through centuries. For usual masonry spandrel arches, no separation can be found between the upper deck and the lower vault: the filling interposed materials easily transfer loads applied upon deck to the main load bearing structure (vault), adding rigidity to the whole system, also increasing the dead loads of a structure in which deck and arch make a monolithic cluster.

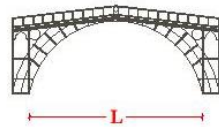
In 18th century, growing live loads due to rail traffic, led designer to take into account other aspects in bridge design, as no-negligible dynamic effects or vibrations, as well as valuing the possibility to use new material or different static schemes. Earliest examples of metal deck arch bridge had a configuration closed to that one of previous masonry bridges, first attempts which didn't exploit effectively the potentialities of materials used. Redundant truss structure characterized earliest deck arch bridges, spanning no more than 50m, almost until Eads (in St.Louis Bridge) succeeded in optimizing structural solution of segmental –truss-deck arch bridge, previously adopted by Telford (in Bonar Bridge), reaching 158m-span.

## ARCH BRIDGETYPE EVOLUTION

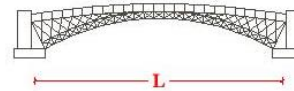
### FROM MASONRY PRECURSOR TO EARLIEST METAL DECK ARCH BRIDGES



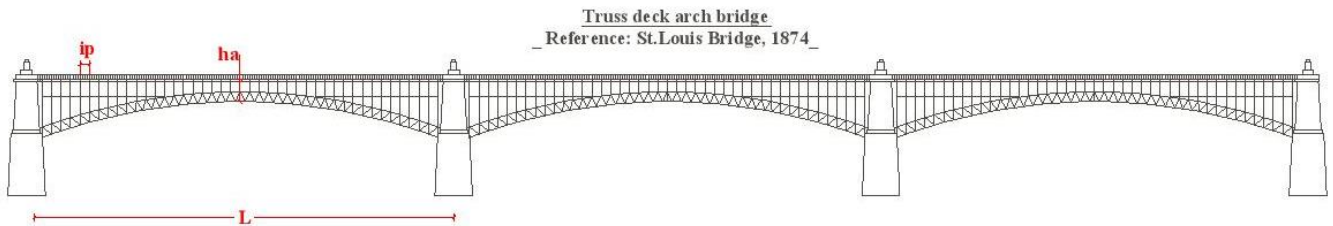
Open spandrel metal arch bridge  
Reference: Coalbrookdale Bridge, 1779



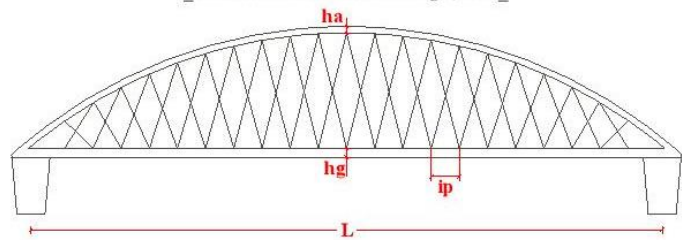
Spandrel masonry arch bridges  
Reference: Bonar Bridge, 1802



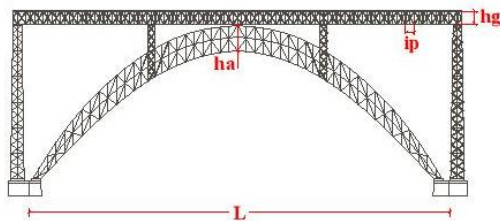
## MODERN STEEL ARCH BRIDGES



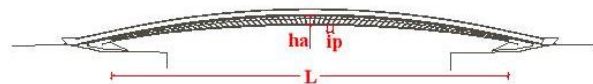
Bowstring arch bridge - Langer system  
Reference: Fehmansund Bridge, 1963



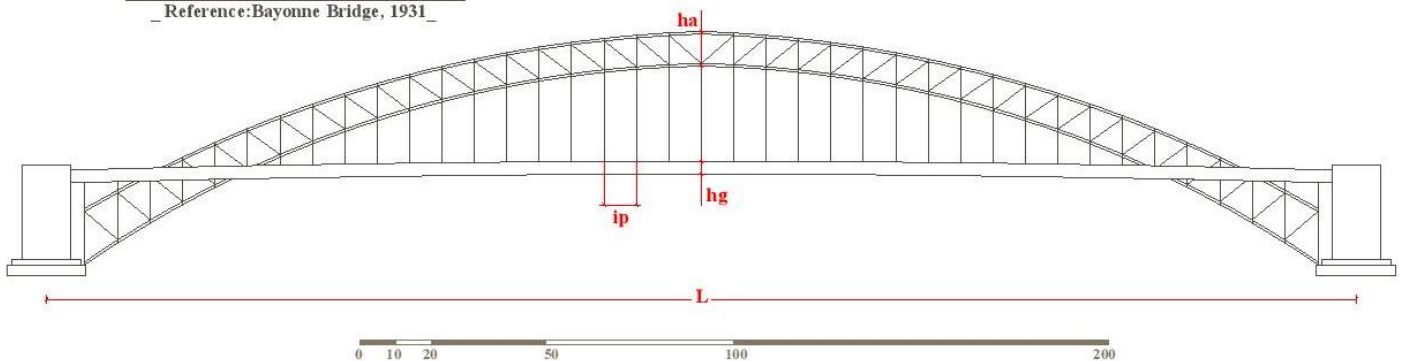
Truss deck arch bridge- hybrid system  
Reference: Garabit Viaduct, 1884



Truss deck arch bridge "pure arch solution"  
Reference: Ponte della Costituzione, 2009



Bowstring arch bridge - rigid arch system  
Reference: Bayonne Bridge, 1931



With a comparable heavy structure (about 3500 tons), covering the same span, Eiffel completely changed the role deck system in Garabit Viaduct. Despite of previous truss girder, whose road-deck was strictly connected to the lower arch by a thick-spaced transverse element system, he made bridge deck clearly distinguishable from the main arch, making the second one prevailing on the slender girder. The introduction of bowstring arch type have given the possibility to increase spans: if the solution with truss upper arch and flexible deck guaranteed to cover more than 550m (as Bayonne Bridge), the pleasant “equilibrium” between aesthetic a functionality has been reached with deck stiffened system, characterized by slender arch. In this case, the improvements of suspension system, particularly the increasing number of hangers used, have led to a better interaction between load bearing structural elements, giving the possibility to reduce deck structural system size.

If Italian designers have given a negligible contribution to steel arch bridge evolution, on the contrary, Calatrava’s experience can be read as turning point in their design approach: he has been capable to completely deny longitudinal girder, “simply decomposing” it in a huge number of deep-closed spaced transverse cross sections; load bearing structural elements size is stripped down, even until there is no need of any filling materials: as in the case of Ponte della Costituzione, Calatrava designs a “pure arch”, whose road deck stands directly upon the main structure.

The evolution of steel arch bridges, starting from their masonry precursors, have seen the succession of different types, inherent both deck-arch and bowstring arch solution; a follows, this “journey into arch typology” wants to analyse changes occurred to deck stiffened system passing from the earliest corbelled stone arches to masonry spandrel deck-ones, from wrought iron truss deck arch bridges to “hybrid” arch structures (ref. “How to read a bridge”, Devison & Stewart, 2012), where the arch and the upper longitudinal girder work in tandem, as in the case of Garabit Viaduct ; the need to cover longer span made the use of bowstring (through or tied) arch bridges necessary, till the innovative split bowstring arch solution.

For each type, geometrical characteristics usually adopted to describe each, have been taken into account; in addition, it has been considered the static coefficient, strictly connected to the value of arch thrust. In particular, for deck arch bridges, the following parameters have been analysed, assuming as  $L$  the main span length, and  $r$  the arch rise:

- $r/L$ : arch rise-to-main span ratio, to define arch lowering
- $L^2/r$ , static coefficient: characterizing segmental arch, is proportional to arch trust value.



For bowstring arch bridges, other design parameters, useful to describe different peculiar aspects, which involve and influence their structural behaviour, has been introduced, as follows:

- ( $i.p./L$ ), cable spacing-to-main arch length ratio, to describe suspension cable distribution;
- ( $h_{arch}/L$ ), arch depth-to span ratio, to define arch slenderness as function of crown section depth;
- ( $h_{girder}/L$ ), girder depth-to span ratio, to characterize longitudinal girder slenderness;
- ( $h^*/L$ ), overall deck depth-to- span ratio (in the case of deck arch bridge), or mean value of arch and deck slenderness (for bowstring arch bridge), considering the whole structure slenderness.

### 3.2 Historical evolution of deck arch bridges: masonry precursors

Considering arch bridge historical evolution, it could be said that, over the centuries, material resources and technologies allowed to build growing main spans. Valuing different and more efficient way to get load-bearing structural elements (arch, stiffening truss, hangers) to interact, new typologies and schemes have been introduced, till the modern complex systems, where arch cooperates with girder: in these cases the main aim is to make the arch working predominantly in extensional regime, carrying only axial forces, minimizing arch cross section; so, all stress due to live loads, above all in the case of asymmetrical distribution, have to be carry by girder. It's emphasized that the arch – to- girder interaction is the main aspect that have influenced arch bridge historical evolution.

Along bridges history, arch represented the optimal solution for its structural efficiency, because when it is designed following the anti-funicular curve of loads, transverse sections are uniformly compressed. This efficiency is the reason of using arches made of materials with good compression strength and bad tensile properties. Till 19th century arches have been built only with stones or bricks and, depending on the length to be saved, they were single or multi-span bridges. Unfortunately in arch bridges it is not possible to avoid totally bending moments, because the thrust line cannot coincide with the geometric axis for all live load combinations, due to the variability of traffic loads. To solve this problem arch cross sections have the right thickness, in order to maintain the thrust line into the central core of inertia and to avoid tensile stresses for all load combinations. The arch behaviour is established when a significant thrust at footings appears, which implies horizontal forces into foundations. When soil is not adequate to receive these forces, it is possible to compensate them through a tie placed between arch footings; in this way only vertical reaction forces can be obtained. So the whole tied-arch structure works as a simply supported beam, in which the arch is a curved

compressed member and the tie is in tension. In bridges with an upper arch, the tie can be provided by the deck itself, that is the link member between arch footings. In this case the deck is suspended to the arch by a number of metallic hangers.

This is the so-called bowstring structure, used either with concrete or steel arches. In the classical solution hangers are vertical, but different arrangements can be found throughout the historical evolution of these bridges, as harp arrangements or network arches. Inclined hangers appeared in XIX and XX centuries following Nielsen solution, in which the global behaviour of the bridge is exactly the same of a truss where the upper member is curved and compressed as an arch. Even if hangers are always in tension for dead loads, the difference between vertical and inclined arrangements can be found in the behaviour for live loads. High compressive forces could appear into inclined hangers for traffic loads combinations, so they need to be pre-tensioned at higher values with respect to vertical ones.

As anticipated, bowstring arch bridges have had a quite recent spreading, deriving from the ancient deck arch bridges. Considering these ones, it's important to understand how, at the beginning of XIX century, the "separation" between arch-extensional regime and girder-flexural regime occurred. A short excursus among the early examples of deck arch bridge, from masonry to steel innovative systems, is appropriate to explain this evolution.

From the earliest times until eighteenth century, stone was the only material known to build durable bridges: designed as permanent structures, according to Palladio, stone bridges replaced wooden ones when men "began to seek the immortality of their name" through construction which "are longer lasting and give greater glory to their builder" [from: "*De i ponti di pietra e di quello che nell'edificarli si deve osservare*" – Cap.X, III Libro, I Quattro Libri dell'Architettura, Palladio (1601)]. Their permanent nature is justified not only because they withstood the passage of time, but also considering that they have resisted to the increase in loads travelling over them, from animal-drawn carts and wagons to the modern vehicles. This type of bridges dominated most of the story, with a technology which remained practically unchanged during centuries.

Stone arch bridges represent one of the first recorded advances in bridge building, illustrating the movement from simple beam spans to use of the structural arch form to better support loads. Historians have traced their first functional precursors to the so-called corbelled arch, used in ancient cultures, as the Mycenaean or Mesopotamian ones; being as rudimentary "arch" constructed of stone courses which project to a peak, resulting in a triangular shape, they consisted in masonry blocks built over a wall opening by uniformly advancing courses from each side until they meet at a midpoint.

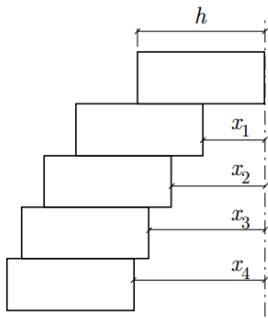


**Fig. 3.1\_ (a)** Corbelled arch\_ scheme\_ **(b)** Arkadiko Corbelled Bridge (1335-1190 B.C.), Peloponnese, Greece. Mycenaean stone corbel bridge.  $L=22\text{m}$ ;  $w=2.50\text{m}$ . **(c)** Eleutherna Bridge (400 - 300 B.C.), Crete, Greece. Stone corbel bridge.  $L=9.35\text{m}$ ;  $w=5.05 - 5.20\text{m}$ .

Considering the following scheme, it was possible to build corbels with large spans but, because of the divergence of the arithmetic series in the equation ( $x_i = x_{i-1} + h/2i$ ), it takes a lot of height to construct. The corbelled arch does not generate any horizontal forces, so called false- arch. (Fig. 3.1.a)

The *Arkadiko Corbelled Bridge*, (Fig. 3.1.b) dating to the Greek Bronze Age 1300–1190 BC, it is one of the oldest arch bridges still in existence and use. The bridge is built of limestone boulders without binding matter in the characteristic Mycenaean masonry called "Cyclopean": the structure is 22m long, 4.00m high at the abutments, 5.30 wide; the width of the roadway at the top is about 2.50m. The *Eleutherna Bridge* (Fig. 3.1.c) is another ancient Greek corbel arch bridge near the Cretan town of Eleutherna, Greece. This well-preserved structure, dating around 3-4th century BC, has a single span of 3.95 m, which is quite large for a false arch. The opening is cut from the unmortared limestone blocks in the shape of an isosceles triangle, the height of which is 1.84 m. The overall length of the bridge measures 9.35 m. Its width varies from 5.05 to 5.2 m, with the structure converging slightly towards its center point above the arch (5.05 m width there). The height is between 4 and 4.2.

**Fig. 3.2** Alcántara Bridge (104-106.), Alcántara, Spain. Semi-circular masonry arch bridge,  $L(\text{main span})=28.8\text{m}$ ;  $w=8.0\text{m}$ .





They reached a degree of perfection that no significant processes got after them, until the innovations introduced by Perronet in 18th century. Roman arches are tunnel or barrel type, with semi-circular shape; characterized by geometrical perfection, most of them are made of all equal voussoirs, from the springings to the keystone. An example of their extreme precision is the *Alcántara Bridge* (Fig.3.2): a semi-circular arch bridge, still in use, it has been finally restored in 1858. The bridge has a total length of 194m (spans: 13.80m – 21.9m – 28.8m – 27.4m – 21.9m – 13.8m), a height of 71m, a width of 8m, 6.7m of them for carriage: for its dimension and composition Alcántara Bridge is unique among stone bridges. Well-known Roman bridges were the aqueduct: extremely high structure were needed to cross valleys, supplying water to large towns.

The Romans overcame this problem building one bridge upon another one, until reaching the height required to create running gravity channel. An example is the *Pont du Gard* (Fig. 3.3), serving the city of Nîmes, in France. Added to the World Heritage List of UNESCO in 1985, the Pont du Gard, dating 1st century, is a three-story semi-circular arch bridge, originally used as aqueduct, with a channel width of 1.20m, and a channel slope of 0.019% (0.19m/km). With a total length of 230m, a height of 47.5m, it's the largest and best-known Roman public work. It's made of two superimposed bridges, having arches 24m spans, three- time greater than that of the top arcades, having a height of 7.40m.

Especially Rome, the Empire capital, saw the construction of multi –span arch bridges. Developing empirical methods for designing arches which still stand more than 2,000 years later, the Romans used a type of construction called voussoir arch with keystone. The weight of the stones, mortared with pozzolana cement, compressed the tapered stones together, making the arch an extremely strong structure: heavy wagons and legions of troops could safely cross a bridge constructed of arches without collapsing the structure.

**Fig. 3.3** Pont du Gard (1st century.), Nîmes, France. Three-story semi-circular masonry arch bridge,  $L(\text{arch}) = 24.4\text{m}$ ;  $h=47.5\text{m}$ .





**Fig. 3.4\_(a)** Ponte Milvio (109 BC), Rome, Italy. - vaulted arch bridge,  $L$  (main span) = 18.70m;  $w = 8.75$ m. **(b)** Ponte Fabricio (64 BC.), Rome, Italy- masonry arch bridge,  $L$  (main span) =  $2 \times 24.5$ m;  $w = 5.50$ m.

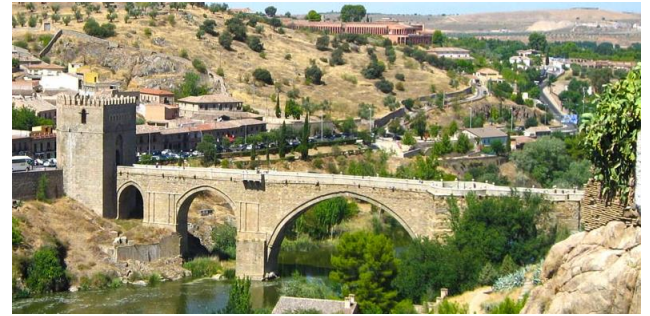
The first ones were built during the Republic, as the Via Flaminia's *Ponte Milvio* (Fig. 3.5.a) constructed in 109 BC over a previous one, a vaulted arch bridge with a total length of 139m (spans: 9.28m – 17.90m – 18.70m – 7.25m). Another example is the *Ponte Fabricio* (Fig. 3.5.b) (64BC): it has two 24.50m long spans; its spandrels are brick clad and the arches limestone-clad. *The Bridge of Tiberius* (Fig. 3.5) is another Roman bridge in Rimini, Italy. It features five semicircular arches with an average span length of ca. 8 m. Construction work started during Augustus' reign and was finished under his successor Tiberius in 20 AD. The bridge is still open to pedestrian and vehicular traffic, with the exception of heavy goods vehicles. Located at the northern end of the main street, Corso d'Augusto, Ponte di Tiberio connects Roman Rimini with the suburbs of San Giuliano. It was built with all Istrian limestone and stretches 70 meters long with five arches. The Doric style bridge was originally built to cross the Marecchia River, but the river was later diverted, shortly before the Second World War. The water seen today is just the "marina" of Rimini. The bridge is quite important given it became a major connector. From it came two consular roads, the Via Emilia and the Via Popilia, which are still in use today.

**Fig. 3.5** Bridge of Tiberio, (20 AD), Rimini.  $L_{tot} = 70$ m\_senicircular Istrian stone arch bridge

Even if the grandeur and prestige of ancient Roman bridges have never been overcome, The Romanesque and Gothic, architectural styles which predominated Medieval Age, saw the construction of noteworthy bridges, still in use. Compared with the previous ones, these more streamlined structures are characterized basically by vaults.







Considering piers width – to- span ratio, during Medieval Age, it reached the average value of  $1/5$  (025%), against the mean Roman one of  $1/2$  (=50%), until the extreme case of *Puente del Diablo* (Fig. 3.6.a) in Martorell with a ratio value of  $1/6.5$  (=15%). Replacing an original Roman bridge, it was rebuilt in the Gothic period (1283 – 1295). It comprises two unequal arches, a pointed vault with two arches on either side: the highest arch has an opening 44.20m high and is quite thin, but the little chapel-shaped building at the top is actually keeping it stable.

Romanesque and Gothic styles saw a substantial decrease of arch voussoirs depth: if Roman bridges had a slenderness ratio in the range  $1/8$  –  $1/18$  (mean value  $1/12.5$ ), Medieval bridge reduced this ratio to  $1/15$ , until extreme Gothic example with a slenderness ratio of  $1/30$ . For instance, the main arch of *San Martin Bridge* (Fig. 3.6b), spanning 38.0m, has a slenderness ratio on  $1/35$ , i.e. the arch depth is only 1.08m at the keystone. Far from Roman bridges perfection, Medieval ones show off an empirical perception of their static behaviour. About this, it's interesting to consider the structural detail usually adopted at the springing section: a quite number of semicircular Gothic arch are made with horizontal curved edge stones to create arch shape; in this way the arch springers are formed, standing upon them the real arch made of radial voussoirs. The classical form adopted for Gothic bridges was the pointed arch, even if also semicircular shape or segmental arches with low rise-to-span ratio were used. As in the case of Avignon Bridge (1185, France), the circular arches of 14th century *Ponte Vecchio* (Fig. 3.7), across Arno in Florence, have a really low rise-to- span ratio. Designed by Neri di Fioravante e Taddeo Gaddi in 1335, its pier width-to-span ratio of only  $1/6.5$  (Heinrich 1983, Brown 1994).

**Fig. 3.6\_(a)** Devil's Bridge (1283), Martorell, Spain. Stone arch bridge.  $L(\text{main span})= 37.3\text{m}$ ;  $L(\text{side span})= 19.1\text{m}$  **(b)** San Martin Bridge (14th century). Toledo, Spain.  $L(\text{main span})= 40\text{m}$

**Fig. 3.7** Ponte Vecchio (1335-1345), Florence. Taddeo Gaddi, Neri di Fioravante. Segmental masonry arch bridge.  $L(\text{main span})= 30\text{m}$ ;  $L(\text{side span}) = 27\text{m}$ ; deck width= 32m

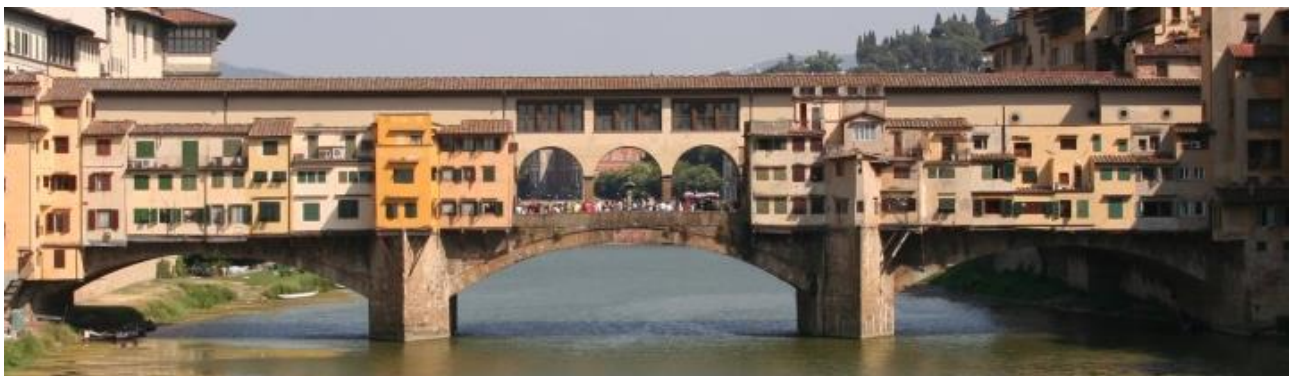






**Fig. 3.8** Scaliger Bridge (1354 - 1356), Verona, Guglielmo Bevilacqua. Vaulted stone arch bridge. L (main span)= 48.70m, deck width= 6m

This segmental arch bridge, with a main span of 30m rising 4.4m above water level, has a rise-to-span ratio of 1/7. The covered way which forms a top story above the shops is added in 1565 to enable the Medici to walk from the Uffizi to the Palazzo Pitti on the other side of the river without descending to street level. *Ponte Vecchio* is one of the most singular bridge ever built, a typical example of inhabited bridge. Another long span arch bridge was the *Scaliger Bridge* (Fig. 3.8) over Adige, in Verona: with a 48.7m main span and a total length of 120, it was destroyed during the Second World War, later rebuilt reproducing the original structure.

As in other form of art, Renaissance meant a return to classical models in bridge design: for instance, the slenderness ratio of the piers and arches were similar to those of Roman bridges; the rules of the Italian architect Leon Battista Alberti during 15th century set the following values: arch slenderness ratio ( $r/L$ ) 1/10; pier slenderness ratio between 1/4- 1/6 of the arch spans. The Renaissance frequently saw bridges with arches decreasing from the center to the end, giving more or less marked humpback profile. Related to the increase in haulage in all European countries, building bridge became necessary in order to allow carriage transit: basket or segmental arches were used, in order to reduce bridge deck sloping, without obstructing passing boats. During the 14th and 15th centuries, the basket arch and circular arch segments were widely used.

**Fig. 3.9** Ponte Santa Trinità (1566-69), Florence\_ Bartolomeo di Antonio Ammannati. Elliptical masonry arch bridge. L (main span)= 32m;





For example, in Italy during that time, many famous bridges were constructed, such as the just mentioned *Ponte Vecchio* in Florence. Only 200 years later, Ammannati designed another famous bridge in Florence, *Ponte di Santa Trinità* (Fig. 3.9): built in 1570, it consists of three basket-handled arches, with spans of 29.3m for the central one, and 26.2m for the others; it's made up of three span with a medium rise-to-span ratio of about 1/7 (as it has been adopted in many Venetian segmental arches).

Another contemporary structure was the *Pont Neuf* (Fig. 3.10) in Paris (1578-1604): with a length of 353m and a width of 23.6m, it's the oldest standing bridge across the river Seine, consisting of 12 three-centered as well as elliptical arches, which span from 14m to 17.55m, with a deck width of 22m. The bridge is composed of two separate spans, one of five arches joining the left bank to the Île de la Cité, another of seven joining the island to the right bank. The bridge had heavy traffic from the beginning. It has undergone much repair and renovation work, including rebuilding of seven spans in the long arm and lowering of the roadway by changing the arches from an almost semi-circular to elliptical form (1848–1855), lowering of sidewalks and faces of the piers, spandrels, cornices and replacing crumbled corbels as closely to the originals as possible.

**Fig. 3.10** Pont- Neuf (1578- 1607), Paris \_ Jacques Ier Androüet du Cerceau Vaulted masonry arch bridge. Ltot= 232m; n of spans=5; span length= 9 – 16.40m; deck width= 22m

**Fig. 3.11** Pulteney Bridge (1769- 1774), Bath\_ Robert Adam. Masonry arch bridge. Ltot= 45m; L (main span)=28m; deck width= 18m



In 1885, one of the piers of the short arm was undermined, removing the two adjacent arches, requiring them to be rebuilt and all the foundations strengthened. The major restoration of the Pont Neuf was begun in 1994 and was completed in 2007, the year of its 400th anniversary. Other contemporary structures to be mentioned are: *Pont Marie*, in Paris (1635), with a width of 23.6m, it consists of five nearly semicircular arches of cut stones, with a maximum 17.6m span and “humpback” profile; Pont Royal, in Paris ((1689), with five basket-handle arches, with decreasing spans of 23.50m in the center down to 20.60m at the end, with a width of 17m. All these bridges reveal as the main characteristic of Renaissance engineering was the improvement of the substructures or foundations, consisting, especially in increasing the use of wood piling and timber grillages, or platforms.

As *Rialto Bridge* (1591), one of only four bridges in the world to have shops across its full span on both sides, is the *Pulteney Bridge* (Fig. 3.11): crossing the River Avon in Bath (England), it was designed by Robert Adam in a Palladian style. It was completed by 1774. Initial plans for the bridge were drawn up by Thomas Paty, who estimated it would cost £4,569 to build, but that did not include the shops. In 1770 the brothers Robert and James Adam, adapted Paty's original design. Robert Adam envisaged an elegant structure lined with shops, similar to the Ponte Vecchio and the Ponte di Rialto he would likely have seen when he visited Florence and Venice. The revised bridge was 15m wide, rather than the 9.1m width envisaged by Paty, which overcame the objections of the local council about the bridge being too narrow. Construction started in 1770 and was completed by 1774 at a cost of £11,000 (more than twice the expected cost). Pulteney Bridge stood for less than 20 years in the form Adam created. In 1792 alterations were made during which the bridge was widened to 18m and the shops enlarged, converting the original sixteen shops into six larger ones. Thomas Telford suggested replacing the bridge with a single span cast iron bridge. However it was rebuilt by John Pinch senior, surveyor to the Pulteney estate, in a less ambitious version of Adam's design. Nowadays the bridge is 45m long and 18m wide: although there have been plans to make pedestrian the bridge, it is still used by buses and taxis.

A remarkable Italian example is the just mentioned *Ponte di Rialto* (Fig. 3.12) (1588-91). Without making any references to various vicissitudes that accompanied bridge design and construction (from 1264 to 1591), it's interesting to consider its final solution, by Antonio Da Ponte: bridge loads estimation and the evaluation of Rialto Bridge static behaviour could help to well define masonry arch bridge. The structural solution adopted (designed by Antonio da Ponte, 1588 – 1591) was similar to the previous wooden one (as it could be seen in Perspective “Bird's eye view, Jacopo de'Barbari, 1500). The span of the bridge is 28.83m; the rise is 7.5m, with a rise-to-span ratio of 1/4; keystone thickness of 1.25m, with a slenderness ratio of 1/23.





This single-span bridge has a width of 22.10m: when it was built, Ponte di Rialto was to be the largest bridge in Venice. Two inclined ramps, occupied by workshops, carry up from the abutments to the keystone section. With a total length of 48m, the bridge is partially covered by arcades. Two inclined ramps, occupied by workshops, carry up from the abutments to the keystone section. With a total length of 48m, the bridge is partially covered by arcades. The main structural problem was related to foundation system: in accordance with the accounting records, drawn up during Rialto Bridge construction (ASV, Provveditori sopra la fabbrica di Rialto, 1588), also argued by Sansovino (in “Venetia città nobilissima et singolare”, 1521) about 6000 elm and alder piles were used for each pier. These, also known as “batudi”, were made on three steps, using 3.5 m long cylindric piles; in addition, in order to create a closed foundation block, about 2000 squared piles, 5m long, were pounded at each side. The system extended 300 square meters at Rialto side, 400 square meters at S.Bartolomio one; for the earliest one a greater number piles seemed to be used: 6050 against 5600 corresponded to a mean number of 20 piles/ square meter at Rialto side against 14 piles/ square meter at S. Bartolomio one.

On April 1588, along Rialto side, works for mud removing started: new piles were put, in order to extract foundation structures of the old wooden bridge. During construction, three bulkhead (Veneatian “palade”) were built, in order to avoid people interfering with bridge building site: put on the river banks, they were made of about a thousand of larch piles, 10-12m long, coming 1 meter up from the water level. Arch abutments stood on huge areas, 30.6mx10.2m on Rialto side, 37.4mx11.9m on San Bortolomio one (Fig. 3.13). The construction of masonry foundations started on 9th July, 1588, using Istrian stones. Each pylon was made up of 5000 blocks, with a length of 1.40m, a width of 0.70m, and a variable height from 0.50m to 0.70m.

**Fig. 3.12** Rialto Bridge, Antonio Da Ponte (1591).  $L=28.83\text{m}$ , rise=7.5 ( $r/L=1/4$ ),  $h(\text{keystone})=1.25\text{m}$  ( $h/L=1/23$ )

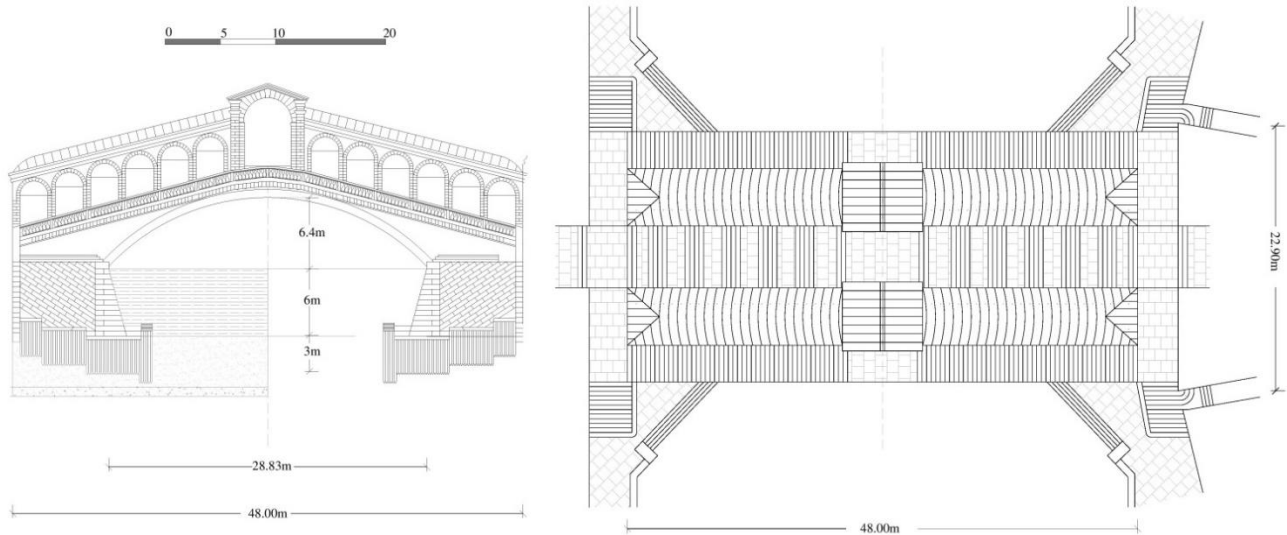


**Fig. 3.13** Ponte di Rialto-1588, Antonio da Ponte – bridge section: detail of foundation system; plan (deck width: 22.90m)

Each block, having a chain of 1.40m – 1.70m, was put along sloping parallel planes, not converging on the geometrical center of the arch, in order to counteract the arch thrust. It's interesting to note that Rialto Bridge needed a particular supporting structure: as it was argued by Rondelet in his treatise on Rialto Bridge [*Traité historique sur le Pont de Rialto*, 1841], its complex wooden arch centering required a great amount of larch: according to the profile designed by Antonio da Ponte, it was built in the convent of the Friars of S. Francesco della Vigna from March to April 1589, before being carried at the site. Miozzi defined it as “circumscribing segments” arch centering (“a segmenti circoscritti”), also known as Perronet’s one: it consisted in a series of wooden struts, put in correspondence with the vertices of a polygon, enclosed in the intrados curve. The Rialto Bridge is a pedestrian structure and has been constructed above the level of the approach spans. The size of the abutments is disproportionately large but to a certain extent necessary, due to the poor ground conditions.

For the first pier a stepped foundation was used; three “tooth” with growing width (2.00m, 4.00m, 5.00m) were made, making no interferences with the foundations of the adjacent historical buildings. For each step, drilling level changed: the largest portion, near the river, reached depth of 26 foot (about 9m), reducing it of about 0.80m, passing from the lowest to the next steps. The deck is inclined at an angle of approximately  $15^\circ$ , and pedestrians are unable to see over the crest. (Fig. 3.14) The stone bricks are relatively smooth to reflect the light and draw attention to the primary structure, whilst the timber is much rougher, as the shops are meant to be a secondary feature.



In terms of the superstructure, the stones forming the arches can be clearly distinguished, expressing the structural system. The spandrel walls on the other hand, are extremely smooth, to the point where the joints are barely visible. This is to reflect the light, making the bridge appear less top-heavy. Analysis concerning Rialto Bridge, described in the appendix B, shows robustness of masonry arch bridges, all designed to carry above all permanent loads, being live ones a little percentage of total vertical loads. It could be said that structural behaviour of masonry arch bridges has had no change through centuries: for this typology dead loads prevailed over live ones, almost until the birth of railroad. In 18th century, increasing live loads due to rail traffic, led designer to consider other aspects in bridge design, as non-negligible dynamic effects or vibrations, as well as valuing the possibility to use new material or different static schemes.

**Fig. 3.14** Rialto Bridge, Antonio Da Ponte (1591).  $L=28.83\text{m}$ ,  $\text{rise}=7.5$  ( $r/L=1/4$ ),  $h(\text{keystone})=1.25\text{m}$  ( $h/L=1/23$ )

### 3.3 18th century revolution: steel deck arch bridges

Built at the end of eighteenth century, first metal arches were designed with no clear idea about resistant behaviour and about how to solve the link between upper deck and arch. The size of cast iron elements in the early arches was really impressive. Producing iron in large amounts, reducing its costs making it suitable as building material, was one of the greatest technical advantages due to Industrial Revolution. It started from Great Britain, where there was a far higher iron-producing capacity than in other countries. Thanks to the use of iron, a radical transformation in building occurred. Its potentialities were much greater than those of the materials known up until then: nowadays, almost 200 years later, it is still the material for large works, especially for bridges.

The first cast iron bridge, the river Severn in Great Britain, was ultimate in 1779. It marked the beginning of a new era for bridge design, giving rise to their development in 19th century. An innovation as the use of iron in construction called for the cooperation of different professionals. The design was by the architect Thomas Farnolls Pritchard; the bridge was partially made by Abraham Derby III's foundry, one of the prestigious in UK, located in *Coalbrookdale*, next to bridge.





**Fig. 3.15** Coalbrookdale Bridge (1775-79), England  
 $L_{tot}=60\text{m}$ ;  $L_{main}$  span= 30.5m. Weight of iron= 378.5tons

Erection works were managed by Ohn Wilkinson. *Coalbrookdale Bridge*, (Fig. 3.15) also known as *Iron Bridge*, is a 30m-span semicircular arch, based on stone bridge. Emulating stone bridges, there was no clear idea in the design of how to lighten the spandrel and this is why segments of a circle were superimposed on the main arch and end at the deck while acting as a support for it. Joints between parts are similar to those used for timber bridges. Despite this lack of clarity for organizing the structure, it is one of the best well known bridge in the world; preserved in a magnificent condition, the UNESCO declared it as part of the Heritage of Mankind in 1986. Simultaneously, two new metal bridges were built in 1796: it was built upon river Sever, designed by Telford, as a 40m span two-hinged arch with low rise-to-span ratio; Sunderland bridge by Wilson, with a 72m span.

In 1802 Telford built *Bonar Bridge* (Fig. 3.16) in Scotland, 45.5m span with a much more correct conception of its structure than previous ones. It was a fundamental step forward in the organization of metal arch bridge structural organization.

The arch was clearly defined by two main bars joined by St. Andrew crosses and vertical members, giving it rigidity to bending which first arches didn't have. The arch-to-deck joint was achieved through an open lattice of much less body than the arch's. Original Bonar bridge no longer remained as it was destroyed by a storm before 1900 (then rebuilt), but several of other bridges designed by Telford are similar to this one.

**Fig. 3.16** Bonar Bridge (1802), Telford. Scotland.  $L_{tot}= 45\text{m}$ , rise=6.2.  $r/L= 1/7.3$





Built in 1815, the 45m-span *Craigelachie Bridge* over river Spey is still in service after being repaired in 1963 when S.Andrew crosses were replaced by rolled metal sections.

Robert Stephenson built *Newcastle (High Level) Bridge* in 1849, one of the largest at the time. It's the first example of bowstring arches, 38m-spanning. It's a two-deck rail and road bridge that crosses the River Tyne north-south. The trains run on the upper level and road vehicles on the lower. The Grade I listed bridge forms one part of a spectacular 1.6km long viaduct system that runs through Newcastle. It remains in daily use after a comprehensive refit.

The bridge is 408m long — 156m of it over water — 12.2m wide and contains some 5,100 tonnes of iron. It has six 38m river spans, supported on masonry piers up to 40m high and 14m by 4.9m in section. The river spans are flanked by four 11m land spans on either side, making 14 spans in total. Each river span consists of four parallel cast iron arch ribs that spring from road level. Horizontal wrought iron bars, visible under the bridge, tie the ends of the arches together. Each rib was cast in five sections. Horizontal and vertical bracing frames provide additional rib stiffness, with diagonal bracing between the spandrels of inner and outer ribs. Longitudinal girders connect the tops of the spandrel pillars and transverse girders cross the ribs, giving a rigid structure. The road deck is hung from the rail deck on wrought iron tension rods enclosed in cast iron box sections, and is 25.9m above high water. Both decks are timber. On the lower deck, a single carriageway road runs between the inner pair of arches, 6.1m apart, with 2m wide pedestrian walkways in the gap between inner and outer arches on each side. It was introduced. Built by James Buchanan Eads, it was completed in 1874, after 7 years work. The bridge consists of three arches of 152m, 157m, 152m, formed by tubular bars joined by Warren truss; it was one of the first bridge where steel was used. A bridge upon the *Mississippi river, at S.Louis* (Fig. 3.18) was something which had not been undertaken until then; it posed some serious problems.

**Fig. 3.17** Newcastle High Level bridge (1846-49), Stephenson, England. Ltot=408m; Clearance=25.92m; Span lengths=6x38.1m



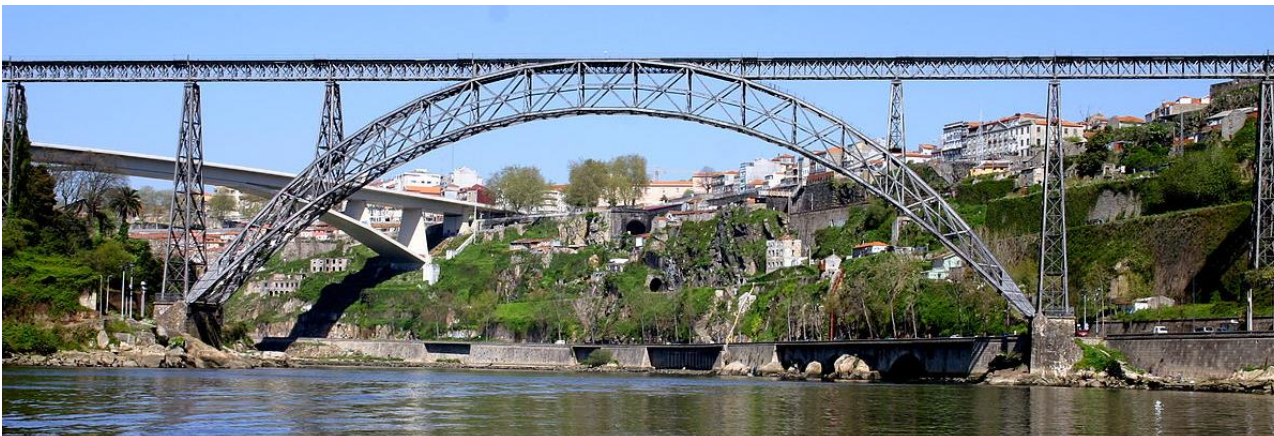


**Fig. 3.18** Saint Louis Bridge (1867-74).  
Bouscaren, Missouri  
(USA) Ltot= 1964m;  
Lmain span= 158.5m;  
Clearance= 16.8m.  
Total weight= 3510m

The first were the foundations because it was necessary to bore down to 42 at East abutment. Compressed air bellies were used, a system used for making deep foundations in the presence of water. The air pressure depends on the underwater depth: it caused the death of several workmen because no one had any idea of the effect of the pressure of over 4 atm (needed in this bridge bell) in human bodies. The second problem regards arch construction. The water and deep foundations made it impossible to erect centering with intermediate supports. Eads invented a new building system, the cantilever method: the half-arches were built with this system in *S. Louis Bridge*, advancing symmetrically from the piers. As arch cross section did not have sufficient capacity to bear its own weight in a cantilever, the problem was solved using provisional stays, attached at wooden towers located upon piers and abutments.

Three years later *S. Louis Bridge* was completed, with a total cost of \$ 10mil (nowadays corresponding to \$ 210\$), Gustave Eiffel built *Maria Pia Bridge* (Fig. 3.19) over river Duoro in Oporto for the Portuguese Railway Company, drawing up the design in cooperation with Theophile Seyrig. It's a very high rise-to span ratio arch, 160m-spanning, a two-hinged arch with a very marked rib depth variation, maximum at the crown and minimum at the springing sections. Becoming the new span length record holder, central the arch was built by advancing the half-arch in the stayed cantilever method. Gustave Eiffel's design proposal, priced at 965,000 French francs, was the least expensive of the four designs considered, around two thirds of the cost of the nearest competitor.

**Fig. 3.19** Maria Pia Bridge (1876-77).  
Eiffel, Porto (Portugal).  
Ltot= 563m; Larch= 160m;  
Clearness= 61.20m



Since the company was relatively inexperienced, a commission was appointed to report on their suitability to undertake the work. Their report was favourable, although it did emphasise the difficulty of the project. Maria Pia bridge is Eiffel's early attempt to separate arch from longitudinal girder, connecting them only to isolated piers, transferring loads acting above the deck firstly to the arch, then at the ground. This is the reason by which he designed a stiffened- two hinged truss arch; its truss piers and deck make unnecessary spandrel, typically used in early metal bridges.

Unlike the bridge at Duoro, the *Garabit Arch* (Fig. 3.20) is separated visually from the thin horizontal girder. Both arches were designed with hinges at their supports so that the crescent shape widens from points at the supports to a deep but light truss at the crown. The hinged design served to facilitate construction and also to produce the powerful visual image intended by Eiffel.

*Garabit Viaduct* span the gorge cut by the river Truy re, 12 km South of the small town of Saint-Flour (France). With its total length of 564.65m, Garabit Viaduct held record for arch bridge for 92 years. This crescent-shaped trussed arch has the following dimensions: central span 165m; rise: 57m; depth of the arch-cross section at the crown: 10m; width of the arch cross section at the crown: 6.28m; width of the arch at springing sections: 20m. The whole construction cost 3.10 mil Francs.

As the trussed arch designed as pinned at the springing (acts like cylindrical bearing with its axis in transverse direction), the structural effective depth of the cross section at this point is zero. In longitudinal direction the system is an elastic two hinged arch with one degree of static indeterminacy. Trussed arch has to withstand bending and axial forces. Garabit Viaduct is based on Maria Pia Bridge design, described before.

**Fig. 3.20** Garabit Viaduct, Loubresse (France) (1881-84)  
 $L_{tot} = 565\text{m}$ ;  $L_{arch} = 165\text{m}$ ; rise = 57m  
 $(r/L = 1/2.8)$ , height = 122 m; Weight = 3249t





The arch axis follows a quadratic parabola; distribution of mass in trussed arch is adapted to suit local loading conditions; trussed girder of the superstructure is separated from trussed arch. Both Eiffel bridges are characterized by a particular solution at the abutments: arch cross section becomes thinner to introduce a pinned connection, while depth increases. This choice is due to the necessity of heaving restraints in longitudinal plane, in order to reduce effective length, minimizing out of plane buckling effects.

Formally similar to Eiffel's masterpieces, different for restraint condition adopted, is the Italian example of *San Michele* (or *Paderno d'Adda*) Bridge, (Fig. 3.21) designed by R  thlisberger in 1887. Towards the end of the 19th century, rapidly growing industrial activities in Lombardia required the further expansion of the existing railway network. In particular, it became necessary to acquire the elevated crossing on the river Adda, North-East from Milano. In 1889, the SNOS completed the construction of the Paderno d'Adda Bridge. It is one of the very first great iron constructions designed through the practical application of the so-called "Theory of the ellipse of elasticity", a graphical-analytical method of structural analysis that was developed by Karl Culmann (1821-1881) and his pupil Wilhelm Ritter (1847-1906) at the Polytechnical School of Z  rich.

The iron bridge crosses the river Adda to a height of approximately 85 m from water. The main upper continuous beam, 5 m wide, is formed by a 266 m long metallic box girder, supported by nine bearings. The girder hosts the railway track in the inner deck, while the road is located on the upper deck. Despite of Eiffel's solution, Italian bridge makes use of a stiffer truss girder, adopting fixed restraint for the arch: in this way buckling effective length is further reduced, if it's compared to pinned French solution.

**Fig. 3.21** San Michele Bridge. Paderno d'Adda (Italy). R  thlisberger (1887-89).  $L_{tot} = 226\text{m}$ ;  $L_{arch} = 150\text{m}$ ; height = 85m

Even if the early 50's saw the spreading of bowstring arch bridge, it's interesting look at one of the most impressive works in the history of engineering built in period, the Viaur Railway Bridge, designed by Bodin in 1895 (Fig. 3.22)





It's a three hinged arch, even if the overall structure works halfway between an arch and a cantilever bridge, as it is formed by two double, almost symmetrical triangulated cantilevers starting from the hinged supports. There are, thus, no stress due to temperature changes over the whole unit and the almost perfect balance of the two double cantilevers practically cancels out the arch effect for own weight. For this reason this type of structure has been called balanced arch. This viaduct was built by free cantilever method with no staying and using the deep depth the overall arch-deck unit generates, joined by triangulations.

**Fig. 3.22(a)** Viaduct (1895-1902)France. Bodin. Ltot= 410m; Larch= 220m; rise= 53.73m ( $r/L=1/4$ ) height above ground= 116m

Another exemplary bridge, that cannot be neglected is Alexandre III Bridge (fig. 3.22b) by Amédée Alby and Jean Résal (Paris, 1896-1900). The structure is a three hinged single steel arch with a main span of 107.5m and total length of 160m. The 40m wide deck supports a road system and the abutments are formed of two masonry viaducts, through which run additional roadway. A key requirement of the design was that it did not obstruct the view along the Invalides and Champs Elysees, the result of this being a very low bridge, only 6m in height, supported by a very shallow arch with a span to depth ratio of 1/17. The arch is constructed of 15 parallel ribs, each with 3 articulation points made up of cast steel voussoirs bolted together. The ribs are braced and connected using a series of steel struts. The design encompasses a large amount of supplementary ornamentation along the deck and at the abutments. The bridge provides a highly symbolic representation of the political situation at the time.

**Fig. 3.22(b)** Alexandre III Bridge by Amédée Alby and Jean Résal (Paris, 1896-1900)Ltot= 160m; Larch= 107.5m; rise= 6m ( $r/L=1/17$ )





Till the end of 18<sup>th</sup> century deck metal arches, both cast iron, and wrought iron or steel ones, have shown a progressive technical improvement, passing from the earliest examples which emulated masonry bridges to the last ones in which an attempt to optimize structural elements was done. However, record spans, built adopting innovative system (as the cantilever one), needed of massive truss structures to carry loads, above all railway ones. Deck type makes the arch to withstand both bending and axial forces, in particular in the case of slender longitudinal girders. A great step forward was done in the last century, when the introduction of bowstring arch bridges revealed an attempt to separate beam flexional regime to arch extensional one, optimizing flow of forces distribution, consequently reducing structural elements size.

### **3.4 The spreading of bowstring arch bridges and the innovative solution of strutted arch by Arenas**

Looking at the previous historical excursus, it could be said that deck arch bridge solution has given the possibility to cover no more than 150m, till the truss arch bridge proposed by Boldin, spanning 220m. The passage from earliest masonry arch bridges to metal deck arch type has been characterized by a progressive separation between arch-extensional regime and girder flexural response, well reaching the perfect combination between these two load bearing structural elements in the “hybrid arch system”, proposed by Eiffel: working in tandem, the upper steel truss beams are supported on pylons, with only the central portion carried by the arch. Bowstring arch bridge solution has become necessary when longer span were required; at the same time, modern construction material and techniques have allowed arch bridge to become increasingly slender: thickening suspension system, the resultant interaction between girder and upper deck has given the possibility contain girder and arch stress state, reducing structural element size.

Bridges have always been considered as works of art in the Structural Engineering domain. Amongst them, bridges with “upper arch” highlight for their first-class aesthetics. Numerous tied-arch bridges have been designed and built over the last 50 years, many of the bowstring type. The term “bowstring” is the outcome of the actual behaviour for this kind of balanced structures. The upper arch “bow”, always strongly compressed, is internally balanced by the tensioned deck, which works as a “string”. From this conjugation bowstring arch bridge results. Vertical or inclined ties (or hangers) connected to the arch support deck from above. The arch and the deck are, thus, locked into each other and the deck acts as a stay for the arch, resisting horizontal forces (thrust) through tension. Considering this scheme, the loads a bowstring arch transmits to its piers are similar to those of a simply supported beam of the same span.. Their spreading is linked to the great innovations introduced by the Industrial Revolution. Tracing bowstring arch bridges evolution, as follows, could be a good way to understand how a clear distinction between arch extensional regime and girder flexural one occurred.



Up until the end of 19<sup>th</sup> century, the only example of bowstring arch bridge was the abovementioned *High Level Newcastle Bridge* (Fig. 3.23) (Tab. 3.1) by Stephenson. A contemporary example was the two-hinged arch, 298m span, *Hell's Gate* railway bridge over the East River in New York (1912-16), being the largest in the world for many years. It was designed by Gustav Lindenthal, while Othmar Amman and Steinman participated as assistants. The steel arch which will span the waters of Hell's Gate will have a span between abutments of 298m, with a clearance below the deck of 41.10m.

<b>L (arch) [m]</b>	298	<b>ip [m]</b>	12
<b>arch rise (r) -to L</b>	1/3.2	<b>ip/L</b>	6.25%
<b>h (girder) [m]</b>	4.40	<b>hg/L</b>	1.5%
<b>h (arch) [m]</b>	12.20	<b>ha/L</b>	4.1%

The depth of the truss at the ends will be 42.7m; at the center, 12.20m ( $h_{\text{arch}}/L = 1/24$ ); and at the quarters 20.1mt. The reverse curve of the upper member of the arch at either end is explained by the necessity of raising the top member of the portal to a sufficient height above the tracks to allow head room for the trains. The floor system is built on the customary method of heavy cross girders and longitudinal stringers. The floor beams are 4.4m ( $h_{\text{girder}}/L = 1/67$ ) in depth by 7.20m in length. This is a deep rib depth, triangulated arch with an intermediate deck finished off by two stone abutments that frame the bridge well. The abutments of the arch are monumental stone and concrete towers, which serve to divide the arch bridge proper from the steel viaduct which forms the approaches to it. These ones have no resistant mission because the hinges are at the springing of the chord forming the arch intrados. Thanks to their weight, they only serve to reduce inclination to the resultant of the arch over the foundations.

High value of arch slenderness is linked to the choice of rigid truss arch, unusual for modern bowstring arch bridge, revealing how this bridge belongs to a period of transition, during which ancient structural forms are mixed to modern static schemes. *Hell's Gate Bridge* was built by advancing the half-arches with the cantilever method from the springing until closing at the crown.

**Fig. 3.23** Hell's Gate Bridge (1912-16). Lindenthal, Steinman, Ammann. New York.  $L_{\text{tot}} = 5200\text{m}$ ;  $L_{\text{arch}} = 298\text{m}$ ,  $\text{rise} = 93\text{m}$  ( $r/L = 1/3.2$ ).  $h_{\text{arch}}/L = 1/24$ .  $h_{\text{girder}}/L = 1/67$

**Tab 3.1** Hell's Gate Bridge (1912-16). Design parameters



**Fig. 3.24** Bayonne Bridge (1928-31). Moisseiff. New York.  $L_{tot}= 1762\text{m}$ ;  $L_{arch}= 510\text{m}$ ,  $rise=98.53\text{m}$  ( $r/L= 1/5$ ).  $h_{arch}/L=1/25$   $h_{girder}/L=1/102$

Being a two-hinged arch bridge, its intrados chords were provisionally anchored in order to advance by cantilevers, such that it was temporarily fixed into springing sections; a provisional stay was also added into the first stretch of each half-arch. The large stone abutments used in *Hell's Gate Bridge* as well as in other large bowstring arch bridges are actually frame elements to finish off the arch. This is obvious from their absence in *Bayonne Bridge* (Fig. 3.24) (Tab. 3.2) over the Kill Van Kull in New York, a 504m span arch, whose abutments were never stone clad as was planned so the bridge is weak at its end, lacking abutments strengthening.

**Tab 3.2** Bayonne Bridge (1928-31) design parameters

<b>L (arch) [m]</b>	510	<b>ip [m]</b>	17
<b>arch rise (r) -to L</b>	1/5	<b>ip/L</b>	3.4%
<b>h (girder) [m]</b>	5	<b>hg/L</b>	1%
<b>h (arch) [m]</b>	20	<b>ha/L</b>	3.8%

The bridge was designed by Othmar Ammann in 1928. A two-hinged half-through bridge with the same structure of *Hell's Gate Bridge*, which is to say with hinges at the arch intrados chord ends, while the triangulation only serves for live loads. Bayonne Bridge differs in shape substantially from the contemporary examples; the arch varies little in rib depth, with no inflected curves at the end of the extrados.

Another interesting example of these earliest bowstring arch bridge is *Sydney Harbour Bridge*; becoming the iconic image of the city, it carries rail, vehicular, bicycle, and pedestrian traffic between the Sydney central business district and the North Shore. Under the direction of Dr John Bradfield of the NSW Department of Public Works, the bridge was built by British firm Dorman Long and Company, under design of Ralph Freeman. Bridge shape and construction method similar to *Hell's Gate* one. The half-arches were built by cantilever method, with no need of provisional stays, thanks to the arch triangulation rib depth. *Sydney Harbour Bridge* (Fig. 3.25) (Tab. 3.3) was finished in 1932, but its 503m span never became the longest in the world because Bayonne Bridge, finished few months before, has 1m more of span. At the crown section, *Sydney Harbour Bridge* (Fig. 3.25) (Tab. 3.3) has the same arch-slenderness of Bayonne.



This characterization underlines a vain attempt to optimize structure: in fact, for a pinned arch with suspended girder, bending moments at the springing sections are zero (considering restraint condition), so that, at the abutments, arch needs a cross section which guarantee it to carry only axial forces; a deep-constant arch cross section could be sufficient, instead of make larger the arch at the abutments. These early examples of bowstring arches were designed as the main rigid arch withstand all moments due to symmetrical and asymmetrical loads, while the slender deck carries only local effect, occurring between two adjacent hangers

<b>L (arch) [m]</b>	503	<b>ip [m]</b>	19
<b>arch rise (r) -to L</b>	1/9	<b>ip/L</b>	3.3%
<b>h (girder) [m]</b>	5	<b>hg/L</b>	1%
<b>h (arch) [m]</b>	20	<b>ha/L</b>	3.8%

**Fig. 3.25** Sydney Harbour Bridge (1923-32). Sir Ralph Freeman. Australia. Ltot= 1150m; Larch= 503m, rise=55m ( $r/L = 1/3.7$ ).  $h_{arch}/L = 1/25$   $h_{girder}/L = 1/100$

**Tab 3.3** Sydney Harbour Bridge (1923-32) design parameters

A step forward was given by the introduction Langer system into bowstring arch bridge design. In 1871, Joseph Langer proposed an inversion of roles between arch and girder: he assumed that the bending effects had to be carried by girder, a deck with high rigidity who acts as a tie for the flexible arches. Even if in the previous examples cable stress distribution is due to live loads acting upon the deck, according to Langer system, is the arch shape (funicular polygon) that governs suspenders stress. Larger girder give the possibility to greatly reduce arch cross section. One of the earliest example of deck-stiffen arch bridge, having slender upper arch, was the *Fremont Bridge* (Fig. 3.26) (Tab 3.4) in Portland (1973). The upper deck carries westbound and southbound traffic. The lower deck carries eastbound and northbound traffic. Because this is an interstate, there is no pedestrian or bicycle traffic allowed. The bridge has two decks carrying vehicular traffic, each with four lanes.

<b>L (arch) [m]</b>	503	<b>ip [m]</b>	19
<b>arch rise (r) -to L</b>	1/9	<b>ip/L</b>	3.3%
<b>h (girder) [m]</b>	5	<b>hg/L</b>	1%
<b>h (arch) [m]</b>	20	<b>ha/L</b>	3.8%

**Tab 3.4** Fremont Bridge (1973) design parameters





**Fig. 3.26** Fremont Bridge (1973) Portland. Parsons Brinckerhoff Quade & Douglas.  $L_{tot} = 656\text{m}$ ;  $L_{arch} = 382.5$ ,  $\text{rise} = 45.5\text{m}$  ( $r/L = 1/8$ ).  $h_{arch}/L = 1/109$   $h_{girder}/L = 1/32$

The centre span of the bridge, where the rib of the arch is above the deck, is 275m long. It was fabricated in California then assembled at Swan Island, 2.7 km downstream. Considering previous examples, Fremont Bridge slenderness ratios are completely inverted. The high deck stiffness is reflected into a girder depth to span ratio of 1/32 (3.1%) against a lower mean value of 1% previously defined for *Bayonne* (Fig. 3.24) (Tab. 3.2) or *Sidney Haurbour Bridges* (Fig. 3.25) (Tab. 3.3).

In the second quarter of 20th century, the Swedish engineer Octavius Nielsen created a system to give rigidity to the bowstring arch, which consisted in inclining the suspenders into two symmetrical direction, so that an improving arch-deck cooperation is created for concentrated or asymmetrical loads: in this way, the dimensions of these two elements are considerably reduced.

Alternate compression and tensile stresses appears in the Nielsen system at the end of suspenders, so they either have to be pre-stressed or not have them when compression stresses have theoretically appeared. In this system, the hangers are inclined and work as a variable-section truss with rigid bottom “flange” Innumerable Nielsen-type bridge have been built all over the world: the best known is the road and railway *Fehmarnsund Bridge* (Fig. 3.27) (Tab. 3.5) by Lohmer (Germany). Construction began in 1958 and the bridge was opened on April 30, 1963. The two steel arches, from which the central span is suspended by cables, are braced with steel cross-beams.

**Fig. 3.27** Fehmarnsund Bridge (1958-63). Lohmer (Germany).  $L_{tot} = 963\text{m}$ ;  $L_{arch} = 248$ ,  $\text{rise} = 45$  ( $r/L = 1/5$ ).  $h_{arch}/L = 1/82$   $h_{girder}/L = 1/100$





<b>L (arch) [m]</b>	248	<b>ip [m]</b>	11
<b>arch rise (r) -to L</b>	1/5	<b>ip/L</b>	4.4%
<b>h (girder) [m]</b>	2.5	<b>hg/L</b>	1%
<b>h (arch) [m]</b>	3	<b>ha/L</b>	1.20%

**Tab 3.5** Fehmansund Bridge (1958-63) design parameters

The arches are 248m in length and reach 45m above the main deck of the bridge. Its slender deck is made of a thin orthotropic deck, standing upon two longitudinal girders. It's a well known example of network arch bridge.

Up until 90s, despite great advantages resulting from using it, network arch was not so widespread. Thanks to increasing cable number, cable sizing could be reduced, becoming invisible from long distances; using box cross section for the arch, both arch and deck became really slender. Recent studies (*Per Tveit*, Norway) underline advantages due to this typology. They are best suited for spans between 80 m and 170 m, but will compete well in a wider range of spans. This results in attractive bridges that do not hide the landscape behind them. A network arch bridge is likely to remain the world's most slender arch bridge. The transverse bending in the slab is usually much greater than the longitudinal bending. Thus the main purpose of the edge beam is to accommodate the hanger forces and the longitudinal pre-stressing cables. The partial pre-stress reduces the cracks in the tie. This is part of the reason why the first network arches are still in good shape after over 50 years. Bridges with vertical hangers are less slim: they have 2 -8 times deeper chords; they use 2-4 times more steel; their welds are 15- 30 times longer.

Considering low deck slenderness ratio, as a result of structural optimization, a special case is the *Roosevelt Lake Bridge* (1990) (Fig. 3.28) (Tab. 3.6) by Howard, Needles, Tammen & Bergendoff. With a 329m span, this bridge is characterized by really low slenderness ratio, 1/160 for the arch, 1/150 for the deck. This extremely thin steel through arch bridge is the result of low live loads acting, having been design only for two traffic lanes, with a total deck width of 10m.

<b>L (arch) [m]</b>	248	<b>ip [m]</b>	11
<b>arch rise (r) -to L</b>	1/5	<b>ip/L</b>	4.4%
<b>h (girder) [m]</b>	2.5	<b>hg/L</b>	1%
<b>h (arch) [m]</b>	3	<b>ha/L</b>	1.20%

**Tab 3.6** Roosevelt Lake Bridge (1990) design parameters

**Fig. 3.28** Roosevelt Lake Bridge (1990) . Howard, Needles, Tammen & Bergendoff. Larch= 329, rise=65 (r/L= 1/5). harch/L =1/160 hgirder/L =1/150





**Fig. 3.29** Lupu Bridge (2003), Shanghai (China). Shanghai Municipal Engineering Design Institute.  
 $L_{\text{tot}}=3600\text{m}$ ;  $L_{\text{arch}}=550\text{m}$ ,  $\text{rise}=100\text{m}$  ( $r/L=1/5$ ).  $h_{\text{arch}}/L=1/40$ ;  $h_{\text{girder}}/L=1/80$

Following a completely opposite trend, many recent bridges, especially in the case of coupled-arch solutions, appear as unnecessary attempts to optimize structure in bowstring arch bridge evolution. A clear example is *Lupu Bridge* in Shanghai (2003) (Fig. 3.29) (Tab. 3.7). It is a three-span steel arch bridge including two side spans of 100 meters and the centre span of 550 meters. It has six lanes and two pedestrian walkways for sightseeing, and has the longest span of arch bridges in the world. Two inclined arch ribs are 100 meters high from the bottom to the crown.

**Tab 3.7** Lupu Bridge (2003) design parameters

<b>L (arch) [m]</b>	550	<b>ip [m]</b>	22
<b>arch rise (r) -to L</b>	1/5.5	<b>ip/L</b>	4%
<b>h (girder) [m]</b>	7.15	<b>hg/L</b>	1.30%
<b>h (arch) [m]</b>	13.5	<b>ha/L</b>	2.40%

The sections are comprised of a 13.5m length of each arch connected by a horizontal wind brace box sections, which create a strong system against lateral buckling opening on abutments, simulating a strutted arch. The arch ribs have as cross section a modified rectangular steel box with a width of five meters and a depth of six meters at the crown and of 9 meters at the base. The central span of the deck (340m) is suspended from two sets of 28 double cables attached to the two inclined arches. The arches were constructed using a cable-stayed cantilever method. Each section of the arch was stayed back to the temporary towers at either side of the arch after being welded to the previous section

A tangible trouble in optimizing arch-to girder transferring system is well perceptible in another recent infrastructure, *Chaotianmen Bridge* (2008) (Fig. 3.30) (Tab. 3.8) a Chongqing( China), which span 552m with a truss massive arch (a the earliest metal arch bridges).

**Tab 3.8** Chaotianmen Bridge (2008) design parameters

<b>L (arch) [m]</b>	552	<b>ip [m]</b>	13.8
<b>arch rise (r) -to L</b>	1/4.3	<b>ip/L</b>	3%
<b>h (girder) [m]</b>	14	<b>hg/L</b>	2.20%
<b>h (arch) [m]</b>	12	<b>ha/L</b>	2.70%



It's a 3-span  $190 + 552 + 190$  m continuous steel truss arch bridge. The full width of main bridge is 36,5 m and that of truss 29,0 m, with truss of variable depth in end span, the middle span is steel truss arch with tie girders. The height from arch top to middle supports is 142m, the lower chord is in quadratic parabola with rise of 128 m. The N-type truss is adopted for the main one with central depth of 14 m, the depths at middle support and at end support are 73,13 m (including the depth of stiffening chord being 40,45 m) and 11,83 m respectively. For upper deck system and both side lanes in lower deck, it is adopted the orthotropic steel plate of 16 mm thick with closed U-type ribs

Even in Europe, no steps towards bowstring arch bridge optimization have been done, as in the case of *Apollo Bridge* (Fig. 3.31) (Tab. 3.9).

<b>L (arch) [m]</b>	231	<b>ip [m]</b>	7
<b>arch rise (r) -to L</b>	1/6.4	<b>ip/L</b>	3%
<b>h (girder) [m]</b>	8	<b>hg/L</b>	3.50%
<b>h (arch) [m]</b>	5	<b>ha/L</b>	2.20%

**Fig. 3.30** Chaotianmen Bridge (2008), China,  $L_{\text{tot}}=1740$ ; Larch=552m, rise=128m ( $r/L=1/3.8$ ). harch/L=1/40; hgirder/L=1/45.

**Tab 3.9** Apollo Bridge, Bratislava (2003-2005) design parameters

**Fig. 3.31** Apollo Bridge, Bratislava (2003-2005) Slovakia. Dopravoprojekt a.s.  $L_{\text{tot}}=854$ m; Larch=231m, rise=36m ( $r/L=1/6.4$ ). harch/L=1/46; hgirder/L=1/30







<b>L (arch) [m]</b>	150	<b>ip [m]</b>	8.55
<b>arch rise (r) -to L</b>	1/7	<b>ip/L</b>	7.6%
<b>h (girder) [m]</b>	3	<b>hg/L</b>	1.60%
<b>h (arch) [m]</b>	2	<b>ha/L</b>	1.30%

This bridge, built in Bratislava (Slovakia), consists of two rhombus shaped main girders, which span the complete length of the bridge, with architecturally shaped cross girders and an orthotropic deck. The two box-shaped arches of the main bridge are inclined inwards. Bridge structure appears redundant: no advantages have been taken from the application of network cable system; on the contrary, the choice a rigid deck system doesn't consider the high contribution to torsional stiffness that cable system could give.

About Italian experiences, design of bowstring arch bridges is often characterized by the precautionary trend to oversize suspension structures, also in the case of small spans. For instance, *Ponte della Musica* (Roma, 2008), (Fig. 3.32) (Tab. 3.10). designed by Petrangeli & Associati, consists of a couple of parabolic arches, individually spanning 186.90m, made of rigid box cross section (arch depth to span ratio of 1/75). Concrete bridge deck is suspended by a stiffen system of steel tension arms, 8.50m spacing, corresponding to an equal distribution of deck cross sections; however, additional intermediate diaphragms, 2.75 – 3m spacing, are used, even more increasing deck stiffness (which is quite comparable to that of the arch).

*Vallecrosia Bridge* (2012) designed by StudioMalerba, consists of a couple of circular arches, individually spanning 26m. ), (Fig. 3.33) (Tab. 3.11).

**Tab 3.11** Vallecrosia Bridge (2012) design parameters

<b>L (arch) [m]</b>	26	<b>ip [m]</b>	2.5
<b>arch rise (r) -to L</b>	1/ 4.3	<b>ip/L</b>	10%
<b>h (girder) [m]</b>	0.50	<b>hg/L</b>	2%
<b>h (arch) [m]</b>	0.50	<b>ha/L</b>	1.80%



Arches are made of steel tubular elements, with variable cross section (arch depth to span ratio of  $1/43$ , quite similar to values used by Eiffel at the end of 19th century). Concrete bridge deck, made of predalles, is suspended by a rod- system, 6m spacing, having a cable-spacing –to –span ratio of 10%.

**Fig. 3.33** Vallecrosia Bridge (2011) Malerba  
Larch= 26m; rise=6m  
( $r/L=1/4.3$ ). harch/L  
= $1/52$ ; hgirder/L= $1/52$

A great contribution to bowstring arch bridge evolution was give by *strutted arch (or split bowstring arch bridge)* introduced by Arenas for *Barqueta Bridge* (Fig. 3.34) (Fig. 3.35) (Tab. 3.12). It was the result of a design competition for one of the bridges built for the 1992 Universal Exposition in Seville, Spain. It is a bowstring steel bridge over the Guadalquivir River with a total length of 198.8 m. The main arch spans 108 meters and it splits into two inclined struts on either end, forming two triangular end frames, covering a total length of 168m. This split arch form is one of the first of its kind, and is an innovative way of increasing the main span of the bridge without decreasing the buckling load of the arch. The triangular frames not only extend the lateral length of the arch bridge as they receive the axial force of the arch, but also allow for an increase in the width of the bridge because of the transverse bracing they provide.

**Fig. 3.34** Barqueta Bridge (Seville), 1992, Apia XXI (Arenas)  
Ltot=198.8m, Larch= 168m, ha/L=  $1/70$ ;  
hgirder/L=  $1/42$







**Fig. 3.35** Barqueta Bridge (Seville) (1992)  
(a) bridge deck\_ (b) inclined struts detail

Even though the bridge seems simple and elegant with minimal number of elements, the geometry of each element as well as the system for load transfer is rather complex. The dead load of the deck as well as the live loads are transferred from the deck via the cables to the main arch. Under the loads, the arch is in compression. The flow of forces in the arch is continued on either end by triangular frames. The two struts of each frame are in compression, and push outwards at the base of the triangle. Therefore, a horizontal tie is required to resist outward forces.

**Tab 3.12** Barqueta Bridge (Seville) (1992) design parameters

<b>L (arch) [m]</b>	168	<b>ip [m]</b>	6
<b>arch rise (r) -to L</b>	1/6	<b>ip/L</b>	6%
<b>h (girder) [m]</b>	4	<b>hg/L</b>	2.3%
<b>h (arch) [m]</b>	2.4	<b>ha/L</b>	1.4%

The deck is connected to the base of the frames, and acts as a tension tie that resists the horizontal forces from the arch. The structure then rests on four concrete piers. The deck has a hollow steel trapezoidal cross-section that is 21.4m wide and 2.4m thick (slenderness ratio  $h_a/L = 1/170$ ). The deck is very thin and the inclined planes of the trapezoidal section create an additional sense of lightness. Transverse stiffening frames made up of steel I-beams in the deck are spaced 4.25m apart along a central truss that runs along the length of the bridge.

### 3.5 Steel arch bridges evolution: parametric analysis

Tracing historical evolution of arch bridges has been an addictive experience to better understand arch bridge behaviour, recognising the way to get a structural as well as economical optimization in bridge design. Technological progress, added to the experimentation of new structural systems, led to innovative solutions, capable to satisfy all sort of requirements, as carrying heavier traffic loads. For many centuries masonry arch bridge appeared the dominant form: the use of steel as structural material has marked a great step foreword, since the end of 18th century.

Masonry arch bridges were designed foreseeing arch deformed shape, trying to balance acting loads at the keystone and at springing sections: their robustness made them capable to support above all permanent load, being live ones a little percentage of total vertical loads. It could be said that structural behaviour of masonry arch bridges has had no change through centuries: for this typology dead loads prevailed over live ones, almost until the birth of railroad.

Following the same principles, first examples of metal arch bridge were built: their redundant structures revealed early designers inability to use material properties in the best way. The attempt to create streamlined structures led to build slender bridges which showed no negligible buckling effects due to accidental loads: the use of spandrel arch solution guaranteed a reduction of relative displacements between arch and deck. A great innovation to arch bridge development was given by Eiffel: in designing long deck arch bridges, he was capable to split arch form girder contribution to carry loads. Unfortunately, his pioneer approach was not applied so easily. Replacing cast iron with steel, as a high-strength material, it has been possible to build bridge with growing spans, from 50m to 500m. A greater interaction between arch and deck was due to the introduction of bowstring arch bridge, even if the earliest examples were characterized by a remarkable difference between arch and girder sizing: rigid truss arches were used to carry almost completely loads, leaving deck to support local effects between cable spacing. Only in the second half of 90s, same attempts to improve arch-to deck transferring system have been done, guaranteed a reduction of bridge dead loads, as well as a high material performance.

A completely innovative approach has been introduced by Santiago Caltrava, who has achieved a great structural optimization for arch and girder, above all in designing footbridges, as it could be seen in the following chapter. His main aim has always been to reduce, almost eliminate, traditional longitudinal load bearing elements, making the structure most slender as possible. This is achieved through a closer discretization of deck structure, using an increasing number of cross section, consequently a reduced spacing between hangers. Bridge deck is fragmented in a huge number transverse load bearing elements, acting as “vertebrae of spine”; as in the emblematic case of Campo de Volantin Bridge, longitudinal girder employed only to carry arch thrust (adopting bowstring arch bridge).

The following table, concerning main design parameters (Tab. 3.13) places Calarava’s contribution in the evolution of steel arch bridge. His paradigmatic experience is clearly distinguishable especially in Ponte della Costituzione design: in this case artist proposes an hybrid solution, a segmental arch bridge which works in extensional regime, spanning 81m.

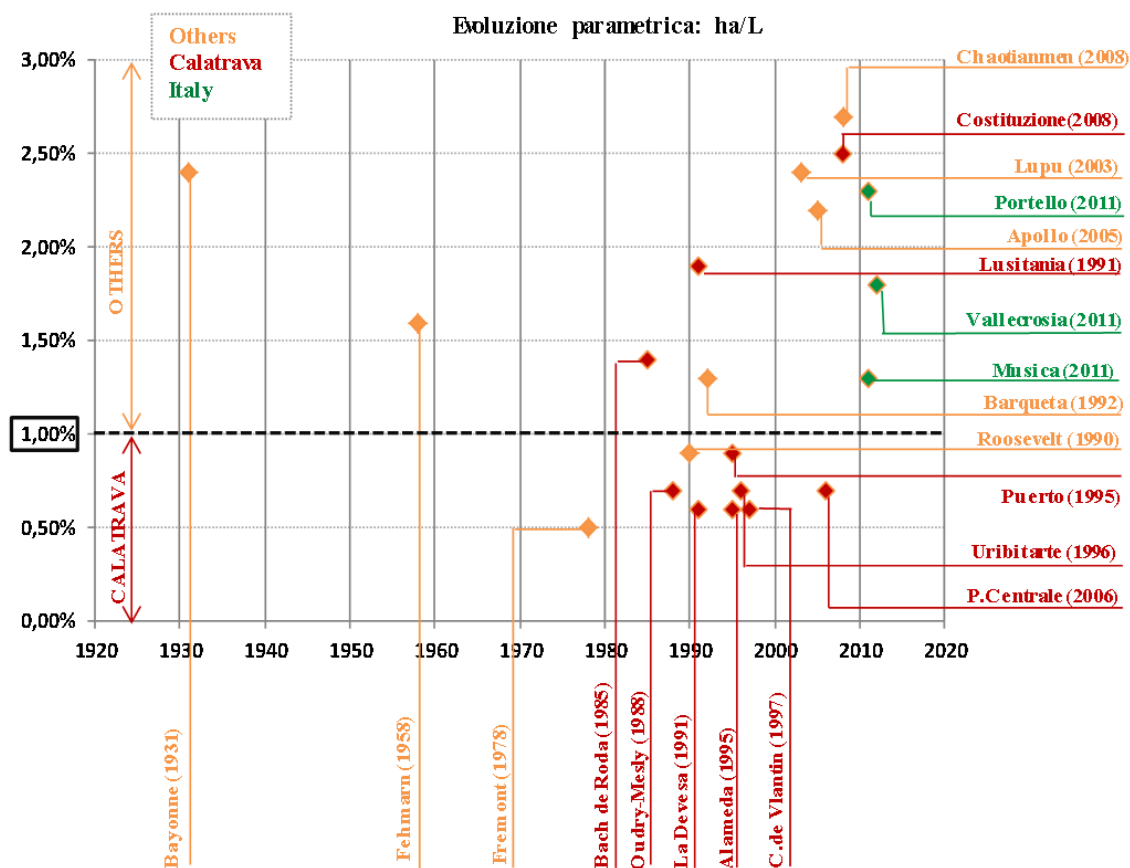
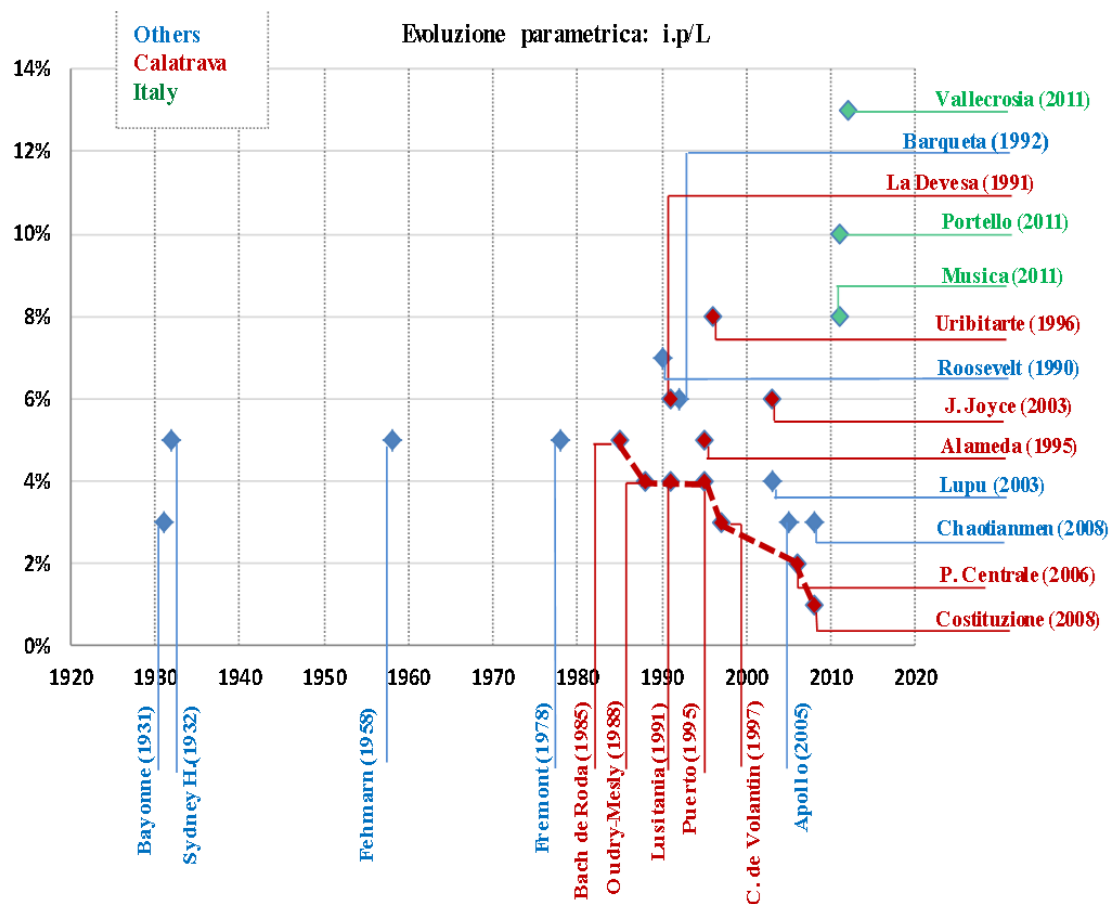


**Fig. 3.36** Ponte della Costituzione, Venice (IT), 2001 - 2007, S. Calatrava.  $L=80.80\text{m}$ ;  $r/L=1/14$ ;  $i_p/L=1.3\%$ ,  $h_a/L=2.5\%$ .

The pure arch of Ponte della Costituzione (Fig. 3.36) is characterized by a imperceptible deck, whose slenderness has been guaranteed by the choose of discretizing it in a great number on cross sections (21 sections,  $i_p/L=4.7\%$  - preliminary design; 32 sections,  $i_p/L=3.1\%$  - final design; 73 sections,  $i_p/L=1.3\%$  - executive design), reducing live loads effects above the deck.

**Tab 3.13** Bowstring arch bridge evolution: summary

		$i_p/l$	$h_a/l$	$h_l/l$	$h^*/l$
<b>1931</b>	Bayonne	3%	2,40%	0,60%	1,50%
<b>1932</b>	Sydney Harbour	5%	3.8%	0,80%	2.30%
<b>1958</b>	Fehmarn	5%	1,60%	1,00%	1,30%
<b>1978</b>	Fremont	5%	0,50%	3,90%	2,20%
<b>1985</b>	<b>Bach de Roda</b>	5%	1,40%	4,10%	2,70%
<b>1988</b>	<b>Oudry-Mesly</b>	4%	0,70%	2,20%	1,40%
<b>1990</b>	Roosevelt	7%	0,90%	1,80%	1,30%
<b>1991</b>	<b>Lusitania</b>	4%	1,90%	2,60%	2,30%
<b>1991</b>	<b>La Devesa</b>	6%6	1.40%	2.30%	1,85%
<b>1992</b>	Barqueta	%	1.00%	1.6%	1.3%
<b>1995</b>	<b>Puerto</b>	4%	0,90%	5,10%	3,00%
<b>1995</b>	<b>Alameda</b>	5%	0,60%	2,00%	1,30%
<b>1996</b>	<b>Uribitarte</b>	8%	0,70%	1,60%	1,10%
<b>1997</b>	<b>Campo de Volantin</b>	3%	0,60%	1,30%	1,00%
<b>2003</b>	Lupu	4%	2,40%	1,30%	1,90%
<b>2003</b>	<b>James Joyce</b>	6%	1.00%	3.25%	2.12%
<b>2005</b>	Apollo	3%	2,20%	3,50%	2,80%
<b>2006</b>	<b>Ponte Centrale</b>	2%	0,70%	1,20%	1,00%
<b>2008</b>	<b>Costituzione</b>	1,00%	2,50%	-	2,5%
<b>2008</b>	Chaotianmen	3%	2,70%	2,20%	3.70%
<b>2011</b>	Musica	8%	1,30%	1,60%	1.45%
<b>2011</b>	Portello	10%	2,30%	2,40%	2.35%
<b>2012</b>	Vallecrosia	13%	1,80%	2,00%	1.90%



### Appendix (B) Case study n.1: static behaviour of Ponte di Rialto (Venice)

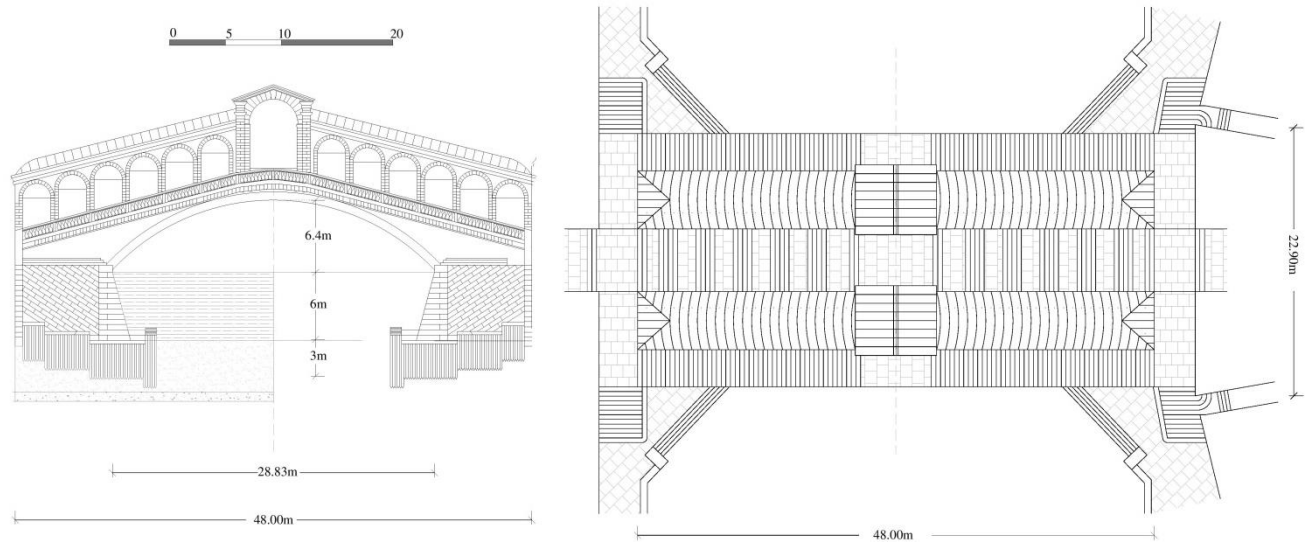
A remarkable Italian example is the just mentioned *Ponte di Rialto* (1588-91). Without making any references to various vicissitudes that accompanied bridge design and construction (from 1264 to 1591), it's interesting to consider its final solution, by Antonio Da Ponte: bridge loads estimation and the evaluation of Rialto Bridge static behaviour could help to well define masonry arch bridge.

The structural solution adopted (Fig. 3.12) (3.13) (designed by Antonio da Ponte, 1588 – 1591) was similar to the previous wooden one (as it could be seen in Perspective “Bird’s eye view, Jacopo de’Barbari, 1500). The span of the bridge is 28.83m; the rise is 7.5m, with a rise-to-span ratio of 1/4; keystone thickness of 1.25m, with a slenderness ratio of 1/23. This single-span bridge has a width of 22.10m: when it was built, Ponte di Rialto was to be the largest bridge in Venice. Two inclined ramps, occupied by workshops, carry up from the abutments to the keystone section. With a total length of 48m, the bridge is partially covered by arcades. Two inclined ramps, occupied by workshops, carry up from the abutments to the keystone section. With a total length of 48m, the bridge is partially covered by arcades. The main structural problem was related to foundation system: in accordance with the accounting records, drawn up during Rialto Bridge construction (ASV, Provveditori sopra la fabbrica di Rialto, 1588), also argued by Sansovino (in “*Venetia città nobilissima et singolare*”, 1521) about 6000 elm and alder piles were used for each pier. These, also known as “batudi”, were made on three steps, using 3.5 m long cylindric piles; in addition, in order to create a closed foundation block, about 2000 squared piles, 5m long, were pounded at each side. The system extended 300 square meters at Rialto side, 400 square meters at S.Bartolomio one; for the earliest one a greater number piles seemed to be used: 6050 against 5600 corresponded to a mean number of 20 piles/ square meter at Rialto side against 14 piles/ square meter at S. Bartolomio one.

**Fig. 3.12:** Rialto Bridge, Antonio Da Ponte (1591).  $L=28.83\text{m}$ ,  $\text{rise}=7.5$  ( $r/L= 1/4$ ),  $h(\text{keystone}) = 1.25\text{m}$  ( $h/L= 1/23$ )







On April 1588, along Rialto side, works for mud removing started: new piles were put, in order to extract foundation structures of the old wooden bridge. During construction, three bulkhead (Venetian “palade”) were built, in order to avoid people interfering with bridge building site: put on the river banks, they were made of about a thousand of larch piles, 10-12m long, coming 1 meter up from the water level. Arch abutments stood on huge areas, 30.6mx10.2m on Rialto side, 37.4mx11.9m on San Bortolomio one. The construction of masonry foundations started on 9th July, 1588, using Istrian stones. Each pylon was made up of 5000 blocks, with a length of 1.40m, a width of 0.70m, and a variable height from 0.50m to 0.70m; each block, having a chain of 1.40m – 1.70m, was put along sloping parallel planes, not converging on the geometrical center of the arch, in order to counteract the arch thrust. It’s interesting to note that Rialto Bridge needed a particular supporting structure: as it was argued by Rondelet in his treatise on Rialto Bridge [Traité historique sur le Pont de Rialto, 1841], its complex wooden arch centering required a great amount of larch: according to the profile designed by Antonio da Ponte, it was built in the convent of the Friars of S.Francesco della Vigna from March to April 1589, before being carried at the site. Miozzi defined it as “circumscribing segments” arch centering (“a segmenti circoscritti”), also known as Perronet’s one: it consisted in a series of wooden struts, put in correspondence with the vertices of a polygon, enclosed in the intrados curve. The Rialto Bridge is a pedestrian structure and has been constructed above the level of the approach spans. The size of the abutments is disproportionately large but to a certain extent necessary, due to the poor ground conditions.

For the first pier a stepped foundation was used; three “tooth” with growing width (2.00m, 4.00m, 5.00m) were made, making no interferences with the foundations of the adjacent historical buildings. For each step, drilling level changed: the largest portion, near the river, reached depth of 26 foot (about

**Fig. 3.13:** Ponte di Rialto-1588, Antonio da Ponte – bridge section: detail of foundation system; plan (deck width: 22.90m)

9m), reducing it of about 0.80m, passing from the lowest to the next steps. According to its design, Rialto Bridge is characterized by a segmental arch, very close to a circular one. Approximated to circumferential arc with a radius of about 18.82m, Rialto Bridge has springer sections forming an angle ( $\alpha$ ) of  $41^\circ$  to the center of hypothesized circumference. This shape is a constant in Venetian bridges because the banks are almost at the water level and the bridge needs to be raised to shape the vaults and leave sufficient clearance for vessels to pass under. Whilst the arch has a fairly low rise, the bridge itself is quite tall. The deck is inclined at an angle of approximately  $15^\circ$ , and pedestrians are unable to see over the crest. The stone bricks are relatively smooth to reflect the light and draw attention to the primary structure, whilst the timber is much rougher, as the shops are meant to be a secondary feature. In terms of the superstructure, the stones forming the arches can be clearly distinguished, expressing the structural system. The spandrel walls on the other hand, are extremely smooth, to the point where the joints are barely visible. This is to reflect the light, making the bridge appear less top-heavy.

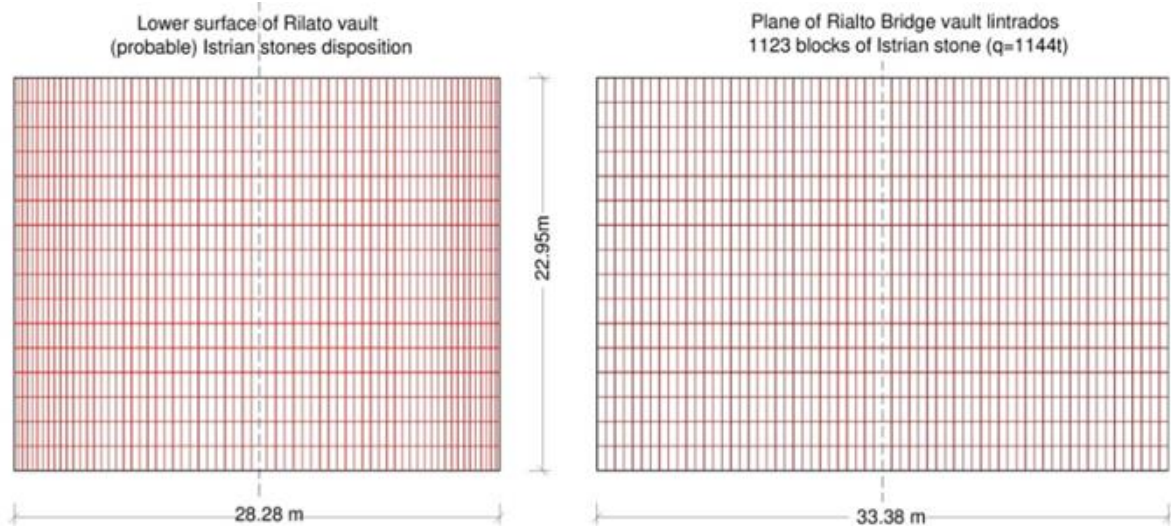
In order to understand bridge static behaviour, also trying to justify the geometrical form chosen for this thrusting structure, it's necessary to define its loads, carrying out from a bridge back analysis. The dead load acting on it can be calculated from the weight of structural elements, as deck, arch rings, spandrel walls and abutments.

In accordance with the accounting records, drawn up during Rialto Bridge construction (ASV, *Provveditori sopra la fabbrica di Rialto*, 1588), it has been possible to define material quantities used for them. A material distinction can be done, considering Istrian stone elements and brick masonry. The main load bearing structure is the vault, whose lower surface is made of Istrian stone blocks, while the upper one consists in brick masonry, putting upon stone springs.

To build bridge piers, Istrian stone blocks of 1.40m x 0.70m x 0.43m (to 0.70m) were used, having an overall weight of 4211 thousands lb (6678t). In addition, 66 stone blocks of exceptional size (2.35m x 1.13m x 0.70m) were required for the springing sections; at last, in order make these ones horizontal, stones of intermediate size, 1.40m x 0.70m (0.80m) x 0.52m (0.70) occurred, increasing piers weight of other 2400miera (1142t, being 1miera= 497kg). valuing a density ( $\delta$ ) of 2690kg/m<sup>3</sup>, the total dead loads for Istrian stone elements at the abutments can be estimated to 8270t, which is to say 4135t for each piers. The same stones had been used for the construction of vault intrados, employing squared section blocks of 1.40m x 0.52m x 0.52m; it seems that 2400miera occurred (1142t), corresponding to 1123 elements of 1.09t each ones.

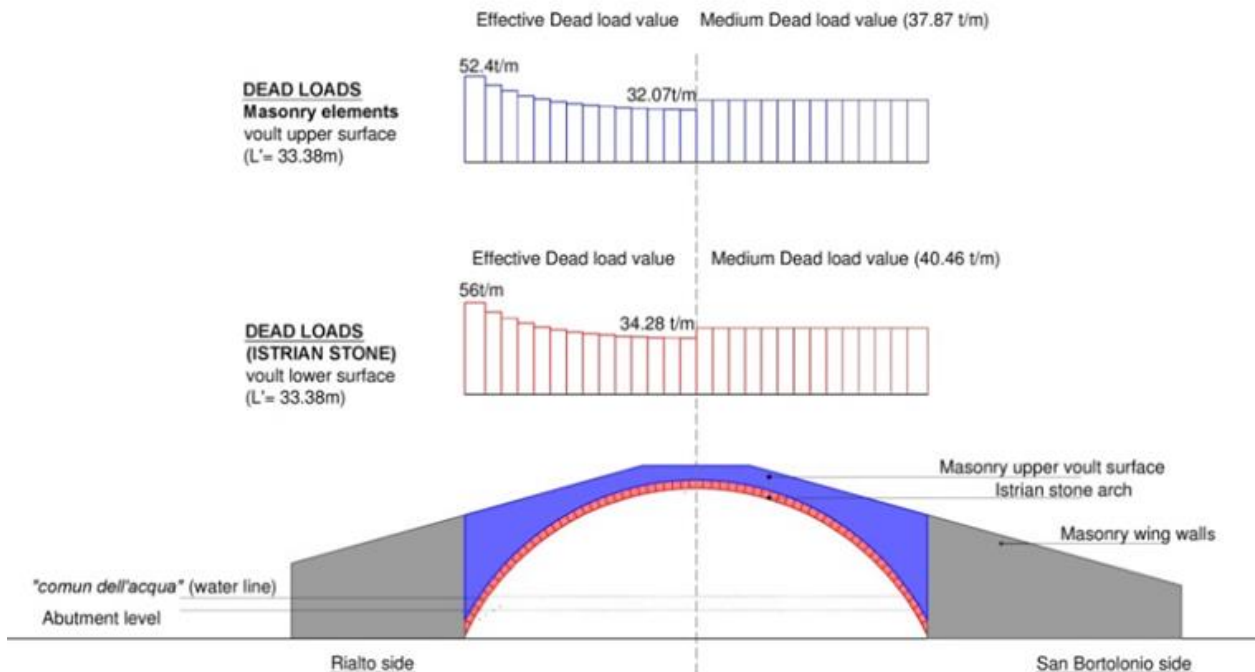
Considering “misura de sottovia”, also known as vault lower surface, an area of 96ft (33.38m) x 66ft (22.95m), or 766m<sup>2</sup>, is estimated; so vault stone intrados has a weight per square meter of 1.49 t/m<sup>2</sup>. (Fig.3.B1)

**Fig. 3.B.1:** Rialto Bridge vault characterization: Istrian stones distribution



Because of bridge symmetrical form, only half span can be considered to define stone dead loads per unit length: 14 different sections, spacing 1.01m one from the other have been considered to define the vault weight along its effective length. This value decreases going through the middle span, passing from 56.00t/m at the abutments to 34.28 t/m at the key stone; with a deck width of 22.95m a medium value of 40.46 t/m can be valued. (Fig.3.B2).

**Fig. 3.B2** Rialto Bridge load definition: VAULT DEAD LOADS distribution



For this thrusting structure, the horizontal (H) and the vertical component (V) of force acting at springing points can be calculated as:

$$H = ql^2/8f \qquad V = ql/2$$

where  $l$  is equal to the span of the arch, which is 28.8m, and  $f$  is taken as the height of the arch (or rise), equal to 6.4m. So, vault intrados generates at the springing sections a thrust of  $H_{DEAD} (I.S) = 632t$ ,  $V_{DEAD} (I.S) = 572t$ .

At the keystone, Rialto Bridge has a cross section 1.40m high, with an arch high-to-span ratio of about 1/20. If the lower part of its vault consists of stone block 0.52m high, at the middle span, a brick masonry upper portion of 0.88m stands, whose high grows to 4.70m at the abutments.

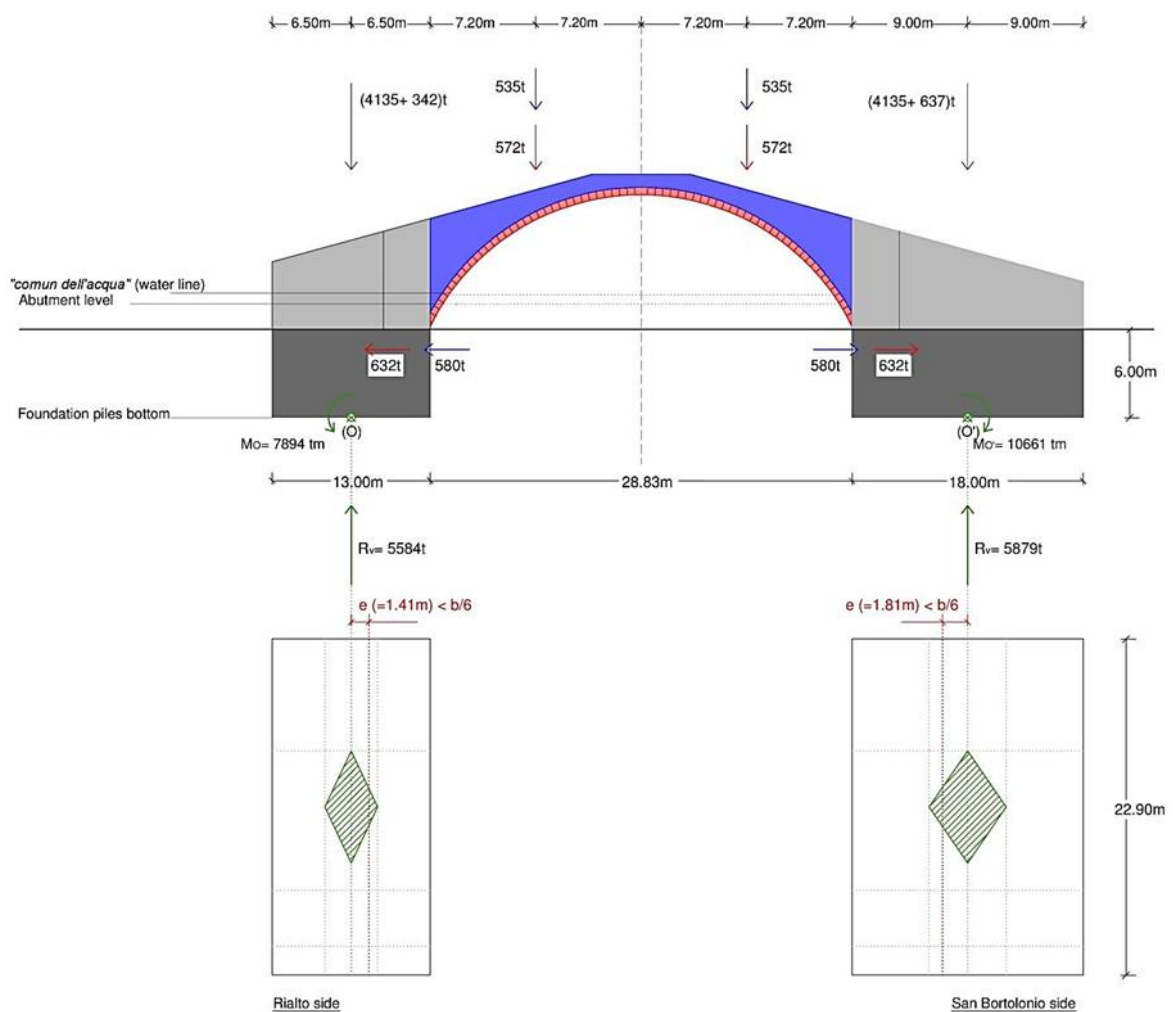
For the extrados a whole volume of 1338m<sup>3</sup> is estimated: with a brick density of 800kg/m<sup>3</sup>, an overall dead load 1070t is assessed, not far from the stone intrados dead load. It corresponds to a weight per square meter of 1.36t/m<sup>2</sup>. As it has been done for the vault upper surface, considering masonry weight distribution along effective arch length, its value increases from 32.07t/m at the middle span, to 52.4t/m at the springing section. With a medium value of 37.87t/m, vault extrados generates at the abutments a thrust of  $H_{DEAD} (M) = 580t$ , almost doubling the previous value. The overall horizontal component of vault ( $H_{DEAD} = 1212t$ ) is balanced by piers and masonry wing walls weight. to fall within pier basis.

Because of adjacent buildings, the buttress wall at Rialto side is 5.00m less wide than the other along San Bortolomio side: for the first one a total volume of 427m<sup>3</sup> is estimated, corresponding to 342t; on the largest side, buttress masonry wall has a volume of 796m<sup>3</sup>, with a total weight of 637t. Considering the previous estimation, the vault transfers a global thrust  $H_{DEAD} = 1212t$  at the abutments, balanced by pier and wing wall weight. Particularly, at Rialto side, thanks to their overall vertical component  $V_{DEAD} = 4477t$  ( $V_{DEAD} = 4772t$  at San Bortolomio), the resultant force at the abutment  $R_{DEAD} = 4613t$  ( $R_{DEAD} = 4916t$  at San Bartolomio) makes an angle of 15° with the vertical plane, so quite inclined.

The superimposed dead loads include the weight of infill material above the arches; parapets, 800mm high; stone walls, 200mm thick; stone arches and timber walls, 300mm thick, as part of shops in elevation; masonry roof covering the workshops, 300mm deep. These volumes have been valued: 1001m<sup>3</sup> for stone arches ( $\delta = 2690 \text{ kg/m}^3$ ), 15m<sup>3</sup> for stone parapets, 127m<sup>3</sup> for masonry roof ( $\delta = 800 \text{ kg/m}^3$ ), 139m<sup>3</sup> for timber elements ( $\delta = 700 \text{ kg/m}^3$ ). They correspond to an overall superimposed dead load of 2390t, increasing in 21% the total dead load (11462t) of the bridge, almost equal to the weight of the only vault (2212t). Added to dead loads, the superimposed ones generate a thrust of  $H(D+SD) = 1212t + 1119t = 2331t$ ; in this case the resultant force at the abutment  $R_{DEAD} = 5542t$  ( $R_{DEAD} = 5786t$  at San Bartolomio) makes an angle of 22° with the vertical plane.

According to Italian legislation (D.M. 14/01/2008 – Norme Tecniche per le Costruzioni), footbridges carry a Live load of  $5 \text{ kN/m}^2$ , eventually increased to  $6 \text{ kN/m}^2$  (+ 20%), considering the high crowding up the bridge: for Rialto Bridge an overall live load of 460t can be estimated (medium value of 20t/m along arch effective length). Considering the previous evaluations, the bridge has an overall permanent load of about 14391t: live loads, above the deck, correspond to 3.1% of permanent ones, with a live-to- dead loads ratio of 1/31. The simultaneous presence of live loads makes the arch thrust growing to  $HTOT = 2643 \text{ t}$ , i.e. only 12% more than the previous value. This means that the massive stone structure of the bridge, whose circular segmental arch is no funicular of loads acting on it, is capable to counterweight the huge thrust at the abutments simply thanks to its high self-weight, making the effect of live loads quiet imperceptible. (Fig.3.B3) (Tab.B.1)

**Fig. 3.B3** Rialto Bridge load definition: VAULT DEAD LOADS distribution





**Tab. B.1** Rialto Bridge load estimation

RIALTO BRIDGE PERMANENT LOADS			
TYPE	ELEMENTS	F [t]	
DEAD LOAD	(2) piers	8270	57.4%
	Vault stone intrados	1142	7.9%
	Vault masonry extrados	1070	7.4%
	Rialto side buttress wall	342	2.4%
	San bartolomio side buttress wall	637	4.4%
SUPERIMPOSED-DEAD LOAD	Stone arches	2693	18.8%
	Stone parapets	40	0.3%
	Shop masonry elements	100	0.7%
	Shop timber elements	97	0.7%
TOT	$\Sigma$ Permanent load	14391	

Concluding these evaluations, it has been verified that at the pier bottom the resultant force due to bridge dead loads falls into pier section central core (of inertia): if “e” is the eccentricity, which is to say the bending moment (M) to resultant force (Rv) ratio, valued at the center of the pier, it should be proved that it was lower than the sixth part of pier width ( $e < w/6$ ); in this way the pressure curve was always inside the pier section, without creating any tensile stress in the masonry. In particular, at Rialto side ( $w=13.00\text{m}$ ), with  $M= 7894\text{ tm}$  compared to  $R_v= 5584\text{t}$ , it has been estimated  $e= M/R_v= 1.4\text{m}$ , lower than  $w/6= 13\text{m}/6= 2.16\text{m}$ ; at S.Bartolomio side ( $w=18\text{m}$ ), with  $M= 10661\text{tm}$  compared to  $R_v= 5879\text{t}$ , it has been estimated  $e= M/R_v= 1.81\text{m}$ , lower than  $w/6= 18\text{m}/6= 3.0\text{m}$ .

Previous analysis concernig Rialto shows robustness of masonry arch bridges, all designed to carry above all permanent lodas, being live ones a little percentage of total vertical loads. It could be said that structural behaviour of masonry arch bridges has had no change through centuries: for this typology dead loads prevailed over live ones, almost until the birth of railroad. In 18th century, increasing live loads due to rail traffic, led designer to consider other aspects in bridge design, as no-negligible dymanic effects or vibrations, as well as valuing the possibility to use new material or different static schemes.

Considering mansonry arch bridges, load-bering system is explained according to the well known litterature (Heyman, Giuffré, Como, et all). As structural type, the arch is a system which transports the applied loads to supports primarily through compression stresses in the arch, eliminating the possibility of tensile ones occurring within the chosen materials. This is

achieved through design of the arch shape above all if it's to match as closely as possible to the line of thrust within the arch, especially in the case of arch bridge with very slender piers and extremely surbased segmental arches.

Forming the basic structural component of the bridge, the arch ring is composed of wedge-shaped voussoirs. Analyzing its structural behaviour, a well-known tool is the construction of funicular polygon: it represents the line of thrust equilibrating the given loading.

Assuming to make a cut at any point of the arch, the equilibrium may be reached introducing the thrust at the cut section, acting along the funicular polygon. This is not necessarily transmitted normally to the abutting faces of the voussoirs: at each section there is a normal force accompanied by a tangential one, and the latter will tend to cause one voussoir to slide upon another. The idea that an arch must have a minimum thickness to contain a line of thrust for given loads proves the key to the establishment of a safety factor for practical construction.

The structural analyses of masonry arches is often based on the application of limit analysis. For the works of many authors, being Heyman and Kooharian two of the most important, the traditional approach to the study of arches, based on the definition of a thrust line, was reformulated and validated by the new theoretical background of limit analysis, based on the concepts of: statically admissible configuration, that is to say an equilibrated state for which the yield condition is not violated at any point; kinematically admissible configuration: any potential failure mechanism for which the external power is positive.

The static theorem (or lower-bound, or safe theorem) states that the load multiplier correspondent to any statically admissible configuration is lower or equal than the collapse load multiplier. ). According this, if a thrust line can be found, for the complete arch, which is in equilibrium with the external loading (including self-weight), and which lies everywhere within the masonry of the arch ring, then the arch is safe. On the other hand, the kinematic theorem states that for a kinematically admissible configuration the load multiplier, for which the work of external loads corresponds to the work done by energy dissipation, is bigger or equal to the collapse load. The uniqueness theorem unifies the two approaches, stating that the load multiplier relative to a configuration that is both statically and kinematically admissible is equal to the collapse load multiplier (Heyman, J, 1982, p.34). Assuming Heyman's hypothesis, that are: (1) masonry has an infinite compressive strength, (2) sliding failures cannot occur, (3) masonry has no tensile strength, a masonry arch could be seen as an assemblage of stones cut to pack together in a coherent structural form, with that form maintained by compressive forces (due to dead and superimposed-dead loads) transmitted within the mass of the material. Live loading will equally be carried by compressive forces, and in all cases these forces are supposed to be high

enough for friction to provide interlocking against slip. Considering that the equilibrium of such an assemblage is impossible to preserve for any kind of load, this means that the voussoirs will take some relative movements which transform the arch into a mechanism. These movements may be both rotations around the edge of the joints or slidings along the surface of the joints.

The main mechanisms through which an arch of the typology studied in this work can collapse are: (1) the envelopment of a mechanism (through the formation of a minimum number of hinges); (2) sliding of the voussoirs, for shear action, eventually combined to formation of hinges; (3) crushing of the material in compression. The most frequent failure mechanism, at least for “regular” arches, is the formation of a mechanism through an adequate number of hinges; for a single span arches the formation of 4 hinges is sufficient to form a mechanism and to lead, consequently, the arch to failure if the applied load is not reduced. The failure configuration corresponds in real cases to the alignment of three of the hinges, condition in which the arch cannot sustain any load. Given these assumptions, indeed, the yielding criteria corresponds to the condition in which the thrust line is tangent to the edge of the section, being it, for the lack of tensile strength, unable to provide a reaction to higher eccentricities. As all the states for which the thrust line is inside the section do not violate any limit criteria, so, a statically compatible state is determined if any thrust line, equilibrated with the external loads, can be found inside the geometrical boundaries of the arch. It's easy to understand how the presence of negligible tensile strength materials can disrupt the behaviour of structures as compared to the common elastic ones. Considering The limit state analysis, the main aspect to value, studying masonry arch bridges is the definition of safety factor related to the most probable failure mechanism due to acting loads. If the applied load stays within a certain 'core' of the section, stresses across the whole section will be only compressed. Because for masonry arch it is the middle third of the section to be relevant, the “middle-third rule” has been supposed by some nineteenth and twentieth centuries engineers to be a prime requirement of design. The rule states that the line of thrust of an arch, expected under the applied loading, should not fall outside the middle third of an arch cross-section (assuming a square or rectangular shaped cross-section). If the applied load stays within this ‘core’ middle third, then the stresses experienced within the section will be compressive (Heyman, J, 1982, p.23). the line of thrust exceeds past the middle third, not only will tensile stresses become present, but the compressive stress on one side of the cross-section at the location of the exceeding thrust line will also increase. This is due to the reduction of contacting area in which the load is passed from one voussoir to another when tensile stress begins to separate voussoirs. So the most effective solution is to design an arch whose middle third section curvature closely mimics that of its line of thrust.

## Bibliography

- [1] Leon Battista Alberti, “Dieci Libri De L’Architettura”, 1546
- [2] Andrea Palladio, “I Quattro Libri dell’Architettura”, Venezia, 1570
- [3] H.Gautier, “Traité de ponts, ou il est parlé de ceux des Romains & de ceux des modernes”, 1716
- [4] Ottavio Bertotti Scamozzi, “Le Fabbriche e i Disegni di Andrea Palladio”, Vicenza, 1796
- [5] Nicola Cavalieri, Istituzioni di architettura statica e idraulica, 1831
- [6] M.Gauthey, “Traite de la construction des ponts”, 1832
- [7] Tveit P., An Introduction to the Network Arch, Technical University of Norway, Trondheim, 1956
- [8] Eugenio Miozzi - “Venezia nei secoli” - Volumes 1-2, Libeccio, Venice - 1957.
- [9] Timoshenko & Gere, Theory of Elastic stability, McGraw Hill, New York 1961.
- [10] G.Krall. Stabilità e vibrazioni. Edizioni Cremonese, Roma, 1968.
- [11] Eugenio Miozzi - “Dal ponte di Rialto al nuovo ponte degli Scalzi” Roma – Stabilimento tipografico del Genio Civile - 1035.1980
- [12] Nascè. Contributi alla Storia della Costruzione metallica.CTA 1981.
- [13] John A. Kouwenhoven. The Designing of the Eads Bridge. Technology and Culture, Vol. 23, No. 4. (Oct., 1982), pp. 535-568.
- [14] Tiziano Rizzo - “I Ponti di Venezia” - Newton Compton – 1983
- [15] G.Ballio- “Il Ponte dell’Accademia a Venezia” – Convegno e mostra: 1889-1989\_ Centenario del Viadotto sull’Adda, MilANO, 15 Novembre – 17 Dicembre 1989\_ Costruzioni Metalliche, n.1, 1990
- [16] H. Bachmann, Walter J. Ammann, F.Deischl, J. Eisenmann, I.Floegl, G.H. Hirsch, G.K. Klein, G.J. Lande, O. Mahrenholtz, H.G. Natke, H. Nussbaumer, A.J. Pretlove, J.H. Rainer, E. Saemann, L. Steinbeisser, Vibration Problems in Structures: Practical Guidelines, 1995
- [17] Frampton K., Webster C., Tischhauser A., Calatrava Bridges, Birkhauser, Berlin,1996
- [18] Menn, C, The Place of Aesthetics in Bridge Design, Structural Engineering International, Volume 6, No. 2, pp. 93-95, 1996
- [19] Nasce' V.; Sabia D., [Teoria e pratica nella costruzione nei ponti in muratura tra XVIII e XIX secolo](#). In: Carlo Bernardo Mosca, 1792-1867 : un ingegnere architetto tra Illuminismo e Restaurazione / Vera Comoli, Laura Guardamagna, Micaela Viglino (cur.). Guerini, Milano, pp. 29-38. ISBN 8878027669 1997
- [20] Menn, C, Functional Shaping of Piers and Pylons, Structural Engineering International, Volume 8, No. 4, pp. 249-251, 1998
- [21] Chen W., Duan L., Bridge Engineering Handbook, CRC Press, 2000
- [22] Menn, C, Stahlbetonbrücken (Reinforced concrete bridges), 2003
- [23] Troyano L.F., Bridge Engineering A global perspective, 2003
- [24] R.W.Clough, J.Penzien. Dynamic of structures. 2003
- [25] F.Mazzolani. STESSA 2003 - Behaviour of Steel Structures in Seismic Areas. Proceedings of the conference on brhaviuor of steel structures in seismic areas, 9-12 giugno 2003, Napoli
- [26] A.Barbieri, V.Chiaradia, A.Di Tommaso (IUAV University of Venice), “Railway masonry arch bridges of Venice lagoon: history, technology and structural behavior”, CIMNE, Barcelona, 2004.

- [27] Arioli M., The Art of Structural Design : a Swiss Legacy: eine Ausstellung im Zürcher "haus konstruktiv", ETH Zürich, Rämistrasse 101, 8092 Zürich, Schweiz, [www.library.ethz.ch](http://www.library.ethz.ch), 2005
- [28] Fjalar Hauksson, LUND University, Master dissertation. Dynamic behaviour of footbridges subjected to pedestrian-induced vibrations, 2005
- [29] Shabanovitz T. B., The Progressive Synthesis of Architecture and Engineering in Modern Bridge Design, Massachussets Institute of Technology, June 2006
- [30] Wilbur J. Watson, "Great Bridges – form Ancient time to the twentieth century", 2006
- [31] Per Tveit. An Introduction to the Network Arch. Lectures at NTNU Trondheim on August 15th 2006
- [32] Fulvio Zezza - "Geologia, proprietà e deformazione dei terreni del centro storico di Venezia"- Second Convention "La riqualificazione delle città e dei territori" - Venice - 2007.
- [33] A. Adão da Fonseca. The Infant Dom Henrique Bridge over the River Douro, at Porto. ARCH'07 – 5th International Conference on Arch Bridges.
- [34] Eckhardt, B., Ott, E., Strogatz, S., Abrams, D., & McRobie, A. (2007). Modeling walker synchronization on the Millennium Bridge Physical Review
- [35] Dobricic S., Siviero E., De pontibus. Un manuale per la costruzione dei ponti, Il Sole 24 Ore, 2008
- [36] Theodore V. Galambos, Andrea E. Surovek. Structural stability of Steel: concepts and applications for structural engineers. John wiley & sons, inc., 2008
- [37] E. Brühwiler, Prof. Dr. Civil Eng. ETH, Ecole Polytechnique Fédérale de Lausanne (EPFL), Switzerland, Christian Menn's recent bridge designs – Reducing structural elements to the simplest solution. . 5th New York City Bridge Conference, Bridge Engineering Association, New York (USA), August 17 – 18, 2009
- [38] D.Proske – P.Gelder, "safety of Historical Stone Arches Bridges", Springer, 2009
- [39] Dirk Proske · Pieter van Gelder , "Safety of Historical Stone Arch Bridges", Spriger, 2009
- [40] M. De Miranda, U.Barbisan, M.Pogacnick, L.Skansi Bridges in Venice - Architectural and Structural engineering aspects, 34<sup>th</sup> IABSE SYMPOSIUM, Venezia 2010
- [41] Theodore V. Galambos, Guide to Stability Design Criteria for Metal Structures, Sixth Edition, John wiley & sons, inc, 20100
- [42] F. Trovò, Università IUAV di Venezia, I sistemi fondali dell'architettura storica di Venezia, Caratteri Costruttivi dell'Edilizia Storica, , 2010
- [43] Kathryn R. Heath, A critical analysis of Ponte della Costituzione, Venice , Proceedings of Bridge Engineering 2 Conference 2011, April 2011, University of Bath, Bath, UK
- [44] Restauro del Ponte di Rialto a Venezia- Relazione Tecnica, Comune di Venezia, Direzione Progettazione ed esecuzione lavori, Arcomai S.n.c, P.Sfamen, D.Busato, 2013
- [45] Eliana Alessandrelli ,distorsioni sistematiche, i ponti "truccati" di Eugenio Miozzi SIXXI 3, Storia dell'ingegneria strutturale in Italia, Gangemi, Roma 2015

#### Web references



- [1] International Database and Gallery of Structures, <http://en.structurae.de>
- [2] [http://www2.comune.venezia.it/lidoliberty/biografie/miozzi\\_e.htm](http://www2.comune.venezia.it/lidoliberty/biografie/miozzi_e.htm)
- [3] [http://mediateca.palladiomuseum.org/palladio/opera\\_immagini.php?id=73&TSK=L&TR=14&RN=0](http://mediateca.palladiomuseum.org/palladio/opera_immagini.php?id=73&TSK=L&TR=14&RN=0)
- [4] <http://fysvenice.weebly.com/rialto-bridge.html>

#### **4. The role of deck stiffened system in long span bridge design: the original contribution of Santiago Calatrava**

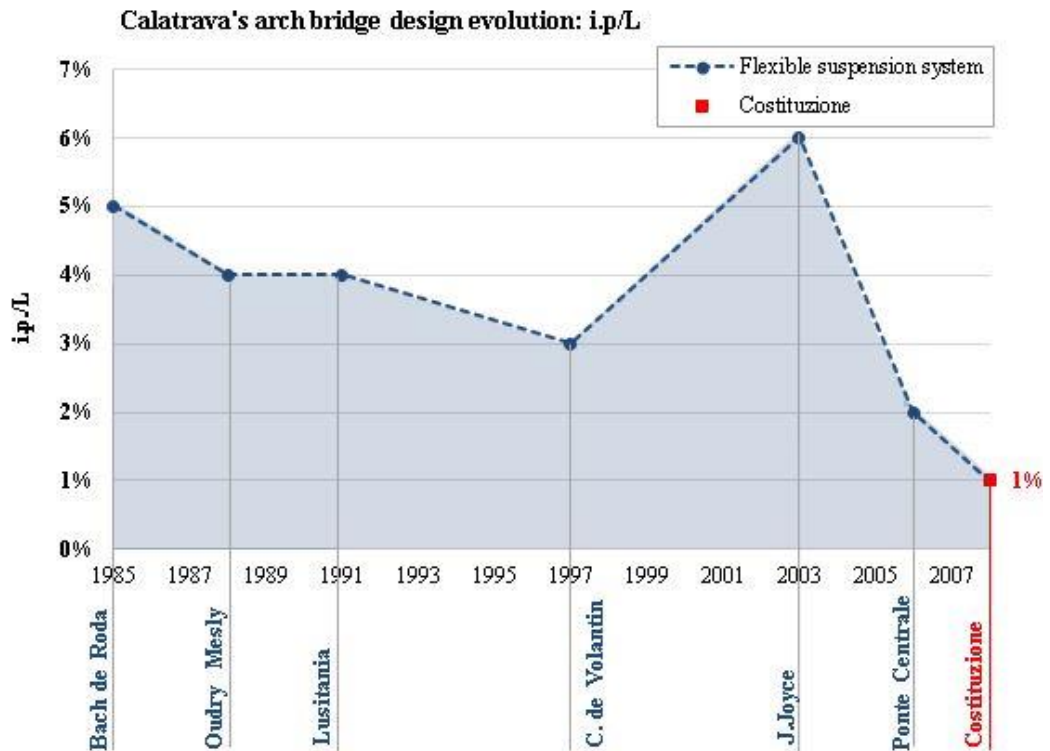
##### **4.1 Calatrava's innovative design approach**

The evolution of long span bridges, described before for suspension and arch solutions, underlines how deck stiffened system role has changed completely: starting from massive deck truss arrangements and open section deck solutions without bracings, the aim of covering longer spans using lighter and slender structures, has led to prefer (aerofoil) box sections; this solution guarantees high torsional stiffness, necessary in the case of structural asymmetrical layout or eccentric load condition. At the same time, the choice of a thickening suspension system, corresponding to an equivalent distribution of deck cross sections, allows to reduce the effective loaded length for structural elements, giving the possibility to reduce their size greatly.

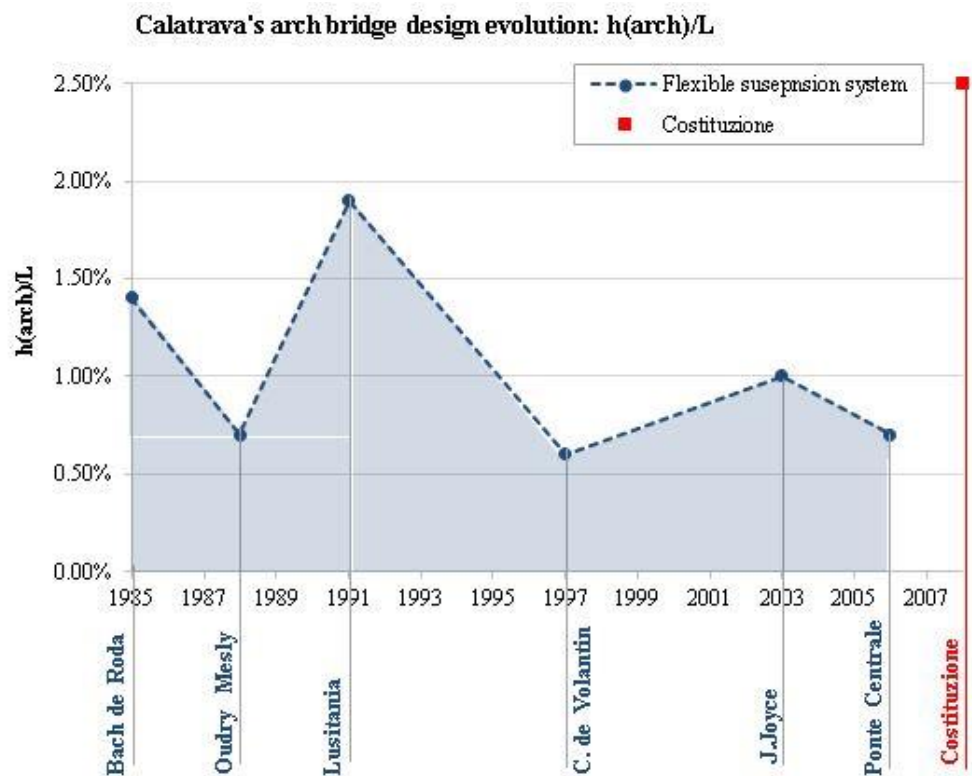
In this route through structural types, investigating the occurred changes in deck stiffened system, the contribution of Santiago Calatrava cannot be neglected, above all in the way this polyhedric artist has been able to combine the role of architect, engineer and urban designer in one person, creating unprecedented works of art. Although he has often been criticised for the excessive formalism of his works, his “structural games” greatly revealed his undeniable technological contribution. His major innovation consists in completely upsetting the traditional role of deck stiffened system both in arch bridge and cable stayed bridge design. Particularly in the case of bowstring arch bridges, his attempt to solve exclusively in extensional regime bridge structural behaviour is put into practice by dematerializing deck stiffened system, “simply” thickening cross section numbers. In this way, the effective loaded length of longitudinal structural elements is significantly reduced, so that acting loads are transferred directly from deck to the upper arch, being carried exclusively through arch thrusts. If bending moments are practically nihil, and torsional effects are often borne by rigid girder box sections, the close succession of deck cross sections, as well as of suspension hangers, accompanied by the choice of particular arch configuration, guarantee the reduction of buckling effects in compressed steel arches, giving also the possibility to trim down size of structural elements. Passing from earliest short footbridges to longer bridges, Calatrava's continuous experimentation is carried out in a progressive optimization of design parameters, heretofore used, which describe the suspension system ( $i.p./L$ ), or arch stiffness ( $ha/L$ ), truss stiffness ( $ht/L$ ), or that of the whole structure ( $h^*/L$ ). Their clear reduction (till  $i.p./L$  of 1%), structurally corresponds to daring and unpredictable solutions, as the innovative “pure arch system” resulting from the evolution of Ponte della Costituzione design. This approach, later define

as “vertebrizzazione”, is well visible in the case of bowstring arch bridge with flexible suspension system (Fig. 4.1).

**Fig. 4.1** Calatrava's design evolution for flexible suspension system :  $ip/L$



**Fig. 4.2** Calatrava's design evolution for flexible suspension system:  $h(\text{arch})/L$



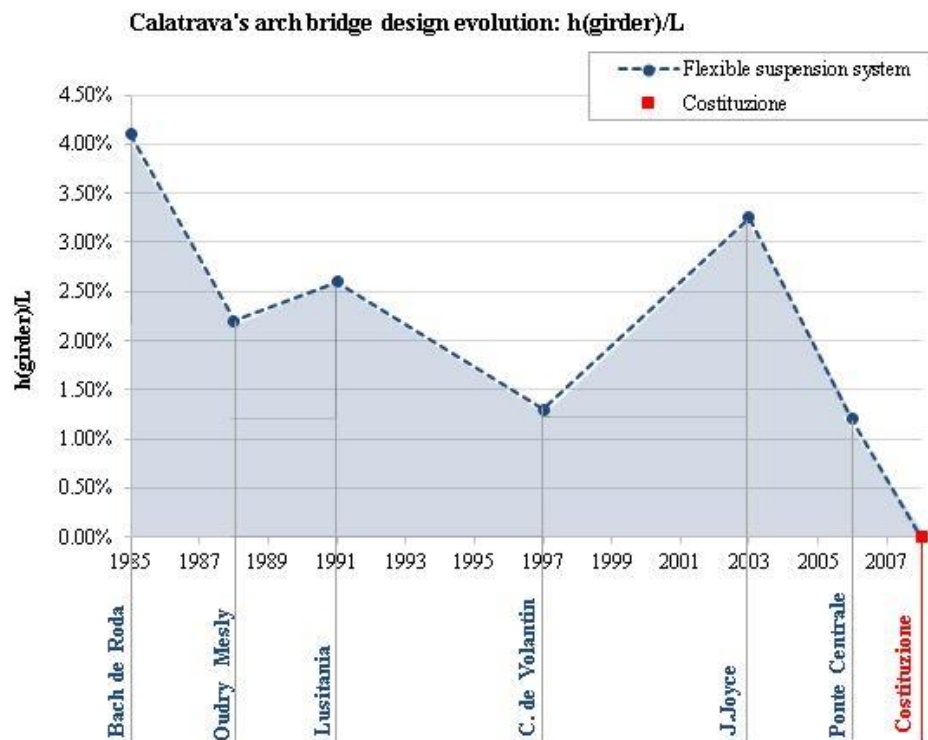


**Fig. 4.3** Calatrava's design evolution for flexible suspension system:  $h(\text{girder})=L$

Calatrava's innovative design approach assures to significantly reduce deck stiffened system size, till completely deny it with the "pure arch" solution of Ponte della Costituzione (Fig. 4.2) (Fig. 4.3): conceptually, this works represent the synthesis of a progressive technological evolution, originally started by Eads and Eiffel two centuries before.

Since the industrial revolution, the *art of bridge design* has undergone radical changes. From short-span masonry arches to streamline-shaped steel box section suspension bridges spanning more the 2000m, the rapid evolution of bridges during the past two centuries reflects the drastic improvements in both material, technologies and analytical method used in their design and construction. The pioneering use of cast-iron in 30m-span Coalbrookdale Bridge of 1779 prophesied changes in bridge design made possible by emerging high-strength materials. During 19<sup>th</sup> century, the unprecedented iron and steel arch bridges by Gustave Eiffel demonstrated the ability of these materials to span distances unheard less than 100 years before. At the turn of 20<sup>th</sup> century, the work of innovators like Freyssinet in France and Maillart in Switzerland demonstrated how another new, high-strength material\_ reinforced concrete\_ would again transform the art of bridge design (as it can be seen in Chapter 67).

As the increased strength of structural material allowed bridges to span ever longer distances, they also encouraged the creation and refinement of new

bridge forms. For instance, steel ability to resist both tension and compression allowed long-span bridges to be made for the first time of trusses, till the choice of resisting wind forces (above all after the paradigmatic collapse of Tacoma Narrow Bridge, 1940) led bridge designers to make deck stiffened system aerodynamically efficient, reducing weight and, therefore, lowering costs, using knife-edge-profile rather than massive truss work. In searching as efficient and economical as possible solutions, a process similar to that employed by Eiffel, Maillart and Freyssinet has been adopted (Ref. Wesber. “New solutions and old problems” in “Calatrava Bridges” by Frampton, 1993): the primary goal of bridge engineering is to solve the problem of span, as economically as possible, in both technical and fiscal sense of the word. This concepts is reflected, for example, in the writings of structural engineer and critic Billington who extols the “engineer ideals as efficiency of materials, economy in construction and elegance in form. In this way he has sketched out a line of thought common between ETH designers, well explain by Menn in writing “Prestressed Concrete Bridges” (1986): *“the fundamental objectives of bridge design are safety, serviceability, economy and elegance. [...] safety and serviceability are achieved through the systematic application of scientific principles. [...] economy and elegance is achieved through non scientific means; they depend entirely on the creativity of the engineer. [...] aesthetically pleasing bridges are distinguished by transparency, slenderness and lack of unnecessary ornamentation, all of which result in an efficient use of material and hence low construction cost”*.

In contrast to this approach, Calatrava does not consider efficiency and economy as design ideals, but as necessary aspects of design: although his use of material and construction technologies is often efficient and economical, the elegance of his bridges derives from a broader set of concerns, rooted on his unusual design method, well visible in Alamillo or Ponte della Costituzione design.

No searching for new structural paradigms, unlike most classic bridges, Calatrava ‘s forms cannot be simply described in term of structural typology. Using his training as engineer, and architect, and his skills as a sculptor, Calatrava brings a broad set of concerns to the problem of bridge design and produces works that transcend issues of engineering. His bridges are both “mega-sculpture” (Frampton) and public place formally defined by a complex intertwinement of plastic expression and structural revelation.

Trained in ETH (Eidgenössische Technishe Hochschule) in graphic statical tradition of Cullman, who founded this section of the Zurich school in 1855, heir to Maillart and Menn, Calatrava has moved away from a rigorous application of ETH principles, in order to achieve more dynamically expressive forms.

His innovative approach characterizes more than 50 bridges, he has design during his career: with single exceptions of the 200m-cable-stayed Alamillo



Bridge and 200m-bowstring –arch solution of Ponte Central (Reggio Emilia), none of these bridge is of mega-engineering scale: however, span alone is not what distinguishes these works; what is more crucial is that these structures display one or more of the following characteristics:\

- (1) they are invariably of mixed-media construction, combining concrete, steel, also glass in a fairly unique way;
- (2) their assembly disposes of static forces in such a way as to produce rather unusual structurally expressive effects;
- (3) his bridges are perfectly integrated into the environment that surrounds it, to such an extent as to totally transform the immediate adjacency
- (4) the structure, rendered as landmark at the regional scale, is detailed and artificially illuminated in such way to emphasize its structural dynamic, conveying a particular sense of arrested motion.

As outlined before, in the last 30 years of his career, this versatile artist has always searched for innovative structural technologies, combining previous aspects in the creation of works of art characterized by naturalistic as anthropomorphic forms (aspect which justifies the term “vertebrizzazione” used in this chapter). Claiming the elegance, identity and recognisability of his structures, Calatrava prefers working in extensional regime also in the case of short spans. In order to guarantee aesthetic qualities to his bridges, as it has been well made by members of ETH, the Valencian artist optimises the interaction between load-bearing structural elements (as arch, stiffening truss, hangers) minimising their dimensions. Thanks to the process of “vertebrizzazione” (which is to say discretizing main structural element into a huge number of cross sections, quite far one from the other) he can successfully “dematerialise” bridge deck, obtaining high slenderness. This result is “simply” achieved increasing hangers as well as cross section number. For these imperceptible decks, built with many transverse stiffening elements, the effect of live loads is practically nihil (as it happens in Ponte della Costituzione, with 90 transverse cross sections).

#### **4.2 Arch bridges structural optimization: the evolution of Calatrava’s design approach form earliest bowstring arch bridges to the “pure arch” system of Ponte della Costituzione**

Since 1985, Calatrava have always given particular attention to arch bridges, deepening cable stayed system since the end of 90s years in designing twelve bridges of this type in the last 15 years. Concerning recent trends for long span arch bridges, works by Santiago Calatrava have cannot be neglected above all in the case of bowstring arch bridges. As emblematic examples in

underlining his extraordinary technical contribution in the evolution of this typology, above all for flexible suspension system, we can consider:

1. Bach de Roda, Barcelona (ES) '85-'87
2. Oudry-Mesly , Créteil (FR) '87-'88
3. Lusitania, Merida (ES) '88-'91
4. Campo de Volantin, Basilea (ES) '94-'97
5. Ponte Centrale, Reggio Emilia (IT) '04-'06
6. Ponte della Costituzione , Venice (IT), '01- '07

Previous historical evaluations suggest that long span arch bridges mainly work in extensional regime, getting longitudinal girder to carry bending effects: the greatest innovation which could be recognised to Calatrava is to have significantly reduced bending deck stress, designing bridges which act only in extensional regime. As it will be seen shortly, increasing cross sections number, as well as using a low-spacing cables system, load transferring structural elements become slender, without using redundant longitudinal girders, till completely dematerializing them. With his free forms, Calatrava has given a great contribution to the evolution of arch bridges, varying in arch- height to optimise its carrying capacity while presenting an aesthetic view to the eye. His works have often become subject of scientific community criticism: the Valencian designer has been accused of showing off a large dose of technical skills, being inclined to indulge in a sort of “structural game” allowed him by latest technological innovations; he has been imputed of acting as a modern archistar, designing a bridge out of a contest, with a modernist-minimalist style . Instead, Calatrava design is based on the idea that bridge “must have its own identity; while being independent of local design, it should harmonise with”, seen as no-redundant landmark giving “energy” to the whole contest. Calatrava bridges are exercises of “Engineering Aesthetic”, where technology merges with beauty. The extraordinary (quite expensive) structural solutions he adopts are really works of art, showing a great cure in details and choosing materials.

He became internationally known from 1987, following completion of the *Bach de Roda* and the Felipe 11 bridges in Barcelona. (Fig. 441, a, b) (Tab. 4.1). Bach de Roda Bridge was commissioned by Unitat Operativa de Proestes Urbans, in 1985, built in 1986-87. After city amplification to hold the '92 Olympic Games, there was a renewed interest in urban transformation: this bridge, well visible from long distances (a point of focus in urban skyline), is part of an urban scale plane to valorise an outlying area. It serves both traffic and pedestrians, covering a total length of 129m. This tied arch bridge is made of two couples of pulled arches, 46m-spanning, having a rise of 10m (rise to- span ratio 1\4.7) and a clearance of 8m above railway tracks. These main arches stand upon walkway, leaving lanes completely clear.



<b>L (arch) [m]</b>	46	<b>ip [m]</b>	2,30
<b>arch rise (r) -to L</b>	1/ 4,7	<b>ip/L</b>	5,50%
<b>h (girder) [m]</b>	1,70	<b>hg/L</b>	1,4%
<b>h (arch) [m]</b>	0,60	<b>ha/L</b>	4.1%

**Tab 4.1** Bach de Roda, Barcelona (1985-87) design parameters

Two slender longitudinal girders support cross sections-warping deck; simultaneously they carry. Girders support the cross beams beneath the concrete road-deck and pedestrian walkways. In elevation, the choice of twin arches supporting the roadway by a set of suspender cables may represent a weakness in its structural design, being this system susceptible to buckling. In plan Calatrava had to solve the problem of having two arches that cross the train below at a skewed angle (approximately  $60^\circ$ ). The easiest but greatly invasive solution to buckling problem should be using horizontally oriented truss connecting two arches. Leaving upper deck completely uncovered, also preserving pedestrian lanes on their own seat, without creating interferences between traffic flows, Calatrava's solution to this structural problem was to place secondary arches of equal height next to the main ones, on either side of the bridge. Standing on the internal side, the secondary arches (Fig. 4.5) (Fig. 4.6\_a,b) are connected to the main ones by rigid fins near their apex, thus bracing both arches against buckling. These upper connections increase lateral stiffness of structural system, greatly reducing the effective length of the arch in order to restrict buckling effects only to arch extremities. (Fig. 4.7)

**Fig. 4.4** Bach de Roda, Barcelona (1985-87), Calatrava\_  $L'=129\text{m}$ ;  $L=46\text{m}$ ;  $r=10\text{m}$ ;  $r/L=1/5$ ;  $ip/L=5.4\%$ ;  $ha/L=1/71$ ;  $ht/L=1/5$ .

**Fig. 4.5** Bach de Roda, Barcelona (1985-87). Double arches system\_ cross section detail, valuing buckling effects

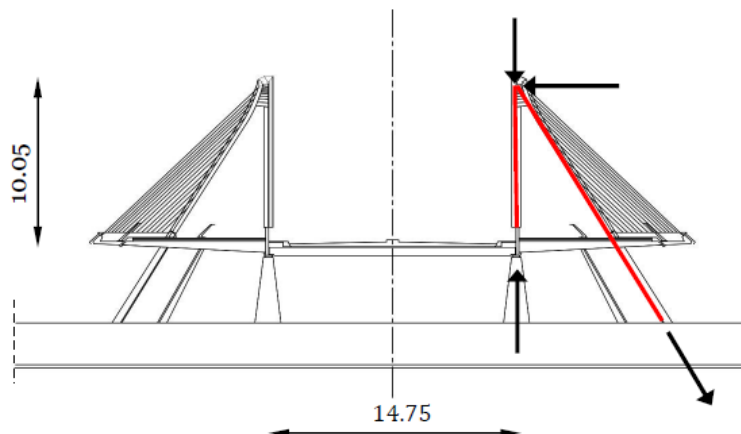


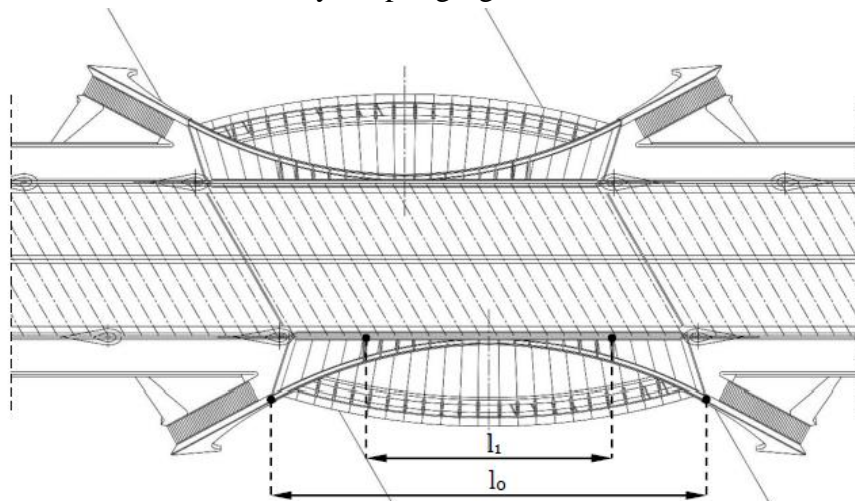


**Fig. 4.6** Bach de Roda, Barcelona (1985-87)\_  
(a) double arches  
system: connection  
details\_ (b) abutments

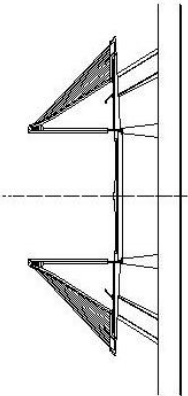
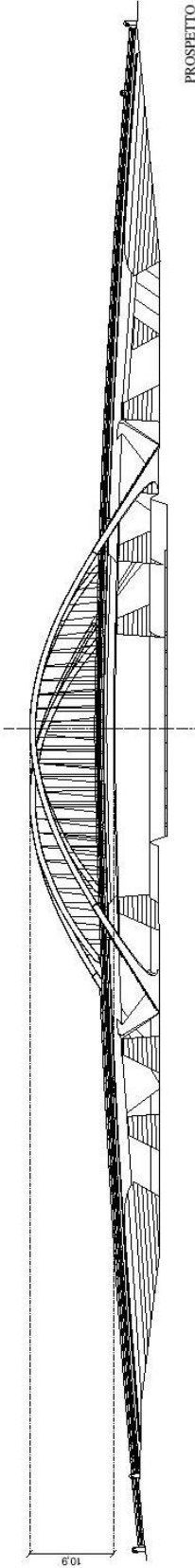
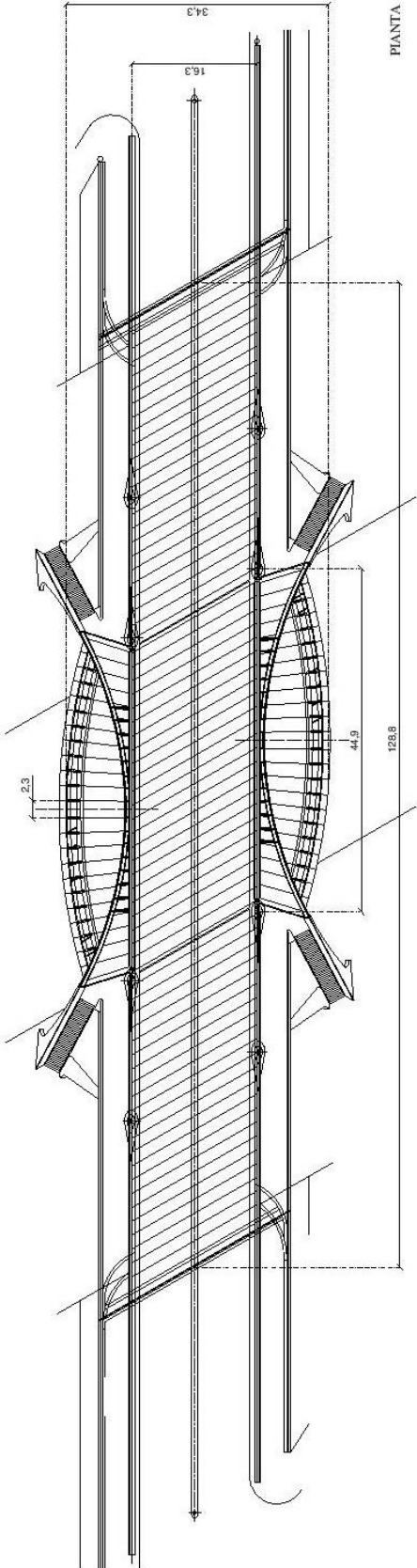
In this case, Calatrava is capable to optimize a solution, proposed before by Fehrmann in 1963: in accordance to classical analytic formulation of Euler's critical load [ $N_{cr} = \pi^2 (EI / l_o^2)$ ], reducing effective length ( $l_o$ ), buckling effects could be better controlled. It's interesting to note that arch connection not only prevent buckling in the arches but also enables the paired arches to split past each other in respect of the skew. Where the outer arch takes its abutment off the strait edge beam, the thrust of the steel-hinged joint of the inner arch is stiffened by the road-bed and abutments buttresses.

The secondary arches have also a purely architectural purpose. Inclined suspenders, lying in the plane of these arches, help to support the pedestrian walkway, whose edge is bowed outward in plan, reflecting the arch elevation, while creating a pedestrian square: the sloped suspender ropes at the walkways edges and the main roadway suspenders themselves define the limit of this plaza. Although secondary arches solve the central structural problem of this bridge, also giving the possibility to transform it in a civic icon, their proportions and details have not been deepened with the same accuracy characterizing bridge structural conception. Even if they are loaded only half pedestrian walkway, they have a cross section similar to that of main arches: their massiveness gives upper deck a lightness appearance. Considering the use of a no much thick suspension system ( $i_p/L = 5,50\%$ ), the choice for a slender deck make necessary adopting rigid arches.

**Fig. 4.7** Bach de Roda, Barcelona (1985-87)\_  
plan view: arches  
effective length



Bach de Roda - Barcellona (SPA) - 1985 - 1987



SEZIONE MEZZERIA







**Fig. 4.8** Oudry- Mesly Bridge, Créteil (1987-88),  $L_{tot}=120\text{m}$ ;  $L_{arch}=53.8\text{m}$ ; rise=8m;  $r/L=1/7$ ;  $ip/L=3.45\%$ ;  $ha/L=0.70\%$ ;  $ht/L=2.20\%$

A great step forward in design optimization is marked by Oudry- Mesly Bridge (Fig. 4.8). Built between February and September 1988, it was commissioned at the beginning of 1987 by SEMEAC, a consortium with includes the City of Créteil (France), to provide a pedestrian link between the suburbs of Créteil and the development area known as Nouveau Créteil, as a point of orientation in an alienating modern *no man's land*.

**Tab 4.2** Oudry- Mesly Bridge, Créteil (1987-88) design parameters

<b>L (arch) [m]</b>	53.8	<b>ip [m]</b>	1.90
<b>arch rise (r) -to L</b>	1/7	<b>ip/L</b>	3.50%
<b>h (girder) [m]</b>	1.20	<b>hg/L</b>	2.20%
<b>h (arch) [m]</b>	0.36	<b>ha/L</b>	0.70%

Its deck steel structure is carried by two 5.20m spacing twin girders, which get close passing form the abutments to the middle span, till jointing here. Girders are hang from the twin steel arches and carry a series of cross beams, on which a continuous concrete walkway has laid. A steel fillet at each end of the arch structure transfers the gravity component to the reinforced concrete foundations and the horizontal component to the steel girder. This load bearing structural system makes Oudry-Mesly a tied arch bridge. Main arches are made of steel tubular elements: these ones were shop fabricated and trial erected before being dismantled into four components to being transported to the side for the final assembly. Following the girders trend, also steel arches joint at the crown, then separating to attach at concrete abutments. Considering reduced spacing between cross sections, as well as the lack of elements which connect diagonally them, torsional effects due to asymmetrical loads are transferred directly from slab to slender longitudinal girders, passing to main arches through hangers.

Suspender cables, supporting the exposed ends of the cross beams, are connected to the arches by sockets and welded gusset plates. These 1.9m-spacing hangers stand vertically from the longitudinal middle-span plane: strictly dividing 53.8m-span, cables give back a low spacing-to-span length ratio ( $ip/L$ ) of about 3.53%. (Tab. 4.2)

Oudry-Mesly - Cret  il (FRA) - 1985 - 1987

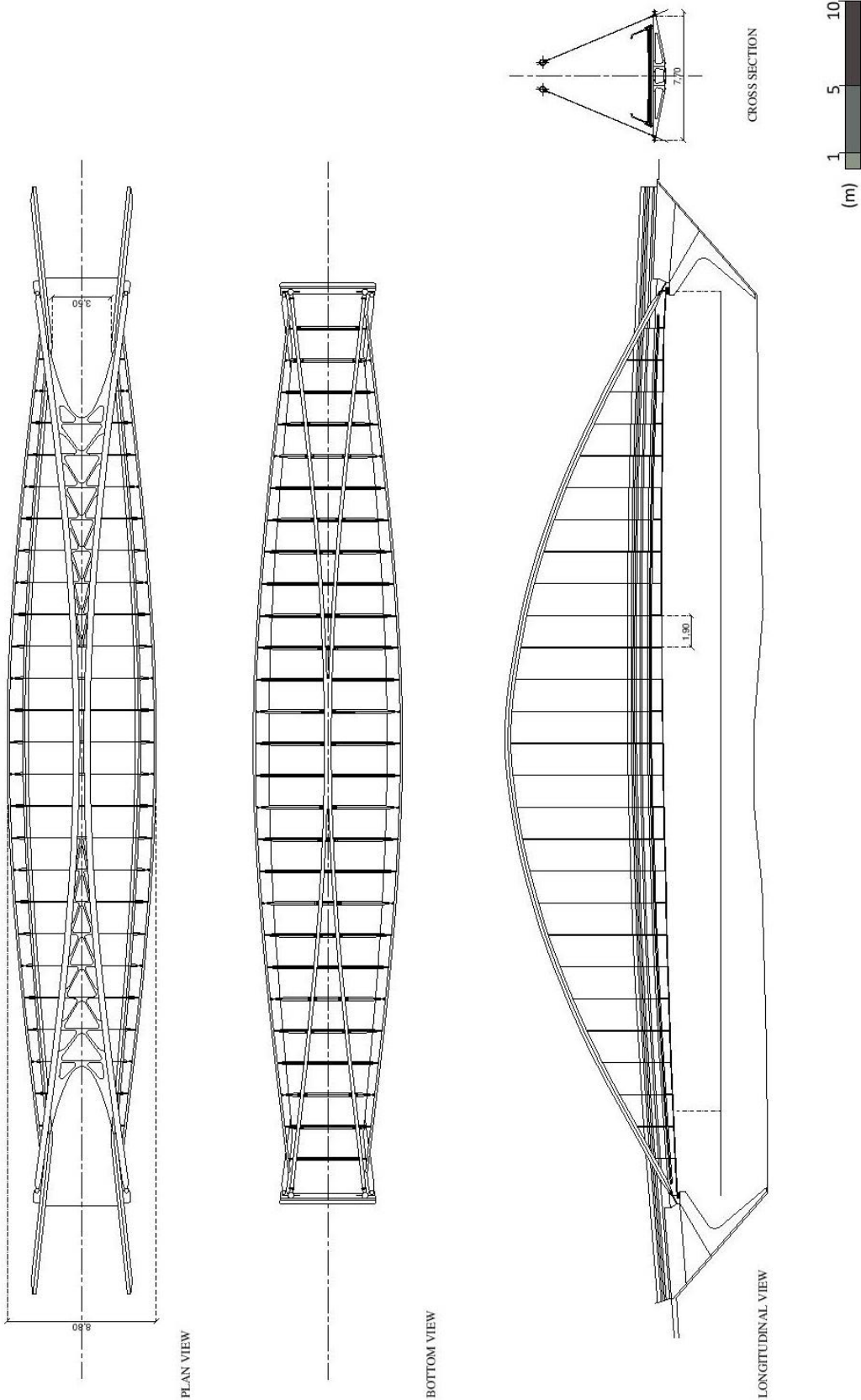




**Fig. 4.9** Oudry- Mesly Bridge, Créteil (1987-88), deck detail

Comparing this bridge with other contemporary ones, it could be said that Calatrava's design approach is really clear since his early works: Oudry-Mesly bridge shows how progressively reducing cross sections spacing, girder and arch moment of inertia can be greatly decreased; in this case, preserving arch slenderness, deck becomes the stiffer (Fig. 4.9).

Deck bottom view reveals an absolute lack of bracing between cross sections: in this case, thanks to the short distance between hangers, local torsional effects due to asymmetrical loads, acting in transverse direction, are transferred directly by the suspenders, from deck system to the upper slender arches.

A completely different structural system can be seen in the contemporary *Lusitania Bridge* (Merida, Spain) (Fig. 4.10) (Tab. 4.3). Built between 1990-91, the bridge was commissioned by the Council of Extremadura, in order to increase regional traffic, following the promotion of Merida to the capital of the autonomous community of western Iberian Peninsula. Connecting the old town of Merida to the newly developed area of Polygon on the Northern side of the River Guadiana, Lusitania Bridge was built to relieve the ancient Roman bridge, which has been declared a footbridge.

**Fig. 4.10** Lusitania Bridge (1988-91),  
 $L_{tot}=465\text{m}$ ;  
 $L_{arch}=189\text{m}$ ; rise=  
 $32\text{m}$ ;  $r/L=1/6$ ;  $ip/L=$   
 $3.7\%$ ;  $ha/L=1.9\%$ ;  
 $ht/L=2.6\%$





<b>L (arch) [m]</b>	189	<b>ip [m]</b>	6.80
<b>arch rise (r) -to L</b>	1/6	<b>ip/L</b>	3.70%
<b>h (girder) [m]</b>	4.75	<b>hg/L</b>	2.60%
<b>h (arch) [m]</b>	3.50	<b>ha/L</b>	1.90%

**Tab 4.3** Lusitania Brigde (1988-91) design parameters

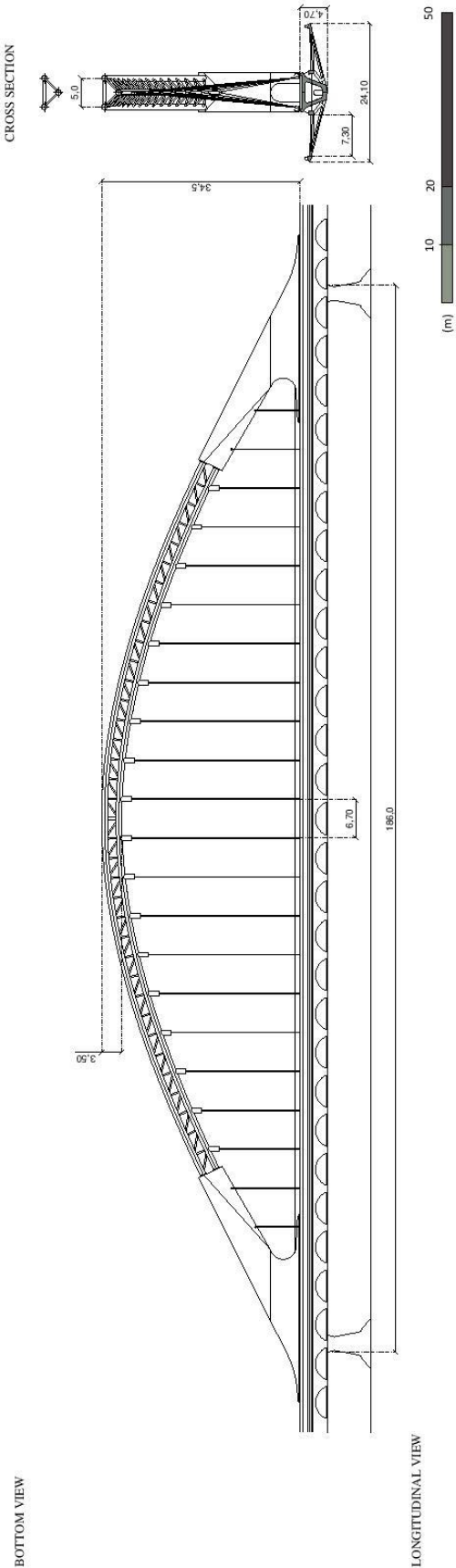
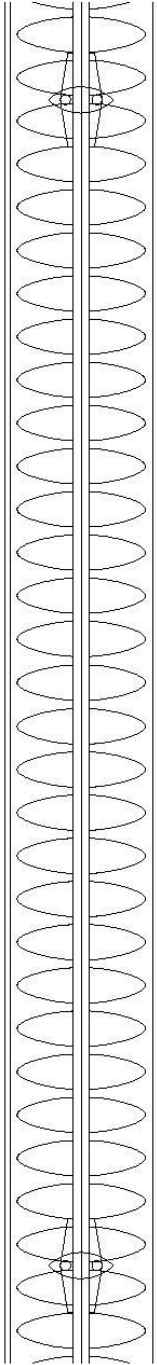
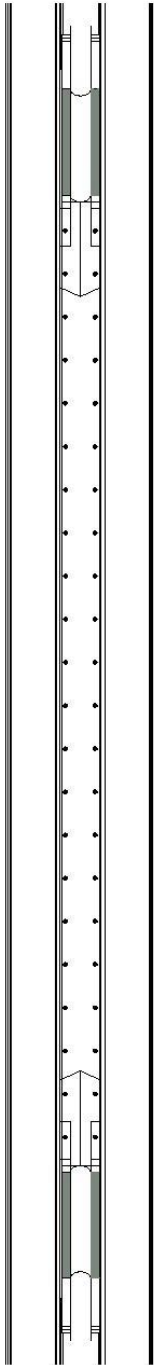
The Lusitania's generous dimensions are dictated by the width of the Rio Guadiana, and both the 139 m side spans are dominated by a 34 m deep central steel arch spanning 189m. Being conceived as an integral structure, the bridge does not make use of expansion joints. Bridge central load bearing element is deck box girder, supporting loads from dual carriageways along each side; it's a torque tube, made of post-tensioned and pre-cast concrete elements. Bridge loads are delivered to two reinforced concrete piers, 45m-spacing. Within the central portion, deck box girder is supported by steel tied arch through 23 couples of cables. Deck pre-stressed wings (Fig. 4.8) support the carriageways, cantilevering from the 4.5m deep concrete box girder. The upper surface of the box girder serve as a 5.5m wide pedestrian and cycling passage, raised centrally above carriageways, through concrete support which were designed as portals for the arch. This upper walkway guarantees an unhindered view of the whole landscape.

One of the most interesting and controversial aspect is the use of steel truss arch which spans upon the central portion (131m), connected to reinforced concrete abutments. These one rises 29m above deck, before joining to the arch, which is made of three steel tubulars, transversely connected. Cable system is fixed to lower tubular element, being anchored on each side of central pedestrian portion, in order to allow users passage. Carriageway loads are transferred, through central girder concrete supports, from cables to steel arch, till being unloaded to concrete abutments and lower piers. Thanks to this system (similar to Haupt one, 1948), the effect of loads, asymmetrically acting into transverse direction, is carried by the central box girder, which bears torsional effects independently: through cable system, arch carries only vertical forces. (Fig. 4.11)

**Fig. 4.11** Lusitania Brigde (1988-91)\_ (a) longitudinal view\_ (b) deck bottom view



Lusitania - Merida (SPA) - SS arch bridge - 1988 - 1991







A completely different approach is used by Calatrava in designing Campo de Volantín Bridge (Fig. 4.12) (Tab.4.4). It provides a strikingly modern pedestrian crossing of the Neruion River estuary, midway between Bilbao's Parque Etxabarria and City Hall and the Guggenheim Museum Bilbao. In 1990, Calatrava created a design for what was then known as the Uribitarte Bridge site, on behalf of a client engaged in an exchange of land with the Municipality of Bilbao. The present design was commissioned in 1994 by a new client — the local government — which was sympathetic to the original idea of making an urban statement but wanted to avoid any association with the project's previous circumstances.

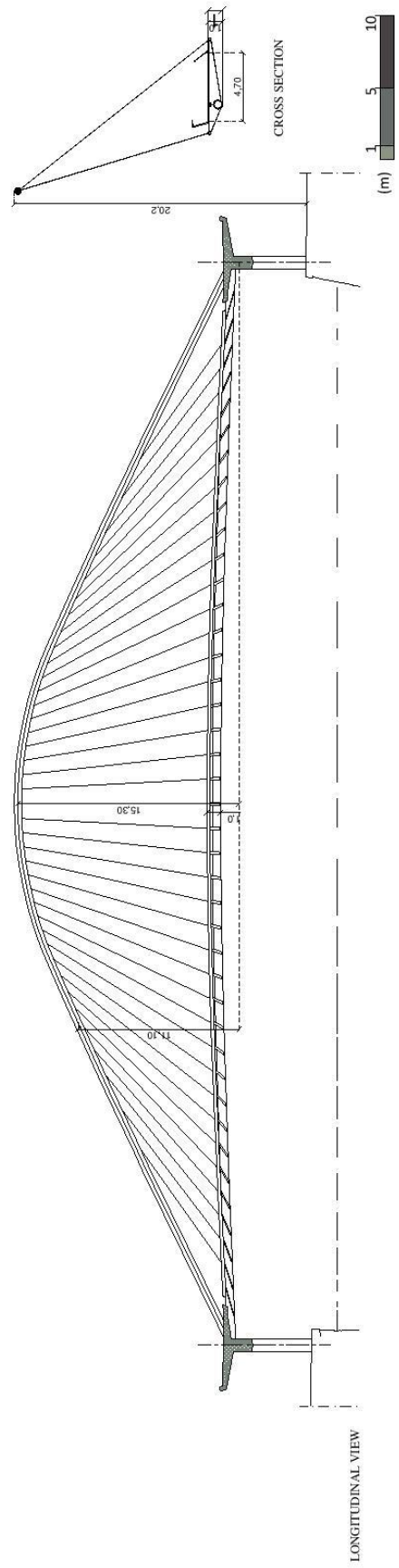
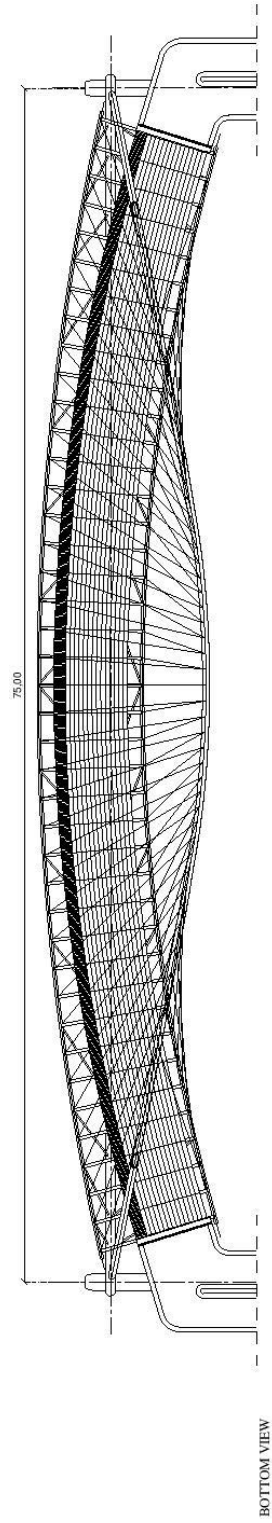
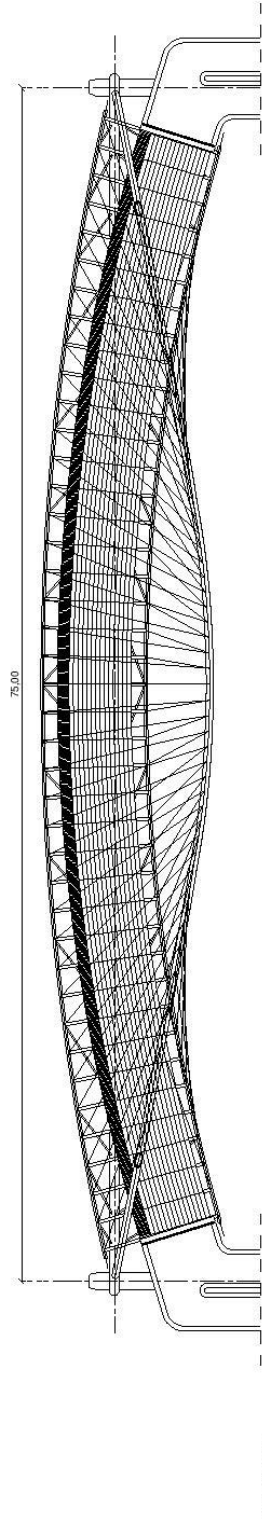
This footbridge could be considered the first example of how Calatrava's design approach is evolved. Since the beginning, this bridge has been characterized by 80° inclined steel arch, 14.5m -rise, with a concrete prefabricated deck. The first proposal consisted of 11-sharp-like tension arms forming suspension system: working as pendulums, these ones were hinged at the arch, spanning 6m one from the other ( $ip/L = 8\%$ ). Final solution (Fig.4.13) completely changes suspension system. Stiffened tension arms have been replaced by cable system; upwards converging, cables, as well as deck cross sections, are 1.5m spaced ( $ip/L = 2\%$ ). Greatly reducing space between cross elements, longitudinal girders are nearly denied: losing their main load bearing function, these ones need only to carry arch thrust, increasing cross section stiffness against torsional effects. The final design (1994) appears more slender and elegant than the previous one, showing a pronounced juxtaposition of material.

<b>L (arch) [m]</b>	75,50	<b>ip [m]</b>	6,00
<b>arch rise (r) -to L</b>	1/5,20	<b>ip/L</b>	3,10%
<b>h (girder) [m]</b>	1,20	<b>hg/L</b>	1,30%
<b>h (arch) [m]</b>	0,50	<b>ha/L</b>	0,60%

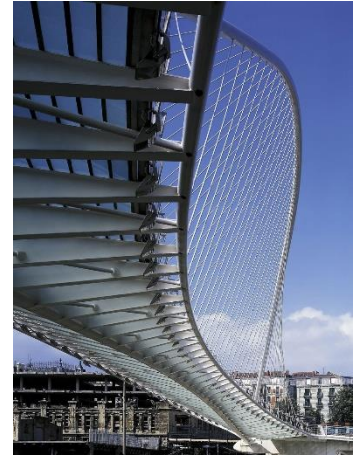
**Fig. 4.12** Campo de Volantín Footbridge (1994-97),  $L_{tot}=L_{arch}=75.5m$ ; rise= 14.5m;  $r/L= 1/5.20$ ;  $ip/L= 3.1\%$ ;  $ha/L= 0.6\%$ ;  $ht/L= 1.3\%$

**Tab. 4.4** Campo de Volantín Footbridge (1994-97), design parameters

Campo de volantin - Basilea (SPA) - 1994 - 1997







The transparency of glass, also used for structural elements, is well combined with concrete abutments heaviness. Its sweeping parabolic form is anchored in the plan of the glass-surfaced deck, giving the bridge a pronounced contrast of materials. The translucent deck has a tighter radius than its supporting cradle, which is reinforced by an inflected steel tube. The tube, placed at right angles to the embankment, is audaciously carried by concrete arms that extend from the approach structure. If Campo de Volantin Bridge (Fig. 4.12) marks the beginning of a new approach in design arch bridge. Assuming a load bearing structural system similar to Haupt's one, as in the case of Lusitania Bridge (Fig. 4.10), the choice of thickening suspension system, adopting a single plane of cable which connects the upper arch to a box girder section, guarantees a slender deck solution in the case of Ponte Centrale (Reggio Emilia).(Fig. 4.15)

In October, 2007, an ensemble of three bridges designed by Calatrava was inaugurated in Reggio Emilia, near Bologna in Italy. These bridges are the first phase of a larger project, which will includes a new high-speed railway station and other infrastructure improvement program. Plans for the bridges originated in 2002 when the city of Reggio Emilia invited Calatrava to design a new train station "Stazione Mediopadana" for the TAV (Treno Alta Velocità) highspeed railway line between Milan and Bologna. (Fig. 4.14)

**Fig. 4.13** Campo de Volantin Footbridge (1994-97), final solution\_ (a) (b) deck upper view\_ (c) deck bottom view

**Fig. 4.14** Caltrava's bridges in Reggio Emilia , A1 Highway (Autostrada del Sole) (2002-2007)





**Fig. 4.15** Ponte Centrale (Reggio Emilia) (2002-2007)  
 $L_{arch}=221\text{m}$ ;  
 $r_{rise}=46\text{m}$ ;  $r/L= 1/4.8$ ;  
 $i_p/L= 1.6\%$ ;  $h_a/L = 0.7\%$ ,  $h_{girder}/L= 1.2\%$

In addition, he was also commissioned to create a master plan for the city's outskirts — a fragmented area called Mancasale —, to improve vehicular access and provide an impressive new gateway from the north.

Calatrava's plan called for integrating the station with three new bridges, designed to connect the Autostrada del Sole (A1) to the city by way of a tree-lined avenue, Viale Trattati di Roma, including a highway toll station for cars leaving the Autostrada. The central bridge has a single symmetrical arch, which rises to a height of 46m and spanning 221m over the highway and railway line. Suspended from the arch by radially-placed cables is a steel box-girder, which cantilever beams project 9.75m at an intervals of 3.5 m. The 25.6-m wide box-girder supports the roadway and accommodates four automobile lanes and two lanes for bicycles and pedestrians, one in either direction. (Tab.4.5) Having a single central plane of cables, it was necessary to use a deck cross section with a high torsional stiffness: so deck has been designed with a central hollow box section, while cantilever ribs span from its edges to carry road deck. Its high torsional stiffness guarantees a reduction of arch stress, giving the possibility of reduce its size: it has to carry only axial forces, being strictly sized to counter buckling effects. The great number of cross sections (as vertebrae of spine), directly loaded by the upper orthotropic deck, as well as the deep-closed cable spacing, led to streamlining and simplifying longitudinal girder.

**Tab. 4.5** Ponte Centrale (Reggio Emilia) (2002-2007) design parameters

<b>L (arch) [m]</b>	221	<b>ip [m]</b>	3,50
<b>arch rise (r) -to L</b>	1/ 4,80	<b>ip/L</b>	1,60%
<b>h (girder) [m]</b>	2,70	<b>hg/L</b>	1,20%
<b>h (arch) [m]</b>	1,45	<b>ha/L</b>	0,70%

Directly to the South and North are other two bridges over the roundabouts and highway access roads. These bridges are 179m long and 13.6-meter m wide and provide one traffic lane in opposite direction. 26 cable-stays supporting the roadbed are arranged strikingly in the shape of a hyperbola.



According to Calatrava's design approach, Ponte della Costituzione shows his capability to create extraordinary structures. He designs a segmental arch spanning 80.81m, whose high thrusts are absorbed by a deep foundation system made of diaphragms, also capable to minimize soil subsiding. As for other works, such as Bach de Roda Bridge (1985-87), Oudry- Mesly Bridge (1985-87) or Campo De Volantin Bridge (1994-97), Calatrava tries to lighten bridge structure, increasing deck slenderness, thanks to the adoption of low spacing cross sections.

Looking for a compromise between the need to guarantee clearance for passing boats with Venetian bad soil conditions, in order to create footbridge without piers along the rivers, arch bridge has been the most commonly used: for this typology Calatrava has been capable to make a significant technical revolution. In the case of Ponte della Costituzione (Appendix B) (Tab. 4.6), instead of the typical deck arch solution, he uses a pure arch bridge, without any filling materials between the load bearing structure and the pedestrian walkway. Dividing the main arch into 73 closely spaced sections, Calatrava is capable to leave out the longitudinal girder; so that the floor is supported directly by a slightly sloping central steel arch. In order to create a work of art, capable to enhance the historical and cultural prestige of Venice, for Ponte della Costituzione Calatrava involves the latest results of his innovative design approach: led by a constant research for technological experimentations, he often tries to optimize element dimensions, creating slender *dynamic structures*, which give visitors the idea of "frozen motion", as if it could have been captured acting displacement. Partially evoking naturalistic as well as anthropomorphic forms, the Valencian artist uses a hybrid material solution, made essentially by steel elements.

**Fig. 4.16** Ponte della Costituzione, Venice (IT), 2001 - 2007, S. Calatrava.  $L = 80.80\text{m}$ ;  $r/L = 1/14$ ;  $i.p/L = 1.3\%$ ,  $ha/L = 2.5\%$ .





**Tab. 4.6** Ponte della Costituzione (2001-2007) design parameters

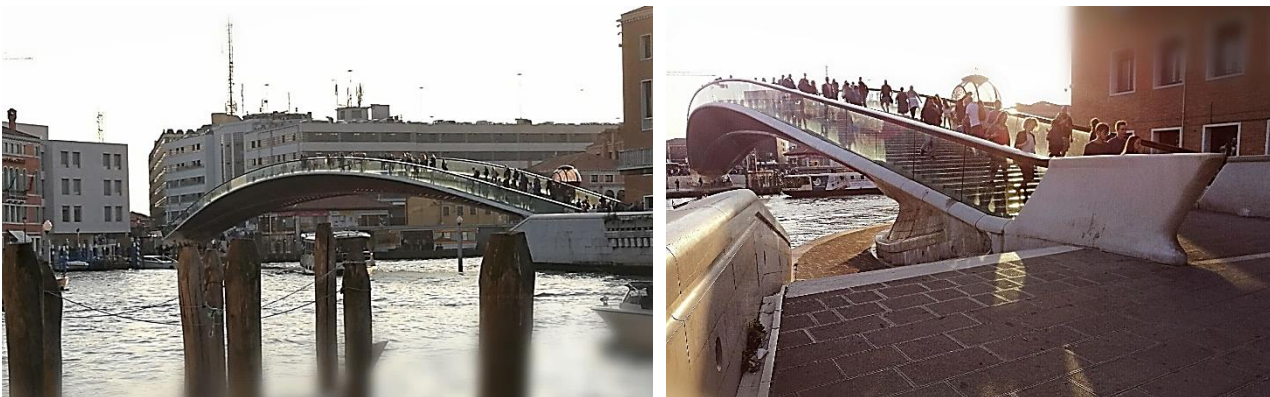
<b>L (arch) [m]</b>	80,80	<b>ip [m]</b>	0,60
<b>arch rise (r) -to L</b>	1/14	<b>ip/L</b>	1,36%
<b>h (arch) [m]</b>	2.08	<b>ha/L</b>	2,50%

Proposing a global view, similar to the Palladian one adopted for Rialto Bridge, Calatrava reveals the intention of including his design in a general planning of urban reorganization: underlying the necessity to guarantee also aesthetic qualities to the structure, the Valencian artist makes his bridge a landmark capable to grab people's attention with its unique feature, increasing urban contest prestige, without being redundant or inappropriate.

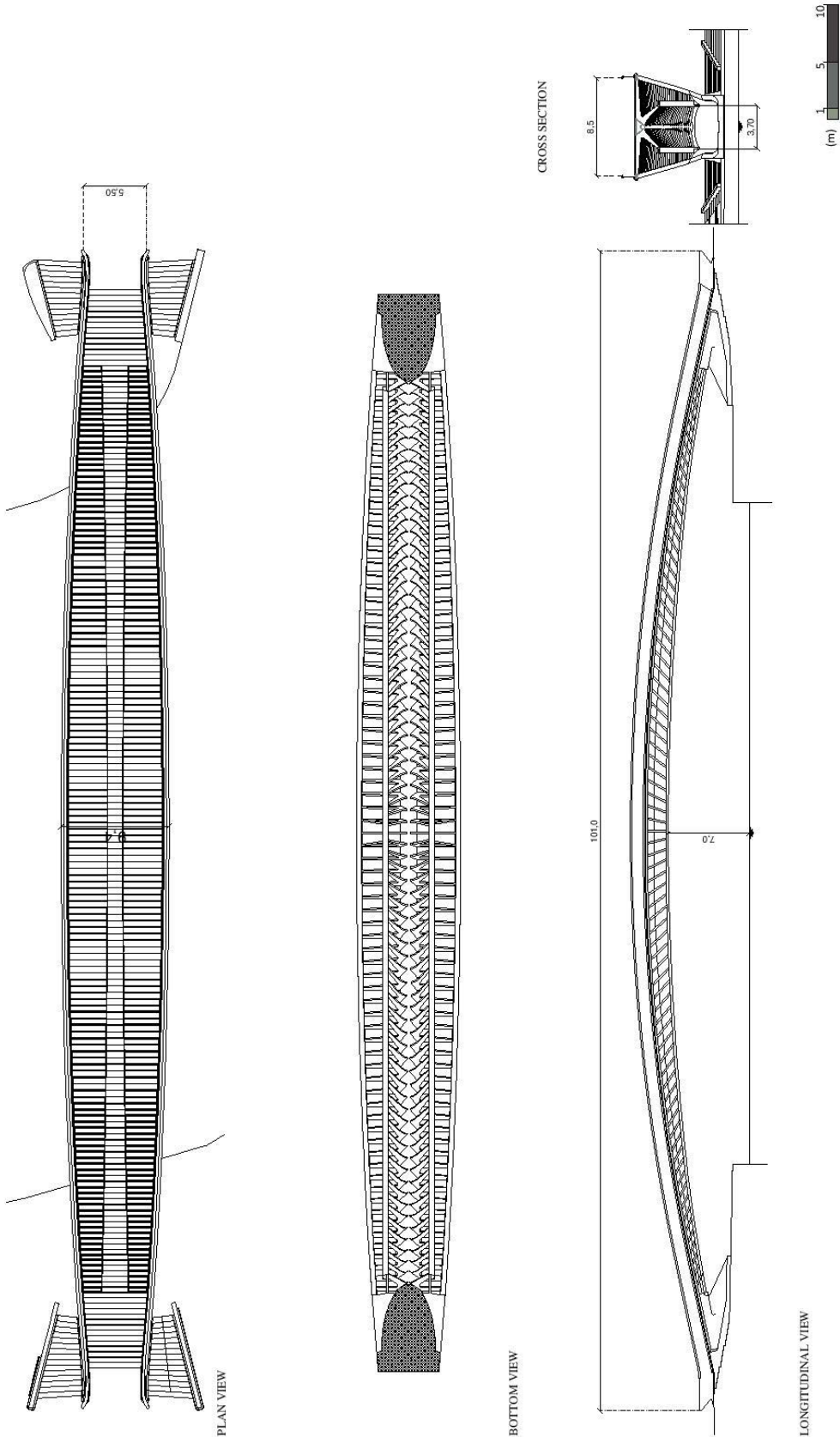
The structural solution includes a bridge spanning 81m over Canal Grande. Its deck overall length is about 93m; it has a variable width, from 6.43m at the abutments to 9.04m at middle span; the arch is characterized by a variable section, with a deck depth changing between 1.70m to 2.08m. To give an idea of the arch geometry, interesting parameters are: (a) rise(r) to span ratio (L):  $r/L = 1/4$ ; (b) cross section spacing (i.p.) to span (L) ratio:  $i.p./L = 1.2$ , corresponding to a partialization of bridge deck in a great number cross section; (c) the span square to rise ratio  $L^2/r = 930$ : known as “static coefficient”, value which characterizes segmental arch, proportionally to its thrust. The value of static coefficient valued for Ponte della Costituzione is six times greater than the one estimated for Ponte degli Scalzi ( $L = 40m$ ,  $r = 6.75m$ ,  $L^2/r = 238$ ); it is very large if we consider that the maximum has been reached with  $L^2/r = 3136$  for the Infant Dom Henrique Bridge ( $L = 280m$ ,  $r = 25m$ , designed by Adão da Fonseca, 2007).

Dematerializing longitudinal truss, Ponte della Costituzione doesn't require secondary load-bearing structures, being built as a “pure” arch. (Fig. 4.17) In this way Calatrava is capable to improve Miozzi's previous solution: the broken line, a three- stretch polygonal which characterized Ponte degli Scalzi, has been divided in a so huge number of sections to be approximated to a continuous arch; at the same time, thanks to the low section spacing, glass floor with anti-skid surface ( $t = 3 \times 10 + 12 = 42 \text{ mm}$ ) can be used, together with traditional Istrian stones

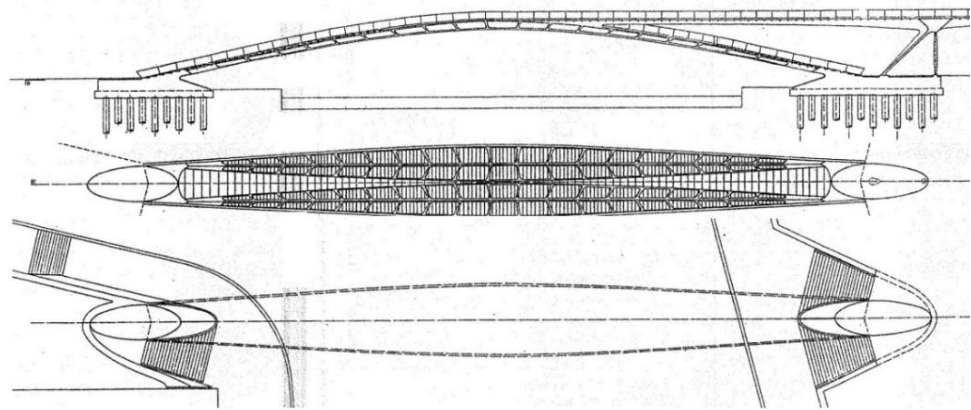
**Fig. 4.17** Ponte della Costituzione, Venice (IT), 2001 – 2007)\_ (a) longitudinal view\_ (b) abutment detail



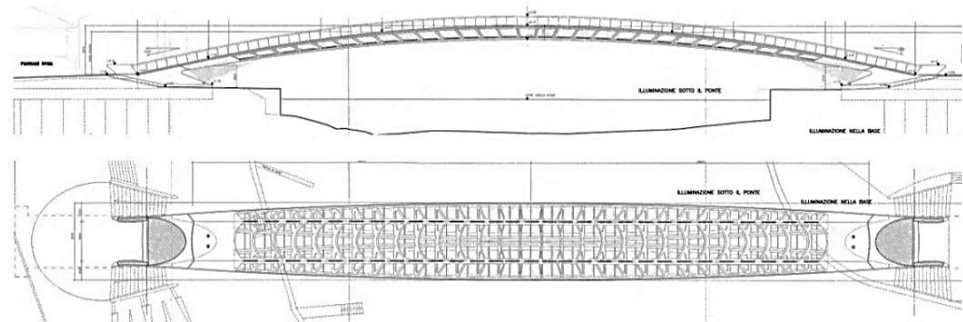
La costituzione - Venezia (ITA) - arch bridge - 2001 - 2007



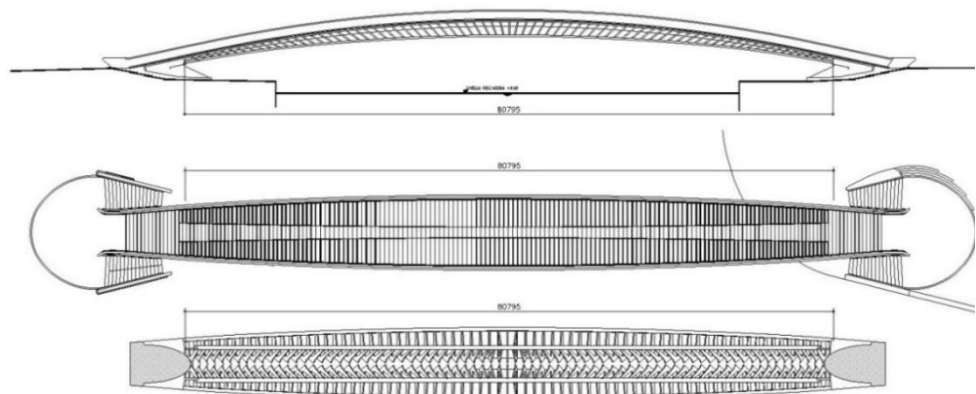
The following design steps show a progressive increasing of cross section number, passing from 21 of Preliminary design, to 32 of Final one, until 73 different cross sections for Executive project; in this way the spacing-to-span ratio ( $i.p./L$ ) is reduced from 4.7% to 3.1% till 1.3%. Thanks to this arrangement, Calatrava can limit structural element sizes, reducing the two trusses of preliminary design into a single torsionally rigid central arch; he adopts a 2m high cross section, lowering arch slenderness to 1/40 of its span.



*Preliminary design ( $i.p./L=4.7\%$ ; 21 sections)*



*Final design ( $i.p./L=3.1\%$ ; 32 sections)*



*Executive design ( $i.p./L=1.3\%$ ; 73 sections)*

### 4.3 Caltrava's experience in rigid tension arm suspension system

Calatrava has given an extraordinary contribution also to rigid suspension system, above all in the way he counteracts buckling effects although using extremely slender arches. As creating urban sculptures, each structural component reaches plastic characterization, easily making perceivable bridge load transferring system.

Flow of forces is clearly evident even for casual observers in the case of *Puerto Bridge* (Fig. 4.18) (Tab. 4.7). This is Calatrava's the first example of tied arch bridge having stiffen suspension system; it directly derives from Larger and Haupt's systems: using the bending stiffen girder which characterized the first, and the continuous box section adopted by the second, Calatrava designs a plastic shape structure, capable to carry bending and torsional effects due to acting loads.

Commissioned by the Municipality of Ajuntament de la Ondarroa, the bridge relieves Ondarroa town from heavy harbor traffic and its walkways offers pedestrians new opportunities to enjoy the formerly interrupted waterfront. An asymmetric steel arch separates the box girder carriage deck from the curved, cantilevered pedestrian deck. The constant width steel arch and suspension cables mark the southern edge of the road deck on the landward side, while steel stiffeners project from the seaward side of the curved pedestrian deck, reaching up to the thrust of the arch. At first glance, this asymmetric arched bridge appears to represent a further investigation by Calatrava into the inclined arch principle. Closer inspection reveals that the arch and suspension cables in fact conform to a vertical plane. Only the stiffeners are inclined to define the curve of the pedestrian deck. The overall minimum width of the deck area is 20.9m reaching 23.7 m at its mid-point.

<b>L (arch) [m]</b>	71,50	<b>ip [m]</b>	3,20
<b>arch rise (r) -to L</b>	1/ 4,70	<b>ip/L</b>	4,10%
<b>h (girder) [m]</b>	4,00	<b>hg/L</b>	5,10%
<b>h (arch) [m]</b>	0,70	<b>ha/L</b>	0,90%

**Tab. 4.7** Puerto Bridge (1988-95), design parameters

**Fig. 4.18** Puerto Bridge (1988-95),  
Larch=71.5m; rise=15m; r/L= 1/5; ip/L= 4.1%; ha/L= 0.9%; ht/L= 5.1%





Puerto Bridge is the first example of rigid tension arms suspension system. Resulting from Langer and Haupt systems (Fig. 4.19): being characterized by a deck system with a high bending stiffness as in Langer system, adopting a rigid box cross section as in Haupt's solution, this structure is capable to carry bending moments due to vertical loads, together with torsional effects caused by sloped arch, always preserving a plastic shape. However, the co-presence of rigid and flexible suspension system in Puerto Bridge, reveals that the system adopted by Calatrava was still in development.

**Fig. 4.19** Comparison between suspension systems

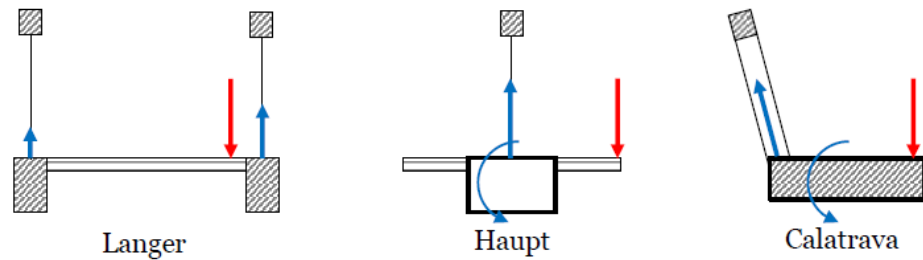


FIGURA 33 - CONFRONTO FRA I TRE SISTEMI DI SOSPENSIONE

A quite similar suspension system is used for *La Devesa* Bridge (Tab. 4.8) (Fig. 4.20). Commissioned by the Ajuntament de la Comtal Vila de Ripoll, north of Barcelona in the Pyrenees, it was designed in 1989 and realized between August 1990 and July 1991. This pedestrian bridge accommodates a height difference of 5 meters. An inclined steel arch spanning 44m is employed to carry the loads of the walkway from the existing retaining wall across to a new concrete pylon — a total distance of 65m. Suspension system is made of steel tension arms: lying within the plane of 6.5m-deep arch, these ones take the walkway load. The arms are canted at an angle of  $65^\circ$ , so that their tension includes both horizontal and vertical components. Looking at the inclined arch (Fig. 4.21), asymmetrically placed, the weight of the wooden deck is not concentrated beneath the arch: this should lead to a rotation of the deck together with the tension arms.

**Fig. 4.20** La Devesa Footbridge, (1989-91),  
 $L_{tot}=65\text{m}$ ;  
 $L_{arch}=42.8\text{m}$ ; rise=  
 $6.5\text{m}$ ;  $r/L=1/6.5$ ;  $ip/L=$   
 $61\%$ ;  $ha/L=0.6\%$ ;  
 $ht/L=1.4\%$







This rotation is prevented by the torque of the tubular spine of the bridge, which collects torsion at each strut and delivers it to the springing points: the pylon and the retaining wall. The tension arms brace the plane of the arch, preventing it from buckling. As gravity loads tend to deflect both walkway and tension arms, the arch is displaced to a more vertical position, slightly stiffening it and protecting it against buckling. Deck bending effects are carried by the steel central tubular, while the cross truss which lies under wooden deck, prevent from distorting laterally. As gravity loads tend to deflect both walkway and tension arms, the arch is displaced to a more vertical position, slightly stiffening it and preventing any buckling effects. Looking at the following design parameters, it seems that torsional stiffness gives them the possibility to make structural elements slender, optimizing element size

<b>L (arch) [m]</b>	42,80	<b>ip [m]</b>	2,55
<b>arch rise (r) -to L</b>	1/6,50	<b>ip/L</b>	6%
<b>h (girder) [m]</b>	0,60	<b>hg/L</b>	1,40%
<b>h (arch) [m]</b>	0,25	<b>ha/L</b>	0,60%

La Devesa reveals Calatrava's capability to use static rules, giving each element a specific role to define bridge static behaviour. Inclined tension arms make suspension system of *Alameda Bridge*. (Tab. 4.9) (Fig. 4.22) (Fig. 4.23)

**Fig. 4.21** La Devesa Footbridge,(1989-91)\_  
(a) Inclined arch\_ (b) wooden deck bottom view

**Tab. 4.8** La Devesa Footbridge,(1989-91)  
design parameters

**Fig. 4.22** Alameda Bridge (1991-95),  
Ltot=163m;  
Larch=130.8m; rise=14m;  
r/L= 1/6.5;  
ip/L=4.4%; ha/L=0.6%; ht/L= 1.4%





**Fig. 4.23** Alameda Bridge (1991-95)\_arch detail

With a total length of 163m, its arch span 130m above River Turia (Valencia) to connect the university district in the north with Valencia's old town off the southern banks, thus providing an all-important pedestrian crossing point for the area. A subway station, aligned on the same longitudinal axis directly below the bridge was constructed at the same time. The steel bridge structure employs an arch inclined at an 70-degree angle, made up of two basic tubes of constant yet different diameter, joined by regularly-spaced welded webs. To ensure the stability of the offset arch, rigid tension arms are placed at regular intervals of 5.84m. The vehicle deck, comprising of four consecutive cells is designed for maximum rigidity, while the pedestrian decks are cantilevered off to each side.

**Tab. 4.9** La Alameda Bridge (1991-95)\_design parameters

<b>L (arch) [m]</b>	130	<b>ip [m]</b>	5,84
<b>arch rise (r) -to L</b>	1/10	<b>ip/L</b>	4,40%
<b>h (girder) [m]</b>	2,85	<b>hg/L</b>	2,10%
<b>h (arch) [m]</b>	0,80	<b>ha/L</b>	0,60%

The white painted structure forms a gentle curve over the piazza-like roof of the Alameda subway station. Externally, the subway is now expressed only as a paved and translucent-glass surface, punctuated by a series of protruding, angled skylights. The approaches to the subway are from either side of the embankment, via ramps and stairs that lead down to the square.

Road-deck stands upon a multiple box cross section, stiffened by internal T-shaped ribs; this characterization gives deck a high torsional stiffness, so that no bending or torsional effects act upon the arch, which is more slender than in the case of La Devesa. Requiring a single arch to span 130m, also deck plane is curved, with a low rise, giving a great scenic effect to the place.

Compared with previous examples, characterized by flexible suspension system, rigid tension arm solutions guarantee to make the upper arch slender, at the expense of a rigid deck, with a slenderness ratio no lower than 1/70.

As it can be seen in (Tab.4.10), Calatrava's attempt to deny bending effects, making his structure acting mostly in extensional regime is realized in the choice of a closed succession of deck cross sections which decomposed the longitudinal girder, always seen as bridge's main load bearing structural element.

	'85	'88	'91	'91	'95	'95	'96	'97	'03	'06	'08
	Bach de Roda	Oudry-Mesly	Lusitania	La Devesa	Puerto	Alameda	Uribitarte	C. de Volantin	J. Joyce	P. Centrale	Costituzione
$i_p/l$	5%	4%	4%	6%	4%	5%	8%	3%	6%	2%	1%
$h_a/l$	1.4%	0.7%	1.9%	0.6%	0.9%	0.6%	0.7%	0.6%	1%	0.7%	2.5%
$h_t/l$	4.1%	2.2%	2.6%	1.4%	5.1%	2.0%	1.6%	1.3%	3.2%	1.2%	0%
$h^*/l$	2.7%	1.4%	2.3%	1.0%	3.0%	1.3%	1.1%	1.0%	2.1%	1.0%	2.5%

**Tab. 4.10** Parametric synthesis of Calatrava's bowstring arch bridges

The corresponding thickening of suspension hangers allows to immediately transfer loads acting upon slender deck to the upper arch, where the short distance between cable anchorages (Fig. 4.24) (Fig. 4.25) (Fig. 4.26) allows to greatly reduce strengths in the arch. Controlling bending effects, structural element size is defined in relation to load-induced axial forces, as well as torsional effects due to eccentric load conditions or asymmetric bridge layout.

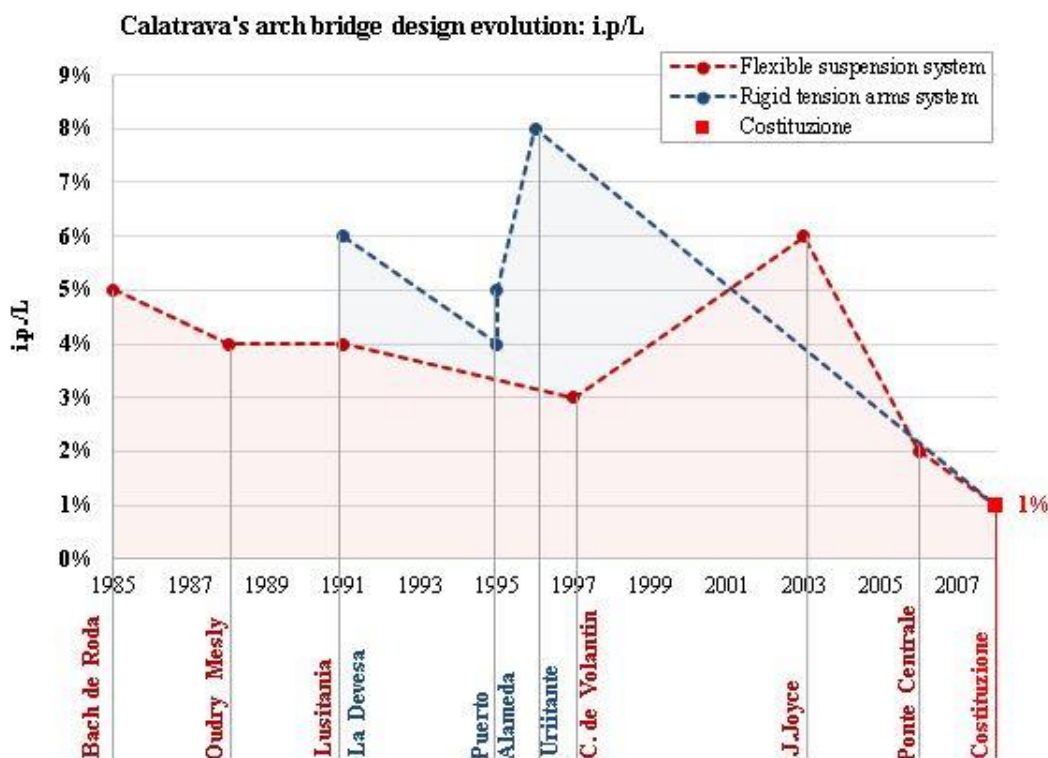


**Fig. 4.24** Parametric synthesis of Calatrava's bowstring arch bridges\_  $i_p/L$



The dynamic shapes adopted by Calatrava make more charged the problem of stability for compressed arches, above all in the case of sloped ones. If rigid tension arm suspenders help to solve it, for flexible suspension system arch buckling can be better controlled thanks to the adding stiffness that a close-spaced suspension system can guarantee.

**Fig. 4.25** Parametric synthesis of Calatrava's bowstring arch bridges\_  $h(\text{arch})/L$

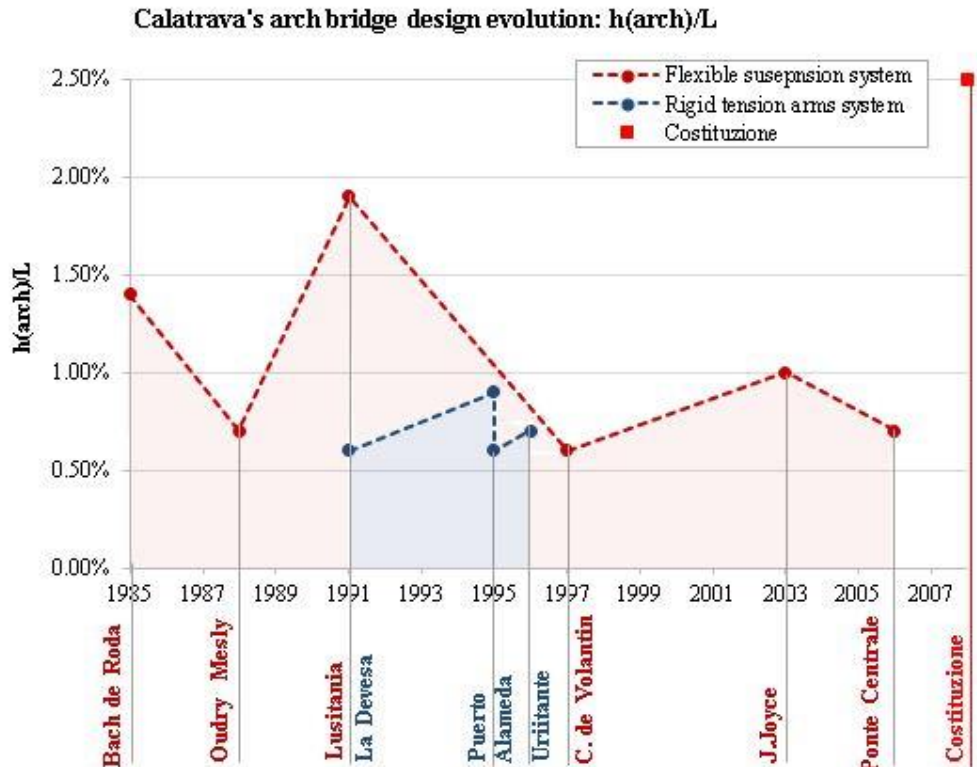
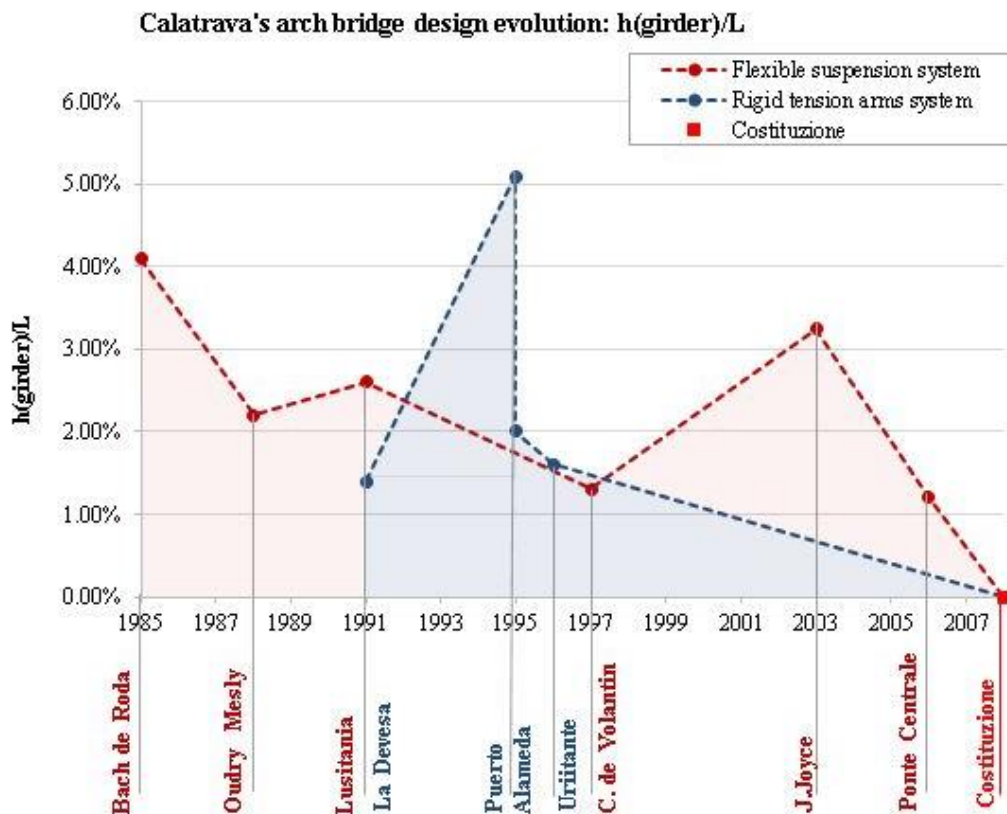


**Fig. 4.26** Parametric synthesis of Calatrava's bowstring arch bridges\_  $h(\text{girder})/L$



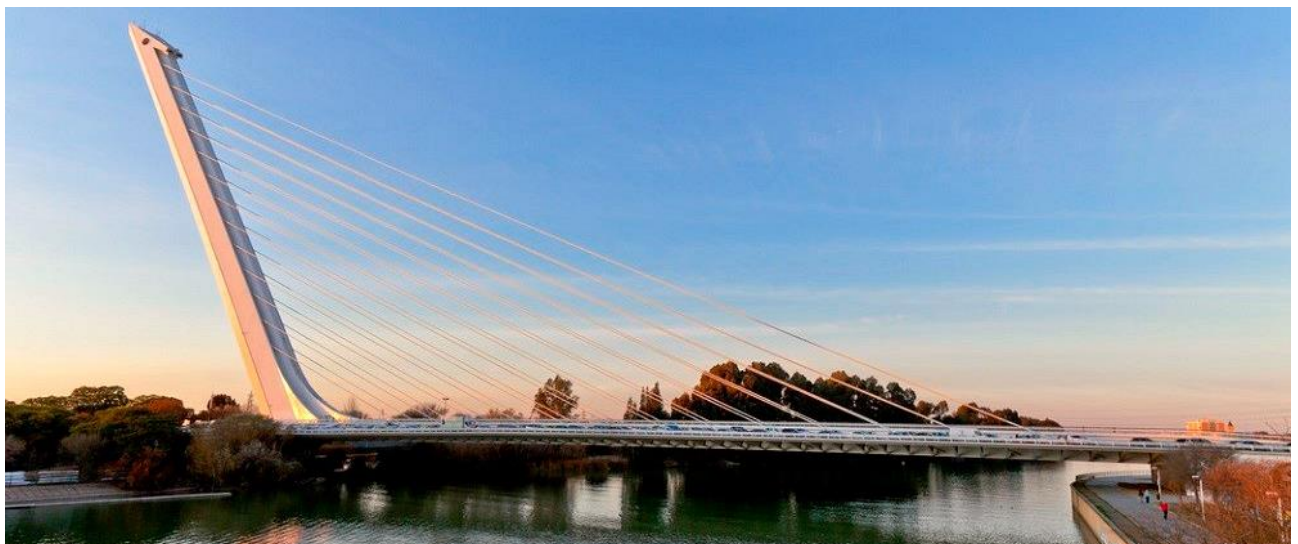
#### 4.4 Calatrava's pioneering approach in design of cable stayed bridges

The innovative approach proposed by Calatrava leads to the construction of spectacular cable-stayed bridges, with unconventional asymmetric structures. As structural type deriving from the oldest suspension bridge, cable stayed bridges (described in Chapter 5) carried acting loads via compression in deck structure, while tensile strength acts in the stays: in the case of symmetrical layout, inconsiderable bending effects occur in the pylons, bearing essentially compression forces from the forestays and the backstays equal to one another. The evolution of this structural type will reveal an improvement in their extensional regime, as well as an optimization in structural element size: this has been achieved reducing cable spacing and, consequently, increasing deck cross section number (till the lowest  $ip/L$  of 2%). This process will lead to completely change the role of deck-stiffened system: minimizing spacing between cable anchorages along the deck corresponds to reduce the effective loaded length of longitudinal elements, so the that lower compression strength requires less deep structural elements, which is to say slender deck.

In line with this modern approach, Calatrava's contribution appear revolutionary. His apparently unbalanced structures, which evoke a sense of dynamism, are governed thanks to the creation of a preventive stress condition (especially in the pylon), as it happens regularly in pre-stressed concrete structure, not only to carry compression or tensile strengths, but also to counteract bending and torsional effects, making their effect practically inconsiderable. His look like instable cable stayed bridges are extraordinary "self-tensioned" structure, whose no balanced forces or moments are absorbed directly by the structure itself.

Form this perspective, Calatrava's *Alamillo Bridge* (Seville, 1987-92) (Fig. 4.27) (Tab. 4.11) is an experimental structure: it is the first cable stayed bridge where the cable supports of the deck are counterbalanced by the sheer weight of the inclined tower, leaning back along the central axis of the bridge.

**Fig. 4.27** Alamillo Bridge (Seville, 1987-92)  $ip/L=6,75\%$ ;  $h/L=1/44$  (2.25%),  $L(\text{main span})=200\text{m}$



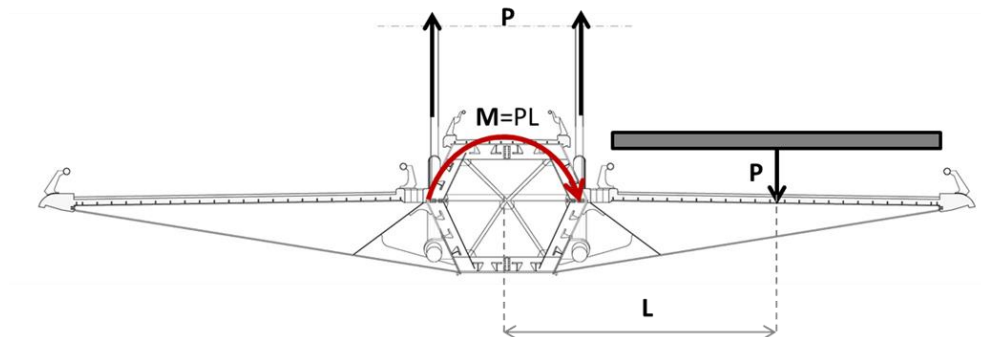


**Tab. 4.11** Alamillo Bridge (Seville,1987-92) design parameters

<b>L<sub>main span</sub> [m]</b>	200,00	<b>L<sub>tot</sub> [m]</b>	250,00
<b>n. of stays</b>	33 couples	<b>Pylon height [m]</b>	142,00
<b>h (girder) [m]</b>	4,50	<b>h/L</b>	1/45
<b>i.p. [m]</b>	13,50	<b>ip/L</b>	6,75%
<b>Deck width (w) [m]</b>	25,00	<b>w/ L</b>	1/8

This 250m long with a maximum span of 200 m is characterized toward La Cartuja Island by a pylon, 142m high and inclined 58 degrees on the horizontal. The pylon supports the bridge way with thirteen pairs of cables. Supporting 33 pair of stays, the pylon was constructed by lifting segments of the steel shell into place with a large, high-capacity crane, then welding them together and filling them with reinforced concrete. The weight of the pylon is sufficient to counter-balance the deck, and back stays are thus not required.

**Fig. 4.28** Alamillo Bridge (Seville,1987-92)\_ bending effects upon deck cross section



The bridge deck consists of a hexagonal, steel box beam spine to which the stay cables are attached. The steel wings, supporting the deck to either side, are cantilevered off this spine, whose 3.75-meter wide top side, elevated some 1.6 meters above road level, serves as an elevated footway and cycle route between the separated traffic lanes. If torsional strengths are carried by the central hexagonal box cross section, the central suspension system, which hugs the central walkway with two cable planes, bears bending effects. (Fig. 4.28) (Fig. 4.29)

**Fig. 4.29** Alamillo Bridge (Seville,1987-92)\_ (a) bridge deck bottom view\_ (b) deck upper view



Alamillo - Siviglia(SPA) - Cable-stayed - 1987-1992

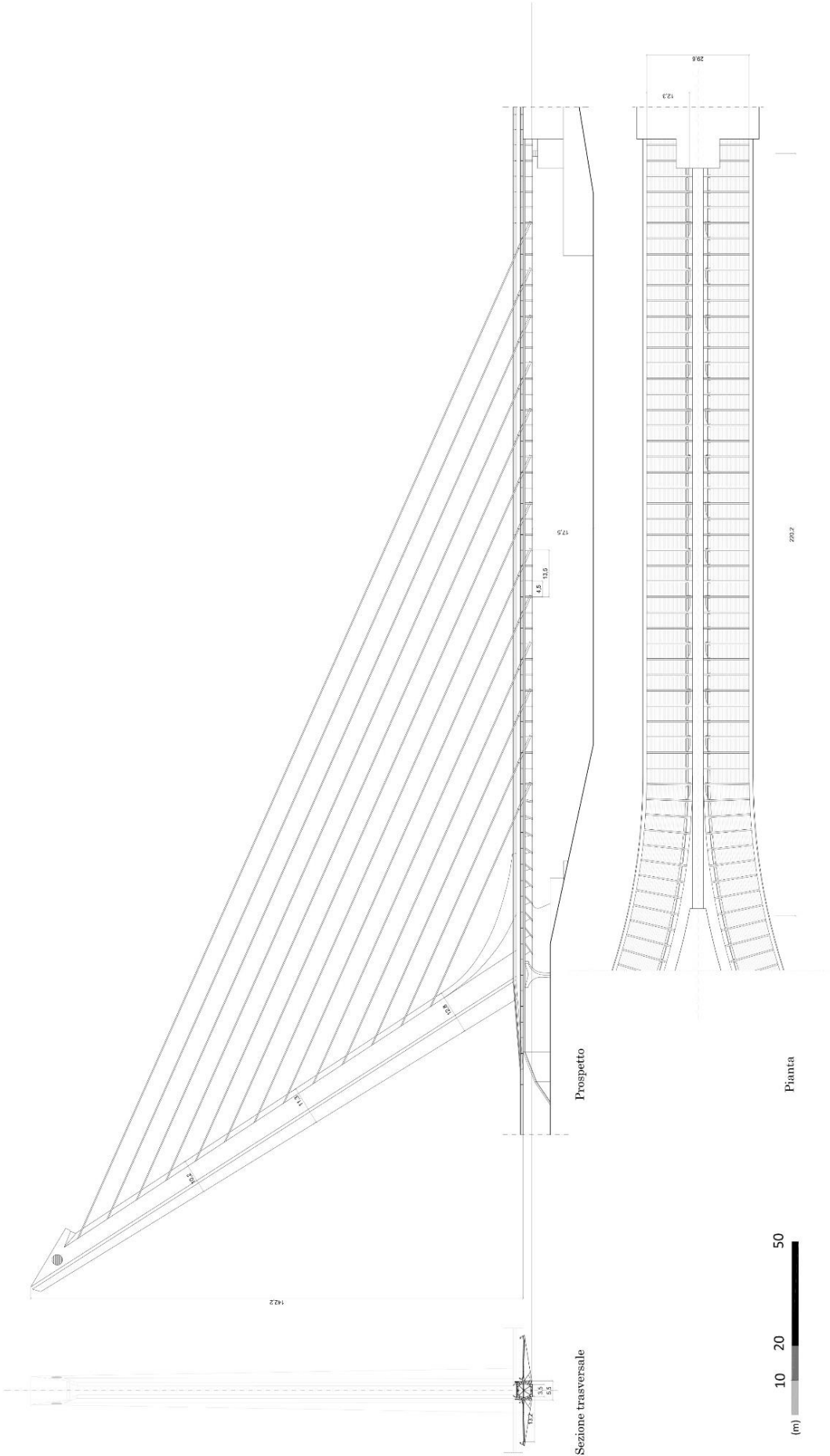




**Fig. 4.30** Trinity Footbridge (Manchester, 1993-95)\_  $L(\text{main span})=54,00\text{m}$ ;  $ip/L=4,20\%$ ;  $h/L=1/78$

In this case, the process of unpacking deck stiffened system in a deep-close spaced succession of transverse cross section (“vertebrizzazione”), as it has been seen firstly for Oudry-Mesly Bridge, is quite stymied by the imposing structure: it requires a high torsional stiffness, having to carry two lateral cantilevered portions. If the main girder is divided into 15 portions, in a shorter number than that of cable anchorages along the main girder, loads acting upon cantilevered beam are not transferred directly to pylon through stays; they are strained through central box section, then transmitted by cables to the sloped tower. The most innovative aspect of this bridge is the use of a pre-stressed structure, capable to take advantages from effective material properties. The asymmetrical cable-stayed *Trinity Footbridge* (Manchester, 1993-95) (Fig. 4.30) (Fig. 32) (Tab. 4.12) that sweeps dramatically across the River Irwell from Salford to central Manchester is another interesting work by Calatrava. Taking its name from nearby Trinity Church, the footbridge is flanked by two traditional stone-arch motor bridges. Trinity Footbridge is a single straight deck over the river supported by a 41m vaguely cigar-shaped pylon on the north bank, all painted white. The deck forks at the pylon, becoming two curved ramps that fit smoothly into the surrounding landscaping. A network of cables and back stays, starting from varying but regular points on the pylon, supports the deck and ramps. The pylon is angled away from the river (62 degrees) in order to reduce the axial forces in the structure. It has a wall thickness of 40mm and a diameter of 550mm at the base and 1.2m at the anchor point of the second-lowest cables. It rests on a 5m high reinforced concrete pillar inclined at the same angle, founded on piles.

**Tab. 4.12** Trinity Footbridge (Manchester, 1993-95) design parameters

<b><math>L_{\text{main span}}</math> [m]</b>	54	<b><math>L_{\text{tot}}</math> [m]</b>	78,50
<b>n. of stays</b>	2 x 8couples	<b>Pylon height [m]</b>	41,00
<b><math>h</math> (girder) [m]</b>	0,70	<b><math>h/L</math></b>	1/78
<b>i.p. [m]</b>	4,50	<b><math>ip/L</math></b>	4,20%
<b>Deck width (w) [m]</b>	25,00	<b><math>w/L</math></b>	1/77

Trinity - Salford (ING) - 1993 -1995

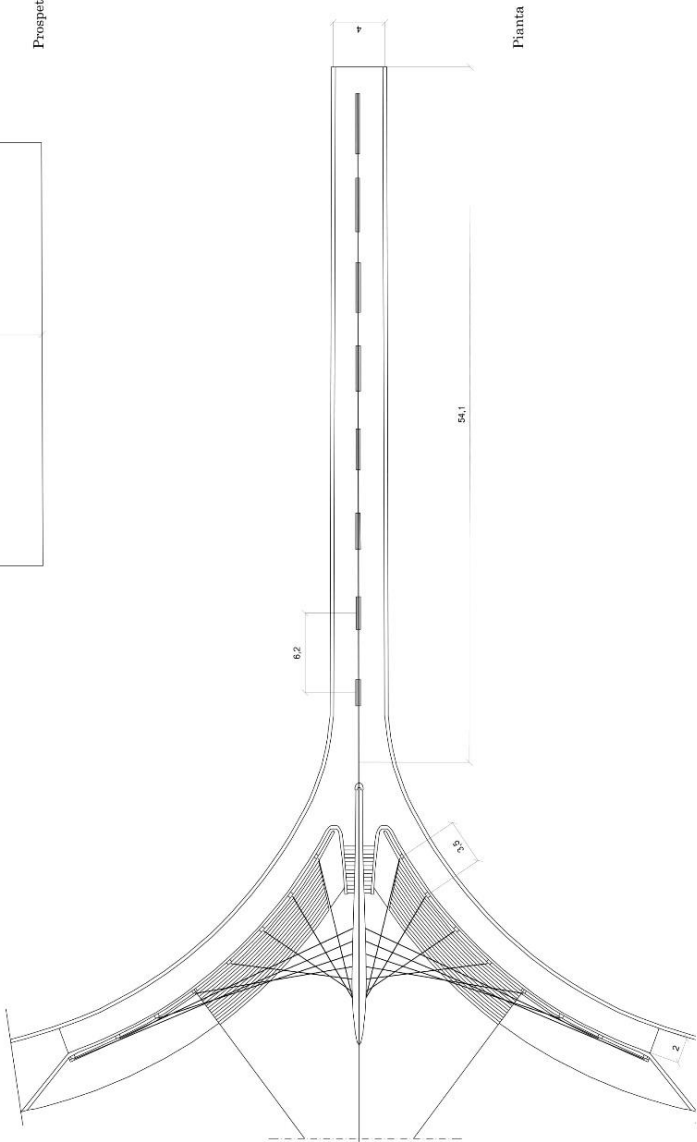
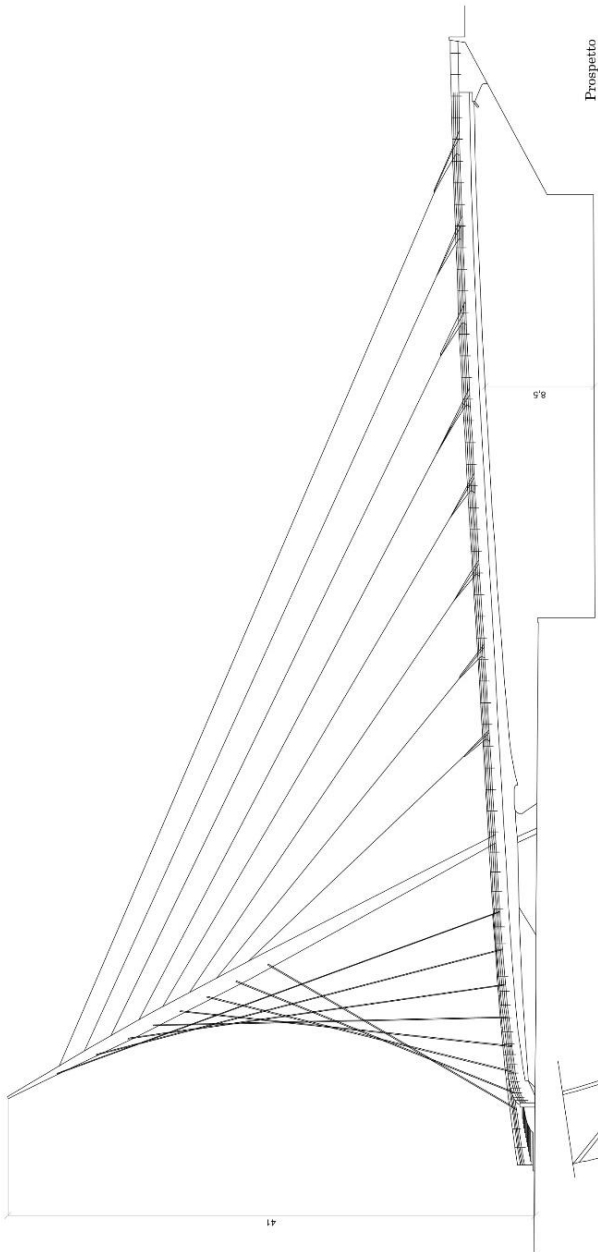






**Fig. 4.31** Trinity Footbridge (Manchester, 1993-95)\_ (a) deck bottom view\_ (b) longitudinal view

The bridge is 78.5m long overall with a 54m river span. The main deck is a triangular section box girder and slopes up 4 degrees towards the south to accommodate the 5m height difference between the two banks. The main cable array consists of eight 30mm diameter cables at angles of between 16 degrees (lowest) and 39 degrees (highest). Their upper anchorages are recessed into the pylon and were welded in place before pylon assembly was completed. The two sets of back stays are also 30mm diameter cables and are designed to resist the horizontal forces from the deck cables. At the ends of the decks are steel tie-downs, stressed to 200 tonnes, which tension the cables.

The bridge key feature is the cable geometry with a un-conventional arrangement on the main span paired with two hyperbolic crossed fans on the twin back spans, each of which curves away from the main bridge deck: these two cable clusters make the inclined pylon stable in the transversal plane, also acting as back stays which equilibrate this dynamic system.

Combining the principle of “vertibrizzazione” to the choice for dynamic shapes capable to revalorize the surrounding contest, Calatrava’s masterpiece in cable stayed bridge design is nowadays considered the *Bridge of Strings (light rail train) Jerusalem (2002-2008)* . (Fig. 4.32) (Tab. 4.13). It is located near the main entrance to the city, near the Central Bus Station. It was built to carry Jerusalem's future light rail lines across a dense urban area, resolving traffic and pedestrian issues, and to create a new landmark for the entrance to the city. To accommodate this difficult site, Calatrava suggested a cable-stayed bridge with a single inclined pylon rising above the urban surroundings. (Fig. 4.33) The bridge deck itself spans over the busy traffic intersection of Shazar Blvd., curving in an elegant s-shape from Jaffa Rd. to Herzl Blvd. This free-spanning structure clears the way for a public plaza below and permits easy pedestrian crossing of the main traffic junction.

**Tab. 4.13** Bridge of Strings (light rail train) Jerusalem (2002-2008) design parameters

<b>L<sub>main span</sub> [m]</b>	160,00	<b>L<sub>tot</sub> [m]</b>	360,00
<b>n. of stays</b>	2 x 33 couples	<b>Pylon height [m]</b>	118,00
<b>h (girder) [m]</b>	3,61	<b>h/L</b>	1/75
<b>i.p. [m]</b>	3,00	<b>ip/L</b>	1,85%
<b>Deck width (w) [m]</b>	13,00	<b>w/ L</b>	1/12





The slender and streamlined triangular-shaped steel box of the pylon is inclined backwards to show visible tension, as well as create a clear visual direction towards the city. The cables are arranged in a parabolic shape, which develops three-dimensionally in space, thus amplifying the impressive visual impact unique to this bridge. Overall the strings and form of this structure suggest a giant harp - the harp of King David as a symbol of the holy city - inspiring residents to refer to it as the "Bridge of Strings."

A sense of precarity is given by the sloped pylon, which is inclined in three planes. This configuration, combined with deck curved girder, cantilevering in transverse direction, characterizes a deep sense of instability and "frozen motion", typical of Caltrava's bridges.

**Fig. 4.32** Bridge of Strings (light rail train) Jerusalem (2002-2008)\_  $L(\text{main span})=160\text{m}$ ;  $i_p/L=1,85\%$ ;  $h/L=1/75$

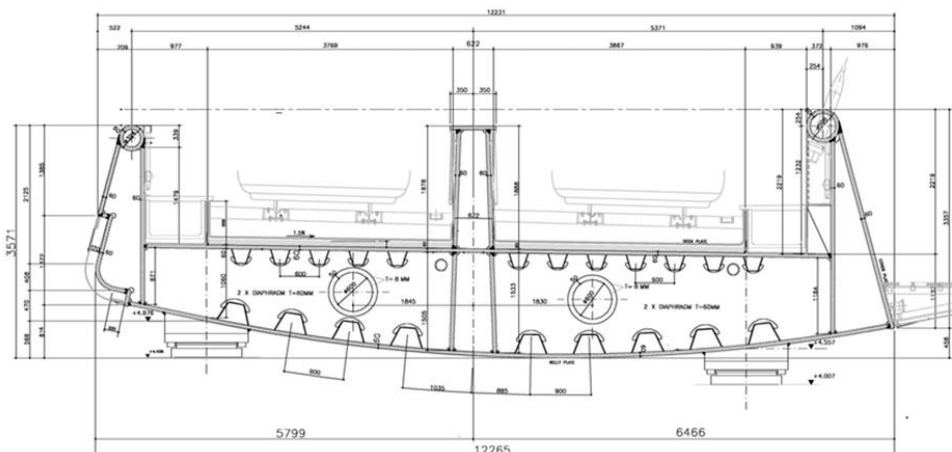


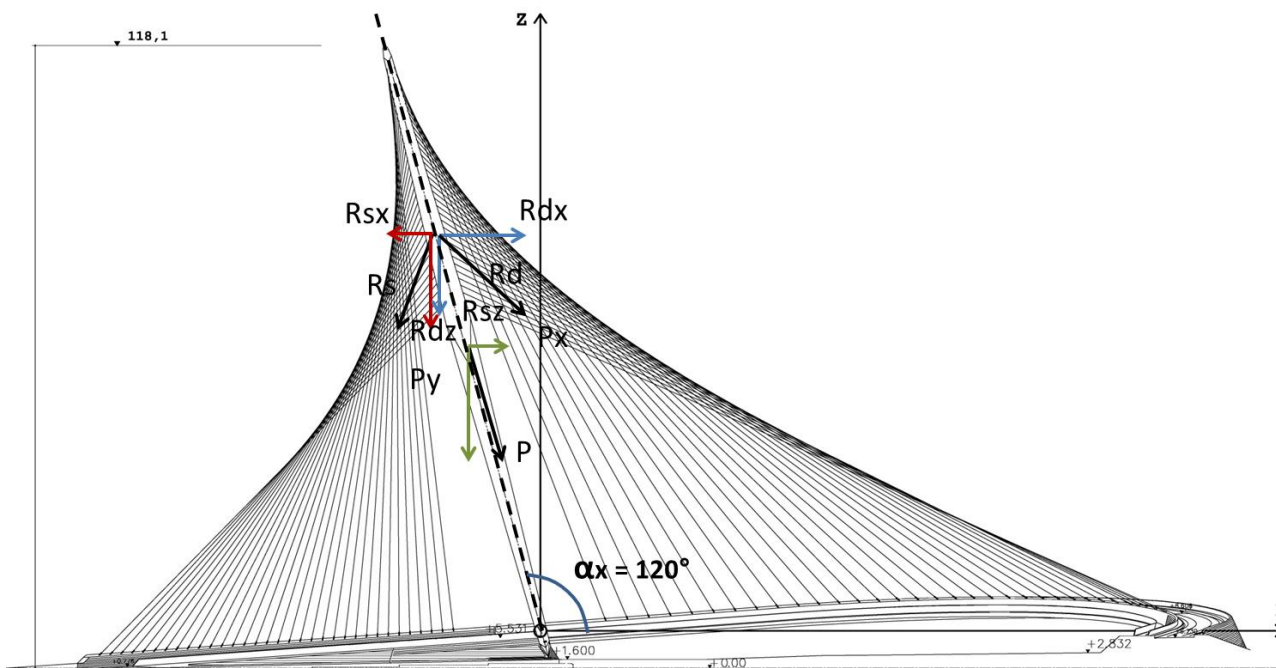
**Fig. 4.33** Bridge of Strings (light rail train) Jerusalem (2002-2008) bridge deck detail

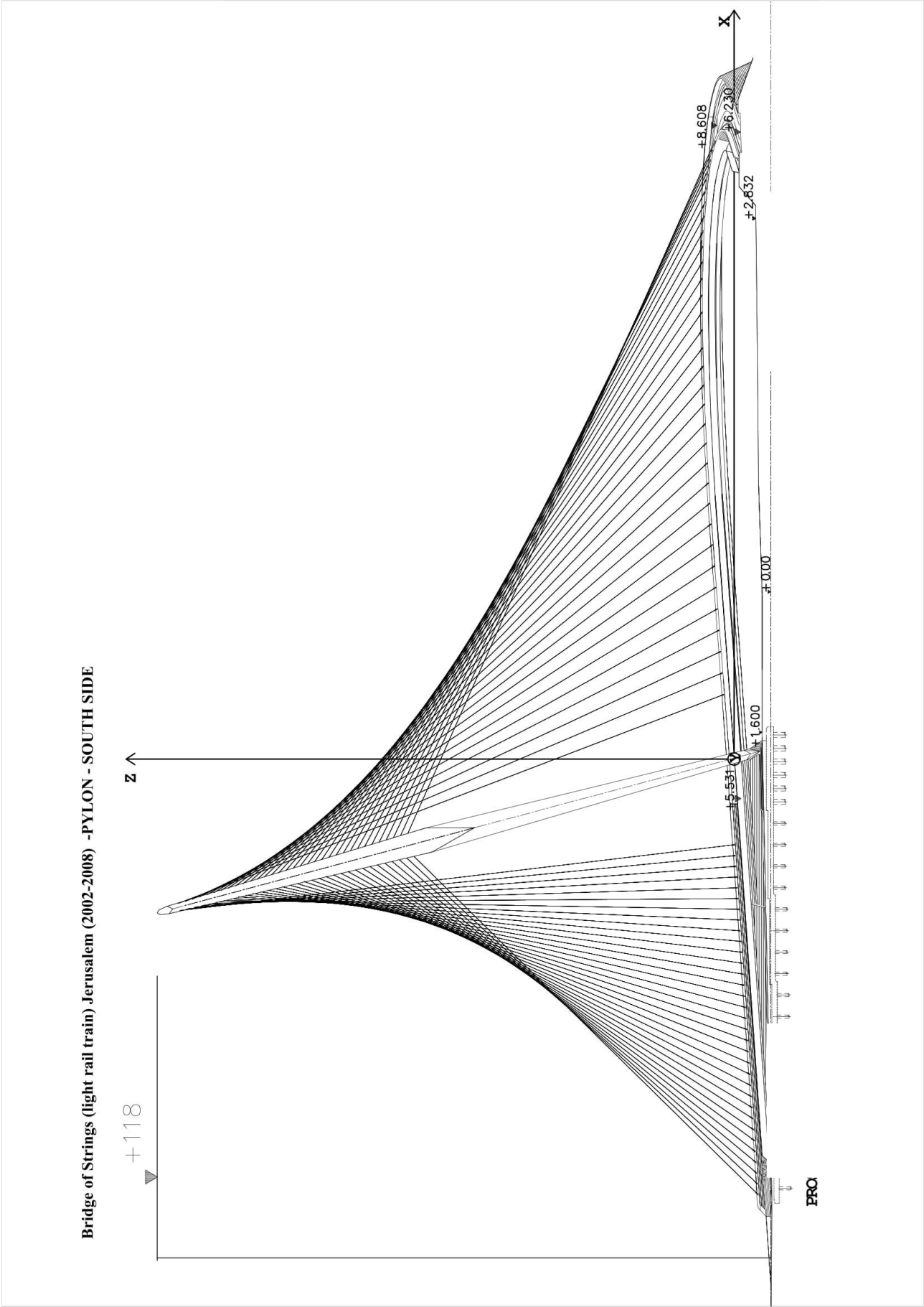
Bridge load bearing structural system is made of a trapezoidal box girder section, 13,50m-wide, characterized by steel plate of variable thickness, reaching also 60mm- thickness. In the central 160m-long portion, bridge deck system is stiffened by diaphragms, put at 4m one from another.

From right edge steel tubular, two clusters of 33 cables run from both side of the inclined pylon, anchored at a mean distances of 3m: considering the asymmetric cable layout, a great portion of deck system cantilevers. This configuration causes no negligible torsional effects, which justify the huge steel plate thickness as well as the high slenderness ratio ( $h_t/L = 1/45$ ). A deep closed spaced cable system ( $i_p/L = 1,85\%$ ) is combined with a rigid deck system, which carries bending and torsional moments, while asymmetric cable system transfers residuary bending moment to the pylon. Short distance between cables give the possibility to use small diameters (3 -5cm) so that suspension system appears diaphanous, imperceptible.

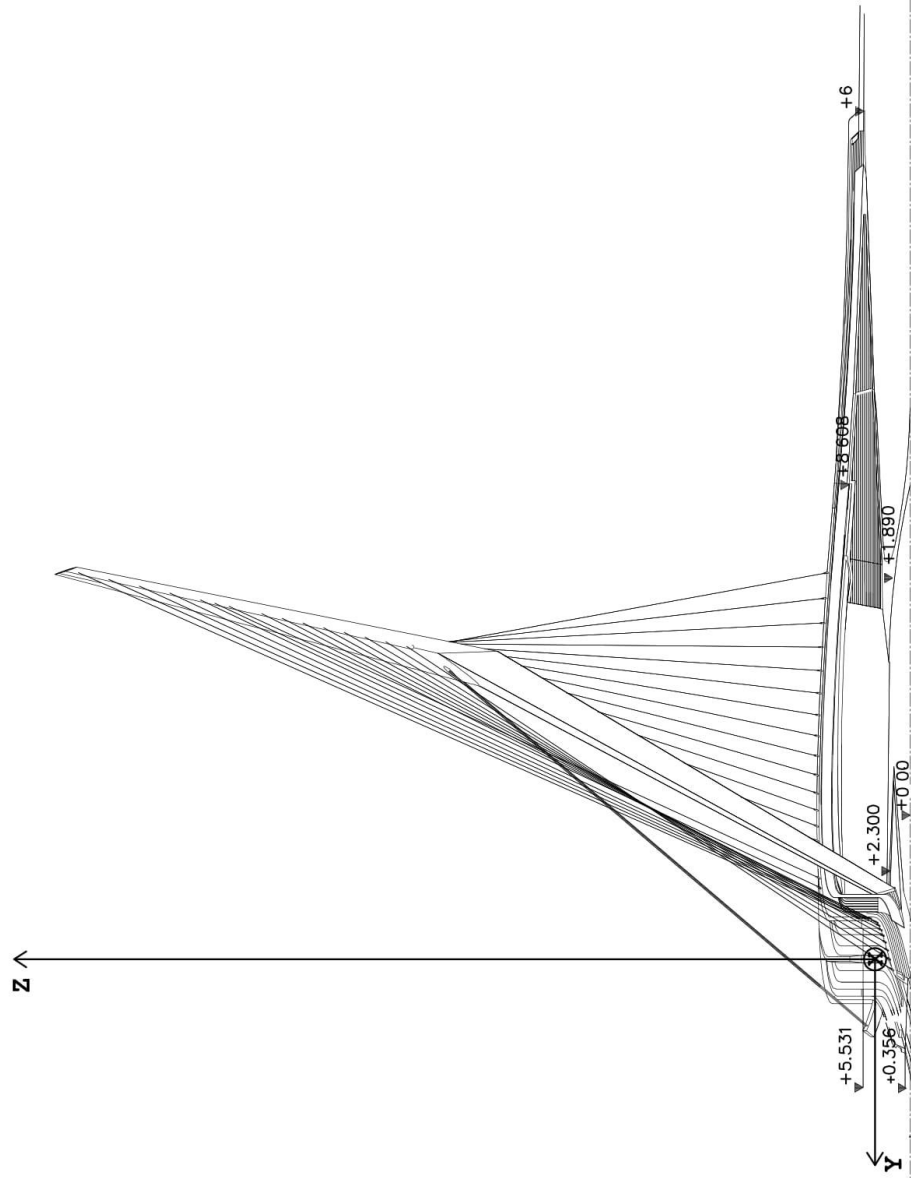
With a total dead load of 2756 tons, and a superimposed aliquot estimated in 1959tons, this heavy steel structure is effects by torsional effects above bending one: this justifies the use of thick steel deck plate, especially next to the central abutment. Even if at first glance this system seems to be instable, this sense of precarity is solved by the innovative use of pre-stressed system, where the structure itself bears no- balanced resultants.(Fig. 4.34)

**Fig. 4.34** Bridge of Strings (light rail train) Jerusalem (2002-2008) \_ force resultants upon the pylon





Bridge of Strings (light rail train) Jerusalem (2002-2008) -PYLON - WEST SIDE



PROSPETTO SUD

### **Appendix (C): Case study n.2: the innovative system of Ponte della Costituzione**

Evolution of bowstring arch bridges reveals Calatrava's ability to create innovative structures, as impressive landmarks, resulting from his attempt to completely change bridge design. Partially evoking naturalistic as well as anthropomorphic forms, the Valencian artist uses hybrid material solution, made essentially by steel elements. His free form design is characterized by the common thread of "dematerializing" main load bearing elements, as bridge longitudinal girder, creating light, slender and unusual structures. He accomplishes this task adopting a revolutionary approach, which has been anticipated by Amman's George Washington Bridge. Completely overturning common assumption in bridge engineering, Calatrava makes use of deep-close cables spacing, as well as of a great number of cross sections, greatly reducing loads effects, consequently sizing, of longitudinal elements. Calatrava's masterpiece, which summarizes this innovative design approach is the well known Ponte della Costituzione in Venice.

Back analysis of previous bridges shows how the "boundary conditions" have always influenced bridge design, strongly effected by the urban contest, its historical stratifications, its culture, its construction traditions. This is true especially in the case of Venice: located in a lagoon, it's made up of 118 islands and 150 canals. Because of this configuration, there has always been the need to ensure a net of walkways to connect "rii". Since XIII century, the lagoon has always been crucial to the survival of Venice. More than 200 original canals have been linked together to form a dense urban network on either side of the curving Grand Canal, which describes a great backward S more than 3-kilometer long, from the railway station to San Marco Basin in front of the Doge's Palace. Venice configuration has limited modern suburban spread beyond the historic center; its framework of canals and narrow medieval streets has prevented the intrusion of automobiles. A portion of the city is connected to the mainland through a 4-km long bridge (Ponte della Libertà), carrying car and railway traffic, whereas the other islets are linked together by footbridges. In his famous treatise on bridge, published in 1716, Henri Gautier described Venice, with its 359 bridges, as the city with highest number of walkways, whose structural forms and technologies were the result of a continuous research for synthesis between architectural and engineering aspects [*"Tratè des ponts, ou il est parlé de ceux dex Romains & de ceux des modernes"* (1716)].

Venice is steeped in history, well known for its architecture, particularly for its bridges. Their design has often been influenced by its historical back ground, as well as its urban contest and soil geological characterization. Venice is one of the world's oldest cultural centers: In 1987, the city and its lagoon were collectively designated a UNESCO World Heritage site. (Fig. 4.B1)

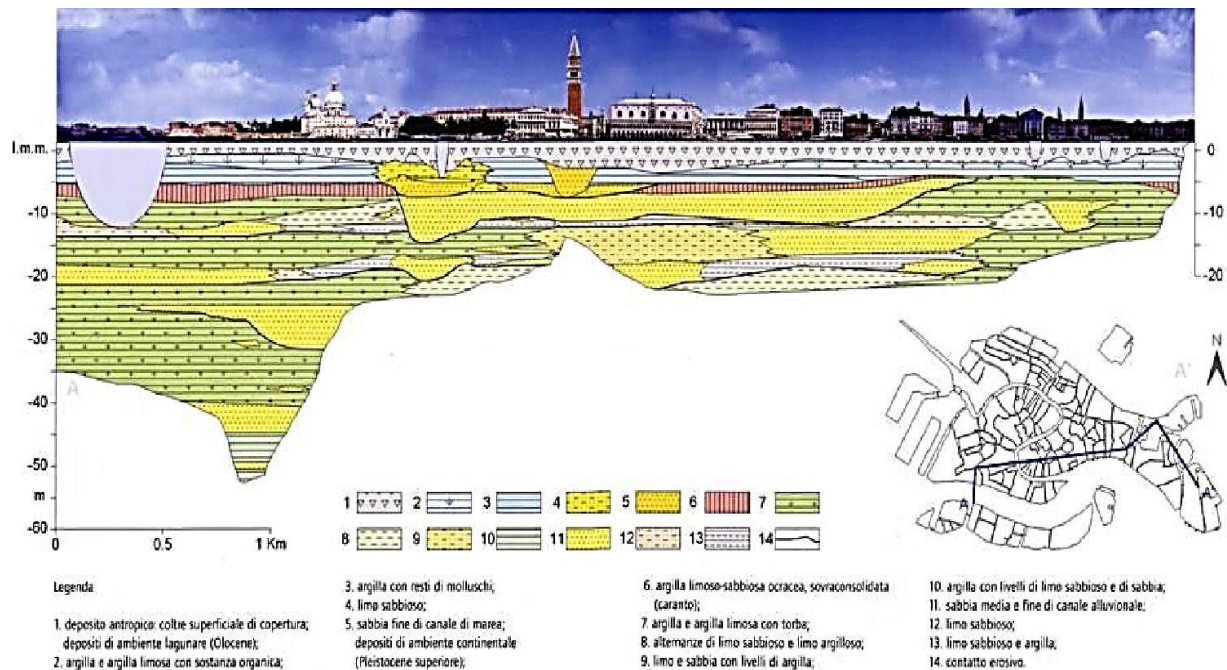




**Fig. 4.B1** Venice aerial map: focus in Gran Canal

Its specific nature is the result of various factors, some due to local traditions, others to its particular environment, and others deriving from different civilizations Venetians came in contact. The local tradition was formed in the lagoon based on Roman style of buildings. Fleeing from barbaric invasions, the communities that made up the first nucleus of Venice came from the Roman towns of Padua, Oderzo, Aquileia, and Altino. The present urban structure of Venice took shape in the early 7th century when migrants from the mainland swelled existing fishing communities on the higher mud flats and sandbanks. Among these early settlements, Rivo Alto, its name corrupted over time to Rialto, was the most central and became the heart of Venice, linking together 118 separate islands with bridges and canals.

Since XIII century, the lagoon has always been crucial to the survival of Venice. More than 200 original canals have been linked together to form a dense urban network on either side of the curving Grand Canal, which describes a great backward S more than 3-kilometer long, from the railway station to San Marco Basin in front of the Doge's Palace. Its width varies from about 30 to 70 meters, and it is lined by buildings that once were the palaces of great merchant families and the public warehouses used in foreign trade. Venice is a city with two completely independent communication networks. The situation of the city on islands has limited modern suburban spread beyond the historic center; its framework of canals and narrow medieval streets has prevented the intrusion of automobiles. A portion of the city is connected to the mainland through a 4-km long bridge (Ponte della Libertà), carrying car and railway traffic, whereas the other islets are linked together by footbridges. In the past, canals held a different status: they were the ways of upper class, while tiny streets on the ground were used by servants; therefore Canal Grande, with its total length of 3800m, became the equivalent of Main Street. This explains why majestic entrances are facing canals whereas pedestrians can hardly find where a building is. Nowadays, instead, canals are mostly used for transportation of goods, public transportation and sightseeing tours on gondolas.



It's interesting also to note that, together with its urban contest, also Venice geological characterization influenced the way the city grew: Structural types and materials used, as well as the choice of foundation typology, were influenced by the poor load-bearing capability of soil. It appears without any regular trend in depth, characterized by a predominant silt fraction; this is always combined with clay and sand, forming a chaotic and erratic interbedding of different sediments coming from variable mineralogy. Below the level of the countryside the following formations can be identified: a first stratum (1÷5 m thick) of fill, a second stratum ( 2÷5 m thick) of clay-loam soil with a low-medium consistency, alternate strata of clay and loamy clay with a medium consistency, formation of over-consolidated loamy-sandy clay (, typically at a depth of between 5 and 8m); below depths varying between 5 and 15 m, the subsoil has enough good loadbearing characteristics. (Fig. 4.B2)

Because of the high soil deformability and its low supporting capability, foundation piling techniques have always been adopted. In the past technology was not yet advanced enough to enable the necessary depths to be reached to ensure solid foundations: the technique involved wooden piles usually made of oak or larch, measuring 3÷6 m, with diameters of 20÷25cm, typically used with a density of 9 piles for square meter. Masonry arch construction constitutes about 70% of the bridges in Venice: this is strange in view of the apparent vulnerability of this type of structure to movement of the foundations, a particular problem in this city. Many innovations were used to help prevent this: vertical loads were reduced by using lighter baked voussoirs and by the omission abutments from the design. Builders had proven rules for construction that came from experience gained over many years; this led to many natural innovations and refinements used to cope with problems

**Fig. 4.B2** Venetian subsoil: sedimentary interbeddings coming from lithostratigraphical analysis of Late Pleistocene- Holocene Era deposits in the historical center of Venice (Giudecca – Canal Grande- San Marco e Sant'Elena) . Taken from: ZEZZA, F., *Geologia, proprietà e deformazione dei terreni del centro storico di Venezia*, “Geologia e progettazione nel centro storico di Venezia – La riqualificazione della città e dei territori”, Padova, 2007, pag.21

encountered. Large foundation slabs and piles were used to prevent the abutments from washing away.

Along Venetian “rivi” two main types were used: girder and arch bridges. Girder bridges are the simplest structural forms that could be used to overcome the canal obstacle, being supported simply by abutment or pier at each end. Differently from arch bridges, they need higher structural deck depth, if span length increases; at the same time, in order to ensure the necessary clearance, they require longer access ramps than arch bridge. Despite this, no moments are transferred throughout the support, hence their structural type is known as simply supported; statically, truss bridges generate mainly vertical reactions on the foundations, making them highly suitable for the city’s soil characteristics. Considering formal and functional restrictions due to girder type, arch bridges are much more prevalent, as they successfully integrate the need for a continuous pedestrian walkway with the necessity to leave sufficient space underneath for boats to pass; they are shaped to follow their function, especially in the case of segmental arch. On the other side arches are thrusting structures that transmit large horizontal forces to the abutments, which, through the foundations, transmit loads to a deformable soil of low bearing capacity. In the history of Venetian bridges, a sort of “natural selection”, influenced by engineering and architectural aspects, shows the passage from girder to arch bridges construction. In this regard, four bridges across Canal Grande (Ponte di Rialto, Ponte dell’Accademia, Ponte degli Scalzi, Ponte della Costituzione), have been analyzed: comparison between main design parameters shows how segmental arch bridge is the most congenial type to create a perfect synthesis between architectural and structural aspects. Looking for a compromise between the need to guarantee clearance for passing boats with Venetian bad soil conditions, in order to create footbridge without piers along the rivers, arch bridge has been the most commonly used: for this typology Calatrava has been capable to make a significant technical revolution. In the case of Ponte della Costituzione, instead of the typical deck arch solution, he uses a pure arch bridge, without any filling materials between the load bearing structure and the pedestrian walkway. Dividing the main arch into 73 closely spaced sections, Calatrava is capable to leave out the longitudinal girder; so that the floor is supported directly by a slightly sloping central steel arch. In order to create a work of art, capable to enhance the historical and cultural prestige of Venice, for Ponte della Costituzione Calatrava involves the latest results of his innovative design approach: led by a constant research for technological experimentations, he often try to optimize element dimensions, creating slender *dynamic structures*, which give visitors the idea of “*frozen motion*”, as if it could have been captured acting displacement. Partially evoking naturalistic as well as anthropomorphic forms, the Valencian artist uses a hybrid material solution, made essentially by steel elements. Proposing a global view, similar to the





Palladian one adopted for Rialto Bridge, Calatrava reveals the intention of including his design in a general planning of urban reorganization: underlying the necessity to guarantee also aesthetic qualities to the structure, the Valencian artist makes his bridge a landmark capable to grab people's attention with its unique feature, increasing urban contest prestige, without being redundant or inappropriate.

**Fig. 4.B3** Ponte della Costituzione, Venice (IT), 2001 - 2007, S. Calatrava.  $L = 80.80\text{m}$ ;  $r/L = 1/14$ ;  $i.p/L = 1.3\%$ ,  $ha/L = 2.5\%$ .

Thanks to its exceptional character, Ponte della Costituzione (Fig. 4.B3) is able to rouse emotions, condensing opposite states, such as beauty and truth, poetry and rationality, or, simply, architecture and engineering; it succeeds in making Venice a model-town of modern art and architecture, which looks at the future, basing on its glorious past. Even if the segmental arch adopted by Calatrava has been considered a poorly adapted form for a walkway across the Venetian canal, it seems to be the most congenial and advantageous one: this form, used previously by Miozzi for Ponte degli Scalzi design, is capable to guarantee the necessary clearance, reducing deck floor slope to make easily pedestrian access above it. Dematerializing longitudinal truss, Ponte della Costituzione doesn't require secondary load-bearing structures, being built as a "pure" arch. In this way Calatrava is capable to improve Miozzi's previous solution: the broken line, a three-stretch polygonal which characterized Ponte degli Scalzi, has been divided in a so huge number of sections to be approximated to a continuous arch; at the same time, thanks to the low section spacing, glass floor with anti-skid surface ( $t = 3 \times 10 + 12 = 42 \text{ mm}$ ) can be used, together with traditional Istrian stones. The choice of a low segmental arch as structural form has often been criticized. The comparison with the remarkable bridges built across Canal Grande over ten centuries, makes the arch option the best one; this structural form, respecting

environmental constraints, guarantees the clearance necessary for navigation, without being excessive or redundant. Because of its form, it has been questioned about real bridge structural behaviour (as girder or arch), valuing its extensional regime against its bending resistance capability. However, the choice for segmental arch is justified by the aim of reach growing spans, passing from 40m of Ponte degli Scalzi to 81m of Ponte della Costituzione.

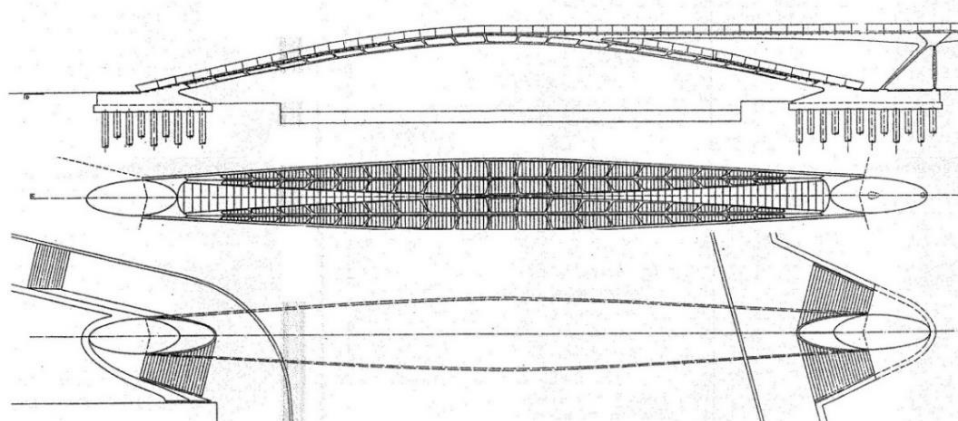
Considering the latest examples, it could be say that the history of Venetian bridges is marked by the constant attempt to achieve a balance between architectural and structural aspects. This dialogue has always taken account of economic constraints, the resources available to build new structures, and the problems associated with the duration of the bridges themselves. So engineers and designers have always been required to solve technical and engineering problems while at the same time producing structures that were in keeping with the city's architectural context and tradition. From Palladio to Calatrava, finding an acceptable compromise between design requirements and Venice cultural background has always been difficult. Over the centuries, arch bridges began the prevalent structural form in Venice: despite girder bridges, they successfully integrated the need for a continuous pedestrian walkway with the need to leave sufficient space underneath for boats to pass. Thanks to scientific and technological development, involving new structural solutions, arch bridges with growing spans have been built. The parametrical analysis carries out an increase of span lengths, joined to a reduction of arch rises; at the same time, according to modern structural trends, bridges with really slender deck are designed in order to reduce environmental impact, particularly in Venetian urban contest, full of cultural and artistic constraints.

Considering walkways across Canal Grande, it's interesting to dwell on Caltrava's bridge, above all for its technological innovation: the Valencian artist proposes an hybrid solution, a segmental arch bridge which works in extensional regime, spanning 81m. The pure arch of Ponte della Costituzione is characterized by a imperceptible deck, whose slenderness has been guaranteed by the choose of discretizing it in a great number on cross sections (21 sections,  $i.p/L = 4.7\%$  - preliminary design; 32 sections,  $i.p/L = 3.1\%$  - final design; 73 sections,  $i.p/L = 1.3\%$  - executive design), reducing live loads effects above the deck (Fig. 4.B4).

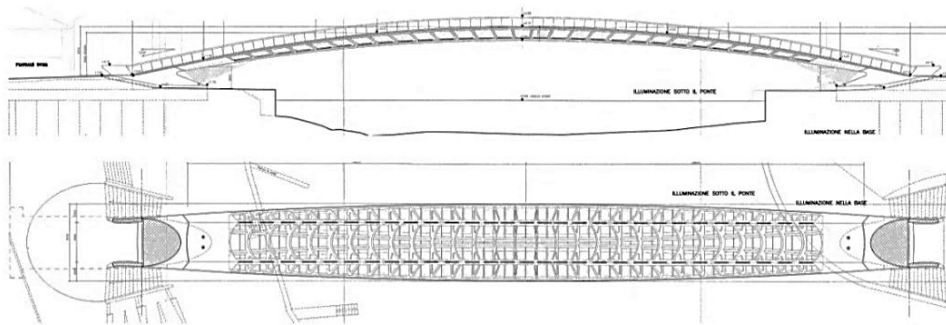
Finally, tracing the historical evolution of arch bridges across Canal Grande, it's interesting to note the progressive reduction of bridges weight, jointed to a rise increase which corresponds to higher thrusts at springing sections. In order to balance it, deeper and bigger foundations are necessary (as it happens for the fourth bridge designed by Calatrava, whose foundation diaphragms are made if  $1040\text{m}^3$  of concrete). Over centuries, growing lighting and slenderness lead to bridge arch form closer to funicular one, passing from tradition segmental circular arch of Rialto bridge, to parabolic one for Ponte della Costituzione, characterized by a lower gap between dead and live loads,



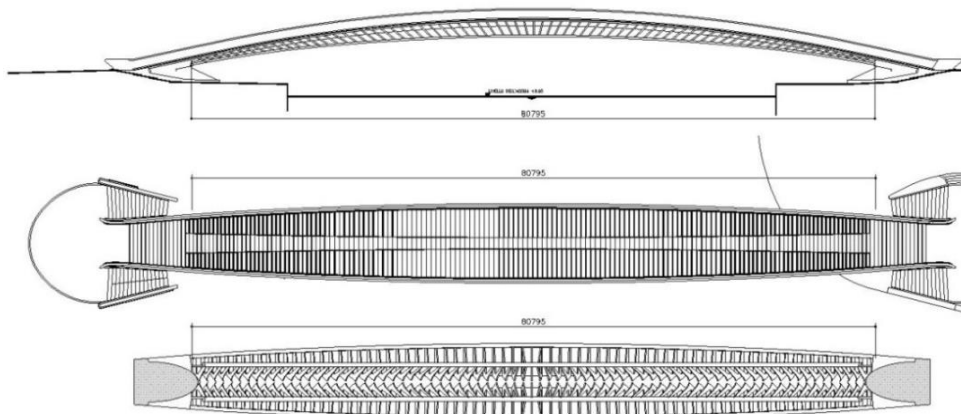
which makes not inconsiderable the effects of the second ones on bridge static behaviour.



*Preliminary design (i.p./=4.7%; 21 sections)*



*Final design (i.p./=3.1%; 32 sections)*



*Executive design (i.p./=1.3%; 73 sections)*

Also known as Fourth Bridge over Canal Grande, it gives people the first perceptible idea of Venice cultural and artistic characterization, welcoming tourist to Venice with a charming panoramic view. As the existing bridges, this walkway has been built in a strategic position: it connects railway station (Stazione Santa Lucia), on the north side with the Piazzale Roma (the City's arrival point by car/bus), on the south side of the Grand Canal. )Fig. 4.B5)

**Fig. 4.B4** Ponte della Costituzione, Venice (IT), 2001 - 2007, design steps

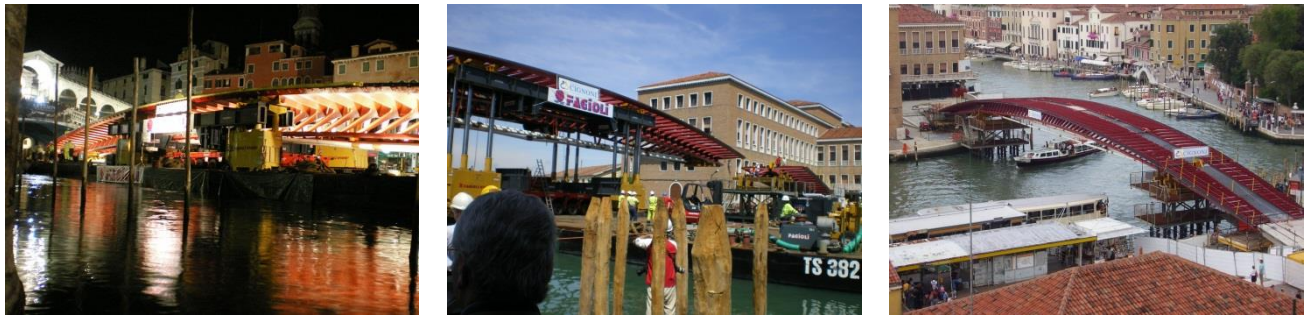


**Fig. 4.B5** Ponte della Costituzione, Venice (IT), 2001 - 2007, S. Calatrava. Bridge deck (glass and Istrian stones flooring)

Perfectly integrated within the overall context, thanks to staircase and flights masking the abutments, it's capable to create a new urban square. Its half-moon shaped abutments, made of concrete as the bridge foundation diaphragms, provide a clear view of bridge deck intrados, without encroaching the canal banks. The load bearing segmental arch is made of stainless steel, in order to resist corrosion by chlorides and sulphates in sea water. The problem of the large horizontal thrust is compensated for by a jacking system at the abutments, installed to cope with any horizontal displacements. The stairway on the bridge is paved with Istrian stone, a stone traditionally used in Venice, alternating with tempered glass steps illuminated from below by fluorescent lights. The parapet is also tempered glass, terminating in a bronze handrail with concealed lighting (LEDs). Particular attention to detail was paid to the finishes to make the bridge as aesthetically pleasing as possible. The proportions of the bridge can also be appreciated when walking over it. The gradient of the slope means that pedestrians cannot see what is on the other side and the widening of the deck in the center opens out to allow people to stop and look at the surroundings. To avoid any architectural barriers to disabled access to this walkway, a platform stair lift (called "ovovia") has recently been installed: this mobile platform is put in a hold over the abutment in order to safeguard it against acts of vandalism.

Considering the rise-to-span ratio ( $r/L$ ), history of walkways across Canal Grande sees structural improvement, passing from 22% valued for Ponte di Rialto (1588), masonry arch bridge with 40m span, to  $r/L=11\%$  for Ponte dell'Accademia (1932), a timber bridge spanning 48m, continuing with a  $r/L=7\%$  for Ponte degli Scalzi (1934), a masonry arch bridge over about 40m, until the lower rise-to-span ratio of 5% valued for della Costituzione. In this last case, the chosen form satisfies functional requirements, as keeping a low slope to guarantee an easy crossing of the walkway.

In June 1999, the Municipality of Venice drafted a preliminary plan for a fourth bridge over the Grand Canal.



Using a public selection process, they commissioned Santiago Calatrava in November 1999 to design the new bridge. Through tendering procedure, execution of the work was entrusted to Cignoni s.r.l.. (Fig. 4.B6)

The construction had suffered enormous delays: if according the initial expectations works should take 456 days to carry out, the bridge construction lasted 6 years. In such a busy area with lots of traffic on the Canal, any prolonged construction works could cause huge problems. In order to cause the least impact possible the steelwork was prefabricated offsite and the erection of the bridge took place over a few days with the Canal traffic being stopped for only two nights. The first step in construction which took place in January 2007 was preparing the foundations: piles were then driven into the ground and substantial reinforcement assembled before pouring the concrete. Once the abutments were finally constructed the steel structure could be brought onto site. The arch was prefabricated in three parts, two side sections and a central span. All the steel was fabricated at a site on the edge of the lagoon so that it could be easily transported by barge. Ever since the beginning of the project the bridge was prone to criticism, both for rising constructions cost and for serious doubts concerning its structural stability, bridge construction began on 28 July 2008, with the arrangement of deck lateral segments using temporary supports. Each section was 15m long and had a weight of around 100tonnes. Once on site the sections were crane lifted into place. A temporary platform with piled foundations for stability was used to support the steel frame and a hydraulic jacking system was installed at the abutment to control the geometry of the section. The central section was around 60m long and around 270tonnes: once on site the barge had to perform a careful rotation so that the section was placed in the right direction. The sections were then quickly welded together. Once welded the temporary supports could be removed as the bridge was self-supporting. The bridge was opened to the public on the night of 11 September 2008. Although it has been criticized, Ponte della Costituzione is an extraordinary example of structural engineering. Considering arch bridge historical evolution, it could be said that, over the centuries, material resources and technologies allowed to build growing main spans: traditionally roadway was identified with the plan of secondary load-bearing transverse girders, no linked to the main structure.

**Fig. 4.B6** (1) Lateral segment transported by barge passing under Rialto Bridge (2) Assembly of central portion (3) Construction end



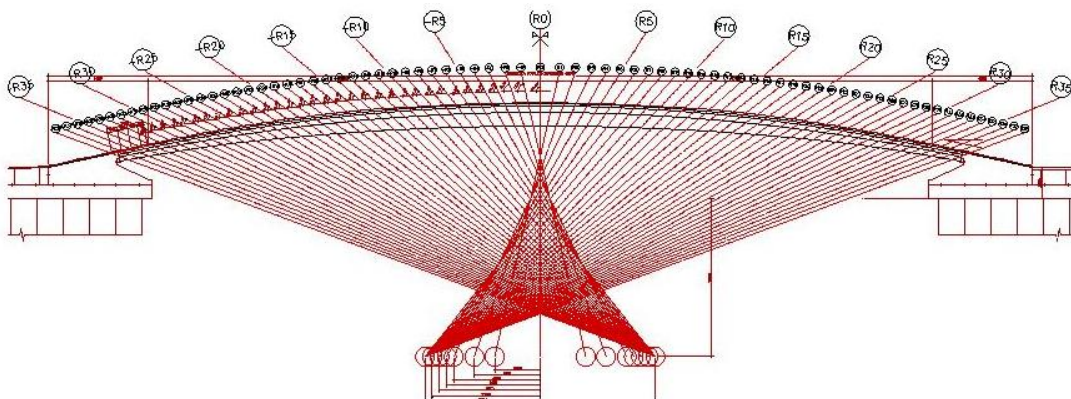


**Fig. 4.B7** Ponte della Costituzione. Bottom view of steel cross sections (i.p.= 1.36%)

*Ponte della Costituzione* (Fig. 4.B7) is a *unicum* for the structural solution adopted. Calatrava is capable to create a pure segmental arch bridge, with no fill between deck and the main load-bearing elements, working in extensional regime on its short span. This extraordinary solution, suited with the past and technically really effective, owes to the segmental arch high thrusts at the abutments: to carry them a tie couldn't be used, interfering with boats shipping. This justifies the use of a deep and expensive foundation system made of diaphragms (30% of the overall cost).

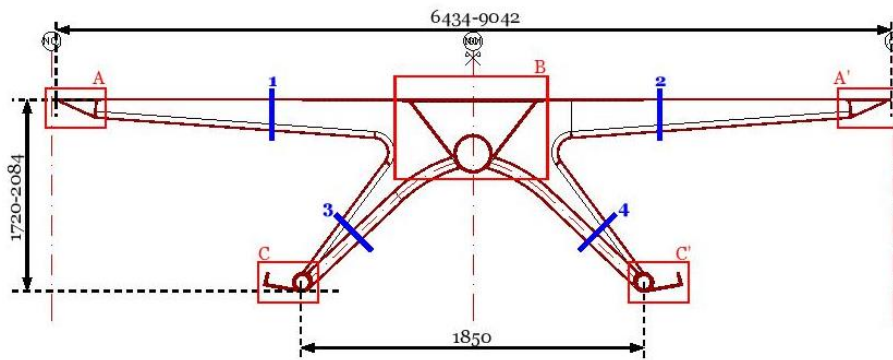
Because of its low rise-to span ratio, load-bearing capacity of Ponte della Costituzione could be assimilated to that of a truss instead of an arch bridge. (Fig. 4.B8) On the contrary, confirming arch structural behaviour of Calatrava's footbridge, it's interesting to note that the outputs of FEM analysis, which have been led to support previous hypothesis concerning bridge behavior, is agree with the calculation of arch thrust, valued using current literature formula for segmental arches

**Fig. 4.B8** Ponte della Costituzione. Radial distribution of deck cross sections



A report about the evaluation of bridge thrust follows. This single span bridge has saddle shape, with 180m- bending radius. Its cross section varies in a non-linear way along bridge axis, passing from 1720x6434mm at the abutments to 2084x9042mm at the midspan. Thin girders link upper to lower arches in a such a way that a certain "structural clearness" is ensured. As it can be seen in the following picture, deck cross section is made of 5 arch-chords (red encircle), connected by four beams, two horizontal beams ( 1 and 2) and other two diagonal (3 and 4). (Fig. 4.B9)

**Fig. 4.B9** Ponte della Costituzione. Deck cross section



A simplification of the real structure occurs to make FEM model. To better understand bridge behaviour a detailed discretization is required, closer, as possible, to the effective structure. So, the following elements have been identified (Fig. 4.10):

- A-A' (upper arches): triangular-shaped box cross section, 15mm-thick, with variable dimensions;
- B (central arch): assembled section, made of three 25mm-thick plates (having variable length), welded to a steel 25mm-thick tubular element, having a 419mm diameter;
- C-C' (lower arches): 40mm-thick tubola sections, having 219mm-diameter;
- 1 – 2 (cantilever): rectangular box cross section beams, with variable dimensions;
- 3 -4 (lengths): lower diagonal beams, having variable rectangular box cross sections.

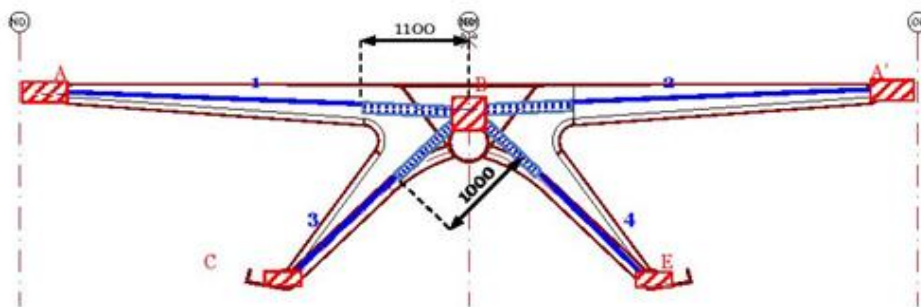


**Fig. 4.B10** FEM model: arch and girders discretization

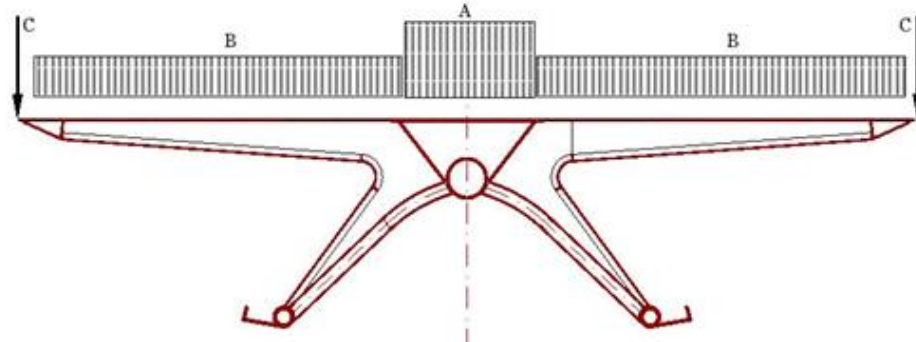
Sap2000 software has been adopted for FEM analysis. Bridge has been discretized as a wireframe model, whose beams and arches have been



represented through their barycentric axis, using end-offset only to define connection to the central arch.

In order to understand bridge static behaviour, a preliminary load analysis is required: it has been valued a dead-to-live loads ratio close to unity. An effective usable surface of 624m<sup>2</sup> has been considered (mean deck width of 7.62m). An effective usable surface of 624m<sup>2</sup> has been considered (mean deck width of 7.62m).

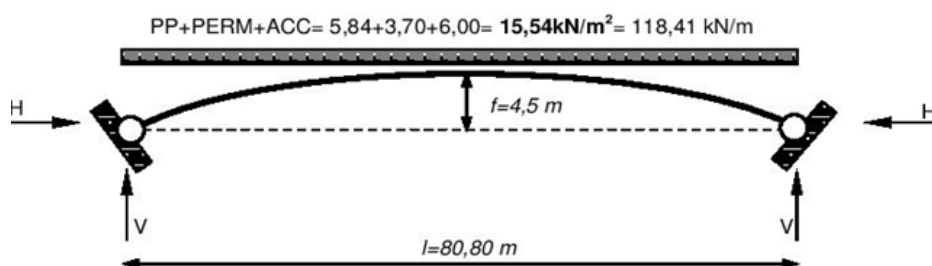
**Fig. 4.B11** FEM model: DEAD and LIVE loads distribution



Taking into account reports given by Lorenzon, bridge construction company, 3600 kN of steel have been used for structural works (this value has been validated by FEM model outputs) , corresponding to a steel-element-dead load (g1) of 5,84 kN/m<sup>2</sup>. Superimposed -dead loads have been calculated considering materials effectively adopted: for Istain stone paving, made of 5cm-high blocks put upon a 14cm-deep concrete slab (specified with “A” in the loading scheme) a load of 4,72 kN/m<sup>2</sup> has been assumed; for glass plates and their corresponding stell supporting structure (specified with “B” in the loading scheme) a load of 2,52 kN/m<sup>2</sup> has been considered; for brass railings, a distributed load of 2,50 kN/m has been considered. Loads have been applied to FEM model frames, considering their effective areas of influence. (Fig. 4.B11) For this crowded footbridge, live loads have been defined according to Itlian Building Code (NTC08): in particular, the value commonly used for compat crowd (5.1.3.3.3 – Schema di Carico 5, folla compatta), i.e. 5 kN/m<sup>2</sup>, has been increased of 20% (to 6 kN/m<sup>2</sup>), considering the high number of tourists visiting Venice.

For symmetrical load pattern, including (dead+ super- imposed dead + live) loads, FEM analysis shows a static behaviour similar to that of a two-hinged segmental arch, with parabolic shape. (Fig. 4.B11)

**Fig. 4.B12** Reference model: two-hinged parabolic arch with (FULL) symmetrical load distribution



The outputs obtained with Sap2000 has been validated with an analytical estimate of arch thrust. In particular, for a parabolic arch, under longitudinally and transversally symmetrical distributed loads, whose axis coincides with funicular curve, its thrust (H) is:

$$\mathbf{H} = \frac{ql^2}{f(1+v)} \frac{5}{6} n^2 \left( 1 - n^2 + \frac{2}{5} n^2 \right)$$

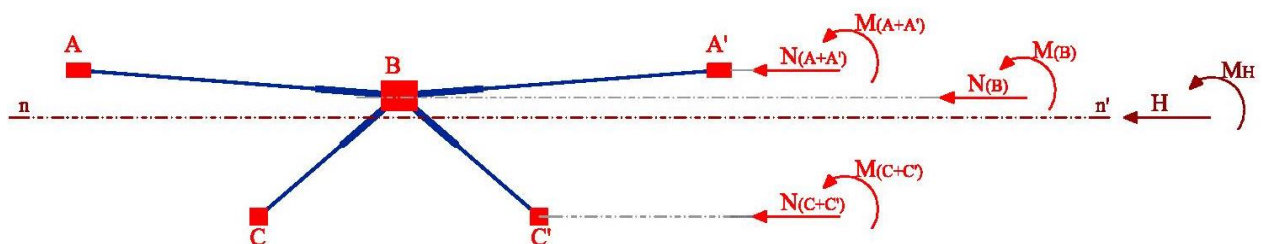
where:

- $n = \frac{x_1}{l}$  ratio between loaded length ( $x_1$ ) and bridge span ( $l = 80.81\text{m}$ ), assumed to be one for symmetrical load pattern ( $X_1 = 1$ ).
- $v = \frac{15}{8} \frac{I_y}{f^2 A_c}$  parameter which considers the deformation due to axial force, defining as  $A_c (= 1.041\text{cm}^2)$  key section area, with a moment of inertia  $I_y (= 7.365.900\text{cm}^4)$ .

Analytically, a thrust  $\mathbf{H} = 20.093 \text{ kN}$  has been valued, not far from  $\mathbf{H}_{\text{FEM}} = 20.166 \text{ kN}$ , obtained with Sap2000 analysis. Matching values (with a difference of 0.36%) confirm that Ponte della Costituzione works in extensional regime, as an arch bridge.

The relationship between flexional and extensional regime could be understood looking at moment and axial forces distribution at the arch-crown section. Considering stress due to bending effects, bending moment equilibrium is calculated, identifying three different contributions, external Moment (ME), internal Moment (MI, as sum of arch-induced moment and moments due to axial forces multiplied by their corresponding arms), finally thrust-induced moment (MH). (Fig. 4.B13)

**Fig. 4.B13** Moment distribution at arch-crown section



It's interesting to note that external Moment, i.e. moment due to acting vertical loads, is counterbalanced by thrust-induced moment, while negligible contributions are given by arch and eccentric axial forces. Moment distribution at the crown section underlines that Ponte della Costituzione has an arch-type static behaviour: about 90% of moment due to external loads is carried in extensional regime, being absorbed as thrust-induced moment; about 7% is counterbalanced by eccentric axial forces-induced moment, while bending contribution (0.70%) are practically nihil. Bridge behaviour doesn't change even if it's modelled as truss arch: added bracing seem to be

unnecessary, as moment distribution doesn't change (atmost, thrust contribution increases of 5%).

### External Moment (ME)

Mq
(kNm) 91440
MV
(kNm) -189900
<b>-98460</b>

### Thrust-induced moment (MH)

MH
(kNm) 90747      92,20%

### Residual Moment (bending)

ME- MH
(kNm) -7713      7,80%

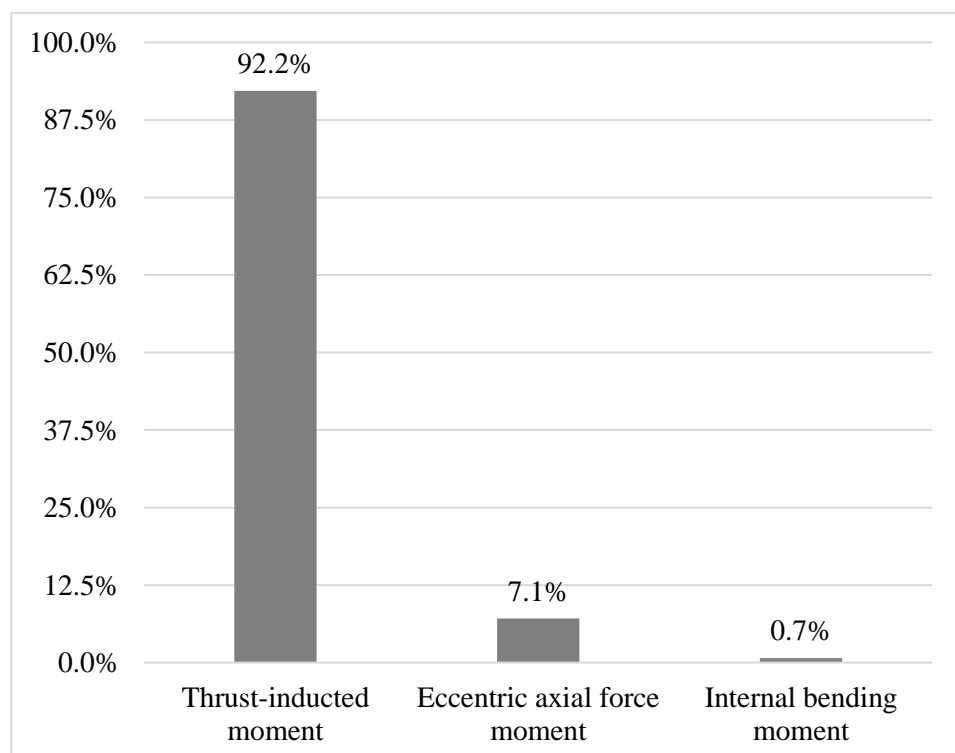
### Internal Moment (MI)

#### a. Arch-induced moments

Moment in A+A'
(kNm) 52      0,05%
Moment in B (kNm) 594      0,60%
Moment in C+C'
(kNm) 43      0,04%
<b>Σ                      689      0,70%</b>

#### b. Moments due to axial forces

Axial contrib. A+A' -
(NA+A' = 2965 kN) 2046      2,10%
Axial contribution in B -
(NB = 13502 kN) 6751      6,80%
Moment in C+C'
(NC+C' = 1480 kN) 1747      1,80%
<b>-</b>
<b>Σ                      7050      7,10%</b>



Other interesting aspects to consider for this segmental parabolic arch, having a low rise-to-span ratio, are potential buckling effects. (Fig. 4.B14)

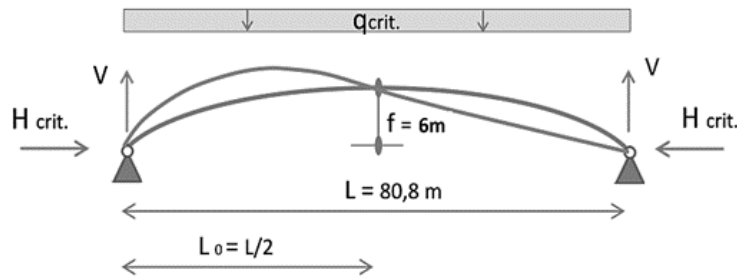


**Fig. 4.B14** Scheme of Ponte della Costituzione: effective length

If a parabolic arch is submitted to the action of an uniformly distributed load ( $q$ ) along the span, there will be axial compression but not bending of the arch, since the parabola is the funicular curve for a uniform load. By a gradual increase of load intensity, it could be reached the condition in which the parabolic form of equilibrium becomes unstable and the arch buckles in a form similar to that for a circular one. In this case, the critical value of load causing arch buckling is strictly dependent from arch shape, restraint conditions, arch cross section characterization ( $E$ ,  $I_y$ ).

Make references to Galambos (*Guide to Stability Design Criteria for Metal Structures*, 6th edition, 2010), as well as to S. Timoshenko e J. M. Gere (*Theory of elastic stability*, 1961), the critical load can be estimated as :

$$q_{crit} = \gamma_4 \frac{EI}{L^3}$$

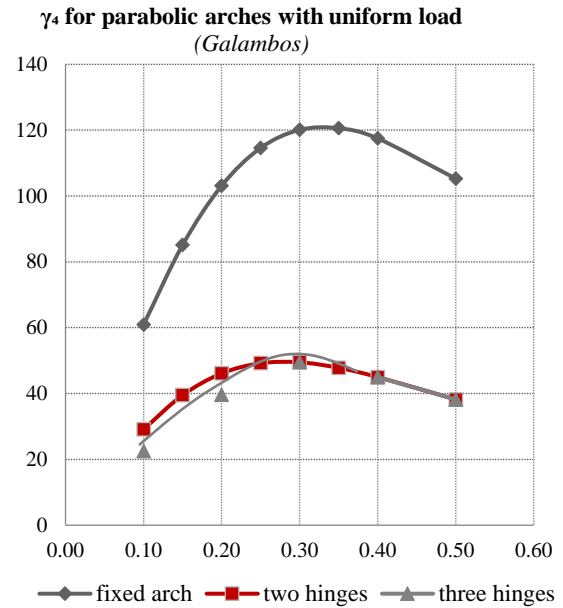
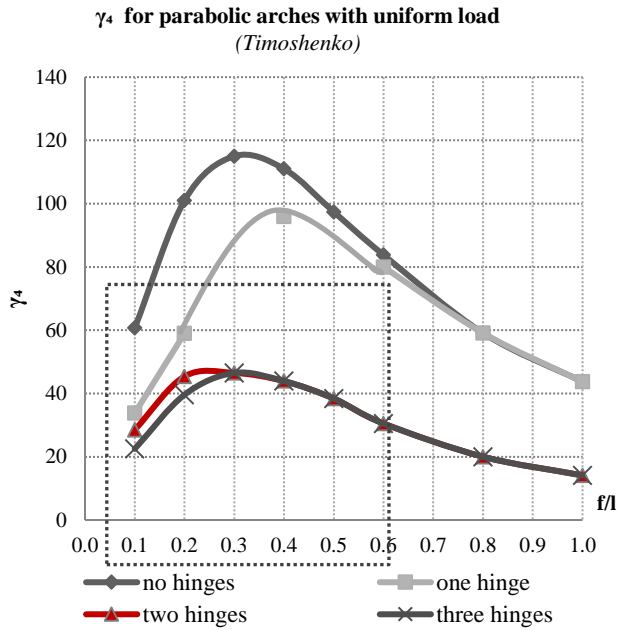
The numerical factor  $\gamma_4$ , depends on rise-to-span ratio ( $r/L$ ), as it can be seen in the following tables.

Ponte della Costituzione is a parabolic two-hinged arch, characterized by a rise-to-span ratio  $r/L = (4.5\text{m}+2.5\text{m})/81 = 0.074$  (nearly 0.1). Looking at the previous tables, it can be seen that critical load decreases when arch rise becomes lower. Overestimating Calatrava's bridge rise-to-span ratio, critical load defined is greater than the effective one.

$$q_{crit} = \gamma_4 \frac{EI}{L^3} = (28.50) \frac{(2.10 \cdot 10^8 \text{ kN/m}^2) \cdot (0.073689 \text{ m}^4)}{(81\text{m})^3} = 830 \text{ kN/m}$$

Analytic calculation gives a critical load value lower than the previous one. Considering the effective arch length  $L_0 = L/2$ , matching Euler classical formulation of critical load with arch-thrust expression, it's obtained:

$$q_{crit} = 32 \frac{EI\pi^2}{L^3} \frac{f}{L} = 510.91 \text{ kN/m}$$



$r/l$	no hinges	One hinge	Two hinges	three hinges
0,1	60,7	33,8	28,5	22,5
0,2	101	59	45,4	39,6
0,3	115	.....	46,5	46,5
0,4	111	96	43,9	43,9
0,5	97,4	.....	38,4	38,4
0,6	83,8	80	30,5	30,5
0,8	59,1	59,1	20,0	20,0
1,0	43,7	43,7	14,1	14,1

$r/l$	fixed arch	two hinges	three hinges
0,10	60,9	29,1	22,5
0,15	85,1	39,5	....
0,20	103,1	46,1	39,6
0,25	114,6	49,2	.....
0,30	120,1	49,5	49,5
0,35	120,6	47,8	.....
0,40	117,5	45,0	45,0
0,50	105,3	38,2	38,2

According to Timoshenko's formulation this critical loads corresponds to  $\gamma_4 = 17.528$ : this numerical factor which coincides with that one obtained interpolating previous scheduled values. *Critical load multiplier (k)* can be defined as  $q_{crit}/q$ : it scales the magnitude acting load till that required to cause buckling. Under overall permanent loads (dead + superimposed dead + live :  $\Sigma = 118,41$  kN/m), (**k**) value of **4.31** is estimated. Considering that in bridge design (**k**) is not greater than **5**, previous considerations underline Calatrava's "freedom to dare", his capability to bring design to unexpected limits, both in structural optimization and in searching a polished and refined beauty for bridge.

Considering the opposing positions developed, as well as taking into account the results of analysis done, it seems appropriate to underline the lack of solidity of all frequently moved objections. The realization costs, together with the long-building times, so far from initial expectations, are in keeping with the specific character of the project. Becoming a sort of Venetian *status symbol*, Calatrava's bridge leads to evaluate the 4.074.000 euro spent for its



construction (the overall cost includes others 2.400.000euro for improvement variations) in relation with bridge serviceability, as well as to the hedonic values it makes the urban contest.

Along this walkway, whose design involves the creation of two new squares, with a total surface of 2200mq, 15.000 – 20.000 people daily transit. In this way Ponte della Costituzione fulfil its public function well, ensuring access to an area of Venice city, which has registered an increasing of trade activities. This bridge, with its overall cost of di 6.609.000euro downstream of 5 variation projects, it's inspired by the need to provide the city something extraordinary, as Foster has done with Millennium Bridge in London, whose cost is of 180000000£ (about six time the sum spent for Venetian bridge).

### Bibliography

- [1] Navier, 1833. Résumé des Lecons
- [2] Timoshenko & Gere, Theory of Elastic stability, McGraw Hill, New York 1961
- [3] Tiziano Rizzo - "I Ponti di Venezia" - Newton Compton – 1983
- [4] F.Leonhardt, 1984. Bridges: Aesthetic and Design
- [5] G.Ballio- "Il Ponte dell'Accademia a Venezia" – Convegno e mostra: 1889-1989\_ Centenario del Viadotto sull'Adda, Milano, 15 Novembre – 17 Dicembre 1989\_ Costruzioni Metalliche, n.1, 1990
- [6] H. Bachmann, Walter J. Ammann, F.Deischl, J. Eisenmann, I.Floegl, G.H. Hirsch, G.K. Klein, G.J. Lande, O. Mahrenholtz, H.G. Natke, H. Nussbaumer, A.J. Pretlove, J.H. Rainer, E. Saemann, L. Steinbeisser, Vibration Problems in Structures: Practical Guidelines, 1995
- [7] H. Bachmann, Walter J. Ammann, F.Deischl, J. Eisenmann, I.Floegl, G.H. Hirsch, G.K. Klein, G.J. Lande, O. Mahrenholtz, H.G. Natke, H. Nussbaumer, A.J. Pretlove, J.H. Rainer, E. Saemann, L. Steinbeisser, Vibration Problems in Structures: Practical Guidelines, 1995
- [8] Frempton, 1996. Calatrava Bridges\_ Second Editio
- [9] Menn, C. 1996. The Place of Aesthetics in Bridge Design, *Structural Engineering International*, Volume 6, No. 2, pp. 93-95.
- [10] Menn, C. 1998. Functional Shaping of Piers and Pylons, *Structural Engineering International*, Volume 8, No. 4, pp. 249-251.
- [11] Dupré, Judith (1997): Bridges. A history of the world's most famous and important spans. Black Dog & Leventhal, New York (USA), pp. 98-99.
- [12] Tzonis, Alexander / Rosselli, Paolo (1999): Santiago Calatrava. The Poetics of Movement. Universe Pub, pp. 240.
- [13] MOLINARI, LUCA / SAMSA, ERIKA / ROSSELLI, PAOLO (2000): Santiago Calatrava. Skira, Milan (Italy), pp. 221.
- [14] Brühwiler, E., Menn, C. 2003. Stahlbetonbrücken (Reinforced concrete bridges)
- [15] Troyano L.F., Bridge Engineering A global perspective, 2003
- [16] A.Barbieri, V.Chiaradia, A.Di Tommaso (IUAV University of Venice), "Railway masonry arch bridges of Venice lagoon: history, technology and structural behavior", CIMNE, Barcelona, 2004.
- [17] Arioli M., The Art of Structural Design : a Swiss Legacy: eine Ausstellung im Zürcher "haus konstruktiv", ETH Zürich, Rämistrasse 101, 8092 Zürich, Schweiz, [www.library.ethz.ch](http://www.library.ethz.ch), 2005

- [18] Fjalar Hauksson, LUND University, Master dissertation. Dynamic behaviour of footbridges subjected to pedestrian-induced vibrations, 2005
- [19] Fulvio Zezza - “Geologia, proprietà e deformazione dei terreni del centro storico di Venezia”- Second Convention “La riqualificazione delle città e dei territori” - Venice - 2007.
- [20] Jodidio, Philip (2007): Calatrava: Complete Works 1979-2007. Taschen Verlag, Cologne (Germany), pp. 519.
- [21] Eckhardt, B., Ott, E., Strogatz, S., Abrams, D., & McRobie, A. (2007). Modeling walker synchronization on the Millennium Bridge Physical Review
- [22] Dobricic S., Siviero E., De pontibus. Un manuale per la costruzione dei ponti, Il Sole 24 Ore, 2008
- [23] Theodore V. Galambos, Andrea E. Surovek. Structural stability of Steel: concepts and applications for structural engineers. John wiley & sons, inc., 2008
- [24] L. Bruno, F. Venuti, Crowd–structure, interaction in footbridges:modelling, application to a real case-study and sensitivity analyses, J. Sound Vib. 323 (2009) 475–493
- [25] M. De Miranda, U.Barbisan, M.Pogacnick, L.Skansi Bridges in Venice - Architectural and Structural engineering aspects, 34th IABSE SYMPOSIUM, Venezia 2010
- [26] Jurado, Henrandez, Nieto, Mosquera. Bridge Aeroelasticity: Sensitivity Analysis and Optimal Design. Boston : WIT Press, 2011
- [27] F. Trovò, Università IUAV di Venezia, I sistemi fondali dell’architettura storica di Venezia, Caratteri Costruttivi dell’Edilizia Storica, , 2010
- [28] Kathryn R. Heath, A critical analysis of Ponte della Costituzione, Venice , Proceedings of Bridge Engineering 2 Conference 2011, April 2011, University of Bath, Bath, UK
- [29] Denison, Edward e Stewart, Ian. Leggere i ponti. Modena : Logos, 2012.
- [30] Restauro del Ponte di Rialto a Venezia- Relazione Tecnica, Comune di Venezia, Direzione Progettazione ed esecuzione lavori, Arcomai S.n.c, P.Sfameni, D.Busato, 2013
- [31] Eliana Alessandrelli ,distorsioni sistematiche, i ponti “truccati” di eugenio miozzi SIXXI 3, Storia dell’ingegneria strutturale in Italia, Gangemi, Roma 2015
- [32] Yozo Fujino, M.ASCE1;Dionysius M. Siringoringo, A Conceptual Review of Pedestrian-Induced Lateral Vibration and Crowd Synchronization Problem on Footbridges, ASCE, 2015.

**Web references**

- [1] International Database and Gallery of Structures, <http://en.structurae.de>
- [2] [http://www2.comune.venezia.it/lidoliberty/biografie/miozzi\\_e.htm](http://www2.comune.venezia.it/lidoliberty/biografie/miozzi_e.htm)
- [3] [http://mediateca.palladiomuseum.org/palladio/opera\\_immagini.php?id=73&TSK=L&TR=14&RN=0](http://mediateca.palladiomuseum.org/palladio/opera_immagini.php?id=73&TSK=L&TR=14&RN=0)
- [4] <http://fysvenice.weebly.com/rialto-bridge.html>
- [5] <https://calatrava.com/>

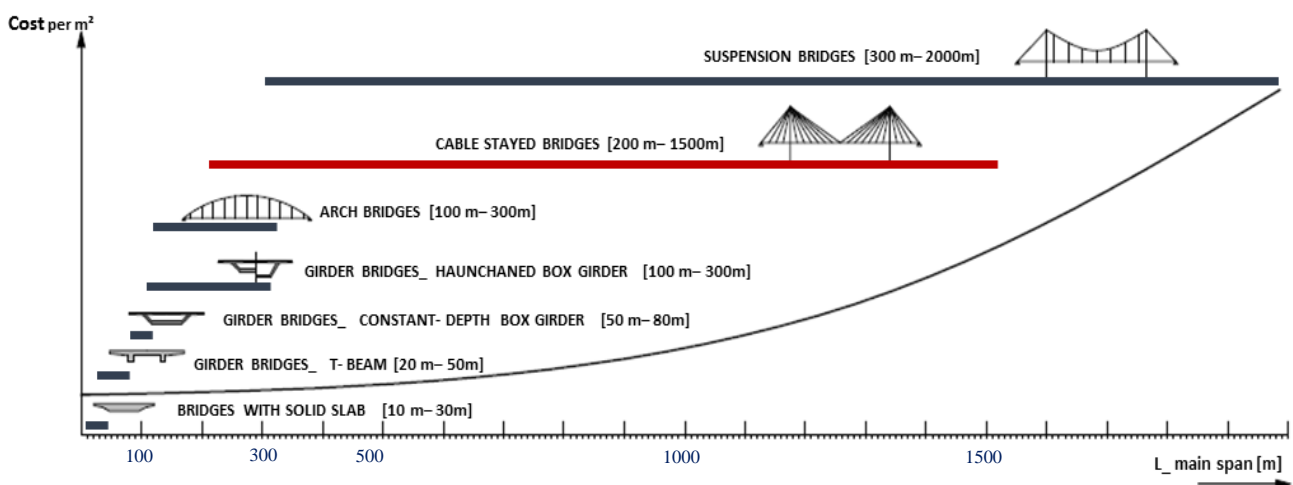
## 5. Cable-stayed bridges

### 5.1 Deck stiffened system: a common mean to read cable stayed bridge evolution

Long span bridge characterization concerns, in particular, suspension and cable-stayed bridges. Cable-stayed bridge are a quiet recent structural typology, even if the principle of supporting a beam or a mast by taught cables goes far back in time. Cable-stayed bridges are currently in fast development, worldwide. While in 1986 about 150 major cable-stayed bridges were known, there number has increased to more than 1000 today. Their span also increased by leaps. From 1975, when the record span was 404m, it jumped to 856m in 1995 and today reached 1104m. The position of cable-stayed bridges within all bridge system is given in the following picture (Fig. 5.1). The economic main span range of cable-stayed bridges thus lies between 100 m with one tower and 1100 m with two towers.

The basic resistant arrangement of cable-stayed bridges is formed by three element: stays, deck and tower (Fig. 5.2) Except for rare cases, two clusters of stays emerge from each tower, namely one main span (or forestay) cable, and side span (or back stay) cable. This second cluster is necessary to stay the side span when necessary, but its main aim is to balance the horizontal forces in the tower to prevent excessive bending effects on it. This is way the resultant of horizontal forces must be equal and opposite in the two clusters. The deck takes part in bridge basic resistant arrangement as it must resist the horizontal components the stays transmit to it. In particular, loads in the main span are carried by the forestays to the tower heads and from there anchored by tension via the concentrated backstays in the anchor piers. The inner stay cables of the side spans receive virtually no forces at all from this loading. The horizontal cable components act in compression in the beam and equal one another out – look forward to. Loads in a side span are transmitted by the side span cables to the tower head and from there via compression (meaning reduction of tensile forces from permanent loads) in the backstays to the anchor piers where they cause compression. The horizontal components of the side spans are balanced by those of the backstays by tension in the side spans.

**Fig. 5.1\_** Economic main range of long span bridges types.[1]





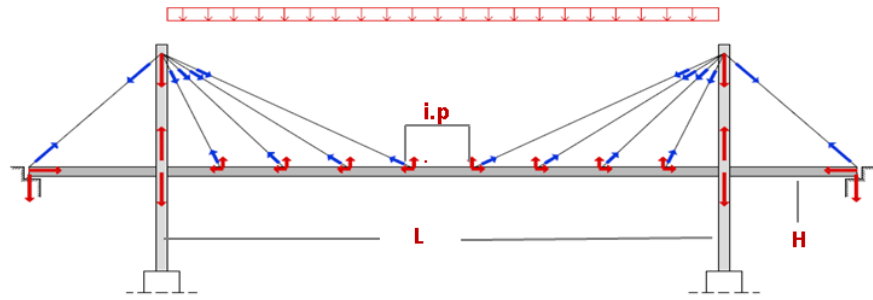


**Fig. 5.2\_** Cable stayed bridge basic resistant arrangement and main design parameters.

The backstays are thus governing the stiffness of a cable-stayed bridge and receive important load changes. The optimum span distribution in cable-stayed bridges led to short side spans, in the order of one-third of the main span; this configuration, leads stay cluster being made asymmetric in many bridges, reducing side span length.

In order to well describe how this typology has changed, underlining its peculiarities and how their variations have had a great influence on bridge behaviour, two main design parameters have been considered, also adopted for other types of long span bridges:

- **(i.p./L)**, cable spacing-to-main span length ratio, to describe suspension cable distribution;
- **(h/L)**, deck depth-to main span ratio, to define bridge slenderness

**Fig. 5.3\_** Cable stayed bridge evolution: proposal for three different generations

Cable-stayed bridge evolution has been traced through the back analysis of 27 existing structures. This thesis proposes their classification into three different “generations”, each one corresponding to a change in bridge static behaviour, as well as in deck stiffened system characterization, as follows. (Tab. 5.3):

First generation (1955-1966)	Second generation (1967-1988)	Third generation (1991-2012)
$L = 150 - 250\text{m}$ $i.p./L = 15 - 20\%$ $h/L = 1/58 - 1/77$	$L = 300 - 450\text{m}$ $i.p./L = 5 - 12\%$ $h/L = 1/80 - 1/150$	$L = 500 - 1100\text{m}$ $i.p./L = 2 - 4 \%$ $h/L = 1/200 - 1/370$
<b>Static behaviour</b> Simply supported beam system with stiffening girders	<b>Static behaviour: Slender deck</b> system standing upon a growing number of intermediate bearings	<b>Static behaviour</b> Light aerofoil deck stiffened system standing upon deep- close spaced elastic supports

Second post-war reconstruction, especially in Germany, gave the opportunity to apply cable-stayed bridge concept, in order to achieve economy of both material and cost. Covering spans no longer than 250m, the earliest examples (first generation: 1955-1966) were characterized by a resistant arrangement similar to that of beam bridges: each of few stays adopted could have been assimilated to an intermediate support of a continuous beam, often characterized by open deck cross sections.

The attempt to cross growing span has been supported by the use of modern multi-stay cable system (second generation: 1967 – 1988): small cable distances resulted in small bending moments from the dead load in the beam; so the live load moments were mostly restraint moments which decreased with the depth of the beam. Therefore, it seemed to be economic to choose a small depth for the beam, which was nearly independent of the span length. In this case, the limiting condition was the safety against buckling of the beam. So, the use of orthotropic system was jointed to the introduction of box girder section, in order to achieve the required torsional stiffness. To reach record spans (third generation: 1991 - 2012) hybrid cable-stayed systems became necessary: thick suspension system adopted guaranteed to greatly reduce deck stiffened system size, while consideration concerning dynamic response to wind effects led the use of aerofoil deck solutions.

In the light of these considerations, it's easy to understand why modern steel cross-sections often comprise an orthotropic deck supported by the main and cross girders (Fig. 5.3). All beam members act together for the local and global loads. From short to medium spans the torsion from eccentric live loads can be carried by a couple in the outer cable planes. Open cross-sections with little torsional resistance can thus be used. Long span system, above all in the case of a central plane of cable, may require, instead, the use of a box girder even with two outer cable planes, as in the case of Sutong Bridge, with a main span of 1088m. Nowadays, the record span The Stonecutters Bridge in Hong Kong represents an unicum: it has a central tower with two outer cable planes. In order to provide the necessary space for the tower, two separate beams connected by cross girders are used.

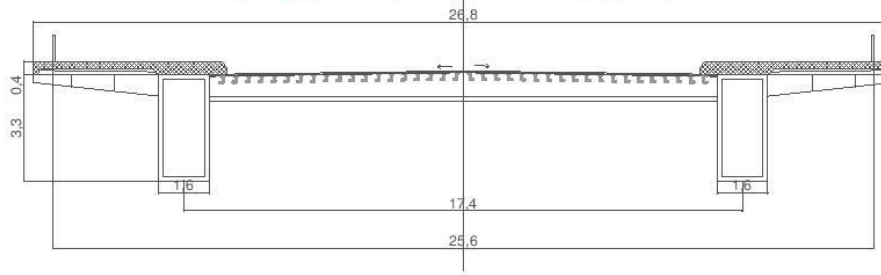
The shape of concrete cross-sections is determined from similar considerations to steel ones. It has, however, to be taken into account that concentrated tensile forces have to be carried by tendons. In the case of two outer cable planes, for two cable planes and medium spans, box girders are generally not required, becoming necessary to cross 500m-longer spans. For smaller spans, solid cross sections may be used: the elastic support of the beam from the stay cables provides a good distribution of heavy single traffic loads. A central cable plane also requires, for concrete beams, a box girder to carry the torsional moments from eccentric live loads.

Hybrid cable-stayed bridges, comprising a steel beam in the main span and a concrete beam in the side spans, is expected to change the way long span bridges are designed. The heavier concrete beam serves as a counterweight to the lighter steel main span. Both cross sections are coupled at or near the tower with shear studs and tendons if the compression force from the cables is not sufficient to overcome local tensile forces from bending.

### CABLE STAYED BRIDGES: DECK CROSS SECTION EVOLUTION

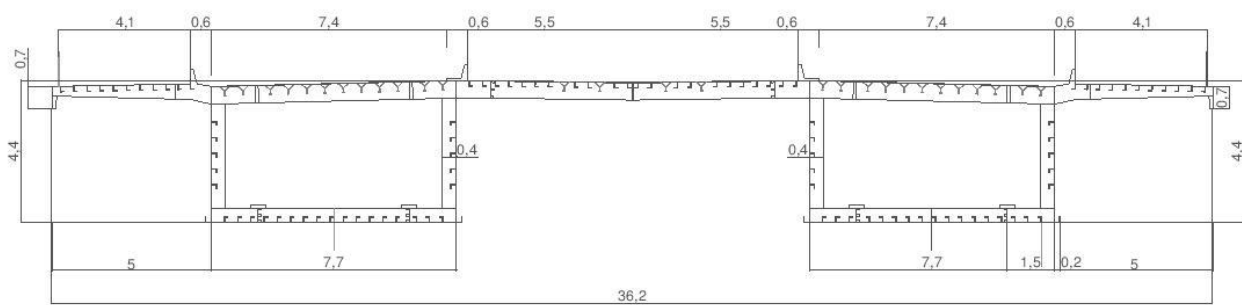
**North Bridge** (Theodor Heuss Bridge) - Dusseldorf, Germania, 1957\_ *Leonhardt, Andrä, Grassl, Wintergerst* (steel structure \_ i.p./L:14% \_ h/L: 1/77)

First generation: orthotropic deck- open section



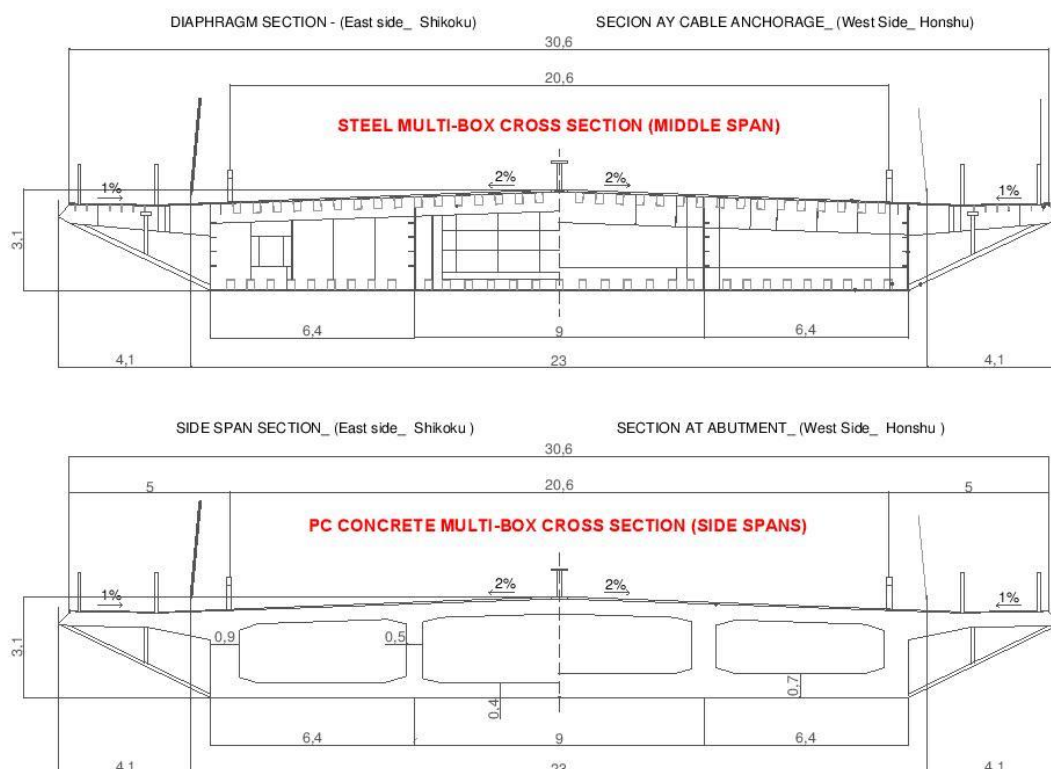
**Rhine River Bridge at Mannheim - Ludwigshafen**, Germania, 1972 \_ *Leonhardt, Andrä* \_ (hybrid structure - i.p./L:20% \_ h/L: 1/64)

Second generation: orthotropic deck with twin box sections



**Tatara Bridge**: Ikuchi- Ohmishima (Japan), 1999 \_ *Komai, Kawada, IHL, Tagagami, Matsuo* (hybrid structure - i.p./L:2% \_ h/L: 1/330)

Third generation: hybrid system with steel multi- box section in the middle span and PC concrete multi-box section at the sides spans



The rapid spread which has contradistinguishes cable stayed bridges is surely due to the advantages characterizing this typology. First of all the bending moments are greatly reduced by the load transfer of the stay cable. By installing the stay cables with their predetermined precise lengths the support conditions for a beam rigidly supported at the cable anchor points can be achieved and thus the moments from permanent loads are minimized. Even for live loads the bending moments of the beam elastically supported by the stay cables remain small. Negative live load moments may occur over the vertical bearings at the towers. They can be avoided by supporting the beam by the stay cables only, including in the tower region. The biggest positive and negative moments occur in the side spans near the hold-down piers, which may require special measures. Shear forces remain small. Large compression forces in the beam are caused by the horizontal components of the inclined stay cables. The normal forces in the main and side span equal one another so that only uplift forces have to be anchored in the abutments which act as hold-down piers.

A second important advantage of cable-stayed bridges is their ease of construction. Arch bridges with large spans are not stable during erection until the arch is closed and the horizontal support forces are anchored. They have to be temporarily supported, e. g. by auxiliary piers or temporary tie-backs. Self-anchored suspension bridges, which may be required when their horizontal cable component cannot economically be anchored due to bad soil conditions, need temporary supports of their beams until the main cables are installed. In cable-stayed bridges, however, the same flow of forces is present during free-cantilever construction stages as after completion.

The third advantage is that, unlike suspension bridges, their resistant arrangement is on its own quite sufficiently rigid for varying traffic loads, which is why the deck needs no additional rigidity to prevent problems of structure deformability that is necessary for suspension bridges. Deck bending is function of its own rigidity, so if deck is made very thin, dimensioning could be only for transversal bending and local effects between stays (whose spacing is here defined as i.p), leading to spectacularly thin slab deck in narrow bridges.

As in the case of suspension bridges, also cable-stayed design is strictly affected by dynamic aspects, especially wind-addicted ones. At the beginning of building major bridges, particularly suspension bridges, many of these early bridges were destroyed by wind effects: *Dryburgh Abbey Bridge* (by John and William Smith, 1818), *Menai Straits Bridge* (by Telford, Wales, 1839), *Tay Bridge* (by Bouch, Scotland, 1879), *Niagara Narrow* (by Keefer, USA, 1889), are only some of the well-known bridges collapses due to wind. The nature of the various dynamic phenomena was not understood for a long time. John R  bling was one of the first engineers, who felt that stiffening the girder of suspension bridges through stay cables should increase the aerodynamic stability of bridges. The destruction of Tacoma Narrows Bridge by wind effects in 1940 attracted great attention. This collapse was the origin of deep scientific research into the

phenomenon of wind-induced bridge oscillations. In cable-stayed bridges, as for any other structure, the natural modes of vibration are of major importance for the susceptibility to dynamic excitation. Low structural frequencies point to a high susceptibility. With growing structural dimensions or larger spans the frequencies decrease, so large bridges are particularly critical.

Also seismic loading is a dynamic excitation, through mostly lateral shaking of the ground. This causes inertial effects and thus time-dependent displacements in cable-stayed bridges. Earthquake loading of cable-stayed bridges could be treated in a way similar to that of other bridges or buildings. Considering high structural deformability, typically periods of vibration of cable-stayed bridges, as for other long-span bridges, are rather long (= low frequencies). For this reason, the hyperbolically decaying branch of the response spectrum is of major importance.

## 5.2 Historical development

History of cable-stayed bridges is highly unique and different from that of other types. Early examples are bridges from natural materials such as bamboo for the beam and lianas for ties. The masts of sailing vessels were always transversely stayed by shrouds. Interestingly, this analogy still exists today in the French name ‘pont a haubans’.

The first conceptual and practical application date back to the 1600s, when a Venetian engineer, Verantius, built a bridge with several diagonal chain stays. This prototype contained main features and basic principles of metal suspension bridges stiffened by stays, later used by Roebling, for Brooklyn Bridge design (1883). These concept were attractive to engineers and builders for many centuries: experimentations and developments continued until its modern-day version. At the end of World War II, West Germany determined that about 15.000 bridges had been destroyed during the conflict. Therefore, the post-war period of rebuilding the crossings gave the opportunity to apply cable-stayed bridge concept, in order to achieve economy of both material and cost. As a result of this emphasis, orthotropic plate design developed, providing a marriage with cable stayed design to produce bridges that were, in some cases 40% lighter than their pre-war counterparts. Efficient use of materials and speed of construction made cable-stayed bridges the most economical type of structure to use for replacements: in a relatively short time, from 1955 to 1974, approximately 60 cable-stayed bridges were built, just less than one-third of the total number in Germany.

### First generation (1955- 1975)

The success of modern cable-stayed bridges as the governing system for long spans started with Dischinger’s publication “*Suspension Bridges for very heavy Loads*” in 1949. In it Dischinger gives for the first time the design basis for stay



cables. The development of high-strength steel for the stays and methods to precisely calculate the forces and the appearance of hydraulic jacks which permit the stressing of the stay cables to their exact precalculated forces on site, finally overcome Navier's rejection of cable stayed bridges due to uncertain flow of forces from 1823. After an initial tentative trial for the construction of suspension bridges (Duisburg-Homberg), the first modern cable-stayed bridges were built in Belgium at Donzière, in Sweden at Strömsund, and in Germany at Büchenau. The comprehensive design of the Düsseldorf Bridge Family started the development in earnest. Decisive for the success of steel cable-stayed bridges was the development of the orthogonal anisotropic lightweight steel deck (orthotropic deck) by Wilhelm Cornelius. Until World War II the different members of the main girders acted independently of the others, the roadway slab now acts together with all other members. In the 1920's, American engineers had already begun to use steel plate riveted to steel beams for large movable bridges. The purpose was to minimize the dead load of the lift span. In 1938, the American Institute of Steel Construction (AISC) began publishing reports on the steel-deck system. AISC called this the "battledeck floor" because it felt the steel deck had the strength of a battleship. The orthotropic deck was a result of the 'battledeck' floor. This floor consisted of a steel deck plate, supported by longitudinal (normally I-beam) stringers. In their turn, these stringers were supported by cross beams. Following World War II, German engineers developed the modern orthotropic bridge design as a response to material shortages during the post-war period. The orthotropic deck reduced the weight of continuous beams considerably and permitted spans and slenderness ratios unknown until then. At first open rib longitudinal stiffeners were used, later the closed stiffeners with a higher torsion stiffness were introduced.

Despite using this technological innovation, earliest examples of cable-stayed bridge had a static behaviour quite similar to that of beam bridges. Few number of stays (corresponding to high value of  $i.p./L$ ) make deck working as simple supported beam. At the same open deck cross section made torsional problem due to asymmetrical load condition not negligible. For these open cross sections with low torsional stiffness double inclined planes of stay, above all with fan arrangement, seem to be necessary to carry eccentric load effect.

*Strömsund Bridge* (Fig. 5.4) (Fig. 5.5) (Tab. 5.2) is generally looked upon as the first modern cable-stayed steel bridge, because the concrete roadway distributes only local wheel loads and is not composite with the steel beam.

**Fig. 5.4** Strömsund Bridge – Strömsund (Sweden), 1955 – Dishinger\_ Longitudinal view

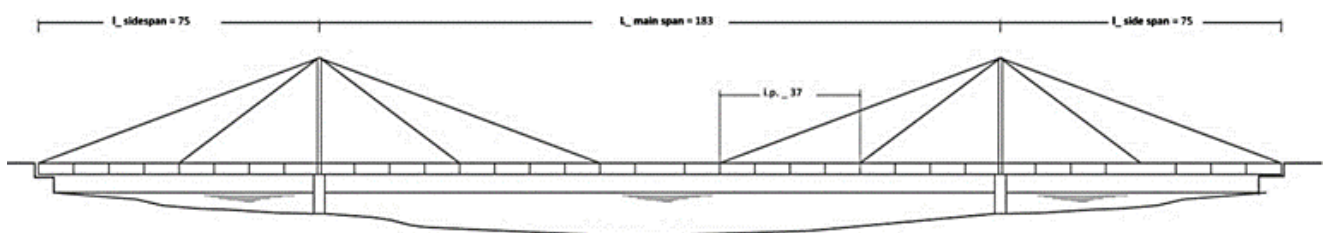




**Fig. 5.5\_** Strömsund  
Bridge \_ Strömsund  
(Sweden), 1955\_  
Dishinger

The concrete slab thus does not participate in carrying the overall beam moments and normal forces, so the Strömsund Bridge is treated under the heading of steel bridges. However, it represents a quantum leap in the development of cable-stayed bridges with the exception of its non-composite roadway slab. 3.2m high girders are supported by group of prestressed cables, forming two vertical planes, having fan arrangement, anchored at the top of trapezoidal towers, which were hinged at the base to allow rocking movements in longitudinal direction.

**Tab. 5.2\_** Strömsund  
1955 design parameters

<b>L (main span) [m]</b>	183	<b>(deck) width [m]</b>	14,30
<b>L (tot) [m]</b>	333	<b>n. of stays</b>	2 x 2 couples
<b>h (girder) [m]</b>	3,20	<b>i.p./L</b>	<b>20%</b>
<b>i.p. [m]</b>	37,0	<b>h/L</b>	<b>1/58 (2%)</b>

In the early cable stayed bridges built from the mid-1950.s to the mid-1970s, the distance between cable anchorages at deck level was generally chosen to be quite large and as a consequence each stay cable had to carry a considerable load. It was therefore necessary to compose each stay of several prefabricated strands joined together. It was necessary to let the multi-strand cable pass over the pylon on a saddle as the space available did not allow the splitting and individual anchoring of each strand, and at the deck the anchoring of the multi-strand cable made it absolutely necessary to split it into individual strands.

*Dusseldorf Bridges* family (Fig. 5.6) is a clear example of how commissioning demand greatly influences bridge design and construction. In 1952 the city of Düsseldorf started to plan three cable-stayed bridges across the Rhine with responsibility given to the architect Friedrich Tamms, and the engineer Erwin Beyer. Tamms requested that the bridges be ‘delicate and light, slender and transparent, with harp arrangement for stay cables, so that they are not only parallel in elevation but also in a skew view.



**Fig. 5.6** Dusseldorf Bridges family, 1958-1969

Even if they are quite different, common characteristics of all three bridges (*North Bridge, Oberkassel Bridge, Knie Bridge*) are the use of orthotropic decks for the beam and the construction by free cantilevering without auxiliary piers and thus without interruption of the dense ship traffic on the Rhine.

*North Bridge* (1958) (Fig. 5.7) (Fig. 5.8) (Fig. 5.9) was the first long span cable-stayed bridge. Its cable, in harp configuration, are in two planes supported by single 40.9m high towers. As one of the first modern cable stayed bridges, the design had relatively few stays, hence the distances created between the elastic supports were large. For this reason, a steel deck was used to provide sufficient stiffness. The bridge deck consists of two stiffening box girders with an orthotropic deck spanning them. Walkways are made of reinforced concrete which cantilevers from the box girders, 3.37m high, giving an overall width of 26.6m for the deck. The box girders are continuous along the deck providing the overall strength and stiffness to the bridge, mostly to resist bending. The orthotropic deck comprises a steel bearing plate, 14.3mm thick, at the top with stiffening members underneath to increase the bending and torsional stiffness of the bridge and help to distribute the concentrated wheel loads on to the box girders (Fig. 5.7\_b). The advantage of using such deck is that the bridge can achieve the maximum strength for the minimum dead weight applied. Three parallel harp stays (Fig. 5.8\_a) are attached to either side of each pylon, at third points along its height. The stays are supported on saddles so that they are continuous through the pylons.

**Fig. 5.7\_** North Bridge (o Theodor Heuss Bridge)\_ Düsseldorf (Germany), 1957\_ Grassl , Leonhardt . Longitudinal view

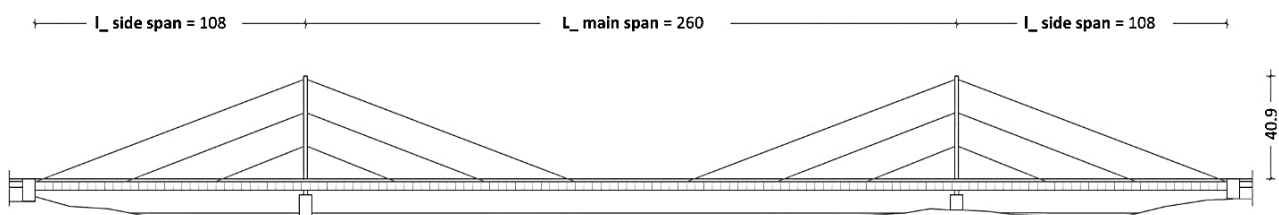






**Fig. 5.8\_** North Bridge (o Theodor Heuss Bridge)\_ Düsseldorf (Germany), 1957\_ Grassl , Leonhardt .

<b>L (main span) [m]</b>	260	<b>(deck) width [m]</b>	25,60
<b>L (tot) [m]</b>	476	<b>n. of stays</b>	2 x 3 couples
<b>h (girder) [m]</b>	3,40	<b>i.p./L</b>	<b>14%</b>
<b>i.p. [m]</b>	36,0	<b>h/L</b>	<b>1/76 (1,30%)</b>

**Tab. 5.3\_** North Bridge (1957)\_ design parameters

The pylons are fixed to the stiffening girder at the base and rise through the roadway as a single cantilever (40.0m) supported by cables. The slenderness of the pylons imply that they are not subjected to large bending moments but are experiencing concentrated cable forces at the saddles due to few cables, thus the saddles must be of high quality. Other than being a lightweight bridge, it would be regarded as impractical to build with few concentrated cable stays today since it does not fully exploit the advantages of a cable stayed bridge design.

Immediately following the North Bridge the same engineers designed the Knie Bridge and the Oberkassel Bridge. The *Knie Bridge* (Fig.5.10) (Tab. 5.4) was designed with Fritz Leonhardt. In order to achieve a visual counterpoint to the highrise buildings on the right bank of the bend in the Rhine, Tamms requested that the towers be placed on the left bank. This resulted in a main span of 320 m, structurally similar to a bridge with a 640 m main span. The stiffness of the main span was increased by connecting each forestay to a backstay that was directly anchored to the beam above the piers in the side span.

**Fig. 5.9\_** North Bridge (1957)\_ deck detail (a) upper view\_ (b) bottom view





<b>L (main span) [m]</b>	319	<b>(deck) width [m]</b>	30,60
<b>L (tot) [m]</b>	561,15	<b>n. of stays</b>	2 x 4 couples
<b>h (girder) [m]</b>	3,45	<b>i.p./L</b>	<b>15%</b>
<b>i.p. [m]</b>	48,75	<b>h/L</b>	<b>1/92 (1,08%)</b>

**Tab. 5.4\_** Knie Bridge (1959) design parameters

**Fig. 5.10\_** Knie Bridge\_ Düsseldorf (Germany), 1969\_ Leonhardt

These piers serve as hold-downs with heavy ballasted concrete footings. (Fig. 5.11) In this bridge the cable system was of the harp configuration with parallel stays, but in contrast to earlier bridges with this system, intermediate supports were arranged under every cable anchor point in the side span. This increased the efficiency of the double harp system to such an extent that it was possible to use a slender deck with an open cross section, i.e. with insignificant torsional stiffness. The anchorages for all four cables are placed outside the main girder webs, while the cable are supported in saddle bearings which allowed limited movement during the erection, being fixed when completed. For Knie Bridge design, whose aerodynamic stability was checked in wind tunnel test (National Physical Laboratory, London), additional component of vertical wind Loads, whose magnitude was comparable to horizontal component, had been taken into account. The orthotropic deck, 30,60m-wide, spans between the plat girder, providing for six traffic lanes, a sidewalk and a cycle track.

**Fig. 5.11\_** Knie Bridge (1969)\_ (a) harp cable arrangement\_ (b) cable anchorage detail\_ (c) hybrid deck solution



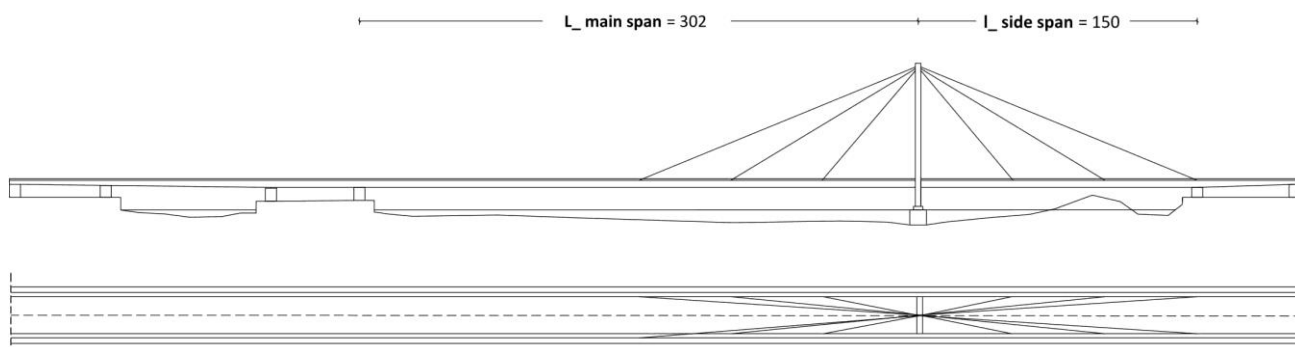




**Fig. 5.12** Severin Bridge\_Cologne(Germany), 1955\_ Grassl & Leonhardt

The *Severin Bridge* (Fig. 5.12) (Fig.5.13) (Tab. 5.5) in Cologne shows more variations of the cable-stayed system: the asymmetrical fan arranged stay cables were placed as a counterpoint to Cologne Cathedral on the opposite river bank; inclined cable planes mitigate the visual intersections of the fan stay cables in a skew view; separate support of the tower and the bridge beam is used. In this bridge, one continuous box type girder of very slender appearance spans the river, standing upon three intermediate elastic supports for each side. The whole superstructure consists of six span continuous beam with a length of  $(49,10 + 89,0 + 47,90 + 302,0 + 150,70 + 52,50)$  metres. The two largest span are stiffened by a system of 12 cables (2 x 3 couples) intersecting at the top of the tower: they converge at one point at the apex of triangular pylon (typical fan arrangement), which is advantageous to the three-dimensional structural behaviour, giving the bridge a restful appearance with no distracting intersections. The beam of the *Severin Bridge* runs freely between the tower legs, which are fixed to independent foundations. In this way the development of the idea of floating beams was initiated. Bridge cross section consists of two box-type main girders (Fig. 5.14), 3.2m wide, with the deck plate spanning between them and cantilevered sidewalks. This 9.5mm deck plate is stiffened by longitudinal flat bars, spaced 0.35m, and transverse cross floor beams, 2.01m spaced apart.

**Fig. 5.13** Severin Bridge\_(1955)\_longitudinal and plan view





Cable system of the Severin Bridge was of the efficient fan-shaped type, which is in good harmony with the A-shaped pylon. . Because of the large compression in the deck due to the one-sided arrangement of the pylon, the application of a steel floor was particularly advantageous in the Severin Bridge, as the axial compression could be distributed over a large cross sectional area. Although it was one of the very first cable stayed bridges, the Severin Bridge still stands as a most successful bridge of this type. The design of the pylon with its pronounced dimensions and the way the deck ‘floats’ through the pylon constitute fine solutions to the design problems faced.

**Fig. 5.14** Severin Bridge\_(1955)\_ (a) longitudinal view\_ (b) deck bottom view

<b>L (main span) [m]</b>	302	<b>(deck) width [m]</b>	29,30
<b>L (tot) [m]</b>	452	<b>n. of stays</b>	2 x 3 couples
<b>h (girder) [m]</b>	4,60	<b>i.p./L</b>	<b>16%</b>
<b>i.p. [m]</b>	50	<b>h/L</b>	<b>1/77 (1,30%)</b>

**Tab. 5.5\_** Severin Bridge\_(1955) design parameters

*Mannheim-Ludwigshafen (Kurt-Schuhmacher) Bridge* (Fig. 5.15) (Tab. 5.6) is a cable-stayed bridge with only one tower, carrying four traffic lanes and two tramway tracks across the Rhine. The beam width increases from 36.9 m on the Ludwigshafen side to 51.9 m for six traffic lanes on the Mannheim side. The 287 m steel main span is balanced by a post-tensioned concrete side span resting on piers at 60 and 65 m spacing. The major span superstructure consists of an orthotropic deck supported on two rectangular box girder, while the minor span, including portion over the pylon piers, is a box girder of prestressed concrete construction. A rigid connection is provided between the steel and concrete superstructure. This asymmetrical structure has stays in radiating configurations. Parallel wire cables were used for the first time in Germany with a unique corrosion protection from polyurethane and zinc chromate inside the PE-pipes, which had later to be replaced. (Fig. 5.16)



**Fig. 5.15** Rhine river bridge at Mannheim Ludwigshafen\_ (Germany), 1969-72 \_ Leonhardt und Andrä

<b>L (main span) [m]</b>	287	<b>(deck) width [m]</b>	30,0
<b>L (tot) [m]</b>	412	<b>n. of stays</b>	2 x clusters
<b>h (girder) [m]</b>	4,50	<b>i.p./L</b>	<b>20%</b>
<b>i.p. [m]</b>	20%	<b>h/L</b>	<b>1/64 (1,57%)</b>

**Tab. 5.6\_** Rhine river bridge at Mannheim Ludwigshafen\_ (1969-72) design parameters

Each parallel wire strand in the stays consists of 295 wires, corresponding to a compacted diameter of 12,70cm. in each sloping plane the stays take the following pattern: top fore-stay, six stands in three layers of two strand each ones; centre forestay, four strands in two layers of two strand each ones; lower forestays and back-stays, two strand in one layer of two; 10 strands in five layer of two strands each. Each strand is individually anchored at the pylon. Bridge deck has a constant depth of 3.80m, producing a depth to span ratio of 1/64. The (Fig. 5.16) A-shaped steel tower with a height of 71.5 m above deck has partially spread legs with two corresponding cable planes to permit the placement of the two tramway tracks inside the tower legs and the 2 x 2 traffic lanes outside. Legs of the pylon pierce side span prestressed concrete box girder of the superstructure to be supported by the pylon pier. (Tab. 5.7)

**Fig. 5.16** Rhine river bridge at Mannheim Ludwigshafen\_ (a) lanes distribution\_ (b) cable system

**Tab. 5.7\_** Rhine river bridge at Mannheim Ludwigshafen\_ (1969-72) dead loads

Element	Material	Weight	q [FL <sup>-2</sup> ]	% tot
Deck	Structural steel	4672,20 t	0.307 t/m <sup>2</sup>	76%
Pylons	Structural steel	845,50 t	0.055 t/m <sup>2</sup>	14%
Stay cables	Cable stayes	655,20 t	0.043 t/m <sup>2</sup>	10%





### Second generation (1976- 1987)

A progressive reduction of cable spacing characterized cable stayed bridges built during 70-80s. The multi-stay solution led cable system to better interact with deck: increasing number of stays anchorages along the deck, as well as deck cross sections, bridge static behaviour corresponds to that of a continuous beam with growing number of intermediate bearings. Lower effective length between stays (i.p.) involves smaller deck compression, so that minimizing section dimensions, bridges appear slender, light, nearly diaphanous. The choice of multi-stay suspension with relatively small spacing (7-15m) greatly facilitates bridge erection and permit the design of bridges with ever-increasing spans. With the aim of covering longer span, new technological solution had to be adopted. This justifies the choice for hybrid structures. Hybrid cable-stayed bridges comprise a steel beam in the main span and a concrete beam in the side spans. The heavier concrete beam serves as a counterweight to the lighter steel main span. Both cross sections are coupled at or near the tower with shear studs and tendons if the compression force from the cables is not sufficient to overcome local tensile forces from bending. As seen before for *Dusseldorf Bridges* family, in order to better integrate structure in the surrounding environment, to guarantee users comfort, above all reducing visual intersections of the stays, single plane cable system was often adopted. It's made of one vertical plane of stay cables, along the middle longitudinal axis of the superstructure, being located in a single vertical strip which is not used for any form of traffic. This arrangement require a hollow box main girder with considerable torsional rigidity in order to keep the change of cross section deformation due to eccentric live load within allowable limits. This system, proposed by Haupt, can be used if there is a median space to separate two opposite traffic lanes; in this way, no extra width is needed for the tower, and the cables at the deck level are protected against accidental impact from cars. This economically and aesthetically acceptable solution also offers the advantage of relatively small piers, because their size is determined by the width of the main girder. What differs from previous examples is also the way cables are anchored. Modern cable-stayed bridges have stay cables with well-defined and tuned cable forces which transfer their loads directly. Their horizontal components are introduced as compression forces into the beam. The forestay cables of the main span are tied back by the backstay cables to the ends of the bridge where they are anchored in hold-down (or anchor) piers. There each cable force is split into two components, the vertical force which is anchored to the ground and the horizontal force which is transmitted into the beam in compression. The compression forces from the forestays and the backstays equal one another out and reach their maximum at the towers. Anchoring backstays at bridge piers, deck compression strength is clearly reduced.



**Fig. 5.17** Friedrich-Erbert Bridge (or Bonn Nord Bridge) – Bonn (Germany), 1967\_Homberg

<b>L (main span) [m]</b>	280	<b>(deck) width [m]</b>	36,60
<b>L (tot) [m]</b>	520	<b>n. of stays</b>	20 couples
<b>h (girder) [m]</b>	4,20	<b>i.p./L</b>	<b>2%</b>
<b>i.p. [m]</b>	4,50	<b>h/L</b>	<b>1/67 (1,50%)</b>

**Tab. 5.8** Friedrich-Erbert Bridge (or Bonn Nord Bridge) (1967) design parameters

It must be pointed out that bridges with only few concentrate stays do not favourably exploit the potential advantages of cable supported structures, especially if heavy concrete deck era used. Hellmut Homberg clearly recognised this fact when, in 1967, he design his innovative *Friedrich Ebert Bridge* (or *Rhine River Bridge Bonn North*). (Fig. 5.17) (Fig. 5.18) (Tab. 5.8) He employed the concept of closely spaced stays , as In many other bridge of the time. The fact that he chose only one cable plane in the bridge axis was not primarily done for aesthetic reasons but because he wanted to reduce the size of pneumatic caisson foundations utilised.

Instead of using only a few concentrated stays consisting of a group of locked coil ropes, he designed many closely spaced individual stays for supporting the beam. The anchorage of the individual stays and their corrosion protection were simplified because, during free-cantilevering, auxiliary tiebacks for bridging the large distances between the concentrated cables were not required any more. Each beam section with a length of 4.5 m – equal to the cable distances at the beam – could be directly connected to its corresponding cable.

**Fig. 5.18** Friedrich-Erbert Bridge (or Bonn Nord Bridge) (1967)\_longitudinal view

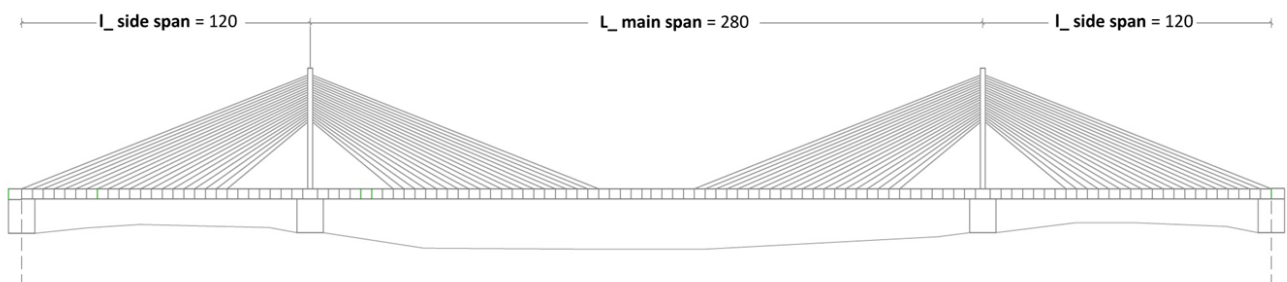






**Fig. 5.19** Friedrich-Erbert Bridge (or Bonn Nord Bridge) (1967)\_  
(a) fan arrangement\_  
(b) deck bottom view longitudinal view

The steel box girders used have a high torsional rigidity, and a high bending stiffness to permit a single plane of cables, removing these next to towers ('Homberg window'). (Fig. 5.19) Multi-cable systems lead to a more continuous support of the deck, and at the same time the cable forces to be transmitted at each anchor point are reduced, so that a local strengthening of the deck at the anchorages can often be avoided. During erection, advantages are to be found due to the much shorter length of the cantilevers required to reach from one anchor point to the next, and in the final structure the smaller stay units will ease a replacement.

In 1975 the span record of 404 m went to the *St Nazaire Bridge across the Loire in France*. (Fig. 5.20) (Fig. 5.21) (Tab. 5.9) The required vertical navigational clearance of 61 m led to a total bridge length of 3356 m in the flat terrain. Due to the nearby airport striped hazard painting appeared necessary, which gives the bridge its characteristic appearance. The approach bridges with lengths of 50.7 m were built from prestressed concrete girders with cast-in roadway slabs. The central steel box girder is continuous over the three stayed spans and has an aerodynamically shaped cross-section. The steel deck of the bridge has a streamline shape: to help with the calculations for the structure, aerodynamic investigation were undertaken, with wind tunnel testing investigations. It consists of box-section girder, of welded plates, 14.8m wide, supporting a 12m-wide carriageway, with two 0.87m-large footways. Deck plating, side plates and bottom plates are stiffened by ribs of prestressed steel throughing, and welded end-to-end.

**Fig. 5.20** Saint Nazaire Bridge\_ Loire (France), 1975\_ SAEM du pont de Saint-Nazaire, longitudinal view

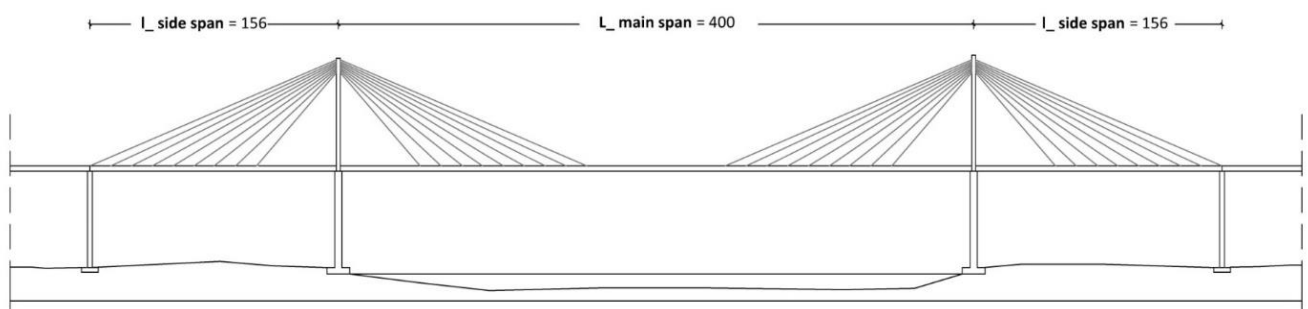




**Fig. 5.21** Saint Nazaire Bridge\_ Loire (France), 1975\_ SAEM du pont de Saint-Nazaire,

At interval of 4m, the diaphragms of the ribbed steel plate prevent any deformation of the box girder. A carriageway paving, with a thickness of 6cm of special composition for orthotropic deck was laid. The towers set up on the main piers appear as inverted V-shapes having a height of 68m above deck plane. (Fig. 5.22) The tower legs have a box cross section of (2.50mx x2m) in welded plate. The stay cables, arranged in sloping planes, are attached at the top to thick steel gusset plates, fixed to either side of the top length of the towers. The steel wire ropes of locked-coil type have a core of round strands with three or four enclosing layers of z-shaped strands, the two other layers being galvanized. These cables vary in diameter from 72mm to 105mm, according to their location in the superstructure.

**Fig. 5.22** Saint Nazaire Bridge (1975)\_ (a) deck upper view\_ (b) deck bottom view

**Tab. 5.9** Saint Nazaire Bridge\_ Loire (France), 1975 design parameters

<b>L (main span) [m]</b>	404	<b>(deck) width [m]</b>	15
<b>L (tot) [m]</b>	3356	<b>n. of stays</b>	2x 9couples
<b>h (girder) [m]</b>	3,20	<b>i.p./L</b>	<b>4%</b>
<b>i.p. [m]</b>	16	<b>h/L</b>	<b>1/126 (0,80%)</b>



The bridge was built with an unusual construction process. The metal structure was made in Marseille and was shipped by the sea around the Iberian Peninsula and along part of west French coast until reaching the mouth of the Loire. The 158m side spans were transported complete and were hoisted into position supported on their ends, with impressive deflections. The main span advanced from them in successive cantilevers, symmetrically staying the main and the side span, which led to recovering the latter's initial deflection.

Cable-stayed concrete bridges with beams from precast elements have not been built very often. The first major examples are the *Pasco-Kennewick Bridge* and the *East Huntington Bridge*, both in the USA, which were completed in 1978 and 1985. *Pasco-Kennewick Bridge* (Fig. 5.23) (Tab. 5.10) cross the Columbia River between the cities of Pasco and Kennewick, replacing a steel truss built in 1921. The fan arrangement of the stay cables requires a minimum of cable steel, produces a high compression in the beam, which is favourable for concrete, and reduces the bending in the towers. Parallel wire cables of high-strength steel permit high stresses and, in combination with their high modulus of elasticity, provide a high stiffness, which creates favourable live load moments in the beam. By using two cable planes anchored at the outside of the bridge beam a torsionally weak open cross-section without bottom slab can be used, which simplifies beam fabrication and construction. The bridge comprises two approaches and the inner three-span symmetrical cable-stayed bridge with a beam supported by 144 cables in two planes. The cables converge closely in steel tower heads. The beam is continuous with a constant shape over the full length of the bridge, fixed in the longitudinal direction at one abutment.

<b>L (main span) [m]</b>	299	<b>(deck) width [m]</b>	24
<b>L (tot) [m]</b>	674	<b>n. of stays</b>	2x 18couples
<b>h (girder) [m]</b>	2,10	<b>i.p./L</b>	<b>2%</b>
<b>i.p. [m]</b>	8,23	<b>h/L</b>	<b>1/142 (0,70%)</b>

**Fig. 5.23** Pasco-Kennewick Bridge\_ Washington (USA), 1978\_ Svensson ,Grant

**Tab. 5.10** Pasco-Kennewick Bridge\_ Washington (USA), 1978\_ Svensson ,Grant







**Fig. 5.24** Brotonne Bridge – Normandie (France), 1977\_ Muller, Mathivat, Combault

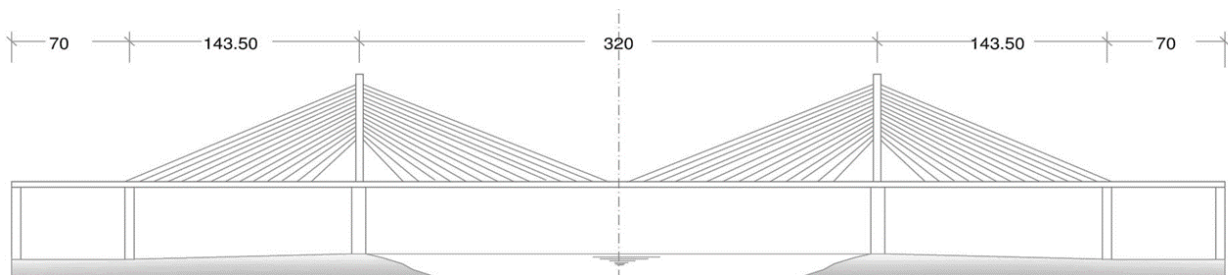
<b>L (main span) [m]</b>	320	<b>(deck) width [m]</b>	19,20
<b>L (tot) [m]</b>	606	<b>n. of stays</b>	12 couples
<b>h (girder) [m]</b>	4,0	<b>i.p./L</b>	<b>2%</b>
<b>i.p. [m]</b>	6,0	<b>h/L</b>	<b>1/80 (1,25%)</b>

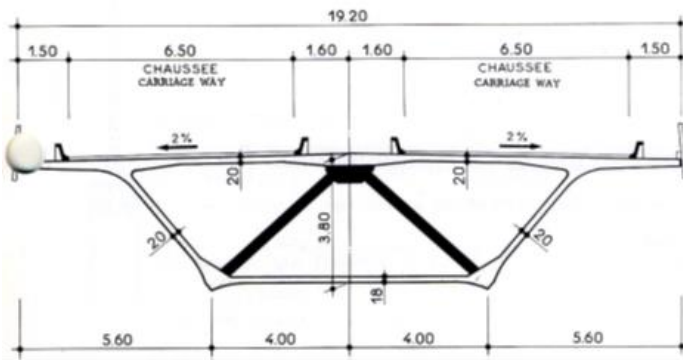
**Tab. 5.11** Brotonne Bridge (1977) design parameters

The beam cross-section comprises two outer triangular boxes and the inner roadway slab supported by cross girders: the shape of shape of the boxes was confirmed by the wind tunnel tests. The precast elements, which are 8.23 m long – equal to the cable anchorage distance – comprise the whole cross-section with a width of 24.3 m.

An interesting example of concrete cable-stayed bridge using only one central plane of cable is *Brotonne Bridge* (1977) (Fig. 5.24) (Fig. 5.25) (Tab. 5.11): in this case a box girder is required to carry torsional moment from eccentric live loads. In particular, cable forces are transmitted to the webs by post-tensioned diagonals. The structure, whose total length is 1278.40m, consists of a cable stayed bridge with a prestressed concrete deck of three span: 143.50m, 320m, 143.50m: is main span created a world record for concrete span. The main cable-stayed bridge uses 12 couples of stays, situated in a single plan along the bridge (varying in length from 84m to 340m); cables are I-towers, with hollow section varying from 4.80mx2.60m at the base to 2.84mx2.60m at the top, having a total length of 124.50m.

**Fig. 5.25** Brotonne Bridge (1977) longitudinal view





The maximum tension in the stays us 750 MPa, as 42% of the ultimate tensile strength: the variation in the letter was about 80MPa, quiet low, given that the structure is heavy and had a maximum deflection of only 0.19m compared with 0.80m for a similar steel structure (Freyssinet international: Brotonne Bidge, 08/1976). The stays were made of parallel seven-wire strands of the type used for tendons in post-tensioned concrete. Corrosion protection was achieved by inserting the parallel strands in stainless steel tubes to be subsequently filled with cement grout. The main structure forms a 5000m radius curve in the vertical plane; the right bank viaduct forms a severe curve ending up horizontally.

**Fig. 5.26** Brotonne Bridge (1977) deck detail

Material	Quantities	Q [FL- <sup>2</sup> ]
Deck concrete	14.400 tons (6000mc)	1.23 tons/m <sup>2</sup>
Steel Stays	522tons	0.044 tons/m <sup>2</sup>
Prestressing steel	150 tons	0.012 tons/m <sup>2</sup>
Reinforcing steel	780 tons	0.067 tons/m <sup>2</sup>

**Tab. 5.12** Brotonne Bridge (1977) dead loads

The left bank approach has nine spans (38.90m + 8x 58.50m), while the right one has three spans (70.00m + 55.50m + 39.00m). The deck has a constant depth of 3.80m, with 6.50m-wide carriageways, separated by 3.20m-wide central reservation. It's a single box with steeply inclined webs: wide cantilevers on the sides make up the total width of 19.20m. (Fig. 2.26) (Tab. 5.12)

The contemporary *Rande Bridge* (Fig. 2.27) (Tab. 5.13) is a steel-reinforced concrete composite cable –stayed bridge, with fan stay system. it's part of a unique project within the Atlantic Highway, which links La Coruña and Vigo, crossing the Ria de Vigo over the Strait of Rande and avoiding a detour of more than 50 km along the estuary. It has a steel deck with a total width of 23.46 m, allowing for traffic flow in both directions, at a height of 50 m above sea level.

L (main span) [m]	400	(deck) width [m]	23,50
L (tot) [m]	694	n. of stays	2 x9 couples
h (girder) [m]	2,70	i.p./L	6%
i.p. [m]	22,0	h/L	1/148 (0.65%)

**Tab. 5.13** Rande Brdige\_Vigo, (1978) design parameters





**Fig. 5.27** Rande Bridge\_Vigo, Spain (1978) \_ De Miranda

Between the central piers and the ground piers, there is a 147.42 m section on both sides, giving the central cable-stayed bridge a total length of 694.98 m. The deck is suspended with straight cables anchored to its edges, and to the heads of the central piers. The central piers, made of reinforced concrete, are 128.10 m above sea level and stand on foundations that extend 20 m below sea level, driven directly into the bedrock of the estuary. The project was completed with two access viaducts, made up of two continuous box girders, on per each side, made of prestressed concrete. The total length of the viaducts is 863 metres. The designers for the project were Florencio del Pozo, Fabrizio de Miranda and Alfredo Passaro. In 1979 it won the European Prize for Best Steel Construction.

The hybrid *Rhine River Bridge at Flehe* (Fig. 5.28) (Tab. 5.14) near Düsseldorf carries a six-lane freeway with a 364 m steel main span and a 780 m concrete approach bridge. The backstays are anchored in the first 240 m of the approach bridge which serves as counterweight for the main span. The bridge was built with only one pylon with a height of 145 one of the river banks. In contrast to the German practice at the time, the pylon was made of concrete, and its lambda ( $\lambda$ ) configuration was chosen to give support to the central cable plane with a harp-shaped cable system in the side span and a semi harp in the main span. In its appearance the pylon of the Flehe Bridge is not very convincing, especially when compared to other, more recent I-shaped pylons. The centre plane of cables is anchored at the top

**Tab. 5.14** Rhine River Bridge at Flehe design parameters

<b>L (main span) [m]</b>	368	<b>(deck) width [m]</b>	41,70
<b>L (tot) [m]</b>	1148	<b>n. of stays</b>	2 x7 couples
<b>h (girder) [m]</b>	3,15	<b>i.p./L</b>	<b>6%</b>
<b>i.p. [m]</b>	6,0	<b>h/L</b>	<b>1/97 (1,25%)</b>



The concrete and steel beam meet at a deep steel cross girder fixed to the tower legs so that a 1148 m continuous beam is created with its fixed point at the tower.. The stays each comprise 19 locked coil ropes with 60–90 mm diameter. Each rope is continuous from mainstay anchorage to backstay anchorage and is diverted in the tower on cable saddles. In the region near the tower the approach beam is provided with an additional inner central beam for the cable anchorages.

**Fig. 5.28** Rhine River Bridge at Flehe – Düsseldorf, Germany (1979) – Grassl

### Third generation (1991 – 2012)

Technological innovations, jointed to new construction methods, lead to design bridges with record spans, mainly characterized by hybrid deck structures. Multi-cable stay system is used to cover growing lengths, adopting locked coil ropes, parallel wire cables and parallel strands. Their high durability is guarantee through specific corrosion protection, including, for each strand later assembled to form cable, the following processes: galvanizing of every single wire in the strand; filling the interstices between the single wires with grease; surrounding each strand with a directly extruded PE-sheath. The installation of these stay cables takes place on site by assembling the individual components. The monostrands are pulled into the PE pipe. Each strand is individually stressed in such way that after complete cable assembly all strands have the same stress. It is possible to restress the complete cable with a large jack. Single strands may be exchanged later individually. For modern long span bridges, construction system becomes one of the decisive factors in designing and building them. The most suited for long span bridges is the cantilever method, just adding new segment and loading stays every time the deck advances. The partial structures being built during the process are stayed in the same way as the complete bridge, with the exception of different stress distribution. In many cases this cantilever

produces stress in the deck which are greater than those bridge will be in service later, which is way they may be decisive in its dimensioning. Different solutions are nowadays, adopted to reduce stresses and preventing bending due to the end of cantilever: reinforcing the cantilever with additional prestressing which is removed later, or by temporary stays; provisionally increasing of the loads in the last stay, which reduces the cantilever negative moment; cantilever advancing with a partial cross section to reduce its weight. Apart from construction upon temporary supports, another method to build cable stayed bridges is the launching one; there are possible ways of actions: the first consist of pushing the bridge with the stay fitted and tensioned to support the front cantilever produced during the launching; he second consists of pushing only the deck, with no stays and using temporary piers.

Among recent cable stayed bridges, *Helgeland Bridge* (Fig. 5.29) (Tab. 5.15) is one of the most slender, a concrete bridge with a main span of 425 m. The aerodynamically shaped beam has a depth of 1.2 m and is 12 m wide. The towers are founded on rock in 30 m depth. The bridge is exposed to severe storms with gusts of up to 77 m/s wind speed. For this bridge, located in Norway on the Artic Circle, CIP concrete beam have been used, with the advantage that no heavy precast elements have to be transported and lifted. In order to reduce the construction period, long beam sections of 12 m, equal to the cable distance, were used. The requirements for low wind resistance, aerodynamic stability and suitability for CIP construction led to an open cross-section with two solid edge girders and a beam depth of 1.2 m, giving a vertical slenderness of  $1/354$ . The towers are A-shaped above the roadway in order to increase the torsional stiffness by coupling the two tower legs; their legs merge on top of the single foundations.

**Fig. 5.29** Helgeland Bridge \_ Sandnessjoen (Norway), 1991 \_ Svensson





<b>L (main span) [m]</b>	425	<b>(deck) width [m]</b>	35,50
<b>L (tot) [m]</b>	11148	<b>n. of stays</b>	2 x 32couples
<b>h (girder) [m]</b>	1,20	<b>i.p./L</b>	<b>3%</b>
<b>i.p. [m]</b>	12,40	<b>h/L</b>	<b>1/354 (0.28%)</b>

**Tab. 5.15** Helgeland Bridge, 1991 design parameters

Cross girders are located at the cable anchorage points at a distance of 12.9 m which contain the only transverse post-tensioning. The 40 cm thick roadway slab spans 12.4 m longitudinally and 7.5 m transversely between the main and cross girders. The sizing of the beam was governed by: permanent loads plus live loads; turbulent wind; loads during construction. The required two lanes of traffic and a walkway resulted in a beam width of only 11.95 m, which leads to the remarkable slenderness in plan of 1:35.6. For the severe wind conditions the shallow, aerodynamically shaped 1.20 m deep cross-section was developed with a slenderness in elevation of 1:354. Non-linear effects in both directions were investigated using realistic non-linear stress-strain relationships (Design of Helgeland Bridge, Svensson, IASBE report, 1991).

Due the location of the bridge on the west coast of Norway, difficult weather conditions had to be taken into account for the construction planning. The problem was not low temperatures, as these were prevented by the influence of the Gulf Stream, but severe storms which regularly occur during winter months. The free cantilevering for 210 m from each tower with a beam depth of only 1.2 m was a very daring undertaking: a storm with wind speeds of up to 70 m/s (252 km/h) occurred during free cantilevering which threw the spray up to beam level.

In 1995 record span was captured by *Normandy Bridge*, (Fig. 5.30) (Tab. 5.16) having main span 856m long. It is a unique structure, 2141 m long from the south abutment to the north abutment. The main span, which crosses the river Seine without support in the stream, is 856 m long. The complete bridge adopts an hybrid solution: approaches, side spans and main span have a similar box girder cross-section with a depth of 3 m (slenderness ratio 1/368).

**Fig. 5.30** Normandy Bridge : La Havre\_Normandie (France), 1995 \_ Virloguex



**Tab. 5.16** Normandy Bridge, 1995 design parameters

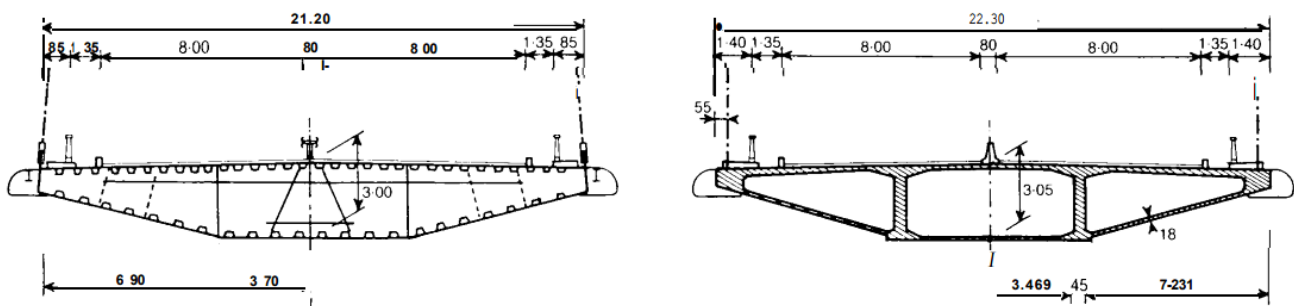
<b>L (main span) [m]</b>	856	<b>(deck) width [m]</b>	22,30
<b>L (tot) [m]</b>	2141	<b>n. of stays</b>	4x 23 couples
<b>h (girder) [m]</b>	3,05	<b>i.p./L</b>	<b>2%</b>
<b>i.p. [m]</b>	18,0	<b>h/L</b>	<b>1/280 (0.35%)</b>

The great difference in weight between the concrete access spans (45 t/m, including equipment) and the steel part in the main span (13 t/m) called for close supports in the access spans, except in the last one before the pylon on each bank, the weight of which is balanced by the weight of the concrete cantilever in the main span. However, this difference in weight avoids uplift reactions on the intermediate supports when the main span is loaded, by traffic loads or wind. (Fig. 5.31) (Tab. 5.17) The deck cross-section has been designed to reduce wind forces on the bridge, and to give a high torsional rigidity; but its shape had to be adapted for both steel and concrete construction. To reduce wind forces, the deck has been streamlined, thus following the ideas developed 25 years ago by Freeman, Fox and Partners for the British suspension bridges. To increase torsional rigidity, a box-girder has been chosen for the deck, with a lateral suspension due to the great span length.

**Tab. 5.17** Normandy Bridge, 1995\_ hybrid system dead loads

<b>Portion</b>	<b>Width [m]</b>	<b>Q [FL<sup>-1</sup>]</b>	<b>q [FL<sup>-2</sup>]</b>
Concrete ramps	22.30	15 t/m	0.67 t/m <sup>2</sup>
Steel main span	21.20	13 t/m	0.61 t/m <sup>2</sup>

The steel deck is evidently an orthotropic box-girder, formed of an external envelope, stiffened by diaphragms-3.93 m apart -and of trapezoidal stringers. The 203 m high concrete A-towers also have box girder cross-sections. The stay cables are anchored at the upper part of the tower in composite boxes. The  $8 \times 23 = 184$  parallel strand stay cables use monostrands: cables, supplied by Freyssinet, are made of parallel strands, 15 mm in diameter, that are individually protected against corrosion. The design of a bridge-especially of such dimensions-is also dependent on the erection techniques; two methods have been adopted: the access spans have been launched incrementally from both abutments, while the steel portion of the main span will be built later by the cantilever method.

**Fig. 5.31** Normandy Bridge, deck cross section\_ (a) steel deck at middle span\_ (b) PC concrete deck at side spans





*Millau Bridge* (Fig. 5.32) (Tab. 5.18) by Virlogeux is a contemporary example of multi-span cable stayed bridge, 2460 meters long (overall structure’s cost: Euro 300 000 000). The roadway of the world’s highest highway bridge is located 270 meters above the river. Each span of the six spaces between the pylons is 342 meters wide.

<b>L (main span) [m]</b>	342	<b>(deck) width [m]</b>	32,0
<b>L (tot) [m]</b>	2460	<b>n. of stays</b>	4x 13 couples
<b>h (girder) [m]</b>	4,20	<b>i.p./L</b>	<b>4%</b>
<b>i.p. [m]</b>	18,0	<b>h/L</b>	<b>1/81 (1,20%)</b>

**Fig. 5.32** Millau Bridge\_ (multi- span cable stayed bridge): Millau (France), 2004\_ Foster

**Tab. 5.18** Millau Bridge, 2004\_ hybrid system dead loads

Diagonal cables carry the road’s weight on the 90 meter high, splayed, steel pylons. The seven pylons each have a cross-section of 200 square meters at their bases, ending at their tops with 30 square meters. For this, an unimaginable 250,000 tons of concrete was poured. The steel deck (Fig. 5.33), which appears very light despite its total mass of around 36,000 tonnes, is 32 m wide. It comprises eight spans. These are composed of 173 central box beams, the spinal column of the construction, onto which the lateral floors and the lateral box beams were welded. This slender orthotropic deck has a ratio (1/81).

**Fig. 5.33** Millau Bridge\_ (2004), deck cross section

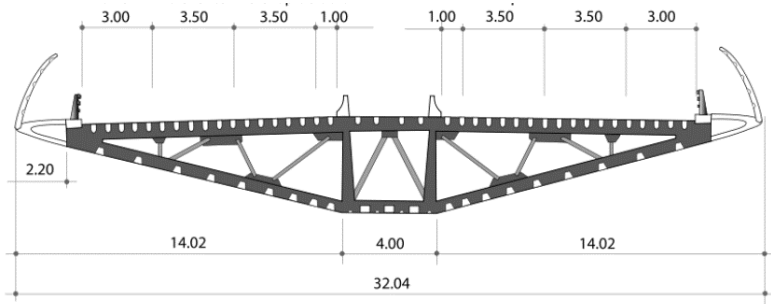




**Fig. 5.34** Millau Bridge\_ (2004)\_ (a) (b) towers\_ (c) cable arrangement

The towers (Fig. 5.34) are 90 m high above the beam with an A-shape in the longitudinal direction in order to achieve the required stiffness and, at the same time, to appear light and transparent.

For aesthetic reasons a central cable plane was selected so that the cables in the shape of a modified fan do not visually intersect. This multi-span cable stayed bridge passes over the Tarn valley at its lowest point. In order to do this it had to become the tallest road bridge in the world creating the world's tallest bridge piers standing at 242m, the structure rising to 343m at the top of the pylon (Fig. 5.34). The bridge also holds the title of the world's longest multi-span cable stayed bridge with a total length of 2460m. There is a slight gradient of 3% from North to South as well as a slight curve about a radius of 20,000m. The piers are of post tensioned reinforced concrete and the deck and pylons are of steel. (Tab. 5.19)

**Tab. 5.19** Millau Bridge\_ (2004), dead loads

Element	Material	Weight /Volume	q [FL <sup>-2</sup> ]	% tot
Deck	Structural steel	36.000 t	0.45 t/m <sup>2</sup>	12.74%
Foundation	Concrete volume	13.000m <sup>3</sup> (75.000t)	0.95 t/m <sup>2</sup>	26.54%
	Reinforcing steel	14.750 tons	0.18 t/m <sup>2</sup>	5.22%
Piers	Concrete volume	53.000 m <sup>3</sup> (127.200t)	1.61 t/m <sup>2</sup>	45.02%
	Prestressing steel	200t	0.002 t/m <sup>2</sup>	0.07%
	Reinforcing steel	10.000t	0.13 t/m <sup>2</sup>	3.54%
Piles	Concrete volume	6.000 m <sup>3</sup> (14.400)	0.18 t/m <sup>2</sup>	5.10%
	Structural steel	4.600t	0.058t/m <sup>2</sup>	1.63%
Stay cables	Structural steel	400t	0.004 t/m <sup>2</sup>	0.14%



In 1999 the span record of 890 m went to the *Tatara Bridge* (Fig. 5.35) (Tab. 5.20) in Japan, which was planned by the Honshu-Shikoku Bridge Authority. The bridge was originally foreseen as a suspension bridge but the costs for the required large abutments for anchoring the cable forces were too high and the design was changed to cable stayed. Tatara Bridge is located in one of the most geologically active parts of the world and designed for some of the world’s biggest typhoons prevalent in Japan. At a cost of \$605.8million it was one of the most expensive bridges out of the 18 major bridges built along the new route.

**Fig. 5.35** Tatara Bridge: Ikuchi- Ohmishima (Japan), 1999 – Komai\_ Kawada, IHI\_ Tagagami\_ Matsuo

<b>L (main span) [m]</b>	890	<b>(deck) width [m]</b>	30,60
<b>L (tot) [m]</b>	1480	<b>n. of stays</b>	4x 21 couples
<b>h (girder) [m]</b>	2,70	<b>i.p./L</b>	<b>2%</b>
<b>i.p. [m]</b>	21,0	<b>h/L</b>	<b>1/330 (0,30%)</b>

**Tab. 5.30** Tatara Bridge(1999), design parameters

Steel towers were selected in order to minimize the foundations in the water (Fig. 5.36) (Fig. 5.37). The slender steel beam, only 26 m above the water, with a total length of 1330 m and a width of only 25.4 m is supported from the two 220 m high towers. A beam depth of 2.7 m (depth to span length ratio of 1/326) proved to be sufficient. (Fig. 5.38)

**Tab. 5.36** Tatara Bridge(1999)\_ (a) deck view – (b) cable arrangement at the tower

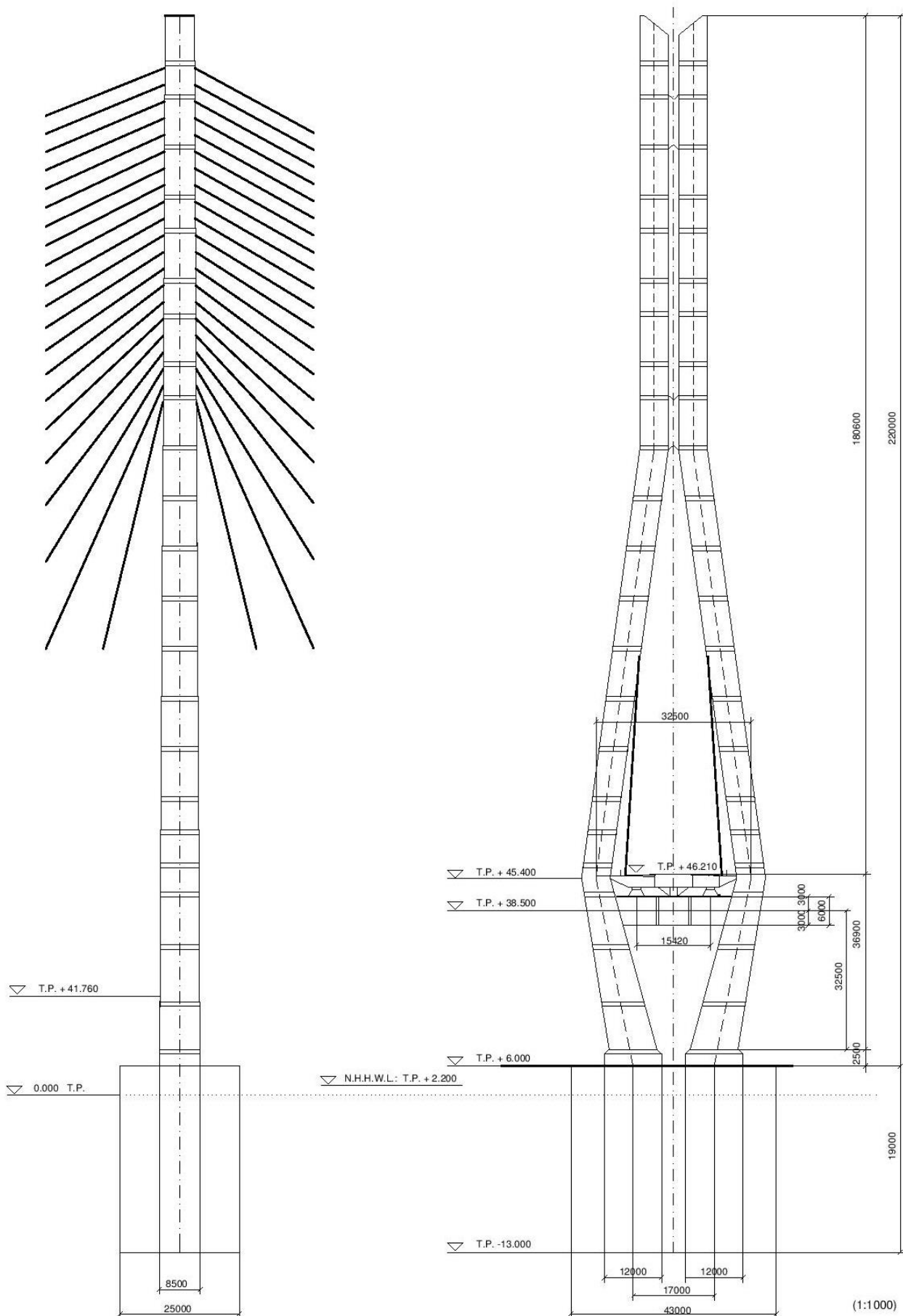


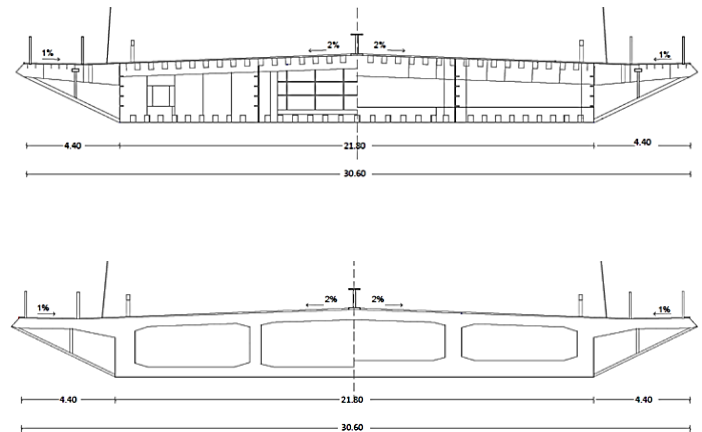
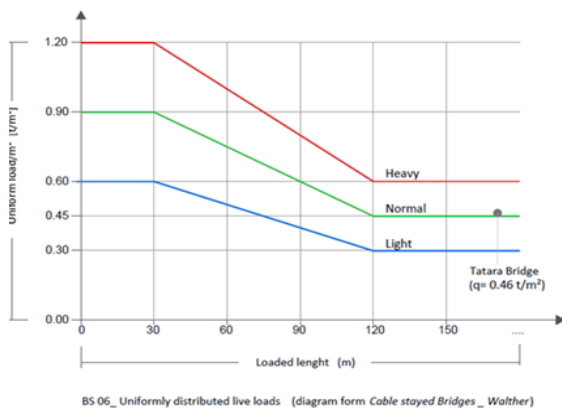


**Fig. 5.37** Tataara  
 Bridge(1999\_  
 detail

Tatara  
 tower

Chapter 5





Load type	[F] (tons)	q [FL <sup>-2</sup> ] (t/m <sup>2</sup> )
Dead load – steel structures	15879	0,40
Dead load- concrete structures	15.870	3,09
Superimposed-dead load	6.376	0,14
Live loads	17.053	0,46

**Tab. 5.31** Tataru Bridge(1999\_ loads characterization

**Fig. 5.38** Tataru Bridge(1999\_ (a) live loads characterization\_ (b) steel deck cross section\_ (c) PC concrete cross section

The main span comprises of a steel box girder with the side spans consisting of steel box and concrete box girders acting as counterweights and against uplift.(Tab. 5.31)

Tataru bridge record span was outclassed by *Sutong Bridge* (Fig. 5.39) (Fig. 5.40) (Tab. 5.32) in China, with a main span of 1088 m and side spans of (2x300m) + (4x100m). It's the main portion of a viaduct, having a total length of 8 km. A balanced cantilever concrete bridge with a main span of 268 m provides a secondary navigation span. The approach bridges have spans varying between 42 m and 75 m. The total costs of the Sutong bridge building project are estimated at around 6.45 billion yuan (approximately US \$ 726 million).

<b>L (main span) [m]</b>	1018	<b>(deck) width [m]</b>	41,0
<b>L (tot) [m]</b>	2088	<b>n. of stays</b>	2x 34 couples
<b>h (girder) [m]</b>	4,0	<b>i.p./L</b>	<b>2%</b>
<b>i.p. [m]</b>	12,17	<b>h/L</b>	<b>1/272 (0,37%)</b>

**Tab. 5.32** Sutong Bridge (China), 2009\_ COWI, design parameters

**Fig. 5.39** Sutong Bridge\_ Jiangsu, China (China), 2009\_ COWI, longitudinal view

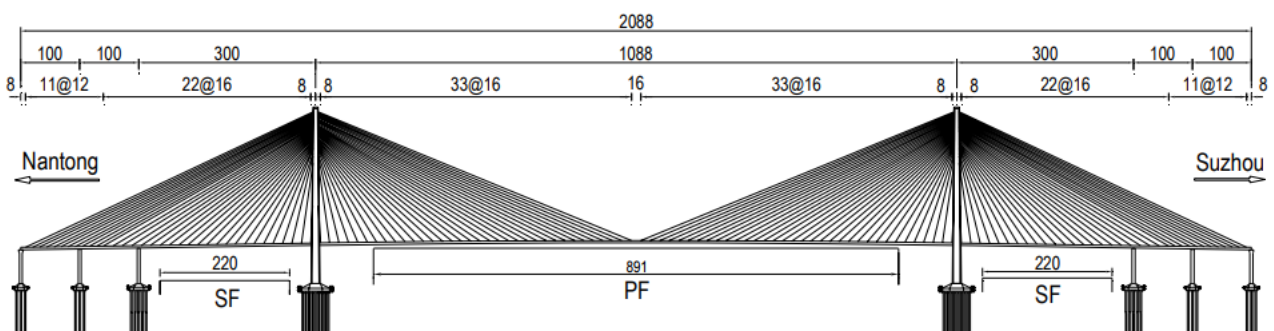






**Fig. 5.40** Sutong Bridge\_ Jiangsu, China (China), 2009\_ COWI

The cable stayed bridge girder is a streamlined closed flat steel box girder, whose high torsional resistance resulting in a good aerodynamic stability. The total width including wind fairing is 41.0 m accommodating dual 8 traffic lanes. The cross-section height is 4.0 m. (Fig. 5.41) (Fig. 5.42) The steel box is generally stiffened in the longitudinal direction with closed steel troughs. Transverse plate diaphragms are provided with a typical distance of 4.m and with smaller distances down to 2.27m locally around the two pylons. The two 300 m high concrete box towers are simply A-shaped. The foundation for each A-shaped pylon consists of 131 drilled shafts, 2.8/2.5 m in diameter.

**Fig. 5.41** Sutong Bridge (2009)\_ steel box cross section detail

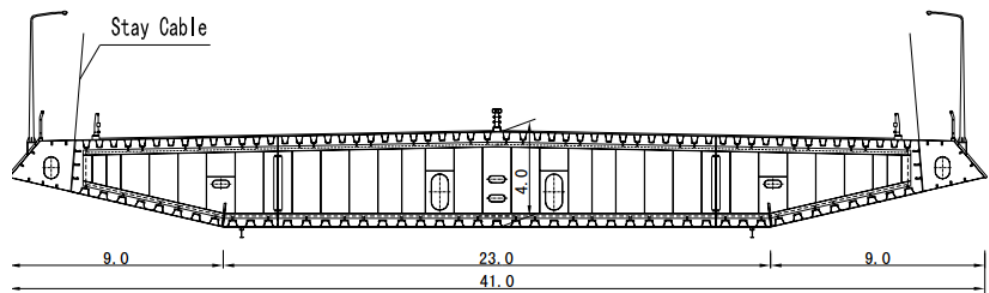


**Fig. 5.42** Sutong Bridge (2009) steel box cross section, construction step





The piers consisted of reinforced, hollow concrete columns with the construction climbing up from the base by integrating a working platform from which the concrete can be poured. The stay cables are arranged in double inclined cable planes with standard spacing of 16 m in the central span and 12 m near the ends of the back spans along the girder. To reduce the effect of wind loads, the cable stay systems are made of the parallel wire strand consisting of 7 mm wires.

**Fig. 5.43** Stonecutters Bridge\_ Hong Kong (China), 2009\_ Yokogawa Bridge Corporation

The *Stonecutters Bridge* (Fig. 5.43) (Tab. 5.40) became the second longest cable-stayed bridge in 2009. It is the new landmark of Hong Kong. The concrete towers are 298 m high and comprise an upwards tapering slender circular cross-section. The beam consists of two separate box girders, which straddle the central towers. The two separate box girders of the superstructure are connected by cross girders at cable distance, creating a girder grid.

<b>L (main span) [m]</b>	1018	<b>(deck) width [m]</b>	53,0
<b>L (tot) [m]</b>	1596	<b>n. of stays</b>	2x 28 couples
<b>h (girder) [m]</b>	3,90	<b>i.p./L</b>	<b>2%</b>
<b>i.p. [m]</b>	22,0	<b>h/L</b>	<b>1/261 (0,38%)</b>

**Tab. 5.40** Stonecutters Bridge (2009) design parameters

The striking profile of Stonecutters Bridge (Fig. 5.44) (Fig. 5.45) (Fig. 4.46) is one of new generation of long span cable stayed bridges. The main span has a unique slender twin orthotropic steel deck 53m wide linked by cross girders at 18m centres giving excellent aerodynamic performance.

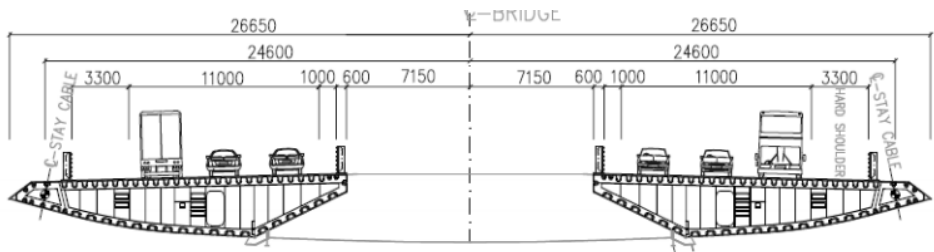


**Fig. 5.44** Stonecutters Bridge (2009, twin box section detail



**Fig. 5.45** Stonecutters Bridge (2009, twin box section\_ (a) detail\_ (b) deck bottom view

A prefabricated parallel wire strand stay cables system was used, which reduced the effect of cable drag. Deck dampers are also being installed to minimize cable vibration. The main span lifting period went through two typhoon seasons, one of which was particularly active, and this involved contingencies at every stage to ensure that safety was not compromised. The 65 steel deck segments weighing a total of 33,200 tonnes were fabricated from high grade S420M or S420ML rolled steel plate in accordance with BS EN 10113 which was procured from Japan and Europe. The segment plates varying in thickness from 10 to 40mm were rolled and cut, and the U-troughs, T stiffeners and anchor boxes added. The reinforced concrete towers start as an oval 24m across at the base and reduce to a circular cross section 7m diameter at 175m level and were built using a jump form system. The upper tower then becomes a composite structure with a stainless steel outer skin and inner steel anchor boxes for the stay cables.

Stonecutter Bridge has been designed to withstand extreme storms and earthquake. Thus, a non conventional restraint system has been used to connect the deck to the pylon in both longitudinal and transverse directions (note from FIP Industriale). At each pylon a group of four 8000kN capacity Shock Transmission Units are installed (displacement 400mm) along the longitudinal direction. To control and mitigate the transversal movements of the main bridge girder, two special lateral spherical bearings connected the girder to each pylon (maximum force 50.600 kN at SLS, 65.000 at ULS)

**Fig. 5.46** Stonecutters Bridge (2009) construction steps







The *Russky Bridge* (2012) (Fig. 5.47) (Tab. 5.41) (Eastern Bosphorus Strait crossing) with is the current recordholder with its main span of 1104 m, connecting City of Vladivostok in Russia with Russky Island. The shape of the both slender concrete towers resembles a narrow-A, height 321m. Along the main span, the bridge deck shape is a round-edged steel box girder, 29.5m wide. The vertical clearance at main span is notably high, 70 m.

**Fig. 5.47** Russky Bridge\_ Vladivostok (Russia), 2012 \_ SIC Mostovik

<b>L (main span) [m]</b>	1104	<b>(deck) width [m]</b>	21,0
<b>L (tot) [m]</b>	1872	<b>n. of stays</b>	2x 19 couples
<b>h (girder) [m]</b>	3,0	<b>i.p./L</b>	<b>2%</b>
<b>i.p. [m]</b>	2,0	<b>h/L</b>	<b>1/368 (0,27%)</b>

**Tab. 5.41** Russky Bridge (2012) design parameters

The design of the bridge crossing has been determined on the basis of two primary factors: (1) shortest coast-to-coast distance in the bridge crossing location 1460 m: navigable channel depth is up to 50 m; (2) the locality of the bridge crossing construction site is characterized by severe climate conditions: temperatures vary from minus 31 to plus 37 degrees, storm wind velocity of up to 36 m/s, storm wave height of up to 6 m, ice formation in winter of up to 70 cm thick. (Fig. 5.48)

**Fig. 5.48** Russky Bridge (2012\_ construction steps in extreme conditions





**Fig. 5.49** Russky Bridge (2012)\_ (b) deck cross section detail

Therefore, the span structure has an aerodynamic cross section to resist squally wind loads. (Fig. 5.48) The deck cross section shape has been determined based on aerodynamic analysis and optimized following the results of experimental wind tunnel testing of the scaled model.

The cable stayed system assumes all static and dynamic loads on the bridge deck. Cable stays are provided with maximum possible protection not only against natural disasters, but also against other adverse effects. The so-called “compact” PSS system has been implemented in the cable-stayed bridge deck; this advanced system differs by denser strands allocation in the sheath. Compact design of cable stays that employs sheaths of smaller diameter makes for wind load reduction by 25-30%. Moreover, the cost of materials for pylons, the stiffening girder and foundations decreases by 35-40%.

#### **New frontier for cable-stayed bridge design: hybrid suspension system**

Cable-stayed bridges are structurally rational and can extend the applicable span length. They are still developing, so new suspension types have been proposed recently to solve problems due to their flexibility (increased with span length) and loss of strength for dynamic loads (traffic and wind). The new overlapping stay system and the hybrid cable solution, are nowadays used to significantly reduce the displacements of the girder and the bending moment of the towers due to live loads.

**Fig. 5.50** New Forth Bridge (Queensferry Crossing). 2011-2017





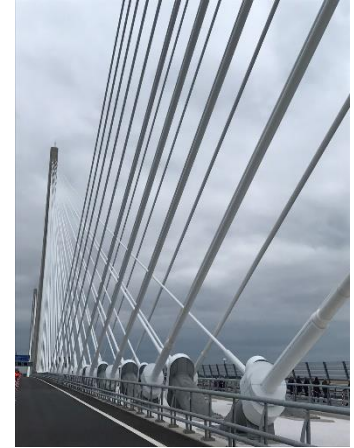


**Fig. 5.51** New Forth Bridge (Queensferry Crossing). 2011-2017

The deflection of the girder with the overlapping stay system due to the train loads decreases by 9.5%, and the hybrid cable system decreases by 10% in comparison with the conventional cable system. The overlapping stay system has been adopted on the New Forth Bridge, or Queensferry Crossing (2011-2017) (Fig. 5.50) (Fig. 5.51) (Tab. 5.42) where the girders are suspended with overlapping stays near the span center in addition to the stays spread on other parts. The Queensferry Crossing is a three-tower cable stay bridge with stay cables crossed at midspan to stabilise the central tower. This is the first use of crossed cables on a large bridge, resulting in three slim mono towers that are visually sympathetic to the existing two towers of the Forth Road Bridge and the three cantilevers of the Railway Bridge. The bridge deck is made up of 122 composite steel/concrete sections.

<b>L (main span) [m]</b>	2x650	<b>(deck) width [m]</b>	39.80
<b>L (tot) [m]</b>	2638	<b>n. of stays</b>	288
<b>h (girder) [m]</b>	4.30	<b>i.p./L</b>	<b>1.7%</b>
<b>i.p. [m]</b>	10.65	<b>h/L</b>	<b>1/151 (0.66%)</b>

**Tab. 5.42** New Forth Bridge (Queensferry Crossing). Design parameters

The Queensferry Crossing is the longest (2.7 kilometres three-tower, cable-stayed bridge in the world, as well as being the largest to feature cables which cross mid-span. The innovative design provides extra strength and stiffness, allowing the towers and deck to be more slender.

**Fig. 5.52** Yavuz Sultan Selim Bridge or Third Bosphorus Bridge (2013-2016)



For hybrid cable system, the girders are suspended by the suspension cables at the center part in addition to the stays on other parts. This hybrid cable system is a combined system of the cable-stayed bridge and the suspension bridge and has been adopted on the Third Bosphorus Bridge, (Fig. 5.52) (Tab. 5.43) a road and railway bridge.

**Tab. 5.43** Third Bosphorus Bridge Design parameters

<b>L (main span) [m]</b>	1408	<b>(deck) width [m]</b>	58.50
<b>L (tot) [m]</b>	1875	<b>n. of stays</b>	176
		<b>n. of hangers</b>	2x34
<b>h (girder) [m]</b>	5.50	<b>Ip/L</b>	1.77%
<b>i.p. [m]</b>	25m	<b>h/L</b>	<b>1/256 (0.37%)</b>

With a main span of 1408m, the so called Yavuz Sultan Selim Bridge combines the hybrid steel-concrete deck solution, typical of modern cable-stay system, to the hybrid suspension cable arrangement which strengthens the stay-cable one with the suspension system at the mid span.

If cable-stayed system was early used (19th century) to stiffen suspension one, above all in the case of more flexible deck bridge, failed on account of insufficient resistance to wind pressure, firstly Roebling understood the huge potential of stay-cable solution: in connection with stiffening truss and efficient lateral bracings, inclined stays proved more effective. However, in Roebling's proposal, cables of suspension bridges were always "assisted" by stays, as efficient and economic mean for stiffening the floor against the cumulative undulations that may be started by the action of the wind. This radiating stay system had primarily the critical function of adding rigidity to the span, ingeniously taking the advantage of the increasing the loading-carrying capacity which they incidentally supplied. But the earliest hybrid system appeared quite redundant; as Roebling said: *"The floor in connection with the stay, will support itself without the assistance of the cable, the supporting power of the stays alone will be ample to hold up the floor. If the cable were removed, the bridge would sink in the centre but would not all"*.

**Fig. 5.53** Third Bosphorus Bridge construction steps





Nowadays, the restatement of the hybrid suspension system, proposed for Third Bosphorus Bridge (2016), has given the possibility to overcome the span record of cable-stayed system, hold by 1104m-long central span of Russky Bridge (Fig. 5.47) up until 2012.

**Fig. 5.54** Third Bosphorus Bridge, suspension system details

The economic, constructive and structural advantages of hybrid suspension solution, agree the request for an extremely short period of design and construction (only 36 months, Virlogeux), creating an iconic and outstanding landmark of Istanbul region, connecting Europe with Asia. In this case, the choice of suspending girder with a parabolic cable in the centre part, in addition to stays on the other part, has been dictated by several reasons: (1) the severe loading scheme (it's the widest and longest hybrid railway bridge, carrying 8 lanes for motorway and 2 lanes of railways on a single level,; live loads are almost 60% of the permanent loads); (2) the need to reduce construction period (Fig. 5.53)(Fig. 5.54); (3) the need to better govern slender deck bridge deflection (compared to usual cable stayed bridge, adding the main parabolic cable guarantees to greatly reduce, of about 10%, displacement of the girder, as well as bending moment of the towers, due to live loads.

French construction master Dr.Michel Virlogeux [35] expressed that the 3<sup>rd</sup> Bosphorus Bridge is a unique structure in many terms. Highlighting the weight of the bridge, he said: *"This bridge has to hold a big weight due to the fact to the fact that there is a railway on. In addition to this there will be an extra weight on the bridge as a result of the heavy traffic in Istanbul."* Concerning earthquake effects, he said: *"Earthquake is a big question in Turkey. Thankfully, the Bosphourusr region is more secure seismically when compared to Izmin shoreline. Our bridge was designed in a way that it will not be affected from any earthquake thanks to its flexibility."*



### 5.3 Critical evaluation of existing cable-stayed bridges: changing role of stiffened girder and its effect on design parameters improvement

Back analysis of 27 existing structures can be summarized as follows:

#### FIRST GENERATION

Bridge	Construction end	Designer	L (m)	i.p. (m)	h (m)	i.p./L	h/L
Strömsund Bridge	1955	Dishinger	183	37	3.2	20%	1\58 1.75%
North Bridge	1957	Grassl Leonhardt	260	36	3.39	14%	1\77 1.30%
Severin Bridge	1959	Lohmer	183	50	3.2	16%	1\66 1.06%
Friedrich-Ebert Bridge	1967	Homberg	302	4.5	4.2	2%	1\67 1.39%
Knie Bridge	1969	Leonhardt	319	48.75	3.45	15%	1\92 1.08%
Rhine River Bridge	1972	Leonhardt Andrä	287	60	4.5	20%	1\64 1.57%

#### SECOND GENERATION

Bridge	Construction end	Designer	L (m)	i.p. (m)	h (m)	i.p./L	h/L
Saint-Nazaire	1975	SAEM	404	16	3.2	5%	1\126 0.79%
Oberkassel Bridge	1976	Andrä – Grass	258	51.55	3.15	19%	1\82 1.22%
Brotonne Bridge	1977	Muller	320	6	4	2%	1\80 1.03%
Rande Bridge	1977	De Miranda	400	22	2.7	6%	1\148 0.68%
Ponte all'Indiano	1978	De Miranda	206	30.5	2.6	12%	1\37 1.26%
Pasco-Kennewick	1978	Grant – Svenson	299	8	2.1	3%	1\142 0.70%
Flehe Bridge	1979	Schambeck	368	9	3.15	5%	1\97 0.85%
Barrios de Luna	1984	Casado	440	8	2.3	2%	1\191 0.52%
Faro-Folster	1985	COWI	290	15	3.5	5%	1\82 1.20%

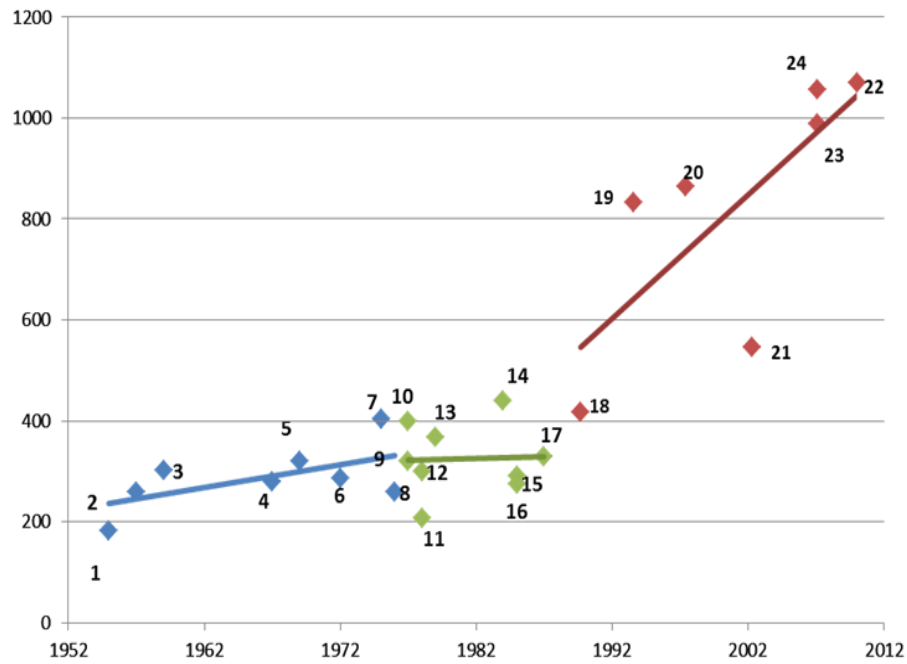


**THIRD GENERATION**

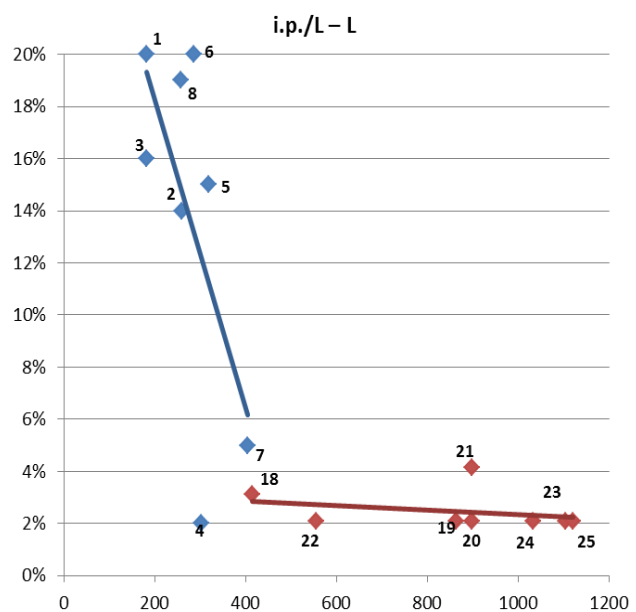
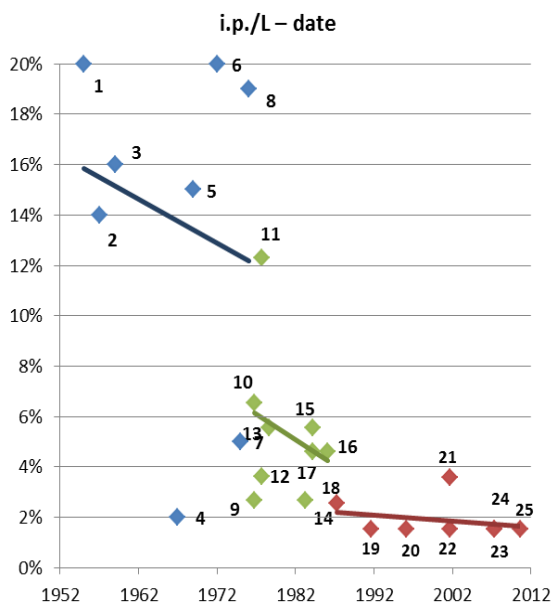
<b>Bridge</b>	<b>Constructi on end</b>	<b>Designer</b>	<b>L (m)</b>	<b>i.p. (m)</b>	<b>h (m)</b>	<b>i.p./ L</b>	<b>h/L</b>
<b>East Huntingto n</b>	1985	Svensson	274	11	1.52	<b>4%</b>	<b>1\180 0.55%</b>
<b>Panarà River</b>	1987	Heckhausen Cabjolsky	330	14	2.93	<b>4%</b>	<b>1\112 0.89%</b>
<b>Helgeland Bridge</b>	1991	Svensson	425	12.4	1.2	<b>3%</b>	<b>1\354 0.28%</b>
<b>Normandy Bridge</b>	1995	Virlogeux	856	18	3.05	<b>2%</b>	<b>1\280 0.35%</b>
<b>Tatara Bridge</b>	1999	Komai – Kawada	890	18	2.7	<b>2%</b>	<b>1\330 0.30%</b>
<b>Millau Bridge</b>	2004	Virlogeux	342	22	4.2	<b>4%</b>	<b>1\81 1.22%</b>
<b>Rion- Antirion Bridge</b>	2004	Pecker Tourtois	560	12.5 1	2.82	<b>2%</b>	<b>1\198 0.50%</b>
<b>Sutong Bridge</b>	2009	COWI	1088	12.1 7	4	<b>2%</b>	<b>1\272 0.370 %</b>
<b>Stonecutte rs Bridge</b>	2009	Halcrow	1018	22	3.9	<b>2%</b>	<b>1\261 0.380 %</b>
<b>Ruski Bridge</b>	2012	SIC Mostovik HIO	1104	23	3	<b>2%</b>	<b>1\368 0.27%</b>

Previous evaluations confirm as this quiet recent typology has had a great improvement in the last 60 years, becoming well competitive to suspension one. Cable stayed bridge historical evolution underlines a progressive span growing, passing from the early examples with little more than 150m long spans, to record bridges which reach 1108m. From the first to the second generation, till the last one, the multi-stay system has been largely adopted: as seen before, increasing cables number leads to a strictly deck –cables interaction; reducing cable spacing (till i.p./L of 2%) results in lower compression strength transferred to deck. Consequently, deck cross section dimensions could be greatly reduced. A closer succession of cross load bearing elements, corresponding to a discretization of the deck in portion having little effective length, as well the use of modern multi-box cross sections, guarantee the required stiffness to deck, making possible the construction of bridge with high slenderness ratio (as 1/354). In this way a perfect optimization, both from a structural and from an aesthetic point of view, is gained.

## GROWING MAIN SPAN\_ L – date: 1955 - 2012

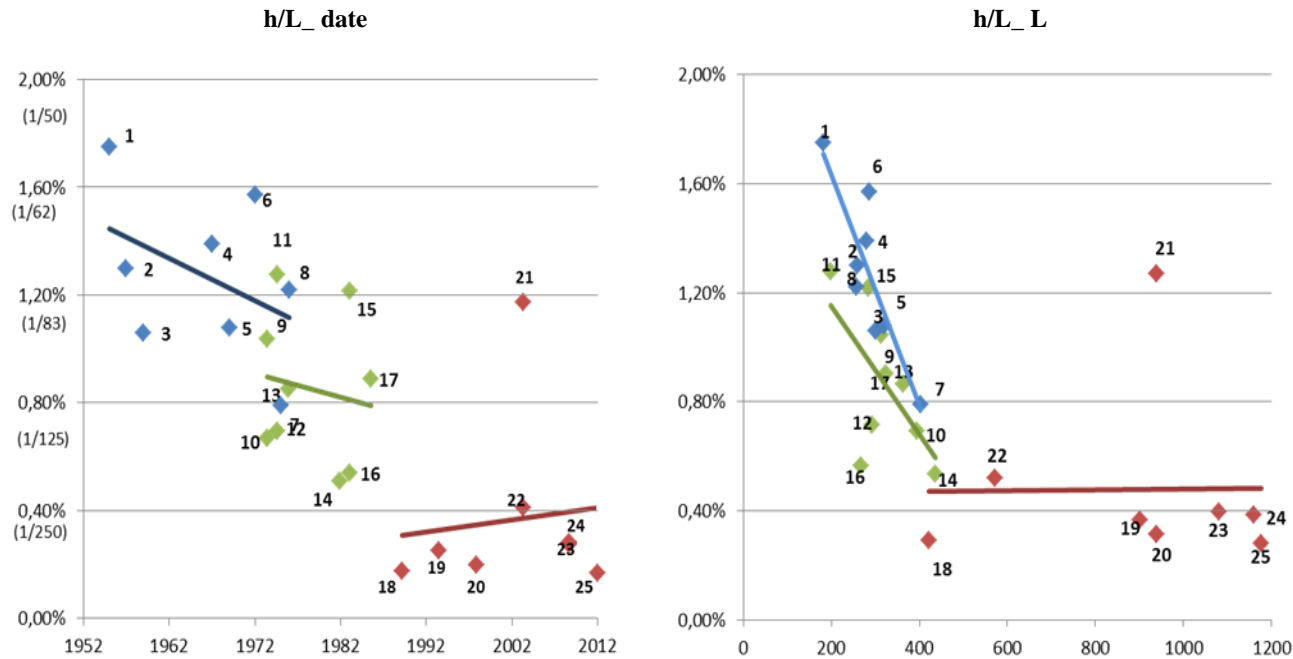


## CHANGING STAY SPACE: 1955 - 2012



n.	date	name	n.	date	name	n.	date	name
1	1955	Strömsund Bridge	9	1977	Brotonne Bridge	17	1987	Panarà River Bridge
2	1957	North Bridge	10	1977	Rande Bridge (Vigo)	18	1991	Helgeland Bridge
3	1959	Severin Bridge	11	1978	Ponte all'Indiano	19	1995	Normandy Bridge
4	1967	Friedrich-Ebert Bridge	12	1978	Pasco- Kennewick Bridge	20	1999	Tatara Bridge
5	1969	Knje Bridge	13	1979	Flehe Bridge	21	2004	Millau Bridge
6	1972	Rhine River Bridge	14	1984	Barrios de Luna Bridge	22	2004	Rion- Antirion Bridge
7	1975	Saint- Nazaire Bridge	15	1985	Faro- Folster Bridge	23	2009	Sutong Bridge
8	1976	Oberkassel Bridge	16	1985	East Huntington Bridge	24	2009	Stonecutters Bridge
						25	2012	Russki Bridge

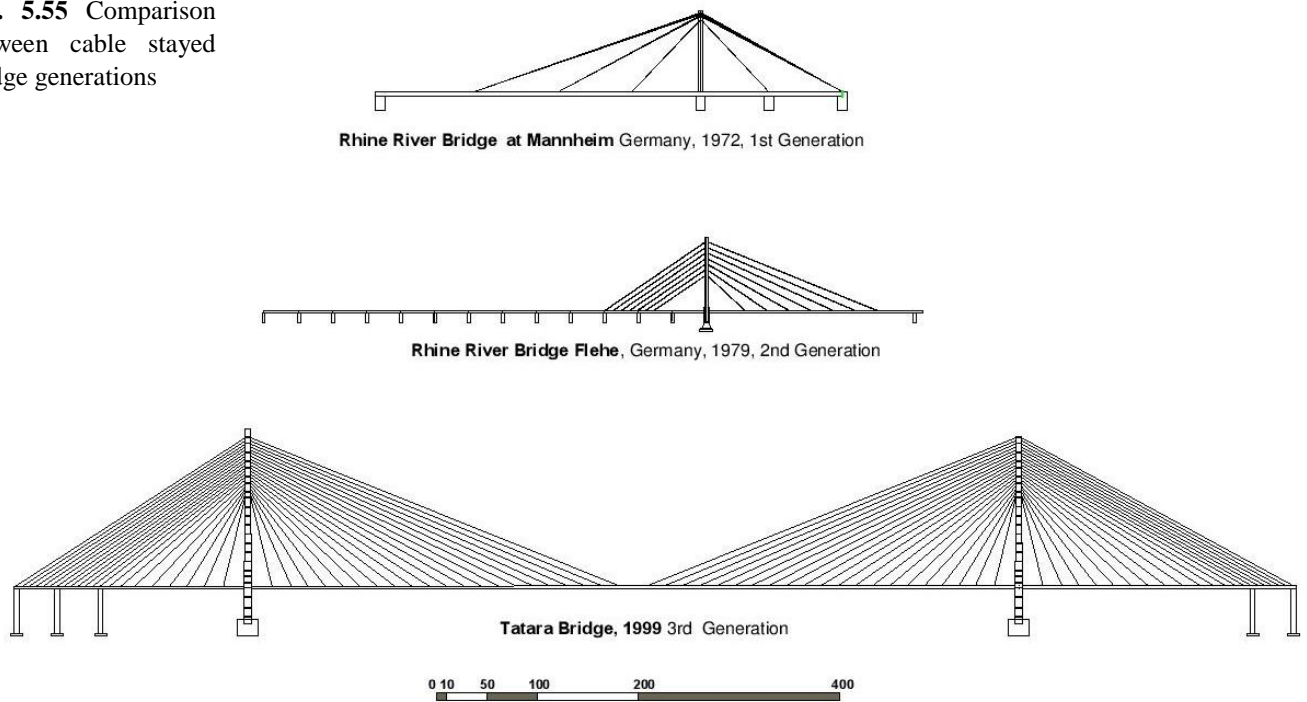
DECK SLENDERNESS : 1955 – 2012



n.	date	name	n.	date	name	n.	date	name
1	1955	Strömsund Bridge	9	1977	Brotonne Bridge	17	1987	Panarà River Bridge
2	1957	North Bridge	10	1977	Rande Bridge (Vigo)	18	1991	Helgeland Bridge
3	1959	Severin Bridge	11	1978	Ponte all'Indiano	19	1995	Normandy Bridge
4	1967	Friedrich-Ebert Bridge	12	1978	Pasco- Kennewick Bridge	20	1999	Tatara Bridge
5	1969	Knie Bridge	13	1979	Flehe Bridge	21	2004	Millau Bridge
6	1972	Rhine River Bridge	14	1984	Barrios de Luna Bridge	22	2004	Rion- Antirion Bridge
7	1975	Saint- Nazaire Bridge	15	1985	Faro- Folster Bridge	23	2009	Sutong Bridge
8	1976	Oberkassel Bridge	16	1985	East Huntington Bridge	24	2012	Stonecutters Bridge
						25	2012	Russki Bridge

Considering the earliest examples of 50-60s years, having a few number of stays, bridge static behaviour can be assimilated to that of a simply supported beam; full advantages of cable stayed system cannot be taken from these earliest solutions, which needed stiffened longitudinal girder to carry loads ( $h/L= 1/60$ ). The introduction of multi-cable stay system, since 70-80s years, has given the possibility to build slender deck for bridges: using closed-cable-spacing, bridge deck can be assimilated to a beam on elastic supports. Multi-cable systems lead to a more continuous support of the deck, and at the same time the cable forces to be transmitted at each anchor point are reduced, so that a local strengthening of the deck at the anchorages can often be avoided. During erection, advantages are to be found due to the much shorter length of the cantilevers required to reach from one anchor point to the next, and in the final structure the smaller stay units will ease a replacement. Full advantage of the continuous support from the multi-cable system is, surely, to reduce the dimensions of the deck: the local bending of the deck becomes insignificant and a very slender deck might therefore be applied if the global stability is achieved without requiring flexural stiffness of the deck.

**Fig. 5.55** Comparison between cable stayed bridge generations



The historical evolution can help to understand how the role of stiffening girder has changed. Considering the last examples, it's easy to note that the attempt to optimize structures has always been reached thickening cable-stay system: this allows to use slender decks, whose streamline box sections guarantee a high torsional stiffness also in the case of asymmetrical live load conditions. Adopting deep-close spacing cables, bending moments are greatly reduced, so that longitudinal girder has to carry only compression strengths.

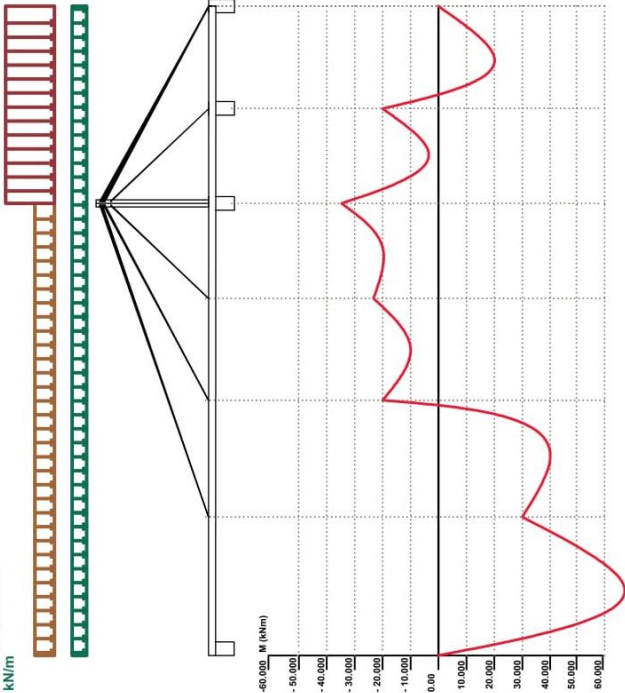
To better realise this extraordinary change in approaching to bridge design, underlining how is changed the load bearing capacity required to girder (especially for bending stress), the comparison between three different cable-stayed bridges, one for each generation, could be useful. (Fig. 5.55)

*Rhine River Bridge at Mannheim* (1972,  $L=287\text{m}$ ), with 3 couples of stay cluster ( $ip/L=20\%$ ) and 4.50m-high girder ( $h/L= 1/64$ ), has been assumed as emblematic case for the first generation, *Rhine River Bridge at Flehe* (1979,  $L=368\text{m}$ ), having 7 couples of stays and 3.15-high girder, has been considered for the second, finally *Tataru Bridge* (1999,  $L=890\text{m}$ ), with 21 couples of stays ( $ip/L=20\%$ ) and 2.70m-high box girded, has been valued for the third generation. A comparison between bending moment diagrams, due to symmetrical (dead + live) loads uniform distribution, follows.



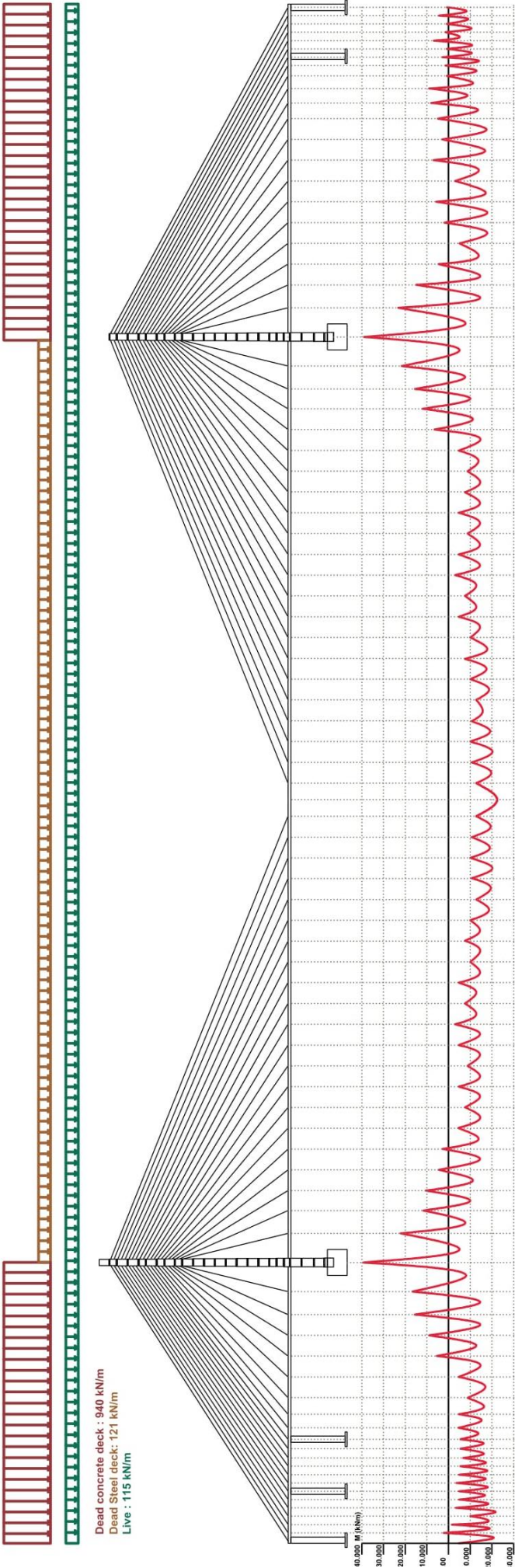
**Rhine River Bridge at Mannheim** Germany, 1972, 1st Generation - Hybrid structure (i.p./L:20%, h/L: 1/64)

Dead concrete deck : 340 kN/m  
Dead Steel deck: 130 kN/m  
Live : 90 kN/m



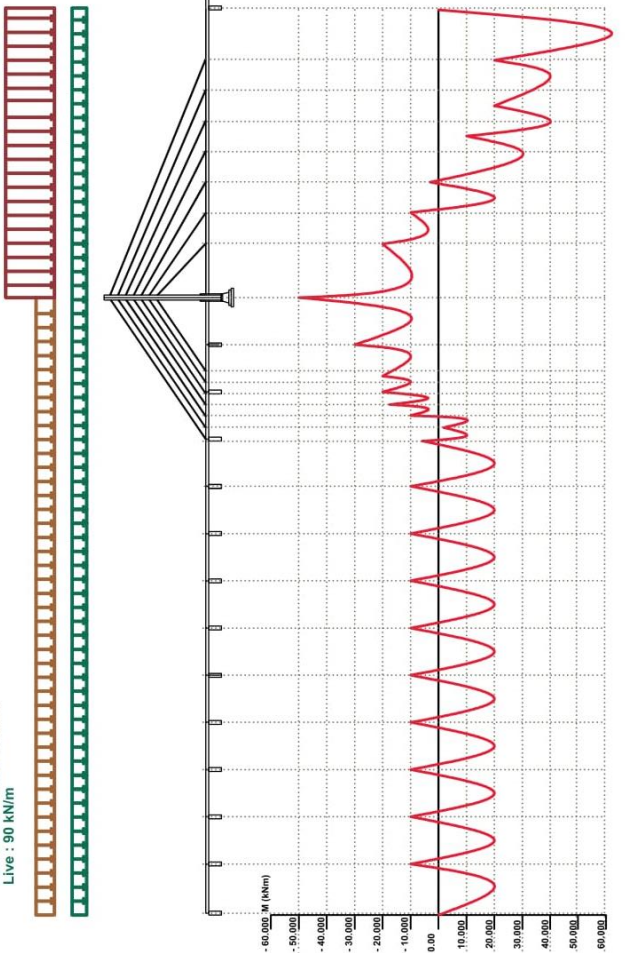
**Tatara Bridge, 1999** 3rd Generation - Hybrid structure (i.p./L:2%, h/L: 1/330)

Dead concrete deck : 940 kN/m  
Dead Steel deck: 121 kN/m  
Live : 115 kN/m



**Rhine River Bridge Flehe** , Germany, 1979, 2nd Generation - Hybrid structure (i.p./L:5%, h/L: 1/97)

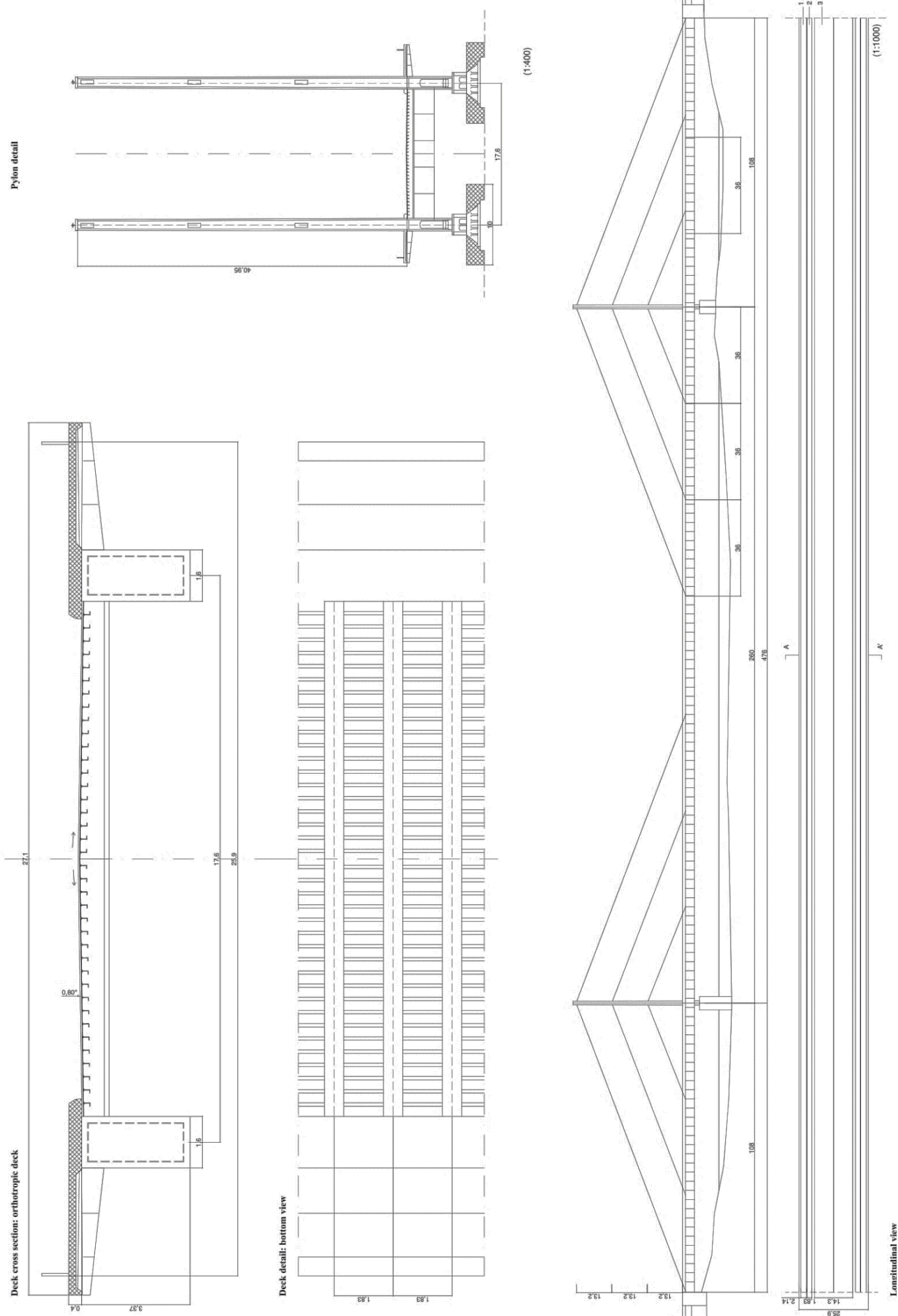
Dead concrete deck : 423 kN/m  
Dead Steel deck: 141 kN/m  
Live : 90 kN/m

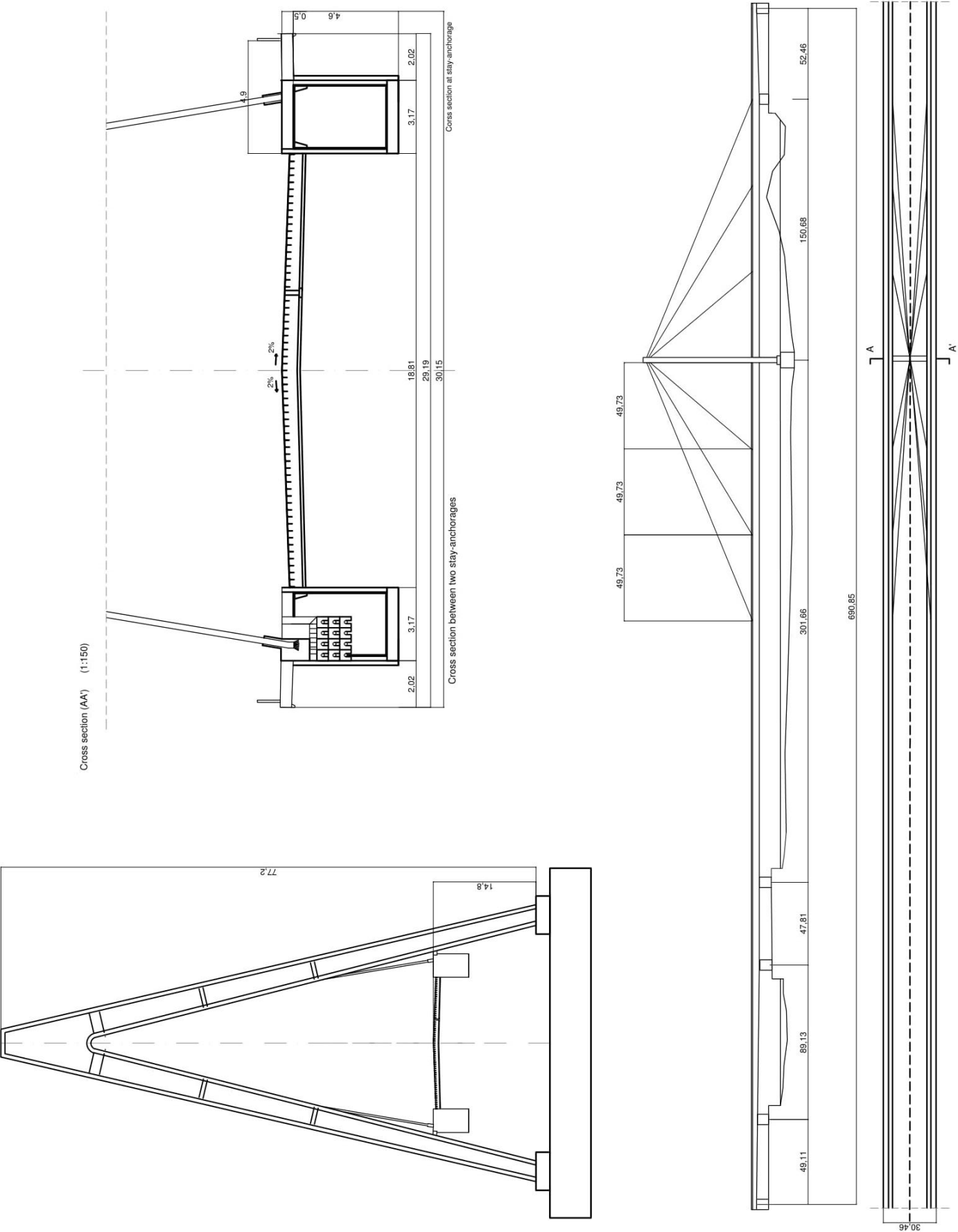


**Appendix (D): Cable stayed bridges Drawings**

- 1. North Bridge (o Theodor Heuss Bridge)\_** Düsseldorf (Germany), 1957\_ *Grassl , Leonhardt*
- 2. Severin Bridge\_** Cologne(Germany), 1955\_ *Grassl \_ Leonhardt*
- 3. Rhine river bridge at Mannheim Ludwigshafen\_** (Germany), 1969-72 \_ *Leonhardt und Andrä*
- 4. Saint Nazaire Bridge\_** Loire (France), 1975\_ *SAEM du pont de Saint-Nazaire*
- 5. Rhine River Bridge at Flehe \_** Düsseldorf, Germany (1979) \_ *Grassl*

North Bridge (Theodor Heuss Bridge) - Düsseldorf, Germany, 1957

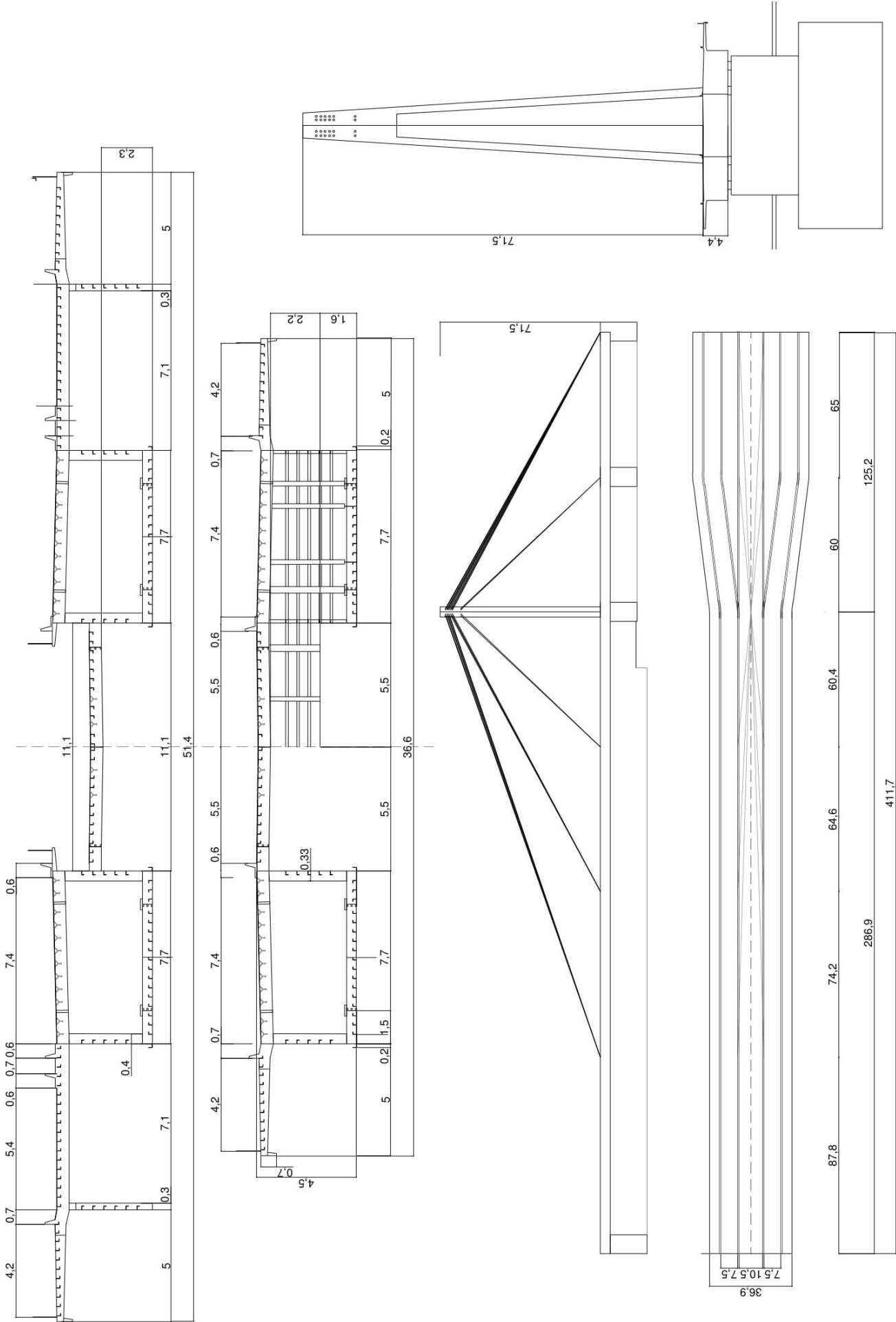




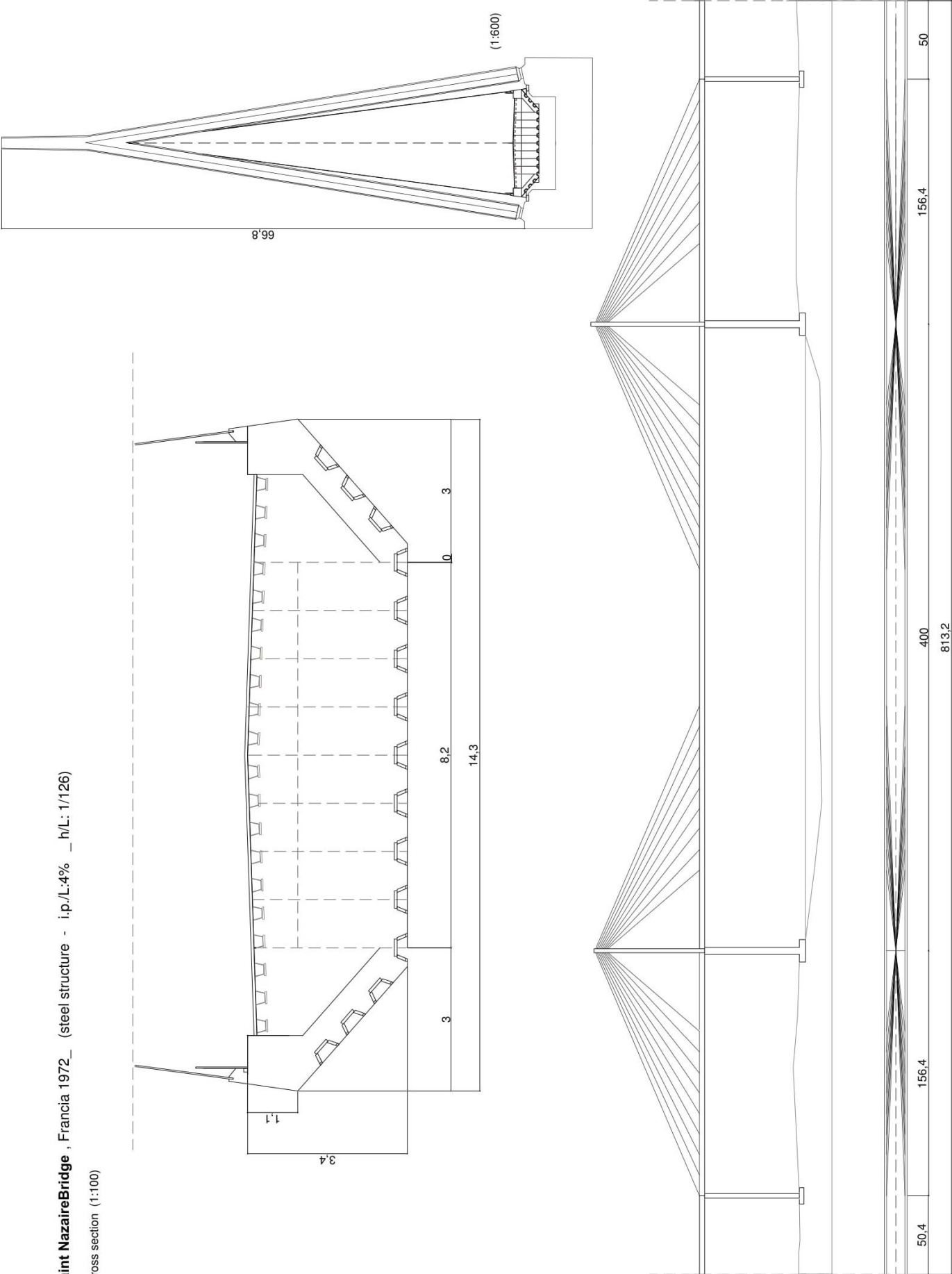


Rhine River Bridge at Mannheim - Ludwigshafen , Germania, 1972 \_ Leonhardt, Andr  \_ (hybrid structure - i.p./L:20%\_ h/L: 1/64)

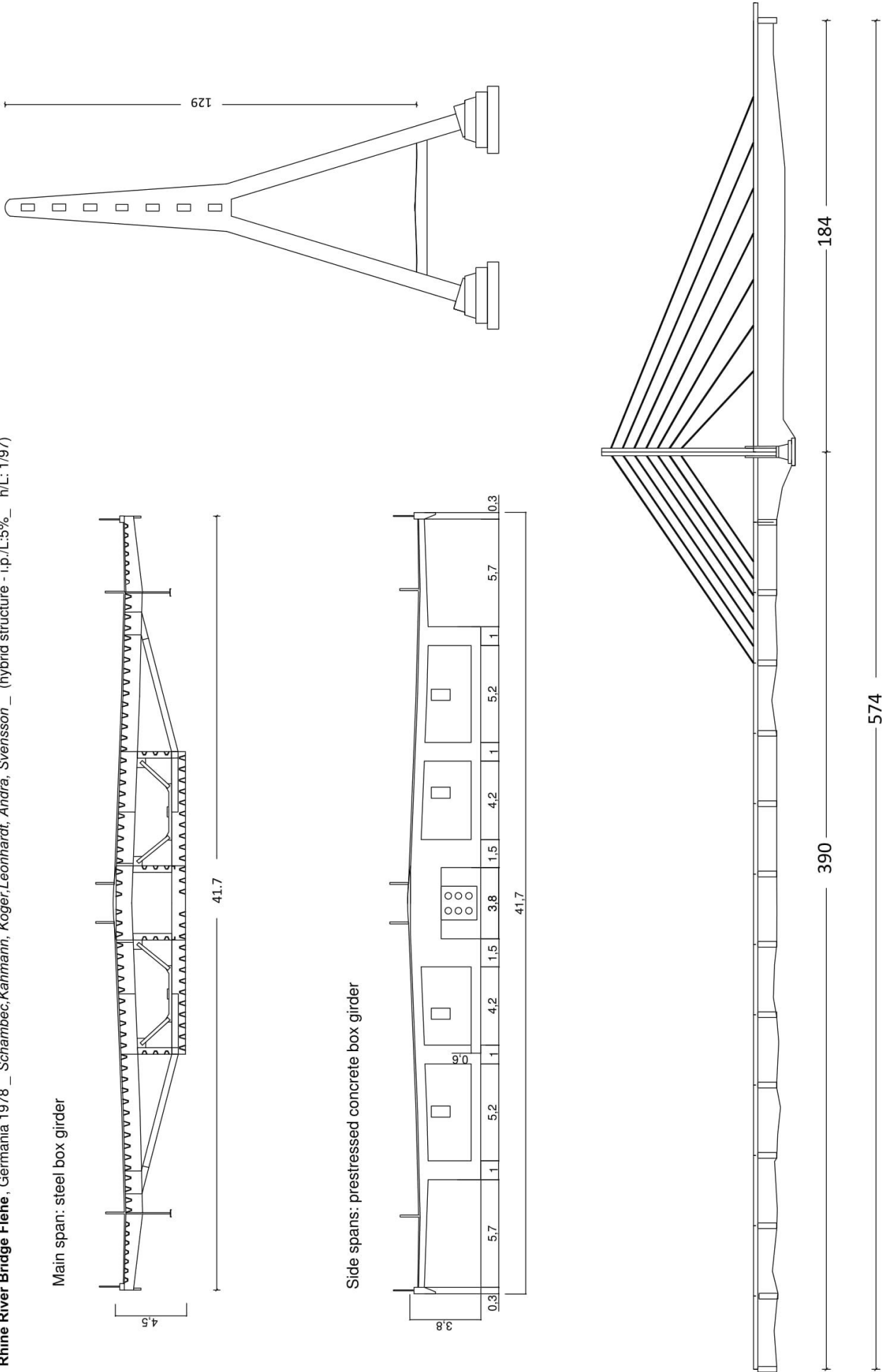
Cross section



**Saint Nazaire Bridge** , Francia 1972\_ (steel structure - i.p./L:4% \_ h/L: 1/126)  
Cross section (1:100)



Rhine River Bridge Flehe, Germania 1978 \_ Schambec,Kahmann, Koger,Leonhardt, Andrä, Svensson \_ (hybrid structure - i.p./L:5%\_ h/L: 1/97)



### Bibliography

- [1] Nicola Cavalieri, Istituzioni di architettura statica e idraulica, 1831
- [2] M.Gauthey, “Traite de la construction des ponts”, 1832
- [3] Navier, 1833. Résumé des Lecons
- [4] Telford, Thomas. Life of Thomas Telford. London : James and Luke G. Hansard and Sons, 1838
- [5] Smiles, Samuel. The Life of Thomas Telford. London : John Murray, 1867
- [6] Tyrrell, Henry Grattan. History of bridge engineering. Chicago, 1911
- [7] Steinman, 1929. Suspension Bridges and cantilevers, their economic proportions and limiting spans.
- [8] Finch, J. K. Wind Failures of suspension bridges or evolution and decay of the stiffening truss. Engineering News Record. 1941, 13.
- [9] E.Mock, 1949. Architecture of Bridges
- [10] G.Krall. Stabilità e vibrazioni. Edizioni Cremonese, Roma, 1968.
- [11] O'Connor, Colin. Design of bridge superstructures. New York : Wiley-Interscience, 1971.
- [12] F.Leonhardt,1974. Latest development of Cable- stayed Bridges for long spans
- [13] Podolny- Scalzi,1976 Construction and design of cable stayed Bridges
- [14] Freyssinet International. Brotonne Bridge.1976. Rep. FI.1013A/08.76
- [15] M.S. Troitsky,1977. Cable- Stayed Bridges. An Approach to Modern Bridge Design
- [16] De Miranda, 1977. Il ponte strallato sull’Arno a Firenze\_ Costruzioni Metalliche
- [17] De Miranda, 1980. Ponti Strallati di grande luce
- [18] Vittorio Nascè, Storia della cosreuzione metallica, 1981
- [19] F.Leonhardt, 1984. Bridges: Aesthetic and Design
- [20] R.Walther, 1988. Cable Stayed Bridges
- [21] Svensson, H.S. / Hopf, S. / Kovacs, I. Dimensioning of the cable-stayed Helgeland bridge. IABSE report. 1991
- [22] Petrangeli, 1996. Progettazione e costruzione di ponti
- [23] Petros P. Xanthakos. 1994. Theory and design of Bridges
- [24] Frempton, 1996. Calatrava Bridges\_ Second Edition
- [25] Menn, C. 1996. The Place of Aesthetics in Bridge Design, *Structural Engineering International*, Volume 6, No. 2, pp. 93-95.
- [26] Menn, C, The Place of Aesthetics in Bridge Design, *Structural Engineering International*, Volume 6, No. 2, pp. 93-95, 1996



- [27] IHI Engineering Rewiw, 1997. Fabrication of Tatara Bridge
- [28] Menn, C, Functional Shaping of Piers and Pylons, Structural Engineering Inter-national, Volume 8, No. 4, pp. 249-251, 1998
- [29] Menn, C. 1998. Functional Shaping of Piers and Pylons, *Structural Engineering International*, Volume 8, No. 4, pp. 249-251.
- [30] IHI Engineering Rewiw, 1997. Fabrication of Tatara Bridge
- [31] M. Virlogeux, Normandie Bridge. Design and construction. Proc. Instn Civ. Engrs Structs & Bldgs, 1993, 99, Aug. 281-302. Structural board paper 10109
- [32] Brühwiler, E., Menn, C. 2003. Stahlbetonbrücken (Reinforced concrete bridges)
- [33] Chen W., Duan L., Bridge Engineering Handbook, CRC Press, 2000
- [34] Troyano L.F., Bridge Engineering A global perspective, 2003
- [35] R.W.Cluogh, J.Penzien. Dynamic of structures. 2003
- [36] F.Mazzolani. STESSA 2003 - Behaviour of Steel Structures in Seismic Areas. Proceedings of the conference on brhaviuor of steel structures in seismic areas, 9-12 giugno 2003, Napoli
- [37] T.Shabanowitz\_ MIT, 2005. The progressive Syntesis of Architecture an Engineering in Modern Bridge Design
- [38] Wilbur J. Watson, "Great Bridges – form Ancient time to the twentieth century", 2006
- [39] A.Wilson\_ Proceedings of Bridge Engineering 2 Conference 2009. A critical analysis of Tatara Bridge
- [40] Atsushi Kaji, Taku Hirai, Rory O’Grady, Robin Sham, An introduction to Stonecutters bridge, Hong Kong: Erection of the steel segments, hydraulic buffers and lateral bearings. IABSE-JSCE Joint Conference on Advances in Bridge Engineering-II, August 8-10, 2010, Dhaka, Bangladesh.
- [41] A.Wilson\_ Proceedings of Bridge Engineering 2 Conference 2009. A critical analysis of Tatara Bridge
- [42] Russell, Lisa (2010): Turkey plans two major suspension bridges. In: Bridge Design & Engineering, v. 16, n. 59 (2nd Quarter 2010), pp. 7
- [43] N.Gimsing, 2011- Cable supported Bridge- Third Edition
- [44] H.Svensson, 2012. Cable-Stayed Bridges: 40 years of experience worldwide
- [45] Connor, Faraji. Fundamentals of structural engineering. 2013
- [46] M. Orçun TOKUÇ and Tamer TUNCA. Construction Techniques of The 3rd Bosphorus Bridge in Istanbul, Turkey. International Symposium on Industrial Chimneys and Cooling Towers, Prague, Oct 8-11, 2014
- [47] Fatema Samim, And Shunichi Nakamura. Study on Serviceability of Cable-Stayed Bridges with New Stay Systems. Proc. Schl. Eng. Tokai Univ., Ser. E

- [48] ASTALDI Report. Third Bosphorus Bridge Completed. Istanbul 2016
- [49] C. Mendez-Galindo & J.C. Rodriguez-Bahen, Max Brüninghold. Cylindrical Pendulum Isolators for the Third Bosphorus Bridge in Turkey. 1<sup>st</sup> Bridge Engineering Workshop, Mexico 2016.
- [50] Jean-Francois Klein, Michel Virlogeux, Thierry Delémont. Third Bosphorus Bridge –. Conceptual design optimized for a fast track construction
- [51] Selcuk Basl, Nurdan M. Apaydin, Alper Ilki and F. Necati Catbas. Wind Analysis of the Bosphorus Suspension Bridge: Numerical and Experimental Investigation. SMAR 2017

### **Web references**

- [1] International Database and Gallery of Structures, <http://en.structurae.de>
- [2] <https://www.theforthbridges.org/queensferry-crossing/facts-and-figures/>
- [3] <https://www.ice.org.uk/events/exhibitions/ice-bridge-engineering-exhibition/the-history-of-bridges/queensferry-crossing>

## 6. Concrete arch bridges

### 6.1 Deck stiffened system: a common mean to read concrete arch bridge evolution

Previous chapter have investigated the changes occurred for deck stiffened system, underlining the corresponding effects on long span bridge structural behaviour. The central thread of this dissertation has been to underline the passage from flexural regime of structures having shorter span, which act like simple beam-bridges, to the extensional regime of slender long span bridges, whose strict succession of deck cross sections guarantee them to carry loads mainly through tensile or compression strength: bending moments are greatly reduced, while torsional effects are often counteracted by rigid deck box sections.

In particular, reviewing the evolution of arch bridges, from the earliest masonry ones to the “pure steel arch” solution proposed by Calatrava, it can be said that the relationship between flexural and extensional regime has greatly changed varying structural materials. For earliest masonry arch bridges with semi-circular shape, upper deck was clearly distinguishable from lower vault, while filling materials help to better transfer acting load from deck to the arch. The semicircular vault remained the preferred form for arch bridge until the Middle Ages, when segmental arch bridges became to be spread: their lower rise-to-span ratio, implying high thrust values, makes more difficult to isolate flexural regime from extensional one. Instead, in the case of metal arch bridges, except from earliest examples with redundant structures, similar to monolithic masonry ones, the distinction between arch and girder load transferring system was somewhat clear, depending only from a few number elements, well distinguishable one from another. In the case of concrete arch, as it will be explained, the just mentioned separation appears more problematic: especially in the case of lower segmental arch bridges, compared with variable depth beam bridges, the split between arch and girder, or extensional and flexural regime, is not easy to define. As it has been seen before also for Ponte della Costituzione, arch bridge behaviour is not easily recognisable for segmental arch bridge, where upper deck tends to match with lower arch, till completely being denied, eliminating all filling materials, as in the aforementioned Fourth Bridge across Canal Grande. Passing through lowered segmental solution, precursor of modern rigid arch system or deck stiffened arch ones, the evolution of concrete arch bridge has often been marked by a progressive attempt to take better advantage from the use of a material that is capable to resist compression and thus, it's ideal for arches, basically working in compression: it's an *artificial stone* (Le Corbusier) making the concrete bridge the direct heir of the stone ones. From the early monolithic examples, potentiality of reinforced concrete technology have been improved, growing arch span until achieving the 420m of *Wanxian Bridge* (Fig. 6.1) over River Yangtze in China.



**Fig. 6.1:** Wanxian Bridge over River Yangtze, China (1997)  
The longest concrete arch bridge in the world  
 $L_{tot}=864.12\text{m}$   
 $L(\text{arch})=420\text{m}$

It's the largest concrete arch bridge built before 2000. Completed in 1997, the deck, 22m-wide, is 133 m above the old river level, with a rise to span ratio of 1:5.

The early use of concrete shows yet another repetition of the cycle associated with the introduction of new materials, which start with the disadvantage of being applied to structural forms better suited to their predecessors. It was inevitable that concrete should initially be regarded as reconstituted stone and used in that context. Reinforced concrete presented an opportunity to adopt structural forms in parallel with those used for steel sections.

Because steel is produced by a rolling process, which gives long lengths of continuous members, the structural forms that were created in steel were inevitably based on linear structural action. To provide adequate support for an area of floor or bridge deck it was necessary to create a grid with a primary, secondary, and sometimes tertiary members spanning at right-angles to one another to cover the area. But the potential merit of concrete is its ability to form shapes which can have a bi-directional structural action, and to be moulded to give economy to suit those two complementary actions. The voided slab or hollow box can be tailored to suit the varying requirements of relative longitudinal and transverse strengths at different points in a bridge deck, representing the effective use of concrete in structural forms which are peculiarly its own and making optimum use of its inherent qualities. The idea of prestressing concrete was a natural progression following the introduction of reinforced concrete. Whereas the latter set out to overcome the lack of strength of concrete in tension by providing steel bars in those areas of the concrete susceptible to tensile stresses, the purpose of prestressing is to induce compression in the concrete which will oppose the tensile stresses that arise due to applied loading, thus ensuring that the whole concrete section remains in compression at all the stages of its working life. One of the early motivations of the idea of prestressing came from the thought of producing a simulated arch.





**Fig. 6.2:** Chatellerault Bridge (river Vienne, France) François Hennebique (1899)  
 $L_{tot}=144\text{m}$   
 $L(\text{arch})=40\text{m}$  rise=4m  
 $(r/L=1:10)$

Whereas the cross-section of a natural arch remains in compression due to the natural thrust which develops at the arch springings, prestressed concrete artificially replaces the force line, which occurs naturally in an arch, by a curved steel tendon which is under stress, thus giving rise to a comparable force system in the member.

The main problem of concrete arch bridges is their construction, above all for their considerable weight. Arch doesn't work until it's closed at the crown, so the intermediate structures being formed during construction process are different to the final one. Due to their construction cost, large concrete arch bridges were practically abandoned, till the only method used in large span was the too expensive centering one. The powerful organization created by Hennebique for his reinforced concrete slab and beam patent registered in 1893 led to construction of many reinforced concrete bridge in all over the world (over 700 bridges built with his patent since the beginning of the century). Among them it could be interesting to focus on the following structures. *Chatellerault Bridge* (1899) (Fig. 6.2) with three-50m- span arches, 8m- wide, was the largest reinforced concrete bridge built during 19th century: its deck is separated from the arch; it's formed by longitudinal ribs joined by a slab and supported on the arch by very slender pier.

*Risorgimento Bridge* over river Tiber in Rome is 100m- span low rise to span ratio arch built in 1911; it was a significant step forward in concrete bridges. It's a spandrel arch with an extraordinary slender arch, which needs the cooperation of spandrels and deck to resist to load, even though this was not provided for in the design. The Giovanni Antonio Porcheddu office in Turin, Italian Hennebique's concessionaire, took part in design and construction.

**Fig. 6.3:** Risorgimento Bridge (Rome), Porcheddu, Hennebique licence (1911),  $L=100\text{m}$ , rise=10m,  $r/L=1:10$



Just as railway bridges were the great structural symbols of the 19th century, highway bridges became the engineering emblems of 20th century. The invention of automobile created an irreversible demand for paved roads and vehicular bridges, which were completely different from those ones needed for locomotive. Many highway bridges carry lighter loads than railway do, so their roadway can be sharply curved or steeply sloping. To meet these needs, many turn-of-the-century bridge designers began working with a new building material, reinforced concrete, whose master was the Swiss structural engineer Robert Maillart. Modern bridge tradition in Switzerland began in 1855 with the foundation of Federal Institute Technology in Zurich and its first professor of civil engineering, Carl Culmann. Swiss topography many bridges in mountains and valley, and since the introduction of railroad these conditions have stimulated engineers to seek new solutions. Thanks to Culmann's successor, Ritter, the research has been for elegance as well as utility. No one achieved that result more successfully than Ritter's student, Maillart, who made an use of reinforced concrete which presents a much-needed view of potential for beautiful design that originates in the imagination of engineers.

Born in Bern in 1872, Maillart studied engineering at the Federal Polytechnical Institute in Zurich from 1890 to 1894 where he came under the influence of one of the greatest teachers of structural engineering, Wilhelm Ritter (1846- 1906). Under Ritter, Maillart learned the scientific basis of structures, the practical context for the profession, and the visual power of form. It was an unusual education upon which he could draw throughout his 46-year career.

When the Museum of Modern Art devoted an entire exhibition in 1947 to the works of Robert Maillart, it only confirmed that he was an artist and that his major works are exemplars of a new art form prototypical of 20th century. *"Museum of Modern Art exhibits Swiss Bridges remarkable for beauty and engineering. Maillart's bridges seem to jump over rivers and abysses with the elegance and swiftness of greyhounds [...] "Heavy vaulting gives the beholder a sense of security; light profiles are more apt to frighten than please him. [...] His bridges were radical in construction and comparable in esthetic importance to the works of great modern sculptors. [...] Maillart's bridges were sometimes on the verge of the impossible, but they were right, they were exciting and they were beautiful",* said Giedion at Maillart's exposition.

Maillart entered the profession at the same time as did a completely new material, the composite of concrete and steel, reinforced concrete. This was a fortunate period to begin designing structures because there were no rules, no codes, no standards, and no tradition. On the other hand, there were millennial years of tradition with stone and wood and a full century of experience with ferrous metal structures. Maillart, more than any other engineer, would find a way to abandon those older traditions and to establish one for this new and intriguing but ill understood material

Maillart's career began in 1894, the year in which he designed his first concrete bridge: a 6m-span bridge made from massive concrete. Reinforcement of concrete opens up the possibility of managing traction forces, and therefore of managing bending. The deviation in thrust lines compared to the locus of the center of gravity of the successive sections gives the bending forces, enabling stresses to be computed. Maillart's method is logical and simple. Firstly, he uses the logic of the thrust line found with masonry, which enables him to design structures where concrete primarily remains compressed, guaranteeing good long-term behavior. Instead of sketching a possible bridge and then calculating it to adapt the geometry of the successive section through the dimensioning – the final geometry resulting from the dimensioning of the successive section – Maillart designs the sections around the expected thrust line. The thrust line is simply obtained by sketching the funicular polygon corresponding to the design loads. The challenge is therefore to devise a regular geometry fitting the trajectory of forces while matching the geometrical constraints of the structure (relative position of the deck compared to the arch, connected or unconnected relative positioning of the arch and the deck structure).

Maillart mastered the reinforced concrete technique and handled all types of bridge structures there were at the time: fixed arch bridges, like *Aaburg* over river Aare; three-hinged bridge as the well-known *Salgina Tobel*; double-cantilever beam with stretch supported in the middle, like 36m-span bridge upon river *Muota*; frames, like 36-m span aqueduct over *Exau-Noires*; continuous beam like the pass over the railway in *Berne*, with a 37m-central span. But he also created a new type of structure: the **arch without rigidity** also called **Maillart-type arch**. This structure consists in reducing the arch thickness so that it has a minimum rigidity to bending and, therefore, support axial stress almost exclusively; the minimum of this rigidity will be that necessary for the arch not to buckle. Concentrated and asymmetrical live loads are distributed through the deck rigidity, which, in this case, must be greater than in normal arch bridges. Its behavior is the inverse of suspension bridge one, because there are only axial stress in the resistant element while bending stress due to traffic load are distributed through the deck. With this method, Maillart was able to develop a new arch form, where the arch and the roadway are separated: each one was supported by columns or cross walls. (Billington, 1979). This form opened up the possibilities of arches, and also drastically reduced the weight of the bridge. Because the arch no longer had to support the weight of the fill underneath the road deck, it could become thinner and use less material. Maillart was also the first to use closed box girder as a reinforced concrete resistant cross section (as it was applied for **hollow box arch bridge**), as in the case of *Zuoz Bridge*, a 30m-span bridge whose cross section is a two-cell-box girder.

## 6.2 Advantages of Maillart's arch- to –beam transferring systems

Maillart's innovative use of concrete, especially in the design of thin arch structures, and his introduction of a wide range of new engineering forms, make him a seminal figure in the history of modern engineering. He rejected the complex mathematical analysis of loads and stress that was adopted by most of his contemporaries. His method was a form of "creative intuition": he had a knack for conceiving new shape to solve classic engineering problems. Working in a highly competitive field, one of his goals was economy (he won design and construction contracts because his structures were reasonably priced, often less costly than all of his rivals' proposals).

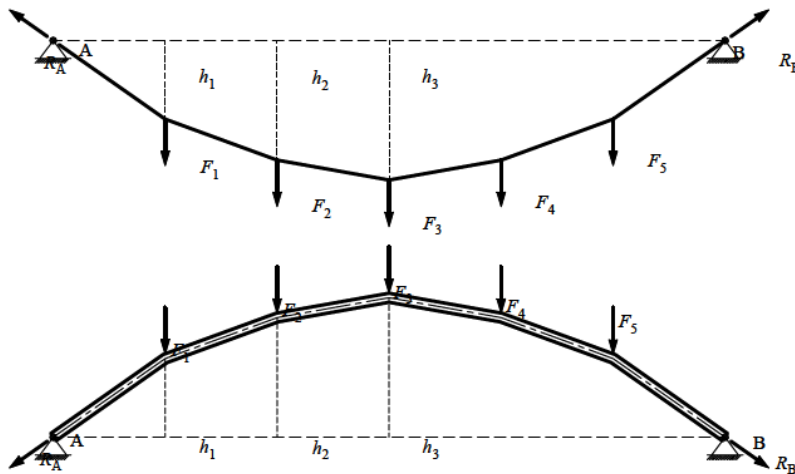
According to Professor Billington *"Robert Maillart, the Swiss bridge designer, developed in 1923 a limited theory for one of his arched bridge types which violated in principle the general mathematical theory of structures and thereby infuriated many Swiss academics between the wars. But Maillart's limited theory worked well for that special type of form. Within that category of type, Maillart's theory was useful and had the virtue of great simplicity; he developed the theory to suit the form, not the form to suit the theory"*. Maillart recognized that there was more than one way to approximate the structural behavior of his deck-stiffened arch systems, and he chose an approximation that exhibited a high degree of conceptual transparency.

Robert Maillart's way of designing the elegant thin concrete arches designed from 1924 to 1934 was controversial. He started from a clear understanding of structural behaviour, and designed these arches so that almost all the live-load bending is taken by the stiff deck, thus leaving the thin arch to carry little more than axial compression. He rejected the complex mathematical analysis of loads and stresses that was being enthusiastically adopted by most of his contemporaries.

Adherence to a general theory in this case was tantamount to the blind application of equations so often observed in the work of engineering students in fundamental classes. Maillart's much simpler approach, however, with its emphasis on new possibilities for arched bridge forms, represents, still now, the heart of creative engineering thinking—creativity not only with respect to the appearance of form, but also with respect to its engineering substance. Even Maillart's calculations were creative. Maillart usually adopted polygonal arch bridges, complex system where the arch, piers or walls and the roadway structure comprise a frame system. The roadway structure is much thicker than the arch, because the deck is resisting any tendency to bend or buckle, leaving the arch chord to resist pure compression. In this way the roadway structure is thinner than a simple beam across the same gap, because its weight is supported by the arch, and the arch can be much thinner than a simple arch, because it is stiffened by the beam. The bending stresses in the area of the arch (between the arch abutment piers) comprise two parts, first the bending moments in the girder for

the unmovable system, and second the frame bending moments from the system displacements. The bending moments in the girder can be easily determined because the girder is behaving like a continuous beam. The arch displacement caused by the settlement is resulting in bending moments both in the girder and in the arch. This happens even for the funicular arches. (Fig. 6.4) The frame bending moments are caused by the displacements from the live-loads. The bending moments in the arch can be accepted with smaller amount of reinforcement compared to the girder due to the natural longitudinal force in the arch.

**Fig. 6.4:** Establishing the shape of the funicular arch



The material required to construct an arch is minimized when all sections along the axis of the arch are in direct stress. For a particular set of loads the arch profile in direct stress is called the funicular arch. By imagining that the loads carried by the arch are applied to a cable, the designer can automatically generate a funicular shape for the loads. If the cable shape is turned upside down, the designer produces a funicular arch. Since dead loads are usually much greater than the live loads, a designer might use part of them to establish the funicular shape. The optimal arch shape is chosen in such a way that for the dead load the bending moments in the arch are smallest as possible, while for the live load some degree of eccentricity of the direct stresses are allowed. The main goal is to exclude tensile forces on the borders of the cross section, allowing them only for exceptional loads.

His design method of slender polygonal arches and stiff girders has two assumptions:

- (1) there are no bending moments from live load in the arch.
- (2) girder bending is numerically identical with the bending of the not-stiffened arch.

With the first assumption that under live loads there are no bending moments in the arch he assumed that the bending stresses in the arch from the live load are



so small that they can be ignored. The result is that the girder has to take all the bending from the live load. With the second assumption the girder bending is numerically identical with the bending the arch would have to take were it not stiffened with the girder. These two assumptions enabled Maillart to design his structures and determine the forces in the arch and in the girder meaning determining the compression stresses in the arch concrete and the quantity of reinforcement in the girder. His design assumptions fit with the chosen shape, and describe the way the structure transfers its loads. His idea is different from the usual assumption that the shape should follow the forces. For this system the forces are traced from the chosen shape. The polygonal arch carries the uniform loads from the dead weight and live loads only with longitudinal forces. The forces are transferred to the arch abutment and the tangential reaction force at the fixed end. Uniform load from the girder is transferred to the arch through vertical longitudinal forces  $F$  in each vertical cross-wall – pier. The polygonal arch transfers these vertical loads into oblique longitudinal forces  $N$  through the arch towards the abutment. The sloped structural elements accept the force  $F$  in the nodes where two arch elements with different slopes and the vertical pier meet. This is the mechanism through which the force passes from the girder, to the piers, to the arch and the arch abutment without bending moments in the arch. By conceiving structures as a whole, Maillart broke away from the atavistic construction principles of 'bearing and loading'. On the contrary he respected the function of every element of the structure, through the monolithic forming of the material. In his bridges, the roadways or railways are no longer loads supported by arches, they become integral parts of the bridge itself serving a constructive function so that there is a great saving of material and a greater degree of safety. His structures are characteristic through their absolute economy of means and through his will to utilize every constituent part to the ultimate.

### 6.2.1 Hollow box arch bridge

Maillart's design ran contrary to the prevailing view that bridges should be massive. He believed massive structures would more easily crack and shrink from temperature fluctuations. He also believed in using the best materials, but using them sparingly. This bridge underscores his view, providing the lowest cost of 19 designs submitted for the bridge's original design competition. His first reinforced concrete arch bridge was, a spandrel three-hinged arch, the **Stauffacher Bridge** (Fig. 6.5) over the Sihl River in Zurich Switzerland, built in 1899. It is an unreinforced concrete arch rib, and reinforced vertical cross walls and deck. (Billington, 1979) This 39.6m-span bridge is faced in masonry that completely conceals the concrete structure. Stone clad to the architectural design, this bridge was always been separated out from Maillart's work as it bears no relationship to it. The Stauffacher Bridge (Stauffacherbrücke) was completed in September 1899 and is still in use today.



**Fig. 6.5:** Stauffacher Bridge, River Sihl, Zurich (1899),  $L=40\text{m}$  – unreinforced concrete

Its arch spans 40m and is effectively a curved concrete slab that transmits loads to the abutments in compression. The arch is 780mm deep at the crown ( $h/L = 1/5$ ), 940mm at the quarter span points and 720mm at the supports. Vertical cross walls support the lightweight reinforced concrete deck. Following the then-accepted idea that an arch spans as long as 39.6m should have hinges, Maillart designed the Stauffacher bridge as a three-hinged arch of unreinforced concrete. He located one hinge at the crown, the highest point which occurs at midspan, and the other two at the support point, where the arch meets the foundations. This three hinged-arch has 3 points that are free to rotate in vertical plane: the arch at those points has no resistance to bending. There are two advantages of such apparent points of weakness: first, as the arch expands (or contracts) with a rise (or fall) in temperature, it rises freely without causing any stresses in the structure thanks to the free rotations of the hinges; second, it is far easier to calculate the stress owing to dead and live loads on the three hinged arch than it is on hingeless or fixed arch. Surely Stauffacher bridge reflects visually the old tradition of stonework rather than the new potentials for reinforced concrete; yet it was for Maillart an important first step in recognizing these potentials, which began to emerge in the next design, the Zuoaz Bridge.

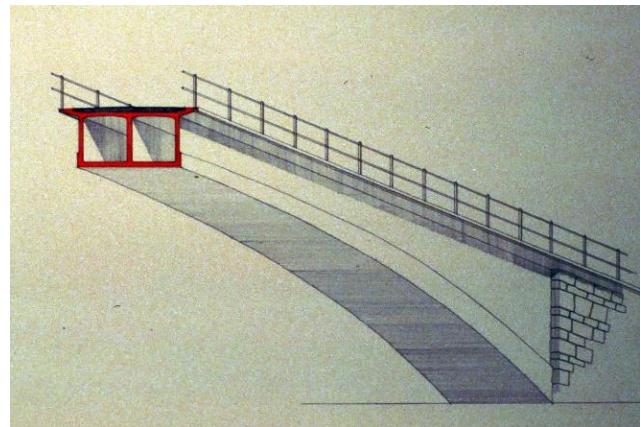
While this is Maillart's first large bridge, it was not until **the Inn River Bridge at Zuoz** (Fig. 6.6) that his design ideas began to take shape. (Billington, 1979) Maillart used "*the arched slab, the longitudinal walls, and the roadway together [to] form the arch,*" meaning that loads are not just transferred from slab to cross wall to arch rib, but the entire system acts together. This **hollow arch system** meant that the slab acts in both directions – carrying live loads to the longitudinal walls and to the abutments, allowing the structure to be thinner and lighter than earlier bridges. In the Zuoz design, the curved three-hinge arch and flat roadway deck are connected to the longitudinal edge walls and a central rib, forming a double-celled hollow box girder of varying depth. The bridge is 38.25m long and 4m wide overall, with a single 30m span. The central hinge is some 3m above the hinges at the abutments. The edges of the deck cantilever from the top of spandrels, a design detail that is characteristic of Maillart's bridges, and of many modern ones.



**Fig. 6.6:** Inn River Bridge at Zuoz (1901),  $L=40\text{m}$  – Reinforced concrete spandrel arch

The deck slab is 200mm thick and the arch varies in thickness from 180mm in the centre to 500mm at the abutments, which are of stone. Because the arch would not have to bear the load alone, it could be much thinner as little as one third as thick as the arch in the conventional bridges. When local authorities wanted a 30m - single span steel bridge, Maillart argued to design a more elegant concrete bridge for about the same cost. For this bridge he adopted a single-arch bridge with hinges at the abutments and the crown (the bridge midpoint) to prevent bending stresses at those sections. His crucial innovation was incorporating the bridge's arch and roadway into a form called the hollow-box arch, which would substantially reduce the bridge expense by minimizing the amount of concrete needed. In a conventional arch bridge the weight of the roadway is transferred by columns to the arch, which must be relatively thick to keep the bending stresses low under the loads resulting from bridge traffic. In Maillart's design, though, the roadway deck and arch were connected by three vertical walls, forming two hollow boxes running under the roadway. The big advantage of this design was that for most of the bridge's span the load would be carried by all three parts of the hollow box: the deck, arch and walls. (Fig. 6.7) (Fig. 6.8) Because the arch would not have to bear the load alone, it could be much thinner as little as one third as thick as the arch in the conventional bridges. Nothing like Zuoz Bridge had been designed before and there was no accepted method of verifying the concept by mathematical calculation.

**Fig. 6.7** (a) Zuoz Bridge, Maillart (1901) three hinged hollow-box arch\_ (b) Billington, Robert Maillart's Bridges (1989)





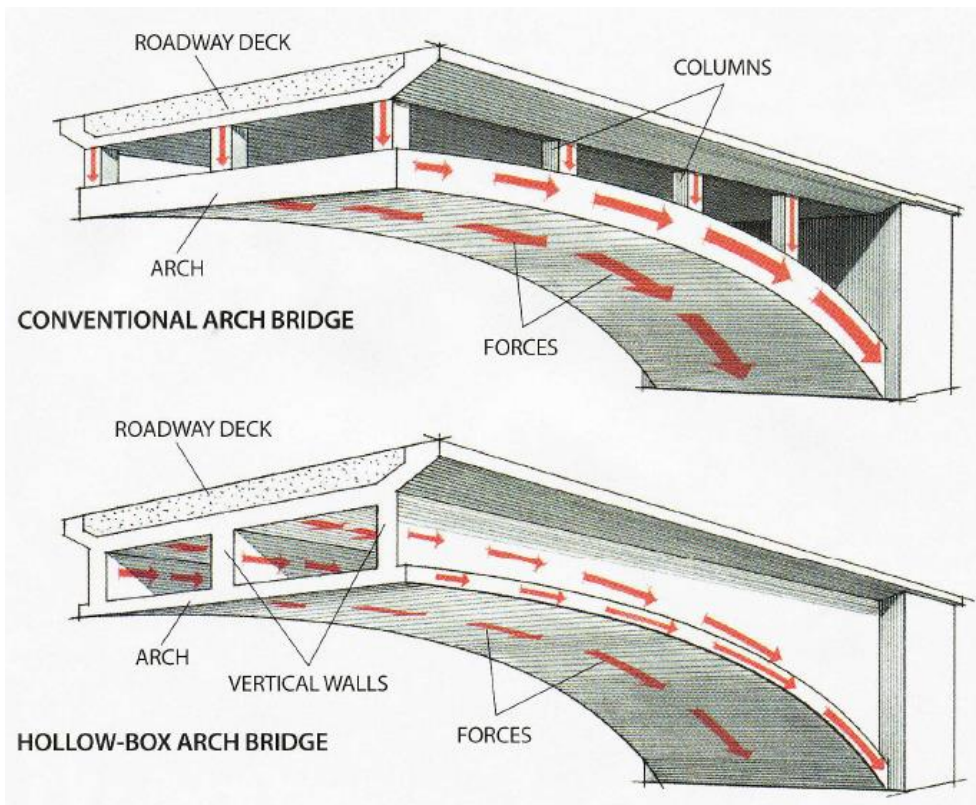


**Fig. 6.8** Comparison between conventional arch bridge and hollow-box arch bridge (Scheme by Billington, "The revolutionary bridges of Robert Maillart" – Scientific America, 2000)

Analysing the distribution of stresses over the box girder's cross section was all but impossible, especially between the quarter spans and the abutments.

Maillart used a simplified graphical analysis to evaluate the feasibility of his design. A rigorous structural analysis could not be performed. When Switzerland's leading authority on structures, Wilhelm Ritter, was called in as a consultant on the Zuoz project, he conceded that he could not mathematically analyze the bridge. Nevertheless, he recognized that Maillart's form was sound and recommended that it be built. The bridge was completed in 1901 and passed a fullscale load test that measured the displacement of the structure when heavy, horse-drawn carts rolled across the span. It was a physical success in spite of being a mathematical mystery. Over the next two years, however, cracks appeared in the vertical walls near the bridge abutments. The cracks resulted from the gradual drying of the structure: tension built in the walls as they tried to contract but were restrained by the arch and deck, which were exposed to moisture and thus dried more slowly. This defect did not threaten the bridge safety, but it motivated Maillart to correct the flaw when he designed his first masterpiece, but it motivated Maillart to correct the flaw when he designed Tavanasa Bridges over the Rhine River in the Swiss Alps (1905), unfortunately destroyed in 1927 by an avalanche. (Fig. 6.9) (Fig. 6.10) In this case, Maillart decided to remove the part of vertical walls near the abutments, which were no necessary to carry loads. In addition, to eliminating the cracking problem, the change produced a slender form, meeting bridge structural requirements.

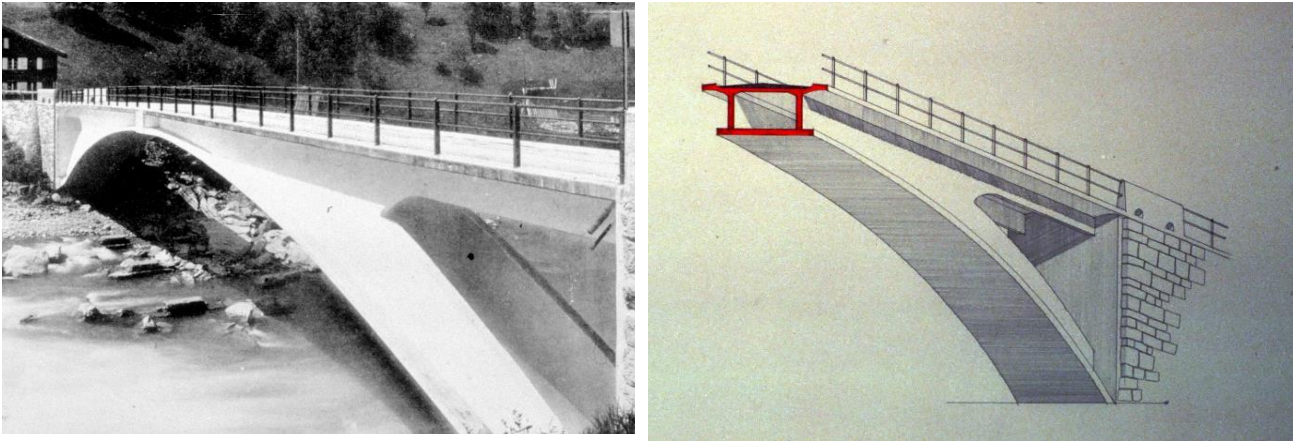
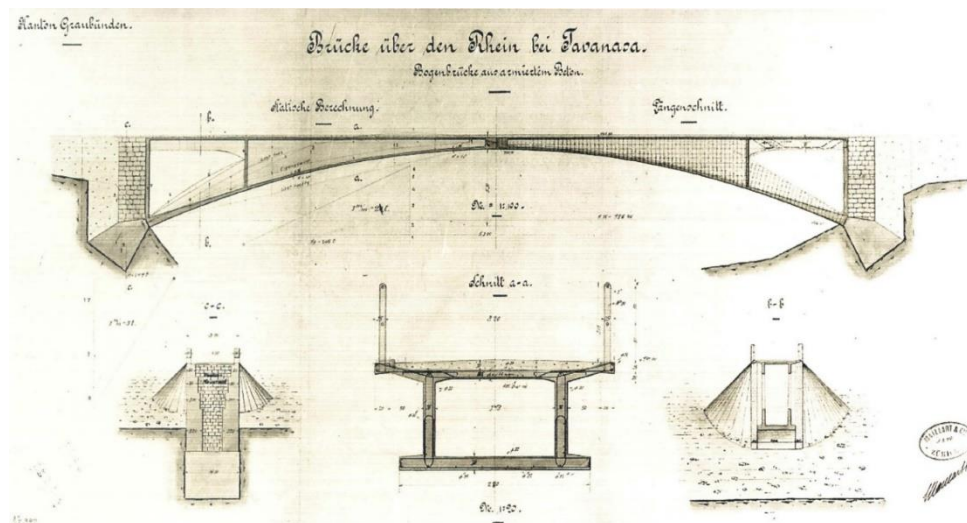


**Fig. 6.9** Tavanasa Bridge, Maillart (1905) three hinged arch (a)deck view\_ (b) Billington, Robert Maillart's Bridges (1989)

It was shallow at the crown and abutments but deep at the quarter span, which is where the live loads have the worst effects on the three hinged arch. Maillart's innovation, characterizing Zuoz and Tavanasa Bridges, didn't gain much notoriety; on the contrary, they aroused strong aesthetic objections from public officials, who were more comfortable with old-fashioned stone faced-bridges.

Classical physics and the chemistry of cement help to explain the performance of the Zuoz Bridge under loading but they do not explain Maillart's choice of form. That choice is the hallmark of design and its origins lie in the imagination. The structural artist is someone who can imagine new forms that safely obey the laws of nature and, in addition, respect the rules of society. Disregard for nature risks collapse, disrespect for society wastes public funds. These were the two disciplines of *structural art*: *safe physical performance with minimum materials* and *reliable construction for competitive cost*. At Zuoz Maillart could have reduced the arch thickness to one-third that of Stauffacher while greatly increasing the bridge's strength and hence safety. At the same time his design was competitive with a steel truss alternative, being slightly less costly to build but more expensive to maintain.

**Fig. 6.10** Maillart's design of Rhine Bridge at Tavanasa (1905), L=51m Three hinged reinforced concrete arch





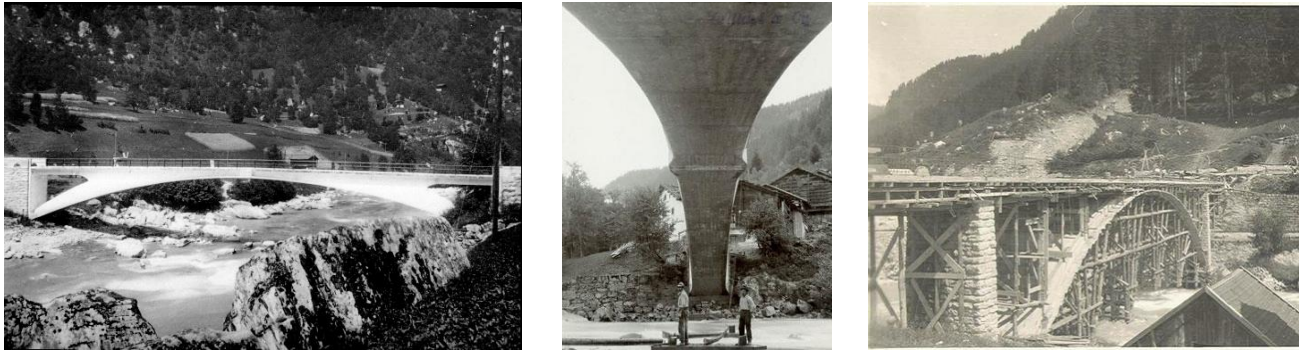


**Fig. 6.11** Rhine Bridge at Tavanasa (1905),  $L=51\text{m}$  Three hinged reinforced concrete arch

It was in 1905, however, that Maillart's genius was fully realized with the **Rhine Bridge at Tavanasa** (Fig. 6.11) (1905). Here the spandrel walls (the longitudinal walls at the outside of the deck) are reduced in height at the abutments, because of cracks that appeared in the earlier bridge at Zuoz. The widening of the arch at the quarter spans, accomplished at Tavanasa by the increasing height of the spandrel walls, was a form that Maillart used regularly at the beginning of his career. This very low rise-to-span ratio arch of 51m-span had a small opening at the end of the facings and the deck was only separated from the arch over the last 7m on each side. It could be considered a transition between spandrel and three hinged arches. (Fig. 6.8) Maillart designed the falsework (or scaffolding system) and formwork to support only the thin curved arch slab. Once hardened that slab could then support by itself the walls and deck of the hollow box. He thus economized on the costly temporary scaffold built in the river. The bridge was 61m long overall and had masonry abutments. The reinforced concrete arch over the Rhine spanned 51.25m, topped by a reinforced concrete deck 3.6m wide (roadway 3.2m). The central hinge was 5.7m above the abutment hinges (rise-to-span ratio 1:10).

Proof of his construction on both bridges was the carefully instrumental full-scale load test carried out before the owners would accept the bridges. These were laboratory tests that often revealed small defects and always allowed Maillart to check his calculated predictions of performance. Unfortunately Tavanasa Bridge no longer remained, being destroyed in 1927 by an avalanche of stones which occurred in a ravine located above. It was rebuilt with a slender arch nothing like the original bridge, spectacular Salginatobel Bridge of 1930. Maillart was then only a designer, having lost his construction business because of an enforced stay in Russia during World War I.

Maillart's reinforced concrete **Aarburg Bridge** (1912) (Fig. 6.12) is similar, in appearance, to Stauffacher ridge (1899), with its fake walls removed, leaving a solid, heavy arch whose thickness is greatest at abutments. Their rise-to-span ratio are quite similar, being 9.75 at Aarburg and 10.7 in Stauffacher; also thicknesses are so close, with 80 to 102 cm at Aarburg and 72 to 95 cm in Stauffacher. Also Aarburg visually appears a strong arch which expresses to be designed to carry the whole bridge loads, without help from walls or deck structure.



**Fig. 6.12** Aarburg Bridge (1912),  $L = 70\text{m}$ , three hinged arch bridge, rise =  $7\text{m}$ ;  $r/L = 1/9.75$

Up until Maillart's death in 1940, almost all concrete arch bridges followed the "Roman concept" of the dominant arch. The main reason for this retrograde attitude of most designers was visual: many of them believed that such massive forms in stone were appropriate to reinforced concrete, continuing a long and distinguished tradition (the arch would support by itself all bridge loads; arch should appear massive as befitted the ancient stone tradition). Maillart, almost alone, between 1900 and 1905, had explored radically new possibilities, both technically and visually original. At Aarburg Maillart designed a thin concrete parapet wall of  $1.65\text{m}$  deep, giving a visual impression in profile of heavy deck structure supported on light columns which rested on the strong arch below.

As at Zuoz and Aarburg, bridge developed unanticipated cracks, this time in the bottom of the deck beam near the column supports, which led Maillart to seek an appropriate technical solution. Such cracks violated the ancient concept of the arch as full support for the deck. Maillart realized that arch and deck had to move together, above all under live loads distributed only upon one half of the deck. Thus the arch would not act alone to support the deck, but rather the two elements had to work together as a deck stiffened arch bridge, since they were connected by columns or cross walls.

**Fig. 6.13** Construction of Salginatobel Bridge (1930), Graubünden canton, Switzerland  $L(\text{arch}) = 90\text{m}$

**Bridge at Salginatobel**, (Fig. 6.13) a particularly fine example of Maillart's hollow box arch with a short width of  $3.50\text{m}$  was dimensioned for light traffic; it showed designer dedication to his project, creating a structure that was beautiful and practical.







**Fig. 6.14** Salginatobel Bridge (1930), Graubünden canton, Switzerland Three-hinged reinforced

The falsework was built by the Graubünden carpenter Richard Coray in late summer 1929, and the rest of the construction started in 1930. The single span soars 90m over the Salginabach (Salgina Brook), its western end carried on five transverse walls above the slope of the gorge. The deck is flanked by solid parapets 1.33m high. Semi-circular drainage holes, 100mm radius and spaced at 3m intervals, are set into the parapet walls at deck level. The arch rises 13m from ends to centre (rise-to span ratio 1:10), to 93m above brook-level. It is thicker and wider at the supports (400mm x 6m) than at the crown (200mm x 3.8m)

(Fig. 6.14) (Fig.6.15) A three-hinge arch was a good choice for the main span, as small movements at the supports can be accommodated, minimising the likelihood of significant cracking. Solid spandrel walls, 290mm thick and 2.58m apart, support the deck directly on the arch over a 53.6m central section of the span, forming a box section. Thereafter the spandrel walls curve downwards, making a trough. The deck is also supported from the arch by tapering I-section (web 120mm wide, flange 600mm) vertical transverse walls, 120mm thick set at 6m centres, with access openings in them. The flanges of these walls curve outwards at the base, joining with the edge of the arch. Maillart derived the final shape graphically using a series of parabolas. As the hinge is central, the design could be determined by evaluating the equilibrium forces on one half of the bridge (the other half being the same). He adjusted the geometry so that bending of the arch was minimised and the concrete was predominantly in compression. In effect, the shape of the arch reflected the bending moment diagram produced by the load path along it. In contemplating his Salginatobel Bridge Maillart recognized an error, not in the physical sense but in the visual expression. He had made the underside of the arch with a continuously smooth curve from one abutment hinge to the other. This was wrong, he later wrote, because the hinge at the crown, representing a discontinuity physically, should be expressed visually. It was this broken arch idea that he then used at Vessy several years later. Another best-known example of Maillart method is Vessy Bridge (6.15) of 1936 on the outskirts of Geneva.



**Fig. 6.15** Vessy Bridge (1936) ,Geneva - Switzerland Three-hinged reinforced concrete arch  $L=56\text{m}$  ,  $r/L=11.7$

Here, after 40 years of practice, Maillart took the classical stone arch form and totally transformed it into shapes impossible to imagine before reinforced concrete. The arch is flat and broken at the crown where the thin vertical slit emphasizes the discontinuity created by a hinge. The buttresses at the abutments meet the arch at narrow points which expose hinges while the arch profile becomes deepest halfway between those hinges and the crown.

The total length of the bridge, between the tops of the abutments, is 79m. Its three-hinge arch spans 56m between the base hinges, with a vertical distance between central and support hinges of 4.8m. The arch supports a deck 10.1m wide overall, carrying a two-lane roadway and two footpaths. The three upstanding longitudinal walls, or ribs, together with the arch form two hollow boxes, closed at the top in the centre of the bridge, where the walls meet the deck. At the outer ends of the span, the ribs become U-shaped channels as the walls decrease in height down to the support hinges, leaving triangular cut-outs between rib, deck and abutment. The ribs are 630mm thick at the central hinge and 440mm thick at the support hinges, while the base of each rib is 150mm thick between hinges. The side walls of each rib are 120mm thick where the section forms a box, and 200-280mm thick where it is a channel. The pattern of form boards tells the knowledgeable observer that the arch is hollow with a curved slab at the bottom and vertical walls that merge with the horizontal deck throughout the central half of the span. The arch, walls, and deck form an integral whole which we now call the hollow box in concrete. It was Maillart's first great innovation and it remains today a major structural form.

**Fig. 6.16** Vessy Bridge Calculation of X-shaped cross walls

*Effet de la température et du retrait*

$$t = 20 + 20 = 40 \quad \Delta l = 11,2 \cdot 0,00001 \cdot 40 = 0,0095 \text{ m.}$$

$$f = \frac{1}{2} \cdot 0,0095 = \frac{6X \cdot 3,20}{19 \cdot 2,000000 \cdot 0,78} = 0,00288 X$$

$$X = \frac{0,00225}{0,00288} = 0,78 \text{ t.} \quad M_0 = 0,78 \cdot 2,2 = 1,72 \text{ mt.}$$



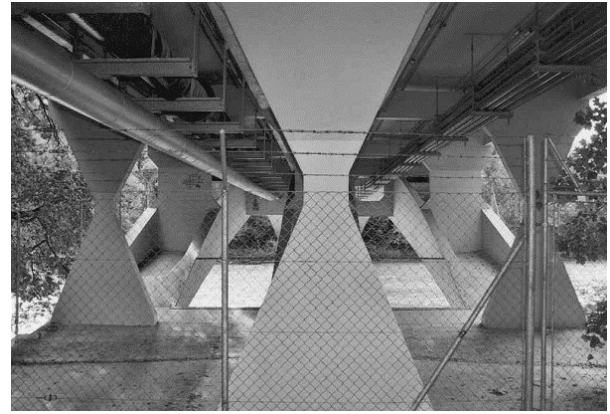


**Fig. 6.17** Vessy Bridge (1936) ,Geneva - Switzerland - Detail of X-shaped cross walls

But we find the most surprising aspect of the Vessy Bridge beneath its deck where the x-shaped cross walls (Fig. 6.17) (Fig. 6.18) give the structure a completely unique image which is, at once a fully rational design and the result of an aesthetic choice by the artist. Maillart's calculations demonstrate how the internal forces in those cross walls varying magnitude exactly as the shape, which is, therefore, a *prototypical example of engineering as a unity of art and science*.

But Maillart bridges could not even have been built had they not been politically acceptable. Indeed they never were in the traditional aesthetic world of the urban designers and politicians. It was only because the highly decentralized Swiss politics allowed local leaders to choose Maillart's designs, but even then only because they were never expensive and often less costly than standard designs. *We thus come to the central idea inherent in Maillart's bridges: that they cannot be understood without some insight into the physics of form, the context of politics, and the concept of structural art. In short, we find in a modest bridge a unity of knowledge that brings together in the terms of the three great liberal arts, natural science, social science, and the humanities* (Billington).

### 6.2.2 Deck- stiffened arch bridges

Starting in 1912, Maillart's firm proposed a second design innovation, the well-known deck stiffened arch. The idea starts from Maillart's analysis of the effect of live loads, when they were added to dead ones. According to Maillart, an arch bridge can be assimilated to an inverted cable. A cable curves downward when a weight is hung from it: the tension in the cable balances the added weight. An arch bridge curves upward to support roadway, and the compression in the arch balances the dead load. Once the arch form has been fixed to fit dead load, the addition of live loads causes the arch to bend, especially in the case of asymmetric load condition. So the arch must be strong and thick to resist to bending. Preserving also aesthetic aspect, Maillart wanted to obtain thinner arch: the innovative solution was to connect the arch to the roadway deck with transverse walls. Maillart assumed that the deck and the arch deform together, and would thus carry bending moments in proportion to their flexural stiff

nesses. He designed the deck to be significantly stiffer than the arch and thus to carry most of the bending in the system. Such a conceptual leap reflects the same level of intellectual quality as the creation of any general theory, and far surpasses the technical exercise of applying such a theory.

**Maillart-type no-rigid arch** (Fig. 6.18) (or deck-stiffened arch bridge) exhibits Maillart's second major bridge innovation, the deck-stiffened arch. This new form in concrete forecasts a thin arch and a relatively stiff deck. Maillart wanted the arch to be as thin as the bridge could be built, but still able to carry all traffic loads safely. A concrete arch can carry permanent loads when it is designed with the proper shape (for a load uniformly distributed over the horizontal bridge deck this shape would be a parabola). The difficulty comes when traffic loads only a part of the span length; then the arch will try to bend into a new shape. Such bending would normally break a very thin concrete arch so that engineers were compelled to design thick, heavy arches. *Maillart reacted against massive concrete as a musician to tone deaf singers* (Billington). Since his modest mountain structures had parapets, he thought, why not use them to prevent the evil bending from damaging his thin sliced arches. This deck-stiffened arch works because the arch and deck are connected firmly together by a series of cross walls. Then as the arch tends to bend when loaded say by traffic over one half of the span, the cross walls make the deck bend to the same new shape as the arch. The bending effect is now shared between arch and deck and, as Maillart further reasoned, that effect will load each part in proportion to its stiffness. (The load required to compress each of two springs the same distance will be proportioned to their stiffnesses.). Thus the arch, made far more flexible than the parapet, will now have very little bending and happily can be both strikingly thin and predictably safe. The arch-and-deck cooperationsuggested to Maillart a differnt view of those elements, of their relative proportion, expecially the arch appearance. Above all Ritter, his former professor, stimulated Maillarto to think in this direction. In a 1883 article concernig deck-stiffened suspension bridges, Ritter developed the parallel idea for arch bridge, not only to improve technical aspects, but also to change visual perception. According to Ritter, when arch and deck act together, the designer could control the forces by first controlling the form. “A stiff deck could remove large forces from the arch, if the arch were designed to be much less stiff tha the deck”(Billington).

**Fig. 6.18** Maillart-type no rigid arch - (Scheme by Billington, “The revolutionary bridges of Robert Maillart” – Scientific America,2000)

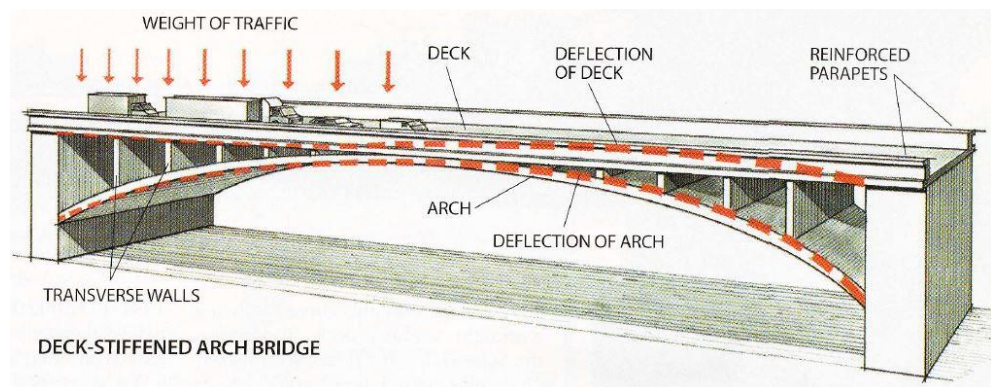






**Fig. 6.19** Flienglabach Bridge (1923, 38.7m-span

In the early example of deck-stiffened arch system, as Flienglabach Bridge (1923, 38.7m-span, thickness at the crown of only 0.25m). Using a much simpler approach to designing deck stiffened arch bridges than was common at the time, when exhaustive theoretical calculations were expected, Maillart designed **Valtschielbach Bridge** (Fig. 6.19) (1925). His concept expressed a far more holistic view of structures. The design of this bridge was encapsulated in just three and a half pages of hypotheses. Based on observing the in-service behaviour of his bridges, Maillart realised that the deck and the arch, when working together, carry bending moments proportional to their flexural stiffness. In this design, the deck is restrained by parapet walls and so is significantly stiffer than the arch. Consequently, the deck can carry practically all the bending moments, producing a structure that is more than eight times as efficient as a simply-supported beam. The shallow arch of the Valtschielbach Bridge (Valtschielbachbrücke) (Fig. 6.20 rises 5.2m and spans 43.2m. The arch is only 230mm deep at midspan, and 290mm at the abutments. Over the central portion of the span, measuring 11.6m long, the arch is fused to the underside of the deck. Where the two diverge, they are braced on each side by four vertical transverse walls, 160mm thick, and at 3.1m centres. The deck structure is a maximum of 1.2m deep overall, with a parapet depth of 1.1m. Each parapet is a solid wall, pierced at roadway level by 14 drainage openings.

**Fig. 6.20** Valtschielbach Bridge (1925)  $L=43.20\text{m}$   
 $h(\text{arch-midspan})=0.23\text{m}$





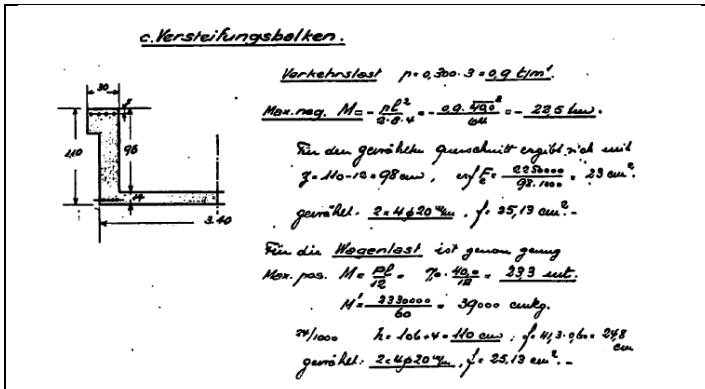


**Fig. 6.21** Maillart's calculations for the bending in the parapet of the Valterschielbach

A projecting lip, 200mm deep and 100mm wide, runs along the top of each parapet, optically correcting the heaviness of the parapets' appearance. The bridge is straight in plan, with sharp transitions in the roadway on either side, leading to two substantial masonry abutments some 6.1m long, each with a central 2.5m wide vaulted arch. The bridge carries a single-track roadway, 3m wide, and is 3.6m wide overall.(Fig. 6.21)

Perhaps the most beautiful of Maillart's bridges is the **Bridge at Schwandbach**. (Fig. 6.22) Built in 1933, the bridge is set high in a valley, arcing from one rock face to the other. The roadway curves over the span of the bridge while the arch is perpendicular to the abutments. The inside of the arch rib follows the inside curve of the roadway, whereas the outside edge is straight. This irregular shape causes the arch to widen at the abutments, where it resists transverse wind load, and narrows at the center, with cross walls that taper to meet the roadway. The arch rib is less than 0.20m thick, the cross walls are 0.16m, contributing to the exceptional lightness of the bridge. The Schwandbach Bridge, which is still in use today, is an exemplar realization of the possibility of reinforced concrete. This reinforced concrete masterpiece is a typical example of **Maillart-type no-rigid arch**: this structure consists in reducing arch rigidity by increasing the deck one. The bridge has a main span of 37 metres, and a total length of 55.6m. The arch is polygonal rather than curved, and is only 200 mm thick. It supports the bridge deck via 160 mm thick reinforced concrete cross walls.

**Fig. 6.22** Schwandbach Bridge (1933) L(main span)=37m, L(tot)=55.60m







The deck is thicker than the arch, and is stiff enough to prevent the slender arch from buckling. The highway deck is curved in plan. The arch varies in width from 4.2 m to 6 m, with one edge forming a straight line between river banks, and the other following the curve of the road. This arrangement helps to resist centrifugal forces from the traffic loads and from the curved deck tendency to twist.

**Fig. 6.23** Reichenau Bridge, C. Menn, Switzerland, 1962. Larch= 100m.; Ltot= 158m; deck width= 8.40m; arch thickness = 0.80 – 1.25m; deck depth= 1.00m; Hgider/L = 1/100; Harch/L= 1/125

### 6.3 The spreading of Maillart-type arch bridges

Maillart reached such of this type are very little different from his one. It's a no frequent solution but has been used on several occasions. Christina Menn's earliest designs clearly reflect the influence of Maillart: making use of prestressed concrete to create really pleasant bridges, his style evolved slowly as he faced the changing conditions of construction during the 1960s. First, the rapid increase of labor cost made the closely spaced vertical cross-walls in deck stiffening system uneconomical. Menn responded by spacing them much more widely apart, as shown in the first arch he built, the 100m-span *Reichenau Bridge* (Fig. 6.23) on the Rhine, featured by total length of 158.00 m, rise of 20.90 m ( $r/L = 1:8$ ), variable arch width of 4.00 - 5.20 m, arch thickness 0.80 - 1.15 m ( $h_a/L = 1:125$ ), deck depth of 1.00m ( $h_d/L = 1:100$ ). The 1962 *Reichenau Bridge* over the Rhine was the first arch bridge with a partially prestressed stiffening girder. Here, the combination of mild and prestressed reinforcement also proved preferable to full prestressing. Stiffening girder was given a relatively weak concentric prestress; mild reinforcement was added as required to resist the live moment peaks, which varied considerably from span to span.

The same design approach has been adopted by Menn for the 96m-span *Via - Mala Gorge Bridge* (Fig. 6.24) on the upper Rhine, having deck width of 10.70m, deck slab thickness of 0.29 m, total girder depth of 1.09 m ( $H/L = 1:88$ ).



**Fig. 6.24** Viamala Gorge Bridge, C. Menn, Switzerland, 1967.  $L_{arch} = 96\text{m}$ ;  $L_{tot} = 179.80\text{m}$ ; deck width =  $10.70$ ; deck slab thickness =  $0.29\text{m}$ ; girder depth =  $1.09\text{m}$ ;  $H_{girder}/L = 1/88$ ;  $H_{arch}/L = 1/331$

Also in this case, this wider spacing, which still permitted the deck to be stiffened, was made economically attractive by a second major factor, the introduction of prestressing: thanks to this technology longer span could be built.

No rigid arch have also been built in other countries, among them the  $100\text{m}$ -span bridge over the *River Costa* in Italy, built by Alfredo Passaro (1961), and the Alagon River Aqueduct, by Casado (1966) in Spain, with four  $60\text{m}$ -span arches.

The cost and difficulties involved in centering for large arches has always been in builders' minds. The *Salginatobel Bridge* by Maillart centering, as seen before, as itself a major piece of engineering work. In 1898, the Czech engineer *Josep Melan* built the first bridge with a system bearing his name: it consists of building an initial metal arch to avoid centering. This initial arch acts as a centering for the concrete arch and will be incorporated into its reinforcement.

The first bridge Melan built with this method was *Schwimmschule Brige* in Steyr in 1898: the initial metal arch was built by the cantiliver method using provisional staying. One of the largest bridges built with this process was the  $130\text{m}$ -span *Echelsbach Bridge* (Fig. 6.25) over the River Ammer in Germany, finished in 1929. This two-hinged reinforced concrete arch bridge has a total length of  $189\text{m}$ , with a  $130\text{m}$ -span arch, having a rise of  $31.80\text{m}$  ( $r/L = 1:4$ ).

**Fig. 6.25** Echelsbach Bridge over the River Ammer in Germany, Heinrich Spangenberg (1929).





The Echelsbach Bridge between Schongau and Oberammergau , designed by Heinrich Spangenberg , spans the deep gorge of the Ammer river. Its construction saved traffic a difficult journey with many bends and gradients of up to 20%. With a self-supporting span of 130 meters, the Echelsbach Bridge was the largest-span reinforced concrete bridge in Germany at the time of its construction. This record, as well as its technical sophistication put it on the list of historic landmarks in civil engineering.

The *Melan system* worst disadvantage is the price, which is why it's currently use in rare occasion. The ammount of steel the metal arch acting as a scaffolding truss requires is much greater than the reinforcement needed by a concrete arch built by stayed cantilevers. This is the reason why most large concrete arches are currently built by this process.

Anyway, *Melan system* spread in all over the world: many bridges were built in USA using this method, above all along Pacific coast. One particular designer, Conde McCullough, built an entire series of bridges for the Oregon Coast Highway between 1932 and 1936. There were also a number of reinforced concrete arched bridges created in California, such as the Russian Gulf Bridge in 1940 and the *Bixby Creek Bridge*(California) in 1933. With a total length of 218m, it consists of a main span of 109.7 m, 79.2m - high above valley floor or water. (Fig. 6.26)

The bridge was retrofitted beginning in 1996 with an analysis by bridge engineering company Buckland & Taylor as part of the Caltrans Phase II seismic retrofit program. In their detailed evaluation of the bridge's seismic vulnerabilities, they were challenged to find a solution that met several difficult issues, including severe load factors, extremely limited physical access, maintaining the appearance of the existing historical structure, and a requirement by the State of California that at least one lane of the bridge remain open at all times. The crux of the design was the longitudinal post-tensioning of the entire bridge deck from end to end.

**Fig. 6.26** Bixby Creek Bridge , Stover, Panhorst & Purcell (1933), California (USA). Larch= 109.70m,  $L_{tot}= 218m$



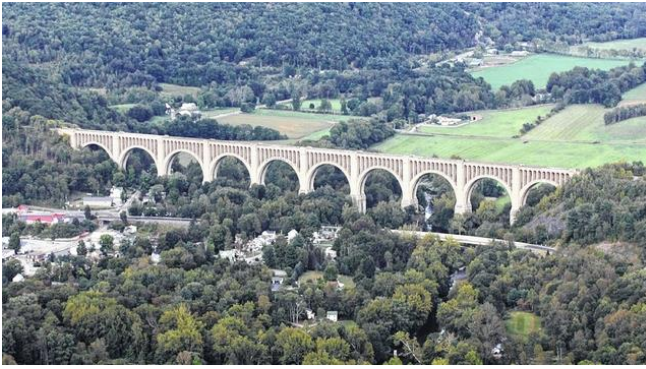


**Fig. 6.27**  
Tunkhannock Viaduct  
in Pennsylvania (1915),  
Abraham Burton Cohen

Perhaps the most impressive concrete arch bridge, in sheer size alone, is the *Tunkhannock Viaduct* (Fig. 6.27) in Pennsylvania (1915) by Abraham Burton Cohen. Spanning across the entire valley for almost half a mile, its massive semicircular arches march inexorably across, bringing to mind its Roman predecessors, and clearly showing their influence. This railway bridge has a total length of 723.9m, made of 10 spans of 54.9m each one, 73.1m-high above the ground. the bridge is owned today by Norfolk Southern Railway and is used daily for regular through freight service.

Tracing concrete arch bridge historical evolution, three different typologies can be identify: spadrrell arch, deck stiffened arch, deck unstiffened arch. Deck unstiffend arch bridge type shows a progressively increase of arch span length, till more than 400m. Slender Maillart arch type bridges (or deck stiffened arch bridge) seems to be the most suitable one for span length of 70 – 80m. Spandrel archs are used for shorter spans. Maillart arch type bridges are characterized by a high rise-to-span ratio, i.e. a low static coefficient: being deck stiffer than the arch, girder has to take all the bending from the live load; in the arch there are no bending moment due to live loads. Arch carries only compressive stress due to dead loads, having as shape the funicular poligon of permanet load (parabolic or catenary arch).

**Fig. 6.28**  
Bisantis  
Brigde, Catanzaro  
(Italy), Riccardo  
Morandi (1962)  
L=231m, rise to span  
ratio 1/3.09







**Fig. 6.29** Arrabida Bridge, Porto (1963) Edgar Cardoso,  $L_{tot}=493.20\text{m}$ ;  $L_{arch}=270\text{m}$

Comparing three typologies, it could be said that deck stiffened arch bridge (as Maillart ones) show the greatest technological improvement, reaching world record spans, as in the case of *Fiumarella Bridge* (1962)(Fig. 6.28) , *Arrabida Bridge* (1963) (Fig. 6.29) or *Infant Dom Henrique Bridge* (Fig. 6.30) over the River Douro (Porto, 2002).

*Fiumarella Bridge* (or Bisantis Bridge), designed by Morandi in 1962, was included among infrastructural works subsidized by Cassa del Mezzogionio during Second post war (50-60s). With an arch length of 272m, a rise of 66m (rise-to-span –ratio 1:3.5), the bridge has a clearance of 112m. central arch is fixed at the springing sections: it's composed of two twin box-section elements, in order to obtain the maximum torsional and bending stiffness, reducing overall dead loads.

*Arrabida Bridge* is an impressive work of art. The two parallel twin arches span 272 m and for a while set a world record for reinforced concrete bridges. Designed by engineer Edgar Cardoso and built with innovative procedures, the opening ceremony on the 22<sup>nd</sup> of June of 1963 was an enthusiastic popular event.

*Infant Dom Henrique Bridge* over the River Douro (Fig. 6.30) (Porto, 2002) was designed by Structural Engineers A. Adão da Fonseca, F. Millanes Mato and J. A. Fernandez Ordoñez. The Bridge is located in a well defined urban space that is full of character and personality; this Bridge intends to avoid any conflict with the consolidated outline of the city, adding no new elements that might change it. The Infant Dom Henrique Bridge is composed of two mutually interacting fundamental elements: a very rigid (slenderness of 1/62.2) prestressed reinforced concrete box beam, 4.50 m in height, supported on a very flexible (slenderness of 1/186.6) reinforced concrete arch, 1.50 m thick. The span between abutments of the arch is 280 m and the rise until the crown of the arch is 25 m, thus with a shallowness ratio greater than 11/1. In the 70 m central segment of the bridge, the arch combines with the deck to form a box section that is 6 m in height. The lateral faces of this section are recessed to give the impression of continuity of both the deck and the arch. The arch has a constant thickness and a width that increases linearly from 10 m at the central span segment up to 20 m at the abutments.



**Fig. 6.30** Infant Dom Henrique Bridge (2002), Cardoso.  $L_{tot}=412.50\text{m}$ ;  $L_{arch}=280\text{m}$

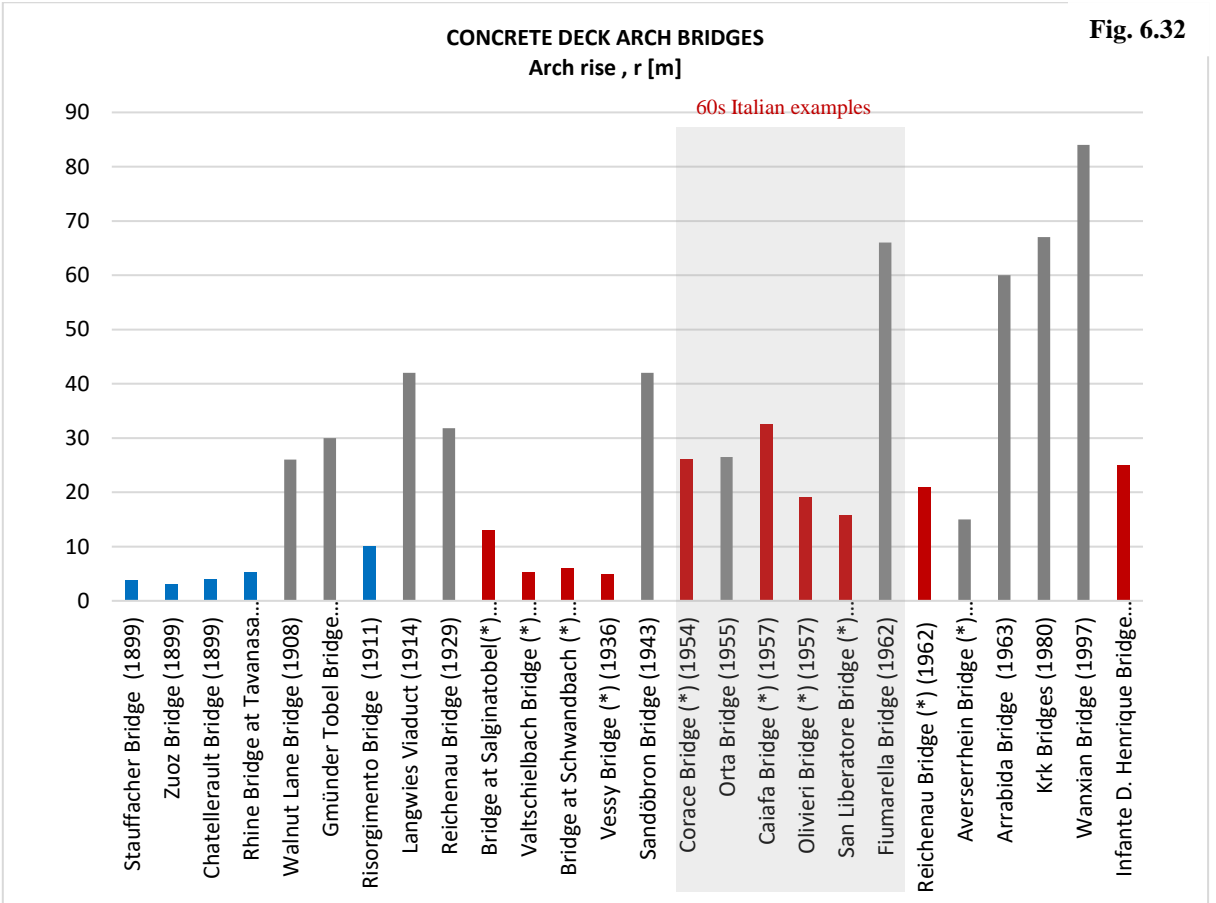
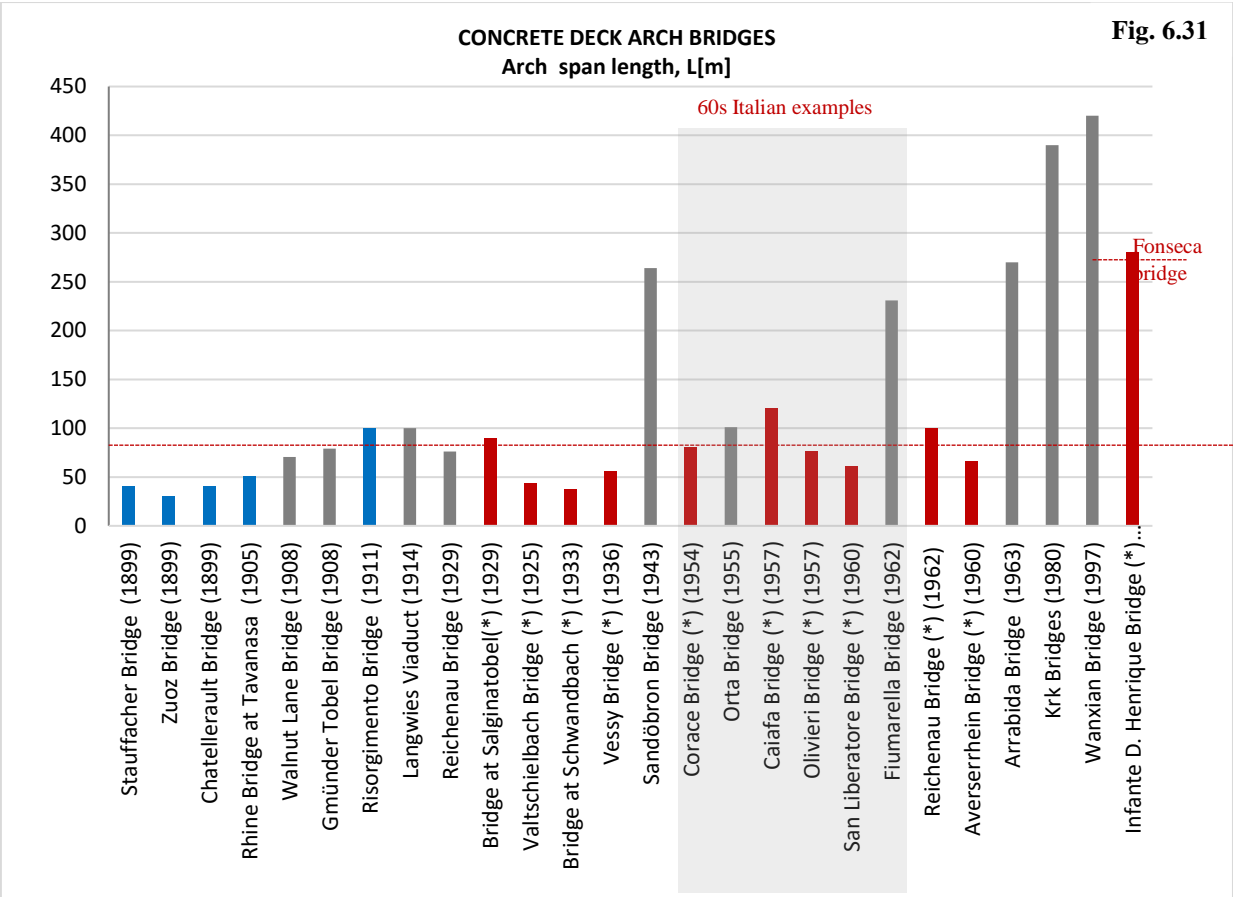
The structural behaviour of the flexible arch – rigid deck combination has the following basic features:

- Absence of important bending moments in the arch except, due to compatibility with its rigid foundations, at its fixed ends.
- Axial force variations carried by the arch are relatively moderate; the tendency of the arch rise to decrease due to thermal actions and creep and shrinkage deformations is hindered by the rigidity of the deck;
- The deck behaves as if it were a continuous beam on elastic supports provided by columns spaced 35 m apart;

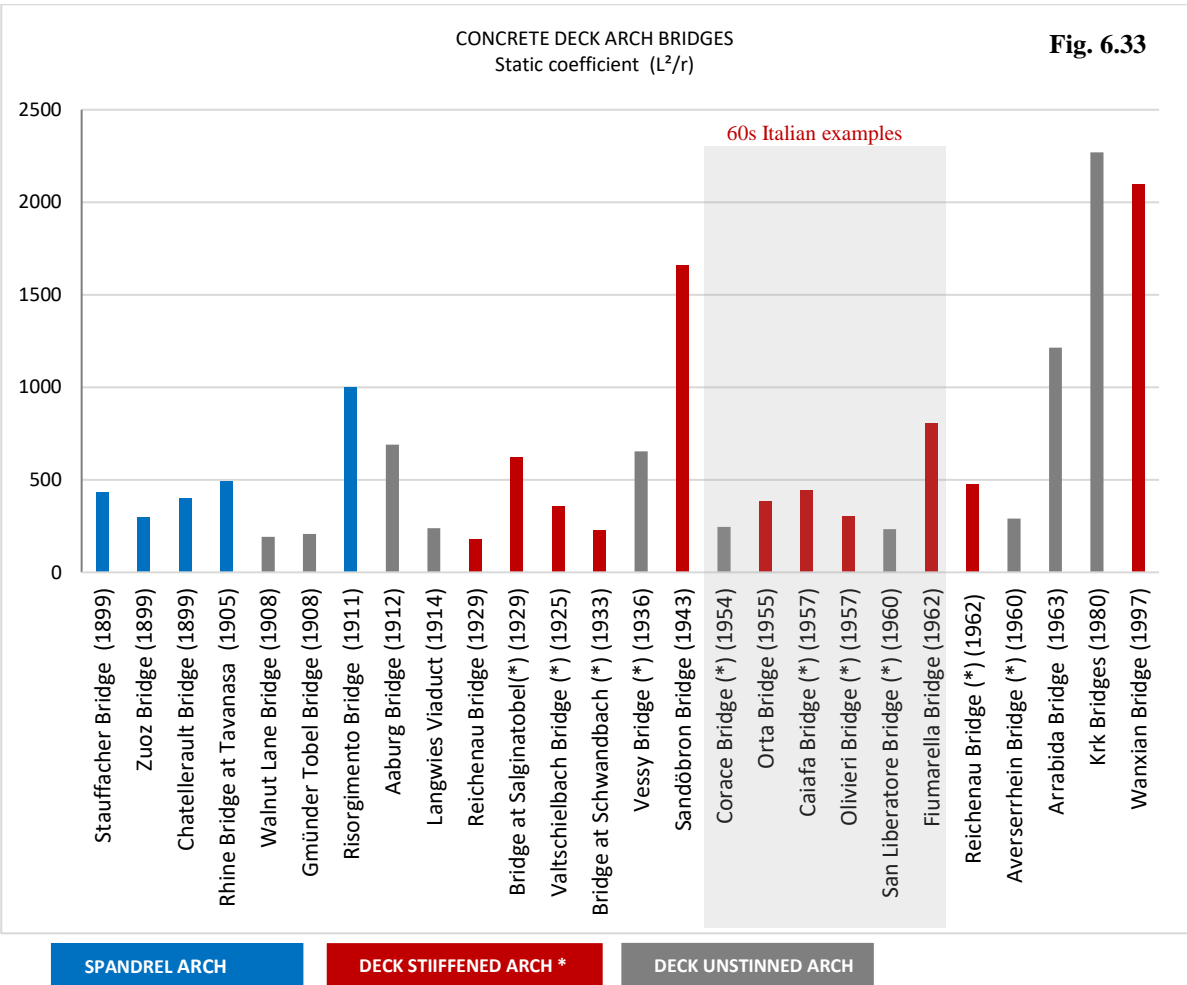
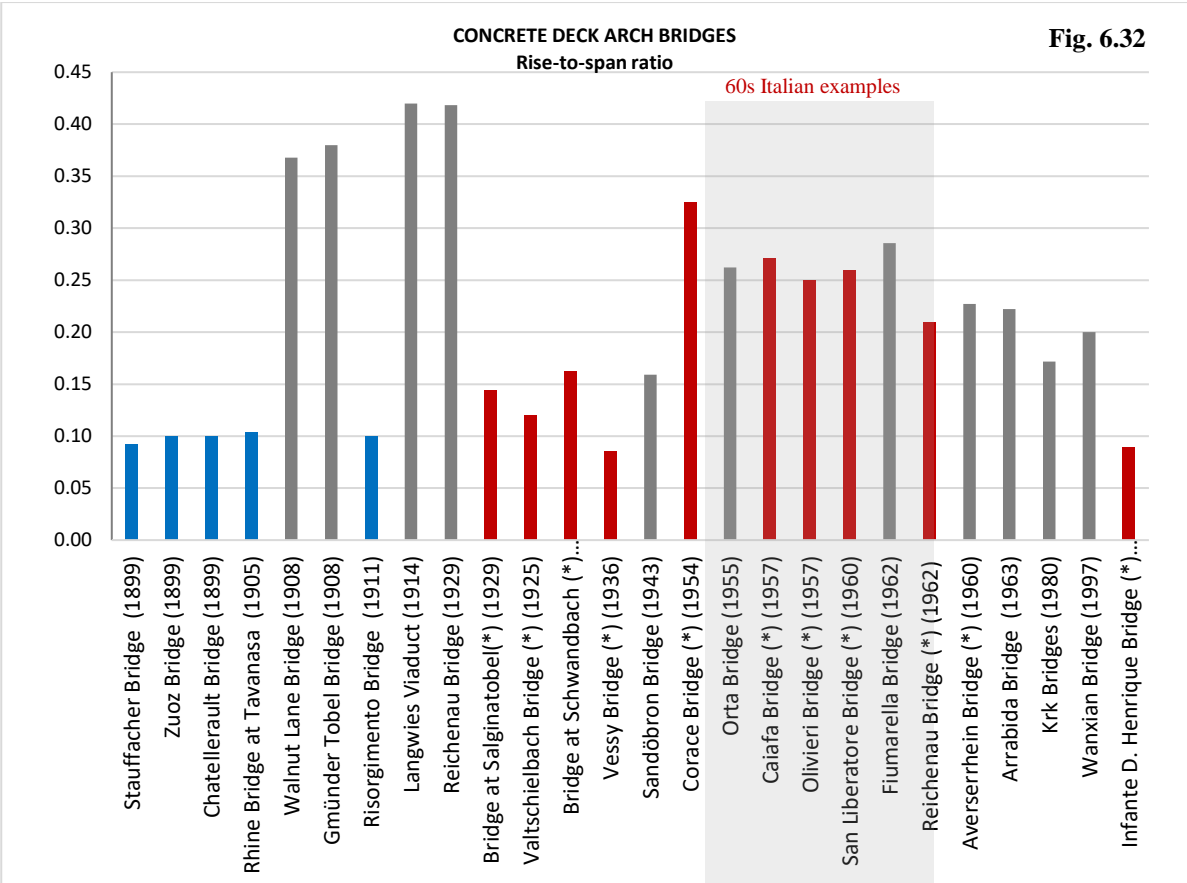
The option for a single box-beam in the 70 m central span, where the arch and deck combine into one single element, was also an important factor in the optimisation of the structure.

The following table summarizes case studies analysed (tab. 6.1) (Fig. 6.30) (fig. 6.31) (Fig. 6.32) (Fig. 6.33):

Bridge	year	Designer	Place	L tot [m]	L - arch span [m]	rise [m]	rise-to- span ratio	L <sup>2</sup> /r
<b>Stauffacher Bridge</b>	1899	Maillart	(Switzerland	40	40.00	3.7	1\11	432
<b>Zuoz Bridge</b>	1899	Maillart	Switzerland	38.25	30.00	3	1\10	300
<b>Chatellerault Bridge</b>	1899	Hennebique	France	144	40.00	4	1\10	400
<b>Tavanasa Bridge</b>	1905	Maillart	Switzerland	51	51.00	5.3	1\10	491
<b>Walnut Lane Bridge</b>	1908	. Webster	Philadelphia	70.7	70.70	26	1\3	192
<b>Gmünder Tobel</b>	1908	Hörsch	Switzerland	79	79.00	30	1\3	208
<b>Risorgimento Bridge</b>	1911	Porcheddu	Italy (Rom)e	100	100.00	10	1\10	1000
<b>Langwies Viaduct</b>	1914	Zublin	Switzerland	100	100.00	42	1\2	238
<b>Reichenau Bridge</b>	1929	Menn	Switzerland	130	76.00	31.8	1\12	182
<b>Salginatobelt (*)</b>	1929	Maillart	Switzerland	132	90.00	13	1\7	623
<b>Valtschielbach Brie (*)</b>	1925	Maillart	Switzerland	43.2	43.20	5.2	1\8	359
<b>Schwandbach (*)</b>	1933	Maillart	Switzerland	55.6	37.00	6	1\6.23	228
<b>Vessy Bridge (*)</b>	1936	Maillart	Switzerland	79	56.00	4.8	1\12	653
<b>Sandöbron Bridge</b>	1943	Skanska	Sweden	810	264.00	42	1\6.2	1659
<b>Corace Bridge (*)</b>	1954	Franciosi, Galli	Italy (CT)	159	80.00	26	1\3.07	246
<b>Orta Bridge</b>	1955	Morandi	Italy (Pescara)	180.3	101.00	26.5	1\3.80	385
<b>Caiafa Bridge (*)</b>	1957	Benini e Schmidt	Italy (Salerno)	210	120.00	32.5	1\3.9	443
<b>Olivieri Bridge (*)</b>	1957	Benini e Schmidt	Italy (Salerno)	136	76.00	19	1\4	304
<b>San Liberatore (*)</b>	1957	Benini e Schmidt	Italy (Salerno)	114	60.80	15.8	1\3.8	234
<b>Fiumarella</b>	1962	Morandi	Italy (CT)	467	231.00	66	1\3.5	809
<b>Reichenau Bridge (*)</b>	1962	Menn	Switzerland	158	100.00	20.9	1\5	478
<b>Averserrhein (*)</b>	1959	Menn	Switzerland	91	66.00	15	1\4.4	290
<b>Arrabida Bridge</b>	1963	Cardoso	Portu gal	493	270.00	60	1\4.5	1215
<b>Krk Bridges</b>	1980	Stojadinovic	Croatia	1430	390	67	1\5.8	2270
<b>Wanxian Bridge</b>	1997	Sichuan Prov.	China	865	420	84	1\5	2100
<b>Infante D. Henrique (*)</b>	2002	A.da-Fonseca	Portugal	412.5	280	25	1\11	3136





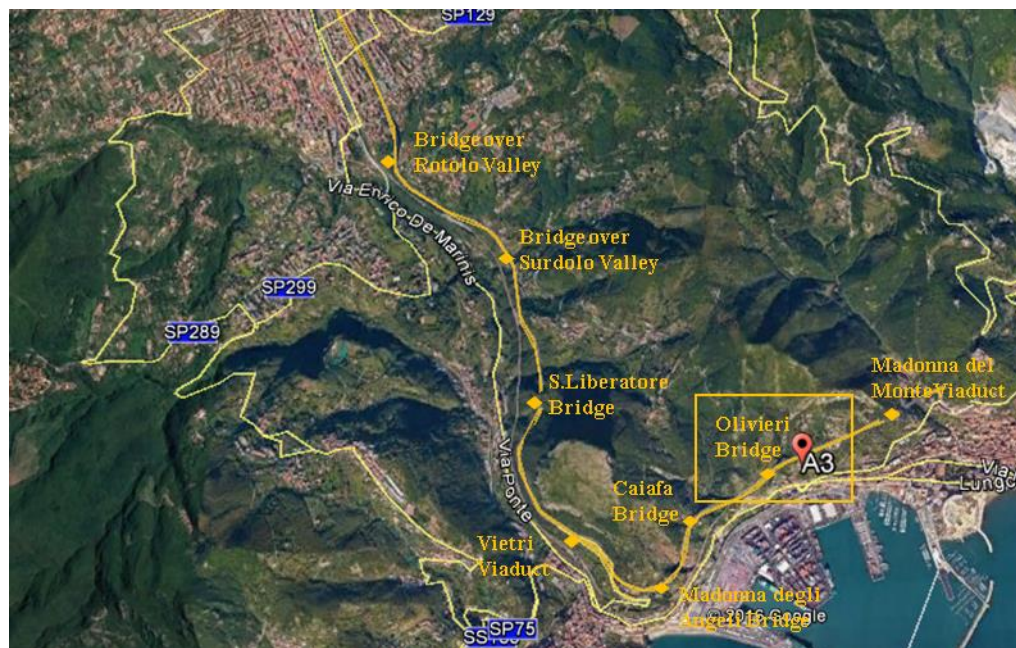


### 7.1.1 1960's Italian concrete arch bridges along Pompei- Salerno highway (A3)

In 1950s, public authority known as Cassa del Mezzogiorno was instituted by Da Gasperi Government to finance industrial initiatives in Southern Italy, with the aim of relaunching its economy and reducing the existing gap with Northern Italy. A plane of measures was drawn up, including environmental renewals and construction of new highways. About 40% of the whole budget was spent to build a new track in one of the most pleasant tourist place, Pompei- Salerno. This highway, as continuum of the existing Napoli-Pompei highway, is 29.33km long: it's characterized by a 19m-wide deck, having two 7.50m- carriageways, two 1.50m-roadside verges and a central 1m-wide bollard. It was built by Società Autostrade Meridionali (SAM), in three steps: Pompei- Cava dei Tirreni early part, Canalone Valley- S.Eremita final portion, then the most difficult one, Cava -Canalone Valley intermediate stretch, where bridges, viaducts and galleries were built. Works financed by Cassa del Mezzogiorno amounted to ITL 382 millions per kilometre, while the other ones completed by SAM cost ITL 293 millions per kilometre. (Fig. 6.30) (Tab. 6.2)

Looking at the extreme local slopes, crossed by rivers, meanwhile the presence of downstream railroad track, the most congenial solution to build Pompei – Salerno highway was to create a line in parallel with the railway. Eight long span bridges were necessary to complete the track, designed by Professor Benini (Rome) and Schmidt (Basilea). Considering boundary conditions, taking into account also the remarkable naturalistic contest, a particular “Z-shapes” deck solution was used, having two staggered carriageways, which allowed to minimize deck width.

**Fig. 6.34** Location of eighth bridges along A3 Pompei- Salerno

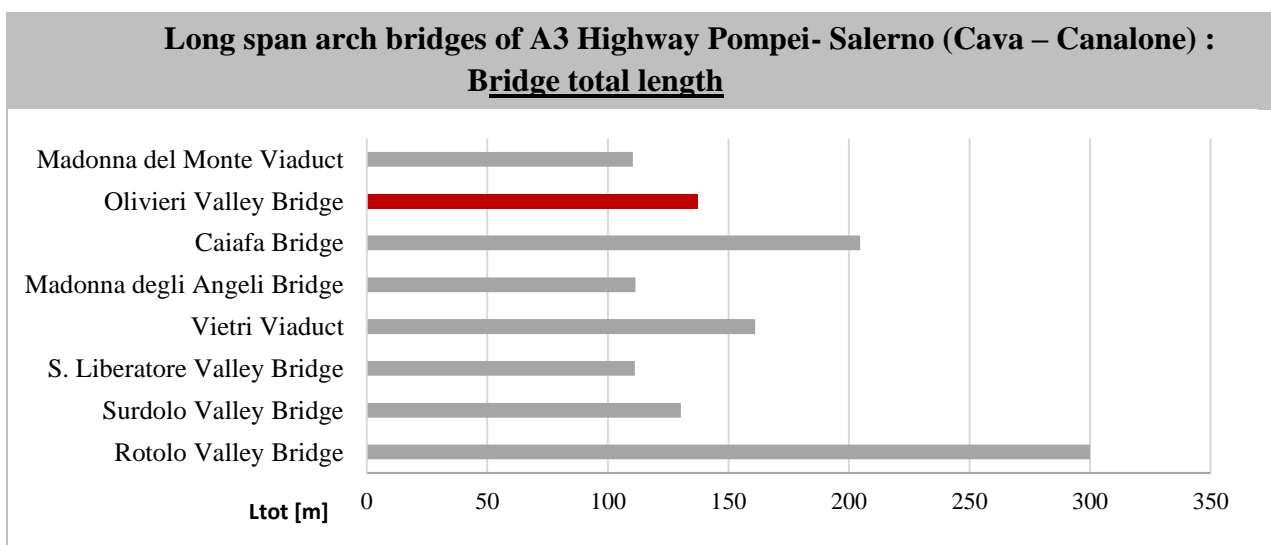


(A3) Pompei – Salerno Highway (Cava – Canalone) : main bridges characterization							
Bridge classification		n. arch	$L_{arch}$ [m]	rise [m]	$L_{tot}$ [m]	r/L	$r^2/f$
1	Rotolo Valley Bridge	2	60	19	300	1/3,15	189
2	Surdolo Valley Bridge	1	60.80	16	130.30	1/3,80	231
3	S. Liberatore Valley Bridge	1	60.80	15.80	111.12	1/3,84	205
4	Vietri Viaduct	Girder bridge, having two separated carriages, staggered one-to another			161.02	-	-
5	Madonna degli Angeli Bridge	1	60.80	18	113.36	1/3,37	205
6	Caiafa Bridge	1	120	32.50	204.60	1/3,69	443
7	Olivieri Valley Bridge	1	76	19.30	137.20	1/3,93	299
8	Madonna del Monte Viaduct	Girder bridge, having two separated carriages, staggered one-to another			110.04	-	-

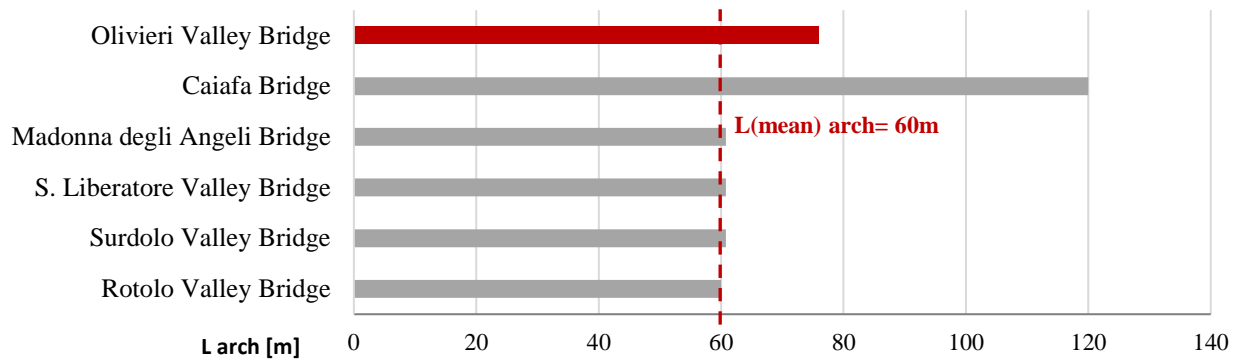
Apart from Rotolo Valley Bridge, all the other infrastructures are characterized by two staggered carriageways, one for travelling direction, each one made of two lanes (7.50m-wide carriageways). This solution led to significant advantages: (1) it avoids discomfort or disability caused by passing cars lamps; (2) deck width is reduced, as the central wall-beam, which links the upper portion to the lower one, is less bulky than the common bollards; (3) considering deck static behavior, “Z-shaped” section is capable to carry stress due to bending moment reversal. (Fig. 6.35) (Fig. 6.36) (Fig. 6.37) (Fig. 3.38) (Fig. 3.39) For bridges along Pompei- Salerno Highway, arch shape was defined considering funicular polygon due to dead loads: considering that Maillart arch type system have been adopted, it could be assumed that all the effects of live load are carried by rigid deck, so there are no additional bending moment in the arch. According to designers’ assumptions, arch-to girder transferring system has been verified, considering second order effects.

**Tab. 6.2** (A3) Pompei – Salerno Highway (Cava – Canalone): main bridges characterization

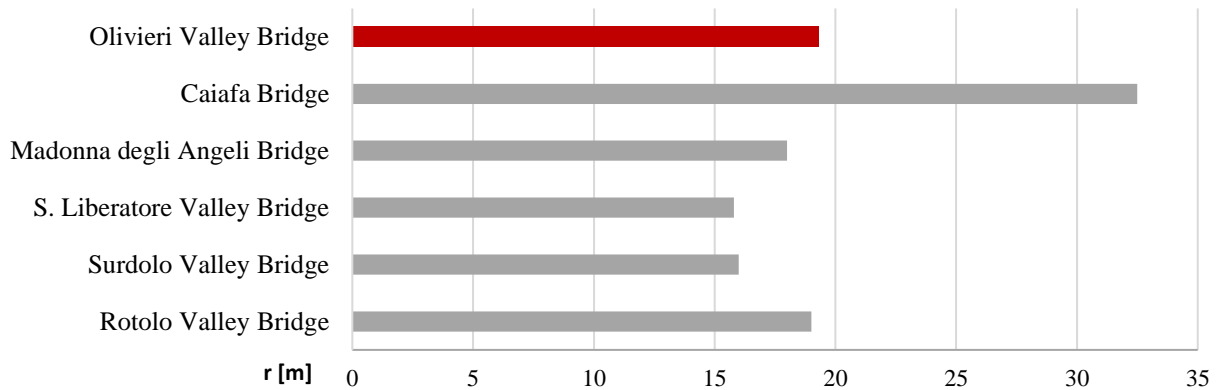
**Fig. 6.35** (A3) Pompei – Salerno Highway Bridges: total length



### Long span arch bridges of A3 Highway Pompei- Salerno (Cava – Canalone) : Arch length (L)



### Long span arch bridges of A3 Highway Pompei- Salerno (Cava – Canalone) : Arch rise (r)



### Long span arch bridges of A3 Highway Pompei- Salerno (Cava – Canalone) : Rise-to-span ratio (r/L)

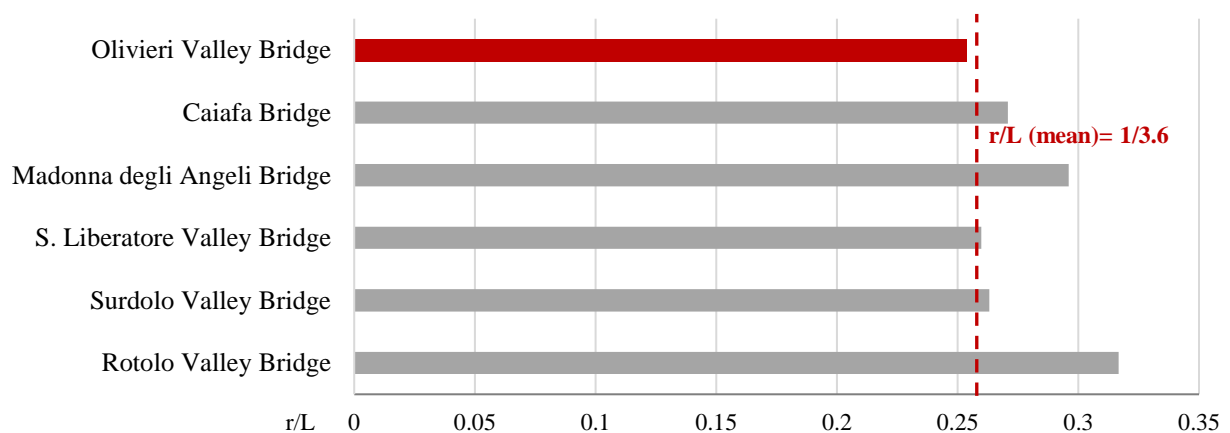
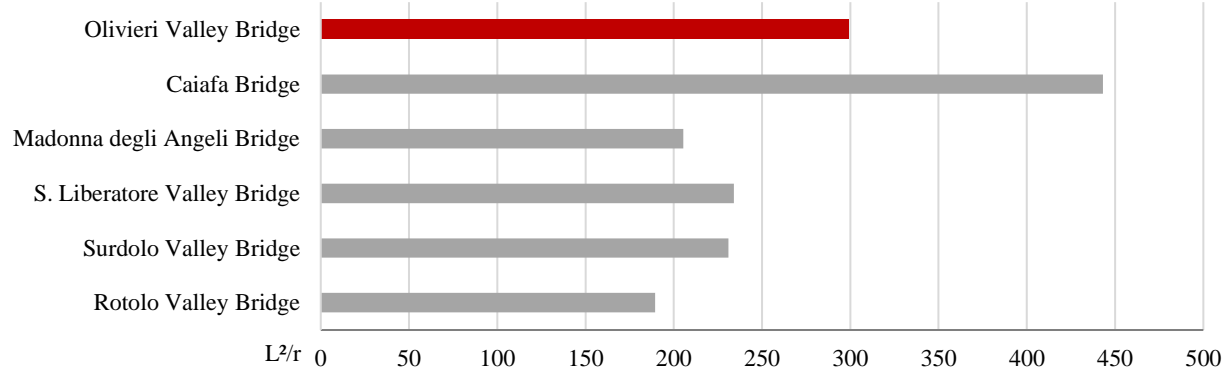


**Fig. 6.36; Fig. 6.37; Fig. 6.38; Fig. 6.39** (A3) Pompei – Salerno Highway Bridges' characterization

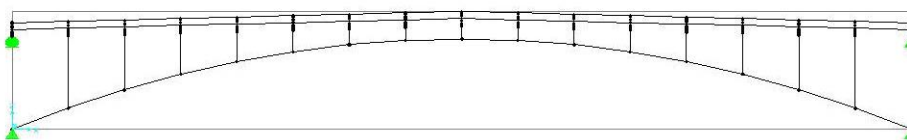


### Long span arch bridges of A3 Highway Pompei- Salerno (Cava – Canalone) : Static coefficient ( $L^2/r$ )



Apart from a visual and compositional uniformity, the choice of building 6 (among 8) bridges using Maillart arch-type has been greatly advantageous from an economical point of view: because arch spans were quite similar (mean value: 60m), bridge constructions proceeded step-by-step in series, adopting quite similar centerings. Bridge construction was quickly completed, thanks to an efficient management of construction side, particularly for using a bridge crane, 1.5tons-carrying, moving upon two main cables, 200m long; this one, stocked by a “boldin” (motorised track), guaranteed casting of concrete in all sides, having a mean production of 8 -10 cubic meters for hour. A water to concrete ratio of 0.50-0.55 was adopted, using fluidifying agents for concrete. [Reference: *Cassa per il Mezzogiorno – Dodici anni 1950 – 1962, La Viabilità*].

Accomplishing to technical, structural and architectural requirements, the choice of Maillart arch type bridge, with a stiffen girder and thin ribbed vault, appeared the most congenial one to cover long span in a so impressive contest. Slender arch is stiffened with a rigid deck, capable to carry bending stress due to accidental loads, while arch supports only compression strengths. Using a “Z-shaped” cross section for bridge deck, arch-to-girder transferring system is guaranteed by a wall-beam, connecting two staged carriageways; at the same time, vertical cross walls, as pendulums, make the arch following deck deformed shape, improving cooperation between load bearing structural elements.



Thanks to this typology, many advantages could be obtained: (1) economy in using materials: strict interaction between arch and girder allows to better use strength coming from different structural elements; (2) effect of concrete shrinkage and settings are negligible, adopting a low-thickness vault; (3) reducing of centering cost, having to support the weight of a slender vault; (4) aesthetic value of a no redundant structure.

## Bibliography

- [1] L.Santarella e E.Miozzi PONTI ITALIANI IN CEMENTO ARMATO - SOLO ATLANTE Ed. 1948
- [2] Luigi Santarella. Prontuario del Cemento Armato. 1962.
- [3] La Viabilità. Dodici anni 1950-1962. Cassa del mezzogiorno. 1962
- [4] Max Bill, Robert Maillart. Robert Maillart Bridges and Constructions. 1969
- [5] D. Billington. The tower and the Bridge: the new Art of Structural Engineering. 1985.
- [6] D.Billington. Robert Maillart's Bridges. 1992
- [7] D.Billington. Robert Maillart and the art of Reinforced concrete. 1990
- [8] Petros P. Xanthakos. 1994. Theory and design of Bridges
- [9] S.E. Thomasen. Seismic strengthening of historic concrete arch bridges. Transactions on the Built Environment vol 15, © 1995 WIT Press, www.witpress.com, ISSN 1743-3509
- [10] Petrangeli M. P., Progettazione e Costruzione di Ponti, C.E. Ambrosiana, Roma, 1996
- [11] Menn, C, The Place of Aesthetics in Bridge Design, Structural Engineering International, Volume 6, No. 2, pp. 93-95, 1996
- [12] Nasce' V.; Sabia D., [Teoria e pratica nella costruzione nei ponti in muratura tra XVIII e XIX secolo](#). In: Carlo Bernardo Mosca, 1792-1867 : un ingegnere architetto tra Illuminismo e Restaurazione / Vera Comoli, Laura Guardamagna, Micaela Viglino (cur.). Guerini, Milano, pp. 29-38. ISBN 8878027669 1997
- [13] David B. McCallen, Charles Noble, Matthew S. Hoehler. The Seismic Response Of Concrete Arch Bridges With Focus On The Bixby Creek Bridge Carmel, California. Technical report N. UCRL - ID - 134419. June, 1999. Lawrence Livermore National Laboratory. California Department of Transportation.
- [14] Chen W., Duan L., Bridge Engineering Handbook, CRC Press, 2000
- [15] Chen e Lian Duan. Bridge Engineering Handbook. Boca Raton : CRC Press LLC, 2000.
- [16] Raj Valluvan, John Stephenson, Don Bergman, Peter Buckland And Dave Pajouhesh. Innovative retrofit techniques for seismic retrofit of concrete arch bridges of earlier vintage. 12WCEE 2000
- [17] D.Billington. The Revolutionary Bridge by Robert Maillart. Scientific America. 2000
- [18] Menn, C, Stahlbetonbrücken (Reinforced concrete bridges), 2003
- [19] R.W.Cluogh, J.Penzien. Dynamic of structures. 2003

- [20] Troyano L.F., Bridge Engineering A global perspective, 2003
- [21] R.W.Cluogh, J.Penzien. Dynamic of structures. 2003
- [22] Arioli M., The Art of Structural Design : a Swiss Legacy: eine Ausstellung im Zürcher "haus konstruktiv", ETH Zürich, Rämistrasse 101, 8092 Zürich, Schweiz, [www.library.ethz.ch](http://www.library.ethz.ch), 2005
- [23] Shabanovitz T. B., The Progressive Synthesis of Architecture and Engineering in Modern Bridge Design, Massachusetts Institute of Technology, June 2006
- [24] Seismic Retrofitting Manual for Highway Structures: Part 1 – Bridges.2006. US Department of Transportation. Federal Highway Administration
- [25] Dobricic S., Siviero E., De pontibus. Un manuale per la costruzione dei ponti, Il Sole 24 Ore, 2008
- [26] Theodore V. Galambos, Andrea E. Surovek. Structural stability of Steel: concepts and applications for structural engineers. John wiley & sons, inc., 2008
- [27] D.Billington. Robert Maillart: Builder, Designer, and Artist. 2008
- [28] E. Brühwiler, Prof. Dr. Civil Eng. ETH, Ecole Polytechnique Fédérale de Lausanne (EPFL), Switzerland, Christian Menn's recent bridge designs – Reducing structural elements to the simplest solution. . 5th New York City Bridge Conference, Bridge Engineering Association, New York (USA), August 17 – 18, 2009
- [29] M.A. Rutherford. A Critical Analysis Of Bixby Creek Bridge. Proceedings of Bridge Engineering 2 Conference 2009 April 2009, University of Bath, Bath, UK
- [30] Tullia Iori, Sergio Poretti. The Golden Age of "Italian Style" Engineering. Proceedings of the Third International Congress on Construction History, Cottbus, May 2009.
- [31] D.Proske – P.Gelder, "Safety of Historical Stone Arches Bridges", Springer, 2009
- [32] Dirk Proske · Pieter van Gelder , "Safety of Historical Stone Arch Bridges", Spriger, 2009
- [33] M. De Miranda, U.Barbisan, M.Pogacnick, L.Skansi Bridges in Venice - Architectural and Structural engineering aspects, 34<sup>th</sup> IABSE SYMPOSIUM, Venezia 2010
- [34] J. Radić and A. Kindij. The polygonal arch bridge. 2010.
- [35] E.C. Kandemira, T. Mazda, H. Nurui, H. Miyamoto. Seismic Retrofit of an Existing Steel Arch Bridge Using Viscous Damper. Elsevier. Procedia Engineering. 2011.
- [36] S. Palaoro, E. Siviero, B. Briseghella, T. Zordan. Concept and construction methods of arch bridges in Italy. ARCH'10 – 6th International Conference on Arch Bridges.
- [37] Denison, Edward e Stewart, Ian. Leggere i ponti. Modena : Logos, 2012.
- [38] D.Billington. FESTSCHRIFT. 2012
- [39] G.Tecchio, F. da Porto, P. Zampieri, C. Modena. Static and seismic retrofit of masonry arch bridges: case studies. Bridge Maintenance, Safety, Management,

Resilience and Sustainability – Biondini & Frangopol (Eds) © 2012 Taylor & Francis Group, London, ISBN 978-0-415-62124-3

- [40] Lily Beyer, University of New Hampshire. Arched Bridges. Spring 2012
- [41] B. Ozden Caglayan, Kadir Ozakgul\* and Ovunc Tezer. Assessment of a concrete arch bridge using static and dynamic load tests. Structural Engineering and Mechanics, Vol. 41, No. 1 (2012) 83-94
- [42] S. De Santis & G. de Felice. Seismic analysis of masonry arches. 15 WCEE. Lisboa 2012.
- [43] Jure Radić Marija Kušter. Aesthetics and sustainability of arch bridges. ARCH13. 7<sup>th</sup> International Conference on Arch Bridges.
- [44] Denis ZASTAVNI, Jean-François CAP, Jean-Philippe JASIENSKI, Corentin FIVET. Load path and prestressing in conceptual design related to Maillart's Vessy Bridge. Proceedings of the IASS-SLTE 2014 Symposium "Shells, Membranes and Spatial Structures: Footprints" 15 to 19 September 2014, Brasilia, Brazil
- [45] Claudio Modena, Giovanni Tecchio, Carlo Pellegrino, Francesca da Porto, Marco Donà, Paolo Zampieri & Mariano A. Zanini. Reinforced concrete and masonry arch bridges in seismic areas: typical deficiencies and retrofitting strategies. Structure and Infrastructure Engineering. 2014
- [46] John Edward Finke. Doctoral Thesis Disserttion. Static and dynamic characterization of tied arch bridge. 2016
- [47] Paolo Lonetti, Arturo Pascuzzo, and Alessandro Davanzo. Dynamic Behavior of Tied-Arch Bridges under the Action of Moving Loads. Hindawi Publishing Corporation. Mathematical Problems in Engineering Volume 2016, Article ID 2749720, 17 pages

### Web references

- [1] International Database and Gallery of Structures, <http://en.structurae.de>
- [2] <http://dx.doi.org/10.1080/15732479.2014.951859>
- [3] <http://dx.doi.org/10.1155/2016/2749720>



## 7. Case study on Maillart-arch-type bridge: seismic behaviour and retrofit proposal for Viadotto Olivieri (SA)

### 7.1 Main scope of the analysis

In line with previous evaluations concerning Maillart-arch-type bridges, this chapter focuses on a specific case study, Viadotto Olivieri (SA). (Fig. 7.1) In the earliest six chapters of this thesis, all typologies often adopted to cover long spans have been taken into account, underlining the way deck stiffened system has changed. Starting from short-span bridges, whose loading transferring system acted in flexural regime, the “revolutionary approach”, which accompanied long span bridge evolution, led to prefer structures working in extensional regime: in this case a close succession of bridge deck cross sections, corresponding to a reduction of the effective loaded length of longitudinal main structural elements, guarantees forces applied to be directly transferred (without additional bending effects) from deck to the main load bearing system, coinciding with the lower arch for deck- arch bridges, the upper arch for bowstring arch bridge, the main cable and hangers system for suspension bridges, the strain stays anchored at the bottom of compressed pylons in the case of cable-stayed bridges. All previous analysis and proposed comparisons check bridges’ static behaviour, underlining the effects of changing deck characterization on bridge response. Considering that no evaluations have been exposed on dynamic behaviour of long span bridges since now, this chapter will debate on this peculiar aspect.

**Fig. 7.1:** Viadotto Olivieri. A3, SA-NA Highway. Beninese design, 1954-1958)

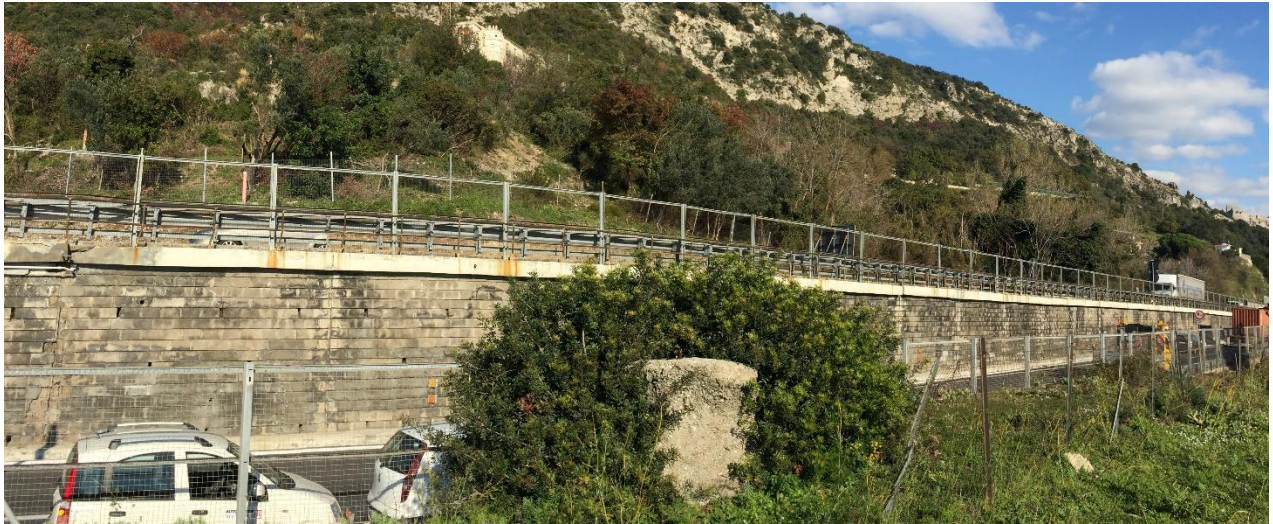


In the following paragraphs, a report of Viadotto Olivieri current state is analysed. In order to better understand bridge static and dynamic response, seven different FEM models have been analysed, valuing the effects due to changing deck configuration or restraint conditions at the base of the cross walls: this approach gives the possibility to check the most vulnerable structural elements, above all acting horizontal force, finding the solution which minimizes out of plane arch over-turning or cross-walls bucking effects. A linear static analysis has been compared to a dynamic linear one, to better define bridge seismic response. A retrofit proposal for the case study testifies that in order to improve bridge seismic response it's not necessary to completely change bridge configuration, introducing isolation system; in fact, as follows, a great reduction of base reactions is obtained "simply" jointing in a stiffer configuration three separated portions, that now compose bridge deck: in this way, stresses occurred both at the bottom of the arch and cross walls are greatly reduced, making the abutments the most affected sections.

## 7.2 Viadotto Olivieri: report of the current state

Olivieri Bridge (Fig. 7.2) (Fig. 7.3) is characterized by a reinforced concrete deck- stiffened parabolic arch, whose access ramps consist of 2-span reinforced concrete beam bridge on Naples side 15.20m long, and 6-span beam bridge on Salerno side, 45.60m long. Bridge deck (having a total length of 136,80m) is separated by two joints, one upon pier n.2 and the other on pier n. 12; its two roadways settle at different grades above the ground, being 4m-staggered one from the other. Olivieri Bridge (Fig. 7.4) main structure is the central Maillart arch-type bridge, having a thin ribbed vault with an upper stiffen girder. 76.00m spanning, this arch reaches 19.30m at the crown, having a rise-to-span ratio ( $r/L$ ) of  $1/4$  (0.25), i.e. a static coefficient ( $L^2/r$ ) of 299. Connection between arch and longitudinal girder is guaranteed by slender cross walls, working as pendulums; each cross wall is made of a thin concrete slab stiffened by 5 columns, whose cross section size grows passing from the middle to the edge of the cross wall





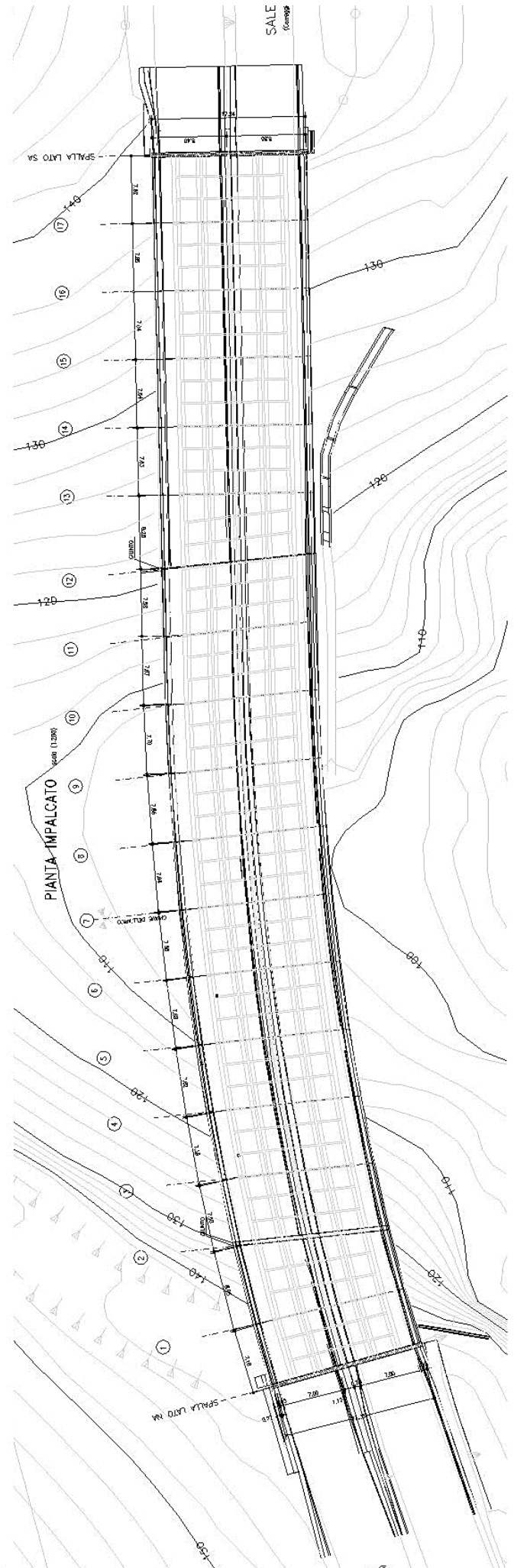
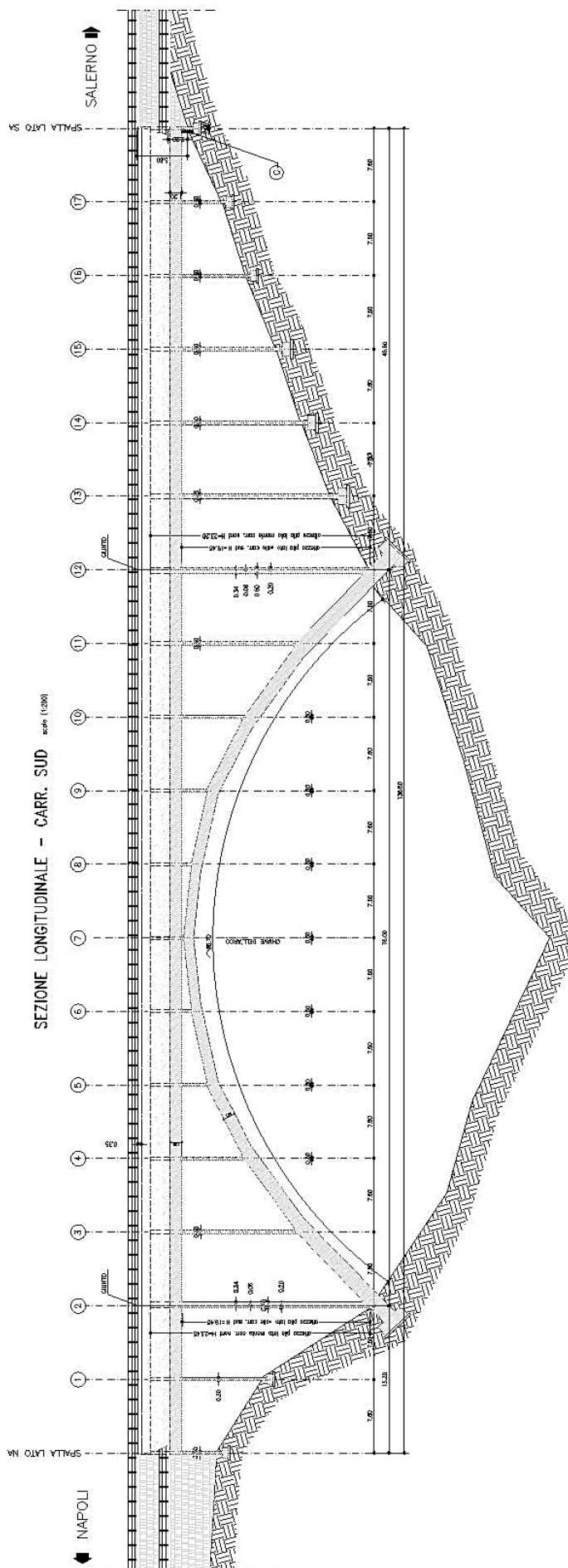
Arch axis matches with the funicular polygon due to permanent loads, passing through the centre of keystone and springing sections. Considering that in a Maillart-arch type bridge, slender vault is not effected by stress due to accidental loads, the usual “*adjustments of thrust line within arch walls*” are not required: these one should be necessary to deviate real arch axis from the funicular curve, reducing moments due to permanent load - induced strain, both at the crown and at springing sections. In this particular case of CIP concrete vault, the effect of viscosity have already served, determining an auto- recentering of thrust curve. Both arch and piers transfer loads to rectangular foundation plinths: each cross wall column and arch rib attaches directly upon them, without any beams to connect them transversely. Foundations stand upon a carbonate bedrock, partially slatted.

**Fig. 7.2:** Viadotto Olivieri. A3, SA-NA Highway. Benine schmidt design, 1954-1958) – Upper deck longitudinal view

**Fig. 7.3:** Viadotto Olivieri. A3, SA-NA Highway. Benine schmidt design, 1954-1958) – Bridge longitudinal view











## 7.3 Loads analysis

### 7.2.1 Dead loads

Arch vault (Fig. 7.5) (Tab. 7.1) is made of a 0.20m-thick concrete slab, stiffened by five ribs, with variable cross section along longitudinal axis; this polygonal arch consists of 10 straight portions, whose section size grow passing from the arch crown to the springing sections: at the midspan arch cross section is characterized by a central rib (100x40), which become (157x40) at the springing section; two intermediate ribs (100x30) which grow to (157x30), two external ribs (100x45) which wide until (157x45) at the springing sections. Bridge deck (Fig. 7.6) consists of two staggered carriageways, each one made of two lanes, connected by a continuous beam-wall ( $\Delta z = 4.00\text{m}$ ). Road-deck is a thin slab, standing upon longitudinal girder, having different size. (Fig. 7.7) (Tab. 7.2)

**Fig. 7.4:** Viadotto Olivieri. A3, SA-NA Highway. Benine schmidt design, 1954-1958) – Bridge upper view

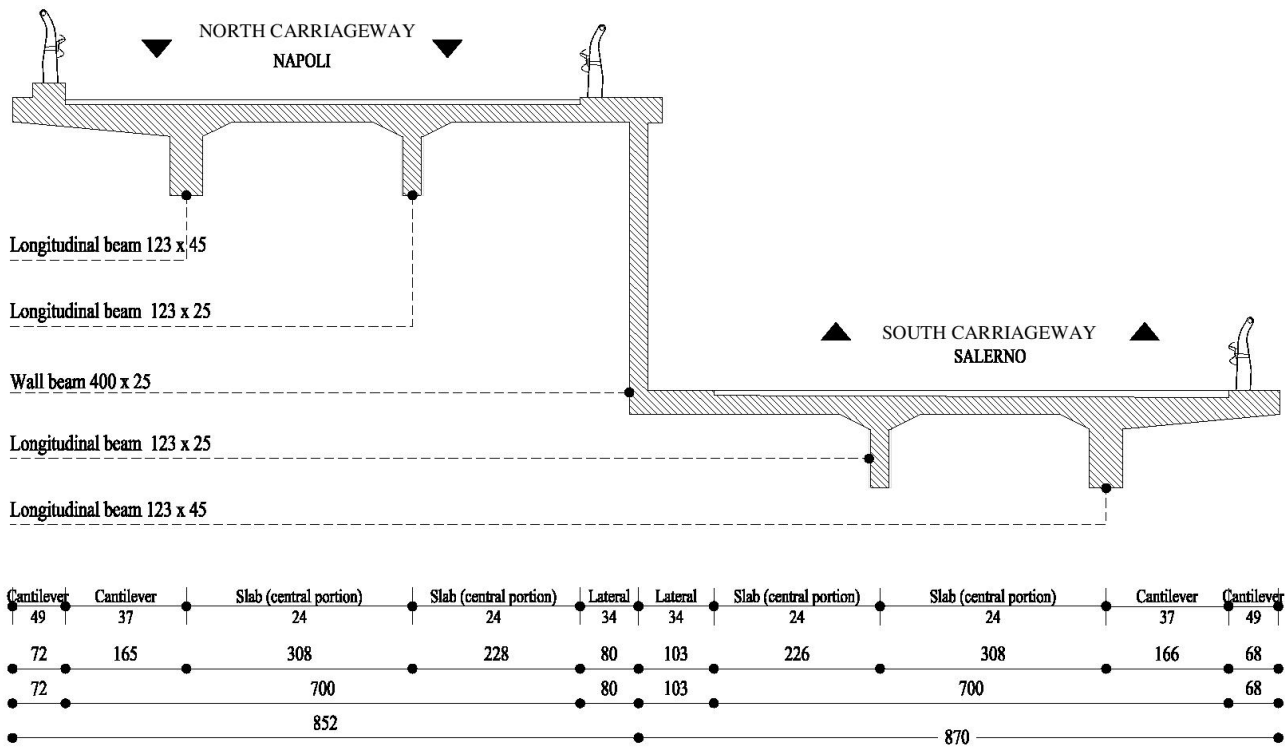
**Fig. 7.5:** Viadotto Olivieri. A3, SA-NA Highway\_ arch vault detail



**Tab. 7.1:** Viadotto Olivieri. arch vault dead load estimation

Dead Loads _ Arch portion							
Element	Height (m)	Depth (m)	Length (m)	Volume (m <sup>3</sup> )	Weight P (kN)	P (t)	% Tot
Rib 100x30	1,00	0,30	15,60	4,68	117,00	11,7	1,19
Rib 100x40	1,00	0,40	15,60	6,24	156,00	15,6	1,58
Rib 100x45	1,00	0,45	15,60	7,02	175,50	17,55	1,78
Rib 113x30	1,13	0,30	15,76	5,34	133,57	13,356	1,35
Rib 113x40	1,13	0,40	15,76	7,12	178,09	17,808	1,81
Rib 113x45	1,13	0,45	15,76	8,01	200,35	20,034	2,03
Rib 125x30	1,25	0,30	16,20	6,08	151,88	15,187	1,54
Rib 125x40	1,25	0,40	16,20	8,10	202,50	20,25	2,05
Rib 125x45	1,25	0,45	16,20	9,11	227,81	22,781	2,31
Rib 138x30	1,38	0,30	17,80	7,37	184,23	18,423	1,87
Rib 138x40	1,38	0,40	17,80	9,83	245,64	24,564	2,49
Rib 138x45	1,38	0,45	17,80	11,05	276,35	27,634	2,80
Rib 157x30	1,57	0,30	32,80	15,45	386,22	38,622	3,92
Rib 157x40	1,57	0,40	32,80	20,60	514,96	51,496	5,22
Rib 157x45	1,57	0,45	32,80	23,17	579,33	57,933	5,87
<b>Rib-subtotal</b>				149,18	<b>3729,4</b>	<b>372,94</b>	<b>37,81</b>
<b>Vault subtotal</b>	12,5	0,2	98,16	245,4	<b>6135</b>	<b>613,50</b>	<b>62,19</b>
<b>TOT Arco</b>					<b>9864,4</b>	<b>986,44</b>	

**Fig. 7.6:** Viadotto Olivieri. A3, SA-NA Highway\_ deck cross section



Each carriageway has cantilever side portions. Apart from avoiding discomfort or disability caused by the passing car lamps and reducing deck depth, this section is capable to carry stress due to bending moment reversal.

Dead Loads _ Bridge Deck						
Element	Height (m)	Depth (m)	Length (m)	V(m <sup>3</sup> )	Weight (kN)	% Tot
Beam 123x45	1,23	0,45	137,10	75,88	1897,12	8,00
Beam 123x25	1,23	0,25	137,1	42,16	1053,96	4,44
Wall beam_25	4,00	0,25	137,1	137,10	3427,50	14,45
<b>Beams- subtotal</b>				<b>255,1</b>	<b>6378,58</b>	<b>26,89</b>
Slab- central portion_ 24	10,70	0,24	137,1	352,07	8801,82	37,11
Slab-laterl _ 34	1,83	0,34	137,1	85,30	2132,59	8,99
Slab- cantilever 37	3,31	0,37	137,1	167,91	4197,66	17,70
Slab- antilever 49	1,40	0,46	137,1	88,29	2207,31	9,31
<b>Slab-subtotal</b>				<b>693,58</b>	<b>17339,38</b>	<b>73,11</b>
<b>TOT Bridge deck</b>				<b>948</b>	<b>23717</b>	

**Tab. 7.2:** Viadotto Olivieri. A3, SA-NA Highway\_ Bridge deck dead load estimation

**Fig. 7.7:** Viadotto Olivieri. Bridge deck \_ (a) bottom view\_ (b) joint detail







**Fig. 7.8:** Viadotto Olivieri. Cross walls\_ (a) longitudinal view\_ (b) connection at foundations

Deck is connected to the arch through vertical cross walls (Fig. 7.8) (Tab. 7.3), 7.60m spaced. These ones are made of a thin concrete membrane (0.12m- thick), stiffened by columns, having different cross sections. Considering low shear stiffness of these vertical elements, cross walls could be assimilated to pendulums.

**Tab. 7.3** Viadotto Olivieri. Cross walls dead loads estimation

Dead Loads _ CROSS WALLS								
Element		Height (m)	Depth (m)	L (m)	V (m³)	Weight P (kN)	P (t)	% Tot
<b>NA- side abutment</b>	Column_45x30	0,45	0,30	12,40	1,67	41,85	4,18	0,36
	Column _40x30	0,40	0,30	12,40	1,49	37,20	3,72	0,32
	Column _ 30x30	0,30	0,30	8,20	0,74	18,45	1,84	0,16
	Slab_12		0,12	12,40	9,30	232,5	23,2	2,00
	<b>NA-abut. tot</b>				<b>13,20</b>	<b>330,00</b>	<b>33,0</b>	<b>2,84</b>
<b>Pier 1</b>	Column _45x30	0,45	0,30	22,80	3,08	76,95	7,69	0,66
	Column _40x30	0,40	0,30	22,80	2,74	68,40	6,84	0,59
	Column _ 30x30	0,30	0,30	13,40	1,21	30,15	3,01	0,26
	Slab_12		0,12	22,80	17,10	427,5	42,7	3,68
	<b>Pier 1 sub-tot</b>				<b>24,12</b>	<b>603,0</b>	<b>60,3</b>	<b>5,19</b>
<b>Pie 2</b>	Column _45x60	0,45	0,60	43,60	11,77	294,3	29,4	2,53
	Column _40x60	0,40	0,60	43,60	10,46	261,6	26,1	2,25
	Column _ 30x60	0,30	0,60	23,80	4,28	107,1	10,7	0,92
	Membrane_12		0,12	43,60	40,88	1022	102	8,80
	<b>Pier 2 sub-tot</b>				<b>67,40</b>	<b>1685</b>	<b>168</b>	<b>14,50</b>



	Element	Height (m)	Depth (m)	L (m)	V (m³)	Weight P (kN)	P (t)	% Tot
<b>Pier 3</b>	Column _45x60	0,45	0,60	27,20	7,34	183,6	18,3	1,58
	Column _40x60	0,40	0,60	27,20	6,53	163,2	16,3	1,40
	Column _ 30x60	0,30	0,60	15,60	2,81	70,20	7,02	0,60
	Membrane_12		0,12	27,20	20,40	510,0	51	4,39
	<b>Pier 3 sub-tot</b>				<b>37,08</b>	<b>927,0</b>	<b>92,7</b>	<b>7,98</b>
<b>Pier 4</b>	Column_45x30	0,45	0,30	17,00	2,30	57,38	5,73	0,49
	Column _40x30	0,40	0,30	17,00	2,04	51,00	5,1	0,44
	Column _ 30x30	0,30	0,30	10,50	0,95	23,63	2,36	0,20
	Membrane_12		0,12	17,00	12,75	318,7	31,8	2,74
	<b>Pier 4 sub-tot</b>				<b>18,03</b>	<b>450,7</b>	<b>45,</b>	<b>3,88</b>
<b>Pier 5</b>	Column _45x30	0,45	0,30	9,20	1,24	31,05	3,10	0,27
	Column _40x30	0,40	0,30	9,20	1,10	27,60	2,76	0,24
	Column _ 30x30	0,30	0,30	6,60	0,59	14,85	1,48	0,13
	Membrane_12		0,12	9,20	6,90	172,50	17,2	1,48
	<b>Pier 5 sub-tot</b>				<b>9,84</b>	<b>246,00</b>	<b>24,6</b>	<b>2,12</b>
<b>Pier 6</b>	Column _45x30	0,45	0,30	5,60	0,76	18,90	1,89	0,16
	Column l_40x30	0,40	0,30	5,60	0,67	16,80	1,68	0,14
	Column _ 30x30	0,30	0,30	4,80	0,43	10,80	1,08	0,09
	Membrane _12		0,12	5,60	4,20	105,00	10,5	0,90
	<b>Pier 6 sub-tot</b>				<b>6,06</b>	<b>151,50</b>	<b>15,1</b>	<b>1,30</b>
<b>Pier 7</b>	Column _45x30	0,45	0,30	4,40	0,59	14,85	1,48	0,13
	Column _40x30	0,40	0,30	4,40	0,53	13,20	1,32	0,11
	Column _ 30x30	0,30	0,30	4,20	0,38	9,45	0,94	0,08
	Membrane_12		0,12	4,40	3,30	82,50	8,25	0,71
	<b>Pier 7 sub-tot</b>				<b>4,80</b>	<b>120,00</b>	<b>12</b>	<b>1,03</b>
<b>Pier 8</b>	Column_45x30	0,45	0,30	5,60	0,76	18,90	1,89	0,16
	Column _40x30	0,40	0,30	5,60	0,67	16,80	1,68	0,14
	Column _ 30x30	0,30	0,30	4,80	0,43	10,80	1,08	0,09
	Membrane_12		0,12	5,60	4,20	105,00	10,5	0,90
	<b>Pier 8 sub-tot</b>				<b>6,06</b>	<b>151,50</b>	<b>15,1</b>	<b>1,30</b>
<b>Pier 9</b>	Column _45x30	0,45	0,30	9,20	1,24	31,05	3,10	0,27
	Column _40x30	0,40	0,30	9,20	1,10	27,60	2,76	0,24
	Column _ 30x30	0,30	0,30	6,60	0,59	14,85	1,48	0,13
	Membrane_12		0,12	9,20	6,90	172,50	17,2	1,48
	<b>Pier 9 sub-tot</b>				<b>9,84</b>	<b>246,00</b>	<b>24,6</b>	<b>2,12</b>

	Element	Height (m)	Depth (m)	L (m)	V (m³)	Weight P (kN)	P (t)	% Tot
<b>Pier 10</b>	Column _45x30	0,45	0,30	17,00	2,30	57,38	5,73	0,49
	Column _40x30	0,40	0,30	17,00	2,04	51,00	5,1	0,44
	Column _ 30x30	0,30	0,30	10,50	0,95	23,63	2,36	0,20
	Membrane _12		0,12	17,00	12,75	318,75	31,8	2,74
	<b>Pier 10 sub-tot</b>				<b>18,03</b>	<b>450,75</b>	<b>45,1</b>	<b>3,88</b>
<b>Pier 11</b>	Column _45x40	0,45	0,40	27,20	4,90	122,40	12,2	1,05
	Column _40x40	0,40	0,40	27,20	4,35	108,80	10,8	0,94
	Column _ 30x40	0,30	0,40	15,60	1,87	46,80	4,68	0,40
	Membrane _12		0,12	27,20	20,40	510,00	51	4,39
	<b>Pier 11 sub-tot</b>				<b>31,52</b>	<b>788,00</b>	<b>78,8</b>	<b>6,78</b>
<b>Pier 12</b>	Column _45x60	0,45	0,60	43,20	11,66	291,60	29,1	2,51
	Column _40x60	0,40	0,60	43,20	10,37	259,20	25,9	2,23
	Column _ 30x60	0,30	0,60	23,60	4,25	106,20	10,6	0,91
	Membrane _12		0,12	43,20	32,40	810,00	81	6,97
	<b>Pier 12 sub-tot</b>				<b>58,68</b>	<b>1467,0</b>	<b>146</b>	<b>12,63</b>
<b>Pier 13</b>	Column _45x45	0,45	0,45	36,20	7,33	183,26	18,3	1,58
	Column _40x45	0,40	0,45	36,20	6,52	162,90	16,2	1,40
	Column _ 30x45	0,30	0,45	20,10	2,71	67,84	6,78	0,58
	Membrane _12		0,12	36,20	27,15	678,75	67,8	5,84
	<b>Pier 13 sub-tot</b>				<b>43,71</b>	<b>1092,7</b>	<b>109</b>	<b>9,41</b>
<b>Pier 14</b>	Column _45x60	0,45	0,60	30,00	8,10	202,50	20,2	1,74
	Column _40x60	0,40	0,60	30,00	7,20	180,00	18	1,55
	Column _ 30x60	0,30	0,60	20,10	3,62	90,45	9,04	0,78
	Membrane _12		0,12	30,00	22,50	562,50	56,2	4,84
	<b>Pier 14 sub-tot</b>				<b>41,42</b>	<b>1035,4</b>	<b>103</b>	<b>8,91</b>
<b>Pier 15</b>	Column _45x60	0,45	0,60	24,80	6,70	167,40	16,7	1,44
	Column _40x60	0,40	0,60	24,80	5,95	148,80	14,8	1,28
	Column _ 30x60	0,30	0,60	14,40	2,59	64,80	6,48	0,56
	Membrane _12		0,12	24,80	18,60	465,00	46,5	4,00
	<b>Pier 15 sub-tot</b>				<b>33,84</b>	<b>846,00</b>	<b>84,6</b>	<b>7,28</b>
<b>Pier 16</b>	Column _45x30	0,45	0,30	18,20	2,46	61,43	6,14	0,53
	Column _40x30	0,40	0,30	18,20	2,18	54,60	5,46	0,47
	Column _ 30x30	0,30	0,30	11,10	1,00	24,98	2,49	0,21
	Membrane _12		0,12	18,20	13,65	341,25	34,1	2,94
	<b>Pier 16 sub-tot</b>				<b>19,29</b>	<b>482,25</b>	<b>48,2</b>	<b>4,15</b>

	Element	Height	Depth	L	V	Weight		
		(m)	(m)	(m)	(m <sup>3</sup> )	P (kN)	P (t)	% Tot
<b>Pier 17</b>	Column _45x30	0,45	0,30	13,20	1,78	44,55	4,45	0,38
	Column _40x30	0,40	0,30	13,20	1,58	39,60	3,96	0,34
	Column _30x30	0,30	0,30	8,60	0,77	19,35	1,93	0,17
	Membrane_12		0,12	13,20	9,90	247,50	24,7	2,13
	<b>Pier 17 sub-tot</b>				<b>14,04</b>	<b>351,00</b>	<b>35,1</b>	<b>3,02</b>
<b>SA-side abutment</b>	Column _45x30	0,45	0,30	9,80	1,32	33,08	3,30	0,28
	Column _40x30	0,40	0,30	9,80	1,18	29,40	2,94	0,25
	Column _30x30	0,30	0,30	5,20	0,47	11,70	1,17	0,10
	Membrane_12		0,12	9,80	4,80	120,00	12	1,03
	<b>Pier 18 sub-tot</b>				<b>7,77</b>	<b>194,18</b>	<b>19,4</b>	<b>1,67</b>

Adding all aliquots, an overall dead load of 4520 tonnes has been estimated: considering all difficulties in finding bridge original drawings, previous evaluations are only based on 3D scanner survey results of current state. Comparing all the percentage, the heaviest portion is the central arch (Tab. 7.4).

Summary of Olivieri Bridge Dead Loads					
	P (t)	L (m)	[FL <sup>-2</sup> ]	[FL <sup>-1</sup> ]	% Tot(D)
<b>Arch</b>	986,44	137,10	0,42	7,20	<b>21,82</b>
<b>Deck</b>	2371,80	137,10	1,00	17,30	<b>52,47</b>
<b>Cross walls</b>	1161,80	137,10	0,49	8,47	<b>25,70</b>
<b>TOT</b>	<b>4520,04</b>	<b>137,10</b>	<b>1,91</b>	<b>32,97</b>	

**Tab. 7.4** Viadotto Olivieri. Dead loads summary

**Fig. 7.9** Viadotto Olivieri. Deck joints, upper view



Bridge deck is articulated in three portions, connected by a 6cm-deep joint: this configuration guarantees the central arch to behave as a typical Maillart-arch-type bridge, having a slender deformable concrete vault, connected to the upper stuffer deck through a series of thin concrete cross walls. The advantage taken from this structure consists in reducing the arch thickness so that it has a minimum rigidity to bending and, therefore, support axial stress almost exclusively; the minimum of this rigidity will be that necessary for the arch not to buckle. Then as the arch tends to bend when loaded say by traffic over one half of the span, the cross walls make the deck bend to the same new shape as the arch. The bending effect is now shared between arch and deck and, as Maillart further reasoned, that effect will load each part in proportion to its stiffness.

### 7.3.2 Superimposed-dead loads

For road deck a flexible paving has been supposed, consisting of a mixture of asphaltic or bituminous material and aggregates placed on a bed of compacted granular material of appropriate quality in layers over the subgrade. The design of flexible pavement is based on the principle that for a load of any magnitude, the intensity of a load diminishes as the load is transmitted downwards from the surface by virtue of spreading over an increasingly larger area, by carrying it deep enough into the ground through successive layers of granular material. Two 7m-wide carriageways are considered, each one made of two lanes. (Fig. 7.5)

**Tab. 7.5** Viadotto Olivieri. Super-Dead loads summary

SUPERIMPOSED-DEAD LOADS (carriageway width:w= 2x 7m)						
	L[m]	w [m]	s (w/2) (m)	[F] _ t	[FL <sup>-1</sup> ]	% Tot
<b>Asphalt surface layer</b>	137,10	14,00	0,04	168,907	12,32	26,9
<b>(2%) slope increment</b>	137,10	-	0,07	36,9484	2,695	5,9
<b>Binder layer</b>	137,10	14,00	0,10	422,268	30,8	67,2
<b>Tot</b>				<b>628,12</b>	<b>45,815</b>	

The following table defines loads for each bridge portion (Fig. 7.6):

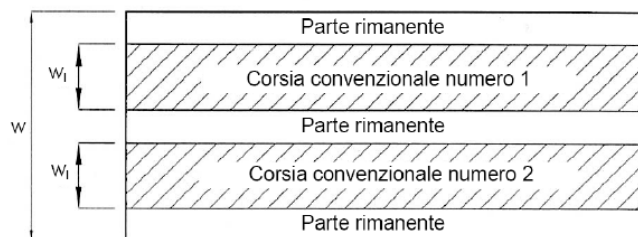


DEAD LOADS & SUPERIMPOSED DEAD LOADS								
	DEAD				SUPER- D.		D+ S.D	
	L (m)	Arch (t)	Deck (t)	Walls (t)	Asph. (t)	Barri er (t)	TOT t)	TOT %)
<b>Section 1 (NA-side)</b>	14,9	0	259,7	261,7	68,24	5,96	595,70	<b>11,4</b>
<b>Section 2 (arch)</b>	76,5	986,4	1333	499,8	350,3	30,6	3200,6	<b>61,3</b>
<b>Section 3 (SA-side)</b>	45,7	0	796,5	400,1	209,3	18,28	1424,3	<b>27,3</b>
<b>TOT</b>	137,1	986,4	2389	1161	627,9	54,84	5220,6	

**Tab. 7.6** Viadotto Olivieri. Summary of vertical loads

### 7.2.2 Live loads: traffic

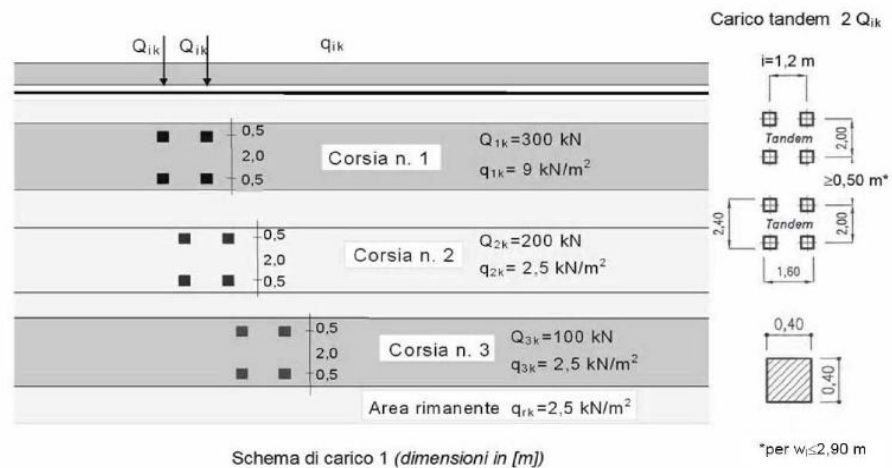
Traffic load is defined in accordance with Italian Building Code (NTC08): preliminarily, conventional lanes have to be individuated. In line with NTC08 (5.1.3.3.2), lane cannot be less wide than 3.00m ( $w > 3\text{m}$ ). Considering deck cross section, made of two staggered planes, carriageways can be seen as separated by a “fixed traffic crash barrier”, so each one is independent from the other, divided into two 3.50m-wide lanes..



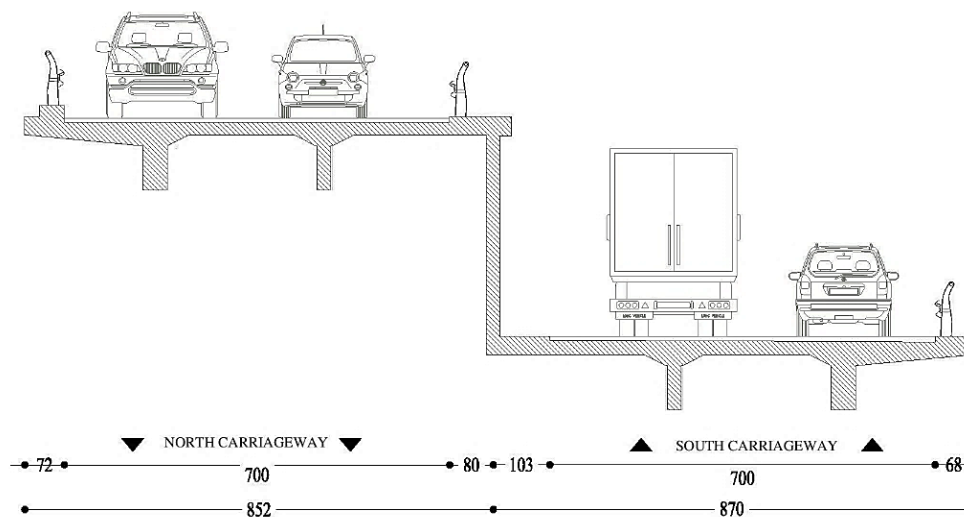
Italian building code (NTC 08): conventional lane scheme

Lanes are placed and numerated in such a way that the worst effect due to live loads can be induced. The loading lane which causes the most unfavourable effect is defined as “Lane 1”, the second one is named “Lane 2”, and so on. For a bridge of “1<sup>st</sup> Category” (i.e. bridge which carries whole traffic load — no reductions are assumed), variable live loads, comprehensive of dynamic effects, consist of concentrated force acting along two tandem axis, upon squared pneumatic tracks (0.40m x 0.40m), and a uniformly distributed load, as follows:

LIVE LOADS (Accidentali da traffico per porzione carrabile: $w = 2 \times 7 \text{ m}$ )							
Lane	L (m)	w (m)	$Q_{ik}$ (t)	$q_{ik}$ (t/m <sup>2</sup> )	F (t)	$FL^{-2}$ (t/m <sup>2</sup> )	$FL^{-1}$ (t/m)
1	171,3	3,5	2 x 30	0,90	599,	1,00	3,500
2	171,3	3,5	2 x 20	0,25	1898	0,32	1,109
3	173,3	3,5	2x 10	0,25	1716	0,282973	0,990
4	171,3	3,5	-	0,25	149	0,25	0,875
TOT	171,3	3,5	-	1,25	749	1,85	5,366



Italian building code (NTC 08): conventional loading scheme of “1<sup>st</sup> Category” bridge



Olivieri Brudge carriageways: traffic load distribution

OVERALL VERTICAL LOADS						
ALIQUOT	P (t)	L (m)	w (m)	[FL <sup>-2</sup> ]	[FL <sup>-1</sup> ]	% Tot
ARCH	1107,1	171,3	14	0,46	26,50	9,07
DECK	2996,2	171,3	14	1,25	9,79	24,54
CROSS WALLS	6572,6	171,3	14	2,74	4,46	53,83
(DEAD) SUB TOTAL	10675,	171,3	14	4,45	2,75	87,43
ASPHALT LAYER	257,20	171,3	14	0,11	1,50	2,11
BINDER	527,60	171,3	14	0,22	3,08	4,32
(SUPER. DEAD) TOT	784,81	171,3	14	0,33	4,58	6,43
DEAD + SUPER.DEAD	11460	171,3	14	4,78	66,90	93,86
LIVE LOADS	749,43	171,3	14	0,3125	4,375	6,14
TOT	12210	171,3	14	5,09	71,28	
L/D	0,065					

Below load estimation, it could be say that live loads are a low percentage of the overall vertical loads (6.14%), having a live-to-dead load ratio **L/D of 0.065 (1/15)**. The choice of parabolic funicular shape for the arch appears really congenial: upon this massive structure the effects of live loads are practically nihil.

### 7.3 FEM modelling: Linear static analysis (Sap 2000)

In order to understand bridge static and dynamic behaviour, particularly defining the effects due to horizontal forces (also valuing the possibility of a seismic retrofit), FEM modelling is required. Make the model matching with the real structure has been no so easy, both for lack of information about this bridge, and for its geometrical and technical complexity: a cloud of points, coming from 3d-scanner relief, has been adopted as guide to modelling the structure. Bridge has been discretized using frame and shell elements: arches and beams, making the “skeleton” of this structure, have been modelled as frame elements, corresponding to their barycentre axis; wall and slab have been defined as shell elements.

Site	Longitude	Latitude	Soil category
Vietri sul Mare (SA)	14.74162	40.67916	B

Nominal life	Usage class	Usage coefficient	Reference period
50years	IV	Cu = 2	100 years

Seismic parameters				
Limit State (NTC 08)	Tr [years]	ag/g	Fo	T*c
Functioning (“Operatività_ SLO)	30	0.038	2.372	0.280
Damage (“Danno”_ SLD)	50	0.048	2.369	0.329
<b>Life Safety</b> <b>(“Salvaguardi vita_ SLV)</b>	<b>475</b>	<b>0.105</b>	<b>2.58</b>	<b>0.439</b>
Collapse preventing (Collasso_ SLC)	975	0.127	2.684	0.459

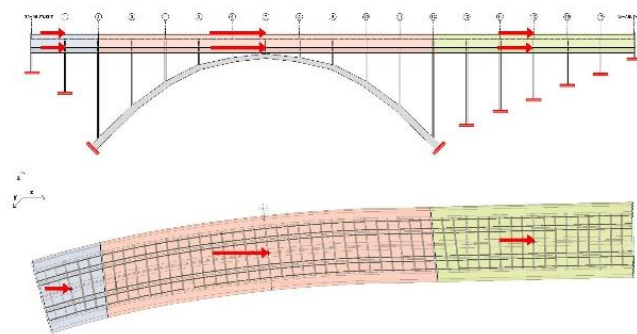
Many options have been considered, changing both constraint conditions at the bottom of the arch and cross walls, and deck characterization. Six different models have been analysed, assuming that a horizontal force ( $F_{OX} = F_{OY} = 10\%P=522t$ ) acts either in longitudinal or in transverse direction. Running a linear static analysis, this indicative value assumed for the horizontal force is useful to understand stress distribution among structural elements, defined as



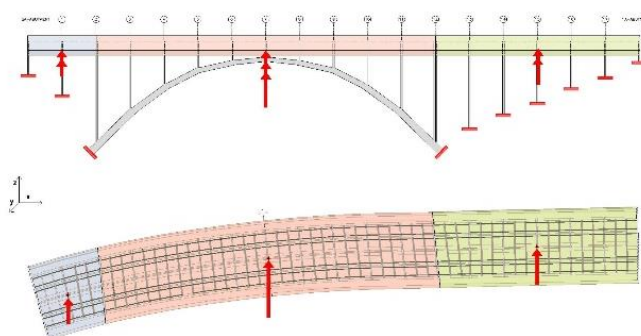
percentage of the overall force applied. After all, the value used, is strictly linked to the seismic parameters which characterize the site (particularly for SLU\_ Ultimate limit state).

Following models have been analysed:

**(1) Three deformable decks model with fixed joints:** it is quiet similar to the real structure, being characterized by three joined portions: access beam-bridge on Napoli-side, central Maillart arch type bridge, access beam bridge on Salerno-side. The overall force has been distributed to each portion, proportionally to its weight, as seen before: NA-side: 11,4%, central arch: 61.3%; SA-side: 27.3%. Considering single portion, the corresponding force has been equally distributed between upper and lower decks, applied at their barycentre. Deck bridge has been modelled as deformable: no diaphragm constraints have been used. Considering that, for each cross walls, as well as for arch springing, 5 ribs attach to foundation plinths, each point that connect structure to foundations has been modelled as ( elastically yielding) fixed joints.

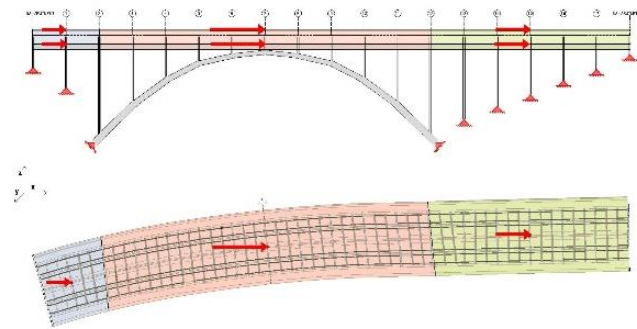


3-deformable decks model with fixed joints: longitudinal horizontal forces

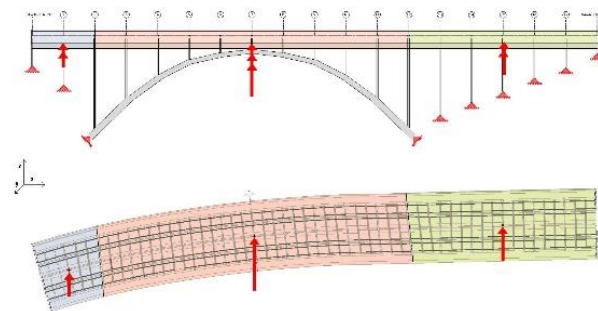


3-deformable decks model with fixed joints: transverse horizontal forces

(2) **Three deformable decks model with hinged joints:** as in the previous case, horizontal force is distributed to each portion, proportionally to its weight: NA-side: 11,4%, central arch: 61.3%; SA-side: 27.3%.. Deck bridge is still modelled as deformable (no diaphragm constraints). In this model, for each cross wall, as for the arch springing section, five points of connection to foundation are modelled as multi-directional hinge: the presence of concrete membrane elements, which make the cross walls stiffer, reduces the possibility for the structure, above all of the arch portion, to rotate out of plane; hinged joints effects is particularly noticeable only along longitudinal direction.



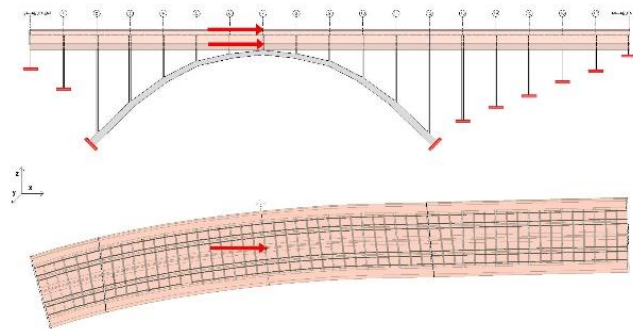
3-deformable decks model with hinged joints: longitudinal horizontal forces



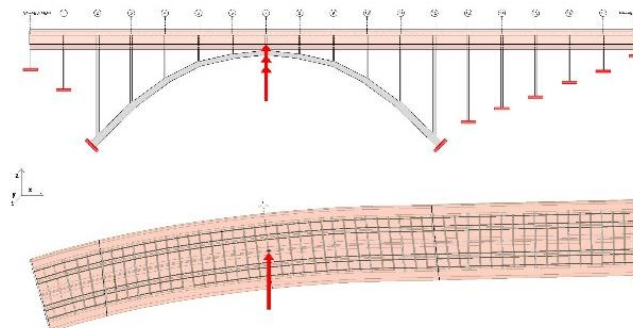
3-deformable decks model with hinged joints: transverse horizontal forces

(3) **Single deformable deck model with fixed joints :** bridge deck is modelled adopting the scheme of kinematic chain, i.e. considering an elastic connection between different portion, both in longitudinal and in transverse direction, so that all deformations occurred along deck are concentrated in a single section, both at the midspan, or at the

abutments. This arrangement reaps the benefits coming from continuous deck system as well as these ones due to simply supported beam one. The deformable continuous deck is modelled without diaphragm constraints. The overall force is applied at the midspan of central arch portion, uniformly divided between two deck levels. Deformable deck is modelled without diaphragm constraints. Connections of the cross walls to foundation plinths are defined as (elastically yielding) fixed joints.



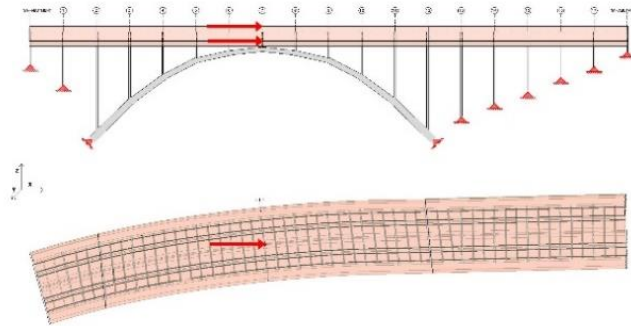
Single deformable deck model with fixed joints: longitudinal horizontal force



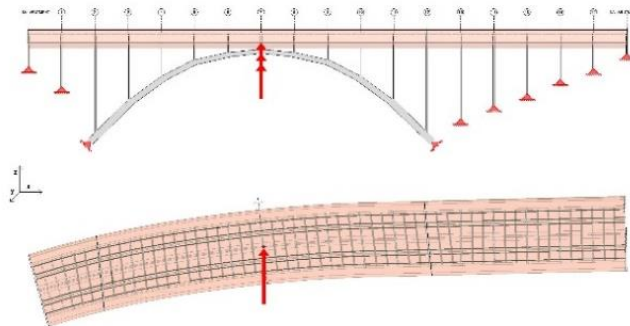
Single deformable deck model with fixed joints: transverse horizontal force

- (4) Single deformable deck with hinged joints:** bridge deck is modelled as continuous, adopting the scheme of kinematic chain. The overall force is applied at the midspan of central arch portion, uniformly divided between two deck levels. The deformable continuous deck is modelled without diaphragm constraints. . Considering that, for each cross walls, as well as for arch springing, 5 ribs attach to foundation plinths, each point that connect structure to

foundations has been modelled as ( elastically yielding) hinged joints.



Single deformable deck model with hinged joints: longitudinal horizontal force



Single deformable deck model with hinged joints: transverse horizontal force

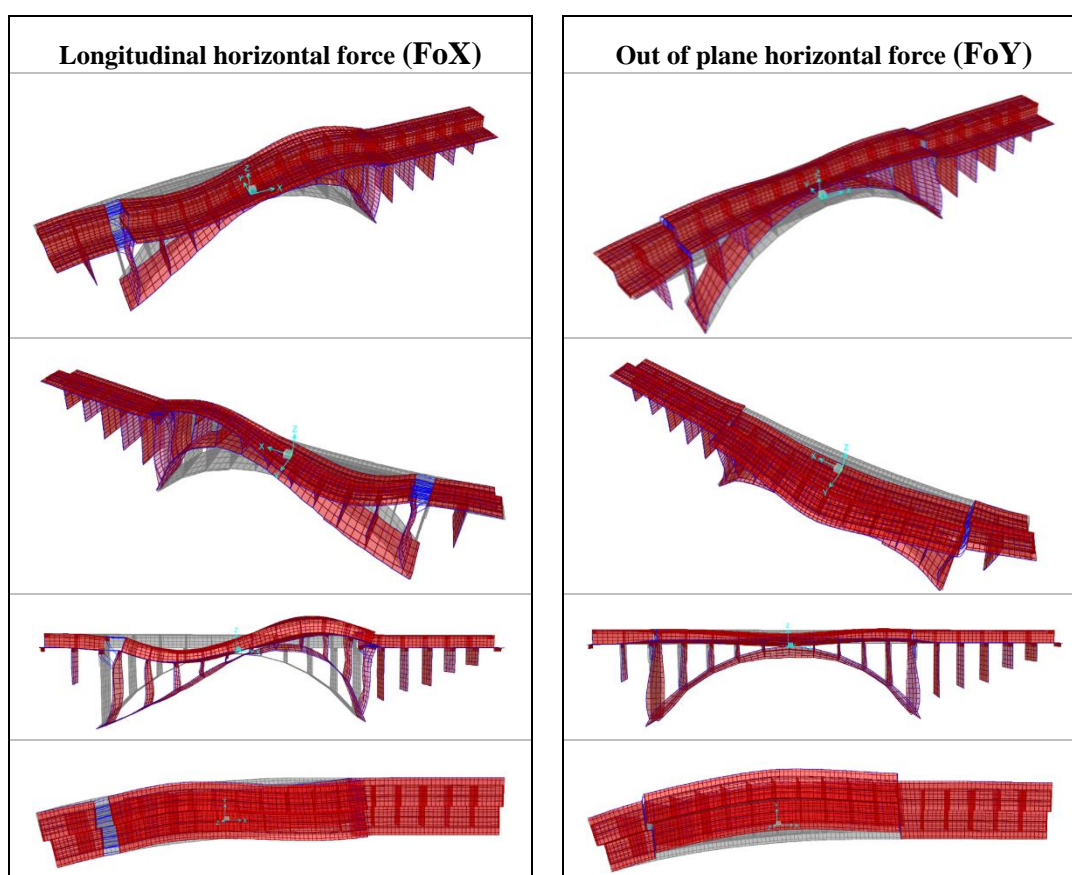
- (5) **Single undeformable deck with fixed joints:** bridge deck is modelled adopting the scheme of kinematic chain, assuming that, for each staggered plane, the whole carriageway moves rigidly. Considering a continuous deck for each level, it's modelled using diaphragm constraints. The overall force is applied at the midspan of central arch portion, uniformly divided between two deck levels. Connections of the cross walls to foundation plinths are defined as (elastically yielding) fixed joints. [For same static scheme, the effect due to a more realistic load distribution has been valued: for each of  $n$ -nodal point along bridge deck, a force equal to  $(F_{tot}/n)$  has been assigned].
- (6) **Single undeformable deck with fixed joints:** as the previous case, undeformable deck is modelled using diaphragm constraints, as in the kinematic chain scheme, assuming that each staggered deck moves



rigidly. The overall force is applied at the midspan of central arch portion, uniformly divided between two deck levels. Connections of the cross walls to foundation plinths are defined as (elastically yielding) hinged joints.

Looking at the deformed shape caused by acting longitudinal forces, the most vulnerable structural elements can be identified.

### 7.3.1 Three deformable decks model with fixed joints



Rotational equilibrium: 3-deformable decks model with fixed joints										
	Ty %	Ty (t)	Mxx (tm)	Mxx %	Mxx (Ty) (tm)	Mxx (Ty) %	M (ΔN) (t m)	M (ΔN) %	M tot (t m)	M Tot %
NA-abut.	2.09	10.91	19.52	7.1	187.4	5.9	-80.9	-0.88	125.9	0.99
Pier 1	10.18	53.13	7.20	2.6	668.5	21.0	635.1	6.89	1310.	10.33
Arch	58.1	303.2	123.1	44.5	470.0	14.7	7337	79.5	7930	62.51
Piers 13-17	28.35	147.9	118.1	42.7	1688	52.9	1408	15.2	3215	25.35
SA-abut.	1.67	8.717	8.73	3.2	175.9	5.5	-81.4	-0.88	103.1	0.81
Σ			276.6		3190		9218		12686	

3-Deformable decks model with fixed joints: joint reactions due to (FoX=0,10P = 522t)										
	Sect.	Column	Fx (t)	Fy (t)	N (t)	Mxx (tm)	Myy (tm)	Mzz (tm)	Fx%	N%
Portion 1 (NA)	NA-abutment	1	-3.13	-9.35	-2.40	0.401	-1.10	-0.55	0.600	0.03
		2	-4.08	-4.53	0.168	0.456	-1.93	0.18	0.782	0.20
		3	-51.7	-1.18	-12.2	46.73	-159	1.06	9.92	0.46
		4	-0.45	1.725	-1.06	-0.05	0.122	0.02	0.087	2.35
		5	-0.08	3.273	-0.48	-0.09	0.105	-0.04	0.016	0.09
	TOT								11.41	
	Pier 1	1	0.001	0.296	-3.66	-0.06	-0.00	0.008	0.002	0.70
		2	0.004	0.642	2.406	-0.13	-0.00	0.004	0.007	0.46
		3	0.000	2.124	9.914	-0.28	-0.01	0.002	0.000	1.90
		4	-0.01	3.513	12.78	-0.44	-0.01	0.001	0.002	2.45
		5	0.003	2.600	13.25	-0.28	-0.53	0.190	0.001	2.54
	TOT								0.002	
Portion 2 (arch)	Pier 2-arch	1	-30.9	-2.04	-19.1	-3.60	-0.40	3.579	5.930	3.68
		2	-25.5	0.307	-18.4	-1.74	-0.19	1.464	4.900	3.54
		3	-34.6	1.852	-25.4	-3.47	-0.54	2.873	6.638	4.88
		4	-33.4	-2.75	-27.5	-1.58	-0.18	1.304	6.398	5.28
		5	-34.1	-2.31	-27.1	-2.60	-0.32	2.063	6.547	5.20
	TOT								30.416	
	Pier 12-arch	1	11.47	-1.93	-28.5	1.387	-0.19	1.959	2.198	5.47
		2	-15.1	6.652	6.480	0.631	-0.06	0.812	2.880	1.24
		3	-36.3	6.867	27.94	0.895	-0.09	1.315	6.966	5.35
		4	-39.7	9.885	46.54	0.394	-0.04	0.583	7.618	8.92
		5	-55.9	10.46	65.91	0.018	-0.01	0.50	10.72	12.63
	TOT								30.385	
Portion 3 (SA)	Pier 13	1	0.007	0.616	-7.19	-0.03	0.001	0.004	0.001	1.38
		2	0.004	0.506	-7.68	-0.08	0.003	-0.02	0.001	1.47
		3	0.003	0.024	-7.37	-0.02	0.001	-0.03	0.001	1.41
		4	0.001	-0.34	-5.61	0.006	0.000	-0.02	0.001	1.08
		5	0.008	-0.38	-3.92	0.015	-0.01	-0.05	0.001	0.75
	TOT								0.003	
	Pier 14	1	-0.02	-0.19	1.956	0.013	0.000	-0.01	0.005	0.37
		2	-0.01	-0.20	1.787	0.009	0.01	-0.06	0.03	0.34
		3	-0.02	-0.13	1.278	0.007	-0.20	-0.01	0.001	0.24
		4	-0.02	-0.09	0.593	0.006	0.001	-0.04	0.005	0.11

		Column	Fx (t)	Fy (t)	N (t)	Mxx (tm)	Myy (tm)	Mzz (tm)	Fx%	N%
		5	-0.04	-0.09	-0.05	0.02	0.001	-0.02	0.002	0.00
		<b>TOT</b>							<b>0.003</b>	
	<b>Pier 15</b>	1	-0.02	-0.07	1.837	0.012	0.001	-0.01	0.001	0.35
		2	-0.02	0.043	1.44	0.003	0.001	-0.02	0.002	0.28
		3	-0.03	0.005	0.522	0.09	0.002	0.001	0.001	0.10
		4	0.001	-0.09	-0.13	0.020	0.000	0.003	0.001	0.02
		5	-0.02	-0.08	-0.48	0.013	-0.03	0.002	0.001	0.09
		<b>TOT</b>							<b>0.002</b>	
	<b>Pier 17</b>	1	-0.02	0.486	1.743	-0.01	0.001	0.001	0.002	0.33
		2	0.002	1.109	0.915	-0.05	0.02	0.002	0.002	0.18
		3	-0.03	0.699	-0.92	-0.04	0.002	0.010	0.004	0.18
		4	-0.0	0.102	-0.11	-0.40	0.002	0.002	0.001	0.02
		5	-0.02	0.012	1.325	-0.68	0.002	0.00	0.001	0.25
		<b>TOT</b>							<b>0.004</b>	
	<b>Pier 18</b>	1	-0.02	1.197	0.557	-0.03	0.002	0.002	0.002	0.11
		2	0.004	2.51	-1.51	-0.18	0.004	0.002	0.009	0.29
		3	-0.05	2.014	-4.33	-0.08	0.002	-0.52	0.001	0.83
		4	-0.01	1.302	-0.81	-0.07	0.002	-0.01	0.002	0.16
		5	-0.02	0.684	3.397	-0.05	0.005	-0.02	0.00	0.65
		<b>TOT</b>							<b>0.008</b>	
	<b>SA-abutment</b>	1	-2.01	2.954	-1.98	0.05	-0.72	-0.34	0.383	0.37
		2	-3.69	7.304	-1.61	-0.07	-1.51	0.074	0.707	0.31
		3	-135	-14.7	9.24	-2.68	-348	-1.33	25.89	1.77
		4	-3.04	-2.71	-1.48	0.009	-1.18	-0.04	0.583	0.28
		5	-1.73	-0.84	-0.73	-0.03	-0.62	0.30	0.333	0.14
		<b>TOT</b>							<b>27.90</b>	

3-Deformable decks model with fixed joints: joint reaction due (FoY=0,10P = 522t)										
	section	Column	Fx (t)	Fy (t)	N (t)	Mxx (tm)	Myy (tm)	Mzz (tm)	Fx%	N%
<b>Portion 1 (NA)</b>	<b>NA-abutment</b>	1	6.310	-0.76	-6.57	-0.51	2.062	0.916	0.14	1.3
		2	7.440	-1.77	-1.95	-0.57	2.699	-0.41	0.34	0.4
		3	-16.1	-5.91	0.621	19.60	-27.6	-4.44	1.13	0.1
		4	-5.04	-1.36	2.957	0.464	-2.06	-0.28	0.25	0.6
		5	-4.12	-1.19	5.698	0.439	-1.47	0.660	0.22	1.1
		<b>TOT</b>							<b>2.08</b>	



	section	Column	Fx (t)	Fy (t)	N (t)	Mxx (tm)	Myy (tm)	Mzz (tm)	Fx%	N%
	Pier 1	1	0.021	-8.08	42.64	0.978	0.001	-0.02	1.55	8.2
		2	0.025	-12.3	24.37	1.662	0.003	-0.01	2.37	4.7
		3	0.02	-13.4	-1.72	1.73	0.003	-0.02	2.57	0.3
		4	0.019	-13.5	-26.3	1.797	0.003	-0.01	2.60	5.0
		5	-0.01	-8.71	-43.5	1.048	0.002	-0.03	1.68	8.3
		TOT								10.77
Portion 2 (arch)	Pier 2-arch	1	247.1	28.15	280.5	0.000	0.000	0.000	5.39	53.7
		2	70.35	-29.1	81.01	0.000	0.000	0.000	5.59	15.5
		3	-19.5	-34.8	-23.5	0.000	0.000	0.000	6.68	4.5
		4	-98.2	-30.1	-114	0.000	0.000	0.000	5.77	21.9
		5	-181	-28.3	-225	0.000	0.000	0.000	5.44	43.1
		TOT								28.87
	Pier 12-arch	1	-251	27.22	278.6	0.000	0.000	0.000	5.22	53.4
		2	-75.7	-27.9	82.26	0.000	0.000	0.000	5.36	15.8
		3	10.99	-39.4	-16.7	0.000	0.000	0.000	7.55	3.2
		4	91.36	-32.1	-108	0.000	0.000	0.000	6.17	20.7
		5	178.6	-28.1	-219	0.000	0.000	0.000	5.39	42.1
		TOT								29.68
Portion 3 (SA)	Pier 13	1	-0.02	-3.32	26.71	0.143	-0.05	0.003	0.64	5.1
		2	-0.02	-4.74	13.50	0.117	-0.05	0.002	0.91	2.6
		3	-0.05	-4.58	-4.16	0.140	-0.05	0.005	0.88	0.8
		4	-0.02	-5.46	-20.9	0.133	-0.05	0.003	1.05	4.0
		5	-0.03	-3.99	-32.8	0.171	-0.06	0.004	0.77	6.3
		TOT								4.24
	Pier 14	1	-0.02	-5.04	32.38	0.297	-0.08	0.003	0.97	6.2
		2	-0.02	-7.79	18.32	0.370	-0.01	0.09	1.49	3.5
		3	-0.02	-7.88	0.520	0.38	-0.01	0.003	1.51	0.1
		4	-0.02	-8.30	-16.7	0.395	-0.01	0.002	1.59	3.2
		5	-0.02	-5.2	-30.7	0.32	-0.08	0.044	1.00	5.9
		TOT								6.57
	Pier 15	1	-0.06	-5.98	35.51	0.761	-0.03	0.008	1.15	6.8
		2	-0.02	-8.9	20.60	1.301	-0.02	0.036	1.71	3.9
		3	-0.02	-9.33	2.008	1.319	-0.03	0.08	1.79	0.4
		4	-0.02	-9.29	-16.2	1.34	-0.03	0.004	1.78	3.1
		5	-0.01	-5.93	-31.5	0.759	-0.01	0.09	1.14	6.0
		TOT								7.56

	section	Column	Fx (t)	Fy (t)	N (t)	Mxx (tm)	Myy (tm)	Mzz (tm)	Fx%	N%
	Pier 17	1	-0.17	-4.95	25.26	0.314	-0.09	-0.06	0.95	4.8
		2	-0.02	-8.46	12.99	0.460	-0.01	0.004	1.62	2.5
		3	-0.01	-9.73	-1.75	0.510	-0.01	0.009	1.86	0.3
		4	-0.03	-10.2	-12.6	0.545	-0.07	0.005	1.97	2.4
		5	-0.12	-5.85	-22.3	0.341	-0.01	0.011	1.13	4.4
		TOT							7.53	
	Pier 18	1	-0.01	-2.51	12.64	0.146	-0.04	0.01	0.48	2.4
		2	-0.01	-4.57	4.308	0.220	-0.06	0.053	0.88	0.8
		3	-0.06	-6.06	-4.17	0.290	-0.08	0.08	1.16	0.8
		4	-0.01	-6.69	-6.07	0.32	-0.00	0.005	1.28	1.2
		5	0.041	-3.54	-10.1	0.17	-0.05	0.01	0.68	1.9
		TOT							4.48	
	SA-abutment	1	-1.55	0.42	-2.69	0.001	-0.55	-0.24	0.08	0.5
		2	-1.84	0.94	0.370	-0.01	-0.74	0.12	0.18	0.1
		3	2.566	4.07	-2.63	-3.96	-5.07	0.80	0.78	0.1
		4	0.970	2.06	-0.51	-0.01	0.377	0.046	0.39	0.5
		5	0.840	1.29	1.150	0.034	0.296	-0.13	0.25	0.2
		TOT							1.68	

In the case of longitudinal horizontal force ( $F_{oX} = 0.10P$ ), it could be said that:

- arch portion records the worst deformative effect, while thin arch follows deck deformed shape.
- shear forces due to acting loads are carried by external abutments (38%) and by the central arch (60%), while intermediate cross walls are quite unloaded.

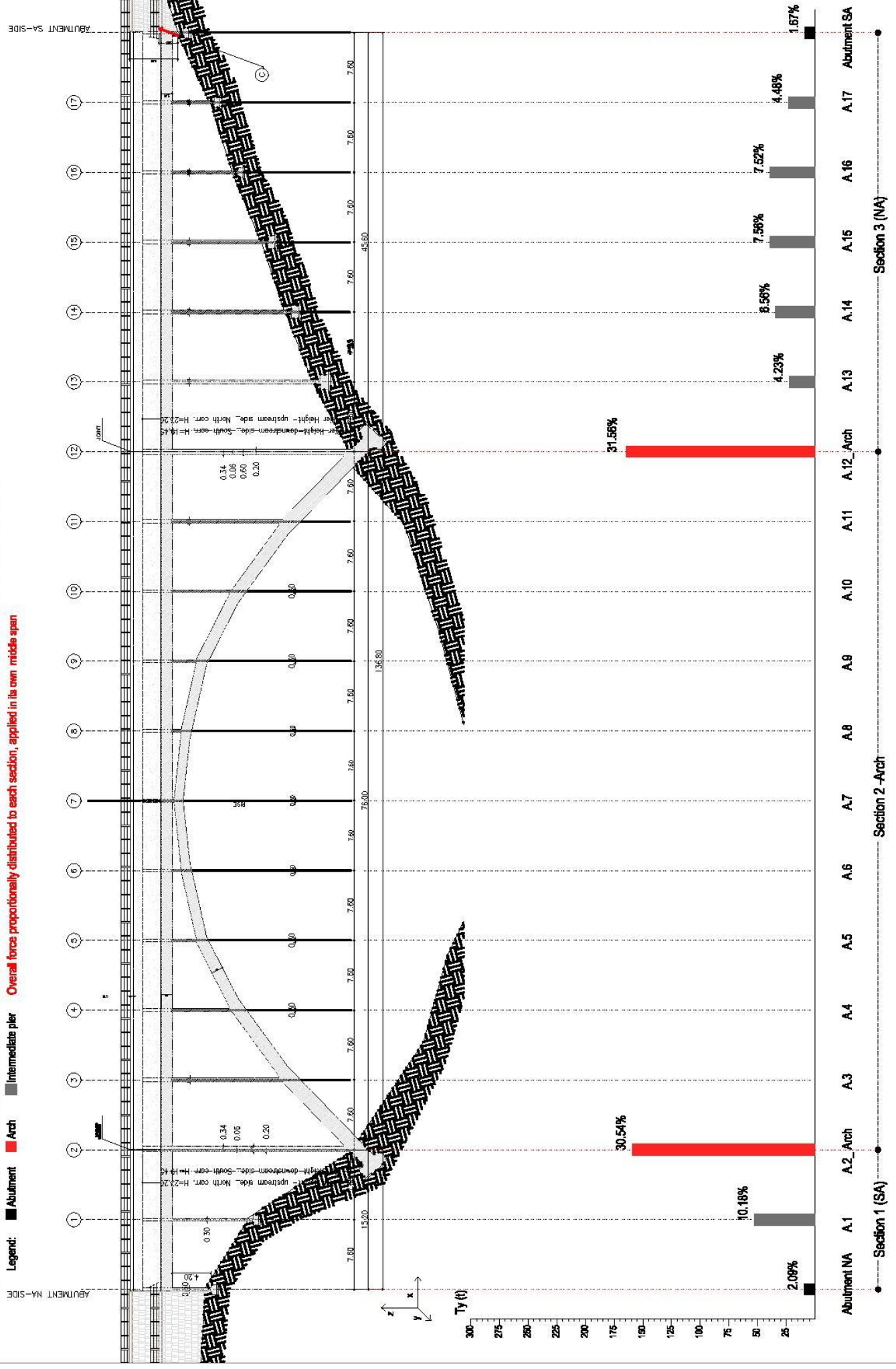
In the case of transversal horizontal force ( $F_{oY} = 0.10P$ ), it could be said that:

- about 60% of shearing force is carried by external arch-cross walls, while deck abutments are the lowest excited sections;
- about 50% of global moment is borne by external arch-cross walls;
- intermediate walls have a quiet uniform distribution of shear (7%);
- the greatest contribution to global moment is due to  $M(\Delta N)$ ;
- Effects due to horizontal out of plane forces (as seismic ones) are not negligible, above all for the central arch.

# Cross walls Shear (Ty) distribution, due to Horizontal forces acting out of plane ( $F_{oy} = 0.10P$ ) - Three-deformable-decks model with fixed joints

Longitudinal section (1:500)

Legend: ■ Abutment ■ Arch ■ Intermediate pier Overall force proportionally distributed to each section, applied in its own middle span



## Longitudinal section (1:500)

DE



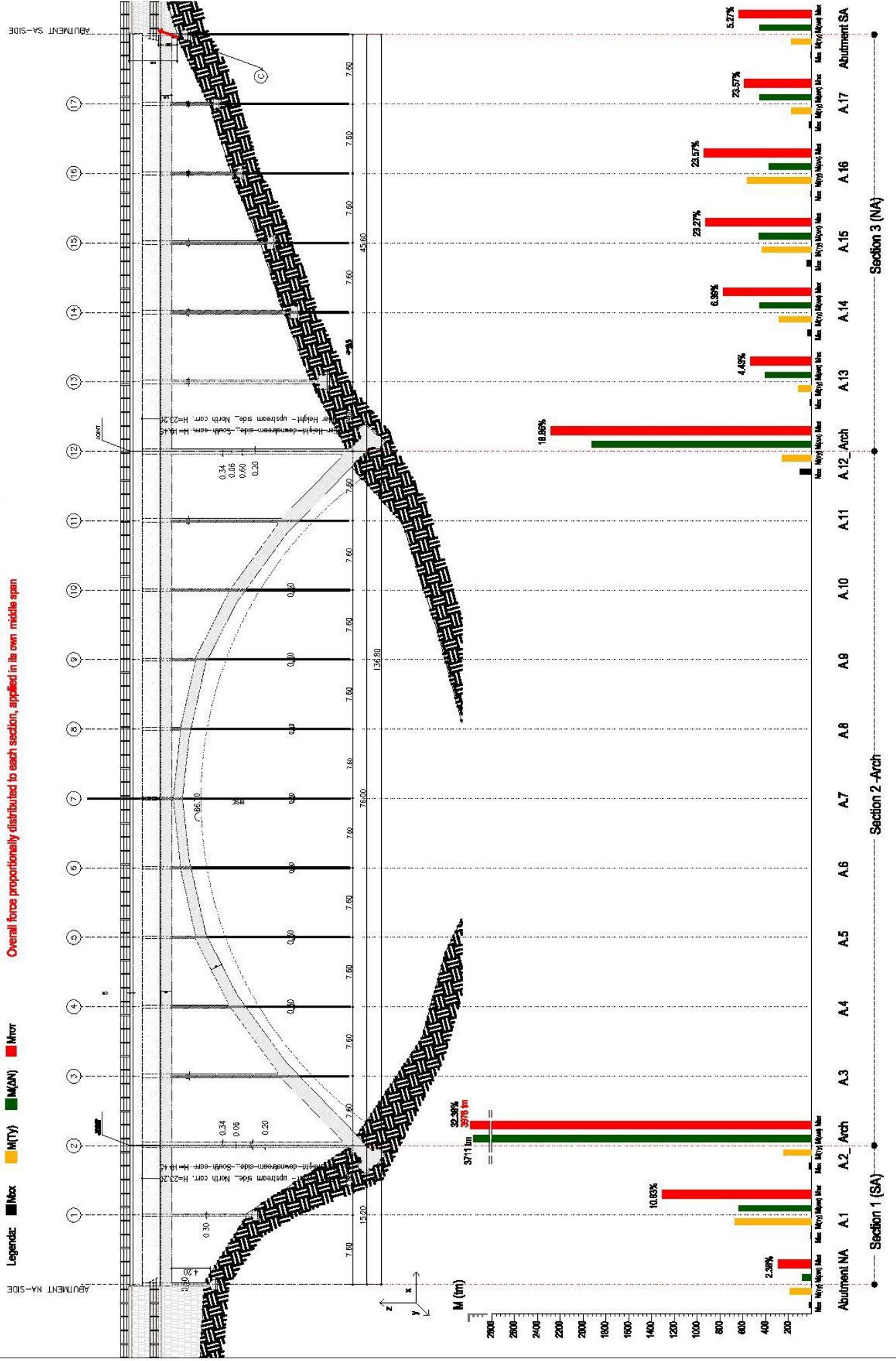


Cross walls Moments (M) distribution, due to Horizontal forces (Foy= 0.10P) acting out of plane - Three-deformable -decks model with fixed joints

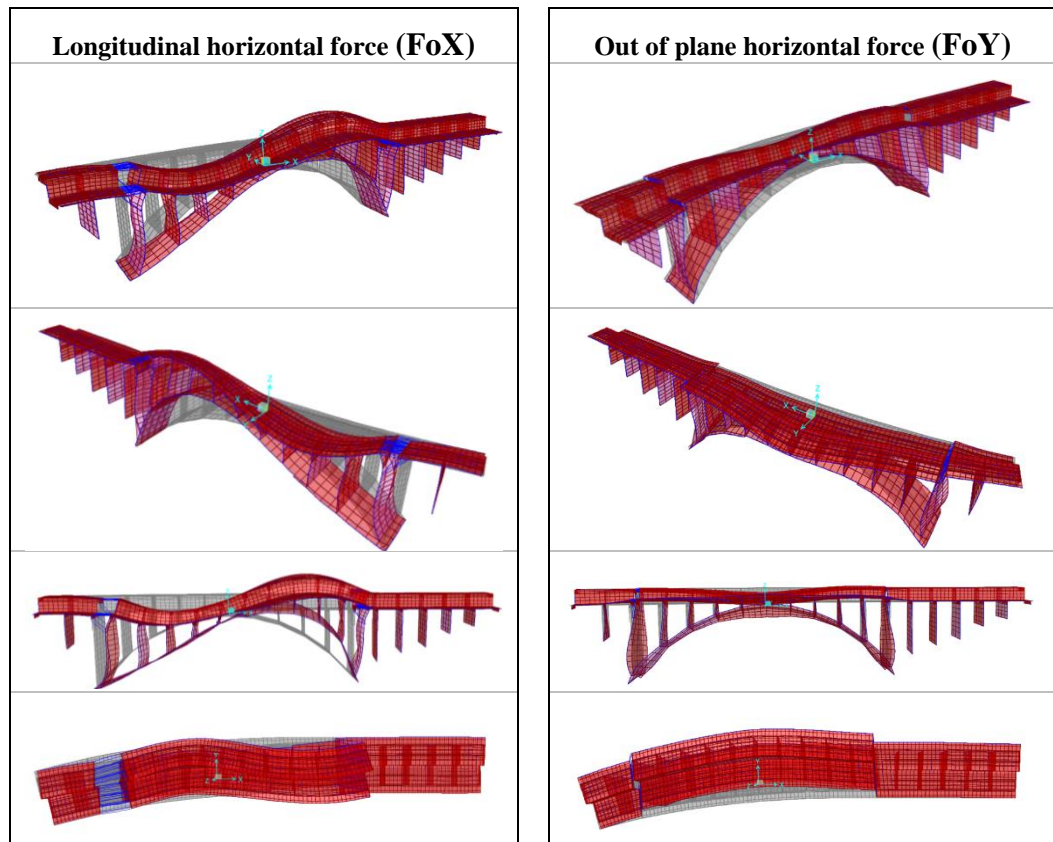
Longitudinal section (1:500)

Overall force proportionally distributed to each section, applied in its own middle span

Legend: ■ Max ■ M(Ty) ■ M(N) ■ M(Tx)



### 7.3.2 Three deformable decks model with hinged joints



3-Deformable decks model: joint reaction due (+FoX=0,10P = 522t)										
	section	Column	Fx (t)	Fy (t)	N (t)	Mxx (tm)	Myy (tm)	Mzz (tm)	Fx%	N%
Portion 1 (NA)	NA-abutment	1	-3.145	-9.373	-2.42	0.402	-1.104	-0.55	0.602	0.03
		2	-4.095	-4.534	0.168	0.457	-1.635	0.18	0.784	0.21
		3	-51.7	-1.184	-12.3	46.805	-159.42	1.07	9.917	0.46
		4	-0.453	1.730	-1.07	-0.059	0.125	0.25	0.086	2.36
		5	-1.803	3.283	-0.45	-0.096	0.107	-0.04	0.345	0.09
		TOT							11.74	
	Pier 1	1	0.001	0.294	-3.65	-0.067	-0.0001	0.0080	0.002	0.70
		2	0.004	0.648	2.439	-0.136	-0.0003	0.0044	0.001	0.47
		3	0.003	2.130	9.970	-0.288	-0.0005	0.0025	0.001	1.91
		4	-0.001	3.524	12.85	-0.441	-0.0008	0.0011	0.002	2.46
		5	0.003	2.609	13.31	-0.287	-0.0005	0.0019	0.006	2.55
		TOT							0.001	

	section	Column	Fx (t)	Fy (t)	N (t)	Mxx (tm)	Myy (tm)	Mzz (tm)	Fx%	N%
Portion 2 (arch)	Pier 2-arch	1	-31.72	-3.89	-20.1	0.0000	0.0000	0.0000	6.077	3.84
		2	-25.68	2.633	-18.6	0.0000	0.0000	0.0000	4.919	3.57
		3	-34.50	0.582	-25.4	0.0000	0.0000	0.0000	6.610	4.88
		4	-33.56	-0.659	-27.6	0.0000	0.0000	0.0000	6.430	5.29
		5	-33.3	-3.69	-26.2	0.0000	0.0000	0.0000	6.379	5.02
		TOT							30.41	
	Pier 12-arch	1	31.26	-1.067	-28.3	0.000	0.000	0.00	5.988	5.43
		2	-31.1	5.984	6.464	0.000	0.0000	0.0000	5.94	1.24
		3	-35.3	7.100	27.98	0.000	0.0000	0.0000	6.777	5.36
		4	-30.7	9.586	46.56	0.000	0.0000	0.0000	5.899	8.92
		5	-35.7	10.38	65.74	0.000	0.0000	0.0000	6.856	12.59
		TOT							31.46	
Portion 3 (SA)	Pier 13	1	0.007	0.61	-7.21	-0.032	0.0001	-0.048	0.004	1.38
		2	0.004	0.508	-7.70	-0.887	0.0000	-0.003	0.001	1.48
		3	0.002	0.024	-7.39	-0.008	0.000	-0.036	0.006	1.42
		4	0.001	-0.347	-5.67	0.0065	-0.0003	-0.021	0.002	1.08
		5	0.001	-0.38	-3.94	0.0158	-0.0001	-0.051	0.001	0.76
		TOT								0.003
	Pier 14	1	-0.002	-0.19	1.96	0.0131	0.0000	-0.019	0.005	0.38
		2	-0.00	-0.20	1.79	0.0092	0.0000	-0.006	0.02	0.34
		3	-0.01	-0.13	1.281	0.0073	-0.0021	-0.05	0.004	0.25
		4	-0.01	-0.099	0.595	0.0061	0.0000	-0.004	0.000	0.11
		5	-0.004	-0.04	-0.02	0.0027	0.0000	-0.006	0.008	0.00
		TOT								0.003
	Pier 15	1	-0.001	-0.079	1.842	0.0121	0.0000	-0.014	0.003	0.35
		2	0.001	0.042	1.451	0.0033	0.0000	-0.004	0.000	0.28
		3	-0.003	0.004	0.522	0.0082	0.0000	0.0010	0.000	0.10
		4	0.001	-0.098	-0.16	0.0203	0.0000	0.0007	0.002	0.02
		5	-0.036	-0.091	-0.48	0.0133	0.0000	0.0021	0.007	0.09
		TOT								0.002
	Pier 17	1	-0.007	4.864	1.745	-0.012	0.0000	0.0001	0.001	0.33
		2	0.002	1.109	0.916	-0.054	0.0002	0.0001	0.004	0.18
		3	-0.003	0.698	-9.17	-0.032	0.001	0.009	0.001	1.76
		4	-0.005	0.101	-0.01	-0.004	0.0000	0.0007	0.001	0.00
		5	-0.007	0.011	1.323	-0.067	0.0000	0.015	0.014	0.25

		<b>TOT</b>							<b>0.004</b>	
	<b>section</b>	<b>Column</b>	<b>Fx (t)</b>	<b>Fy (t)</b>	<b>N (t)</b>	<b>Mxx (tm)</b>	<b>Myy (tm)</b>	<b>Mzz (tm)</b>	<b>Fx%</b>	<b>N%</b>
	<b>Pier 18</b>	<b>1</b>	-0.009	1.194	0.556	-0.034	0.0001	0.0023	0.002	0.11
		<b>2</b>	0.004	2.517	-1.51	-0.107	0.0003	0.0014	0.009	0.29
		<b>3</b>	-0.005	2.014	-4.38	-0.084	0.0003	-0.005	0.001	0.83
		<b>4</b>	-0.009	1.301	-0.81	-0.078	0.0002	-0.011	0.002	0.16
		<b>5</b>	-0.013	0.684	3.395	-0.048	0.001	-0.014	0.001	0.65
		<b>TOT</b>							<b>0.008</b>	
	<b>SA-abutment</b>	<b>1</b>	-2.001	2.955	-1.99	0.020	-0.7241	-0.348	0.383	0.37
		<b>2</b>	-3.691	7.306	-1.61	-0.077	-1.515	0.0747	0.707	0.31
		<b>3</b>	134.1	-14.7	9.248	-2.692	-348.10	-1.335	25.70	1.77
		<b>4</b>	-3.046	-2.713	-1.48	0.009	-1.1862	-0.045	0.583	0.28
		<b>5</b>	-1.739	-0.844	-0.73	-0.032	-0.6215	0.303	0.333	0.14
		<b>TOT</b>							<b>27.71</b>	

3-Deformable decks model: joint reaction due to transverse horizontal force (FoY=0,10P = 522t)										
	<b>section</b>	<b>Column</b>	<b>Fx (t)</b>	<b>Fy (t)</b>	<b>N (t)</b>	<b>Mxx (tm)</b>	<b>Myy (tm)</b>	<b>Mzz (tm)</b>	<b>Fx%</b>	<b>N%</b>
<b>Portion 1 (NA)</b>	<b>NA-abutment</b>	<b>1</b>	6.310	-0.706	-6.579	-0.512	2.062	0.916	0.14	1.3
		<b>2</b>	7.440	-1.774	-1.957	-0.574	2.699	-0.416	0.34	0.4
		<b>3</b>	-16.05	-5.917	0.621	19.60	-27.67	-4.448	1.13	0.1
		<b>4</b>	-5.045	-1.306	2.957	0.464	-2.046	-0.258	0.25	0.6
		<b>5</b>	-4.127	-1.159	5.698	0.439	-1.471	0.660	0.22	1.1
		<b>TOT</b>							<b>2.08</b>	
	<b>Pier 1</b>	<b>1</b>	0.021	-8.087	42.64	0.978	0.001	-0.026	1.55	8.2
		<b>2</b>	0.025	-12.36	24.37	1.662	0.003	-0.013	2.37	4.7
		<b>3</b>	0.023	-13.40	-1.727	1.730	0.003	-0.021	2.57	0.3
		<b>4</b>	0.019	-13.59	-26.33	1.797	0.003	-0.013	2.60	5.0
		<b>5</b>	-0.001	-8.791	-43.51	1.048	0.001	-0.025	1.68	8.3
		<b>TOT</b>							<b>10.77</b>	

<b>Portion 2 (arch)</b>	<b>Pier 2-arch</b>	<b>1</b>	247.1	28.15	280.5	0.000	0.000	0.000	5.39	53.7
		<b>2</b>	70.35	-29.18	81.01	0.000	0.000	0.000	5.59	15.5
		<b>3</b>	-19.52	-34.87	-23.54	0.000	0.000	0.000	6.68	4.5
		<b>4</b>	-98.20	-30.14	-114.5	0.000	0.000	0.000	5.77	21.9



		Colu mn	Fx (t)	Fy (t)	N (t)	Mxx (tm)	Myy (tm)	Mzz (tm)	Fx%	N%
		5	-181.9	-28.38	-225.0	0.000	0.000	0.000	5.44	43.1
		TOT								28.87
Pier 12- arch	1	-251.2	27.22	278.6	0.000	0.000	0.000	5.22	53.4	
	2	-75.07	-27.99	82.26	0.000	0.000	0.000	5.36	15.8	
	3	10.99	-39.41	-16.79	0.000	0.000	0.000	7.55	3.2	
	4	91.36	-32.18	-108.1	0.000	0.000	0.000	6.17	20.7	
	5	178.6	-28.12	-219.8	0.000	0.000	0.000	5.39	42.1	
	TOT								29.68	
Portion 3 (SA)	Pier 13	1	-0.015	-3.321	26.71	0.143	-0.000	0.003	0.64	5.1
		2	-0.019	-4.746	13.50	0.117	-0.000	0.002	0.91	2.6
		3	-0.015	-4.586	-4.168	0.140	-0.005	0.004	0.88	0.8
		4	-0.016	-5.461	-20.94	0.133	-0.051	0.003	1.05	4.0
		5	-0.002	-3.999	-32.82	0.171	-0.066	0.038	0.77	6.3
		TOT								4.24
	Pier 14	1	-0.014	-5.043	32.38	0.297	-0.083	0.003	0.97	6.2
		2	-0.022	-7.796	18.32	0.370	-0.001	0.001	1.49	3.5
		3	-0.021	-7.889	0.520	0.381	-0.001	0.002	1.51	0.1
		4	-0.023	-8.303	-16.76	0.395	-0.001	0.001	1.59	3.2
		5	-0.015	-5.240	-30.78	0.300	-0.085	0.003	1.00	5.9
		TOT								6.57
	Pier 15	1	-0.015	-5.983	35.51	0.761	-0.001	0.008	1.15	6.8
		2	-0.021	-8.920	20.60	1.301	-0.002	0.003	1.71	3.9
		3	-0.021	-9.333	2.008	1.319	-0.003	0.008	1.79	0.4
		4	-0.020	-9.299	-16.28	1.345	-0.003	0.004	1.78	3.1
		5	-0.010	-5.936	-31.54	0.759	-0.001	0.009	1.14	6.0
		TOT								7.56
	Pier 17	1	-0.017	-4.955	25.26	0.314	-0.000	-0.009	0.95	4.8
		2	-0.027	-8.463	12.99	0.460	-0.001	0.004	1.62	2.5
		3	-0.031	-9.733	-1.705	0.510	-0.001	0.009	1.86	0.3
		4	-0.030	-10.27	-12.63	0.545	-0.001	0.005	1.97	2.4
		5	-0.012	-5.875	-22.83	0.341	-0.001	0.011	1.13	4.4
		TOT								7.53

	section	Column	Fx (t)	Fy (t)	N (t)	Mxx (tm)	Myy (tm)	Mzz (tm)	Fx%	N%
	<b>Pier 18</b>	<b>1</b>	-0.011	-2.516	12.64	0.146	-0.004	0.010	0.48	2.4
		<b>2</b>	-0.014	-4.577	4.308	0.220	-0.064	0.005	0.88	0.8
		<b>3</b>	-0.063	-6.062	-4.174	0.290	-0.000	0.008	1.16	0.8
		<b>4</b>	-0.014	-6.692	-6.070	0.326	-0.000	0.005	1.28	1.2
		<b>5</b>	0.003	-3.548	-10.13	0.170	-0.050	0.01	0.68	1.9
		<b>TOT</b>							<b>4.48</b>	
	<b>SA-abutment</b>	<b>1</b>	-1.558	0.42	-2.697	0.001	-0.553	-0.241	0.08	0.5
		<b>2</b>	-1.848	0.94	0.370	-0.010	-0.748	0.102	0.18	0.1
		<b>3</b>	2.566	4.07	-2.639	-3.968	-5.079	0.800	0.78	0.1
		<b>4</b>	0.970	2.06	-0.512	-0.012	0.377	0.046	0.39	0.5
		<b>5</b>	0.840	1.29	1.150	0.034	0.296	-0.131	0.25	0.2
		<b>TOT</b>							<b>1.68</b>	

Rotational equilibrium: 3-deformable decks model with hinged joints										
	Ty %	Ty (t)	Mxx (tm)	Mxx %	Mxx (Ty) (tm)	Mxx (Ty) %	M (ΔN) (t m)	M (ΔN) %	M tot (t m)	M Tot %
<b>NA-abut.</b>	<b>2.08</b>	10.86	19.41	<b>46.3</b>	186.5	<b>5.6</b>	-90.6	-0.87	115.31	<b>0.84</b>
<b>Pier 1</b>	<b>10.77</b>	56.22	7.22	<b>17.2</b>	707.2	<b>21.3</b>	686.0	6.60	1400	<b>10.1</b>
<b>Arch</b>	<b>56.55</b>	295.1	0.00	<b>0.0</b>	457.5	<b>13.8</b>	7732	74.43	8190	<b>59.5</b>
<b>Piers 13-17</b>	<b>30.38</b>	158.5	11.32	<b>27.0</b>	1791	<b>54.0</b>	2081	20.04	3884	<b>28.2</b>
<b>SA-abut.</b>	<b>1.68</b>	8.77	3.96	<b>9.4</b>	176.9	<b>5.3</b>	-20.9	-0.20	159.9	<b>1.16</b>
<b>Σ</b>			<b>41.90</b>		<b>3319</b>		<b>10389</b>		<b>13750</b>	

In the case of longitudinal horizontal force ( $F_{oX}=0.10P$ ), it could be said that:

- arch portion records the worst deformative effect, while thin arch follows deck deformed shape.

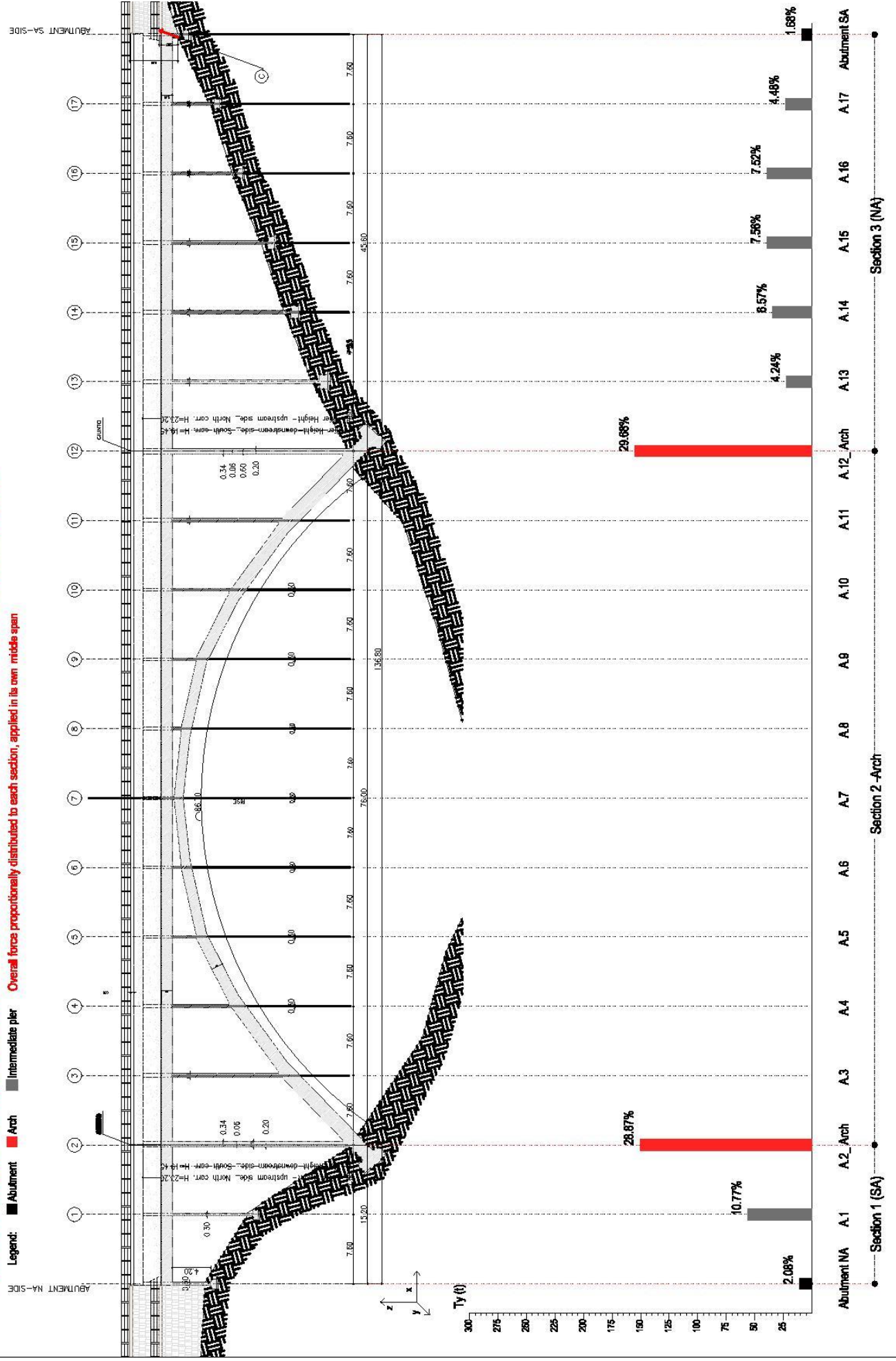
- shear forces due to acting loads are carried by external abutments (38%) and by the central arch (60%), while intermediate cross walls are quite unloaded.

In the case of transversal horizontal force ( $F_{oY} = 0.10P$ ), it could be said that:

- about 60% of shearing force is carried by external arch-cross walls, while deck abutments are the lowest excited sections;
- about 50% of global moment is borne by external arch-cross walls;
- intermediate walls have a quiet uniform distribution of shear (7%);
- the greatest contribution to global moment is due to  $M(\Delta N)$ ;
- Effects due to horizontal out of plane forces (as seismic ones) are not negligible, above all for the central arch

# Cross walls Shear (Ty) distribution, due to Horizontal forces acting out of plane ( $F_{oy} = 0.10P$ ) - Three-deformable -decks model with hinged joints

Longitudinal section (1:500)



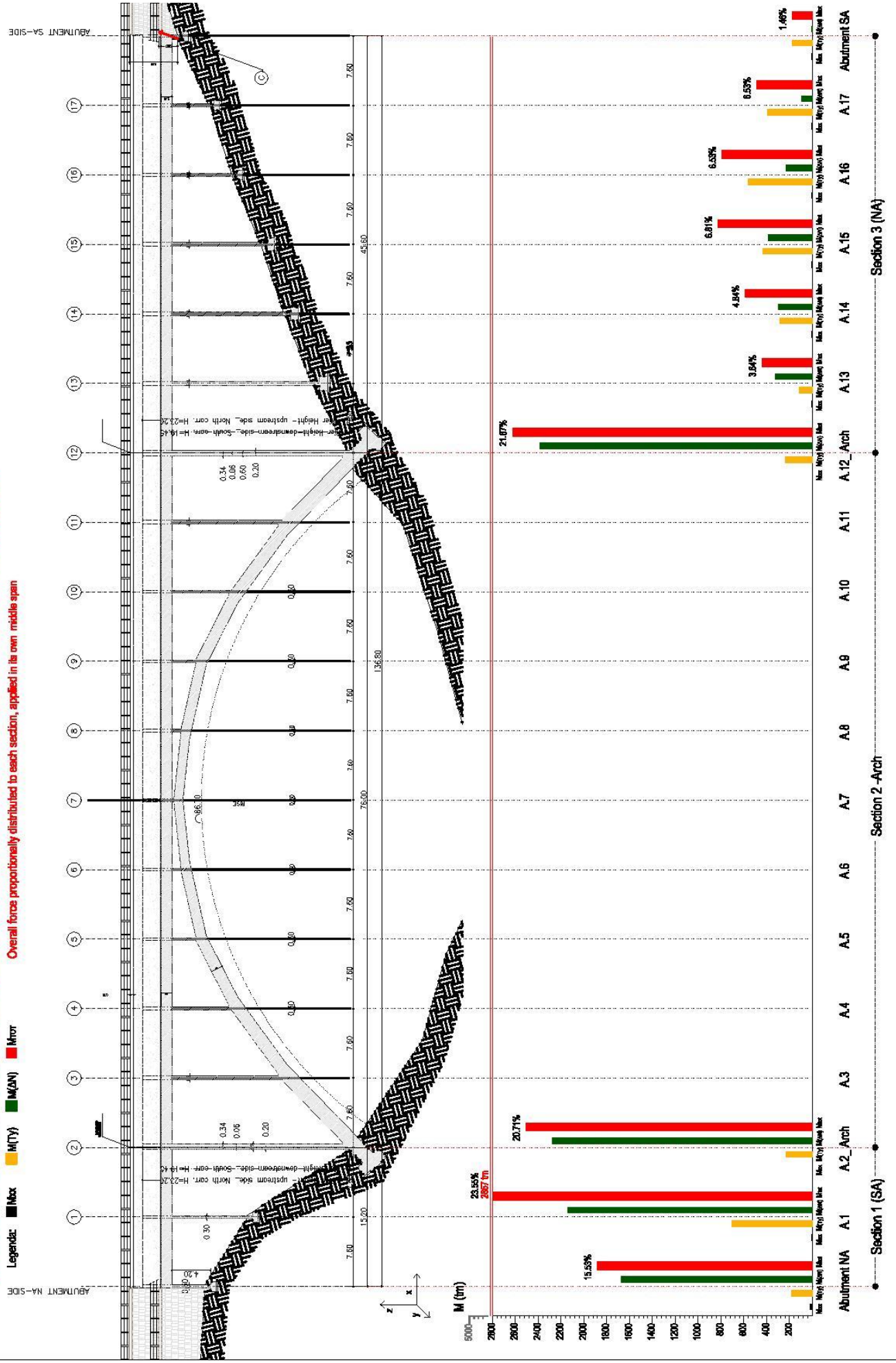




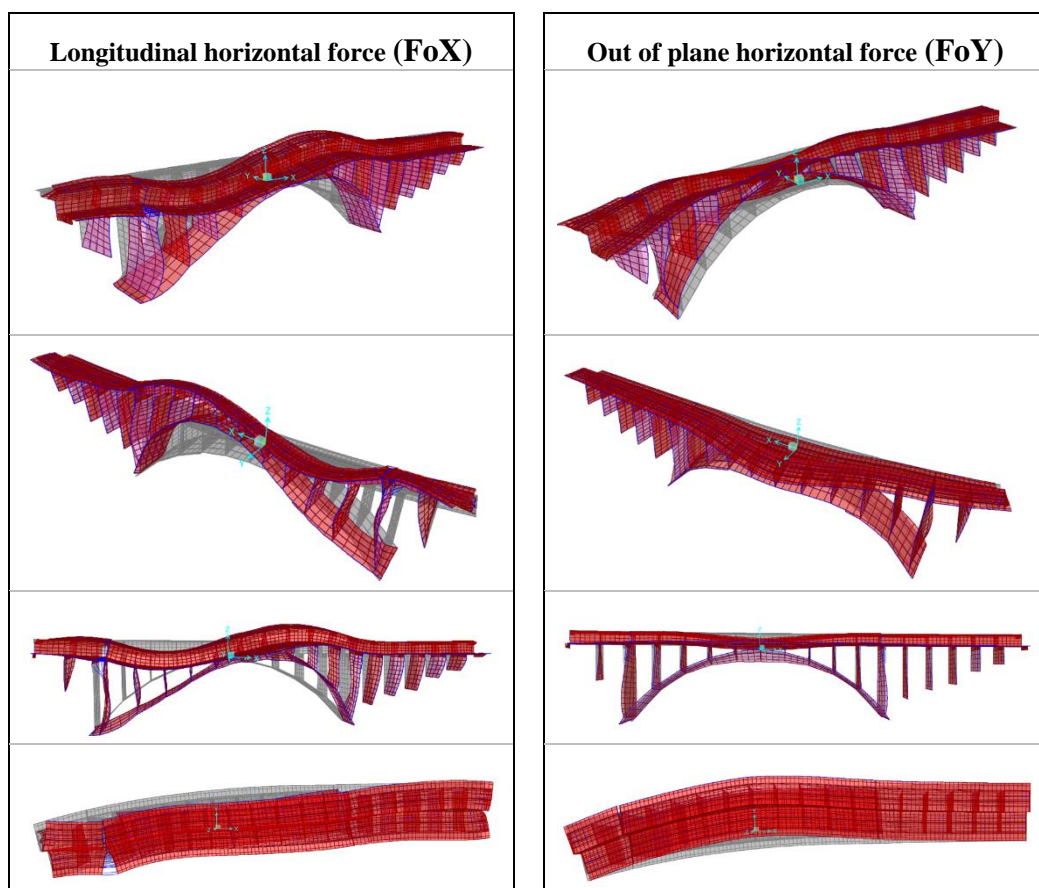
# Cross walls Moments (M) distribution, due to Horizontal forces (Foy= 0.10P) acting out of plane - Three-deformable -decks model with hinged joints

Longitudinal section (1:500)

Overall forces proportionally distributed to each section, applied in its own middle span



### 7.3.3 Single undeformable deck with fixed joints



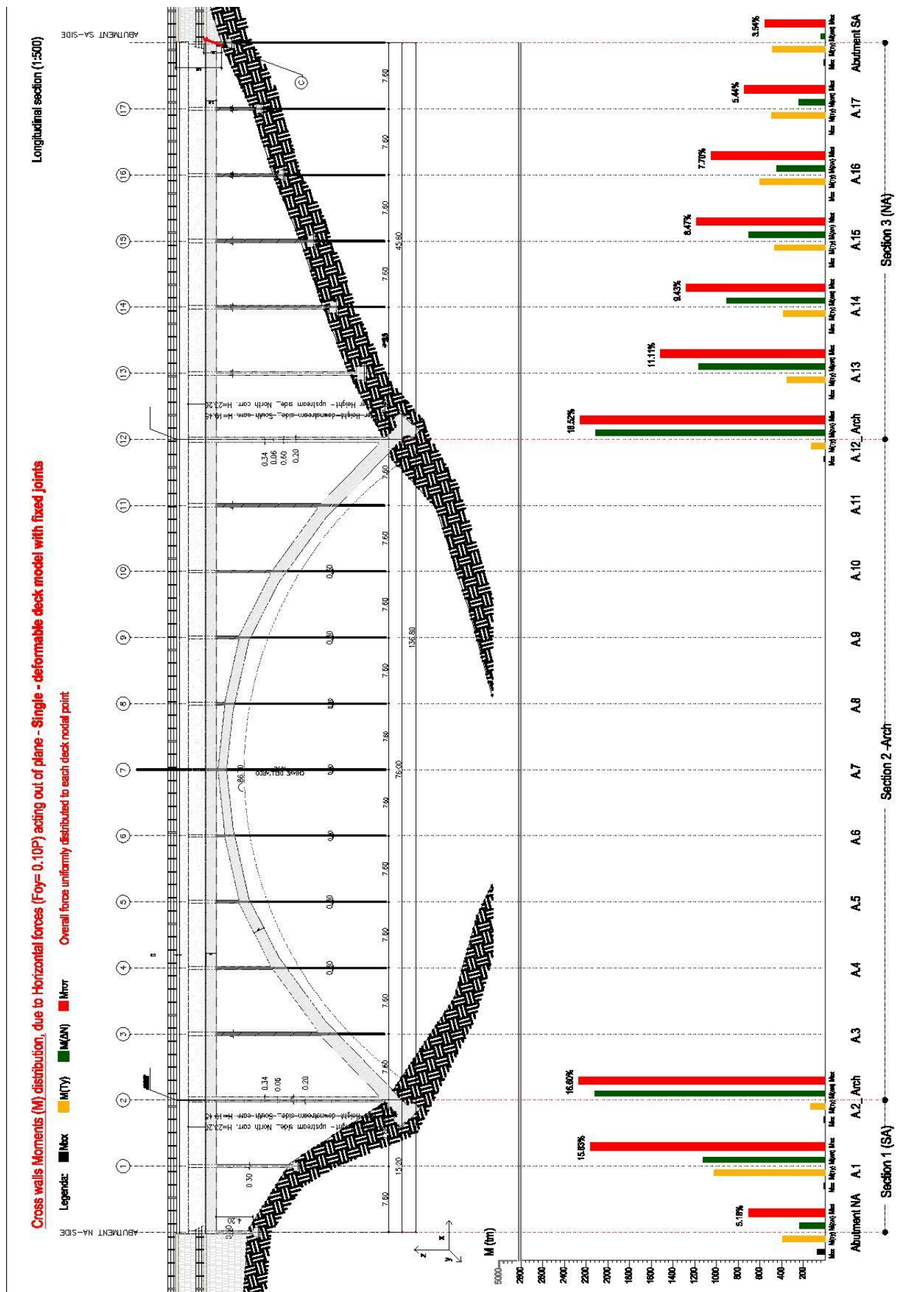
Rotational equilibrium: Single deformable deck model with fixed joints under uniformly distributed forces										
	Ty %	Ty (t)	Mxx (tm)	Mxx %	Mxx (Ty) (tm)	Mxx (Ty) %	M (ΔN) (t m)	M (ΔN) %	M tot (t m)	M Tot %
NA- abut.	4.42	23.07	76.90	50.8	396.3	8.9	234.1	2.59	707.4	5.18
Pier 1	15.58	81.33	13.29	8.8	1023	22.9	1126	12.47	2163	15.83
Arch	32.76	171	28.62	18.9	265.0	5.9	4231	46.81	4525	33.11
Piers 13 - 17	43.46	226.8	15.85	10.5	2305	51.5	3465	38.33	5786	42.34
SA-abut.	4.6	24.01	16.63	11.0	484.5	10.8	-17.7	-0.20	483.4	3.54
Σ			151.2		4474		9040		13666	



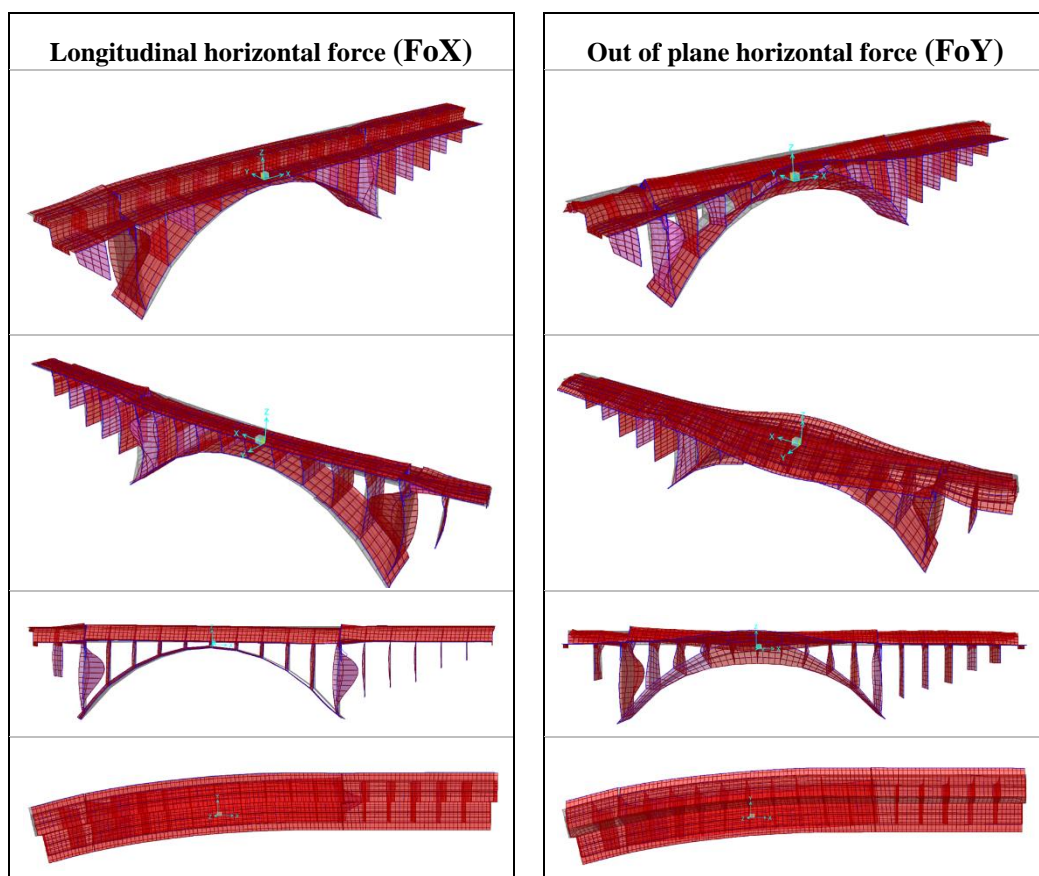








### 7.3.4 Single undeformable deck with hinged joints



Rotational equilibrium: single undeformable deck model with fixed joints										
	Ty %	Ty (t)	Mxx (tm)	Mxx %	Mxx (Ty) (tm)	Mxx (Ty) %	M (ΔN) (t m)	M (ΔN) %	M tot (t m)	M Tot %
NA-abut.	2.09	10.91	19.52	7.1	187.43	5.9	-80.98	-0.88	125.97	0.99
Pier 1	10.18	53.1396	7.20	2.6	668.50	21.0	635.11	6.89	1310.8	10.33
Arch	58.1	303.282	123.11	44.5	470.09	14.7	7337.34	79.59	7930.5	62.51
Piers 13 -17	28.35	147.98	118.08	42.7	1688.7	52.9	1408.8	15.28	3215.6	25.35
SA-abut.	1.67	8.7174	8.73	3.2	175.92	5.5	-81.47	-0.88	103.18	0.81
Σ			276.64		3190.6		9218.8		12686	











Considering single undeformable deck (FEM) models, a comparison between the outputs obtained for different restraint conditions follows.

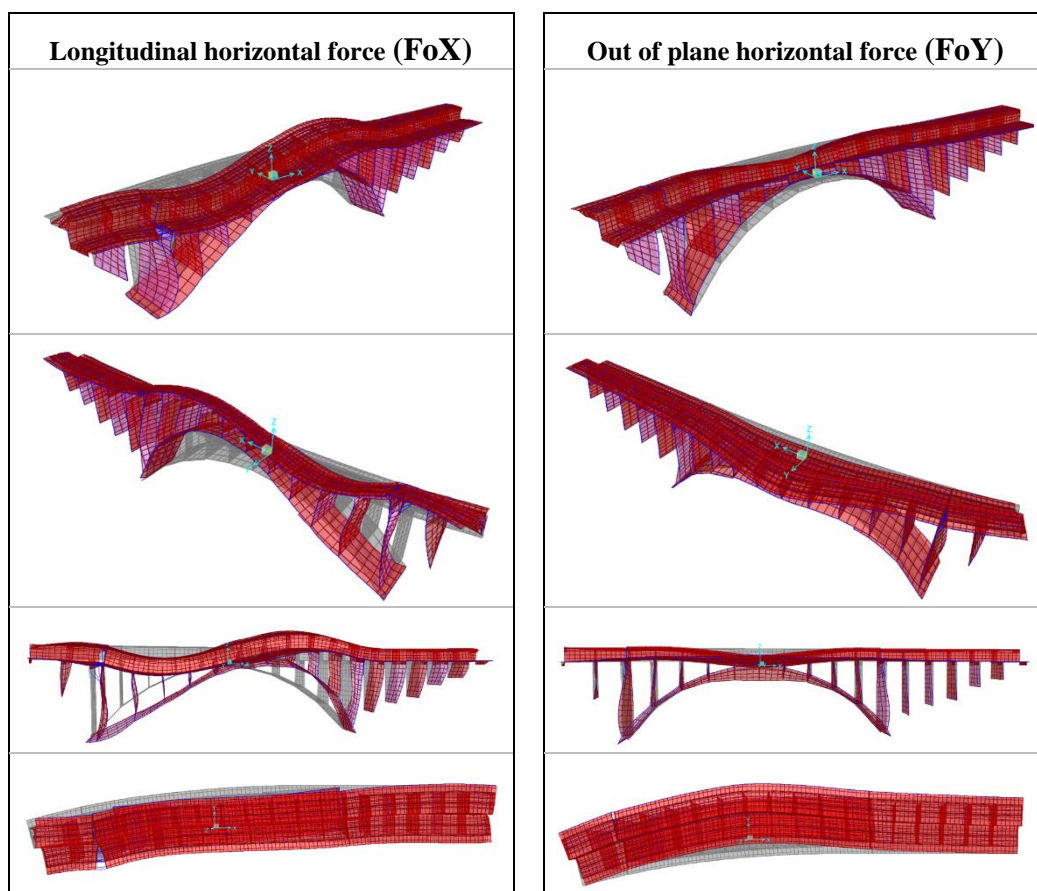
In the case of longitudinal horizontal force ( $F_{oX} = 0.10P$ ), it could be said that:

- for both cases, arch portion records the worst deformative effects;
- the most vulnerable elements are arch cross walls.

In the case of transversal horizontal force ( $F_{oY} = 0.10P$ ), it could be said that:

- more than 50% of shear force is carried by abutments in fixed-joints model;
- introducing hinged restraints, about 95% of shear force is carried by abutments, being the other cross walls less excited;
- uplift effect is almost negligible, except for abutments
- about 70% of global moment is borne by abutments
- the greatest contribution to global moment is due to  $m(T_y)$  and not to  $M(\Delta N)$
- for rigid continuous deck option, cross wall stress is considerably reduced
- the most excited sections are the abutments.

### 7.3.5 Single deformable deck model with fixed joints



Rotational equilibrium: Single deformable deck model with fixed joints										
	Ty %	Ty (t)	Mxx (tm)	Mxx %	Mxx (Ty) (tm)	Mxx (Ty) %	M (ΔN) (t m)	M (ΔN) %	M tot (t m)	M Tot %
NA-abut.	5.01	26.15	89.06	41.5	449.2	11.6	-256.0	-2.80	282.2	2.23
Pier 1	8.53	44.53	11.95	5.6	560.1	14.5	1018	11.14	1590	12.54
Arch	47.14	246.0	38.61	18.0	381.4	9.9	5032	55.07	5452	42.98
Piers 13 -17	34.00	177.4	43.34	20.2	1897	49.0	3459	37.86	5399	42.57
SA-abut.	5.53	28.87	31.70	14.8	582.5	15.1	-115.5	-1.26	498.7	3.93
Σ			214.6		3870		9138		13223	



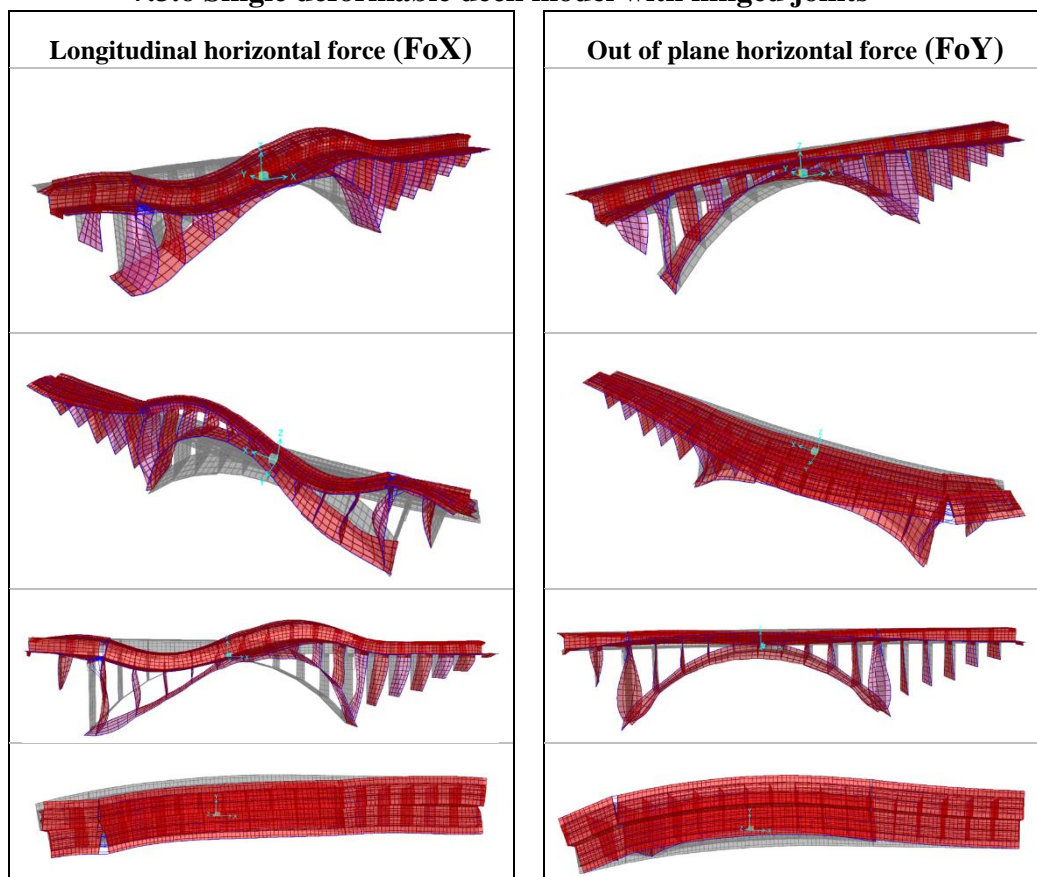






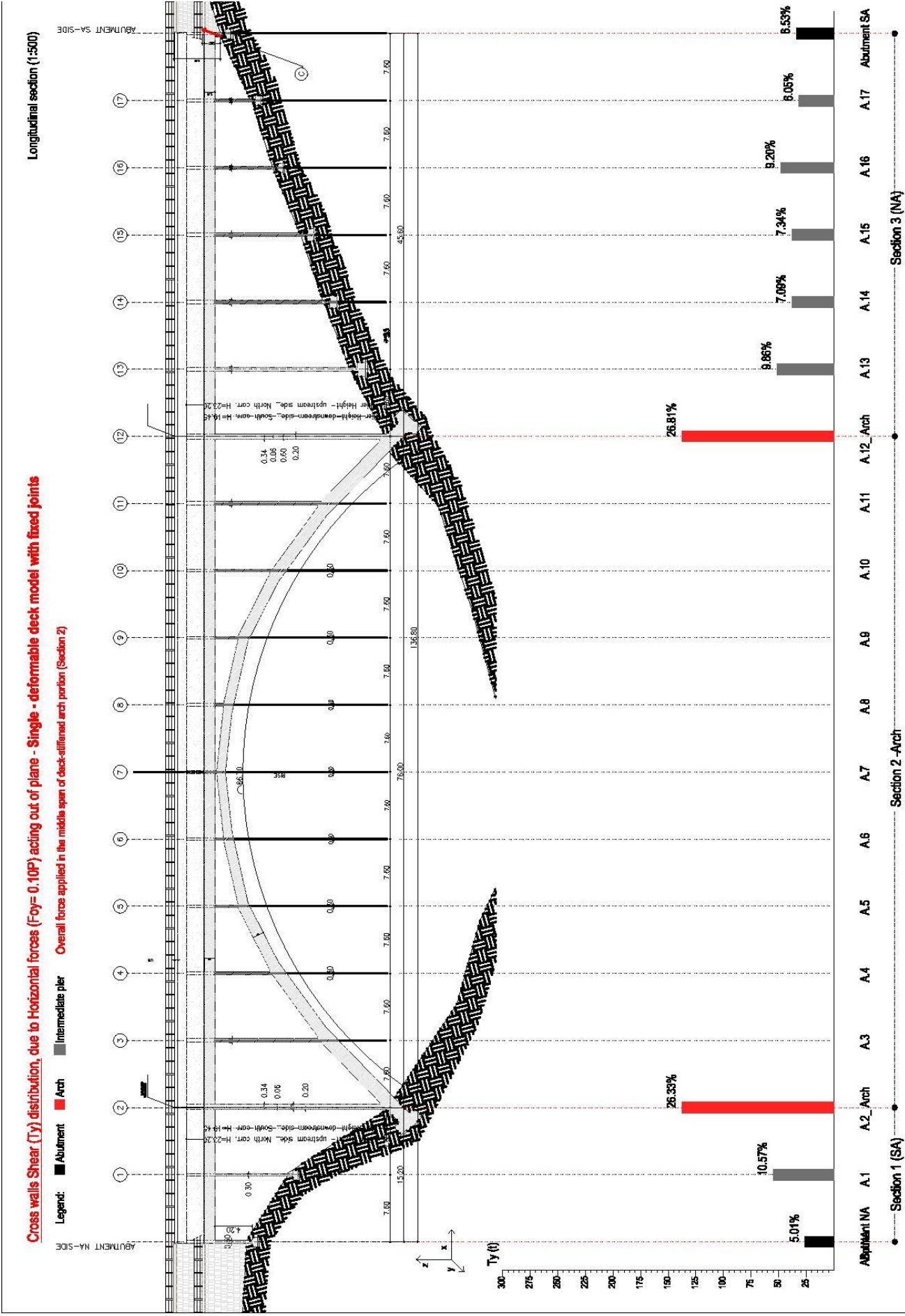


### 7.3.6 Single deformable deck model with hinged joints



Rotational equilibrium: single deformable deck model with hinged joints										
	Ty %	Ty (t)	Mxx (tm)	Mxx %	Mxx (Ty) (tm)	Mxx (Ty) %	M (ΔN) (t m)	M (ΔN) %	M tot (t m)	M Tot %
NA- abut.	12.93	67.49	121.1	66.90	1159	18.2	57.10	1.16	1337.8	11.64
Pier 1	18.26	95.32	11.99	6.62	1199	18.8	1206	24.46	2417	21
Arch	8.82	46.04	0.00	0.00	71.36	1.1	-16.44	-0.33	54.92	0.48
Piers 13 - 17	46.99	245.2	16.16	8.92	2577	40.4	3066	33.26	5660	49.2
SA-abut.	13.07	68.23	31.80	17.56	1376	21.6	618.3	12.54	2026.	17.6
Σ			181.1		6384		4931		11497	





**Longitudinal section (1:500)**

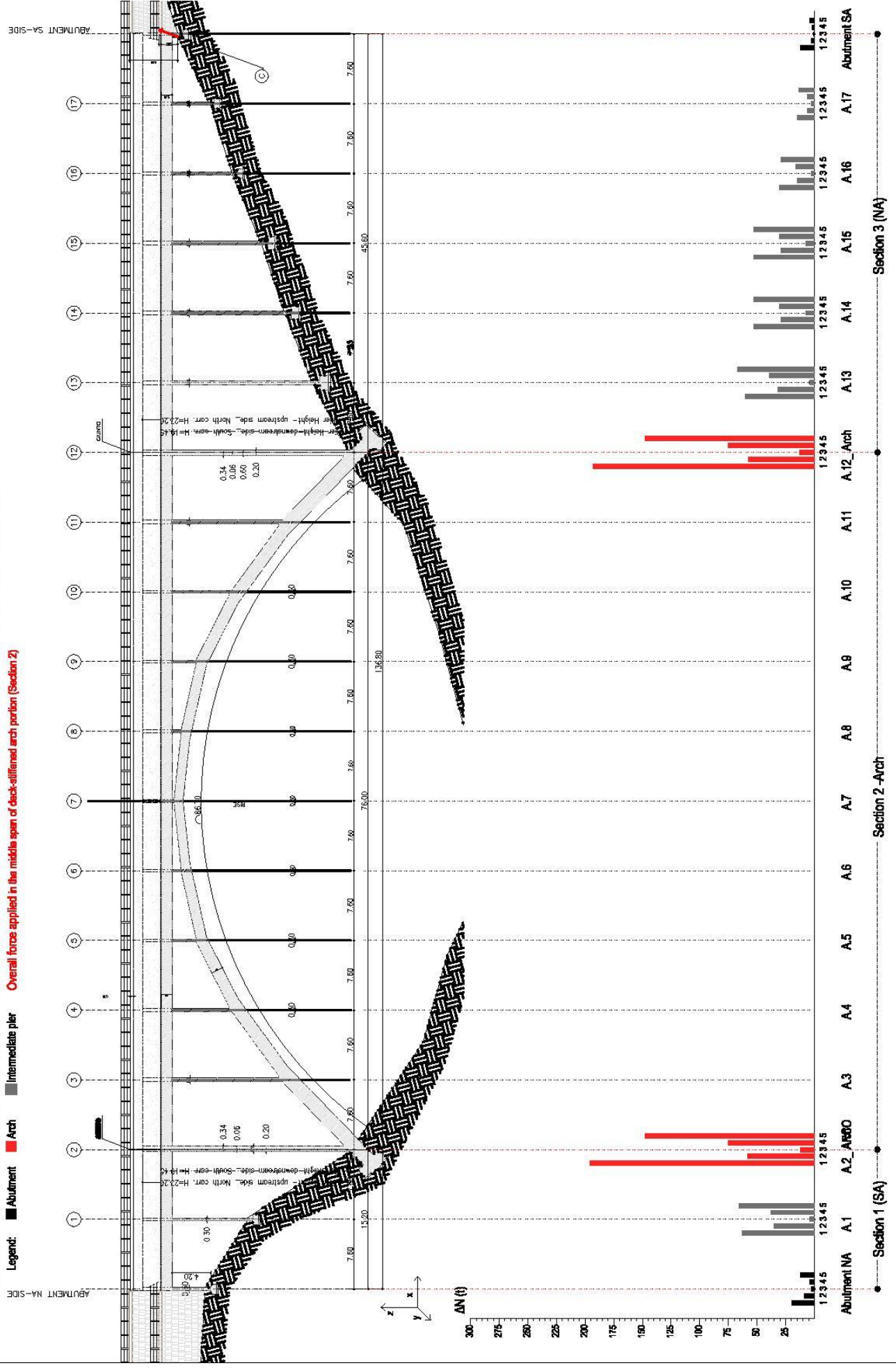
Overall force applied in the middle span of deck-stiffened arch portion (Section 2)

**Legend:** ■ Abutment ■ Arch ■ Intermediate pier

**Arach**

## Conclusion

■  
三





### 7.3.7 Model comparison

Looking at **three-deformable-decks models**, changing restraint condition at the base of the cross walls, it ascertains that:

- arch portion records the worst deformations, for both loading conditions;
- acting longitudinal horizontal forces, stiffer side spans show little sliding motions; while arch, as the most vulnerable portion, follows decks deformed shape, slender cross walls are effected by buckling effects;
- out of plane forces cause arch uplift, while side spans preserve their initial condition;
- for transverse force load condition, about 60% of shearing force is carried by external arch cross section; deck abutments are the lowest excited sections; the highest variation of axial force is carried by external arch cross walls;
- central arch is the main load bearing structural element;
- arch-hinged joints leads to a low  $\delta n$ -increase compared to fixed model ;
- about 50% of global moment is borne by external arch-cross walls;
- the greatest contribution to global moment is due to  $m(\Delta N)$ ;
- for fixed joints model, restraint contribution to global moment is nihil.

Looking at **single-undeformable-deck model**, changing restraint condition at the base of the cross walls, it ascertains that:

- acting longitudinal horizontal forces, the most vulnerable structural element is the thin central arch: in this case, deck sliding leads to buckling effects for slender cross walls, at the external portions of the arch;
- for both load conditions, hinged joints restraints make the structure more flexible;
- more than 50% of shear force is carried by abutments in fixed-joints model;
- introducing hinged restraints, about 95% of shear force is carried by abutments, being the other cross walls less excited;
- arch is the lowest excited portion;
- continuous deck guarantee a reduction of  $\Delta N$ ;
- uplift effect is almost negligible, except for abutments;
- arch-hinged joints leads to a low  $\Delta N$ -increase compared to fixed model ; about 70% of global moment is borne by abutments;
- the greatest contribution to global moment is due to  $m(T_y)$  and not to  $M(\Delta N)$ ;
- for rigid continuous deck option, cross wall stress is considerably reduced;
- the most excited sections are the abutments.



Looking at **single-deformable-deck model**, changing restraint condition at the base of the cross walls, it ascertains that:

- for both loading conditions, arch portion records the worst sliding and overturning effects;
- high deformability of continuous deck involves all cross walls into deformed shape;
- acting longitudinal horizontal cross walls, the most vulnerable elements are bridge cross walls;
- this is the only deck option which causes a force distribution strictly related to bottom restraint conditions;
- the fixed joints model makes the arch stiffer than the side portions, so the arch carries about 60% of shear force;
- shear-force distribution completely changes for hinged joints model: shear-force is quite uniformly distributed, reaching peak at abutments;
- for fixed joints model, arch carries about 50% of total moment;
- for hinged joint model, abutments are the worst moment-excited sections;
- hinged restraint condition leads a quite uniform distribution of moment among cross walls;
- for fixed joint model, arch is the main load bearing structural element;
- instead, for hinged joint model, the most excited sections are the abutments.



## 7.4 FEM modelling: modal analysis (Sap 2000)

### 7.4.1 Three deformable decks model with fixed joints

Modal analysis is performed considering 100 vibration modes:

Modal analysis output: Three deformable decks with fixed joints													
Mode	T [sec]	UX (%)	UY (%)	UZ (%)	Sum UX	Sum UY	Sum UZ	RX (%)	RY (%)	RZ (%)	Sum RX	Sum RY	Sum RZ
<b>1</b>	<b>0.6743</b>	<b>31.376</b>	0.157	0.013	31.37	0.157	0.013	1.307	<b>9.009</b>	0.565	1.307	9.009	0.565
2	0.6547	0.623	0.0011	4.82E-	31.99	0.158	0.013	0.0015	0.045	0.0090	1.308	9.054	0.574
3	0.5632	0.247	1.7E-	1.35E-	32.24	0.158	0.013	2.31E-	0.0026	0.0034	1.308	9.057	0.578
4	0.5325	0.193	0.0008	0.0003	32.43	0.159	0.013	0.0072	0.0021	1.3E-05	1.316	9.059	0.578
5	0.5288	0.0020	0.247	0.012	32.44	0.406	0.026	0.069	0.021	0.106	1.384	9.08	0.683
6	0.5153	0.02	0.225	0.0050	32.46	0.631	0.031	0.016	0.051	0.011	1.4	9.131	0.694
<b>7</b>	<b>0.4725</b>	<b>0.242</b>	<b>49.726</b>	0.238	32.70	50.35	0.268	<b>8.339</b>	<b>0.056</b>	<b>5.499</b>	9.739	9.188	6.194
8	0.4667	0.367	0.875	0.0037	33.06	51.23	0.272	0.151	0.0040	0.128	9.89	9.192	6.322
9	0.4553	0.228	0.0001	2.25E-	33.2	51.23	0.272	1.1E-05	0.0014	0.00114	9.89	9.193	6.323
10	0.4302	0.192	0.123	0.0007	33.48	51.35	0.273	0.0025	0.24	14.664	9.893	9.433	20.98
11	0.4277	0.361	0.0020	3.5E-05	33.85	51.35	0.273	8.7E-06	0.019	0.079	9.893	9.452	21.06
12	0.4152	0.258	0.0052	0.0001	34.10	51.36	0.273	0.0003	0.014	0.03	9.893	9.466	21.09
13	0.4035	0.029	0.289	0.0042	34.13	51.65	0.277	0.054	0.0059	0.485	9.947	9.472	21.58
14	0.3966	0.473	0.022	0.0003	34.61	51.67	0.278	0.0026	0.066	2.439	9.95	9.538	24.02
15	0.3955	0.132	8.1E-05	4.5E-06	34.74	51.67	0.278	0.0002	0.0002	0.061	9.95	9.539	24.08
16	0.3614	0.187	0.038	0.0055	34.92	51.71	0.283	8.5E-02	0.0007	0.076	9.95	9.54	24.15
17	0.3607	0.0014	0.049	0.022	34.93	51.76	0.305	0.0008	0.0028	0.039	9.951	9.542	24.19
18	0.3580	0.54	0.0008	0.0007	35.47	51.76	0.306	0.0010	0.0018	0.203	9.952	9.544	24.39
19	0.3550	0.156	4.2E-05	7.3E-07	35.62	51.76	0.306	3.4E-05	4.27E-	0.00178	9.952	9.544	24.40
20	0.3507	0.065	0.0017	0.0016	35.69	51.76	0.308	0.0014	0.019	3.2E-05	9.953	9.563	24.40
21	0.3474	0.045	0.0031	1.5E-05	35.73	51.76	0.308	0.0011	0.0017	0.027	9.954	9.565	24.42
22	0.3457	0.061	0.0065	1.7E-06	35.79	51.77	0.308	1.3E-05	0.0019	0.016	9.954	9.567	24.44
23	0.34224	0.081	0.0055	0.0006	35.87	51.77	0.308	0.0062	0.038	0.00011	9.961	9.605	24.44
24	0.3414	0.262	1.2E-05	7.3E-07	36.14	51.77	0.308	2.9E-06	0.0045	0.00034	9.961	9.61	24.44
25	0.3269	0.204	9.1E-05	6.6E-07	36.34	51.77	0.308	1.4E-05	0.0040	5.8E-05	9.961	9.614	24.44
26	0.3197	0.173	0.0004	9.7-08	36.56	51.77	0.308	0.0002	0.0008	0.0043	9.961	9.615	24.44
27	0.3035	0.0009	0.206	0.351	36.51	51.98	0.66	0.0003	0.054	0.016	9.961	9.669	24.46
28	0.2950	0.208	3.2E-06	0.0054	36.72	51.98	0.665	5.2E-05	0.0089	0.00863	9.961	9.678	24.47
29	0.2753	0.151	0.0068	0.0004	36.87	51.99	0.666	0.0008	0.0001	0.00233	9.962	9.678	24.47
30	0.2739	0.037	0.012	0.163	36.91	52.00	0.829	0.0073	0.033	0.021	9.97	9.711	24.49
31	0.2729	0.286	6.3E-05	0.022	37.2	52.00	0.851	5.6E-05	0.0045	0.033	9.97	9.716	24.52
32	0.26335	0.228	5.6E-06	2.6E-06	37.42	52.00	0.851	9.0E-06	0.00208	0.00033	9.97	9.718	24.53
33	0.26241	0.132	0.00976	0.00020	37.56	52.01	0.851	0.00022	0.00051	0.00240	9.97	9.718	24.53
34	0.24954	0.295	0.00352	0.00638	37.85	52.01	0.858	0.00229	0.064	0.00082	9.972	9.783	24.53
35	0.24693	0.189	0.00035	2.1E-06	38.04	52.01	0.858	9.8E-05	0.00208	1.4E-05	9.972	9.785	24.53
36	0.24278	0.334	0.00072	0.013	38.37	52.01	0.871	0.017	0.041	0.00168	9.989	9.826	24.53
37	0.24088	0.124	0.00239	1.5E-06	38.50	52.02	0.871	0.00111	1.8E-08	0.00038	9.99	9.826	24.53
38	0.23438	0.27	0.00585	0.01	38.77	52.02	0.881	0.012	0.14	0.00051	10.00	9.966	24.53
39	0.22884	0.167	0.00430	1.2E-05	38.93	52.03	0.881	0.00151	0.00343	0.00036	10.00	9.969	24.53
40	0.22362	0.923	0.00212	0.027	39.86	52.03	0.908	0.053	0.285	0.00494	10.05	10.25	24.54
41	0.22321	0.144	0.00146	1.0E-06	40.00	52.03	0.908	0.00070	0.00013	5.6E-05	10.05	10.25	24.54
<b>42</b>	<b>0.21530</b>	<b>11.704</b>	0.094	7.1E-05	51.71	52.12	0.908	0.57	4.28	0.045	10.62	14.53	24.58

Mode	T [sec]	UX (%)	UY (%)	UZ (%)	Sum UX	Sum UY	Sum UZ	RX (%)	RY (%)	RZ (%)	Sum RX	Sum RY	Sum RZ
43	0.20996	0.467	0.00217	0.069	52.17	52.13	0.977	0.022	0.316	0.00044	10.64	14.85	24.58
44	0.20670	2.409	0.00391	0.382	54.58	52.13	1.359	0.059	0.24	0.012	10.70	15.09	24.59
45	0.20495	0.591	0.00679	0.223	55.17	52.14	1.581	0.012	0.027	0.00028	10.72	15.11	24.59
46	0.20246	0.019	0.00347	7.5E-05	55.19	52.14	1.581	0.00163	0.00458	0.00165	10.72	15.12	24.60
47	0.20113	1.513	0.036	0.059	56.70	52.18	1.64	0.066	0.355	0.00174	10.78	15.47	24.60
48	0.19714	0.978	0.00251	0.076	57.6	52.18	1.716	0.00086	0.294	0.065	10.78	15.77	24.66
49	0.19483	0.528	2.431	0.042	58.21	54.61	1.758	1.235	0.016	4.464	12.02	15.78	29.13
50	0.19112	0.362	8.3E-05	0.054	58.57	54.61	1.812	0.103	0.634	0.068	12.12	16.42	29.20
<b>51</b>	0.18276	0.079	0.158	0.021	58.65	54.77	1.832	<b>1.249</b>	<b>6.736</b>	0.181	13.37	23.15	29.38
52	0.17708	0.178	0.097	0.04	58.83	54.86	1.873	0.095	0.00564	0.023	13.47	23.16	29.40
<b>53</b>	<b>0.17577</b>	<b>0.095</b>	<b>7.733</b>	0.171	58.92	62.60	2.044	3.734	0.00394	<b>9.045</b>	17.20	23.16	38.45
54	0.17399	0.014	1.055	0.137	58.94	63.65	2.181	0.597	0.00511	1.293	17.80	23.17	39.74
<b>55</b>	<b>0.17252</b>	0.248	0.693	<b>5.648</b>	59.19	64.35	7.829	1.214	0.57	1.279	19.01	23.74	41.02
<b>56</b>	<b>0.17213</b>	0.026	1.143	<b>41.374</b>	59.21	65.49	49.20	0.381	4.767	0.439	19.39	28.50	41.46
57	0.16523	8.3E-07	0.068	0.00602	59.21	65.56	49.20	0.00129	0.00154	0.062	19.39	28.51	41.52
<b>58</b>	<b>0.16211</b>	0.036	<b>5.845</b>	3.97	59.25	71.40	53.17	<b>9.076</b>	0.488	0.16	28.47	28.99	41.68
59	0.15814	0.238	0.066	0.099	59.49	71.47	53.27	0.229	0.063	0.00636	28.70	29.06	41.69
60	0.15618	0.036	1.056	1.166	59.52	72.52	54.44	3.978	0.058	0.174	32.68	29.12	41.86
61	0.15247	0.024	0.017	0.00872	59.55	72.54	54.45	0.065	0.189	0.107	32.74	29.3	41.97
62	0.15084	0.013	0.264	1.154	59.56	72.81	55.60	1.382	0.121	0.153	34.12	29.43	42.12
63	0.14923	0.00215	0.041	1.774	59.56	72.85	57.38	0.114	0.229	0.026	34.24	29.65	42.15
64	0.14553	0.322	0.00089	0.00198	59.88	72.85	57.38	0.023	0.112	0.017	34.26	29.77	42.16
65	0.14300	0.00035	0.018	0.00089	59.88	72.87	57.38	0.00140	7.8E-05	0.049	34.26	29.77	42.21
66	0.14206	0.014	0.03	0.035	59.90	72.9	57.41	0.015	0.013	0.00084	34.28	29.78	42.21
67	0.13498	0.225	0.00043	0.048	60.12	72.9	57.46	0.049	0.063	0.00083	34.33	29.84	42.21
68	0.13049	0.075	0.00140	0.547	60.20	72.90	58.01	0.028	0.00116	8.3E-07	34.36	29.84	42.21
69	0.12854	0.016	0.00154	2.539	60.21	72.90	60.55	0.094	0.365	0.011	34.45	30.21	42.22
70	0.12431	0.072	0.024	0.014	60.29	72.92	60.56	0.014	0.00653	0.019	34.46	30.22	42.24
71	0.12054	0.028	0.00121	0.00013	60.31	72.92	60.56	0.013	6.2E-05	0.017	34.48	30.22	42.26
72	0.11045	0.369	0.00837	0.019	60.68	72.93	60.58	0.041	0.232	0.00980	34.52	30.45	42.27
73	0.10829	0.749	0.053	0.017	61.43	72.99	60.60	0.027	0.305	0.021	34.54	30.75	42.29
74	0.10690	2.742	0.00482	0.00575	64.17	72.99	60.60	0.00305	0.102	0.234	34.55	30.85	42.53
75	0.10252	0.946	0.00590	0.511	65.12	73	61.11	0.014	0.121	0.036	34.56	30.98	42.56
76	0.10161	0.41	0.00041	0.00153	65.53	73.00	61.12	0.068	0.272	3.34	34.63	31.25	45.90
<b>77</b>	<b>0.09981</b>	<b>12.709</b>	0.012	0.072	78.24	73.01	61.19	0.0003	0.17	0.273	34.63	31.42	46.19
78	0.08888	1.652	0.03	0.105	79.89	73.03	61.29	0.351	0.685	0.041	34.98	32.10	46.22
79	0.08574	0.00946	0.598	0.728	79.90	73.64	62.02	0.113	0.049	0.339	35.09	32.15	46.55
80	0.08443	0.782	0.728	0.046	80.68	74.36	62.07	0.127	0.00121	1.505	35.22	32.15	48.06
81	0.08224	0.473	0.288	0.025	81.15	74.65	62.09	0.023	0.355	3.661	35.24	32.51	51.72
<b>82</b>	<b>0.07689</b>	0.2	4.824	0.071	81.35	79.48	62.16	0.645	1.123	<b>6.981</b>	35.89	33.63	58.70
83	0.07436	0.016	0.032	0.361	81.37	79.51	62.53	5.631	0.064	2.404	41.52	33.69	61.11
84	0.07129	0.023	0.00379	2.314	81.39	79.51	64.84	0.166	0.069	0.00084	41.69	33.76	61.11
85	0.06495	3.121	0.303	0.299	84.51	79.81	65.14	2.593	1.788	0.00135	44.28	35.55	61.11
<b>86</b>	<b>0.0637</b>	0.277	3.072	0.00386	84.79	82.89	65.14	<b>9.561</b>	0.725	0.16	53.84	36.28	61.27
<b>87</b>	<b>0.05794</b>	0.375	0.584	<b>8.607</b>	85.17	83.47	73.75	0.143	2.216	3.719	53.98	38.49	64.99
88	0.05557	0.336	1.174	1.522	85.50	84.64	75.27	0.99	0.029	2.252	54.97	38.52	67.24

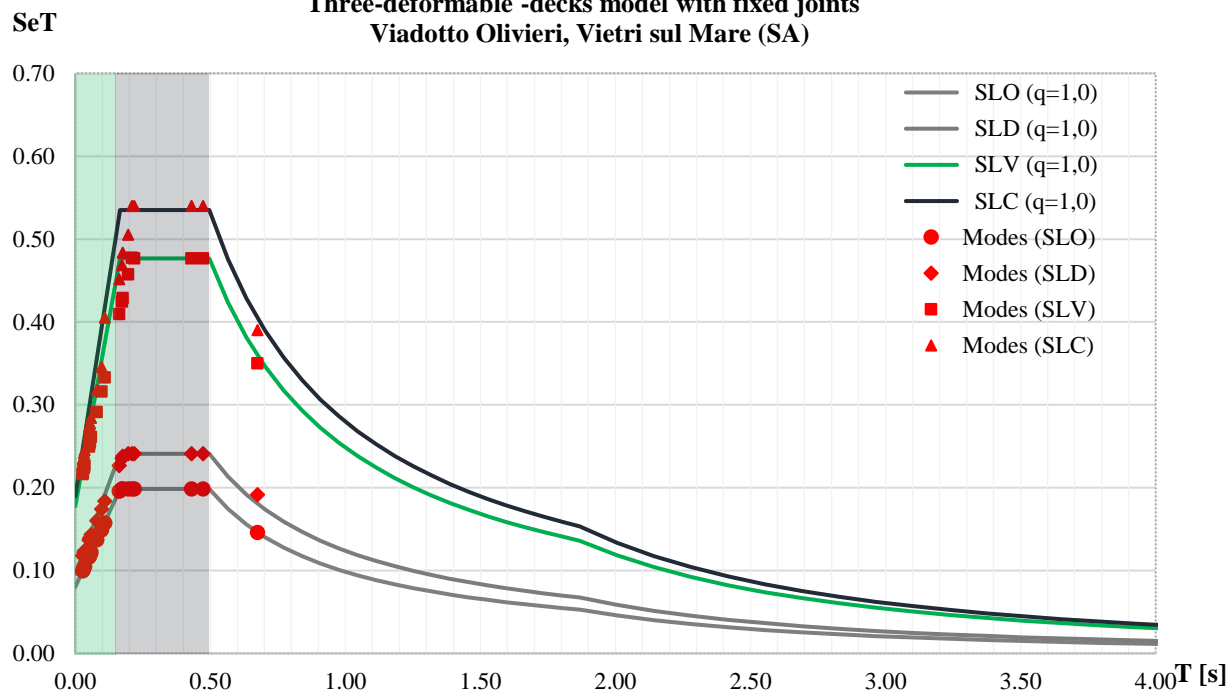


Mode	T [sec]	UX (%)	UY(%)	UZ (%)	Sum UX	Sum UY	Sum UZ	RX (%)	RY /%	RZ (%)	Sum RX	Sum RY	Sum RZ
<b>89</b>	<b>0.05217</b>	<b>5.532</b>	0.1	0.151	91.03	84.74	75.42	1.595	1.228	0.605	56.57	39.75	67.84
90	0.04609	1.317	2.632	0.726	92.35	87.38	76.15	1.758	0.641	0.26	58.33	40.39	68.10
<b>91</b>	<b>0.04465</b>	0.316	0.00688	<b>9.605</b>	92.67	87.38	85.75	0.00046	<b>5.289</b>	0.895	58.33	45.68	69.00
<b>92</b>	<b>0.04141</b>	0.00206	0.83	0.05	92.67	88.21	85.80	0.021	0.125	<b>6.453</b>	58.35	45.80	75.45
93	0.03837	3.04	0.046	0.018	95.71	88.26	85.82	0.675	1.783	0.052	59.02	47.59	75.50
<b>94</b>	<b>0.03288</b>	0.021	0.813	7.321	95.73	89.07	93.14	0.129	1.847	0.115	59.15	49.43	75.62
<b>95</b>	<b>0.03102</b>	0.251	<b>5.029</b>	0.553	95.98	94.10	93.69	1.422	0.867	0.878	60.57	50.30	76.50
<b>96</b>	0.02976	0.271	0.138	0.00547	96.25	94.24	93.70	0.385	0.137	<b>13.043</b>	60.96	50.44	89.54
97	0.01741	2.47	0.015	0.038	98.72	94.25	93.74	0.094	0.251	0.014	61.05	50.69	89.55
<b>98</b>	0.01624	0.013	4.261	0.16	98.73	98.52	93.92	<b>6.111</b>	0.072	0.015	67.18	50.76	89.57
<b>99</b>	<b>0.01548</b>	0.034	0.066	0.00059	98.77	98.58	93.90	0.393	0.057	<b>7.955</b>	67.56	50.82	97.52
<b>100</b>	0.01418	0.02	0.051	3.876	<b>98.79</b>	<b>98.63</b>	<b>97.77</b>	0.465	0.00731	0.00039	<b>68.02</b>	<b>50.83</b>	<b>97.53</b>

Considering previous output data, it could be said that:

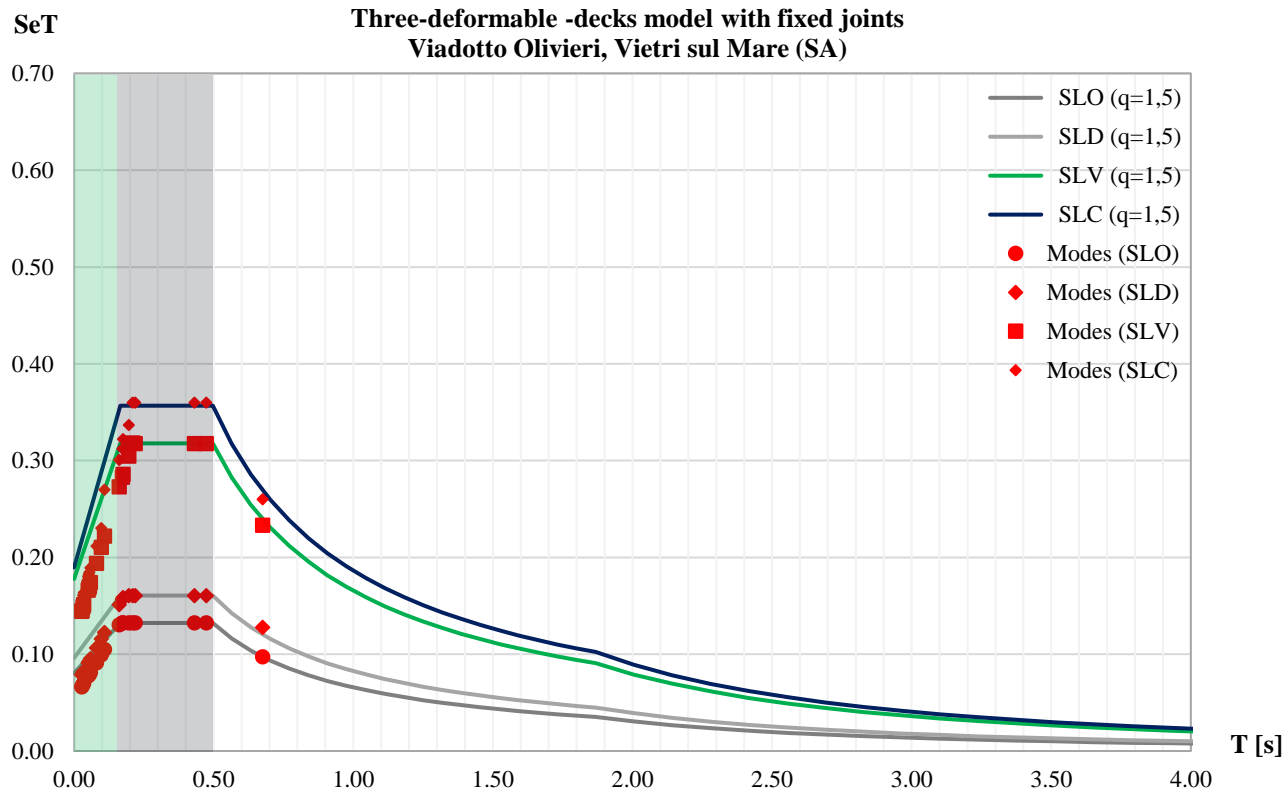
- modes with relatively high effects represent translational local modes, both in longitudinal and in transverse direction;
- apart from Rz component, rotational contribution can be neglected;
- despite this bridge is a complex multi- degree of freedom system, 100 modes are sufficient to involve about 100% of participating mass;
- period associated to main modes are lower than 1sec, characterizing a really rigid structure;
- modes fall within the first two spectrum section, above all in the highest amplification one.

**ACCELERATION DESIGN RESPONSE SPECTRUM**  
**Three-deformable -decks model with fixed joints**  
**Viadotto Olivieri, Vietri sul Mare (SA)**



Importance class (NTC 08): IV. Nominal life: 100 years % damping: 5% Soil class: B **q= 1,0**

**ACCELERATION DESIGN RESPONSE SPECTRUM**  
**Three-deformable -decks model with fixed joints**  
**Viadotto Olivieri, Vietri sul Mare (SA)**



Importance class (NTC 08): IV. Nominal life: 100 years % damping: 5% Soil class: B **q= 1,5**

### 7.3.2 Three deformable decks model with hinged joints

Modal analysis is performed considering 100 vibration modes:

Modal analysis output: Three deformable deck with hinged joints													
Mode	T [sec]	UX (%)	UY (%)	UZ (%)	Sum UX	Sum UY	Sum UZ	RX (%)	RY (%)	RZ (%)	Sum RX	Sum RY	Sum RZ
<b>1</b>	<b>0.675</b>	<b>31.404</b>	0.153	0.013	31.404	0.153	0.013	1.312	9.024	0.551	1.312	9.024	0.551
2	0.655	0.617	0.001	0.000	32.021	0.154	0.013	0.001507	0.044	0.008813	1.313	9.068	0.56
3	0.563	0.247	0.000	0.000	32.268	0.154	0.013	2.32E-05	0.00266	0.00345	1.313	9.071	0.563
4	0.533	0.193	0.001	0.000	32.46	0.155	0.013	0.007512	0.002174	6.22E-08	1.321	9.073	0.563
5	0.529	0.00199	0.257	0.012	32.462	0.412	0.026	0.071	0.022	0.113	1.392	9.095	0.676
6	0.515	0.02	0.235	0.005	32.482	0.647	0.031	0.017	0.052	0.013	1.409	9.147	0.689
<b>7</b>	<b>0.474</b>	0.256	<b>50.036</b>	0.235	32.738	50.68	0.266	<b>8.365</b>	0.054	<b>5.624</b>	9.774	9.201	6.313
8	0.467	0.354	0.570	0.002	33.092	51.25	0.268	0.099	0.005087	0.097	9.873	9.206	6.41
9	0.455	0.228	0.000	0.000	33.32	51.25	0.268	8.05E-06	0.001483	0.001066	9.873	9.208	6.411
<b>10</b>	<b>0.433</b>	0.217	0.143	0.001	33.537	51.39	0.269	0.00175	0.251	<b>15.022</b>	9.875	9.458	21.43
11	0.428	0.34	0.001	0.000	33.877	51.39	0.269	2.84E-05	0.015	0.017	9.875	9.473	21.45
12	0.415	0.256	0.005	0.000	34.133	51.40	0.269	0.000383	0.013	0.024	9.875	9.486	21.47
13	0.404	0.029	0.278	0.004	34.162	51.68	0.273	0.051	0.005743	0.455	9.926	9.492	21.92
14	0.397	0.432	0.024	0.000	34.595	51.70	0.274	0.002054	0.059	2.139	9.928	9.551	24.06
15	0.396	0.146	0.000	0.000	34.74	51.70	0.274	0.000160	0.000504	0.04	9.928	9.552	24.10
16	0.361	0.189	0.039	0.006	34.93	51.74	0.279	7.28E-05	0.000869	0.074	9.928	9.553	24.18
17	0.361	0.00128	0.049	0.022	34.931	51.79	0.301	0.000944	0.002867	0.038	9.929	9.556	24.22
18	0.358	0.543	0.001	0.001	35.474	51.79	0.302	0.001093	0.001997	0.187	9.93	9.558	24.40
19	0.355	0.156	0.000	0.000	35.63	51.79	0.302	3.42E-05	4.27E-05	0.001786	9.93	9.558	24.41
20	0.351	0.065	0.002	0.002	35.695	51.79	0.304	0.001355	0.019	0.000050	9.931	9.577	24.41
21	0.347	0.045	0.003	0.000	35.74	51.79	0.304	0.001122	0.001732	0.025	9.933	9.578	24.43
22	0.346	0.061	0.006	0.000	35.801	51.80	0.304	1.62E-05	0.001898	0.015	9.933	9.58	24.45
23	0.342	0.081	0.006	0.001	35.882	51.81	0.304	0.006351	0.038	0.000106	9.939	9.619	24.45
24	0.341	0.262	0.000	0.000	36.143	51.81	0.304	2.96E-06	0.004575	0.000344	9.939	9.623	24.45
25	0.327	0.204	0.000	0.000	36.347	51.81	0.304	1.42E-05	0.004023	0.000058	9.939	9.627	24.45
26	0.320	0.173	0.000	0.000	36.52	51.81	0.304	0.000254	0.00081	0.004281	9.939	9.628	24.45
27	0.304	0.00104	0.207	0.349	36.521	52.01	0.653	8.96E-05	0.053	0.016	9.939	9.681	24.47
28	0.295	0.208	0.000	0.005	36.73	52.01	0.658	4.45E-05	0.008899	0.008498	9.939	9.69	24.47
29	0.275	0.151	0.007	0.001	36.881	52.02	0.659	0.000819	0.000164	0.002329	9.94	9.69	24.48
30	0.274	0.035	0.013	0.165	36.916	52.03	0.824	0.007353	0.033	0.022	9.947	9.724	24.50
31	0.273	0.288	0.000	0.021	37.204	52.03	0.846	5.97E-05	0.00478	0.033	9.948	9.728	24.53
32	0.263	0.228	0.000	0.000	37.432	52.03	0.846	9.08E-06	0.002083	0.000330	9.948	9.731	24.53
33	0.262	0.132	0.010	0.000	37.564	52.04	0.846	0.000226	0.000515	0.002427	9.948	9.731	24.53

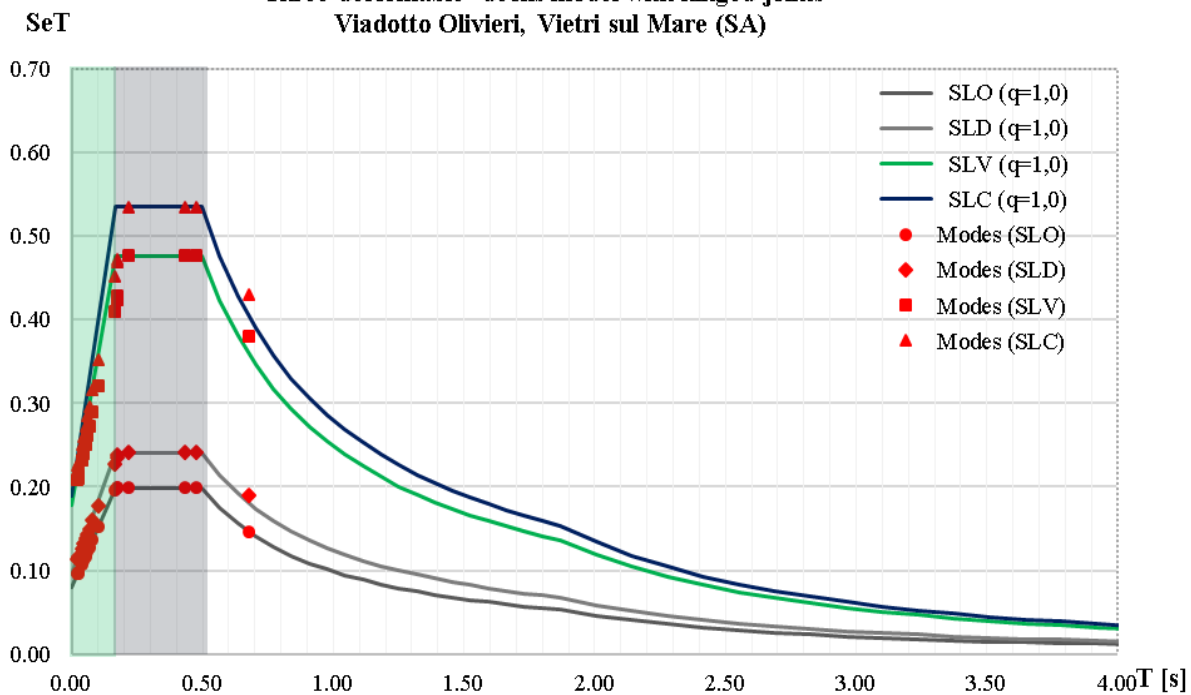
Mode	T [sec]	UX (%)	UY (%)	UZ (%)	Sum UX	Sum UY	Sum UZ	RX (%)	RY (%)	RZ (%)	Sum RX	Sum RY	Sum RZ
34	0.250	0.294	0.003	0.006	37.858	52.05	0.852	0.002375	0.064	0.000809	9.95	9.795	24.54
35	0.247	0.189	0.000	0.000	38.047	52.05	0.852	9.82E-05	0.002081	0.000014	9.95	9.797	24.54
36	0.243	0.334	0.001	0.013	38.381	52.05	0.865	0.017	0.041	0.001641	9.967	9.838	24.54
37	0.241	0.124	0.002	0.000	38.504	52.05	0.865	0.001117	1.60E-08	0.000387	9.968	9.838	24.54
38	0.234	0.27	0.006	0.010	38.775	52.06	0.875	0.012	0.14	0.000536	9.98	9.978	24.54
39	0.229	0.167	0.004	0.000	38.942	52.06	0.875	0.001516	0.003434	0.000368	9.982	9.982	24.54
40	0.224	0.927	0.002	0.027	39.868	52.06	0.902	0.053	0.286	0.00504	10.03	10.26	24.54
41	0.223	0.144	0.001	0.000	40.013	52.06	0.902	0.000702	0.000135	0.000056	10.03	10.26	24.54
<b>42</b>	<b>0.215</b>	<b>11.714</b>	0.094	0.000	51.726	52.16	0.903	0.57	4.281	0.047	10.60	14.54	24.59
43	0.210	0.476	0.002	0.071	52.202	52.16	0.973	0.021	0.32	0.000408	10.62	14.86	24.59
44	0.207	2.408	0.004	0.381	54.61	52.16	1.354	0.059	0.238	0.012	10.68	15.10	24.60
45	0.205	0.584	0.007	0.225	55.195	52.17	1.58	0.013	0.028	0.000300	10.69	15.13	24.60
46	0.202	0.019	0.003	0.000	55.214	52.17	1.58	0.001637	0.004575	0.001663	10.7	15.14	24.61
47	0.201	1.505	0.035	0.059	56.719	52.21	1.639	0.065	0.352	0.001796	10.76	15.49	24.61
48	0.197	0.976	0.003	0.077	57.695	52.21	1.715	0.000689	0.292	0.066	10.76	15.78	24.67
49	0.195	0.527	2.425	0.043	58.222	54.64	1.758	1.239	0.016	4.461	12.00	15.8	29.13
50	0.191	0.363	0.000	0.055	58.584	54.64	1.813	0.104	0.639	0.069	12.10	16.43	29.20
<b>51</b>	<b>0.183</b>	0.076	0.156	0.016	58.661	54.79	1.829	1.234	<b>6.767</b>	0.174	13.34	23.20	29.38
52	0.177	0.177	0.097	0.040	58.838	54.89	1.869	0.095	0.005408	0.023	13.43	23.21	29.40
<b>53</b>	<b>0.176</b>	0.095	7.698	0.195	58.933	62.59	2.064	3.787	0.005664	<b>9.074</b>	17.22	23.21	38.47
54	0.174	0.014	1.032	0.163	58.947	63.62	2.227	0.606	0.006939	1.282	17.83	23.22	39.76
<b>55</b>	<b>0.173</b>	0.233	0.509	<b>8.545</b>	59.18	64.13	10.77	1.321	0.883	1.119	19.15	24.10	40.88
57	0.165	3.0E-06	0.071	0.005	59.221	65.57	48.99	0.001756	0.001302	0.062	19.41	28.51	41.54
<b>58</b>	<b>0.162</b>	0.036	<b>5.903</b>	4.200	59.257	71.47	53.19	<b>9.076</b>	0.511	0.156	28.49	29.02	41.69
59	0.158	0.238	0.062	0.095	59.495	71.53	53.28	0.221	0.06	0.006221	28.71	29.08	41.70
60	0.156	0.037	1.052	1.121	59.532	72.58	54.40	4.029	0.055	0.177	32.74	29.13	41.88
61	0.153	0.022	0.017	0.008	59.554	72.60	54.41	0.058	0.193	0.106	32.8	29.33	41.98
62	0.151	0.012	0.272	1.582	59.565	72.87	55.99	1.466	0.163	0.166	34.26	29.49	42.15
63	0.149	0.0023	0.022	1.405	59.568	72.89	57.40	0.041	0.2	0.012	34.30	29.69	42.16
64	0.146	0.326	0.002	0.004	59.894	72.90	57.40	0.021	0.103	0.016	34.32	29.79	42.18
65	0.143	0.00026	0.016	0.001	59.894	72.91	57.40	0.001815	1.85E-05	0.051	34.33	29.79	42.23
66	0.142	0.0065	0.033	0.035	59.90	72.95	57.44	0.013	0.016	0.0009	34.34	29.81	42.23
67	0.135	0.244	0.000	0.037	60.14	72.95	57.48	0.051	0.061	0.0008	34.39	29.87	42.23
68	0.130	0.055	0.001	0.758	60.20	72.95	58.24	0.041	0.007447	0.0000	34.44	29.88	42.23
69	0.129	0.018	0.001	2.316	60.22	72.95	60.55	0.081	0.36	0.0110	34.52	30.24	42.24
70	0.124	0.067	0.025	0.018	60.29	72.98	60.57	0.012	0.00732	0.0160	34.53	30.25	42.26
71	0.121	0.043	0.000	0.000	60.33	72.98	60.57	0.017	0.001056	0.0180	34.55	30.25	42.28



Mode	T [sec]	UX (%)	UY (%)	UZ (%)	Sum UX	Sum UY	Sum UZ	RX (%)	RY (%)	RZ (%)	Sum RX	Sum RY	Sum RZ
72	0.111	0.362	0.007	0.018	60.69	72.99	60.59	0.041	0.249	0.0130	34.59	30.50	42.29
73	0.108	0.526	0.056	0.018	61.22	73.04	60.61	0.031	0.331	0.0300	34.62	30.83	42.32
74	0.107	3.133	0.003	0.008	64.35	73.04	60.62	0.001072	0.07	0.2240	34.62	30.90	42.55
75	0.103	1.041	0.005	0.507	65.39	73.05	61.12	0.013	0.121	0.0270	34.63	31.02	42.57
76	0.102	0.33	0.000	0.001	65.72	73.05	61.12	0.068	0.274	3.4240	34.70	31.29	46.00
<b>77</b>	<b>0.100</b>	<b>12.568</b>	0.012	0.076	78.29	73.06	61.20	0.000756	0.166	0.2440	34.70	31.46	46.24
78	0.089	1.572	0.040	0.129	79.86	73.10	61.33	0.352	0.674	0.0440	35.05	32.13	46.29
79	0.086	0.01	0.653	0.672	79.87	73.75	62.00	0.163	0.027	0.4220	35.22	32.16	46.71
80	0.084	0.841	0.648	0.065	80.71	74.40	62.07	0.106	0.003074	1.5300	35.32	32.16	48.24
81	0.082	0.459	0.306	0.033	81.17	74.71	62.10	0.015	0.358	3.4990	35.34	32.52	51.74
<b>82</b>	<b>0.077</b>	0.195	4.837	0.056	81.36	79.55	62.16	0.602	1.145	<b>6.9090</b>	35.94	33.67	58.65
<b>83</b>	<b>0.074</b>	0.021	0.026	0.400	81.39	79.57	62.56	<b>5.731</b>	0.071	2.5220	41.67	33.74	61.17
84	0.071	0.031	0.013	2.244	81.42	79.58	64.80	0.094	0.073	0.0006	41.76	33.81	61.17
85	0.065	2.94	0.484	0.358	84.36	80.07	65.16	3.51	1.99	0.0000	45.27	35.80	61.17
<b>86</b>	<b>0.064</b>	0.47	2.887	0.000	84.83	82.96	65.16	8.757	0.543	0.1640	54.03	36.34	61.33
<b>87</b>	<b>0.058</b>	0.404	0.563	<b>8.583</b>	85.23	83.52	73.74	0.162	2.122	3.6850	54.19	38.46	65.02
88	0.056	0.254	1.227	1.450	85.48	84.75	75.19	1.089	0.052	2.3400	55.28	38.52	67.36
<b>89</b>	<b>0.052</b>	5.53	0.090	0.229	91.01	84.84	75.42	1.574	1.321	0.5410	56.85	39.84	67.90
90	0.046	1.368	2.606	0.569	92.38	87.44	75.99	1.774	0.522	0.3070	58.63	40.36	68.21
<b>91</b>	<b>0.045</b>	0.32	0.018	<b>9.712</b>	92.70	87.46	85.70	0.009182	<b>5.335</b>	0.8520	58.64	45.69	69.06
<b>92</b>	<b>0.041</b>	0.00212	0.839	0.038	92.70	88.30	85.74	0.02	0.135	<b>6.4680</b>	58.66	45.83	75.53
93	0.038	3.013	0.048	0.028	95.72	88.35	85.77	0.658	1.871	0.0490	59.32	47.70	75.58
<b>94</b>	<b>0.033</b>	0.018	0.861	<b>7.330</b>	95.74	89.21	93.10	0.149	1.813	0.1100	59.46	49.51	75.69
95	0.031	0.258	4.976	0.589	95.99	94.18	93.69	1.443	0.878	0.9150	60.91	50.39	76.60
<b>96</b>	<b>0.030</b>	0.265	0.146	0.008	96.26	94.33	93.69	0.392	0.126	<b>13.0320</b>	61.30	50.52	89.63
97	0.017	2.47	0.012	0.047	98.73	94.34	93.74	0.087	0.247	0.0120	61.39	50.76	89.64
<b>98</b>	<b>0.016</b>	0.011	4.188	0.172	98.74	98.53	93.91	<b>6.004</b>	0.076	0.0017	67.39	50.84	89.65
<b>99</b>	<b>0.016</b>	0.031	0.101	0.000	98.77	98.63	93.91	0.301	0.052	<b>7.9410</b>	67.69	50.89	97.59
<b>100</b>	0.014	0.024	0.058	3.859	<b>98.79</b>	<b>98.69</b>	<b>97.77</b>	0.497	0.006349	0.0000	<b>68.19</b>	<b>50.90</b>	<b>97.59</b>

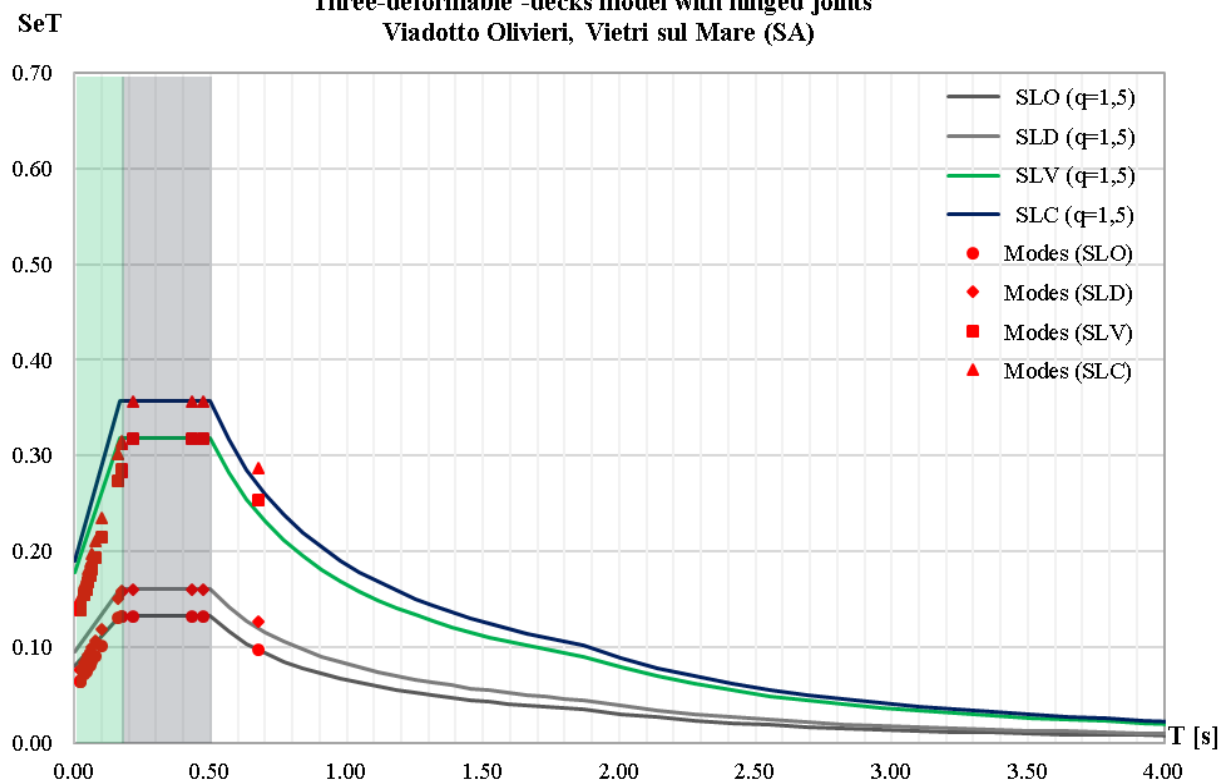
Considering previous output data, it could be said that: modes with relatively high effects represent translational local modes; periods associated to main modes are lower than 1sec, characterizing a really rigid structure; comparing different modal deformed shapes, it seems that only few macro-elements are involved in each mode; Modes fall within the first two spectrum section, above all in the previous one.

**ACCELERATION DESIGN RESPONSE SPECTRUM**  
**Three-deformable -decks model with hinged joints**  
**Viadotto Olivieri, Vietri sul Mare (SA)**



*Importance class (NTC 08): IV. Nominal life: 100 years % damping: 5% Soil class: B  $q=1,0$*

**ACCELERATION DESIGN RESPONSE SPECTRUM**  
**Three-deformable -decks model with hinged joints**  
**Viadotto Olivieri, Vietri sul Mare (SA)**



*Importance class (NTC 08): IV. Nominal life: 100 years % damping: 5% Soil class: B  $q=1,5$*

### 7.3.3 Single undeformable deck with fixed joints

Modal analysis is performed considering 100 vibration modes:

Modal analysis output: Three- deformable - decks model with fixed joints													
Mode	T [sec]	UX (%)	UY (%)	UZ (%)	Sum UX	Sum UY	Sum UZ	RX (%)	RY /%)	RZ (%)	Sum RX	Sum RY	Sum RZ
1	0.51	0.2540	0.0000	0.0000	0.2540	0.0000	0.0000	0.000	0.010	0.004	0.000	0.010	0.004
2	0.43	0.2660	0.0000	0.0000	0.5210	0.0000	0.0000	0.000	0.009	0.001	0.000	0.019	0.005
3	0.42	0.1970	0.0000	0.0000	0.7180	0.0000	0.0000	0.000	0.004	0.003	0.000	0.023	0.008
4	0.41	0.1950	0.0000	0.0001	0.9130	0.0000	0.0001	0.000	0.006	0.000	0.000	0.029	0.008
5	0.41	0.5460	0.0040	0.0092	1.4600	0.0040	0.0093	0.007	0.092	0.003	0.007	0.121	0.011
6	0.41	0.5570	0.0036	0.0110	2.0170	0.0076	0.0200	0.012	0.061	0.003	0.020	0.182	0.014
7	0.36	0.1930	0.0000	0.0002	2.2100	0.0076	0.0200	0.000	0.010	0.009	0.020	0.192	0.022
8	0.36	0.1320	0.0060	0.0000	2.3420	0.0140	0.0200	0.001	0.002	0.007	0.021	0.194	0.029
9	0.36	0.5780	0.0040	0.0061	2.9200	0.0180	0.0260	0.014	0.084	0.005	0.035	0.278	0.034
10	0.35	0.4680	0.0033	0.0087	3.3880	0.0210	0.0350	0.003	0.047	0.004	0.038	0.325	0.038
11	0.34	0.2060	0.0000	0.0000	3.5940	0.0210	0.0350	0.000	0.006	0.000	0.038	0.331	0.038
12	0.34	0.1710	0.0015	0.0010	3.7640	0.0220	0.0360	0.009	0.053	0.000	0.048	0.383	0.039
13	0.34	0.0069	0.0000	0.0190	3.7710	0.0220	0.0550	0.000	0.000	0.000	0.048	0.383	0.039
14	0.33	0.1790	0.0000	0.0000	3.9510	0.0220	0.0550	0.000	0.003	0.003	0.048	0.386	0.041
15	0.33	0.1780	0.0000	0.0000	4.1290	0.0220	0.0550	0.000	0.004	0.000	0.048	0.391	0.042
16	0.32	0.5520	0.0040	0.0300	4.6810	0.0260	0.0850	0.046	0.213	0.008	0.093	0.603	0.050
17	0.32	0.2850	0.0019	0.0580	4.9660	0.0280	0.1430	0.010	0.200	0.004	0.103	0.803	0.054
18	0.29	0.1310	0.0000	0.0010	5.0960	0.0280	0.1440	0.000	0.001	0.002	0.103	0.804	0.056
19	0.29	0.1570	0.0000	0.0000	5.2530	0.0280	0.1440	0.000	0.004	0.006	0.103	0.808	0.062
20	0.28	0.1190	0.0060	0.0001	5.3730	0.0340	0.1440	0.001	0.000	0.004	0.104	0.808	0.066
21	0.27	0.6630	0.0042	0.0170	6.0360	0.0390	0.1610	0.080	0.500	0.011	0.183	1.309	0.077
22	0.27	0.2070	0.0015	0.0750	6.2430	0.0400	0.2360	0.003	0.077	0.003	0.187	1.386	0.080
23	0.26	0.1850	0.0000	0.0000	6.4280	0.0400	0.2360	0.000	0.003	0.000	0.187	1.388	0.080
24	0.26	0.1230	0.0053	0.0000	6.5510	0.0450	0.2360	0.001	0.001	0.000	0.188	1.389	0.080
25	0.26	0.3770	0.0033	0.0032	6.9280	0.0490	0.2390	0.021	0.130	0.002	0.209	1.519	0.083
26	0.25	0.3810	0.0023	0.0008	7.3090	0.0510	0.2400	0.022	0.190	0.002	0.231	1.709	0.085
27	0.25	0.1510	0.0000	0.0000	7.4600	0.0510	0.2400	0.000	0.003	0.000	0.231	1.712	0.085
28	0.25	0.0920	0.0040	0.0001	7.5520	0.0550	0.2400	0.002	0.004	0.009	0.232	1.715	0.094
29	0.23	0.1410	0.0000	0.0000	7.6930	0.0550	0.2400	0.000	0.007	0.006	0.232	1.723	0.099
30	0.23	0.1380	0.0000	0.0000	7.8310	0.0550	0.2400	0.000	0.005	0.002	0.232	1.728	0.101
<b>31</b>	<b>0.22</b>	<b>6.0290</b>	<b>0.0440</b>	<b>0.0540</b>	<b>13.8600</b>	<b>0.0990</b>	<b>0.2940</b>	<b>2.426</b>	<b>17.840</b>	<b>0.014</b>	<b>2.658</b>	<b>19.568</b>	<b>0.115</b>
32	0.22	0.0390	0.0001	0.0001	13.8990	0.0990	0.2940	0.006	0.035	0.001	2.664	19.604	0.117
33	0.21	0.0750	0.0003	0.0002	13.9730	0.0990	0.2950	0.177	1.331	0.001	2.841	20.934	0.118
34	0.20	0.0007	0.0001	0.0170	13.9740	0.0990	0.3110	0.087	0.623	0.000	2.929	21.558	0.118
35	0.20	0.0064	0.0001	0.0012	13.9800	0.0990	0.3130	0.056	0.382	0.003	2.984	21.939	0.121
36	0.19	0.0280	0.0001	0.0150	14.0090	0.0990	0.3280	0.020	0.159	0.002	3.005	22.098	0.123
37	0.18	0.0200	0.0011	0.0250	14.0290	0.1000	0.3520	0.016	0.244	0.002	3.021	22.342	0.125
38	0.18	0.0390	0.0000	0.0800	14.0680	0.1000	0.4320	0.030	0.091	0.001	3.050	22.433	0.126
39	0.18	0.0930	0.0037	0.0200	14.1610	0.1040	0.4520	0.001	0.001	0.000	3.052	22.434	0.126
40	0.17	0.1120	0.0000	0.0000	14.2730	0.1040	0.4520	0.000	0.002	0.002	3.052	22.436	0.128
41	0.17	0.0014	0.0310	53.4750	14.2740	0.1350	53.9270	0.022	5.877	0.003	3.073	28.313	0.131
42	0.16	0.0000	0.0240	0.0780	14.2740	0.1590	54.0050	0.001	0.014	0.002	3.074	28.327	0.133
43	0.16	0.1100	0.0000	0.0000	14.3840	0.1590	54.0050	0.000	0.000	0.000	3.074	28.327	0.134
44	0.16	0.0007	0.0000	0.0007	14.3850	0.1590	54.0060	0.000	0.002	0.000	3.074	28.329	0.134

Mode	T [sec]	UX (%)	UY (%)	UZ (%)	Sum UX	Sum UY	Sum UZ	RX (%)	RY /%)	RZ (%)	Sum RX	Sum RY	Sum RZ
45	0.15	0.0270	0.0001	1.7450	14.4110	0.1600	55.7500	0.005	0.368	0.000	3.079	28.697	0.134
46	0.15	0.0094	0.0004	1.7340	14.4210	0.1600	57.4840	0.003	0.115	0.000	3.082	28.812	0.134
47	0.15	0.0670	0.0000	0.0001	14.4880	0.1600	57.4840	0.000	0.000	0.003	3.082	28.812	0.137
48	0.14	0.0890	0.0000	0.0000	14.5780	0.1600	57.4840	0.000	0.000	0.000	3.082	28.813	0.137
49	0.14	0.0450	0.0007	0.1340	14.6230	0.1610	57.6180	0.000	0.002	0.003	3.082	28.815	0.140
50	0.14	0.0210	0.0011	0.0540	14.6440	0.1620	57.6720	0.002	0.067	0.000	3.084	28.882	0.140
51	0.14	0.0025	0.0001	1.0350	14.6470	0.1620	58.7070	0.008	0.100	0.000	3.092	28.982	0.141
52	0.14	0.0890	0.0000	0.1610	14.7360	0.1620	58.8680	0.023	0.000	0.005	3.115	28.982	0.145
53	0.14	0.0100	0.0001	0.0540	14.7460	0.1620	58.9220	0.003	0.000	0.001	3.118	28.982	0.146
54	0.13	0.0290	0.0000	1.3450	14.7760	0.1620	60.2670	0.019	0.111	0.001	3.137	29.093	0.148
55	0.13	0.0510	0.0038	0.4970	14.8270	0.1660	60.7640	0.028	0.080	0.001	3.165	29.173	0.149
56	0.13	0.0560	0.0000	0.1140	14.8830	0.1660	60.8780	0.019	0.108	0.000	3.183	29.281	0.149
57	0.13	0.0003	0.0000	0.0008	14.8830	0.1660	60.8780	0.002	0.001	0.000	3.185	29.282	0.149
58	0.12	0.0039	0.0000	0.0006	14.8870	0.1660	60.8790	0.000	0.004	0.000	3.186	29.286	0.149
59	0.12	0.2260	0.0002	0.0078	15.1120	0.1660	60.8870	0.063	1.209	0.020	3.248	30.494	0.169
60	0.12	0.0009	0.0085	0.3020	15.1130	0.1740	61.1890	0.540	0.002	0.002	3.788	30.496	0.171
61	0.11	0.0890	0.0002	0.0001	15.2030	0.1750	61.1890	0.005	0.017	0.000	3.793	30.514	0.171
62	0.11	0.0480	0.0057	0.0021	15.2500	0.1800	61.1910	0.096	0.592	0.024	3.889	31.105	0.194
<b>63</b>	<b>0.11</b>	0.0014	0.6470	0.0099	15.2520	0.8270	61.2010	<b>23.091</b>	0.000	0.185	26.980	31.106	0.379
64	0.10	0.0047	0.0510	0.0540	15.2560	0.8780	61.2540	1.208	0.009	0.017	28.188	31.114	0.396
65	0.10	0.1900	0.0025	0.0550	15.4460	0.8810	61.3090	0.002	0.009	0.001	28.190	31.123	0.398
66	0.10	0.0340	0.0013	0.0310	15.4810	0.8820	61.3410	0.007	0.000	0.003	28.197	31.124	0.401
67	0.10	0.0015	0.0790	0.3210	15.4820	0.9610	61.6610	1.017	0.013	0.024	29.214	31.136	0.425
68	0.10	0.1800	0.0025	0.0018	15.6620	0.9640	61.6630	0.054	0.001	0.002	29.268	31.138	0.427
69	0.09	0.1360	0.0150	0.0011	15.7980	0.9780	61.6640	0.006	0.171	0.004	29.275	31.308	0.431
70	0.09	0.0480	0.0005	0.0190	15.8460	0.9790	61.6830	0.023	0.123	0.122	29.297	31.431	0.553
71	0.09	0.0084	0.0024	0.0088	15.8550	0.9810	61.6920	0.000	0.109	0.674	29.298	31.540	1.227
72	0.08	0.0059	0.0047	0.0190	15.8610	0.9860	61.7110	0.249	0.856	0.378	29.547	32.396	1.605
73	0.08	0.2370	0.0001	0.0016	16.0980	0.9860	61.7130	0.009	0.035	0.000	29.556	32.431	1.605
74	0.08	0.0014	0.0570	0.0100	16.0990	1.0430	61.7230	0.348	0.383	0.043	29.904	32.815	1.648
75	0.07	0.0350	0.0410	0.4360	16.1340	1.0840	62.1590	0.587	0.678	0.003	30.491	33.493	1.651
76	0.07	0.0074	1.2540	0.1400	16.1420	2.3380	62.2990	9.585	0.003	0.169	40.077	33.496	1.819
77	0.07	1.8560	0.0025	0.0750	17.9970	2.3410	62.3740	0.152	2.558	0.153	40.229	36.054	1.972
78	0.07	0.1010	0.5640	2.8580	18.0990	2.9050	65.2320	0.814	0.201	0.009	41.042	36.255	1.982
79	0.06	0.0220	0.0001	0.1430	18.1200	2.9050	65.3740	0.559	0.653	0.769	41.601	36.908	2.751
<b>80</b>	<b>0.06</b>	0.0540	<b>5.0330</b>	1.9080	18.1740	7.9380	67.2820	<b>6.062</b>	3.663	0.148	47.663	40.571	2.899
<b>81</b>	<b>0.06</b>	<b>8.7810</b>	0.0350	0.0360	26.9550	7.9730	67.3190	0.013	1.048	0.009	47.676	41.619	2.908
<b>82</b>	<b>0.06</b>	0.0940	0.5630	<b>4.1640</b>	27.0490	8.5360	71.4830	1.840	0.641	0.203	49.516	42.260	3.111
83	0.05	0.0160	0.0770	1.2460	27.0660	8.6120	72.7290	0.053	3.474	1.536	49.569	45.734	4.647
<b>84</b>	<b>0.05</b>	0.0002	<b>7.9210</b>	1.2380	27.0660	16.5330	73.9670	0.036	0.996	0.168	49.605	46.730	4.815
<b>85</b>	<b>0.05</b>	2.1150	0.0160	<b>4.6110</b>	29.1800	16.5490	78.5770	1.435	0.529	0.634	51.040	47.258	5.449
86	0.05	2.6920	0.2890	3.5120	31.8730	16.8380	82.0900	0.954	0.455	0.162	51.994	47.713	5.611
87	0.04	0.0002	0.6260	0.0000	31.8730	17.4640	82.0900	0.425	0.693	7.480	52.419	48.407	13.091
<b>88</b>	<b>0.04</b>	0.2230	<b>28.2880</b>	0.5980	32.0950	45.7530	82.6880	0.051	0.425	0.075	52.470	48.832	13.167
<b>89</b>	<b>0.04</b>	0.4020	0.8200	<b>8.0460</b>	32.4970	46.5720	90.7350	0.113	3.294	1.353	52.583	52.126	14.520
<b>90</b>	<b>0.03</b>	2.2950	0.2200	0.2120	34.7920	46.7920	90.9470	0.149	0.026	<b>29.147</b>	52.732	52.153	43.666
91	0.03	1.2380	5.0490	0.0400	36.0300	51.8410	90.9860	0.726	0.220	3.484	53.457	52.372	47.151
<b>92</b>	<b>0.03</b>	<b>7.0890</b>	1.2700	0.2480	43.1200	53.1110	91.2340	0.029	0.135	0.534	53.487	52.507	47.684

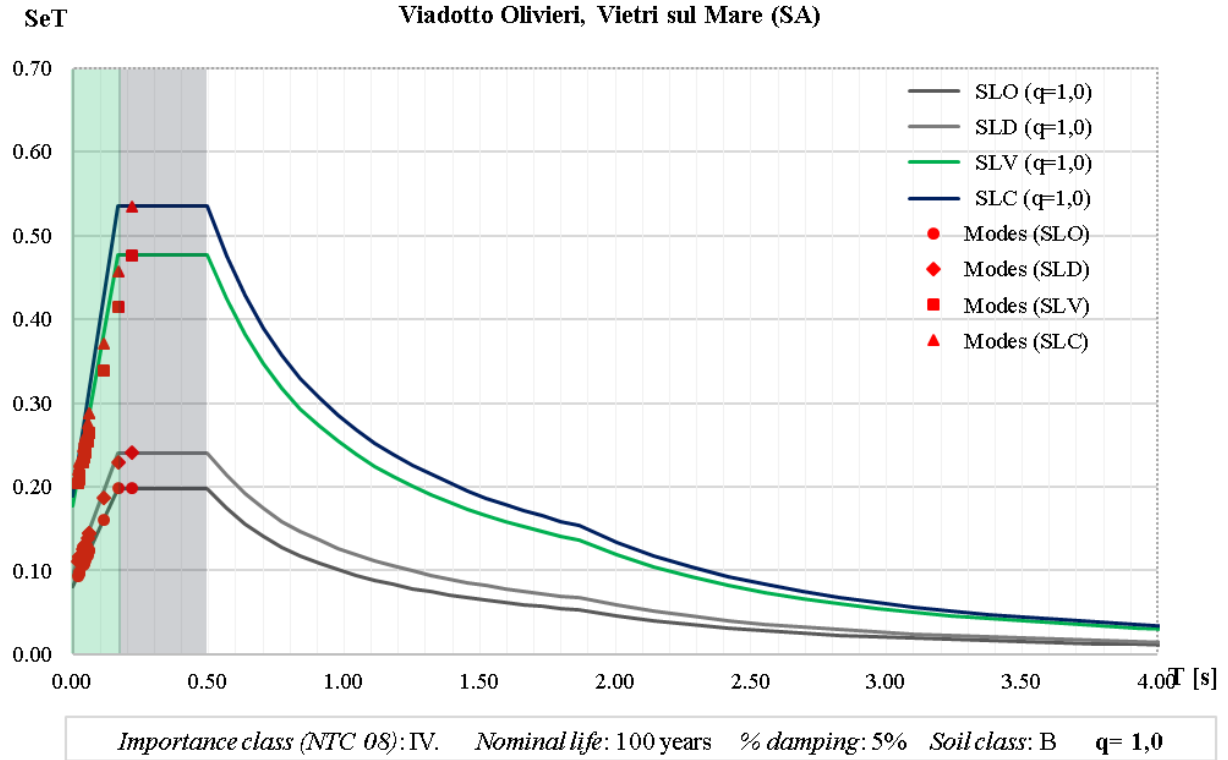


Mode	T [sec]	UX (%)	UY (%)	UZ (%)	Sum UX	Sum UY	Sum UZ	RX (%)	RY /%)	RZ (%)	Sum RX	Sum RY	Sum RZ
93	0.03	7.6590	0.2560	2.3740	50.7790	53.3670	93.6080	0.040	1.794	0.016	53.527	54.301	47.700
94	0.03	15.3470	0.0420	0.9380	66.1250	53.4080	94.5460	0.294	0.441	0.177	53.821	54.742	47.877
95	0.02	0.0770	2.0450	0.1000	66.2020	55.4530	94.6460	0.001	0.171	6.794	53.822	54.913	54.670
96	0.02	0.0330	8.5630	0.0018	66.2350	64.0170	94.6480	0.901	0.110	1.863	54.723	55.023	56.534
97	0.01	0.2160	0.0160	3.5560	66.4510	64.0330	98.2030	0.021	0.084	0.135	54.744	55.107	56.668
98	0.01	0.9690	0.0350	0.1260	67.4200	64.0680	98.3290	0.057	0.012	7.839	54.802	55.120	64.507
99	0.01	5.0230	0.0096	0.0470	72.4430	64.0780	98.3760	0.062	0.001	1.967	54.864	55.120	66.474
100	0.01	0.0100	8.6410	0.0004	72.4530	72.7190	98.3760	0.522	0.003	0.094	55.386	55.123	66.568

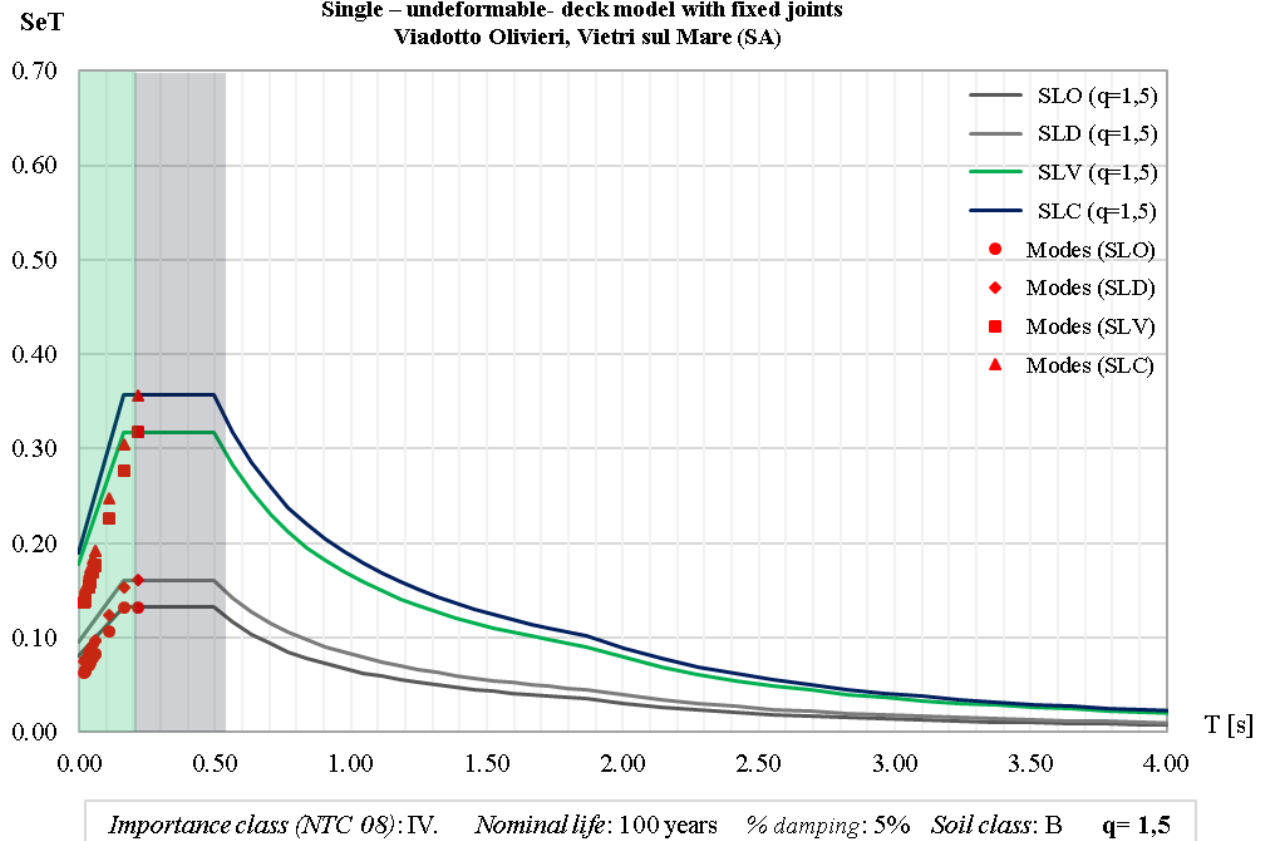
Considering previous output data, it could be said that:

- considering that the assumption of continuous rigid deck increases static redundancy, 100 modes are not sufficient to involve all participating mass;
- modes with relatively high effects represent translational local modes, above all in vertical direction;
- periods associated to main modes are lower than 1sec, characterizing a really rigid structure;
- comparing different modal deformed shapes, it seems that only few macro-elements are involved in each mode;
- modes fall within the first two spectrum sections, above all in the previous one

**ACCELERATION DESIGN RESPONSE SPECTRUM**  
**Single – undeformable- deck model with fixed joints**  
**Viadotto Olivieri, Vietri sul Mare (SA)**



**ACCELERATION DESIGN RESPONSE SPECTRUM**  
**Single – undeformable- deck model with fixed joints**  
**Viadotto Olivieri, Vietri sul Mare (SA)**



### 7.3.4 Single undeformable deck with hinged joints

Modal analysis is performed considering 100 vibration modes:

Modal analysis output: Single undeformable deck with hinged joints													
Mode	T [sec]	UX (%)	UY (%)	UZ (%)	Sum UX	Sum UY	Sum UZ	RX (%)	RY (%)	RZ (%)	Sum RX	Sum RY	Sum RZ
1	0.512	0.254	0.0000	0.0000	0.2540	0.000	0.0000	2.15E-06	0.00950	0.00419	2.1E-06	0.009	0.0041
2	0.427	0.266	0.0000	0.0000	0.5210	0.000	0.0000	0.000010	0.00904 4	0.00055	0.0001	0.019	0.0047
3	0.420	0.197	0.0000	0.0000	0.7180	0.000	0.0000	6.09E-08	0.00426	0.00331	0.0001	0.023	0.0080
4	0.415	0.195	0.0000	0.0001	0.9130	0.000	0.0001	0.000542	0.00604 6	0.00036	0.0006	0.029	0.0084
5	0.412	0.547	0.0040	0.0092	1.4600	0.004	0.0094	0.007298	0.093	0.00248	0.0736	0.121	0.011
6	0.407	0.557	0.0036	0.0110	2.0170	0.007	0.0200	0.012	0.061	0.00261	0.02	0.182	0.014
7	0.365	0.193	0.0000	0.0002	2.2110	0.007	0.0200	0.000075	0.01	0.00851	0.02	0.192	0.022
8	0.363	0.132	0.0060	0.0000	2.3430	0.014	0.0200	0.001306	0.00196	0.00726	0.021	0.194	0.029
9	0.356	0.578	0.0040	0.0061	2.9210	0.018	0.0270	0.014	0.085	0.00494	0.035	0.279	0.034
10	0.354	0.468	0.0033	0.0087	3.3890	0.021	0.0350	0.003456	0.047	0.00371	0.038	0.326	0.038
11	0.341	0.206	0.0000	0.0000	3.5950	0.021	0.0350	3.88E-06	0.00570	0.00046	0.039	0.332	0.038
12	0.340	0.17	0.0015	0.0011	3.7650	0.020	0.0360	0.009343	0.053	0.00008	0.048	0.385	0.039
13	0.337	0.006	0.0000	0.0190	3.7720	0.020	0.0550	0.000079	5.2E-06	0.00002	0.048	0.385	0.039
14	0.327	0.179	0.0000	0.0000	3.9510	0.022	0.0550	2.57E-06	0.00307	0.00286	0.048	0.388	0.041
15	0.327	0.178	0.0000	0.0000	4.1290	0.022	0.0550	0.000001	0.00441	0.00027	0.048	0.392	0.042
16	0.323	0.554	0.0041	0.0300	4.6830	0.026	0.0850	0.046	0.214	0.00785	0.094	0.606	0.05
17	0.322	0.285	0.0019	0.0580	4.9680	0.028	0.1430	0.009321	0.201	0.00388	0.103	0.807	0.053
18	0.295	0.13	0.0000	0.0010	5.0990	0.028	0.1440	0.000267	0.00102	0.00221	0.104	0.808	0.056
19	0.295	0.157	0.0000	0.0000	5.2560	0.028	0.1440	3.38E-06	0.00401	0.00622	0.104	0.812	0.062
20	0.275	0.119	0.0060	0.0001	5.3750	0.034	0.1440	0.000513	3.2E-05	0.00353	0.104	0.812	0.065
21	0.274	0.665	0.0042	0.0180	6.0400	0.039	0.1620	0.08	0.504	0.011	0.184	1.316	0.076
22	0.273	0.209	0.0015	0.0750	6.2480	0.040	0.2370	0.003278	0.078	0.00308	0.188	1.394	0.079
23	0.263	0.185	0.0000	0.0000	6.4340	0.040	0.2370	2.84E-07	0.00275	0.00038	0.188	1.397	0.08
24	0.262	0.123	0.0053	0.0000	6.5560	0.045	0.2370	0.001132	0.00101	0.00032	0.189	1.398	0.08
25	0.257	0.378	0.0033	0.0032	6.9340	0.049	0.2400	0.021	0.131	0.00223	0.21	1.529	0.082
26	0.249	0.381	0.0023	0.0009	7.3150	0.051	0.2410	0.022	0.191	0.00211 9	0.232	1.719	0.085
27	0.247	0.151	0.0000	0.0000	7.4660	0.051	0.2410	3.56E-07	0.00255	0.00022	0.232	1.722	0.085
28	0.246	0.092	0.0040	0.0001	7.5580	0.055	0.2410	0.001571	0.00380	0.00894	0.233	1.726	0.094
29	0.230	0.141	0.0000	0.0000	7.6990	0.055	0.2410	0.000231	0.00734	0.00552	0.233	1.733	0.099
30	0.229	0.138	0.0000	0.0000	7.8370	0.055	0.2410	0.000018	0.00506	0.00184	0.233	1.738	0.101
<b>31</b>	<b>0.219</b>	<b>6.024</b>	0.0440	0.0530	13.862	0.098	0.2940	2.429	<b>17.897</b>	0.014	2.663	19.63	0.115
32	0.217	0.042	0.0001	0.0001	13.903	0.099	0.2940	0.0053	0.031	0.00131	2.668	19.66	0.116
33	0.208	0.071	0.0003	0.0002	13.975	0.099	0.2940	0.174	1.311	0.00100	2.841	20.97	0.117
34	0.202	0.001	0.0000	0.0170	13.975	0.099	0.3110	0.086	0.616	0.00040	2.928	21.59	0.117
35	0.197	0.006	0.0001	0.0013	13.982	0.099	0.3120	0.055	0.378	0.00252	2.982	21.97	0.12
36	0.191	0.029	0.0001	0.0150	14.010	0.099	0.3270	0.02	0.158	0.00230	3.003	22.12	0.122
37	0.184	0.02	0.0011	0.0260	14.031	0.100	0.3530	0.016	0.243	0.00171	3.018	22.37	0.124
38	0.178	0.039	0.0000	0.0810	14.070	0.100	0.4340	0.03	0.09	0.00135	3.048	22.46	0.125
39	0.177	0.093	0.0037	0.0200	14.163	0.104	0.4540	0.001185	0.00055	0.00003	3.049	22.46	0.125

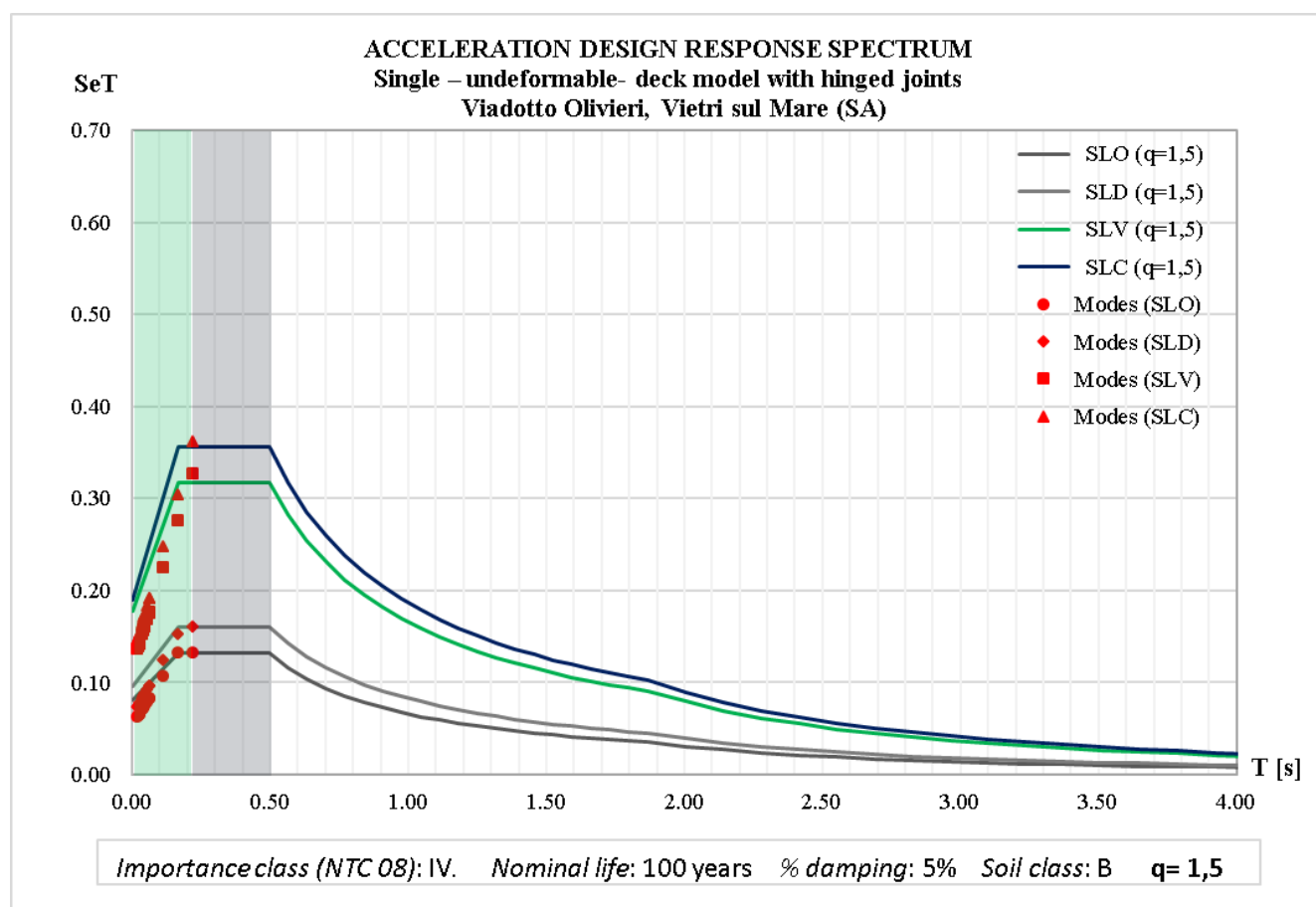
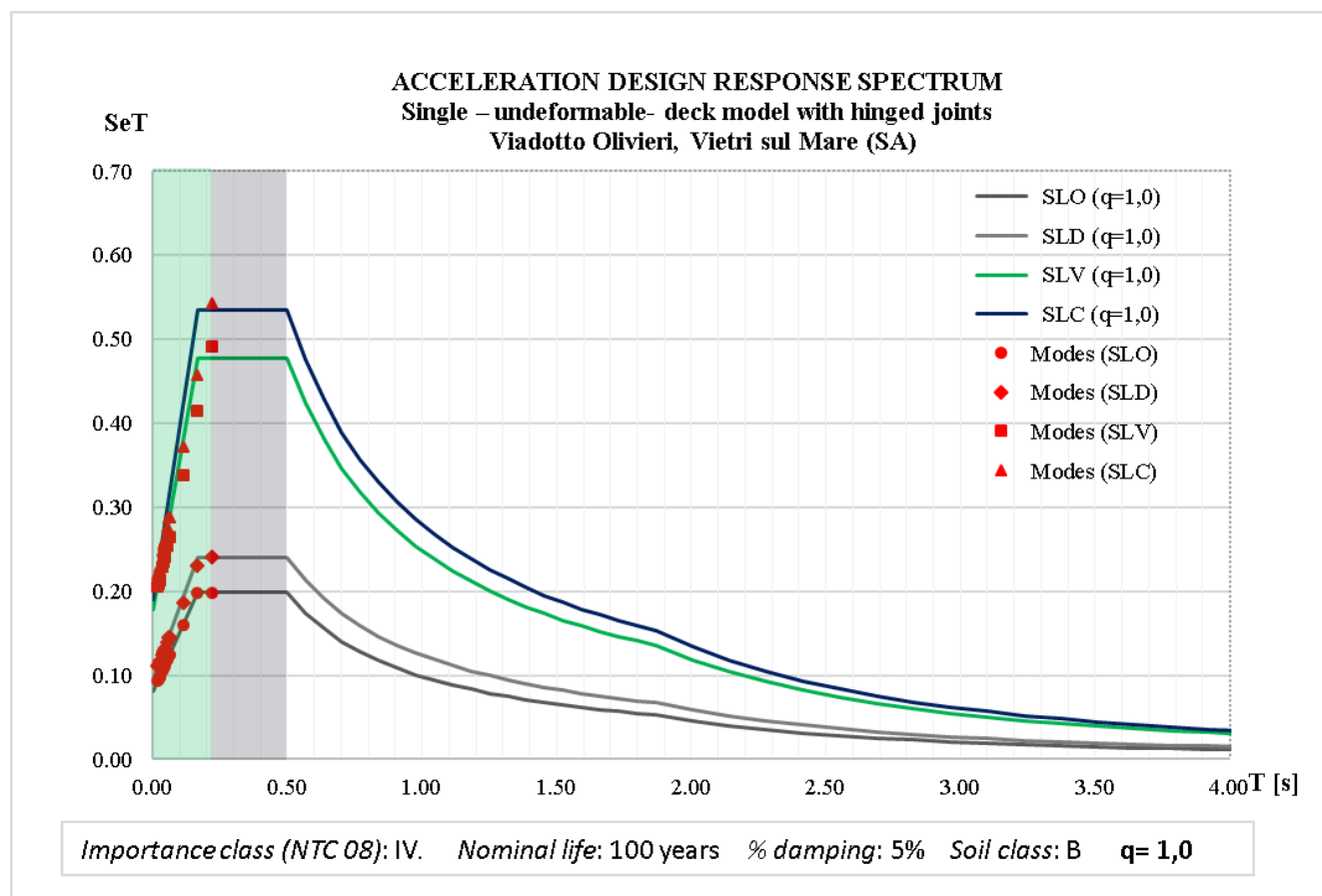
Mode	T [sec]	UX (%)	UY (%)	UZ (%)	Sum UX	Sum UY	Sum UZ	RX (%)	RY (%)	RZ (%)	Sum RX	Sum RY	Sum RZ
40	0.173	0.112	0.0000	0.0000	14.275	0.104	0.4540	1.59E-07	0.00176	0.00161	3.049	22.46	0.127
<b>41</b>	<b>0.165</b>	0.001	0.0280	53.260	14.276	0.132	53.714	0.02	<b>5.839</b>	0.00289	3.07	28.30	0.13
42	0.164	3E-05	0.0280	0.3270	14.276	0.160	54.041	0.000207	0.048	0.00277	3.07	28.35	0.133
43	0.159	0.11	0.0000	0.0000	14.380	0.160	54.041	5.6E-07	0.00035	0.000254	3.07	28.35	0.133
44	0.157	0.0006	0.0000	0.0007	14.387	0.160	54.041	9.18E-06	0.00205	6.40E-06	3.07	28.35	0.133
45	0.153	0.027	0.0001	1.7350	14.414	0.160	55.777	0.004444	0.367	0.000361	3.074	28.72	0.133
46	0.148	0.0094	0.0004	1.7200	14.423	0.161	57.497	0.003355	0.113	0.000455	3.078	28.83	0.134
47	0.147	0.067	0.0000	0.0001	14.491	0.161	57.497	8.4E-06	7.2E-05	0.002955	3.078	28.83	0.137
48	0.142	0.089	0.0000	0.0000	14.580	0.161	57.497	5.27E-07	0.00043	0.000124	3.078	28.83	0.137
49	0.141	0.045	0.0007	0.1340	14.625	0.161	57.631	0.000059	0.0024	0.002717	3.078	28.83	0.139
50	0.140	0.022	0.0011	0.0550	14.647	0.162	57.686	0.002221	0.067	0.000451	3.08	28.90	0.14
51	0.139	0.0024	0.0001	1.0340	14.649	0.162	58.719	0.008667	0.1	0.000075	3.089	29.00	0.14
52	0.138	0.089	0.0001	0.1580	14.739	0.162	58.878	0.023	0.00013	0.005049	3.112	29.00	0.145
53	0.136	0.01	0.0001	0.0540	14.749	0.163	58.932	0.003266	0.00036	0.00107	3.115	29.00	0.146
54	0.135	0.029	0.0000	1.3450	14.778	0.163	60.277	0.019	0.111	0.001222	3.134	29.11	0.147
55	0.134	0.051	0.0039	0.4930	14.829	0.166	60.770	0.029	0.079	0.000863	3.163	29.19	0.148
56	0.132	0.056	0.0000	0.1130	14.885	0.167	60.883	0.018	0.108	0.000197	3.181	29.30	0.148
57	0.128	0.0003	0.0000	0.0007	14.885	0.167	60.884	0.002033	0.00065	1.93E-06	3.183	29.31	0.148
58	0.125	0.0038	0.0000	0.0007	14.889	0.167	60.885	0.000223	0.00395	0.000022	3.184	29.30	0.148
59	0.121	0.226	0.0001	0.0085	15.115	0.167	60.893	0.06	1.205	0.022	3.244	30.51	0.171
60	0.116	0.0009	0.0077	0.3010	15.116	0.174	61.194	0.511	0.00184	0.001372	3.755	30.51	0.172
61	0.115	0.093	0.0003	0.0002	15.209	0.175	61.195	0.006571	0.024	1.46E-08	3.761	30.53	0.172
62	0.114	0.043	0.0059	0.0021	15.252	0.181	61.197	0.1	0.582	0.024	3.861	31.12	0.197
<b>63</b>	<b>0.112</b>	0.0014	0.6590	0.0100	15.254	0.839	61.207	<b>23.259</b>	0.00043	0.186	27.12	31.12	0.383
64	0.105	0.3044	0.0530	0.0540	15.258	0.892	61.261	1.213	0.00879	0.017	28.333	31.12	0.4
65	0.104	0.192	0.0024	0.0540	15.450	0.894	61.315	0.001697	0.00959	0.001705	28.334	31.14	0.402
66	0.101	0.031	0.0011	0.0300	15.480	0.895	61.345	0.005264	3.0E-05	0.003738	28.339	31.14	0.405
67	0.098	0.0021	0.0830	0.3190	15.482	0.978	61.66	1.016	0.013	0.024	29.356	31.15	0.43
68	0.096	0.182	0.0029	0.0020	15.665	0.981	61.666	0.059	0.00082	0.002061	29.415	31.15	0.432
69	0.094	0.136	0.0150	0.0013	15.801	0.996	61.667	0.0055	0.1750	0.0042	29.420	31.32	0.436
70	0.089	0.048	0.0005	0.0190	15.849	0.997	61.687	0.0210	0.1150	0.1300	29.441	31.44	0.566
71	0.087	0.0088	0.0026	0.0084	15.858	0.999	61.695	0.0000	0.0900	0.7050	29.441	31.53	1.271
72	0.084	0.0073	0.0048	0.0200	15.865	1.004	61.715	0.2470	0.8340	0.3600	29.688	32.36	1.631
73	0.081	0.235	0.0002	0.0023	16.100	1.004	61.717	0.0140	0.0330	0.0000	29.701	32.40	1.631
74	0.079	0.0023	0.0570	0.0081	16.102	1.061	61.725	0.3430	0.4030	0.0450	30.044	32.80	1.675
75	0.075	0.037	0.0350	0.4460	16.139	1.096	62.171	0.5150	0.6960	0.0019	30.559	33.49	1.677
<b>76</b>	<b>0.072</b>	0.0095	1.2960	0.1260	16.149	2.392	62.297	<b>9.7510</b>	0.0060	0.1710	40.310	33.50	1.848
77	0.069	1.859	0.0014	0.0740	18.007	2.393	62.371	0.1330	2.5190	0.1480	40.443	36.02	1.996
78	0.067	0.1	0.5620	2.8680	18.107	2.955	65.239	0.8250	0.2020	0.0089	41.268	36.22	2.005
79	0.063	0.024	0.0004	0.1250	18.131	2.955	65.364	0.5260	0.6350	0.7780	41.794	36.86	2.783
<b>80</b>	<b>0.060</b>	0.055	<b>5.0080</b>	1.9110	18.186	7.963	67.276	<b>6.1130</b>	3.7060	0.1630	47.907	40.56	2.946
<b>81</b>	<b>0.058</b>	<b>8.772</b>	0.0360	0.0370	26.959	8.000	67.313	0.0140	1.0560	0.0093	47.920	41.62	2.956
82	0.056	0.09	0.6310	4.1000	27.049	8.631	71.413	1.8230	0.6110	0.2230	49.744	42.23	3.179
83	0.055	0.02	0.1130	1.3500	27.069	8.744	72.763	0.0700	3.5410	1.5610	49.814	45.77	4.740
<b>84</b>	<b>0.053</b>	0.0001 9	<b>7.8970</b>	1.2190	27.069	16.64	73.981	0.0390	0.9210	0.1420	49.853	46.69	4.882
85	0.047	2.181	0.0150	4.5000	29.250	16.65	78.482	1.3970	0.5160	0.6440	51.250	47.21	5.526
86	0.046	2.626	0.2880	3.6200	31.876	16.94	82.102	0.9920	0.4700	0.1490	52.242	47.68	5.675



Mode	T [sec]	UX (%)	UY (%)	UZ (%)	Sum UX	Sum UY	Sum UZ	RX (%)	RY (%)	RZ (%)	Sum RX	Sum RY	Sum RZ
87	<b>0.044</b>	0.0001	0.7290	0.0001	31.876	17.67	82.102	0.4440	0.6630	<b>7.5020</b>	52.686	48.34	13.177
88	<b>0.042</b>	0.221	<b>28.142</b>	0.5930	32.097	45.82	82.695	0.0480	0.4420	0.0940	52.734	48.78	13.272
89	<b>0.037</b>	0.408	0.8100	<b>8.0410</b>	32.504	46.62	90.736	0.1110	3.2990	1.3750	52.845	52.084	14.647
90	<b>0.034</b>	2.272	0.2230	0.2160	34.777	46.84	90.952	0.1520	0.0260	<b>29.1480</b>	52.997	52.11	43.794
91	<b>0.033</b>	1.175	<b>5.1060</b>	0.0410	35.952	51.95	90.992	0.7790	0.2250	3.4370	53.776	52.335	47.231
92	<b>0.031</b>	<b>7.157</b>	1.2180	0.2480	43.108	53.17	91.240	0.0290	0.1380	0.5440	53.805	52.473	47.775
93	<b>0.027</b>	<b>7.759</b>	0.2530	2.3590	50.867	53.42	93.599	0.0410	1.7960	0.0160	53.846	54.269	47.791
94	<b>0.025</b>	<b>15.267</b>	0.0440	0.9470	66.134	53.47	94.546	0.2960	0.4370	0.1870	54.142	54.706	47.978
95	0.023	0.068	2.1200	0.1020	66.202	55.59	94.648	0.0017	0.1700	<b>6.7280</b>	54.144	54.876	54.706
96	0.021	0.033	<b>8.4950</b>	0.0021	66.235	64.08	94.650	0.9050	0.1110	1.9140	55.048	54.988	56.619
97	0.011	0.227	0.0170	3.5410	66.462	64.10	98.190	0.0190	0.0850	0.1540	55.068	55.073	56.774
98	<b>0.011</b>	0.906	0.0290	0.1370	67.368	64.13	98.327	0.0580	0.0120	<b>7.8750</b>	55.125	55.085	64.649
99	0.010	5.072	0.0140	0.0500	72.440	64.14	98.377	0.0560	0.0007	1.8530	55.182	55.085	66.502
100	<b>0.009</b>	0.012	<b>8.5990</b>	0.0003	<b>72.452</b>	<b>72.74</b>	<b>98.377</b>	0.4570	0.0033	0.1120	<b>55.639</b>	<b>55.089</b>	<b>66.614</b>

Considering previous output data, it could be said that:

- considering that the assumption of continuous rigid deck increases static redundancy, 100 modes are not sufficient to involve all participating mass;
- modes with relatively high effects represent translational local modes, above all in vertical direction;
- periods associated to main modes are lower than 1sec: they fall within the first two spectrum sections
- comparing different modal deformed shapes, it seems that only few macro-elements are involved in each mode;



### 7.3.5 Single deformable deck model with fixed joints

Modal analysis is performed considering 100 vibration modes:

Modal analysis output: Single undeformable deck with hinged joints													
Mode	T [sec]	UX (%)	UY (%)	UZ (%)	Sum UX	Sum UY	Sum UZ	RX (%)	RY (%)	RZ (%)	Sum RX	Sum RY	Sum RZ
1	0.655	0.3	0.0001	0.0001	0.3	3.E-06	1.E-05	0.0001	0.0063	0.0040	14E-05	0.006	0.0040
2	0.563	0.274	0.0001	0.0001	0.575	1.E-05	11E-05	0.0001	0.0047	0.0032	2.E-05	0.011	0.0073
3	0.532	0.166	0.0014	0.0006	0.741	0.0014	7.E-05	0.0019	0.0003	0.0033	0.0019	0.011	0.011
4	0.525	0.774	0.014	0.0031	1.515	0.016	0.0031	0.012	0.126	0.022	0.014	0.138	0.033
5	0.510	0.872	0.0043	0.0062	2.387	0.02	0.0094	0.041	0.136	0.0074	0.055	0.274	0.04
6	0.467	0.238	0.0019	0.0001	2.625	0.022	0.0095	0.0006	0.0041	0.0073	0.056	0.278	0.048
7	0.455	0.277	0.0001	0.0007	2.902	0.022	0.0095	0.0002	0.0059	0.0022	0.056	0.284	0.05
8	0.428	0.373	0.0030	8.E-09	3.275	0.025	0.0095	0.0128	0.016	0.0005	0.058	0.3	0.05
9	0.415	0.479	0.065	0.0004	3.754	0.09	0.0099	0.027	0.05	0.0059	0.085	0.35	0.056
<b>10</b>	<b>0.408</b>	<b>8.483</b>	<b>1.46</b>	<b>0.029</b>	<b>12.237</b>	<b>1.549</b>	<b>0.039</b>	<b>2.121</b>	<b>4.904</b>	<b>0.0025</b>	<b>2.206</b>	<b>5.253</b>	<b>0.058</b>
11	0.404	1.156	1.38	0.064	13.393	2.929	0.103	0.756	0.633	0.112	2.961	5.886	0.171
12	0.396	0.587	0.048	0.0007	13.98	2.977	0.104	0.05	0.131	0.0006	3.011	6.018	0.171
<b>13</b>	<b>0.394</b>	<b>5.508</b>	<b>9.525</b>	<b>0.11</b>	<b>19.488</b>	<b>12.502</b>	<b>0.214</b>	<b>4.741</b>	<b>4.093</b>	<b>0.883</b>	<b>7.752</b>	<b>10.111</b>	<b>1.054</b>
<b>14</b>	<b>0.373</b>	<b>1.041</b>	<b>41.414</b>	<b>0.35</b>	<b>20.529</b>	<b>53.916</b>	<b>0.563</b>	<b>3.896</b>	<b>4.119</b>	<b>4.158</b>	<b>11.648</b>	<b>14.23</b>	<b>5.213</b>
15	0.361	0.101	0.626	0.0065	20.63	54.542	0.57	0.075	0.0040	0.047	11.723	14.234	5.259
16	0.355	0.124	0.0017	0.0000	20.754	54.544	0.57	0.0000	0.0021	0.0001	11.723	14.236	5.259
17	0.353	0.016	0.736	0.034	20.77	55.28	0.604	0.106	0.0003	3E-07	11.83	14.237	5.259
18	0.350	9E-05	0.294	0.0009	20.771	55.573	0.604	0.0007	0.313	0.073	11.83	14.549	5.333
19	0.344	0.016	0.186	0.0059	20.787	55.759	0.61	0.0087	0.016	0.151	11.839	14.565	5.483
20	0.342	0.007	0.101	8E-07	20.794	55.86	0.61	0.06	0.076	0.014	11.899	14.641	5.498
21	0.341	0.153	0.013	0.0002	20.947	55.873	0.61	0.0035	0.0025	4E-05	11.902	14.643	5.498
22	0.341	0.223	0.315	0.0053	21.17	56.189	0.615	0.0018	0.286	0.021	11.904	14.929	5.519
23	0.339	0.073	0.08	0.0004	21.243	56.269	0.616	0.031	0.02	0.068	11.935	14.949	5.587
24	0.327	0.176	0.0079	0.0002	21.419	56.277	0.616	0.0032	0.0005	0.0002	11.939	14.95	5.587
25	0.320	0.168	0.0011	0.0001	21.586	56.278	0.616	0.0004	0.0003	0.0001	11.939	14.95	5.587
26	0.298	0.024	3.224	0.204	21.61	59.502	0.82	0.214	0.0032	0.707	12.153	14.953	6.294
27	0.295	0.198	0.0007	0.0058	21.808	59.502	0.826	0.0006	0.0030	0.0003	12.153	14.956	6.295
28	0.276	0.453	0.081	0.085	22.262	59.583	0.91	0.0001	0.015	2.206	12.153	14.971	8.5
29	0.275	0.069	0.0024	0.0079	22.33	59.586	0.918	0.0005	0.0002	0.134	12.154	14.972	8.634
30	0.263	0.254	0.0040	0.0000	22.584	59.59	0.918	0.0017	0.0001	0.014	12.156	14.972	8.648
31	0.262	0.087	0.0072	0.0000	22.671	59.597	0.918	0.0093	0.0010	0.279	12.165	14.973	8.927
32	0.260	0.474	0.172	0.072	23.145	59.769	0.99	0.032	0.0003	3.685	12.197	14.973	12.612
<b>33</b>	<b>0.252</b>	<b>0.168</b>	<b>0.643</b>	<b>0.018</b>	<b>23.314</b>	<b>60.413</b>	<b>1.008</b>	<b>0.11</b>	<b>0.018</b>	<b>22.668</b>	<b>12.307</b>	<b>14.991</b>	<b>35.28</b>
34	0.249	0.311	0.065	0.0043	23.625	60.478	1.012	0.0061	0.022	1.226	12.313	15.013	36.506
35	0.247	0.208	0.0038	0.0001	23.833	60.482	1.012	0.0012	0.0003	0.012	12.314	15.013	36.518
36	0.243	0.203	0.0031	0.013	24.036	60.485	1.025	0.0064	0.0017	0.045	12.321	15.015	36.563
37	0.241	0.092	0.0031	0.0001	24.128	60.488	1.025	0.0000	0.0000	0.138	12.321	15.015	36.702
38	0.234	0.121	0.0070	0.012	24.249	60.495	1.037	0.0030	0.044	0.0021	12.324	15.059	36.704
39	0.229	0.211	0.0072	0.0003	24.46	60.502	1.038	0.0018	0.0006	0.019	12.326	15.06	36.723
40	0.223	0.144	0.0018	0.021	24.603	60.503	1.059	0.0047	0.014	0.0005	12.331	15.074	36.723
41	0.223	0.134	5E-07	0.0001	24.737	60.503	1.059	0.0009	0.0004	0.013	12.331	15.074	36.737
42	0.209	0.339	0.0001	0.05	25.075	60.503	1.108	0.028	0.282	0.098	12.359	15.356	36.835
43	0.208	0.113	0.027	0.178	25.188	60.53	1.286	0.024	0.224	0.125	12.382	15.58	36.959

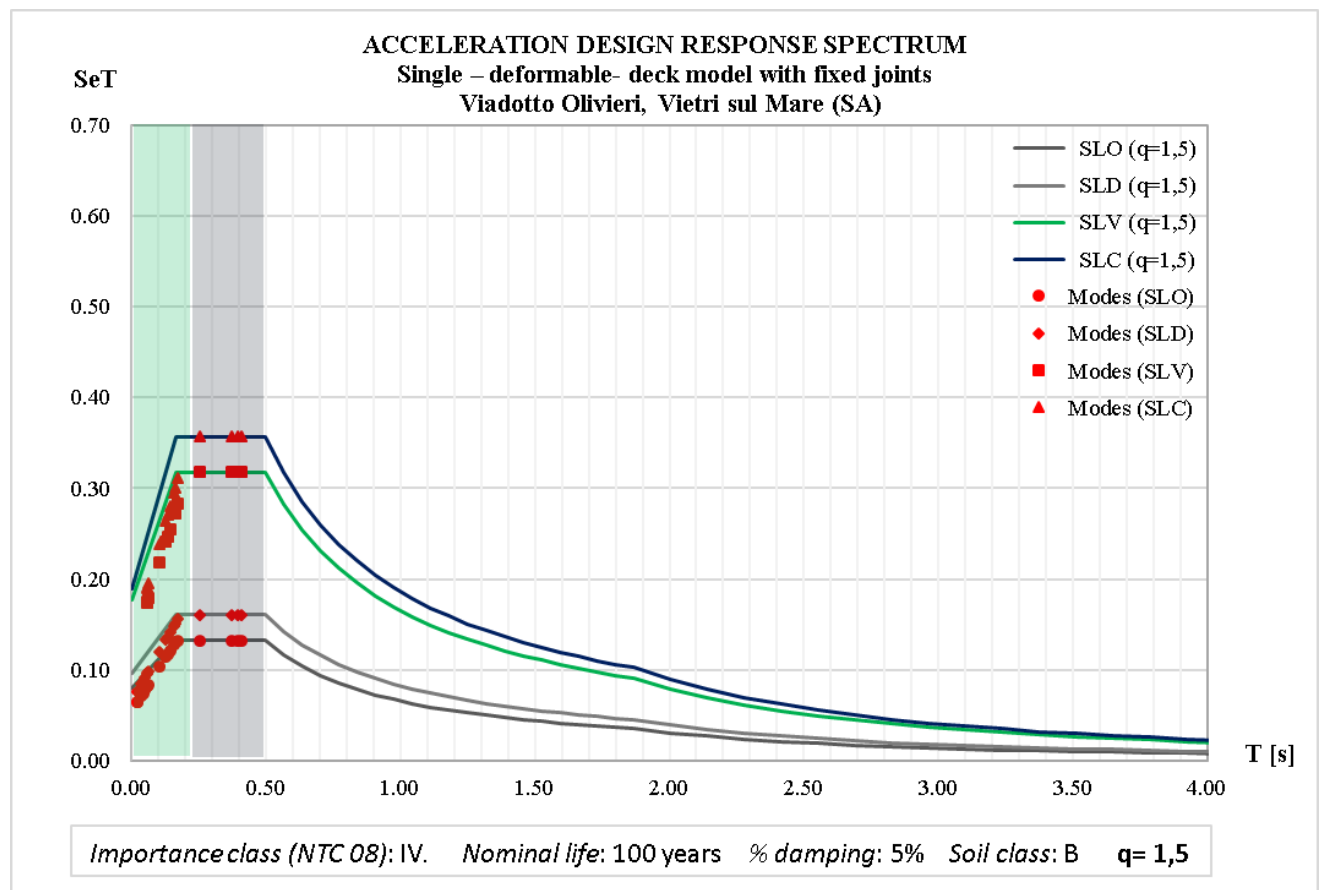
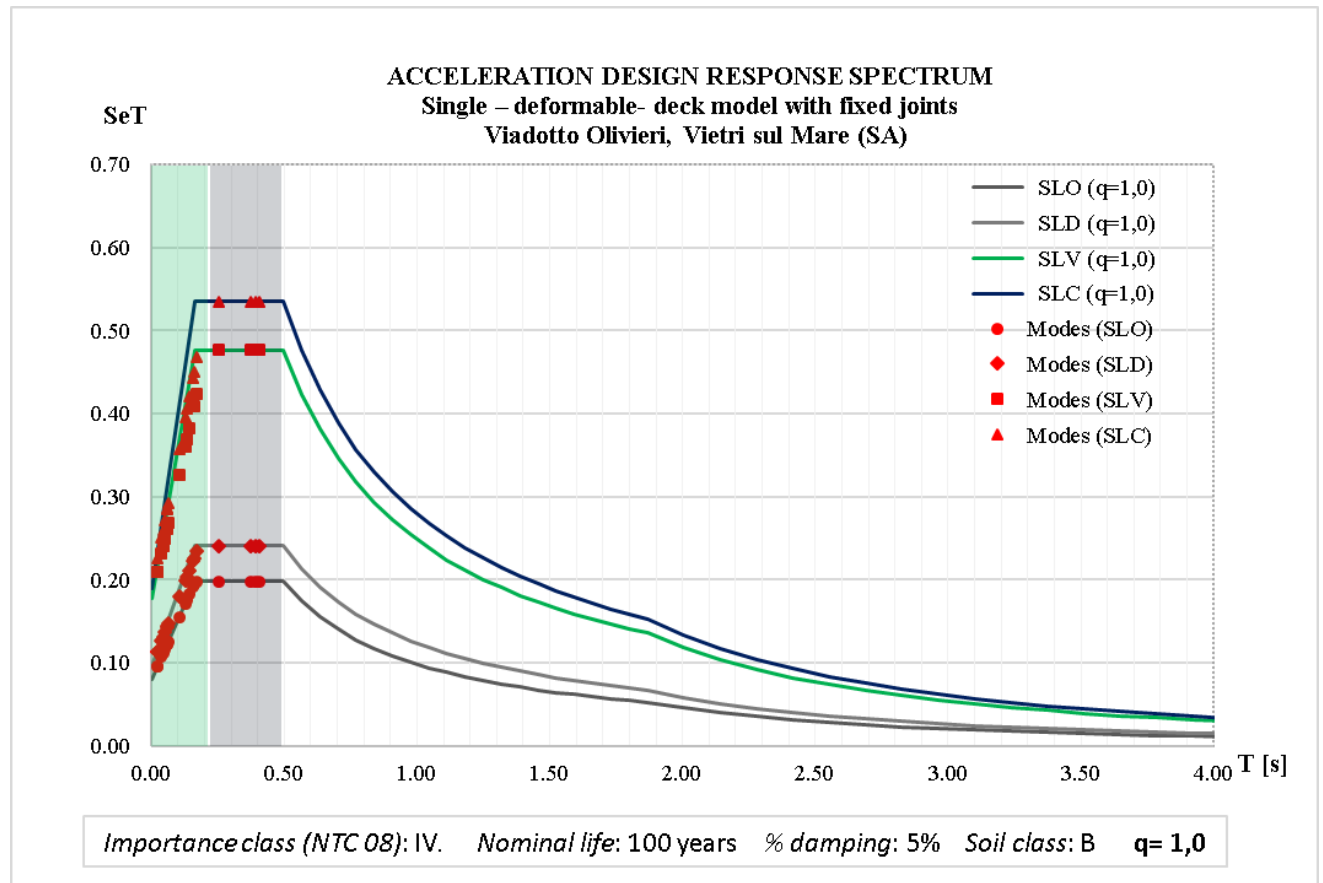
Mode	T [sec]	UX (%)	UY (%)	UZ (%)	Sum UX	Sum UY	Sum UZ	RX (%)	RY (%)	RZ (%)	Sum RX	Sum RY	Sum RZ
44	0.205	0.034	0.035	0.381	25.222	60.565	1.668	0.006	0.064	0.016	12.389	15.644	36.975
45	0.203	0.406	0.0070	0.106	25.628	60.572	1.773	0.0019	0.0045	0.035	12.391	15.649	37.01
46	0.202	0.014	0.0001	0.0005	25.642	60.572	1.774	0.0003	0.0079	0.0027	12.391	15.657	37.013
47	0.198	0.325	0.02	0.033	25.967	60.592	1.807	0.0029	0.0049	0.0002	12.394	15.662	37.013
48	0.192	0.478	0.0059	0.077	26.445	60.598	1.884	0.062	0.115	0.027	12.456	15.776	37.041
49	0.182	1.649	0.013	0.0066	28.094	60.612	1.891	0.522	4.753	0.033	12.978	20.529	37.073
50	0.177	0.21	0.017	0.31	28.304	60.628	2.201	0.0070	0.0004	0.067	12.985	20.53	37.141
51	0.174	0.038	0.0024	0.053	28.342	60.631	2.254	0.0088	0.037	0.0007	12.994	20.566	37.141
52	0.173	0.367	0.0030	1.073	28.709	60.634	3.327	0.049	0.08	0.0034	13.043	20.646	37.145
<b>53</b>	<b>0.172</b>	<b>0.1</b>	<b>0.376</b>	<b>45.781</b>	<b>28.809</b>	<b>61.01</b>	<b>49.108</b>	<b>2.142</b>	<b>4.347</b>	<b>0.271</b>	<b>15.185</b>	<b>24.993</b>	<b>37.415</b>
54	0.166	0.046	0.0006	0.147	28.855	61.011	49.255	0.0054	0.044	0.036	15.19	25.037	37.451
<b>55</b>	<b>0.162</b>	<b>0.614</b>	<b>1.09</b>	<b>2.127</b>	<b>29.469</b>	<b>62.1</b>	<b>51.382</b>	<b>9.263</b>	<b>0.761</b>	<b>1.185</b>	<b>24.454</b>	<b>25.798</b>	<b>38.636</b>
56	0.160	0.411	0.504	1.03	29.881	62.604	52.412	3.813	0.031	0.307	28.266	25.829	38.943
57	0.157	0.053	3.544	0.25	29.934	66.148	52.662	3.604	3E-06	0.0002	31.87	25.829	38.943
58	0.156	1.577	0.832	0.13	31.511	66.98	52.792	0.225	0.0067	0.179	32.095	25.836	39.123
59	0.153	1.025	0.398	0.101	32.536	67.378	52.893	0.046	0.038	0.017	32.141	25.874	39.14
60	0.151	0.334	0.976	0.794	32.871	68.354	53.687	0.014	0.074	0.25	32.155	25.948	39.39
61	0.151	0.492	1.778	3.652	33.362	70.132	57.339	0.164	1.066	0.333	32.319	27.014	39.723
62	0.150	1.326	0.13	0.3	34.688	70.262	57.639	0.0002	0.328	0.07	32.319	27.341	39.794
63	0.142	0.032	0.0052	0.214	34.72	70.267	57.852	0.014	0.036	0.0045	32.333	27.377	39.798
<b>64</b>	<b>0.142</b>	<b>10.65</b>	<b>0.464</b>	<b>0.14</b>	<b>45.379</b>	<b>70.731</b>	<b>57.992</b>	<b>0.3</b>	<b>0.325</b>	<b>0.013</b>	<b>32.633</b>	<b>27.702</b>	<b>39.811</b>
65	0.139	0.481	0.015	0.065	45.86	70.746	58.057	0.018	0.212	0.068	32.651	27.914	39.88
66	0.137	0.603	0.142	0.0004	46.464	70.888	58.058	0.074	0.038	0.0031	32.725	27.952	39.883
<b>67</b>	<b>0.133</b>	<b>16.47</b>	<b>0.565</b>	<b>0.115</b>	<b>62.934</b>	<b>71.453</b>	<b>58.172</b>	<b>0.58</b>	<b>0.801</b>	<b>0.0076</b>	<b>33.305</b>	<b>28.753</b>	<b>39.89</b>
<b>68</b>	<b>0.128</b>	<b>15.23</b>	<b>0.343</b>	<b>0.026</b>	<b>78.171</b>	<b>71.796</b>	<b>58.199</b>	<b>0.454</b>	<b>1.241</b>	<b>0.0003</b>	<b>33.759</b>	<b>29.993</b>	<b>39.891</b>
69	0.127	0.132	0.164	2.511	78.303	71.959	60.71	0.404	0.362	0.046	34.163	30.356	39.937
70	0.124	2.659	0.155	0.0016	80.962	72.115	60.711	0.209	0.373	0.027	34.372	30.728	39.964
71	0.112	0.15	0.005	0.004	81.11	72.12	60.72	0.0006	0.046	0.0038	34.373	30.775	39.968
72	0.108	0.537	0.022	0.037	81.65	72.14	60.75	0.0290	0.241	0.044	34.401	31.016	40.012
73	0.106	0.416	0.336	0.009	82.07	72.48	60.76	0.6150	1.379	2.994	35.016	32.394	43.006
<b>74</b>	<b>0.103</b>	<b>0.032</b>	<b>0.125</b>	<b>0.117</b>	<b>82.10</b>	<b>72.60</b>	<b>60.88</b>	<b>0.0064</b>	<b>0.779</b>	<b>5.122</b>	<b>35.023</b>	<b>33.173</b>	<b>48.129</b>
75	0.101	0.006	0.040	0.357	82.10	72.64	61.24	0.0230	0.413	0.555	35.046	33.586	48.684
76	0.098	0.433	0.160	0.000	82.54	72.80	61.24	0.3070	0.195	0.058	35.353	33.781	48.742
77	0.095	0.068	2.090	0.117	82.61	74.89	61.35	0.4890	0.019	1.33	35.842	33.8	50.071
78	0.087	0.001	0.718	0.518	82.61	75.61	61.87	0.0140	6E-06	0.651	35.855	33.8	50.722
79	0.084	0.053	1.353	0.367	82.66	76.96	62.24	0.0650	0.549	0.778	35.92	34.35	51.5
80	0.083	0.17	0.003	0.064	82.83	76.97	62.30	0.6590	0.397	0.22	36.58	34.746	51.72
<b>81</b>	<b>0.080</b>	<b>1.01</b>	<b>0.704</b>	<b>0.231</b>	<b>83.84</b>	<b>77.67</b>	<b>62.53</b>	<b>2.8420</b>	<b>1E-06</b>	<b>6.63</b>	<b>39.422</b>	<b>34.746</b>	<b>58.35</b>
82	0.073	0.013	0.005	0.405	83.85	77.68	62.94	1.4960	0.014	1.372	40.918	34.76	59.722
<b>83</b>	<b>0.069</b>	<b>0.01</b>	<b>3.731</b>	<b>0.461</b>	<b>83.86</b>	<b>81.41</b>	<b>63.40</b>	<b>5.9470</b>	<b>0.027</b>	<b>0.0086</b>	<b>46.865</b>	<b>34.788</b>	<b>59.731</b>
84	0.068	0.032	0.008	1.841	83.89	81.42	65.24	0.0067	0.967	0.886	46.872	35.754	60.616
85	0.063	3.102	0.151	0.295	87.00	81.57	65.53	0.4200	1.238	0.077	47.292	36.993	60.693
86	0.059	0.042	1.166	0.131	87.04	82.73	65.67	4.5450	1.411	0.776	51.838	38.404	61.469
<b>87</b>	<b>0.057</b>	<b>0.076</b>	<b>1.002</b>	<b>6.108</b>	<b>87.11</b>	<b>83.74</b>	<b>71.77</b>	<b>0.0110</b>	<b>3.262</b>	<b>4.224</b>	<b>51.849</b>	<b>41.666</b>	<b>65.693</b>
88	0.056	1.045	1.261	2.847	88.16	85.00	74.62	2.2810	0.136	0.644	54.13	41.803	66.337
<b>89</b>	<b>0.050</b>	<b>5.019</b>	<b>0.042</b>	<b>0.497</b>	<b>93.18</b>	<b>85.04</b>	<b>75.12</b>	<b>1.3370</b>	<b>0.072</b>	<b>1.26</b>	<b>55.467</b>	<b>41.875</b>	<b>67.597</b>
<b>90</b>	<b>0.045</b>	<b>0.338</b>	<b>1.180</b>	<b>9.075</b>	<b>93.52</b>	<b>86.22</b>	<b>84.19</b>	<b>0.0710</b>	<b>4.906</b>	<b>0.492</b>	<b>55.538</b>	<b>46.781</b>	<b>68.089</b>



Mode	T [sec]	UX (%)	UY (%)	UZ (%)	Sum UX	Sum UY	Sum UZ	RX (%)	RY (%)	RZ (%)	Sum RX	Sum RY	Sum RZ
91	0.043	0.081	1.443	1.273	93.60	87.66	85.47	0.0230	0.0033	4.442	55.561	46.785	72.531
92	0.042	0.019	1.057	0.846	93.62	88.72	86.31	1.2410	0.58	2.375	56.802	47.364	74.905
93	0.035	1.879	0.035	0.451	95.50	88.75	86.76	0.1150	0.096	1.562	56.917	47.46	76.468
<b>94</b>	<b>0.032</b>	0.059	0.069	<b>6.751</b>	95.55	88.82	93.51	0.0790	3.873	0.135	56.996	51.333	76.602
<b>95</b>	<b>0.030</b>	0.109	<b>5.450</b>	0.245	95.66	94.27	93.76	1.1560	0.042	1.048	58.152	51.375	77.65
96	0.030	0.712	0.234	0.002	96.38	94.51	93.76	0.2300	0.02	11.747	58.382	51.395	89.397
97	0.017	2.138	0.448	0.038	98.51	94.96	93.80	1.0990	0.244	0.317	59.481	51.638	89.715
<b>98</b>	<b>0.016</b>	0.278	1.103	0.002	98.79	96.06	93.80	0.3190	0.032	<b>6.249</b>	59.801	51.671	95.964
<b>99</b>	<b>0.015</b>	0.044	2.598	0.015	98.83	98.66	93.82	<b>6.0100</b>	0.0021	1.532	65.811	51.673	97.496
<b>100</b>	0.014	0.02	0.064	4.011	<b>98.85</b>	<b>98.72</b>	<b>97.83</b>	0.0230	0.0022	0.0016	<b>65.833</b>	<b>51.675</b>	<b>97.498</b>

Considering previous output data, it could be said that:

- modes with relatively high effects represent translational local modes, above all in transverse and vertical directions
- rotational contributions don't prevail on translational ones;
- under the assumption of continuous deformable deck, 100 modes are quite sufficient to involve all mas;
- comparing different modal deformed shapes, it seems that only few macro-elements are involved in each mode;
- period referring to interesting modes fall within the first two spectrum section, above all in the highest amplification one.



### 7.3.6 Single deformable deck model with hinged joints

Modal analysis is performed considering 100 vibration modes:

Modal analysis output: Single deformable deck with hinged joints													
Mode	T [sec]	UX (%)	UY (%)	UZ (%)	Sum UX	Sum UY	Sum UZ	RX (%)	RY (%)	RZ (%)	Sum RX	Sum RY	Sum RZ
1	0.655	0.3	0.0003	1E-05	0.3	3.4E-06	1.E-05	1.-05	0.0063	0.0040	1.4E-05	0.0063	0.0040
2	0.563	0.274	9E-06	1.E-06	0.575	1.3E-05	1.E-05	1E-05	0.0047	0.0032	2.8E-05	0.011	0.0073
3	0.532	0.166	0.0014	6.-05	0.741	0.00144	7.E-05	0.0019	0.0004	0.0033	0.00198	0.011	0.011
4	0.525	0.777	0.014	0.0031	1.518	0.015	0.0032	0.012	0.127	0.022	0.014	0.139	0.033
5	0.510	0.873	0.0042	0.0062	2.391	0.019	0.0095	0.041	0.137	0.0073	0.056	0.275	0.04
6	0.467	0.238	0.0019	9.E-05	2.629	0.021	0.0095	0.0006	0.0041	0.0073	0.056	0.279	0.047
7	0.455	0.277	0.0000	7.E-06	2.907	0.021	0.0096	0.0002	0.0060	0.0022	0.057	0.285	0.049
8	0.428	0.374	0.0031	2.E-11	3.281	0.025	0.0096	0.0013	0.016	6.E-05	0.058	0.302	0.05
9	0.415	0.487	0.069	0.0004	3.768	0.093	0.01	0.029	0.052	0.0062	0.087	0.353	0.056
<b>10</b>	<b>0.408</b>	<b>8.646</b>	1.589	0.031	12.415	1.682	0.041	2.21	<b>5.001</b>	0.0009	2.296	5.354	0.057
11	0.404	1.131	1.409	0.064	13.546	3.091	0.105	0.76	0.619	0.119	3.057	5.973	0.176
12	0.396	0.665	0.087	0.0012	14.211	3.178	0.106	0.074	0.164	0.0025	3.131	6.137	0.178
<b>13</b>	<b>0.394</b>	<b>5.233</b>	9.702	0.109	19.445	12.88	0.215	4.692	3.9	0.922	7.824	10.037	1.101
<b>14</b>	<b>0.373</b>	1.098	<b>41.101</b>	0.344	20.543	53.981	0.559	3.794	4.21	4.129	11.61	14.247	5.23
15	0.361	0.101	0.595	0.0061	20.644	54.577	0.565	0.071	0.0036	0.044	11.68	14.25	5.274
16	0.355	0.124	0.0017	3E-05	20.768	54.579	0.565	0.0004	0.0021	0.0001	11.68	14.252	5.274
17	0.353	0.016	0.74	0.034	20.783	55.318	0.599	0.108	0.0004	5.E-08	11.79	14.253	5.274
18	0.350	8.E-05	0.287	0.0001	20.784	55.606	0.599	0.0005	0.311	0.072	11.79	14.564	5.346
19	0.344	0.016	0.188	0.0059	20.8	55.794	0.605	0.0090	0.016	0.153	11.80	14.58	5.498
20	0.342	0.0071	0.1	4.E-07	20.807	55.893	0.605	0.059	0.075	0.014	11.86	14.655	5.513
21	0.341	0.152	0.013	0.0002	20.959	55.906	0.606	0.0034	0.0027	4.E-05	11.86	14.658	5.513
22	0.341	0.223	0.308	0.0052	21.183	56.215	0.611	0.0015	0.285	0.02	11.87	14.942	5.533
23	0.339	0.073	0.077	0.0004	21.256	56.292	0.611	0.03	0.02	0.069	11.9	14.963	5.602
24	0.327	0.176	0.0078	0.0002	21.432	56.3	0.611	0.0032	0.0006	0.0002	11.90	14.963	5.602
25	0.320	0.168	0.0010	0.0001	21.6	56.301	0.612	4.E-05	0.0004	0.0001	11.90	14.964	5.602
26	0.298	0.025	3.24	0.202	21.625	59.541	0.813	0.222	0.0035	0.715	12.12	14.967	6.317
27	0.295	0.198	0.0004	0.0055	21.822	59.542	0.819	0.0006	0.0038	0.0002	12.12	14.97	6.318
28	0.276	0.433	0.086	0.088	22.255	59.628	0.907	0.0002	0.015	2.37	12.12	14.985	8.687
29	0.275	0.092	0.0042	0.0050	22.347	59.632	0.912	0.0050	5.E-05	0.076	12.12	14.985	8.764
30	0.263	0.254	0.0041	1.E-05	22.602	59.636	0.912	0.0017	0.0004	0.015	12.12	14.985	8.779
31	0.262	0.085	0.0080	5.E-05	22.687	59.644	0.912	0.0097	0.0011	0.304	12.13	14.986	9.083
32	0.260	0.48	0.18	0.071	23.166	59.824	0.984	0.034	0.0004	3.902	12.17	14.987	12.985
<b>33</b>	<b>0.252</b>	0.164	0.647	0.018	23.331	60.471	1.002	0.11	0.019	<b>22.517</b>	12.28	15.006	35.502
34	0.249	0.3	0.058	0.0044	23.63	60.529	1.006	0.0052	0.021	1.022	12.28	15.027	36.524
35	0.247	0.208	0.0037	0.0001	23.838	60.533	1.006	0.0012	0.0003	0.011	12.28	15.027	36.535
36	0.243	0.201	0.0029	0.013	24.039	60.536	1.019	0.0061	0.0017	0.041	12.29	15.029	36.576
37	0.241	0.093	0.0030	0.0001	24.132	60.539	1.019	5.E-05	69E-05	0.132	12.29	15.029	36.708
38	0.234	0.121	0.0070	0.012	24.253	60.546	1.031	0.0033	0.044	0.0021	12.29	15.072	36.71
39	0.229	0.211	0.0072	0.0003	24.463	60.553	1.032	0.0018	0.0006	0.019	12.3	15.073	36.729
40	0.223	0.144	0.0001	0.021	24.607	60.553	1.053	0.0047	0.014	0.0005	12.30	15.087	36.73
41	0.223	0.134	4.E-07	0.0001	24.741	60.553	1.053	9.E-05	0.0004	0.013	12.30	15.088	36.743
42	0.209	0.336	0.0001	0.052	25.077	60.553	1.105	0.028	0.291	0.1	12.33	15.379	36.842
43	0.208	0.116	0.027	0.177	25.194	60.58	1.282	0.023	0.222	0.121	12.35	15.601	36.963

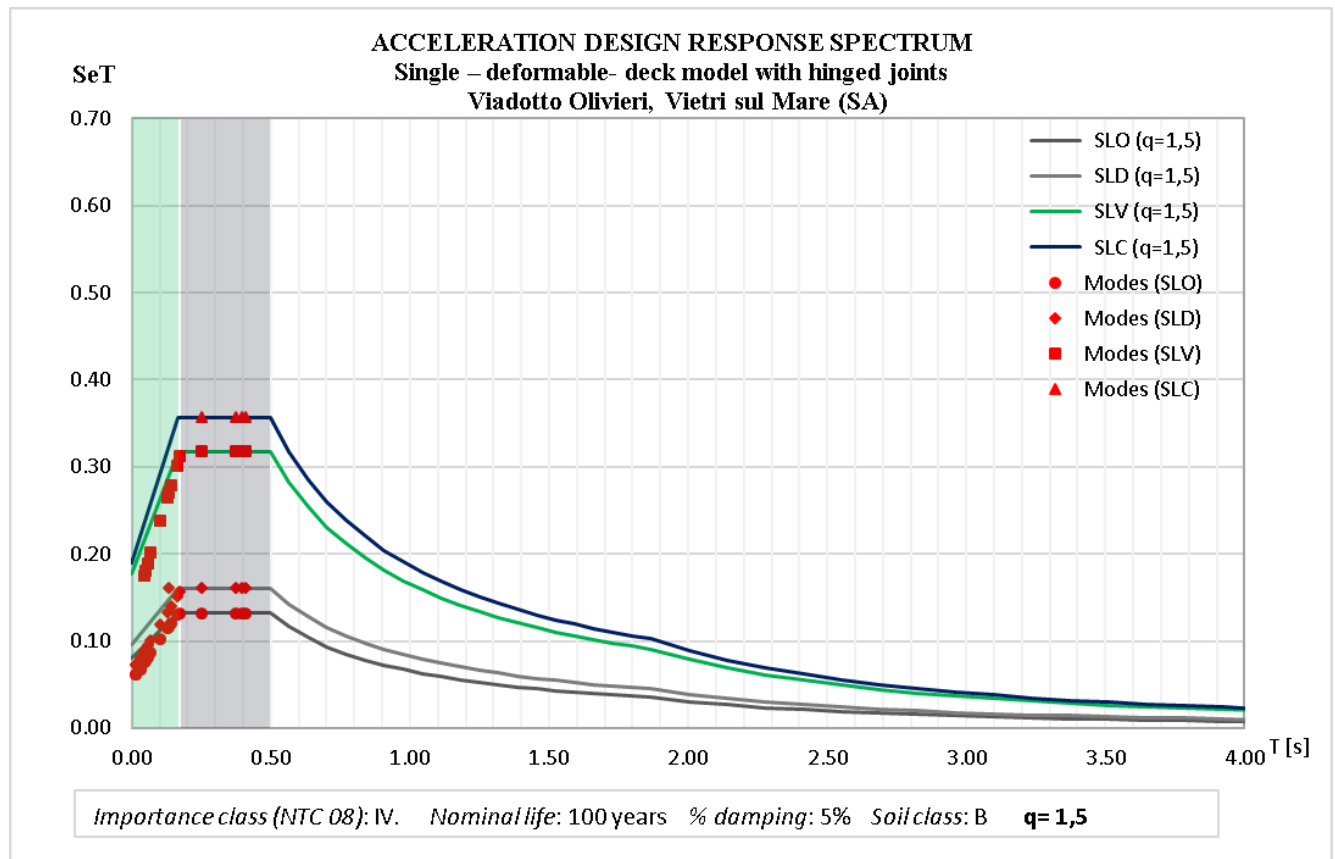
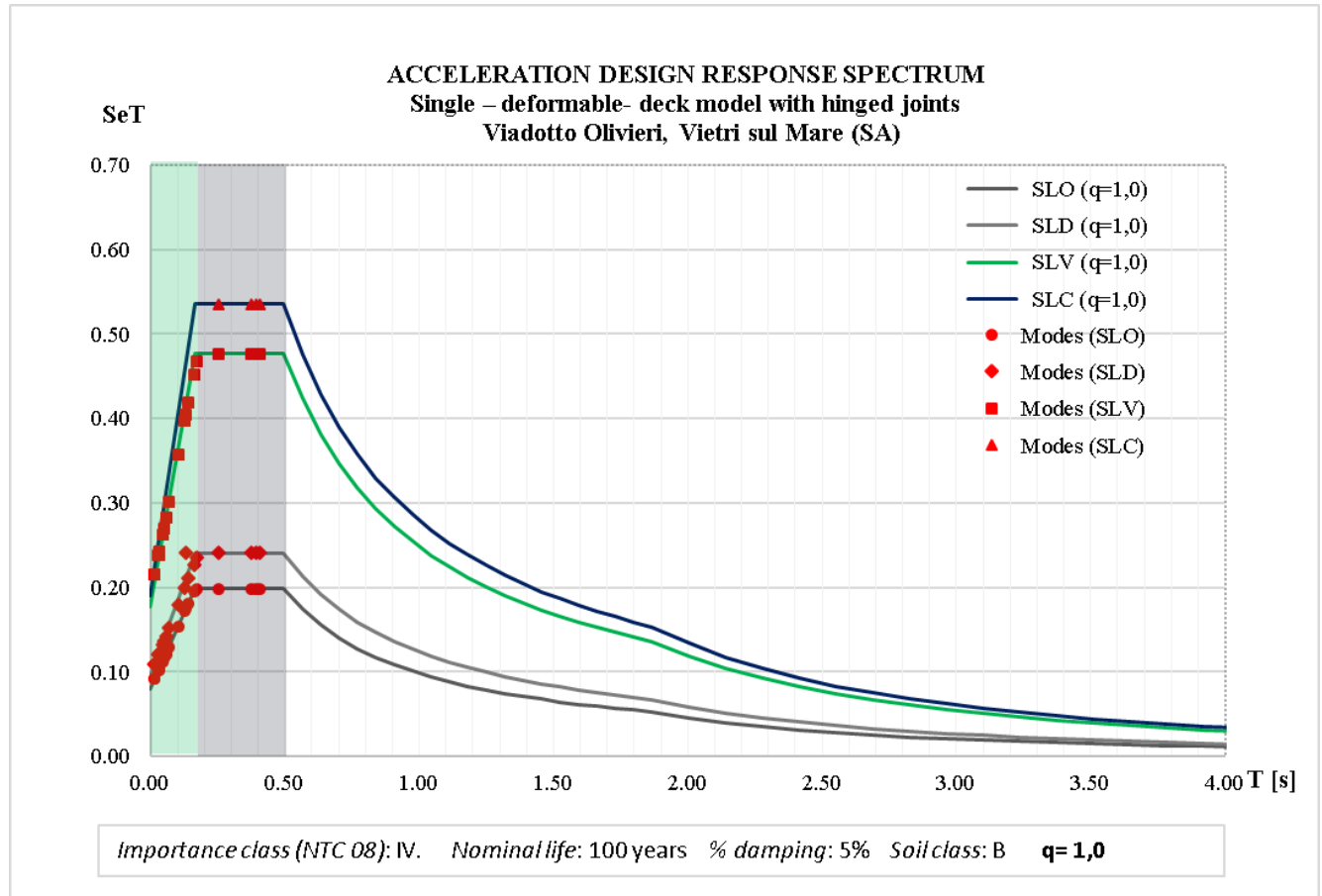
Mode	T [sec]	UX (%)	UY (%)	UZ (%)	Sum UX	Sum UY	Sum UZ	RX (%)	RY (%)	RZ (%)	Sum RX	Sum RY	Sum RZ
44	0.205	0.034	0.036	0.383	25.228	60.616	1.665	0.0068	0.064	0.016	12.36	15.665	36.979
45	0.203	0.407	0.0069	0.106	25.634	60.623	1.771	0.0019	0.0046	0.035	12.36	15.67	37.014
46	0.202	0.014	0.0001	0.0005	25.648	60.623	1.772	0.0003	0.0079	0.0027	12.36	15.678	37.017
47	0.198	0.326	0.02	0.033	25.974	60.643	1.805	0.0030	0.0052	0.0002	12.36	15.683	37.017
48	0.192	0.48	0.0058	0.078	26.454	60.649	1.883	0.063	0.117	0.027	12.43	15.8	37.044
49	0.182	1.642	0.013	0.0045	28.096	60.662	1.887	0.517	4.77	0.033	12.95	20.57	37.078
50	0.177	0.208	0.017	0.317	28.304	60.678	2.204	0.0076	0.0007	0.068	12.96	20.571	37.145
51	0.174	0.038	0.0025	0.057	28.342	60.681	2.26	0.0091	0.037	0.0006	12.96	20.608	37.146
52	0.173	0.37	0.0036	1.191	28.712	60.685	3.452	0.056	0.089	0.0041	13.02	20.697	37.15
<b>53</b>	<b>0.172</b>	0.096	0.374	<b>45.546</b>	28.808	61.059	48.998	2.158	4.303	0.278	15.17	25	37.428
54	0.166	0.047	0.0008	0.152	28.855	61.06	49.15	0.0068	0.045	0.037	15.18	25.046	37.465
<b>55</b>	<b>0.162</b>	0.574	1.161	2.333	29.43	62.221	51.482	<b>9.783</b>	0.786	1.234	24.96	25.831	38.699
56	0.160	0.454	0.461	0.948	29.884	62.682	52.431	3.428	0.021	0.264	28.39	25.852	38.963
57	0.157	0.043	3.422	0.235	29.926	66.105	52.666	3.476	1.4E-5	0.0002	31.87	25.852	38.963
58	0.156	1.521	0.953	0.119	31.447	67.058	52.785	0.29	0.0069	0.173	32.16	25.859	39.136
59	0.153	1.1	0.35	0.116	32.547	67.408	52.901	0.05	0.034	0.026	32.21	25.893	39.162
60	0.151	0.187	0.776	0.462	32.734	68.184	53.363	0.0056	0.022	0.188	32.21	25.915	39.35
61	0.151	0.598	2.012	4.012	33.332	70.196	57.375	0.166	1.132	0.39	32.38	27.047	39.741
62	0.150	1.342	0.119	0.283	34.675	70.315	57.658	5.E-05	0.316	0.068	32.38	27.363	39.809
63	0.142	0.056	0.0030	0.209	34.731	70.318	57.867	0.012	0.04	0.0043	32.39	27.403	39.813
<b>64</b>	<b>0.142</b>	<b>10.693</b>	0.466	0.146	45.425	70.784	58.013	0.303	0.324	0.014	32.69	27.727	39.827
65	0.139	0.482	0.014	0.065	45.906	70.798	58.078	0.017	0.212	0.068	32.71	27.939	39.894
66	0.137	0.599	0.142	0.0005	46.506	70.94	58.079	0.076	0.036	0.0034	32.79	27.975	39.898
<b>67</b>	<b>0.133</b>	<b>16.652</b>	0.567	0.115	63.157	71.506	58.193	0.58	0.81	0.0078	33.37	28.785	39.906
<b>68</b>	<b>0.128</b>	<b>14.834</b>	0.33	0.024	77.991	71.836	58.218	0.438	1.215	0.0003	33.81	30	39.906
69	0.127	0.129	0.16	2.499	78.121	71.997	60.717	0.397	0.359	0.045	34.20	30.359	39.951
70	0.124	2.845	0.161	0.0017	80.966	72.158	60.719	0.22	0.393	0.028	34.42	30.753	39.979
71	0.112	0.13	0.01	0.00	81.10	72.16	60.72	0.001	0.040	0.004	34.42	30.793	39.983
72	0.108	0.56	0.02	0.04	81.66	72.19	60.76	0.030	0.245	0.036	34.45	31.038	40.019
73	0.106	0.41	0.35	0.01	82.07	72.53	60.77	0.609	1.336	3.101	35.06	32.374	43.120
<b>74</b>	<b>0.103</b>	0.04	0.11	0.12	82.10	72.64	60.88	0.009	0.801	<b>5.069</b>	35.07	33.175	48.188
75	0.101	0.01	0.04	0.36	82.11	72.68	61.24	0.026	0.426	0.547	35.10	33.602	48.735
76	0.098	0.43	0.19	0.00	82.54	72.86	61.24	0.315	0.174	0.036	35.41	33.776	48.770
77	0.095	0.07	2.07	0.12	82.61	74.93	61.36	0.470	0.015	1.342	35.88	33.791	50.112
78	0.087	0.00	0.73	0.52	82.61	75.66	61.88	0.012	0.000	0.671	35.89	33.791	50.783
79	0.084	0.06	1.38	0.35	82.67	77.04	62.23	0.080	0.514	0.795	35.97	34.305	51.578
80	0.083	0.17	0.01	0.07	82.84	77.05	62.30	0.660	0.441	0.251	36.63	34.746	51.829
<b>81</b>	<b>0.080</b>	1.00	0.68	0.23	83.84	77.72	62.54	2.948	0.000	<b>6.616</b>	39.58	34.746	58.445
82	0.073	0.02	0.01	0.42	83.86	77.73	62.95	1.495	0.012	1.341	41.08	34.758	59.787
<b>83</b>	0.069	0.02	3.80	0.51	83.87	81.53	63.46	<b>6.079</b>	0.014	0.002	47.15	34.771	59.789
84	0.068	0.03	0.00	1.75	83.91	81.53	65.21	0.045	0.970	0.916	47.20	35.741	60.705
85	0.063	3.10	0.13	0.32	87.01	81.66	65.53	0.383	1.198	0.072	47.58	36.939	60.778
86	0.059	0.05	1.19	0.21	87.05	82.86	65.74	4.480	1.641	0.660	52.06	38.580	61.437
<b>87</b>	<b>0.057</b>	0.07	0.93	<b>6.08</b>	87.12	83.79	71.81	0.001	3.128	4.330	52.06	41.708	65.767
88	0.056	1.04	1.30	2.80	88.17	85.09	74.61	2.352	0.119	0.658	54.42	41.827	66.424
<b>89</b>	<b>0.050</b>	<b>5.02</b>	0.04	0.52	93.19	85.13	75.13	1.334	0.068	1.256	55.75	41.894	67.680
<b>90</b>	<b>0.045</b>	0.34	1.14	<b>9.16</b>	<b>93.52</b>	86.27	84.29	0.063	4.965	0.473	55.81	46.860	68.153
91	0.043	0.08	1.49	1.22	93.60	87.76	85.50	0.029	0.005	4.450	55.84	46.865	72.603



Mode	T [sec]	UX (%)	UY (%)	UZ (%)	Sum UX	Sum UY	Sum UZ	RX (%)	RY (%)	RZ (%)	Sum RX	Sum RY	Sum RZ
92	0.042	0.02	1.06	0.79	93.62	88.81	86.29	1.273	0.538	2.402	57.12	47.403	75.004
93	0.035	1.87	0.03	0.50	95.49	88.84	86.79	0.111	0.081	1.546	57.23	47.483	76.551
<b>94</b>	<b>0.032</b>	0.07	0.06	<b>6.73</b>	95.56	88.90	93.53	0.078	3.873	0.150	57.30	51.356	76.700
<b>95</b>	<b>0.030</b>	0.11	<b>5.46</b>	0.23	95.67	94.37	93.76	1.195	0.040	1.027	58.50	51.397	77.728
<b>96</b>	<b>0.030</b>	0.71	0.23	0.00	96.38	94.60	93.76	0.233	0.017	<b>11.769</b>	58.73	51.414	89.497
97	0.017	2.13	0.46	0.04	98.51	95.06	93.80	1.123	0.238	0.309	59.85	51.652	89.806
98	0.016	0.27	1.04	0.00	98.78	96.10	93.80	0.261	0.031	6.335	60.12	51.683	96.140
<b>99</b>	<b>0.015</b>	0.05	2.62	0.01	98.83	98.72	93.81	<b>5.872</b>	0.004	1.416	65.99	51.687	97.556
<b>100</b>	0.014	0.02	0.05	4.01	<b>98.86</b>	<b>98.77</b>	<b>97.83</b>	0.015	0.003	0.001	<b>66.00</b>	<b>51.689</b>	<b>97.558</b>

Considering previous output data, it could be said that:

- modes with relatively high effects represent translational local modes, both in longitudinal and in transverse direction;
- apart from Rz component, rotational contribution can be neglected;
- period associated to main modes are lower than 1sec, characterizing a really rigid structure;
- comparing different modal deformed shapes, it seems that only few macro-elements are involved in each mode;
- period referring to interesting modes fall within the first two spectrum section, above all in the highest amplification one.



### Considerations

Static and dynamic evaluation about Olivieri Bridge lead to the following observations.

1. FEM analysis points out that the effects of horizontal forces, above all acting out of plane, cannot be neglected.
2. Out of plane horizontal force lead significant overturning problems, especially for the central arch.
3. Considering bridge structural characterization, as a Maillart arch type bridge, made of stiffen deck and thin vault, arch deformed shape is completely influenced by upper girder behavior.
4. Acting horizontal forces, the central arch portion is the most vulnerable one; the elements which record the worst deformation are the thinnest cross walls, put upon the arch: for them, buckling effects have to be considered.
5. According to modal analysis outputs, bridge is rigid enough: modes with relatively high effects are characterized by really short period, falling within the first two spectrum section, above all in the highest amplification one.
6. Modes with relatively high effects represent translational local modes, both in longitudinal and in transverse direction: except rare cases, rotational contribution is quite negligible
7. Comparing modal deformed shapes, it seems that few macro elements are involved in each mode.

Previous considerations suggest the following measures:

- a. Structural maintenance works, to guarantee bridge serviceability;
- b. Bridge structural improvement to guarantee a correct behaviour, acting horizontal forces, as:
  - b.1 strengthening existing structure
  - b.2 applying retrofit proposal (as jointing in a single deck the three portions, cutting cross walls at the top, putting combined system of isolators and dampers, capable to transfers the allowable stress to each cross walls

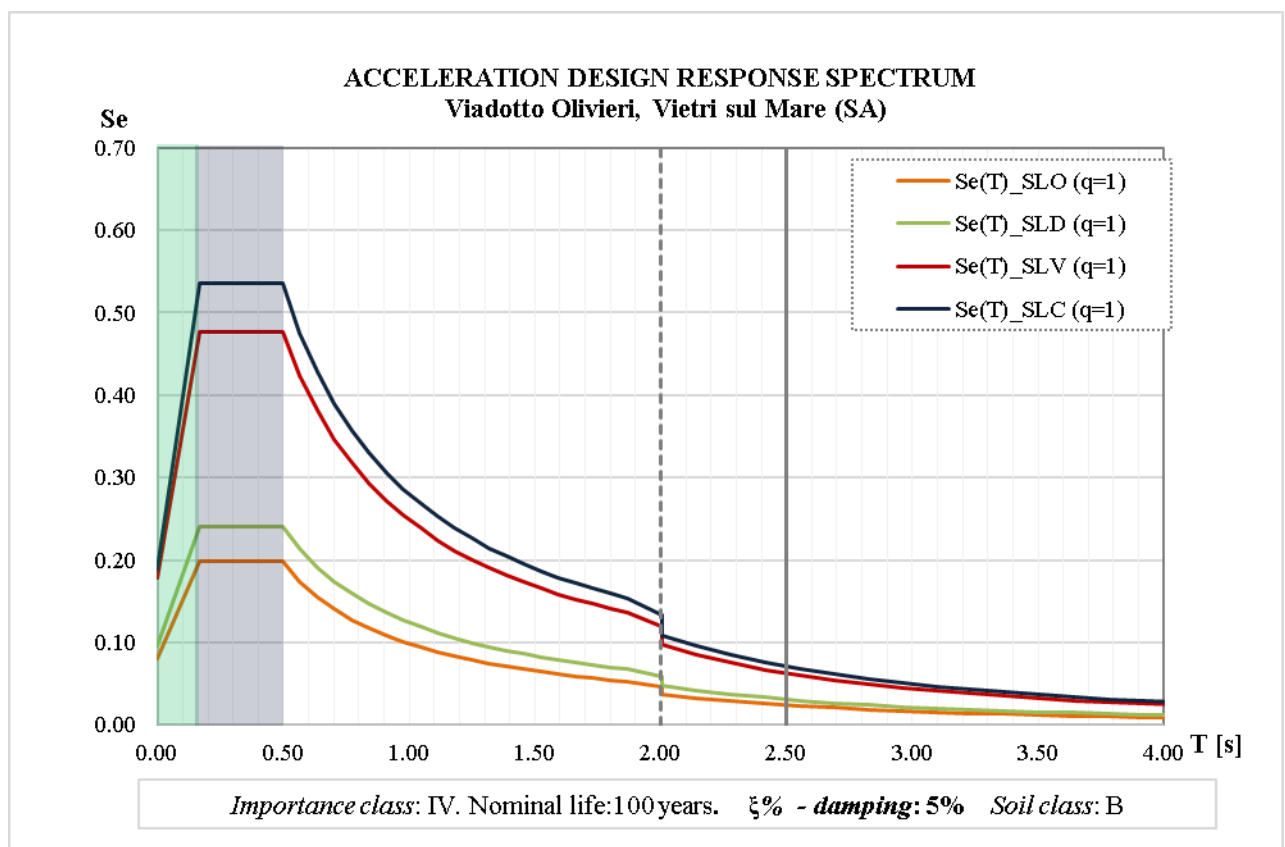
### 7.5 Retrofit proposal for Viadotto Olivieri

In order to prove that this structure has a great seismic capacity, also valuing the event that three portions now forming bridge deck would be jointed creating a stiffer structure, a retrofit solution is proposed as comparison.

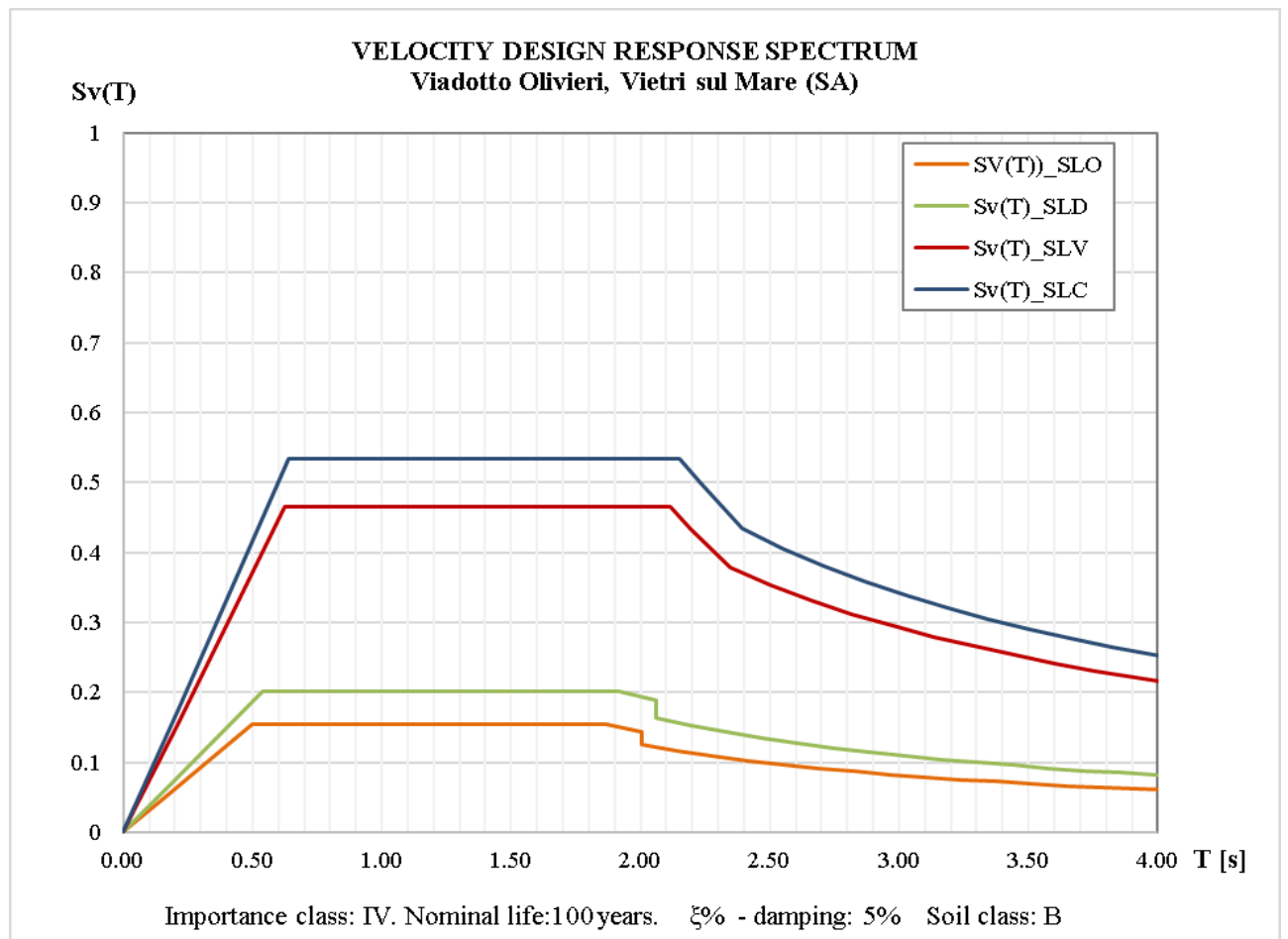
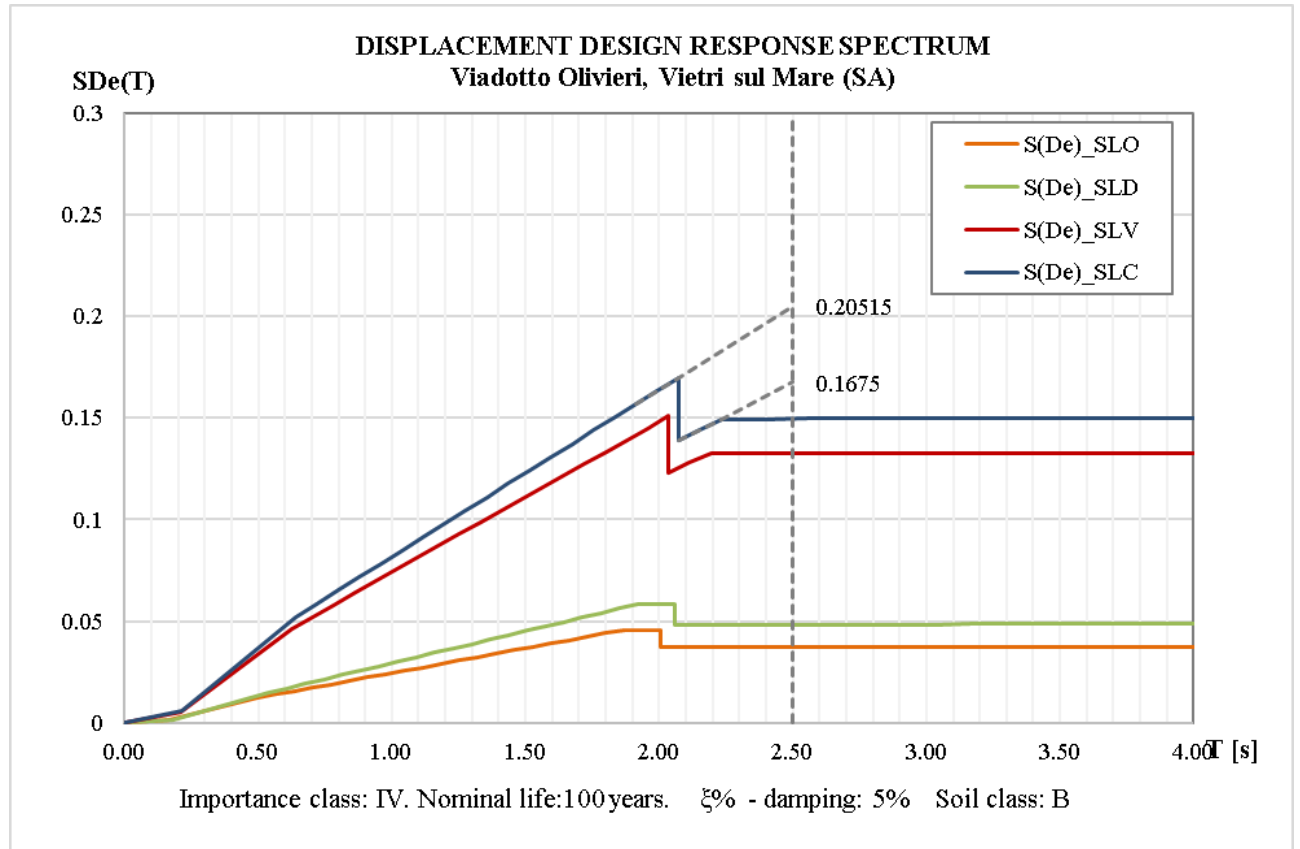
An isolated system (IS) made of High D Rubber Bearing, also known as HDR, is hypothesized, assuming to insert them by cutting the cross walls at the top. HDRB isolator solution has the following advantages: great reduction of base reactions; no damage to the structure that remains in the elastic response due to high intensity earthquakes with no interruption of the structural function; capacity to reduce the seismic energy from the ground to the structure.

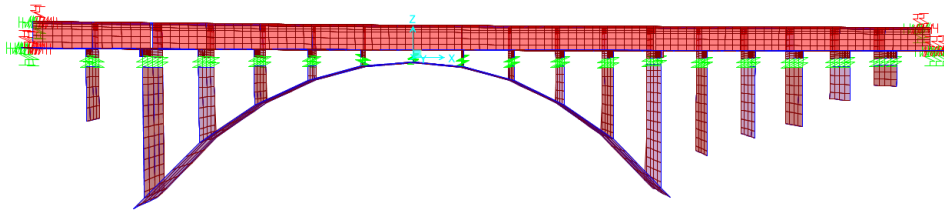
Regrettably, in this way, the original static scheme of a Maillart-arch-type bridge will be completely modified. It points out that the following retrofit proposal would not be built really, being simply assumed as a double check of Olivieri Bridge great seismic response.

A pre-dimensioning of isolation system has been done assumed a period  $T_{IS}=2.50\text{sec}$ , corresponding to a maximum displacement of 250mm.










The effective seismic weight,  $W$ , that needs to be used in the determination of the seismic base shear is the total weight of the building and that part of the other gravity loads that might reasonably be expected to be acting on the building at the time it is subjected to the design earthquake. According to Italian building code (NTC08, CH. 5.1.3.8), for busy urban bridges, in addition to Dead and Super-Dead loads, 20% of overall Live loads can be considered in defining seismic weight,  $W$ . Putting the IS system between deck and cross walls, only the first aliquot, approximately corresponding to 60% of the overall (Dead+ Super-Dead) load, has to be considered:

Load type	Fk [t]	$\gamma$	$\gamma Fk$ [t]
Dead (G1k)	2371.80	1.00	2371.80
Super- D- (G2k)	628.12	1.00	628.12
Live (Qk)	749.43	0.20	149.88
Tot	3749.35	-	<b>3149.80</b>

Considering that each of 17 cross walls is cut at the top, as close as possible to the upper deck, a HDRB isolator is used for each column that ribs the walls; overall,  $n=5 \times 17 = 85$  HDRB will be used: every single isolator will carry a vertical load of 37t.

Assuming an isolation period ( $T_{ISO}$ ) of 2.50sec, the overall stiffness of IS can be defined as:  $K_{ISO,tot} = W \cdot (4\pi^2) / (T_{ISO})^2 = 19876$  kN/m; for each HDRB isolator  $K_i = K_{ISO,tot} / n = 233$  kN/m. Considering the displacement the it's supposed to be accommodated, FIP HDRB SI-N 350/100 could be sufficient, a single HDRB will support a compression strength  $\sigma$  of about 37 kg/cm<sup>2</sup>: it's underlined that isolator dimensions are greatly limited by the cross wall geometry. In the following table, main design characteristic of the chosen FIP HDRB are described.

<b>HDRB – FIP Industrial – Displacement: +/- 250mm</b>										
<b>SI-N</b>	<b>V KN</b>	<b>Fzd kN</b>	<b>Ke kNmm</b>	<b>Kv kNmm</b>	<b>Dg [mm]</b>	<b>te mm</b>	<b>h mm</b>	<b>H mm</b>	<b>Z mm</b>	<b>W kg</b>
<b>350/100</b>	200	1680	0.62	478	350	125	213	263	400	138

<b>V</b>	Maximum vertical load at load combination including the seismic action	
<b>Fzd</b>	Maximum vertical load at non-seismic load condition (ULS)	
<b>Ke</b>	Effective horizontal stiffness	
<b>Kv</b>	Vertical Stiffness	
<b>Dg</b>	Elastomer diameter	
<b>te</b>	Total elastomer thickness	
<b>h</b>	Height excluding outer steel plates	
<b>H</b>	Total height including outer steel plates	
<b>Z</b>	Side length out outer steel plates	
<b>W</b>	Isolator weight excluding anchoring elements	

HDRB are reinforced rubber bearings made of alternating layers of steel laminates and hot vulcanized rubber, usually of circular form. They are characterized by low horizontal stiffness, high vertical stiffness and suitable damping capacity. These characteristics permit to increase the fundamental period of vibration of the structure, to resist to vertical loads without appreciable setting and to limit horizontal displacements in seismically isolated structures.

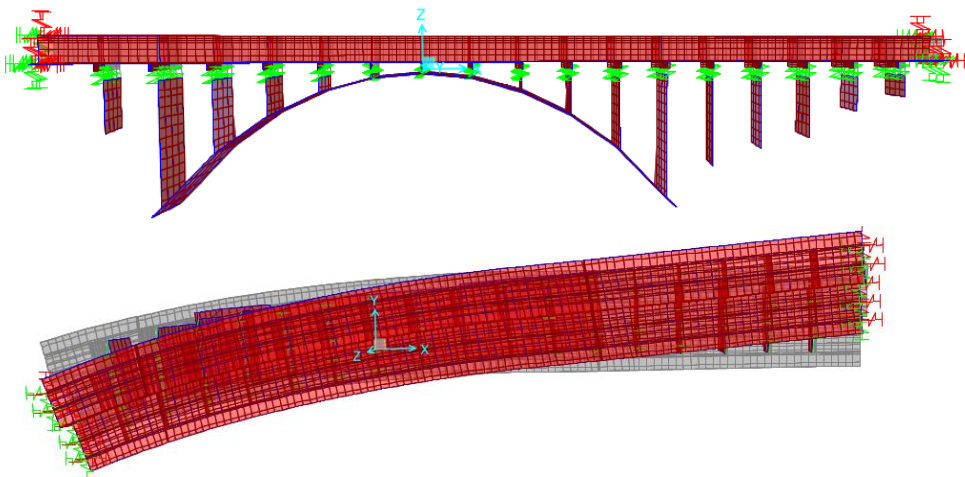
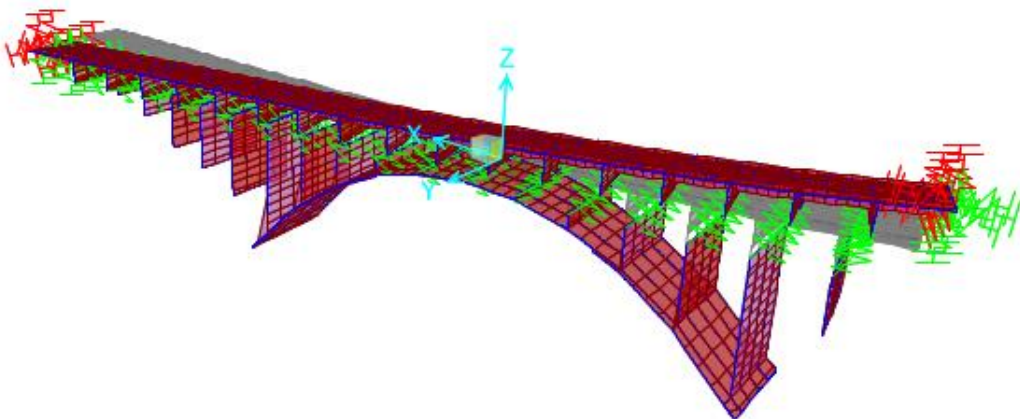
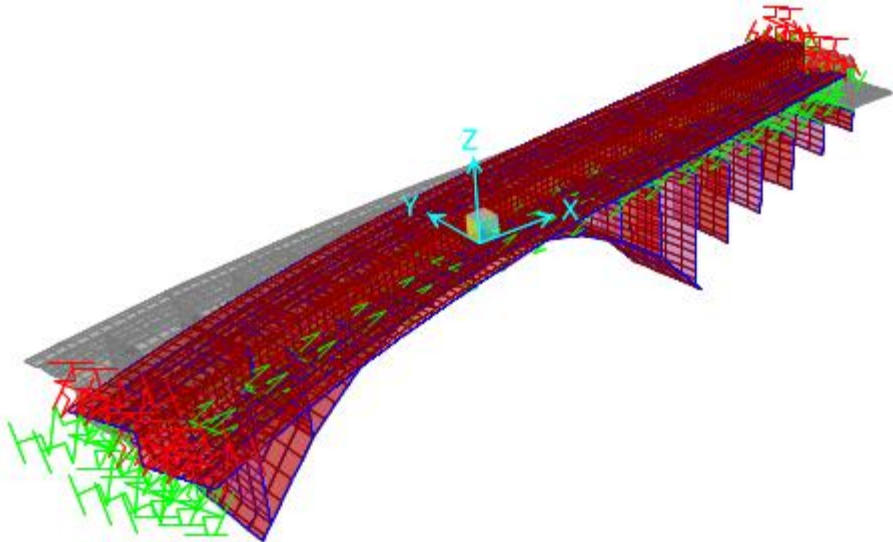
Following table concerns modal analysis outputs for (IS) system, remarking the increasing vibration period of the structure, in the case of fixed restraint conditions at the base of the cross walls. Despite of current structural solution, (IS)-one guarantees a more “regular” dynamic behaviour: earliest three modes includes about 70% of mass participation mass ratio, involving deck torsional displacements, as well as sliding motions in longitudinal and transversal directions.

Modal analysis output: (IS Model) Three deformable decks with fixed joints													
Mode	T [sec]	UX %	UY%	UZ%	ΣUX%	ΣUY%	ΣUZ%	RX	RY	RZ	ΣRX%	ΣRY%	ΣRZ%
1	1.507527	0.1	0.234	1.4E-07	0.1	0.234	1.4E-07	0.073	0.0057	<b>69.347</b>	0.073	0.0057	69.347
2	1.432480	<b>61.72</b>	0.161	2.5E-08	61.819	0.395	1.7E-07	0.044	0.919	0.159	0.117	0.925	69.506
3	1.428163	0.177	<b>61.595</b>	2.5E-06	61.996	61.99	2.7E-06	16.724	0.00288	1.469	<b>16.84</b>	0.928	70.975
4	0.418229	7.8E-05	0.006617	0.00181	61.997	61.996	0.00181	0.0006	0.00094	2.4E-05	16.841	0.928	70.975
5	0.321103	0.37	0.00251	0.00032	62.366	61.999	0.00212	0.004	0.027	0.00378	16.845	0.955	70.979
6	0.300164	0.379	0.002595	0.00044	62.745	62.002	0.00256	0.0037	0.029	6.8E-05	16.848	0.984	70.979
7	0.283025	0.492	0.003307	0.00046	63.237	62.005	0.00302	0.0033	0.032	0.00356	16.852	1.016	70.982
8	0.280385	0.304	0.002006	0.00037	63.541	62.007	0.00339	0.0032	0.021	0.00223	16.855	1.037	70.984
9	0.267153	0.34	0.002273	0.00047	63.882	62.009	0.00386	0.0028	0.023	6.4E-05	16.858	1.06	70.984
10	0.266486	0.328	0.00227	0.0005	64.209	62.011	0.00436	0.003	0.029	0.00164	16.861	1.089	70.986
11	0.244932	0.269	0.001809	0.00055	64.478	62.013	0.00491	0.0045	0.023	0.00984	16.865	1.112	70.996
12	0.217332	1.5E-05	9.65E-05	0.026	64.478	62.013	0.031	0.019	0.108	0.00141	16.884	1.221	70.997
13	0.214393	0.307	0.002086	0.00129	64.785	62.015	0.032	0.0059	0.026	0.00732	16.89	1.247	71.005
14	0.208321	0.278	0.001857	0.00069	65.063	62.017	0.033	0.0013	0.021	0.00959	16.891	1.268	71.014
15	0.197725	0.285	0.001934	0.00172	65.347	62.019	0.034	0.002	0.036	0.00672	16.893	1.304	71.021
16	0.182232	0.273	0.001854	4.2E-06	65.62	62.021	0.034	0.0004	0.00384	4.8E-07	16.893	1.308	71.021
17	0.181731	0.103	0.000753	3.1E-06	65.723	62.022	0.034	0.0001	0.00136	0.00091	16.894	1.309	71.022
18	0.181101	0.126	0.00079	1.8E-06	65.849	62.023	0.034	0.0002	0.00179	0.00137	16.894	1.311	71.023
19	0.159991	0.243	3.67E-06	3.3E-18	66.092	62.023	0.034	2E-06	0.00815	0.00056	16.894	1.319	71.024
20	0.149856	0.111	0.000533	1.2E-06	66.203	62.023	0.034	8E-05	0.00155	0.00277	16.894	1.321	71.027
21	0.145241	0.267	4.03E-06	5.3E-18	66.471	62.023	0.034	2E-06	0.00895	0.00039	16.894	1.33	71.027
22	0.144817	0.266	3.98E-06	1.8E-17	66.737	62.023	0.034	2E-06	0.0089	0.00464	16.894	1.339	71.032
23	0.143263	0.103	0.000954	1.4E-06	66.839	62.024	0.034	0.0002	0.00137	0.00224	16.894	1.34	71.034
24	0.139241	4.3E-06	4.96E-06	0.031	66.839	62.024	0.066	0.191	8E-05	6.8E-06	17.085	1.34	71.034
25	0.129776	6.1E-06	2.32E-05	0.523	66.839	62.024	0.589	0.176	0.429	1.8E-05	17.261	1.769	71.034
26	0.117517	0.197	2.95E-06	2.3E-16	67.036	62.024	0.589	2E-06	0.0066	0.00286	17.261	1.776	71.037
27	0.117516	0.197	2.95E-06	2.3E-16	67.233	62.024	0.589	2E-06	0.00659	0.00906	17.261	1.782	71.046
28	0.111700	0.012	7.95E-05	0.00864	67.245	62.024	0.597	0.011	0.053	6.5E-05	17.272	1.835	71.046
29	0.107206	0.12	0.005459	1E-05	67.365	62.03	0.597	0.0008	0.00092	0.00277	17.273	1.836	71.049
30	0.106355	0.117	0.005304	3.7E-06	67.482	62.035	0.597	0.0009	0.00101	0.00663	17.274	1.837	71.055
31	0.103898	1.5E-11	4.16E-06	3.487	67.482	62.035	4.084	0.518	0.663	2.2E-05	17.792	2.501	71.055
32	0.103441	4.8E-05	1.62E-05	0.397	67.482	62.035	4.481	1.991	14.937	1.4E-05	19.782	17.438	71.055
33	0.103125	0.195	1.58E-06	1.8E-17	67.677	62.035	4.481	6E-07	0.00412	0.00045	19.782	17.442	71.056
34	0.103064	0.013	0.000101	0.013	67.69	62.035	4.494	0.0094	0.038	5.2E-05	19.792	17.48	71.056
35	0.101588	0.031	0.00019	0.02	67.72	62.035	4.514	0.011	0.103	2.2E-07	19.803	17.583	71.056
36	0.098175	0.012	6.39E-05	0.013	67.733	62.035	4.527	0.0024	0.058	7.2E-05	19.805	17.641	71.056
37	0.097830	0.014	9.26E-05	0.02	67.747	62.035	4.547	0.0034	0.054	1.6E-05	19.809	17.695	71.056
38	0.097346	9.6E-08	3.71E-05	0.226	67.747	62.035	4.773	0.585	0.41	9.6E-05	20.394	18.104	71.056
39	0.096755	0.00552	4.31E-05	0.00346	67.753	62.035	4.777	0.0021	0.00844	4.9E-06	20.396	18.113	71.056
40	0.094299	4.4E-07	2.14E-05	0.321	67.753	62.035	5.098	1.796	0.329	5.7E-05	22.191	18.442	71.056
41	0.093618	0.214	1.73E-06	3E-15	67.967	62.035	5.098	7E-07	0.00453	0.00031	22.191	18.446	71.056
42	0.093344	0.213	1.72E-06	2.6E-15	68.179	62.035	5.098	7E-07	0.0045	0.00373	22.191	18.451	71.06
43	0.092298	1.6E-06	3.41E-06	0.993	68.179	62.035	6.091	0.321	0.061	1.4E-07	22.512	18.512	71.06
44	0.086184	0.032	0.00029	0.024	68.211	62.036	6.114	0.033	0.099	0.00047	22.545	18.611	71.061
45	0.084295	0.074	0.003319	6.5E-10	68.285	62.039	6.114	0.0006	0.00076	0.00759	22.546	18.611	71.068
46	0.080348	5.3E-06	2.92E-07	0.215	68.285	62.039	6.329	0.056	1.353	2.1E-07	22.602	19.964	71.068
47	0.079858	0.08	0.001827	0.071	68.365	62.041	6.4	0.069	0.109	0.0007	22.671	20.074	71.069
48	0.077113	0.036	5.98E-05	0.032	68.401	62.041	6.431	9E-06	0.057	0.00046	22.671	20.131	71.069
49	0.075748	0.05	4.05E-07	3.6E-07	68.451	62.041	6.431	8E-08	0.00098	0.00937	22.671	20.132	71.079
50	0.075747	0.288	1.08E-06	0.00035	68.739	62.041	6.432	2E-07	0.012	0.00015	22.671	20.145	71.079



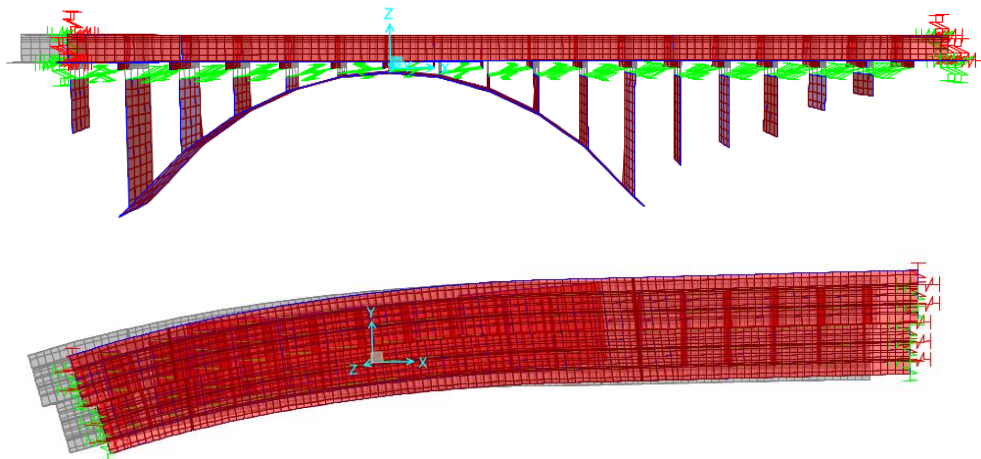
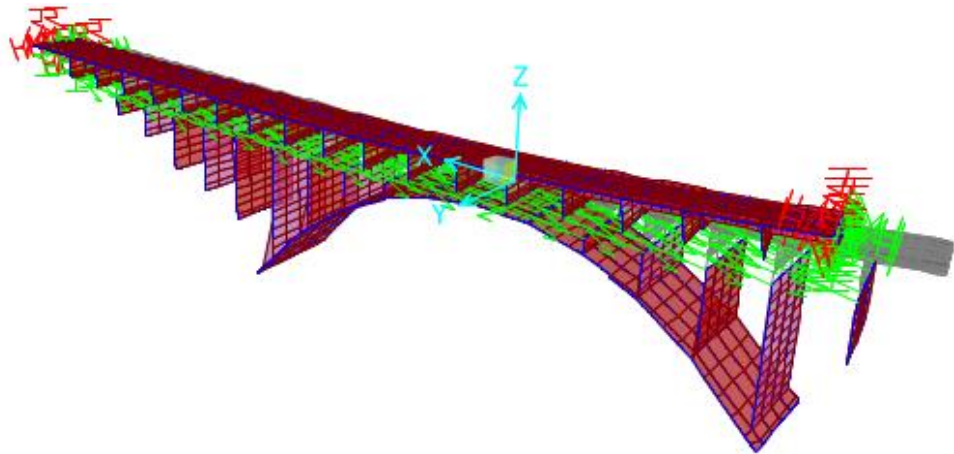
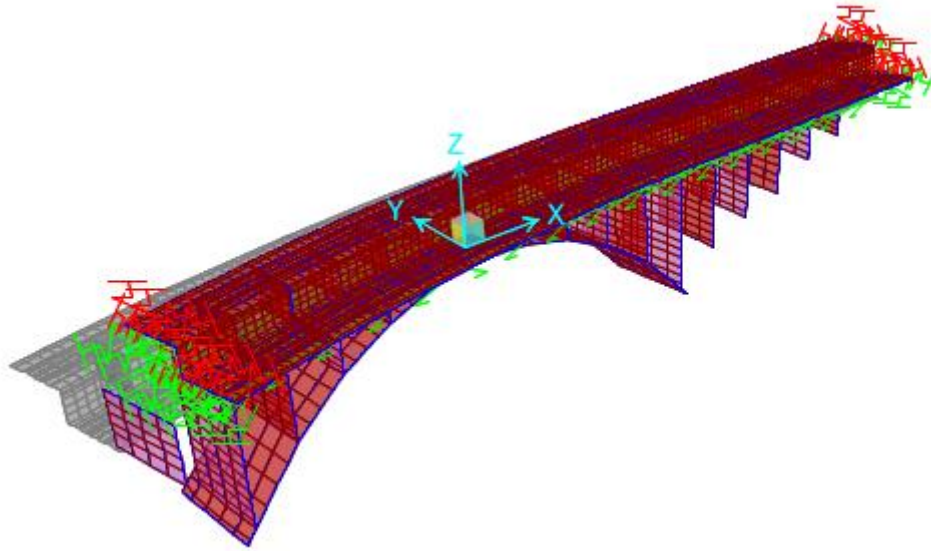
Mode	T [sec]	UX %	UY%	UZ%	ΣUX%	ΣUY%	ΣUZ%	RX	RY	RZ	ΣRX%	ΣRY%	ΣRZ%
51	0.075720	0.469	0.000185	0.388	69.208	62.041	6.82	0.0039	1.21	0.00103	22.675	21.354	71.08
52	0.074244	5.1E-08	8.75E-05	2.521	69.208	62.041	9.341	8.081	0.422	2.5E-05	30.756	21.776	71.08
53	0.072032	4.7E-06	2.68E-05	1.336	69.208	62.041	10.677	2.231	1.309	3.8E-05	32.987	23.085	71.08
54	0.068533	0.515	0.001567	0.341	69.723	62.043	11.019	0.142	1.287	0.00036	33.129	24.372	71.08
55	0.068166	0.017	2.08E-05	0.323	69.74	62.043	11.342	0.207	0.359	2.4E-05	33.336	24.732	71.08
56	0.067022	0.047	3E-06	0.00034	69.787	62.043	11.342	0.042	0.569	0.00048	33.378	25.301	71.081
57	0.066486	0.878	0.00018	0.577	70.666	62.043	11.919	0.0023	1.495	0.00039	33.381	26.796	71.081
58	0.063734	2.313	0.065	1.606	72.978	62.108	13.525	0.726	1.444	0.00176	34.106	28.24	71.083
59	0.063665	0.2	0.018	0.00152	73.178	62.126	13.527	0.964	0.697	0.00206	35.07	28.938	71.085
60	0.062848	0.00069	5.92E-05	0.613	73.179	62.126	14.14	0.27	1.261	0.00013	35.34	30.199	71.085
61	0.058705	0.006	0.004353	0.094	73.185	62.131	14.234	0.151	0.121	0.00215	35.491	30.32	71.087
62	0.057624	0.058	0.041	0.066	73.243	62.172	14.299	0.105	0.186	0.00557	35.596	30.506	71.093
63	0.056572	0.00515	0.004062	10.398	73.248	62.176	24.697	5.096	0.00036	0.00077	40.692	30.506	71.094
64	0.055632	0.069	0.002622	0.00593	73.318	62.178	24.703	0.021	0.15	0.00436	40.713	30.656	71.098
65	0.054954	0.081	0.021	2.235	73.399	62.199	26.939	0.011	0.02	0.014	40.724	30.676	71.112
66	0.052559	0.178	0.00031	14.282	73.577	62.199	41.221	0.1	1.364	0.01	40.824	32.04	71.122
67	0.052017	0.24	0.007875	16.243	73.818	62.207	57.464	0.0005	0.091	0.00264	40.824	32.131	71.125
68	0.051292	0.227	0.003791	1.07	74.045	62.211	58.534	0.061	0.465	0.00592	40.886	32.596	71.131
69	0.049718	0.137	0.166	1.413	74.181	62.377	59.947	0.464	0.356	0.052	41.35	32.952	71.182
70	0.048785	2.402	0.004694	0.00028	76.583	62.381	59.947	0.0002	1.056	0.089	41.35	34.008	71.271
71	0.047336	9E-05	0.005304	2.59	76.583	62.387	62.538	0.605	0.881	0.00288	41.955	34.889	71.274
72	0.045765	0.585	0.617	0.181	77.168	63.004	62.719	1.088	0.024	0.197	43.043	34.913	71.471
73	0.045535	0.297	1.152	0.015	77.466	64.156	62.734	2.96	0.238	0.427	46.003	35.151	71.898
74	0.044042	0.474	0.249	0.00742	77.94	64.405	62.741	0.458	0.149	0.126	46.461	35.3	72.024
75	0.041162	0.101	5.193	0.23	78.041	69.597	62.971	6.331	0.031	0.33	52.792	35.331	72.354
76	0.040664	0.00183	0.467	0.698	78.043	70.065	63.669	0.299	0.052	3.212	53.091	35.382	75.566
77	0.039953	0.078	4.429	0.489	78.121	74.494	64.158	6.932	0.116	4.843	60.023	35.498	80.409
78	0.039008	0.041	4.612	0.041	78.163	79.106	64.199	3.964	0.019	0.658	63.986	35.517	81.068
79	0.038369	0.021	2.022	0.209	78.183	81.128	64.408	1.518	4.9E-05	3.502	65.505	35.517	84.569
80	0.035488	1.253	0.022	0.035	79.437	81.15	64.443	0.0094	0.124	0.00261	65.514	35.641	84.572
81	0.034006	0.00117	0.001386	4.198	79.438	81.152	68.641	0.129	0.093	0.00501	65.644	35.734	84.577
82	0.031763	1.206	0.133	0.065	80.644	81.284	68.706	0.313	0.092	0.095	65.957	35.826	84.672
83	0.031084	0.083	0.32	0.171	80.727	81.604	68.877	0.289	0.025	0.353	66.246	35.851	85.025
84	0.029533	0.456	0.065	0.373	81.183	81.669	69.25	0.283	0.02	0.087	66.529	35.871	85.112
85	0.027818	0.094	0.057	4.93	81.277	81.726	74.18	0.0041	0.411	4.6E-05	66.533	36.282	85.112
86	0.024611	0.00711	0.000649	0.00218	81.284	81.727	74.182	0.004	0.031	2.287	66.537	36.313	87.4
87	0.023690	3.679	0.144	0.00123	84.963	81.871	74.184	0.013	0.199	0.00314	66.55	36.512	87.403
88	0.023143	0.066	2.527	0.125	85.029	84.399	74.309	1.003	0.094	0.37	67.553	36.606	87.773
89	0.021414	0.00352	0.091	9.018	85.032	84.49	83.326	0.105	0.949	0.017	67.658	37.555	87.79
90	0.020866	5.932	0.037	0.023	90.964	84.527	83.349	0.23	0.973	0.128	67.888	38.528	87.918
91	0.017694	0.04	0.742	0.038	91.004	85.27	83.387	0.322	1E-04	1.647	68.21	38.528	89.565
92	0.017059	0.00749	3.344	0.011	91.012	88.614	83.398	1.276	0.015	0.773	69.485	38.543	90.338
93	0.014217	0.0009	0.078	5.436	91.012	88.692	88.834	0.0005	0.366	0.01	69.486	38.908	90.348
94	0.012132	0.00612	1.751	0.00017	91.019	90.443	88.834	0.886	0.015	2.264	70.372	38.923	92.612
95	0.011882	1.795	0.316	0.00083	92.814	90.76	88.835	0.063	0.016	0.222	70.435	38.94	92.834
96	0.011159	0.461	3.091	0.024	93.275	93.851	88.859	0.752	0.021	1.033	71.187	38.961	93.867
97	0.007330	1.276	1.765	0.017	94.551	95.616	88.876	0.05	0.029	1.524	71.236	38.99	95.391
98	0.007110	3.803	0.398	0.046	98.353	96.014	88.922	0.061	0.00315	0.499	71.297	38.993	95.89
99	0.006650	0.00727	2.23E-05	7.556	98.361	96.014	96.478	0.0012	0.3	0.027	71.298	39.293	95.917
100	0.006278	0.00191	2.078	0.018	98.363	98.092	96.497	0.119	0.024	2.963	71.417	39.317	98.879

(1) Mode 1: T= 1.51 sec, UX= 31.376% , RZ=69.35%



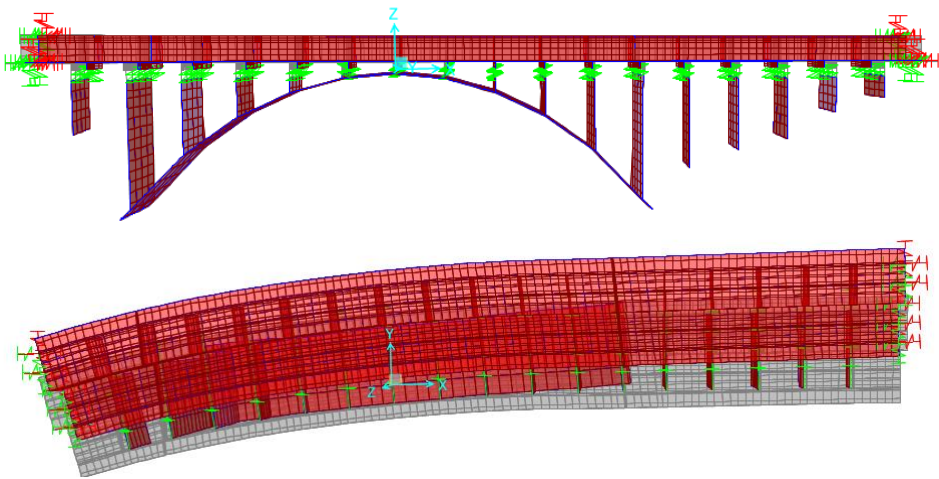
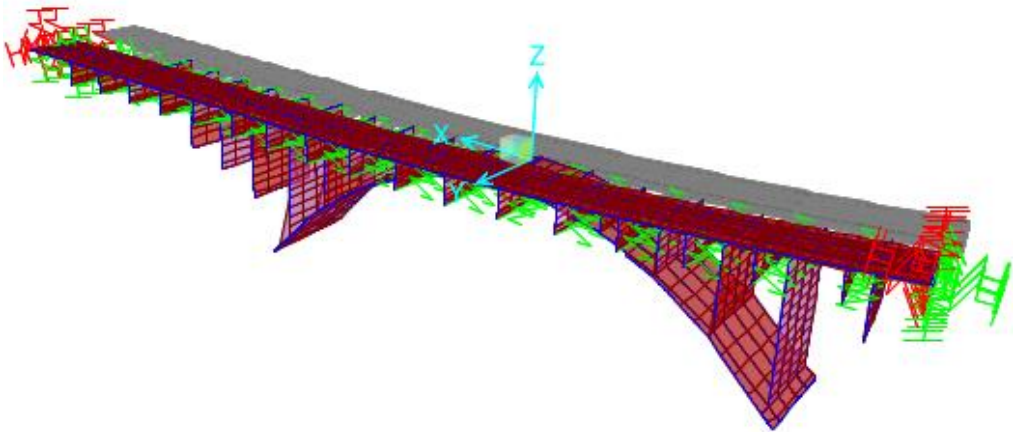
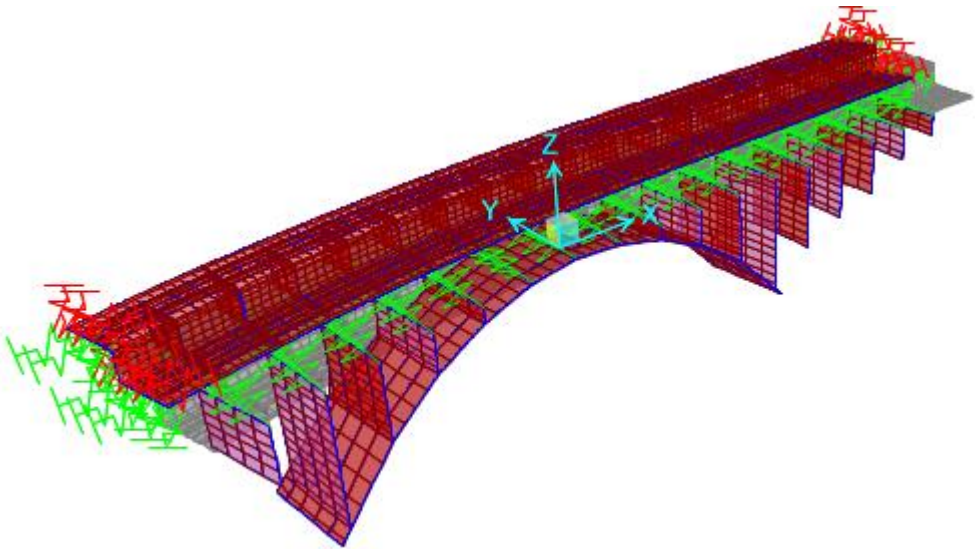
Mode	T [sec]	Ux (%)	UY (%)	UZ (%)	Sum UX	Sum UY	Sum UZ
1	1.51	0.1	0.234	1.4E-07	0.10	0.234	1.4E-07
Modo	T [sec]	RX (%)	RY (%)	RZ (%)	Sum RX	Sum RY	Sum RZ
1	1.51	0.073	0.0057	69.347	0.073	0.0057	69.347

(2) Mode 2: T= 1.43 sec, UX= 61.72%



Mode	T [sec]	Ux (%)	UY (%)	UZ (%)	Sum UX	Sum UY	Sum UZ
2	1.43	61.72	0.161	2.5E-08	61.819	0.395	1.7E-07
Modo	T [sec]	RX (%)	RY (%)	RZ (%)	Sum RX	Sum RY	Sum RZ
2	1.43	0.044	0.919	0.159	0.117	0.925	69.506

(3) Mode 3: T= 1.428 sec, UY= 61.59%, RY=16.84%



Mode	T [sec]	Ux (%)	UY (%)	UZ (%)	Sum UX	Sum UY	Sum UZ
3	1.428	0.177	61.595	2.5E-06	61.996	61.99	2.7E-06
Modo	T [sec]	RX (%)	RY (%)	RZ (%)	Sum RX	Sum RY	Sum RZ
3	1.428	16.724	0.00288	1.469	16.84	0.928	70.975

In order to test its efficiency, a comparison between (IS)-Fixed-cross-wall-model and (IS)-Hinged-Cross-wall-model follows, both considering global base reactions coming from Modal response spectrum analysis (in X-X and Y-Y directions), and comparing the percentage carried by single element. It's easy to note that the greatest changes occurred for shear forces, varying cross wall-bottom-restraint conditions.

Base Reactions - IS Model - Fixed Joints: Modal XX - Output						
GlobalFX	GlobalFY	GlobalFZ	GlobalMX	GlobalMY	GlobalMZ	GlobalM( $\Delta N$ )
KN	KN	KN	KN-m	KN-m	KN-m	KN-m
3468.92	263.75	2364.65	190.28	4262.01	107.29	8985.69

Base Reactions - IS Model - Hinged Joints: Modal XX - Output						
GlobalFX	GlobalFY	GlobalFZ	GlobalMX	GlobalMY	GlobalMZ	GlobalM( $\Delta N$ )
KN	KN	KN	KN-m	KN-m	KN-m	KN-m
4945.74	375.78	2336.29	0.00	0.00	0.00	8877.91

Base Reactions - IS Model - Fixed Joints: Modal YY - Output						
GlobalFX	GlobalFY	GlobalFZ	GlobalMX	GlobalMY	GlobalMZ	GlobalM( $\Delta N$ )
KN	KN	KN	KN-m	KN-m	KN-m	KN-m
3421.76	373.22	2098.74	2644.38	252.59	62.36	7975.20

Base Reactions - IS Model - Hinged Joints: Modal YY - Output						
GlobalFX	GlobalFY	GlobalFZ	GlobalMX	GlobalMY	GlobalMZ	GlobalM( $\Delta N$ )
KN	KN	KN	KN-m	KN-m	KN-m	KN-m
3598.12	452.21	3129.81	0.00	0.00	0.00	11893.27

As follows, both models are compared again, valuing, at NA-abutment, SA-Abutment, arch-pier n.2, and arch-pier n.12, the corresponding carried aliquot, in term of shear force [Fx, Fy], uplift reactions [ $\Delta N$ ], global Moment [Mxx, Myy, Mzz, M( $\Delta N$ )].



FX- distribution: Modal XX (Fixed-joints IS-model)								
Column	Abut. NA Fx [kN]	%tot	Pier 2 Fx [kN]	% tot	Pier 12 Fx [kN]	%tot	Abut. SA Fx [kN]	%tot
<b>1</b>	0.33	0.01	35.21	1.02	39.43	1.14	0.33	0.010
<b>2</b>	0.33	0.01	42.5	1.23	43.63	1.26	0.33	0.010
<b>3</b>	0.33	0.01	52.36	1.51	53.88	1.55	0.33	0.010
<b>4</b>	0.33	0.01	44.91	1.29	46.13	1.33	0.33	0.010
<b>5</b>	0.33	0.01	70.74	2.04	63.62	1.83	0.33	0.010
<b>TOT</b>	<b>1.65</b>	<b>0.05</b>	<b>245.72</b>	<b>7.08</b>	<b>246.69</b>	<b>7.11</b>	<b>1.65</b>	<b>0.048</b>

FX- distribution: Modal XX (Hinged-joints IS-model)								
Column	Abut. NA Fx [kN]	%tot	Pier 2 Fx [kN]	% tot	Pier 12 Fx [kN]	%tot	Abut. SA Fx [kN]	%tot
<b>1</b>	200.85	4.06	34.71	0.70	39.28	0.79	210.53	4.256
<b>2</b>	203.23	4.11	42.45	0.86	43.7	0.88	210.05	4.247
<b>3</b>	205.71	4.16	52.11	1.05	53.93	1.09	209.56	4.237
<b>4</b>	207.61	4.20	44.62	0.90	46.02	0.93	209.83	4.242
<b>5</b>	209.98	4.25	72.34	1.46	63.92	1.29	209.36	4.233
<b>TOT</b>	<b>1027.38</b>	<b>20.7</b>	<b>246.23</b>	<b>4.98</b>	<b>246.85</b>	<b>4.99</b>	<b>1049.33</b>	<b>21.22</b>

FX- distribution: Modal YY (Fixed-joints IS-model)								
Column	Abut. NA Fx [kN]	%tot	Pier 2 Fx [kN]	% tot	Pier 12 Fx [kN]	%tot	Abut. SA Fx [kN]	%tot
<b>1</b>	0.0043	0.00	41.83	9.92	37.57	8.91	0.0012	0.0002
<b>2</b>	0.0029	0.00	10.93	2.59	4.54	1.08	0.0013	0.0003
<b>3</b>	0.0015	0.00	5.71	1.35	4.52	1.07	0.0013	0.0003
<b>4</b>	0.0001	0.00	2.15	0.51	8.71	2.07	0.0015	0.0003
<b>5</b>	0.0001	0.00	27.28	6.47	39.71	9.42	0.0033	0.0007
<b>TOT</b>	<b>0.0089</b>	<b>0.00</b>	<b>87.9</b>	<b>20.8</b>	<b>95.05</b>	<b>22.5</b>	<b>0.0086</b>	<b>0.00</b>

FX- distribution: Modal YY (Hinged-joints IS-model)								
Column	Abut. NA Fx [kN]	%tot	Pier 2 Fx [kN]	% tot	Pier 12 Fx [kN]	%tot	Abut. SA Fx [kN]	%tot
<b>1</b>	42.24	7.06	42.98	7.19	38.63	6.46	18.72	3.12982
<b>2</b>	27.79	4.65	10.98	1.84	4.15	0.69	10.2	1.70535
<b>3</b>	12.76	2.13	5.74	0.96	4.53	0.76	2.48	0.41463
<b>4</b>	4.08	0.68	2.14	0.36	8.57	1.43	4.87	0.84222
<b>5</b>	11.17	1.87	28.18	4.71	40.59	6.79	13.27	2.21862
<b>TOT</b>	<b>98.04</b>	<b>16.39</b>	<b>90.02</b>	<b>15.05</b>	<b>96.47</b>	<b>16.13</b>	<b>49.54</b>	<b>8.28</b>

FY- distribution: Modal XX (Fixed-joints IS-model)								
Column	Abut. NA FY [kN]	%tot	Pier 2 FY [kN]	% tot	Pier 12 FY [kN]	%tot	Abut. SA FY [kN]	%tot
1	0.0012	0.00	5.3	2.01	5.58	2.12	0.0018	0.0007
2	0.001	0.00	7.18	2.72	3.97	1.51	0.0018	0.0007
3	0.001	0.00	11.06	4.19	4.43	1.68	0.0018	0.0007
4	0.001	0.00	12.73	4.83	4.63	1.76	0.0018	0.0007
5	0.001	0.00	7.64	2.90	9.6	3.64	0.0017	0.0006
<b>TOT</b>	<b>0.0052</b>	<b>0.00</b>	<b>43.91</b>	<b>16.65</b>	<b>28.21</b>	<b>10.70</b>	<b>0.0089</b>	<b>0.003</b>

FY- distribution: Modal XX (Hinged-joints IS-model)								
Column	Abut. NA FY [kN]	%tot	Pier 2 FY [kN]	% tot	Pier 12 FY [kN]	%tot	Abut. SA FY [kN]	%tot
1	13.24	3.52	5.79	1.54	5.53	1.47	3.3	0.8782
2	13.79	3.67	7.86	2.09	4.06	1.08	3.3	0.8782
3	14.36	3.82	11.03	2.94	4.14	1.10	3.3	0.8782
4	14.62	3.89	15.68	4.17	6.01	1.60	3.31	0.8808
5	15.16	4.03	6.84	1.82	10.12	2.69	3.31	0.8808
<b>TOT</b>	<b>71.17</b>	<b>18.94</b>	<b>47.2</b>	<b>12.56</b>	<b>29.86</b>	<b>7.95</b>	<b>16.52</b>	<b>4.40</b>

FY- distribution: Modal YY (Fixed-joints IS-model)								
Column	Abut. NA FY [kN]	%tot	Pier 2 FY [kN]	% tot	Pier 12 FY [kN]	%tot	Abut. SA FY [kN]	%tot
1	0.34	0.01	27.41	0.89	27.31	0.89	0.34	0.011063
2	0.34	0.01	43.66	1.42	45.01	1.46	0.34	0.011063
3	0.34	0.01	51.84	1.69	53.03	1.73	0.34	0.011063
4	0.34	0.01	49.02	1.60	49.71	1.62	0.34	0.011063
5	0.34	0.01	36.16	1.18	35.77	1.16	0.34	0.011063
<b>TOT</b>	<b>1.7</b>	<b>0.06</b>	<b>208.09</b>	<b>6.77</b>	<b>210.83</b>	<b>6.86</b>	<b>1.7</b>	<b>0.06</b>

FY- distribution: Modal YY (Hinged-joints IS-model)								
Column	Abut. NA FY [kN]	%tot	Pier 2 FY [kN]	% tot	Pier 12 FY [kN]	%tot	Abut. SA FY [kN]	%tot
1	152.71	3.77	25.51	0.63	25.6	0.63	151.87	3.747829
2	149.43	3.69	46.02	1.14	48.33	1.19	151.85	3.747335
3	146.01	3.60	51.06	1.26	52.73	1.30	151.82	3.746595
4	143.97	3.55	52.21	1.29	53.86	1.33	153.06	3.777195
5	140.68	3.47	33.19	0.82	33.09	0.82	153.03	3.776455
<b>TOT</b>	<b>732.8</b>	<b>18.08</b>	<b>207.99</b>	<b>5.13</b>	<b>213.61</b>	<b>5.27</b>	<b>761.63</b>	<b>18.80</b>

<b>ΔN- distribution: Modal XX (Fixed-joints IS-model)</b>								
<b>Column</b>	<b>Abut. NA ΔN [kN]</b>	<b>%tot</b>	<b>Pier 2 ΔN [kN]</b>	<b>% tot</b>	<b>Pier 12 ΔN [kN]</b>	<b>%tot</b>	<b>Abut. SA ΔN [kN]</b>	<b>%tot</b>
<b>1</b>	0.002	0.00	71.06	3.01	64.99	2.75	0.00092	4E-05
<b>2</b>	0.0018	0.00	94.81	4.01	89.81	3.80	0.00092	4E-05
<b>3</b>	0.0014	0.00	108.85	4.60	98.69	4.17	0.001	4E-05
<b>4</b>	0.0015	0.00	83.34	3.52	84.87	3.59	0.001	4E-05
<b>5</b>	0.0015	0.00	90.43	3.82	84.18	3.56	0.001	4E-05
<b>TOT</b>	<b>0.0082</b>	<b>0.00</b>	<b>448.49</b>	<b>18.9</b>	<b>422.54</b>	<b>17.8</b>	<b>0.00484</b>	<b>0.00</b>

<b>ΔN- distribution: Modal XX (Hinged-joints IS-model)</b>								
<b>Column</b>	<b>Abut. NA ΔN [kN]</b>	<b>%tot</b>	<b>Pier 2 ΔN [kN]</b>	<b>% tot</b>	<b>Pier 12 ΔN [kN]</b>	<b>%tot</b>	<b>Abut. SA ΔN [kN]</b>	<b>%tot</b>
<b>1</b>	1.56	0.07	71.14	3.04	64.97	2.78	1.31	0.056
<b>2</b>	1.41	0.06	94.63	4.05	89.96	3.85	1.42	0.060
<b>3</b>	1.26	0.05	108.39	4.64	98.76	4.23	1.65	0.070
<b>4</b>	1.11	0.05	82.91	3.55	84.87	3.63	1.42	0.060
<b>5</b>	0.97	0.04	91.62	3.92	84.51	3.62	1.43	0.061
<b>TOT</b>	<b>6.31</b>	<b>0.27</b>	<b>448.69</b>	<b>19.2</b>	<b>423.07</b>	<b>18.1</b>	<b>7.23</b>	<b>0.31</b>

<b>ΔN- distribution: Modal YY (Fixed-joints IS-model)</b>								
<b>Column</b>	<b>Abut. NA ΔN [kN]</b>	<b>%tot</b>	<b>Pier 2 ΔN [kN]</b>	<b>% tot</b>	<b>Pier 12 ΔN [kN]</b>	<b>%tot</b>	<b>Abut. SA ΔN [kN]</b>	<b>%tot</b>
<b>1</b>	0.0008	0.00	43.61	2.08	39.2	1.87	0.0038	0.00018
<b>2</b>	0.001	0.00	13.52	0.64	7.84	0.37	0.004	0.00019
<b>3</b>	0.005	0.00	9.68	0.46	8.06	0.38	0.0048	0.00022
<b>4</b>	0.0015	0.00	5.87	0.28	10.8	0.51	0.0091	0.00043
<b>5</b>	0.0019	0.00	28.39	1.35	40.64	1.94	0.0013	6.1E-05
<b>TOT</b>	<b>0.0102</b>	<b>0.00</b>	<b>101.07</b>	<b>4.8</b>	<b>106.54</b>	<b>5.08</b>	<b>0.023</b>	<b>0.00</b>

<b>ΔN- distribution: Modal YY (Hinged-joints IS-model)</b>								
<b>Column</b>	<b>Abut. NA ΔN [kN]</b>	<b>%tot</b>	<b>Pier 2 ΔN [kN]</b>	<b>% tot</b>	<b>Pier 12 ΔN [kN]</b>	<b>%tot</b>	<b>Abut. SA ΔN [kN]</b>	<b>%tot</b>
<b>1</b>	12.23	0.39	44.42	1.42	39.89	1.27	7.84	0.2504
<b>2</b>	12.22	0.39	13.11	0.42	7.59	0.24	6.84	0.2185
<b>3</b>	12.23	0.39	9.53	0.30	8.15	0.26	5.85	0.1869
<b>4</b>	12.21	0.39	5.83	0.19	10.81	0.35	5.69	0.1818
<b>5</b>	12.2	0.39	29.25	0.93	41.48	1.33	4.58	0.1463
<b>TOT</b>	<b>61.09</b>	<b>1.95</b>	<b>102.14</b>	<b>3.26</b>	<b>107.92</b>	<b>3.45</b>	<b>30.8</b>	<b>0.98</b>

M( $\Delta$ N)- distribution: Modal XX (Fixed-joints IS-model)								
Column	Abut. NA M( $\Delta$ N) kNm]	%tot	Pier 2 M( $\Delta$ N) kNm]	% tot	Pier 12 M( $\Delta$ N) kNm]	%tot	Abut. SA M( $\Delta$ N) kNm]	%tot
1	0.0124	0.00	440.572	4.90	402.938	4.48	0.005704	6.35E-05
2	0.00684	0.00	360.278	4.01	341.278	3.80	0.003496	3.89E-05
3	0	0.00	0	0.00	0	0.00	0	0.00E+00
4	0.00465	0.00	258.354	2.88	263.097	2.93	0.0031	3.45E-05
5	0.0093	0.00	560.666	6.24	521.916	5.81	0.0062	6.90E-05
TOT	0.05084	0.00	1619.87	18.03	1529.229	17.02	0.0185	0.00

M( $\Delta$ N)- distribution: Modal XX (FHinged-joints IS-model)								
Column	Abut. NA M( $\Delta$ N) kNm]	%tot	Pier 2 M( $\Delta$ N) kNm]	% tot	Pier 12 M( $\Delta$ N) kNm]	%tot	Abut. SA M( $\Delta$ N) kNm]	%tot
1	9.672	0.11	441.068	4.97	402.814	4.54	8.122	0.0915
2	5.358	0.06	359.594	4.05	341.848	3.85	5.396	0.0608
3	0	0.00	0	0.00	0	0.00	0	0.0000
4	3.441	0.04	257.021	2.90	263.097	2.96	4.402	0.0496
5	6.014	0.07	568.044	6.40	523.962	5.90	8.866	0.0999
TOT	39.122	0.28	1625.727	18.31	1531.721	17.25	26.786	0.30

M( $\Delta$ N)- distribution: Modal YY (Fixed-joints IS-model)								
Column	Abut. NA M( $\Delta$ N) kNm]	%tot	Pier 2 M( $\Delta$ N) kNm]	% tot	Pier 12 M( $\Delta$ N) kNm]	%tot	Abut. SA M( $\Delta$ N) kNm]	%tot
1	0.00496	0.00	270.382	3.39	243.04	3.05	0.02356	0.000295
2	0.0038	0.00	51.376	0.64	29.792	0.37	0.0152	0.000191
3	0	0.00	0	0.00	0	0.00	0	0
4	0.00465	0.00	18.197	0.23	33.48	0.42	0.02821	0.000354
5	0.01178	0.00	176.018	2.21	251.968	3.16	0.00806	0.000101
TOT	0.06324	0.00	515.973	6.47	558.28	7.00	0.07503	0.00

M( $\Delta$ N)- distribution: Modal YY (Hinged-joints IS-model)								
Column	Abut. NA M( $\Delta$ N) kNm]	%tot	Pier 2 M( $\Delta$ N) kNm]	% tot	Pier 12 M( $\Delta$ N) kNm]	%tot	Abut. SA M( $\Delta$ N) kNm]	%tot
1	75.826	0.64	275.404	2.32	247.318	2.08	48.608	0.408702
2	46.436	0.39	49.818	0.42	28.842	0.24	25.992	0.218544
3	0	0.00	0	0.00	0	0.00	0	0
4	37.851	0.32	18.073	0.15	33.511	0.28	17.639	0.148311
5	75.64	0.64	181.35	1.52	257.176	2.16	28.396	0.238757
TOT	378.758	1.98	524.645	4.41	566.847	4.77	120.635	1.01

Mxx- distribution: Modal XX (Fixed-joints IS-model)								
Column	Abut. NA Mxx [kNm]	%tot	Pier 2 Mxx [kNm]	% tot	Pier 12 Mxx [kNm]	%tot	Abut. SA Mxx [kNm]	%tot
1	0.0001	0.00	3.08	1.62	1.74	0.91	0.0001	5.2E-05
2	0.0001	0.00	1.47	0.77	0.9	0.47	0.0001	5.2E-05
3	0.0001	0.00	3.77	1.98	1.97	1.04	0.0001	5.2E-05
4	0.0001	0.00	1.84	0.97	1.28	0.67	0.0001	5.2E-05
5	0.0001	0.00	3.39	1.78	2.67	1.40	0.0001	5.2E-05
TOT	0.0005	0.00	13.55	7.12	8.56	4.50	0.0005	0.00

Mxx- distribution: Modal YY (Fixed-joints IS-model)								
Column	Abut. NA Mxx [kNm]	%tot	Pier 2 Mxx [kNm]	% tot	Pier 12 Mxx [kNm]	%tot	Abut. SA Mxx [kNm]	%tot
1	0.001	0.00	2.97	0.11	3.27	0.12	0.0013	4.9E-05
2	0.001	0.00	2.07	0.08	2.23	0.08	0.0014	5.2E-05
3	0.001	0.00	3.26	0.12	3.61	0.14	0.0013	4.9E-05
4	0.001	0.00	2.13	0.08	2.77	0.10	0.0011	4.1E-05
5	0.001	0.00	5.16	0.20	5.6	0.21	0.0013	4.9E-05
TOT	0.005	0.00	15.59	0.59	17.48	0.66	0.0064	0.00

MYX- distribution: Modal XX (Fixed-joints IS-model)								
Column	Abut. NA MYX[kNm]	%tot	Pier 2 MYX [kNm]	% tot	Pier 12 MYX [kNm]	%tot	Abut. SA MYX [kNm]	%tot
1	0.0002	0.00	0.363	0.01	0.149	0.00	0.002	4.6E-05
2	0.0001	0.00	0.15	0.00	0.072	0.00	0.002	4.6E-05
3	0.0001	0.00	0.54	0.01	0.18	0.00	0.002	4.6E-05
4	0.0001	0.00	0.18	0.00	0.103	0.00	0.002	4.6E-05
5	0.0001	0.00	0.33	0.01	0.208	0.00	0.002	4.6E-05
TOT	0.0006	0.00	1.563	0.04	0.712	0.02	0.01	0.00

MYX- distribution: Modal YY (Fixed-joints IS-model)								
Column	Abut. NA MYX[kNm]	%tot	Pier 2 MYX [kNm]	% tot	Pier 12 MYX [kNm]	%tot	Abut. SA MYX [kNm]	%tot
1	0.002	0.00	0.35	0.14	0.28	0.11	0.005	0.001979
2	0.002	0.00	0.18	0.07	0.15	0.06	0.005	0.001979
3	0.002	0.00	0.43	0.17	0.3	0.12	0.005	0.001979
4	0.002	0.00	0.19	0.08	0.165	0.07	0.005	0.001979
5	0.002	0.00	0.45	0.18	0.36	0.14	0.005	0.001979
TOT	0.01	0.00	1.6	0.63	1.255	0.50	0.025	0.01



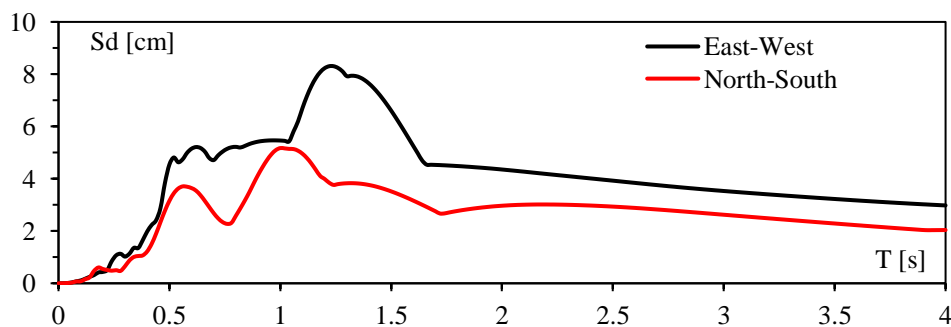
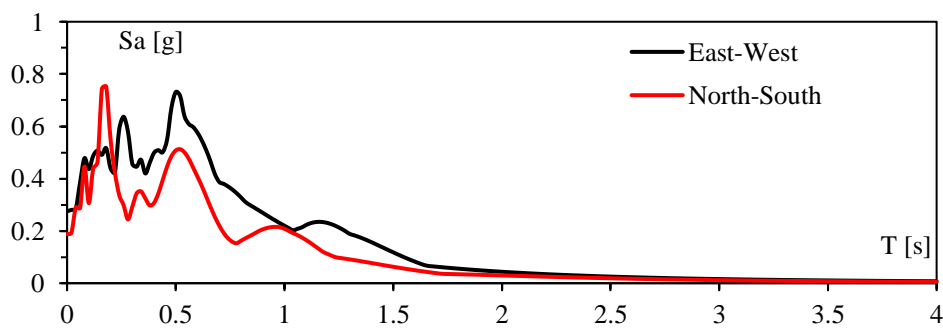
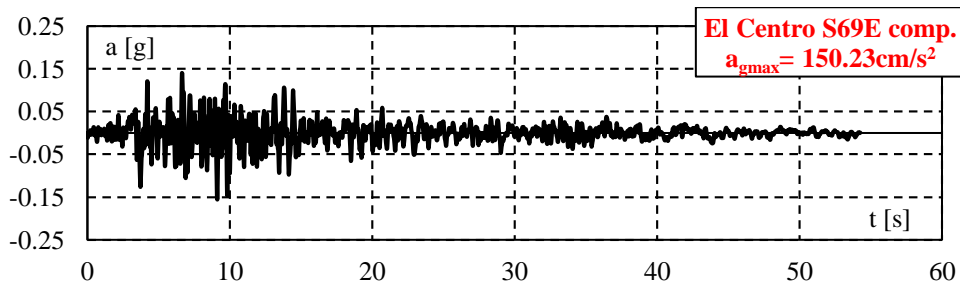
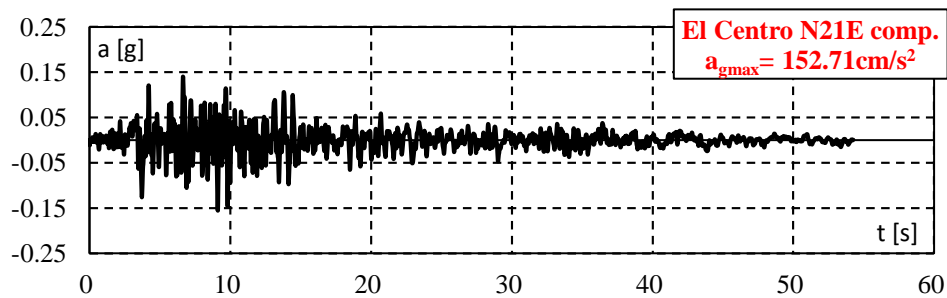
MZZ- distribution: Modal XX (Fixed-joints IS-model)								
Column	Abut. NA Mzz [kNm]	%tot	Pier 2 Mzz [kNm]	% tot	Pier 12 Mzz [kNm]	%tot	Abut. SA Mzz [kNm]	%tot
<b>1</b>	0.0003	0.00	2.88	2.68	2.51	2.34	0.003	2.8E-03
<b>2</b>	0.0001	0.00	1.02	0.95	0.68	0.63	0.003	2.8E-03
<b>3</b>	0.0001	0.00	2.13	1.99	1.039	0.97	0.003	2.8E-03
<b>4</b>	0.0001	0.00	1.41	1.31	0.78	0.73	0.003	2.8E-03
<b>5</b>	0.0003	0.00	7.01	6.53	3.73	3.48	0.003	2.8E-03
<b>TOT</b>	<b>0.0009</b>	<b>0.00</b>	<b>14.45</b>	<b>13.47</b>	<b>8.739</b>	<b>8.15</b>	<b>0.015</b>	<b>0.01</b>

MZZ- distribution: Modal YY (Fixed-joints IS-model)								
Column	Abut. NA Mzz [kNm]	%tot	Pier 2 Mzz [kNm]	% tot	Pier 12 Mzz [kNm]	%tot	Abut. SA Mzz [kNm]	%tot
<b>1</b>	0.0045	0.01	3.55	5.69	3.87	6.21	0.0065	0.010423
<b>2</b>	0.0045	0.01	2.16	3.46	2.29	3.67	0.0065	0.010423
<b>3</b>	0.0045	0.01	3.73	5.98	4.01	6.43	0.0065	0.010423
<b>4</b>	0.0045	0.01	2.25	3.61	2.45	3.93	0.0065	0.010423
<b>5</b>	0.0045	0.01	6.03	9.67	6.74	10.81	0.0065	0.010423
<b>TOT</b>	<b>0.0225</b>	<b>0.04</b>	<b>17.72</b>	16.52	<b>19.36</b>	18.04	<b>0.03</b>	0.030291

Looking at the previous tables it's deducible that for both restraint conditions, (IS) solution guarantees to reduce the percentage of global reaction carried by the arch, passing from a mean value of 60% for the current structure, to 30% of (IS) solution. There is, however, a downside: outputs from modal response spectrum analysis in X-X direction show that only 20-25% of  $F_x(\text{tot})$  and  $F_y(\text{tot})$  burden arch, while 20-30% is carried by the external abutments: this means that cross walls are overloaded (+40%), in comparison to the current state. Similar evaluation can be done considering outputs from modal response spectrum analysis in Y-Y direction: for both restraint condition, 40% of  $F_x(\text{tot})$  is carried by arch and 20% by abutments, while the remaining 40% burden cross walls; on the contrary, only 20% of global  $F_y$  is carried by arch, i.e. that, apart from the abutments(20%), again cross walls are overloaded (+50%), in comparison to the current state.

Therefore, in order to value the effective requirement of IS solution, a comparison follows, considering both the current state (three-decks solution, 3D), and possible changes occurring to this one (single deformable/undeformable deck solutions, SD and SUD), finally and (IS)-proposal: outputs are related to the highest base reactions, estimated for:

1. Modal response Spectrum (NTC08) analysis, in X-X direction
2. Modal response Spectrum (NTC08), analysis in Y-Y direction
3. Time History analysis, considering El Centro EQ in X-X direction
4. Time History analysis, considering El Centro EQ in Y-Y direction



Base Reactions - (3 decks) IS Model - Fixed Joints							(IS_F)
OutputCase	StepType	GlobalFX	GlobalFY	GlobalFZ	GlobalMX	GlobalMY	GlobalMZ
		KN	KN	KN	KN-m	KN-m	KN-m
ElCentro x	Max	2261.04	154.04	206.06	8150.50	19025.17	40486.04
ElCentro x	Min	-3542.79	-154.09	-234.89	-7911.61	-24612.11	-57243.04
ElCentro y	Max	253.81	3025.89	393.26	23977.86	2023.90	63346.99
ElCentro y	Min	-253.08	-4305.65	-420.02	-26641.79	-1475.38	-16154.01
Modal Spectrum_XX	Max	4678.93	640.36	133.24	7050.01	80506.25	31759.48
Modal Spectrum_YY	Max	540.34	5664.86	219.19	21814.23	10182.66	64144.39

Base Reactions -(3 decks) IS Model - Hinged Joints							(IS_H)
OutputCase	StepType	GlobalFX	GlobalFY	GlobalFZ	GlobalMX	GlobalMY	GlobalMZ
		KN	KN	KN	KN-m	KN-m	KN-m
ElCentro x	Max	2143.22	63.67	186.65	1858.23	19503.72	10129.04
ElCentro x	Min	-3560.31	-52.63	-93.44	-1885.43	-25212.30	-7001.03
ElCentro y	Max	61.23	2966.64	25.98	23959.79	1981.22	22488.86
ElCentro y	Min	-51.74	-4486.93	-27.57	-39229.52	-1829.04	-21765.01
Modal Spectrum_XX	Max	4892.27	572.41	46.05	1030.80	21326.36	8117.67
Modal Spectrum_YY	Max	572.23	4476.57	17.16	16074.07	1118.34	49048.09

Base Reactions - (3 decks) FIXED BASE Model - Fixed Joints							(3D-F)
OutputCase	StepType	GlobalFX	GlobalFY	GlobalFZ	GlobalMX	GlobalMY	GlobalMZ
		KN	KN	KN	KN-m	KN-m	KN-m
ElCentro x	Max	6346.24	997.82	364.38	13827.58	54854.90	60179.56
ElCentro x	Min	-6963.84	-965.14	-580.84	-18053.41	-70112.35	-122033.60
ElCentro y	Max	915.54	4767.44	1144.03	32029.04	86196.10	115027.05
ElCentro y	Min	-875.99	-5063.85	-1033.80	-36716.38	-65487.71	-120217.14
Modal Spectrum_XX	Max	7181.93	960.05	234.60	12694.20	133269.59	49698.04
Modal Spectrum_YY	Max	955.92	10241.82	617.00	31216.38	22637.42	103373.00

Base Reactions -(3 decks) FIXED BASE Model - Hinged Joints							(3D-H)
OutputCase	StepType	GlobalFX	GlobalFY	GlobalFZ	GlobalMX	GlobalMY	GlobalMZ
		KN	KN	KN	KN-m	KN-m	KN-m
ElCentro x	Max	4556.12	532.51	442.26	11063.80	83494.60	15691.22
ElCentro x	Min	-5405.61	-309.88	-271.23	-9719.71	-89249.97	-18123.18
ElCentro y	Max	622.50	3384.39	1102.18	46362.82	45163.14	167049.11
ElCentro y	Min	-320.06	-4922.14	-837.45	-60275.83	-56245.13	-197656.26
Modal Spectrum_XX	Max	8355.75	944.41	210.71	12281.66	133994.86	40973.10
Modal Spectrum_YY	Max	944.49	10060.27	686.92	33827.84	20691.91	108891.76

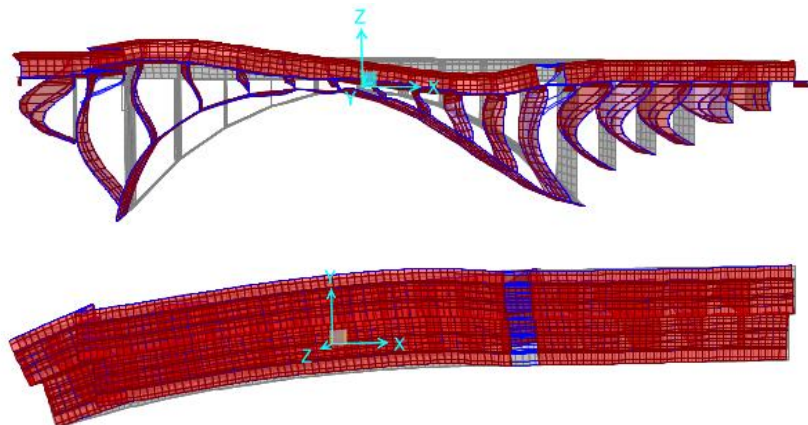
Base Reactions - (Single Undeformable -deck) FIXED BASE Model - Fixed Joints							(SUD-F)
OutputCase	StepType	GlobalFX	GlobalFY	GlobalFZ	GlobalMX	GlobalMY	GlobalMZ
		KN	KN	KN	KN-m	KN-m	KN-m
ElCentro x	Max	5673.66	700.35	543.64	10126.72	48915.44	51819.41
ElCentro x	Min	-6868.02	-380.48	-779.47	-7852.83	-51972.47	-55560.44
ElCentro y	Max	821.90	1469.76	893.05	21017.82	44432.61	46577.32
ElCentro y	Min	-480.48	-2700.63	-690.85	-27354.88	-27395.05	-75014.53
Modal Spectrum_XX	Max	6505.22	821.15	215.51	8242.37	94105.20	34209.12
Modal Spectrum_YY	Max	911.61	7247.28	452.91	12033.54	35635.01	99032.96

Base Reactions -(Single Undeformable deck) FIXED BASE Model - Hinged Joints							(SUD-H)
OutputCase	StepType	GlobalFX	GlobalFY	GlobalFZ	GlobalMX	GlobalMY	GlobalMZ
		KN	KN	KN	KN-m	KN-m	KN-m
ElCentro x	Max	1390.84	133.96	122.41	4803.30	37380.63	8581.98
ElCentro x	Min	-1891.03	-81.89	-102.66	-4437.07	-36649.83	-13595.28
ElCentro y	Max	164.35	2005.61	549.11	37371.39	13174.38	107800.58
ElCentro y	Min	-118.15	-2851.13	-424.00	-28626.92	-27936.59	-64467.93
Modal Spectrum_XX	Max	8672.44	1177.13	686.90	18452.89	133837.08	53024.09
Modal Spectrum_YY	Max	1873.39	11306.37	1566.68	35135.35	74959.34	70196.21

Base Reactions - (Single Deformable -deck) FIXED BASE Model - Fixed Joints							(SD-F)
OutputCase	StepType	GlobalFX	GlobalFY	GlobalFZ	GlobalMX	GlobalMY	GlobalMZ
		KN	KN	KN	KN-m	KN-m	KN-m
ElCentro x	Max	2444.28	646.69	400.03	9431.63	83365.05	35285.10
ElCentro x	Min	-4884.28	-1074.76	-409.34	-11617.14	-74617.05	-43331.92
ElCentro y	Max	707.63	8217.00	1246.61	37297.11	79415.40	268350.47
ElCentro y	Min	-1080.76	-8254.06	-986.92	-49608.45	-71701.85	-294334.91
Modal Spectrum_XX	Max	13334.60	2032.31	216.34	10786.48	123572.31	57888.46
Modal Spectrum_YY	Max	2032.71	11249.25	1127.83	39508.57	30233.44	206685.56

Base Reactions -(Single Undeformable deck) FIXED BASE Model - Hinged Joints							(SD-H)
OutputCase	StepType	GlobalFX	GlobalFY	GlobalFZ	GlobalMX	GlobalMY	GlobalMZ
		KN	KN	KN	KN-m	KN-m	KN-m
ElCentro x	Max	17579.73	969.94	487.97	3097.20	98673.01	88969.82
ElCentro x	Min	-11610.79	-1036.14	-321.63	-9417.09	-24617.63	-125638.24
ElCentro y	Max	747.49	21106.46	1371.66	20629.01	50683.64	307507.08
ElCentro y	Min	-1008.23	-14373.25	-1355.42	-9984.42	-39901.86	-178306.65
Modal Spectrum_XX	Max	10967.25	1840.99	310.33	15229.27	167490.38	63262.45
Modal Spectrum_YY	Max	1850.35	10433.02	1325.93	36298.37	22887.64	138170.21

Looking at modal deformed shapes, it's easy to note that, even if out of plane overturning problems seem to be reduced for central arch portion, (IS) solution emphasises deck sliding effects, in longitudinal direction, worsening slender cross walls buckling.





However, despite of single deck solution, current bridge deck partition (into three segments) makes out of plane overturning effects more controllable.

Valuing FEM analysis outputs, it's pointed out that the (IS) solution, that is quite invasive in changing bridge structural characterization, is not the best one to improve seismic capacity of Viadotto Olivieri. As planned in designing (IS) , this solution guarantees to greatly reduce base reactions, of about 25% in X-X direction, and of about 35% in Y-Y, compared to current state. But, a more interesting aspect concerns SUD, i.e. single-undeformable-deck solution, which assures base reactions decreasing of about 20%. This means that, apart from a gap of 10%, the choice of jointing current deck improve bridge capacity almost as much as (IS) solution.

## **Bibliography**

- [1] L.Santarella e E.Miozzi PONTI ITALIANI IN CEMENTO ARMATO - SOLO ATLANTE Ed. 1948
- [2] Luigi Santarella. Prontuario del Cemento Armato. 1962.
- [3] La Viabilità. Dodici anni 1950-1962. Cassa del mezzogiorno. 1962
- [4] Max Bill, Robert Maillart. Robert Maillart Bridges and Constructions. 1969
- [5] D. Billington. The tower and the Bridge: the new Art of Structural Engineering. 1985.
- [6] D.Billington. Robert Maillart and the art of Reinforced concrete. 1990
- [7] Kelly JM (1990), Base isolation: Linear theory and design, Earthquake Spectra, 1990; 6(2): 223–244.

- [8] D.Billington. Robert Maillart's Bridges. 1992
- [9] Roberto Ramasco. DINAMICA DELLE STRUTTURE scienza delle costruzioni ingegneria sismica. 1993
- [10] Petros P. Xanthakos. 1994. Theory and design of Bridges
- [11] S.E. Thomasen. Seismic strengthening of historic concrete arch bridges. Transactions on the Built Environment vol 15, © 1995 WIT Press, www.witpress.com, ISSN 1743-3509
- [12] Petrangeli M. P., Progettazione e Costruzione di Ponti, C.E. Ambrosiana, Roma, 1996
- [13] Menn, C, The Place of Aesthetics in Bridge Design, Structural Engineering International, Volume 6, No. 2, pp. 93-95, 1996
- [14] Kelly JM (1997) *Earthquake Resistant Design with Rubber*, Springer-Verlag: London.
- [15] Nasce' V.; Sabia D., [Teoria e pratica nella costruzione nei ponti in muratura tra XVIII e XIX secolo](#). In: Carlo Bernardo Mosca, 1792-1867 : un ingegnere architetto tra Illuminismo e Restaurazione / Vera Comoli, Laura Guardamagna, Micaela Viglino (cur.). Guerini, Milano, pp. 29-38. ISBN 8878027669 1997
- [16] Naeim F, Kelly J (1999) *Design of Seismic Isolated Structures: From Theory to Practice*, John Wiley and Sons, Inc.:New York, NY, USA.
- [17] David B. McCallen, Charles Noble, Matthew S. Hoehler. The Seismic Response Of Concrete Arch Bridges With Focus On The Bixby Creek Bridge Carmel, California. Technical report N. UCRL - ID - 134419. June, 1999. Lawrence Livermore National Laboratory. California Department of Transportation.
- [18] Chen W., Duan L., *Bridge Engineering Handbook*, CRC Press, 2000
- [19] Chen e Lian Duan. *Bridge Engineering Handbook*. Boca Raton : CRC Press LLC, 2000.
- [20] Raj Valluvan, John Stephenson, Don Bergman, Peter Buckland And Dave Pajouhesh. Innovative retrofit techniques for seismic retrofit of concrete arch bridges of earlier vintage. 12WCEE 2000
- [21] D.Billington. The Revolutionary Bridge by Robert Maillart. Scientific America. 2000
- [22] Menn, C, *Stahlbetonbrücken (Reinforced concrete bridges)*, 2003
- [23] R.W.Cluogh, J.Penzien. *Dynamic of structures*. 2003
- [24] Troyano L.F., *Bridge Engineering A global perspective*, 2003
- [25] R.W.Cluogh, J.Penzien. *Dynamic of structures*. 2003
- [26] Arioli M., *The Art of Structural Design : a Swiss Legacy: eine Ausstellung im Zürcher "haus konstruktiv", ETH Zürich, Rämistrasse 101, 8092 Zürich, Schweiz, www.library.ethz.ch*, 2005

- [27] Shabanovitz T. B., The Progressive Synthesis of Architecture and Engineering in Modern Bridge Design, Massachusetts Institute of Technology, June 2006
- [28] Seismic Retrofitting Manual for Highway Structures: Part 1 – Bridges.2006. US Department of Transportation. Federal Highway Administration
- [29] Dobricic S., Siviero E., De pontibus. Un manuale per la costruzione dei ponti, Il Sole 24 Ore, 2008
- [30] Theodore V. Galambos, Andrea E. Surovek. Structural stability of Steel: concepts and applications for structural engineers. John wiley & sons, inc., 2008
- [31] D.Billington. Robert Maillart: Builder, Designer, and Artist. 2008
- [32] N.Hoang, Y.Fujino, P.Warnichai. Optimal tuned mass damper for seismic applications and practical design formulas. Engineering Structures. 2008
- [33] E. Brühwiler, Prof. Dr. Civil Eng. ETH, Ecole Polytechnique Fédérale de Lausanne (EPFL), Switzerland, Christian Menn's recent bridge designs – Reducing structural elements to the simplest solution. . 5th New York City Bridge Conference, Bridge Engineering Association, New York (USA), August 17 – 18, 2009
- [34] M.A. Rutherford. A Critical Analysis Of Bixby Creek Bridge. Proceedings of Bridge Engineering 2 Conference 2009 April 2009, University of Bath, Bath, UK
- [35] Tullia Iori, Sergio Poretti. The Golden Age of “Italian Style” Engineering. Proceedings of the Third International Congress on Construction History, Cottbus, May 2009.
- [36] D.Proske – P.Gelder, “Safety of Historical Stone Arches Bridges”, Springer, 2009
- [37] Dirk Proske · Pieter van Gelder , “Safety of Historical Stone Arch Bridges”, Spriger, 2009
- [38] M. De Miranda, U.Barbisan, M.Pogacnick, L.Skansi Bridges in Venice - Architectural and Structural engineering aspects, 34<sup>th</sup> IABSE SYMPOSIUM, Venezia 2010
- [39] J. Radić and A. Kindij. The polygonal arch bridge. 2010.
- [40] E.C. Kandemira, T. Mazda, H. Nurui, H. Miyamoto. Seismic Retrofit of an Existing Steel Arch Bridge Using Viscous Damper. Elsevier. Procedia Engineering. 2011.
- [41] S. Palaoro, E. Siviero,B. Briseghella, T. Zordan. Concept and construction methods of arch bridges in Italy. ARCH'10 – 6th International Conference on Arch Bridges.
- [42] Denison, Edward e Stewart, Ian. Leggere i ponti. Modena : Logos, 2012.
- [43] D.Billington. FESTSCHRIFT. 2012

- [44] G.Tecchio, F. da Porto, P. Zampieri, C. Modena. Static and seismic retrofit of masonry arch bridges: case studies. Bridge Maintenance, Safety, Management, Resilience and Sustainability – Biondini & Frangopol (Eds) © 2012 Taylor & Francis Group, London, ISBN 978-0-415-62124-3
- [45] Lily Beyer, University of New Hampshire. Arched Bridges. Spring 2012
- [46] B. Ozden Caglayan, Kadir Ozakgul\* and Ovunc Tezer. Assessment of a concrete arch bridge using static and dynamic load tests. Structural Engineering and Mechanics, Vol. 41, No. 1 (2012) 83-94
- [47] S. De Santis & G. de Felice. Seismic analysis of masonry arches. 15 WCEE. Lisboa 2012.
- [48] Jure Radić Marija Kušter. Aesthetics and sustainability of arch bridges. ARCH13. 7<sup>th</sup> International Conference on Arch Bridges.
- [49] Denis ZASTAVNI, Jean-François CAP, Jean-Philippe JASIENSKI, Corentin FIVET. Load path and prestressing in conceptual design related to Maillart's Vessy Bridge. Proceedings of the IASS-SLTE 2014 Symposium "Shells, Membranes and Spatial Structures: Footprints" 15 to 19 September 2014, Brasilia, Brazil
- [50] Claudio Modena, Giovanni Tecchio, Carlo Pellegrino, Francesca da Porto, Marco Donà, Paolo Zampieri & Mariano A. Zanini. Reinforced concrete and masonry arch bridges in seismic areas: typical deficiencies and retrofitting strategies. Structure and Infrastructure Engineering. 2014
- [51] John Edward Finke. Doctoral Thesis Dissertion. Static and dynamic characterization of tied arch bridge. 2016
- [52] Paolo Lonetti, Arturo Pascuzzo, and Alessandro Davanzo. Dynamic Behavior of Tied-Arch Bridges under the Action of Moving Loads. Hindawi Publishing Corporation. Mathematical Problems in Engineering Volume 2016, Article ID 2749720, 17 pages

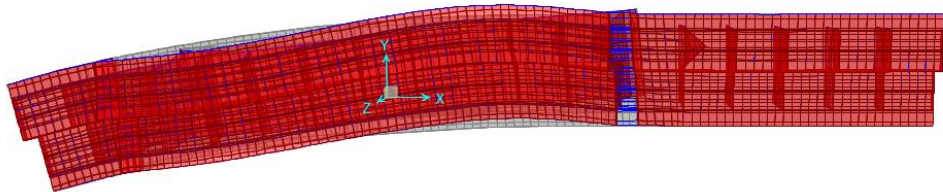
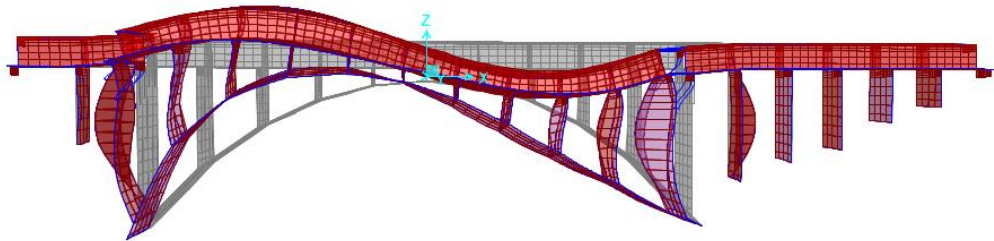
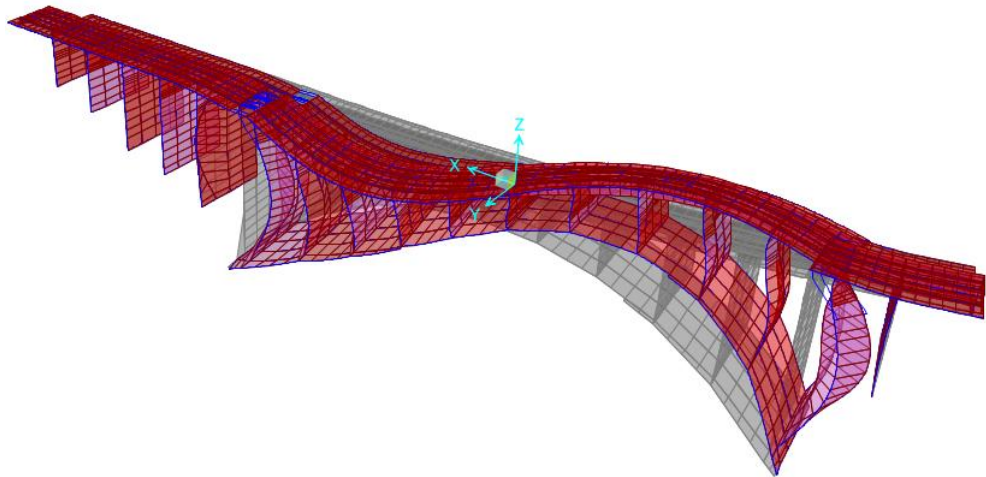
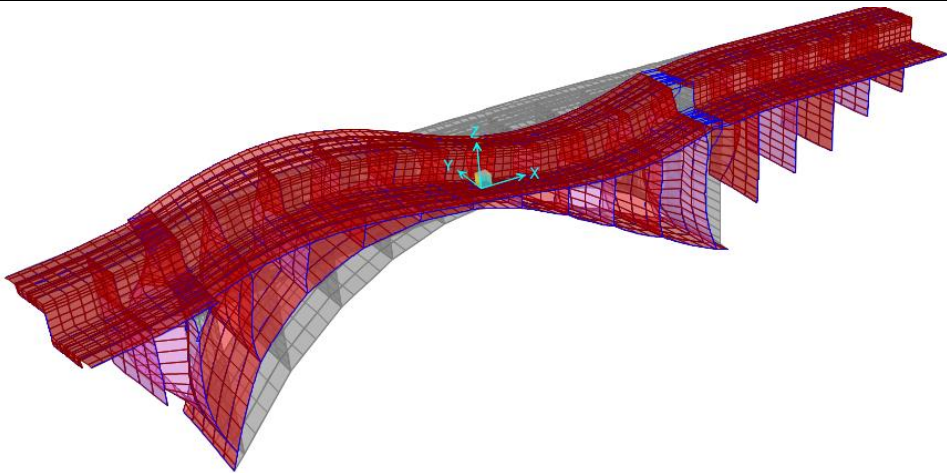
### Web references

- [1] International Database and Gallery of Structures, <http://en.structurae.de>
- [2] <http://dx.doi.org/10.1080/15732479.2014.951859>
- [3] <http://dx.doi.org/10.1155/2016/2749720>

Appendix (E): Seismic behaviour and retrofit proposal for Viadotto Olivieri (SA) – modal deformed shapes

(1.1) Three- deformable - decks model with fixed joints

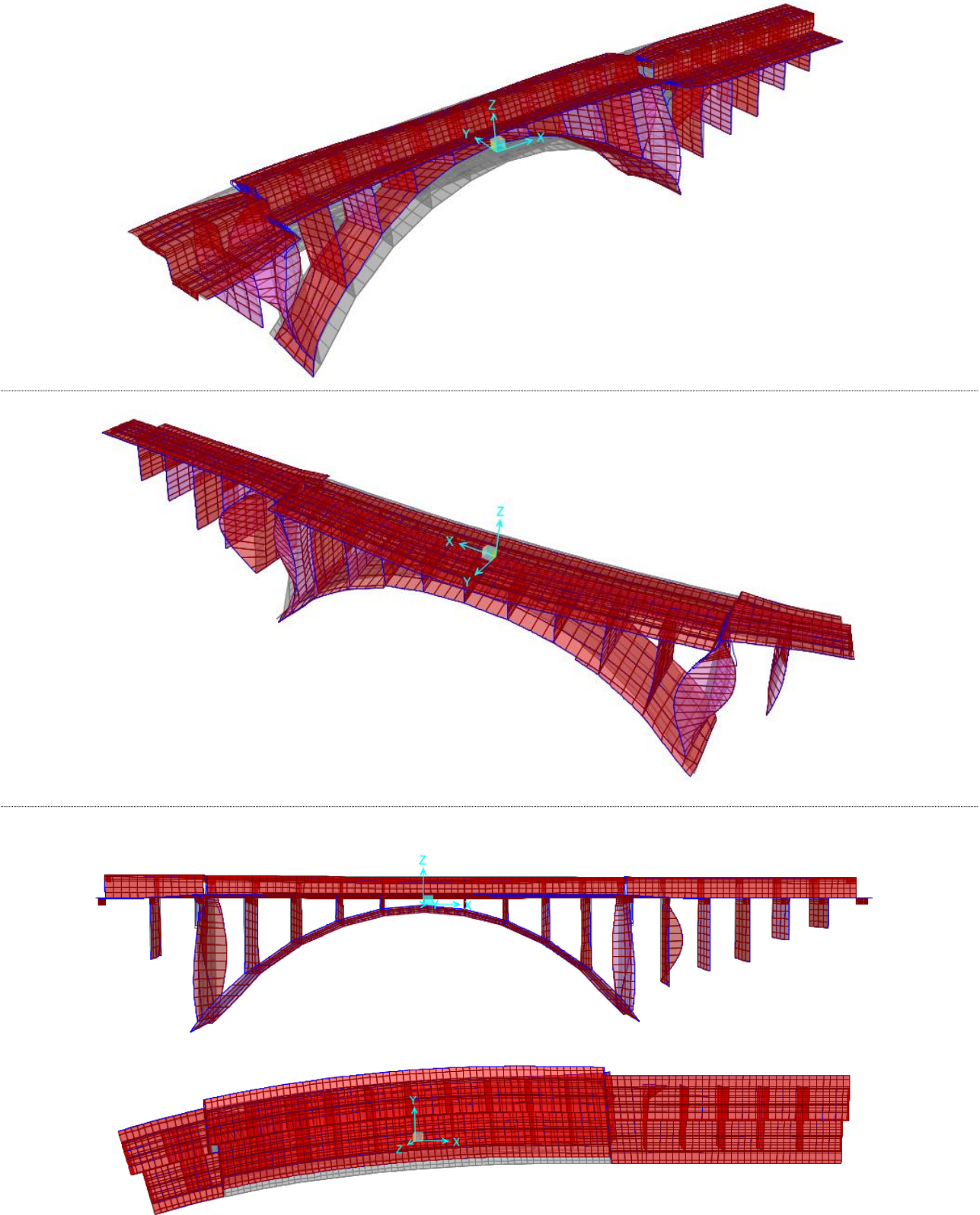
(1) Modo 1: T= 0.674 sec, UX= 31.376% , Ry= 9.009%



Modo	T [sec]	Ux (%)	UY (%)	UZ (%)	Sum UX	Sum UY	Sum UZ
1	0.6743	31.376	0.157	0.013	31.376	0.157	0.013
Modo	T [sec]	RX (%)	RY (%)	RZ (%)	Sum RX	Sum RY	Sum RZ
1	0.6743	1.307	9.009	0.565	1.307	90.009	0.565

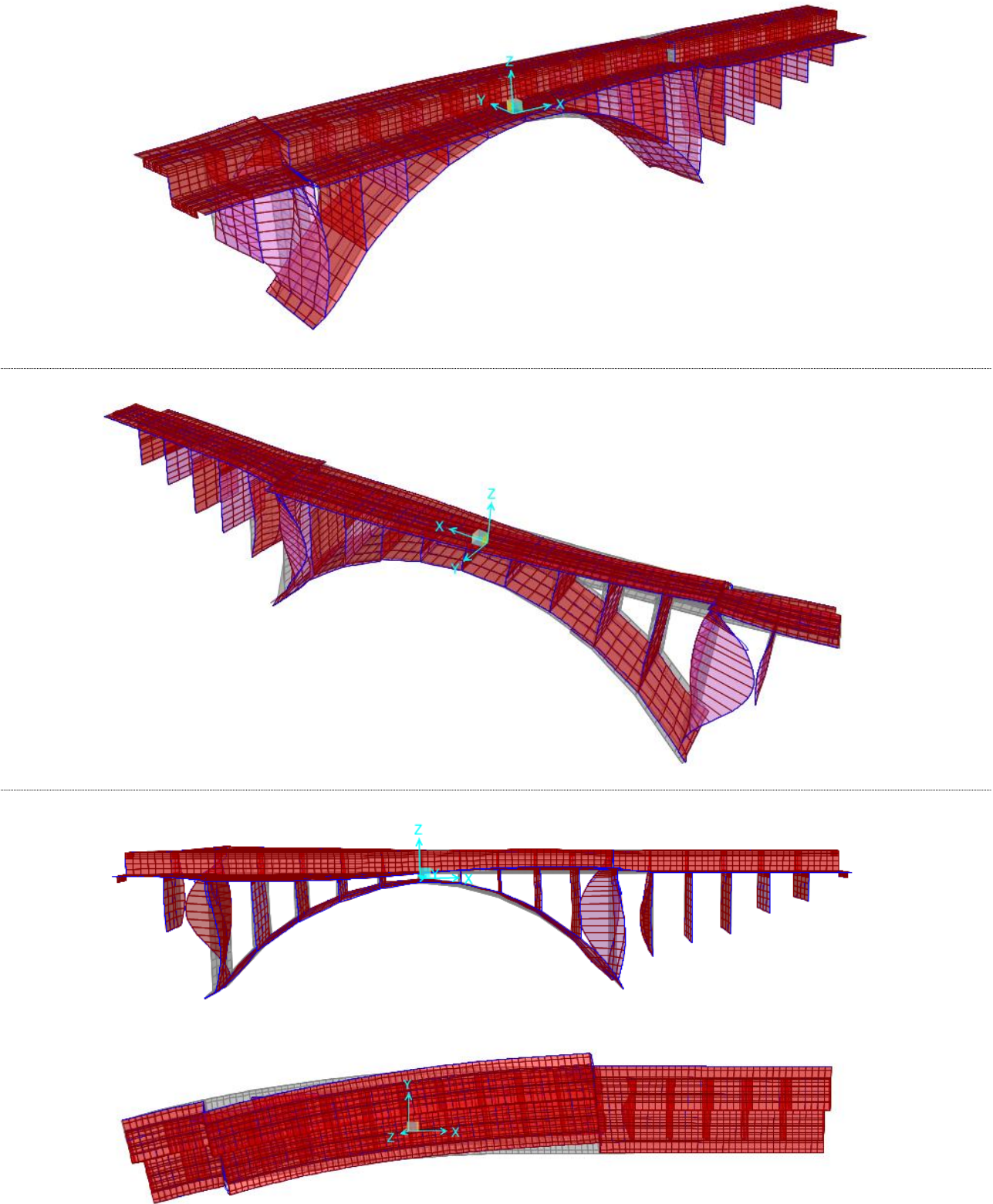


**Modo 7: T= 0.472sec; UY= 49.726% - RX= 8.34% - RZ= 5.499%**



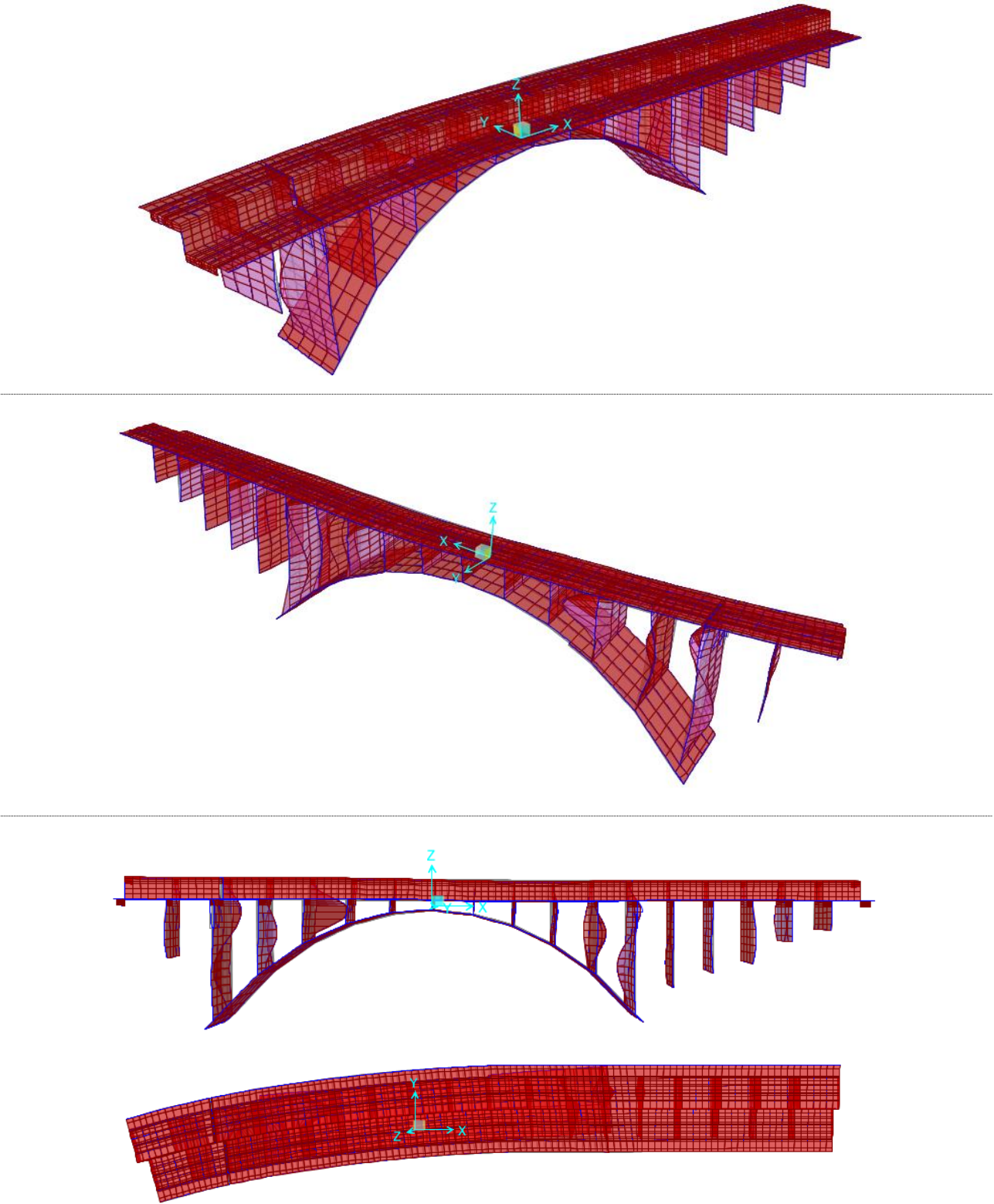
Modo	T [sec]	Ux (%)	UY (%)	UZ (%)	Sum UX	Sum UY	Sum UZ
7	0.4725	0.242	49.726	0.238	32.701	50.357	0.268
Modo	T [sec]	RX (%)	RY (%)	RZ (%)	Sum RX	Sum RY	Sum RZ
7	0.4725	8.339	0.056	5.499	9.739	9.188	6.194

Modo 10: T= 0.4302 sec, RZ= 14.664%



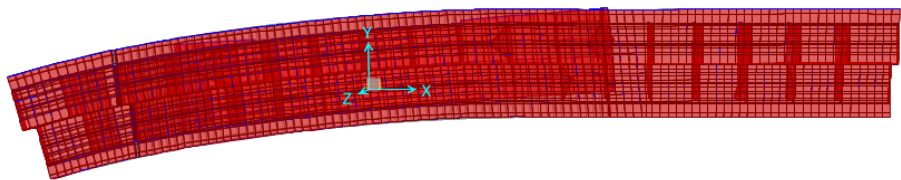
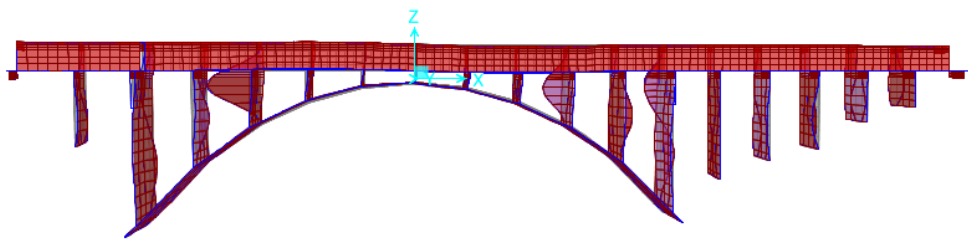
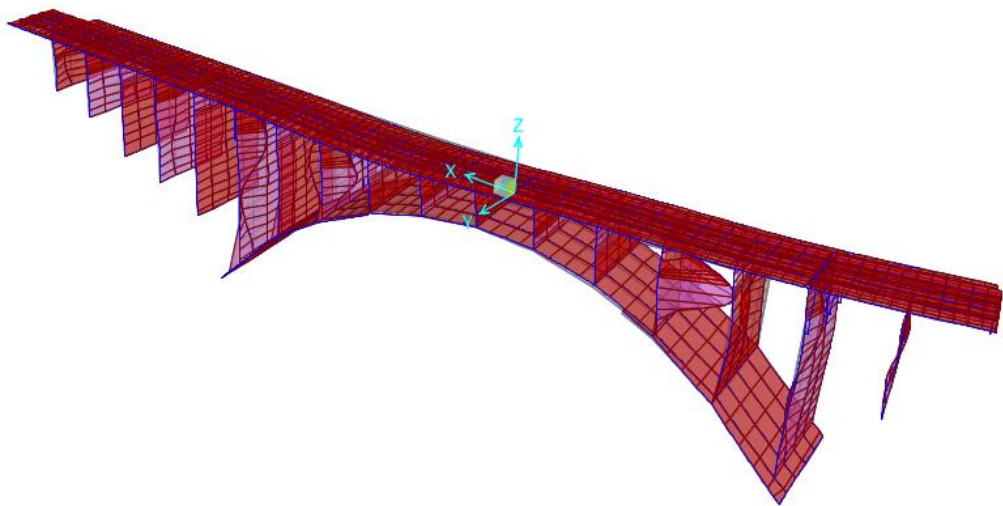
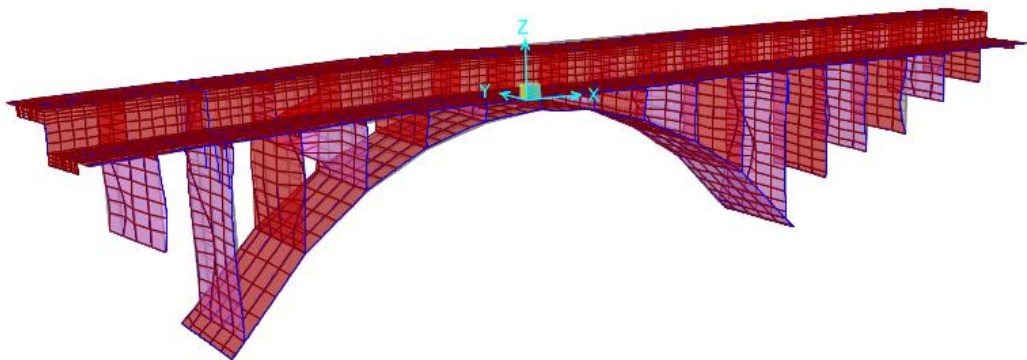
Modo	T [sec]	Ux (%)	UY (%)	UZ (%)	Sum UX	Sum UY	Sum UZ
10	0.4302	0.192	0.123	0.00079	33.489	51.355	0.273
Modo	T [sec]	RX (%)	RY (%)	RZ (%)	Sum RX	Sum RY	Sum RZ
10	0.4302	0.00255	0.24	14.664	9.893	9.433	20.987

**Modo 40: T= 0.2180 sec, UX= 8.16%**



Modo	T [sec]	Ux (%)	UY (%)	UZ (%)	Sum UX	Sum UY	Sum UZ
40	0.2180	8.16	0.054	0.017	47.291	52.085	0.915
Modo	T [sec]	RX (%)	RY (%)	RZ (%)	Sum RX	Sum RY	Sum RZ
40	0.2180	0.513	3.417	0.037	10.518	13.483	24.573

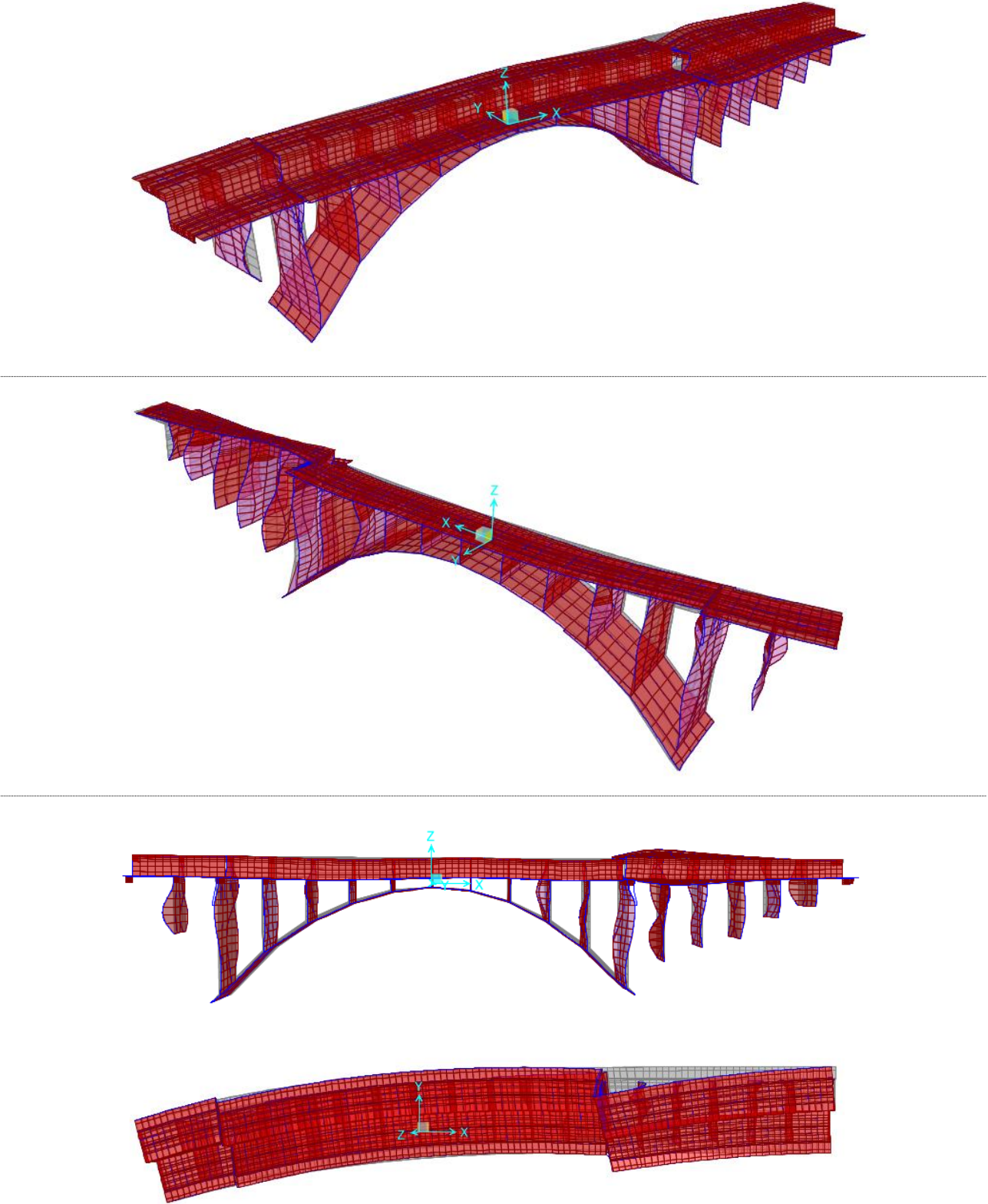
Modo 41: T= 0.2091 sec, UX= 8.593%



Modo	T [sec]	Ux (%)	UY (%)	UZ (%)	Sum UX	Sum UY	Sum UZ
41	0.2091	8.593	0.08	0.001	55.884	52.165	0.916
Modo	T [sec]	RX (%)	RY (%)	RZ (%)	Sum RX	Sum RY	Sum RZ
41	0.2091	0.175	1.485	0.022	10.694	14.968	24.595



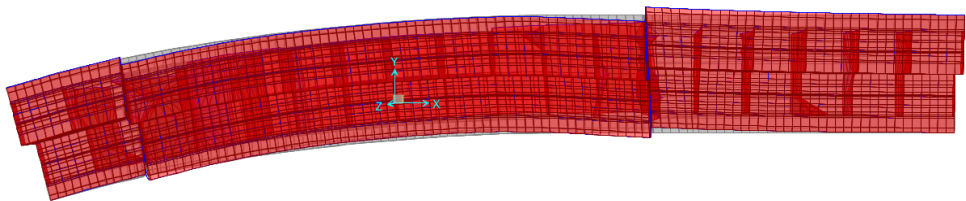
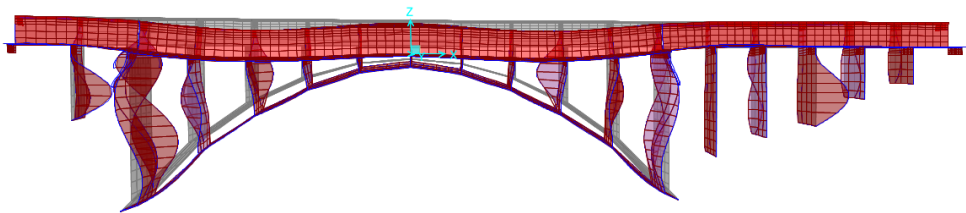
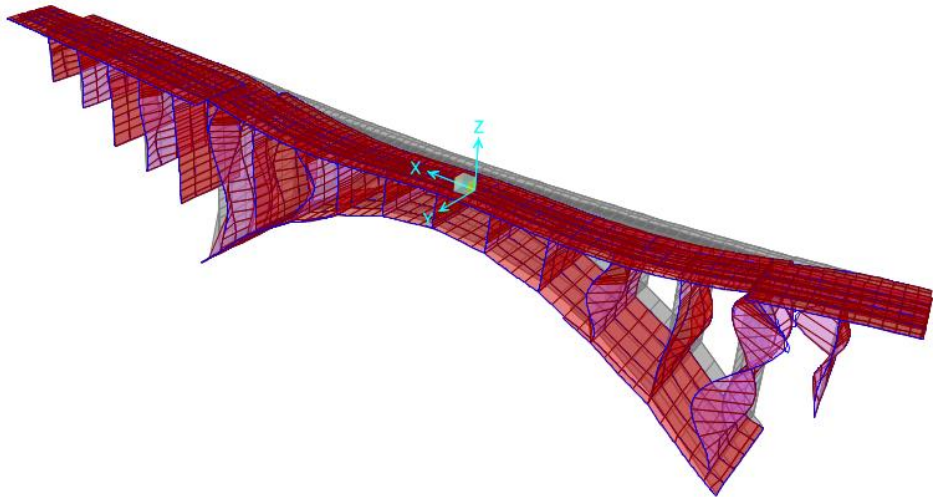
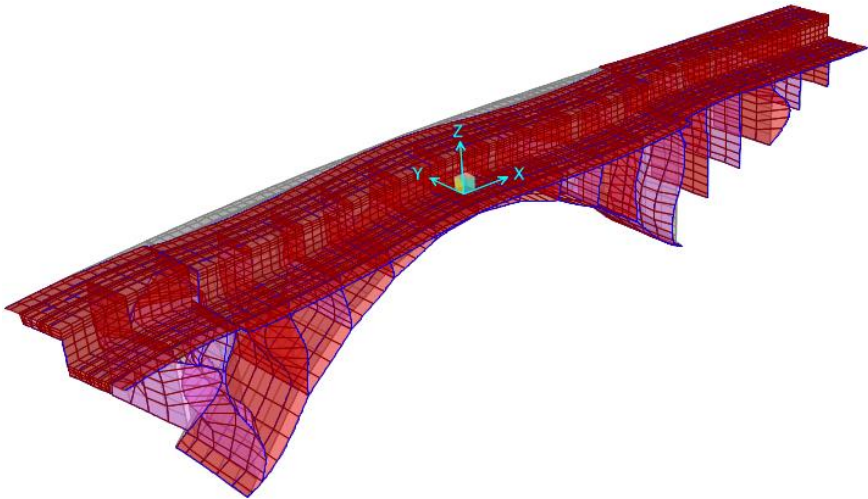
**Modo 47: T= 0.1752 sec, UY=9.524%, RX= 5.288%**



Modo	T [sec]	Ux (%)	UY (%)	UZ (%)	Sum UX	Sum UY	Sum UZ
47	0.1752	0.144	9.524	0.904	59.089	64.586	3.125
Modo	T [sec]	RX (%)	RY (%)	RZ (%)	Sum RX	Sum RY	Sum RZ
47	0.1752	5.288	0.058	11.648	18.216	19.995	41.058



**Modo 48: T= 0.1721 sec, UZ=45.088%, RY= 5.544%**



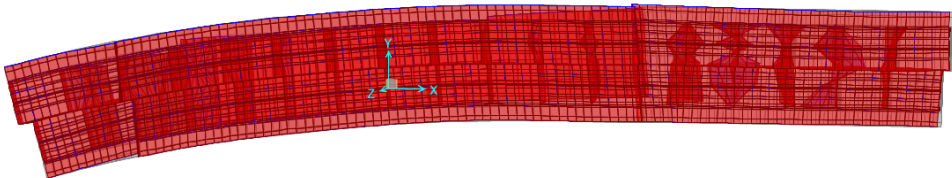
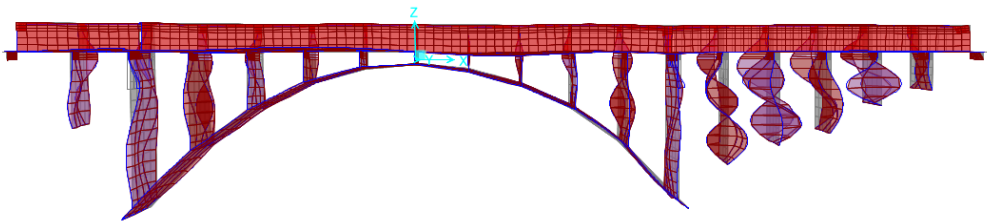
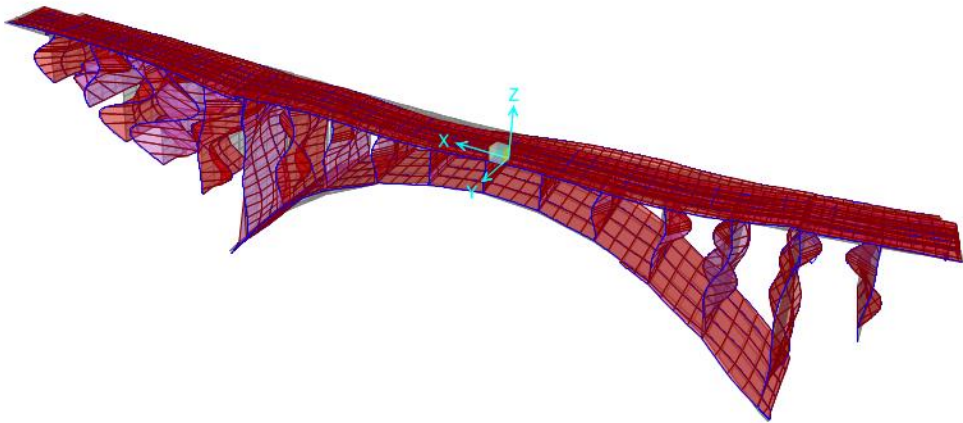
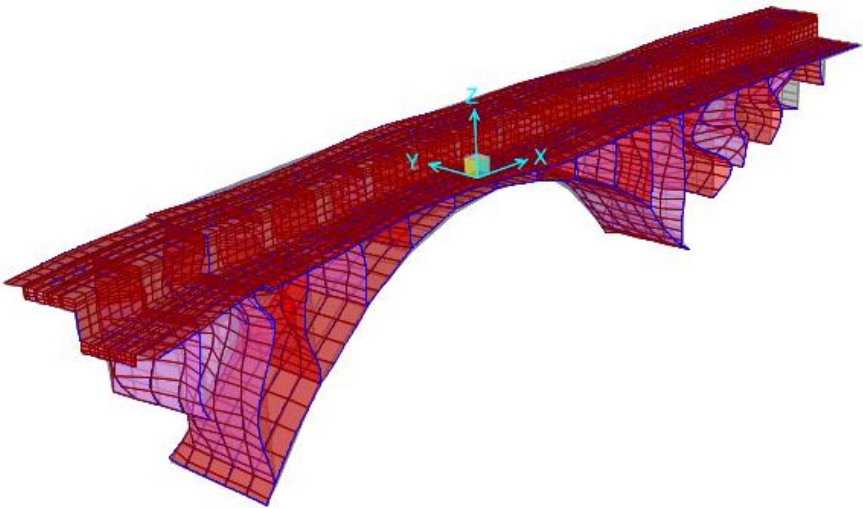
Modo	T [sec]	UX (%)	UY (%)	UZ (%)	Sum UX	Sum UY	Sum UZ
48	0.1721	0.013	0.825	45.088	59.103	65.411	48.213
Modo	T [sec]	RX (%)	RY (%)	RZ (%)	Sum RX	Sum RY	Sum RZ
48	0.1721	0.658	5.544	0.267	18.874	25.54	41.325

**Modo 50: T= 0.1616 sec, UY=6.855%, RX= 10.733%**



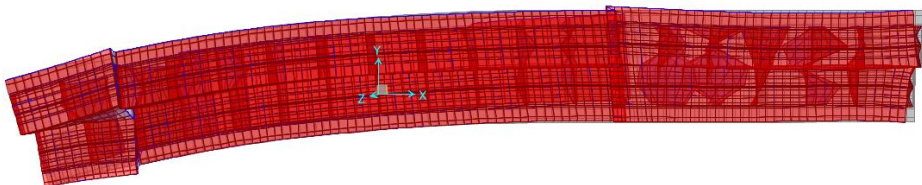
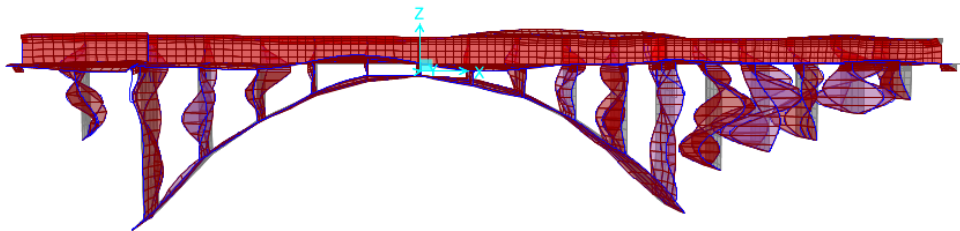
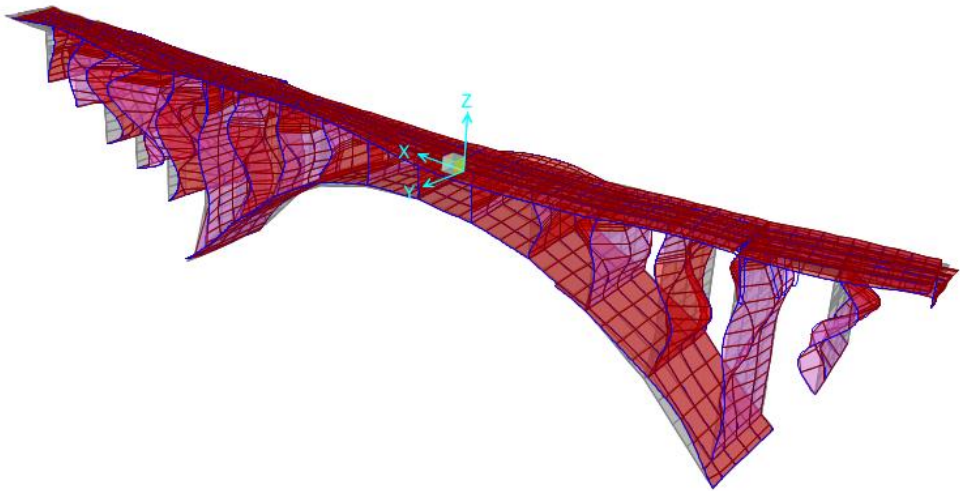
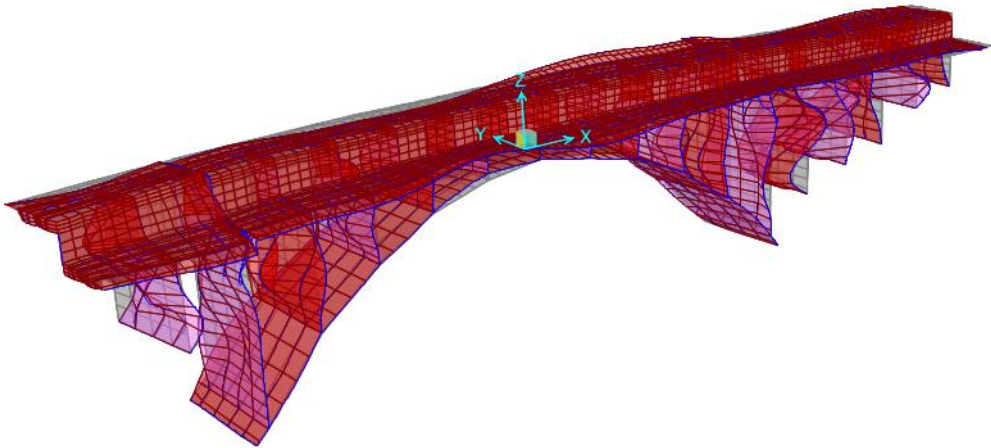
Modo	T [sec]	UX (%)	UY (%)	UZ (%)	Sum UX	Sum UY	Sum UZ
50	0.1616	0.02	6.855	4.589	59.307	72.266	54.498
Modo	T [sec]	RX (%)	RY (%)	RZ (%)	Sum RX	Sum RY	Sum RZ
50	0.1616	10.733	0.555	0.208	29.678	26.391	41.768

Modo 56: T= 0.1083 sec, UX=6.663%



Modo	T [sec]	UX (%)	UY (%)	UZ (%)	Sum UX	Sum UY	Sum UZ
56	0.1083	6.663	0.0067	0.0030	66.725	72.932	60.888
Modo	T [sec]	RX (%)	RY (%)	RZ (%)	Sum RX	Sum RY	Sum RZ
56	0.1083	0.041	0.025	0.175	34.043	27.172	42.419

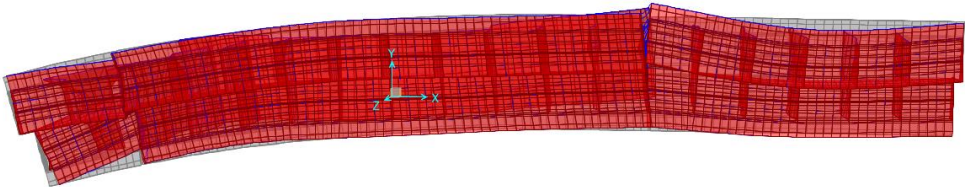
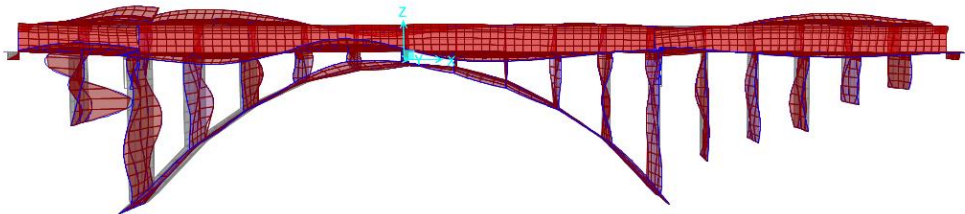
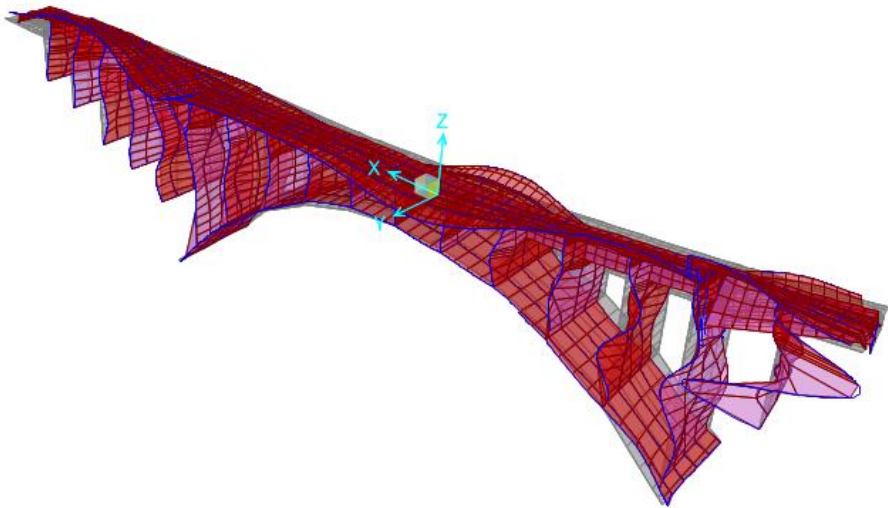
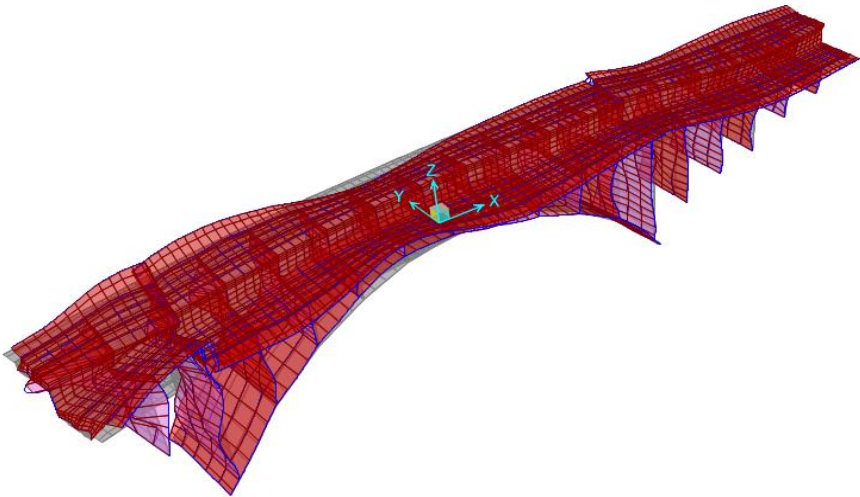
**Modo 58: T= 0.0963sec, UX=13.475%**



Modo	T [sec]	UX (%)	UY (%)	UZ (%)	Sum UX	Sum UY	Sum UZ
57	0.0963	13.475	0.0009	0.016	80.764	72.935	60.917
Modo	T [sec]	RX (%)	RY (%)	RZ (%)	Sum RX	Sum RY	Sum RZ
57	0.0963	0.184	0.344	0.432	34.351	27.649	46.587



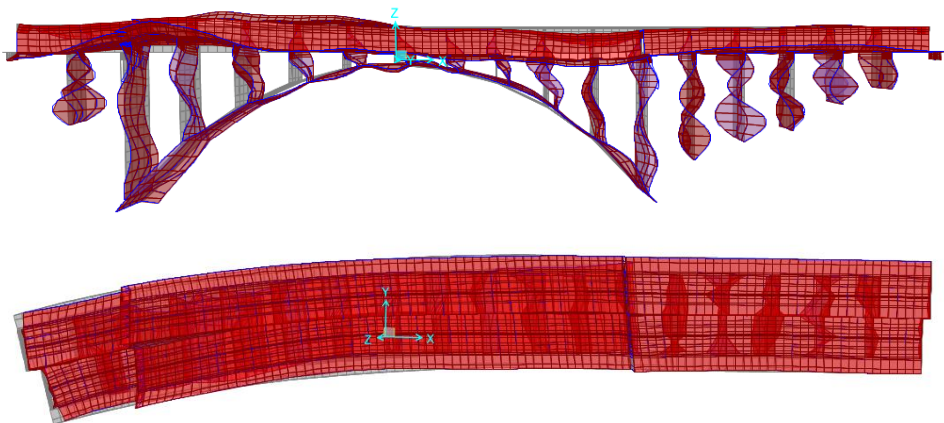
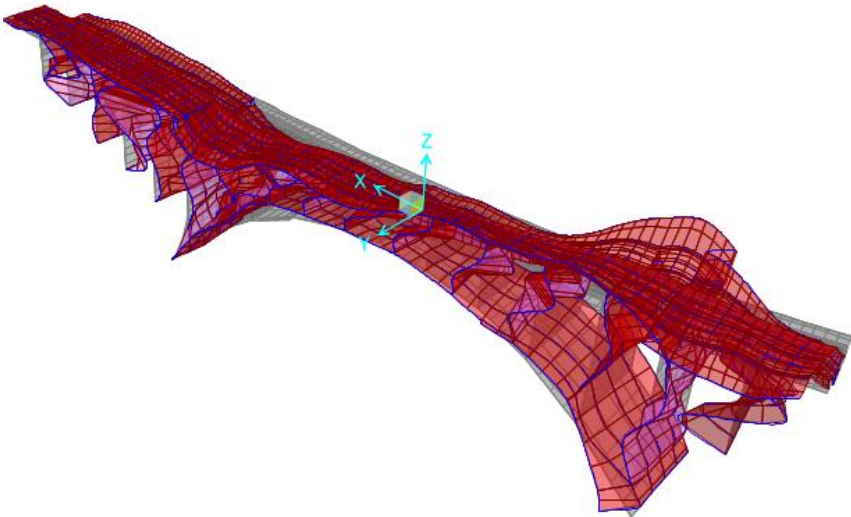
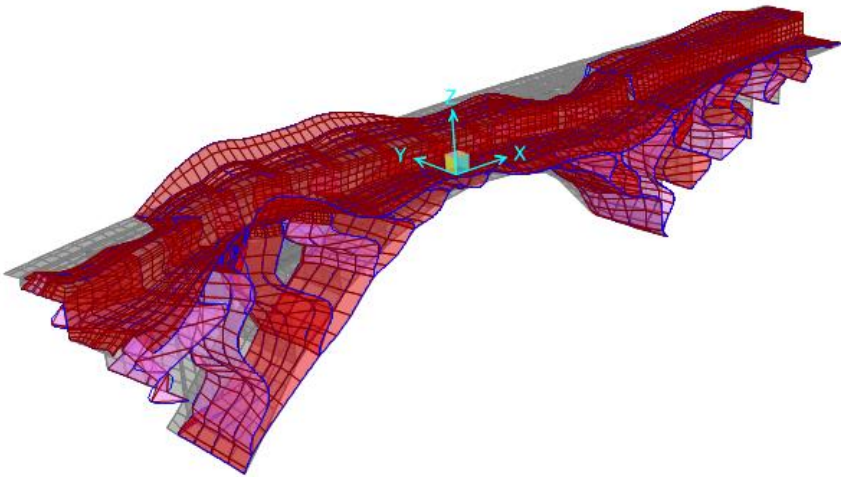
Modo 60: T= 0.0791sec, RX=5.923%, RZ= 11.31%



Modo	T [sec]	UX (%)	UY (%)	UZ (%)	Sum UX	Sum UY	Sum UZ
60	0.0791	0.631	0.0070	0.373	81.396	73.607	61.7
Modo	T [sec]	RX (%)	RY (%)	RZ (%)	Sum RX	Sum RY	Sum RZ
60	0.0791	5.923	0.0003	11.31	40.387	27.674	57.901

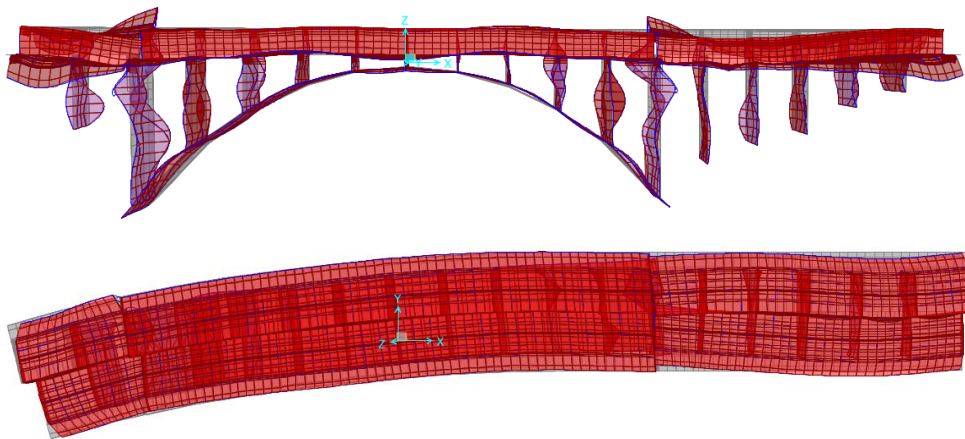
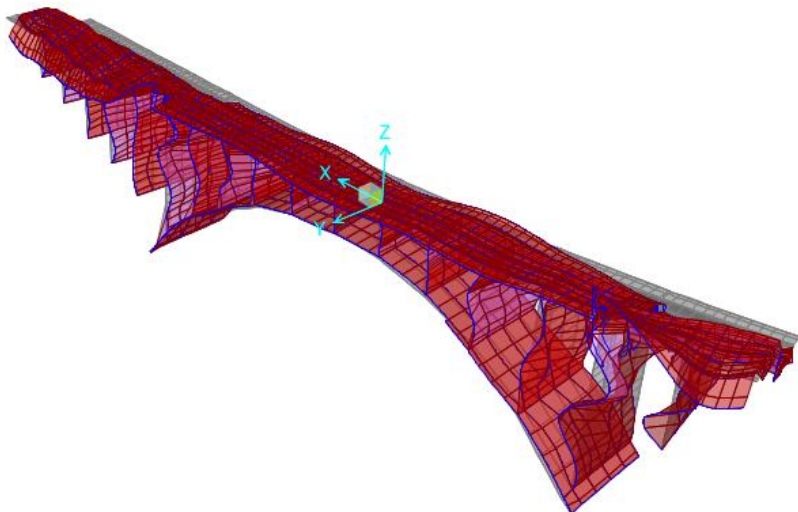
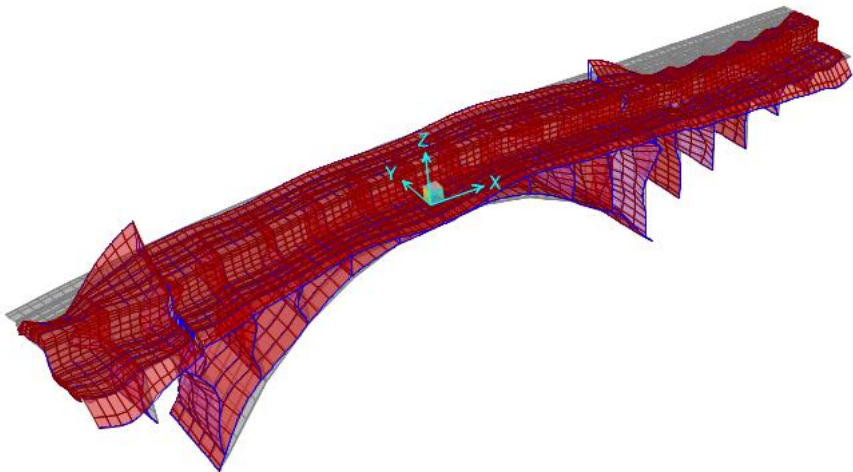


Modo 63: T= 0.0583sec, UX= 8.159%, RX=5.017%



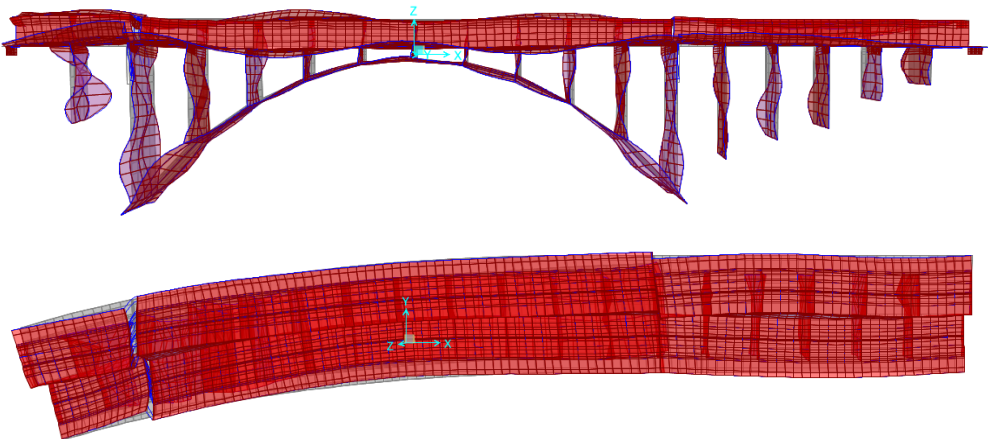
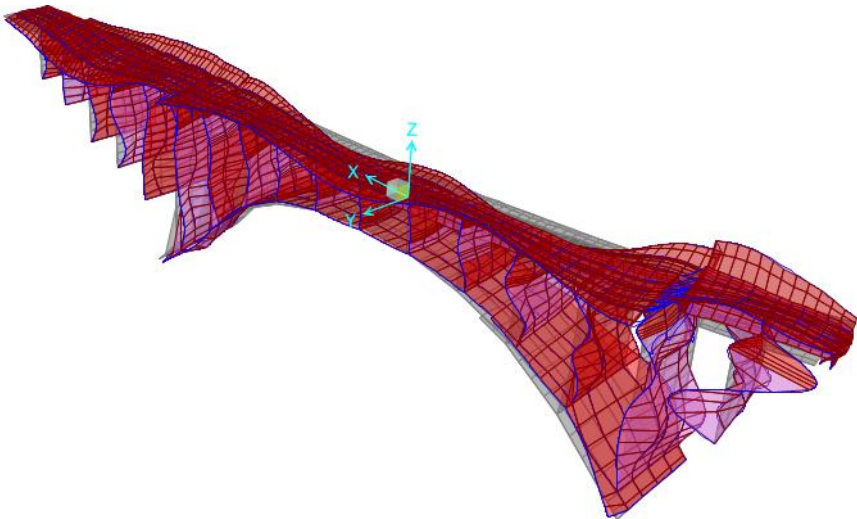
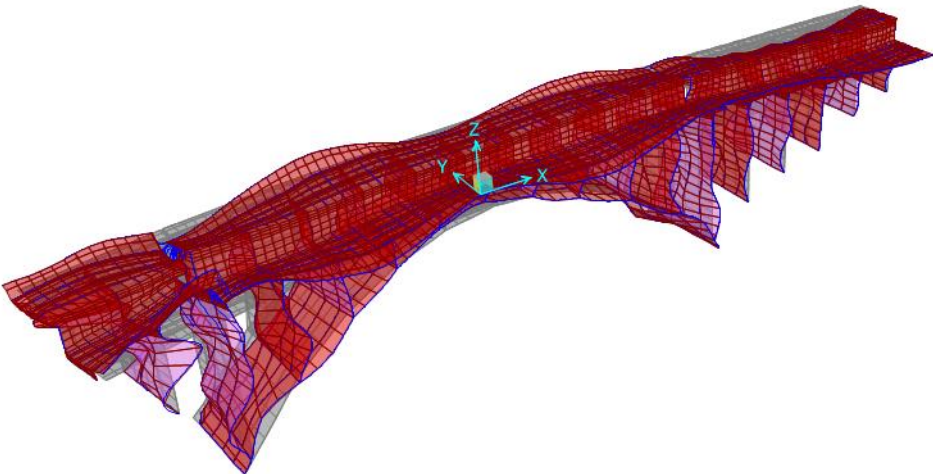
Modo	T [sec]	UX (%)	UY (%)	UZ (%)	Sum UX	Sum UY	Sum UZ
63	0.0583	8.159	0.092	0.02	89.591	81.375	64.948
Modo	T [sec]	RX (%)	RY (%)	RZ (%)	Sum RX	Sum RY	Sum RZ
63	0.0583	5.017	2.374	0.132	46.206	30.411	61.655

**Modo 64: T= 0.0541sec, UZ= 15.276%**



Modo	T [sec]	UX (%)	UY (%)	UZ (%)	Sum UX	Sum UY	Sum UZ
64	0.0541	0.00	0.267	15.276	89.591	81.642	80.223
Modo	T [sec]	RX (%)	RY (%)	RZ (%)	Sum RX	Sum RY	Sum RZ
64	0.0541	0.02	7.079	2.752	46.226	37.46	64.407

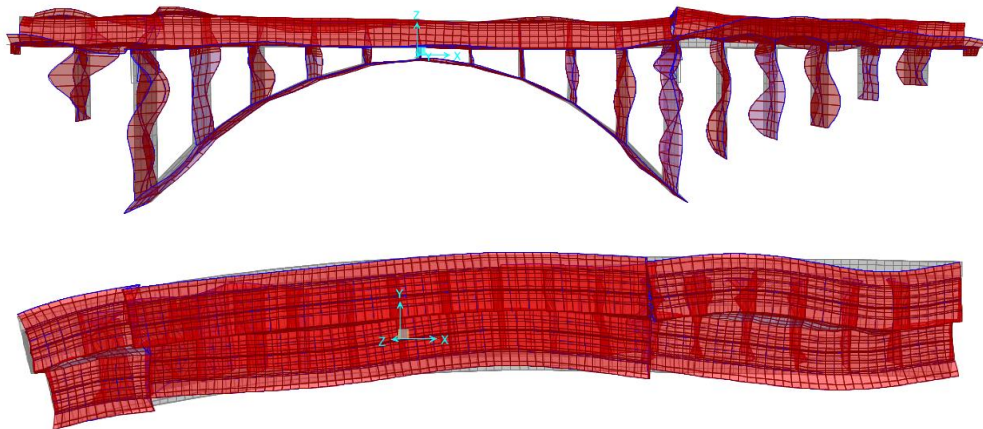
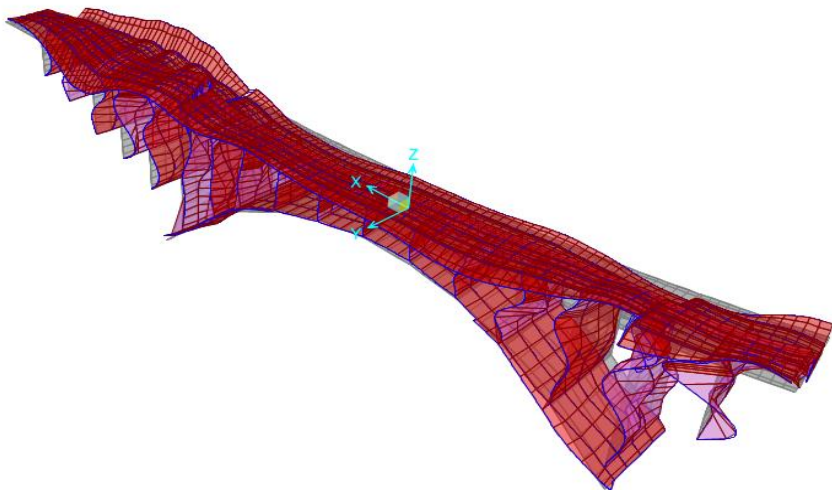
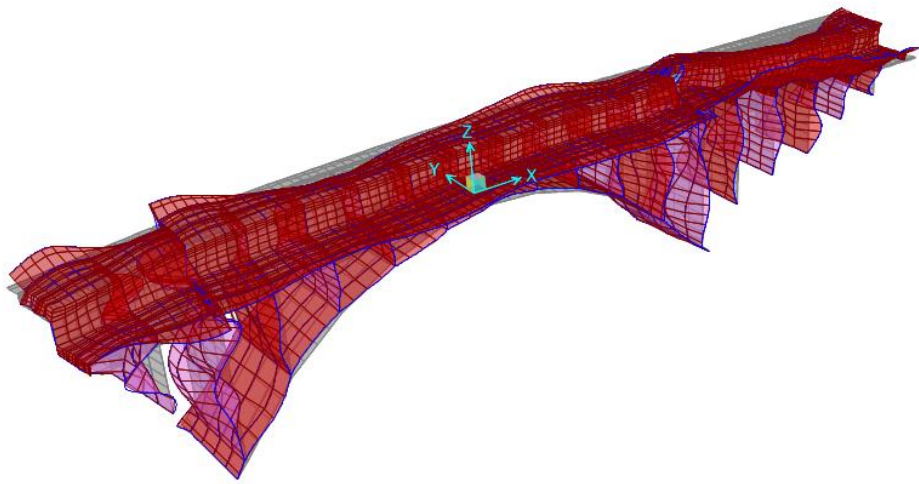
**Modo 65: T= 0.0521sec, UY= 5.688%, RX= 8.46%**



Modo	T [sec]	UX (%)	UY (%)	UZ (%)	Sum UX	Sum UY	Sum UZ
65	0.0521	1.648	5.688	0.143	91.238	87.33	80.366
Modo	T [sec]	RX (%)	RY (%)	RZ (%)	Sum RX	Sum RY	Sum RZ
65	0.0521	8.46	0.243	0.00	54.686	37.703	64.407

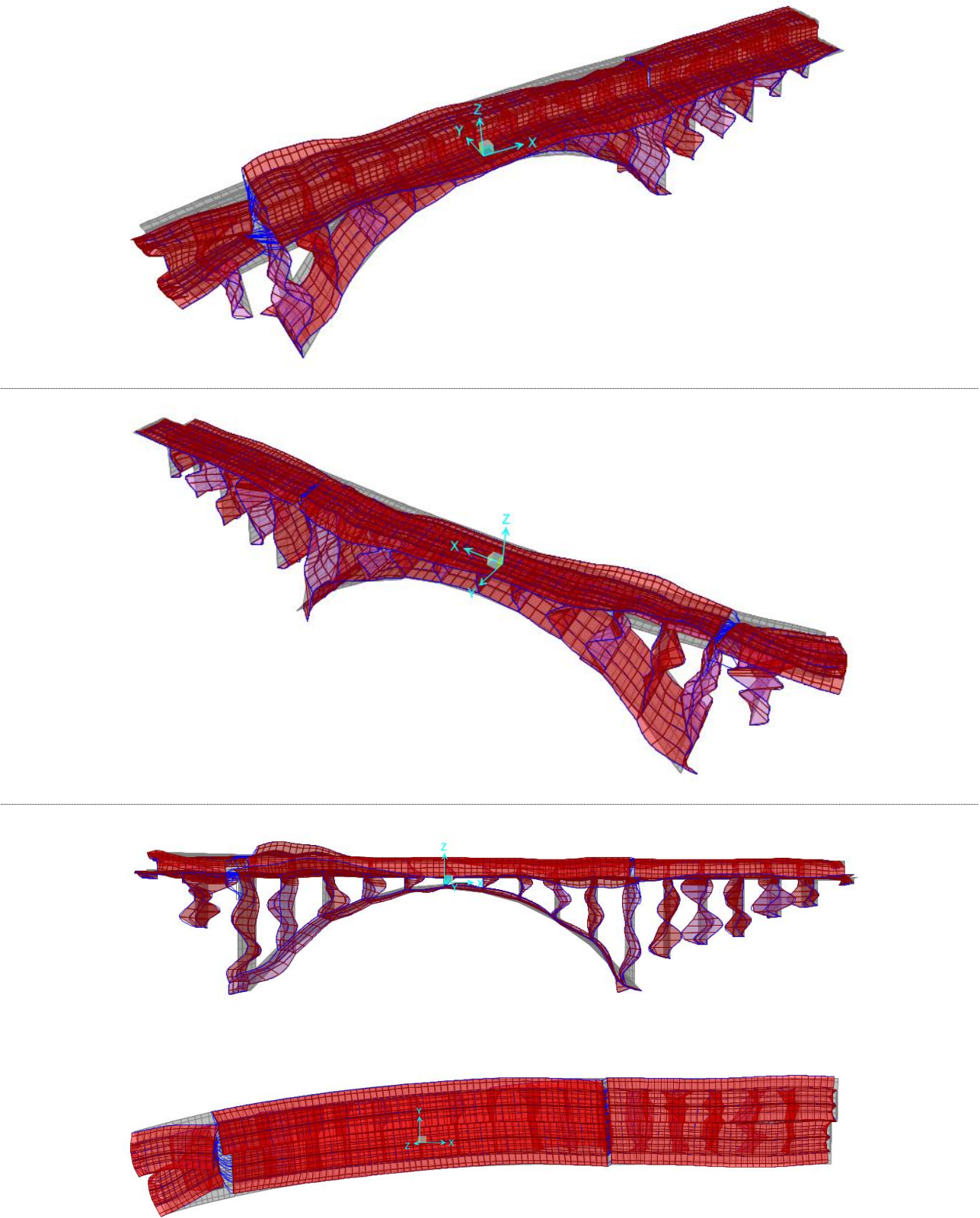


**Modo 66: T= 0.0500 sec, RZ= 8.945%**



Modo	T [sec]	UX (%)	UY (%)	UZ (%)	Sum UX	Sum UY	Sum UZ
66	0.0500	0.384	0.714	2.286	91.622	88.044	82.652
Modo	T [sec]	RX (%)	RY (%)	RZ (%)	Sum RX	Sum RY	Sum RZ
66	0.0500	0.0048	0.282	8.945	54.691	37.985	73.352

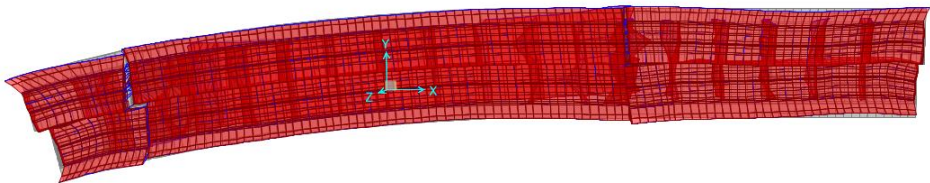
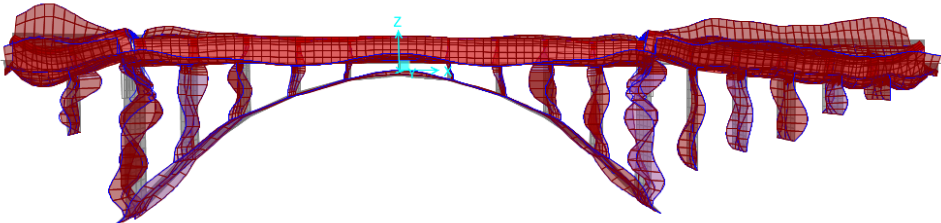
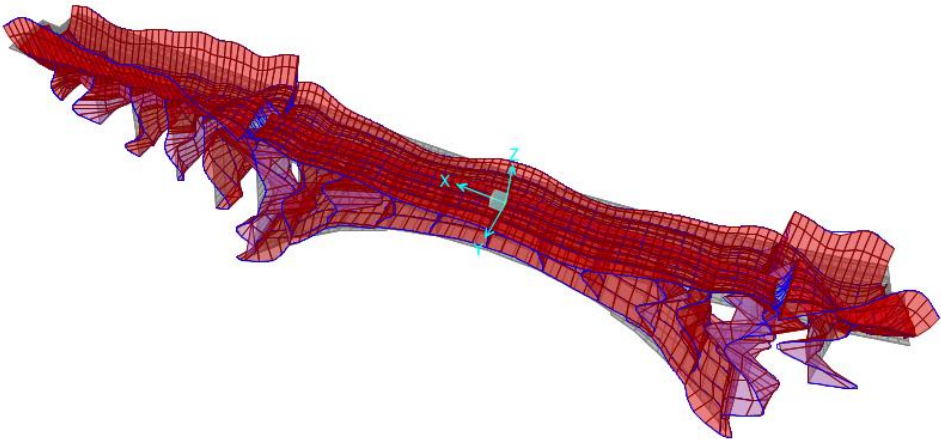
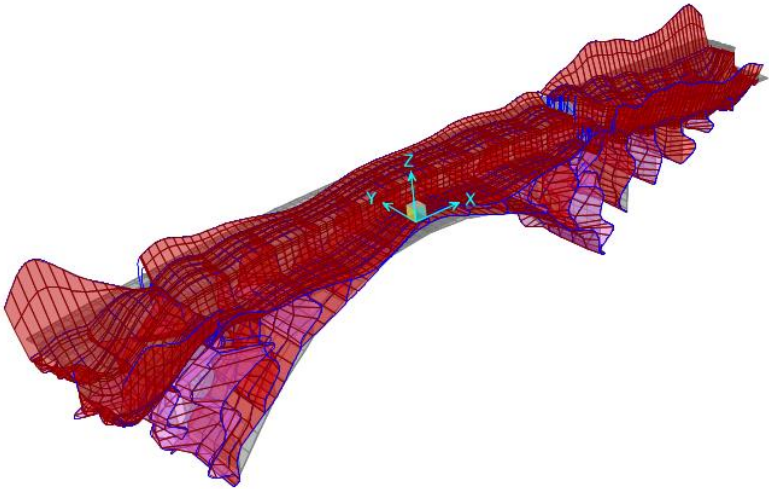
**Modo 67: T= 0.0343sec, UX= 5.62%**



Modo	T [sec]	UX (%)	UY (%)	UZ (%)	Sum UX	Sum UY	Sum UZ
67	0.0343	5.62	0.044	0.0079	97.242	88.088	82.66
Modo	T [sec]	RX (%)	RY (%)	RZ (%)	Sum RX	Sum RY	Sum RZ
67	0.0343	0.493	1.029	0.16	55.184	39.014	73.926

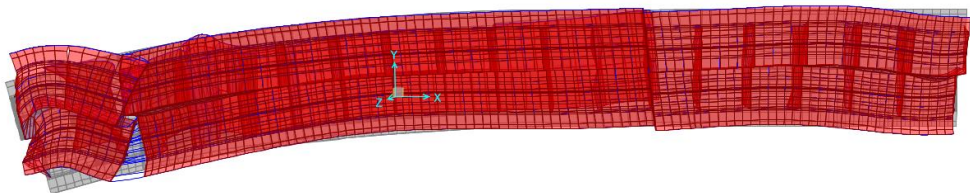
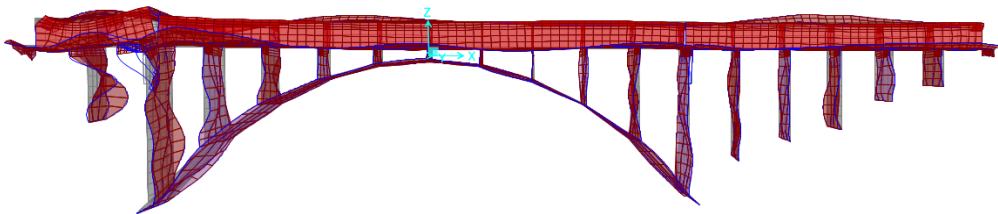
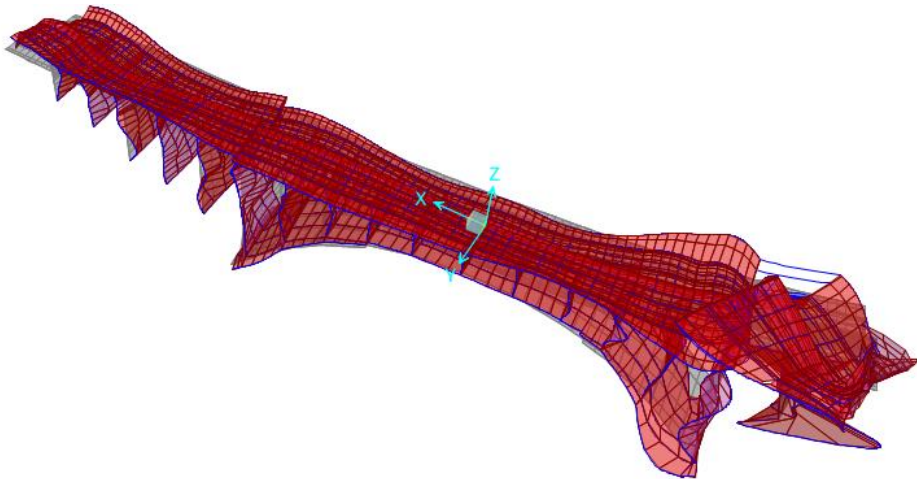
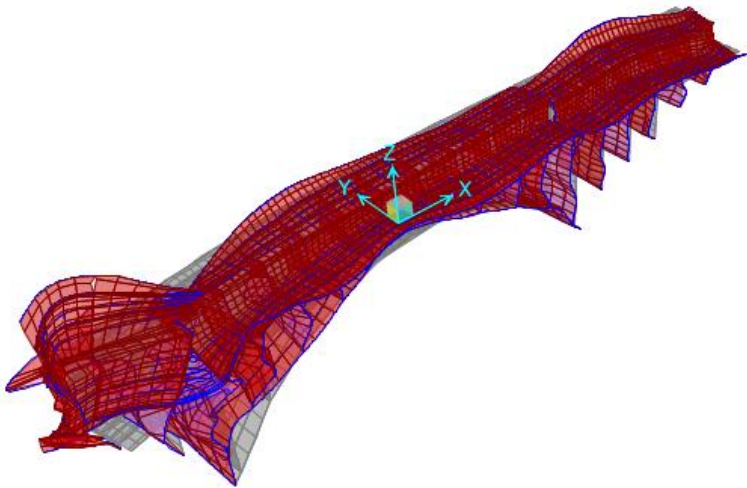


Modo 68: T= 0.0320sec, UZ= 12.806%



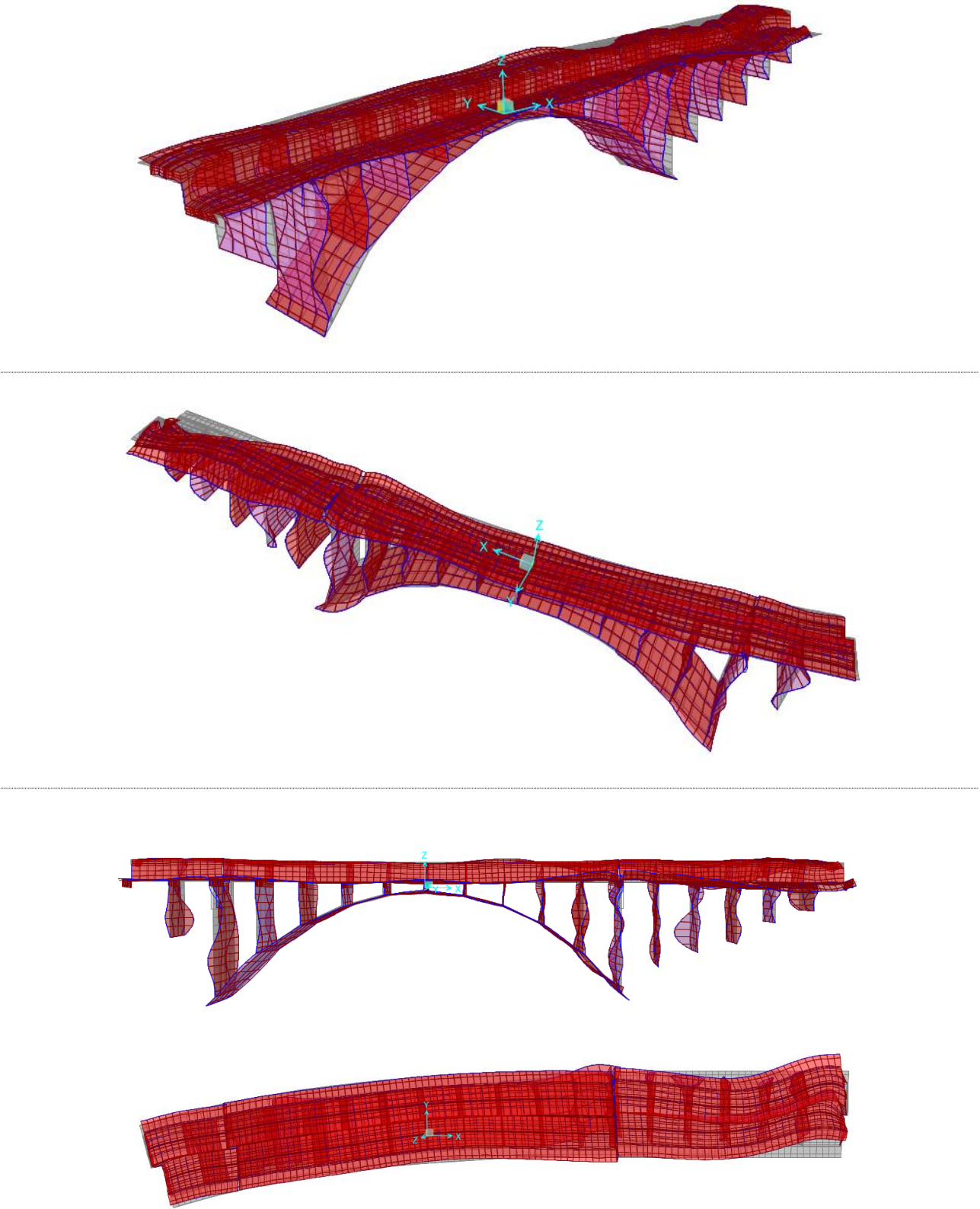
Modo	T [sec]	UX (%)	UY (%)	UZ (%)	Sum UX	Sum UY	Sum UZ
68	0.0320	0.00	0.007	12.809	97.243	88.096	95.467
Modo	T [sec]	RX (%)	RY (%)	RZ (%)	Sum RX	Sum RY	Sum RZ
68	0.0320	0.103	4.215	0.413	55.287	43.228	73.926

**Modo 69: T= 0.028027, RZ= 14.966%**



Modo	T [sec]	UX (%)	UY (%)	UZ (%)	Sum UX	Sum UY	Sum UZ
69	0.028027	0.466	2.34	0.013	97.708	90.436	95.48
Modo	T [sec]	RX (%)	RY (%)	RZ (%)	Sum RX	Sum RY	Sum RZ
69	0.028027	0.573	0.338	14.966	55.86	43.566	88.891

**Modo 70: T= 0.02698sec, UY= 6.768%, RZ= 5.619%**

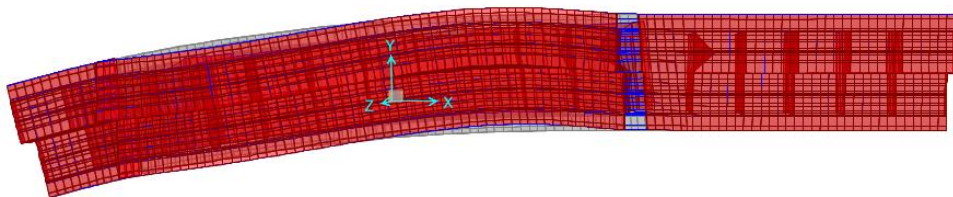
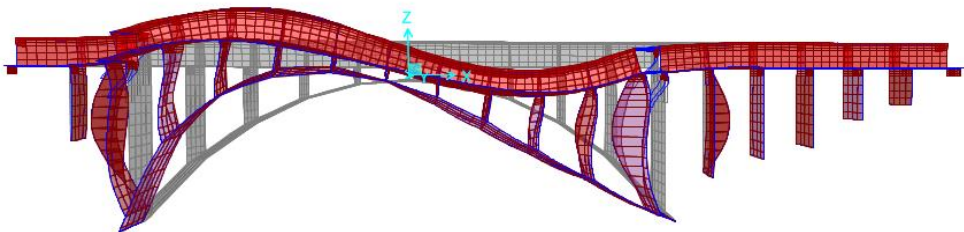
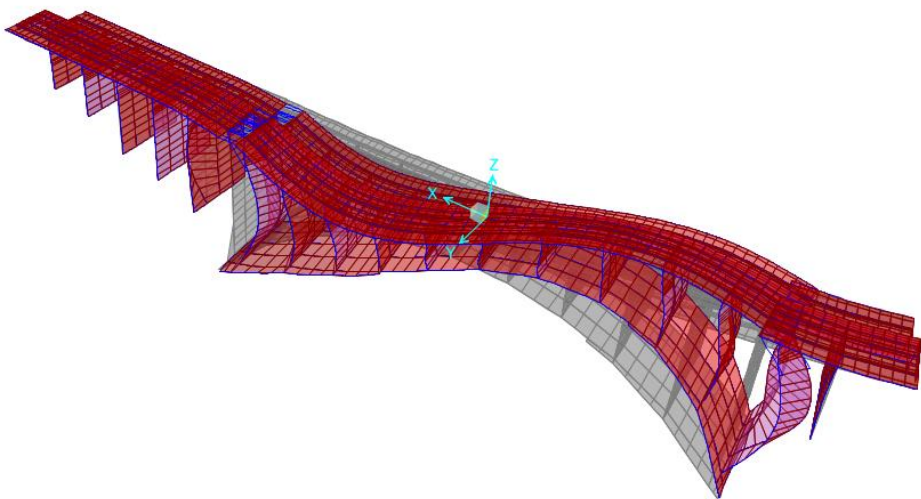
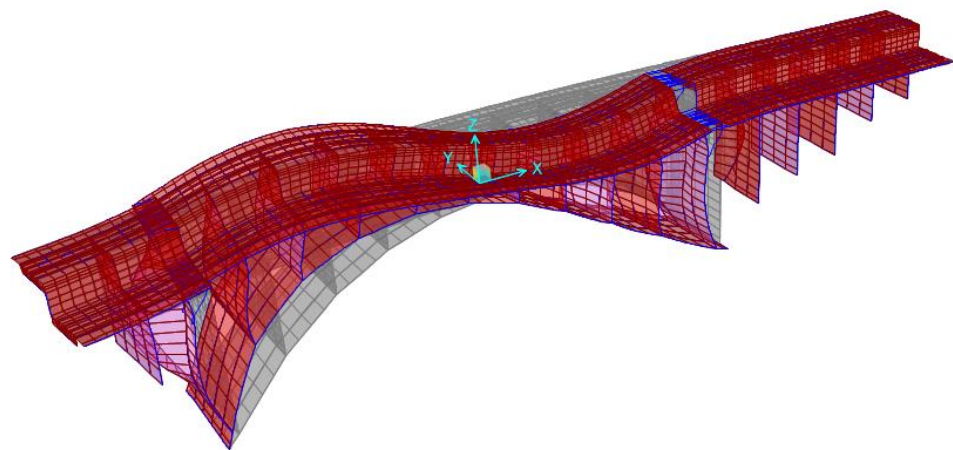


Modo	T [sec]	UX (%)	UY (%)	UZ (%)	Sum UX	Sum UY	Sum UZ
70	0.0269	0.0022	6.768	0.167	97.711	97.204	95.647
Modo	T [sec]	RX (%)	RY (%)	RZ (%)	Sum RX	Sum RY	Sum RZ
70	0.0269	2.163	0.382	5.619	58.024	43.948	94.511



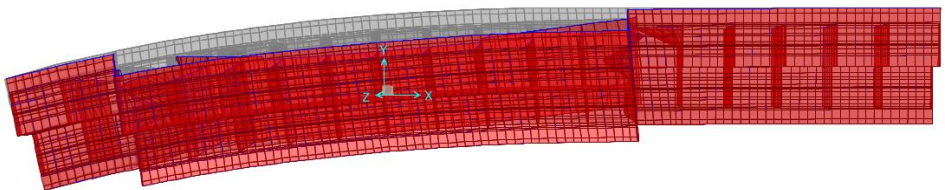
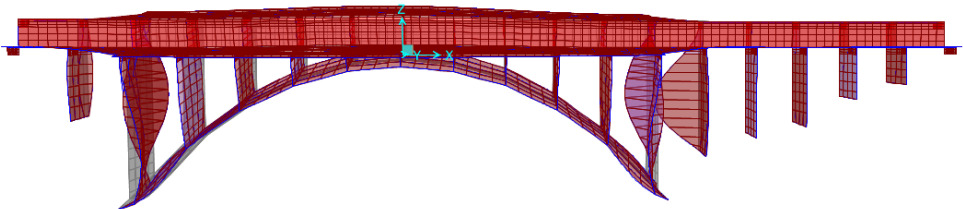
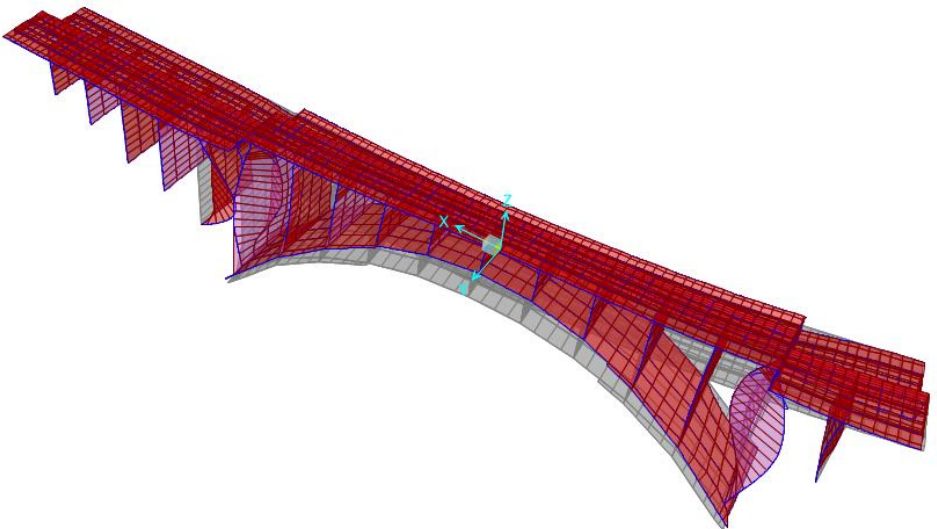
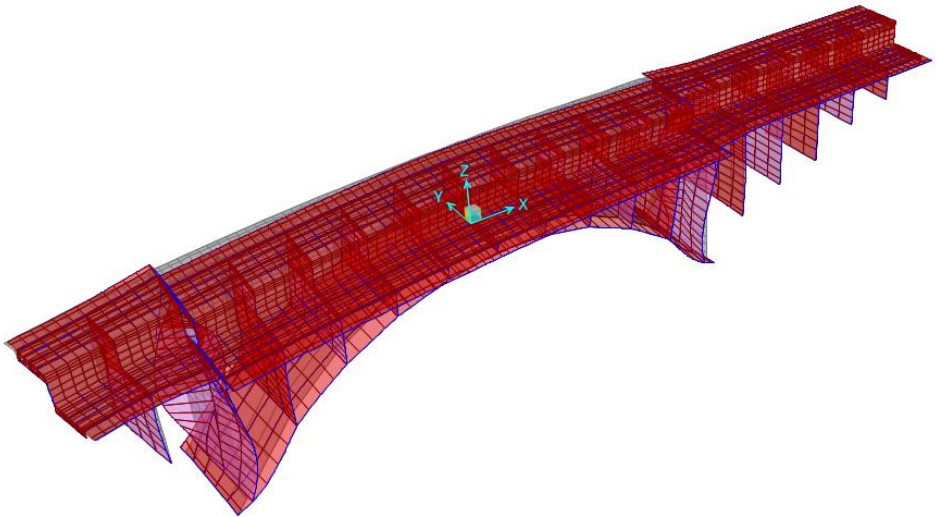
(2.1) Three- deformable - decks model with hinged joints

Modo 1: T= 0.674 sec, UX= 31.404% , RY= 9.024%



Modo	T [sec]	UX (%)	UY (%)	UZ (%)	Sum UX	Sum UY	Sum UZ
1	0.6746	31.404	0.153	0.013	31.404	0.153	0.013
Modo	T [sec]	RX (%)	RY (%)	RZ (%)	Sum RX	Sum RY	Sum RZ
1	0.6746	1.312	9.024	0.551	1.312	9.024	0.551

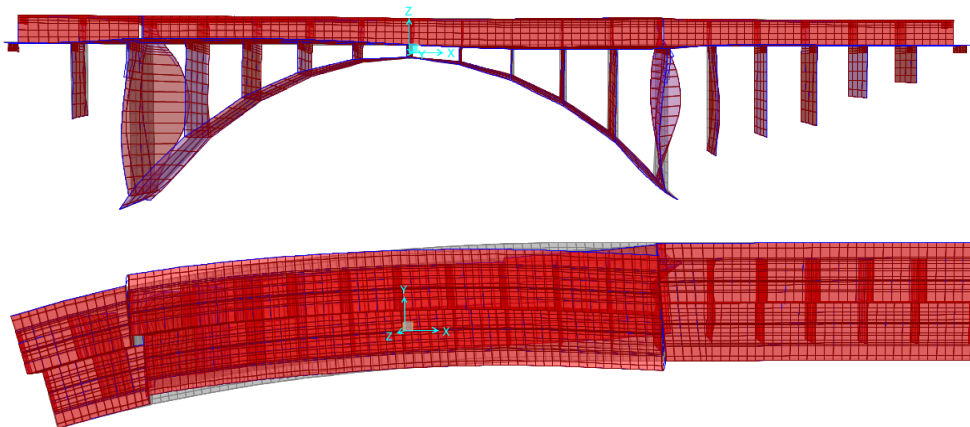
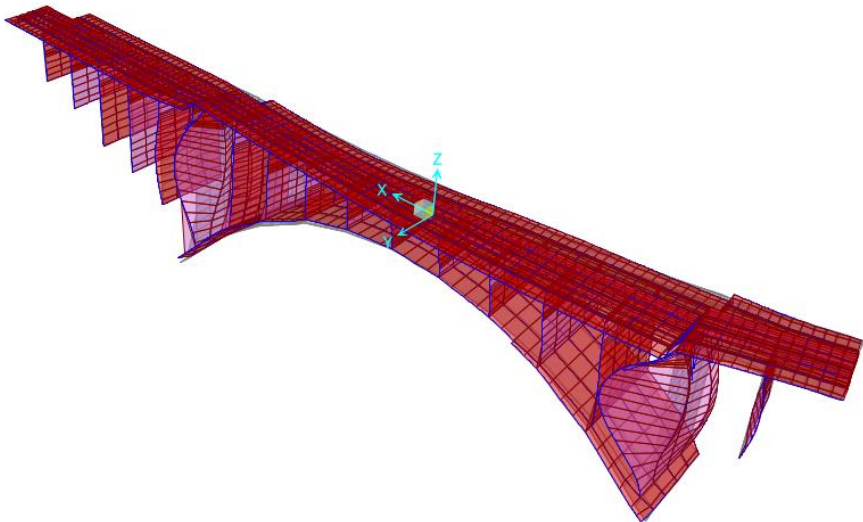
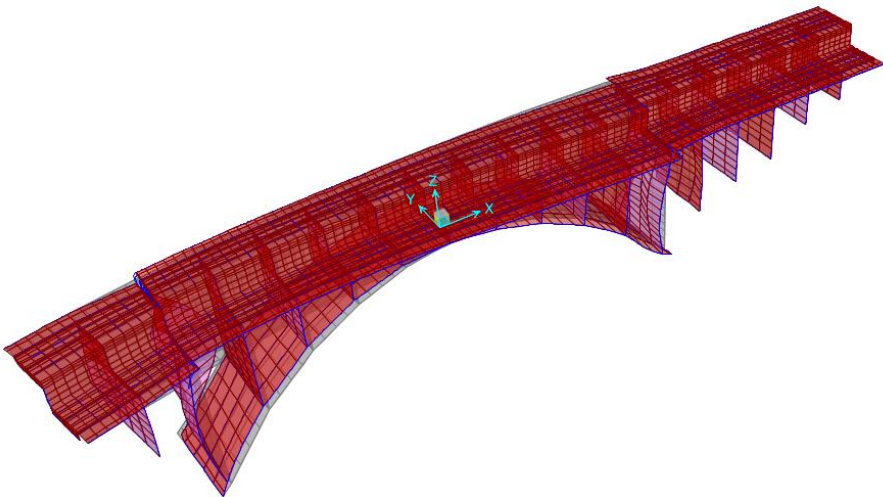
Modo 7: T= 0.4737 sec, UY= 50.036% , RX= 8.365%



odo	T [sec]	UX (%)	UY (%)	UZ (%)	Sum UX	Sum UY	Sum UZ
7	0.4737	0.256	50.036	0.235	32.738	50.683	0.266
Modo	T [sec]	RX (%)	RY (%)	RZ (%)	Sum RX	Sum RY	Sum RZ
7	0.4737	8.365	0.054	5.624	9.774	9.201	6.313

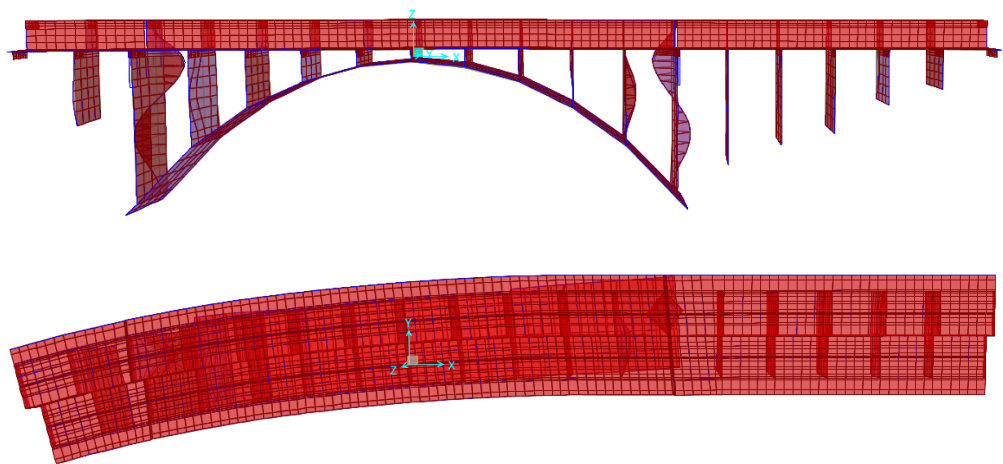
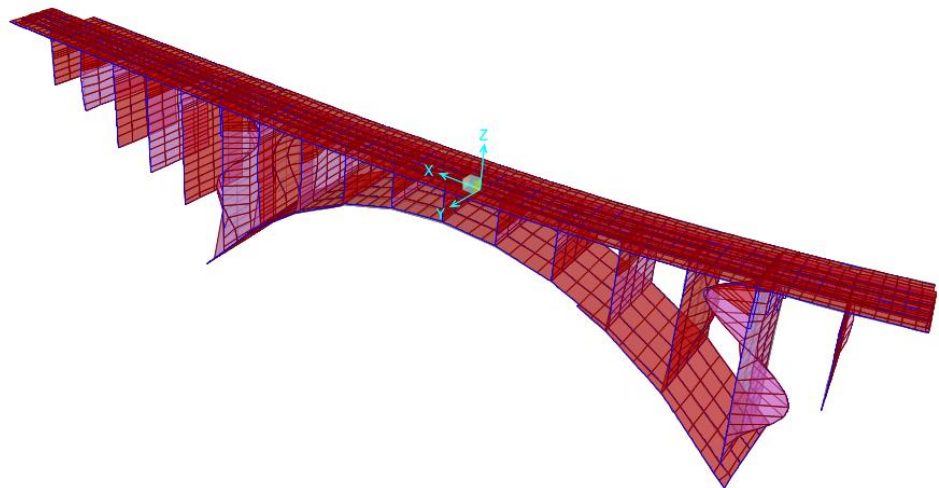
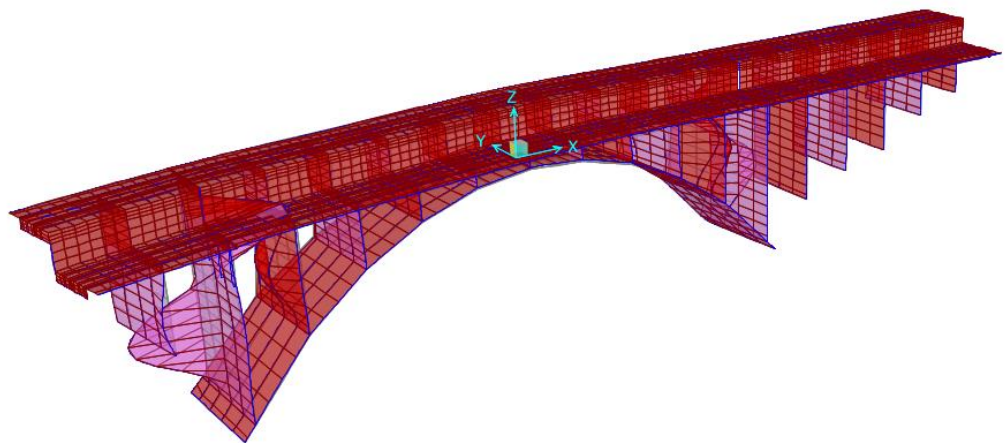


Modo 10: T= 0.4727 sec, RZ= 15.02%



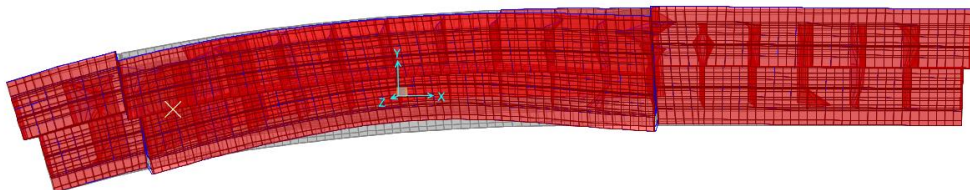
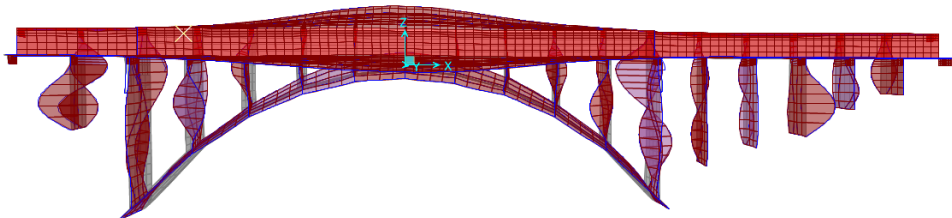
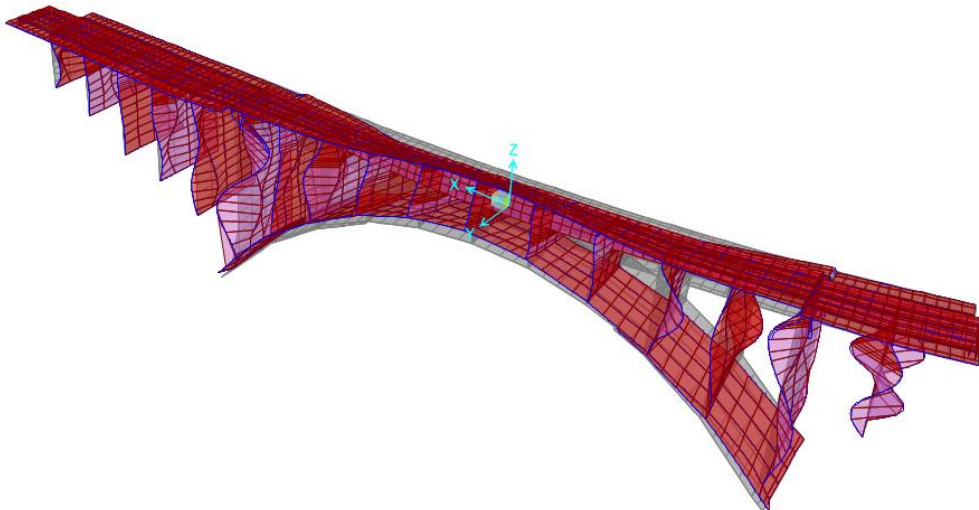
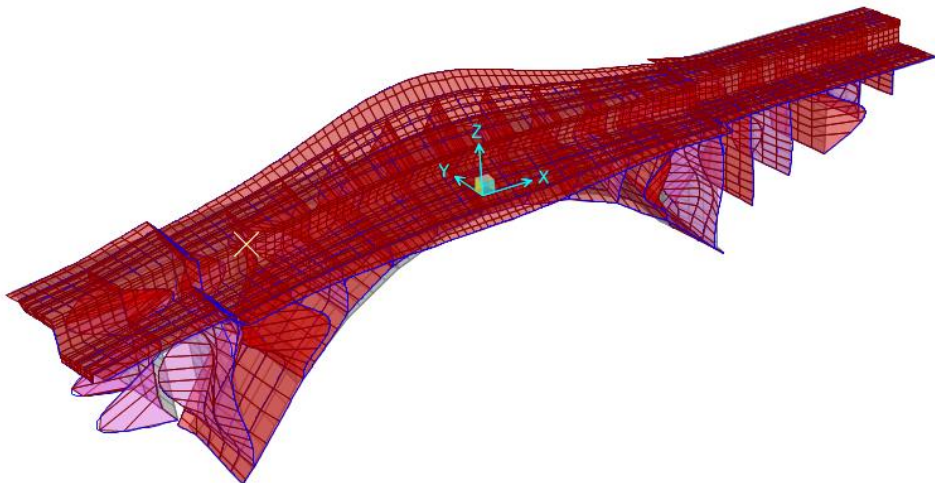
Modo	T [sec]	UX (%)	UY (%)	UZ (%)	Sum UX	Sum UY	Sum UZ
10	0.4327	0.217	0.143	0.001	33.537	51.396	0.269
Modo	T [sec]	RX (%)	RY (%)	RZ (%)	Sum RX	Sum RY	Sum RZ
10	0.433	0.00175	0.251	15.022	9.875	9.458	21.433

Modo 42: T= 0.2151 sec, UX= 11.25%



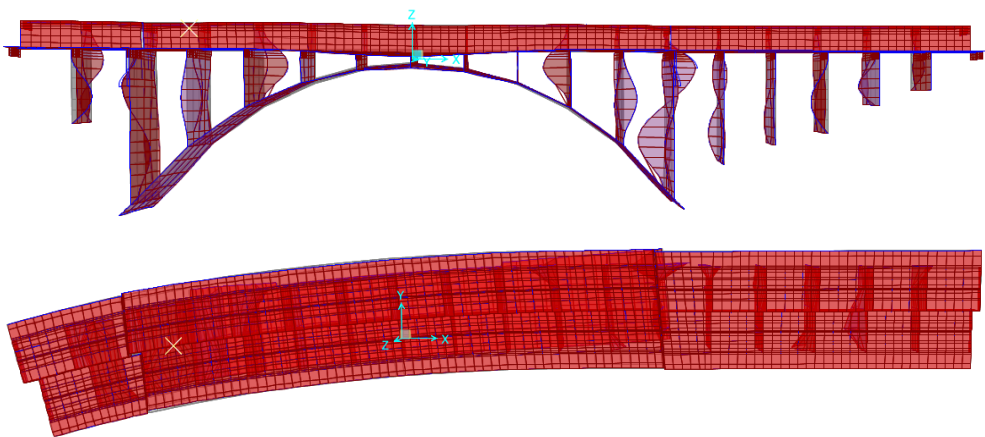
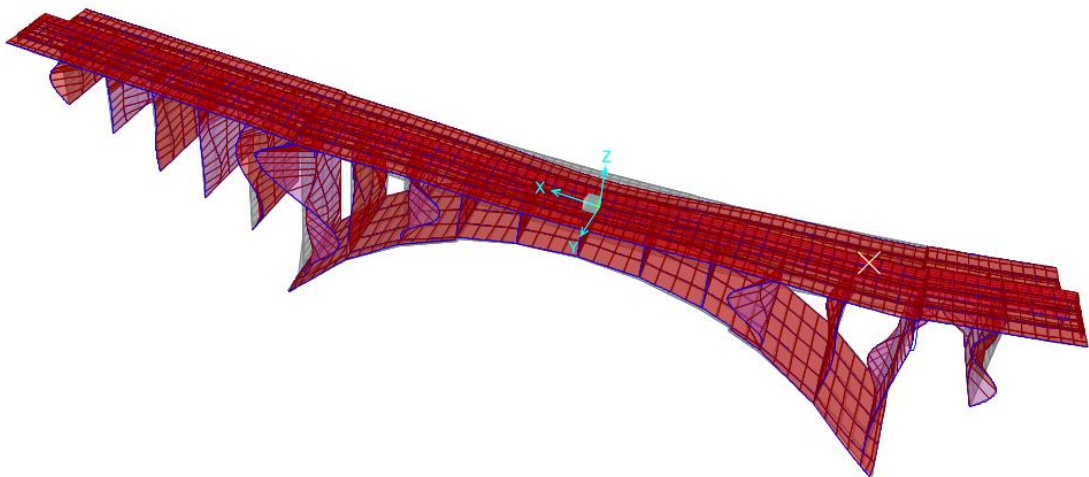
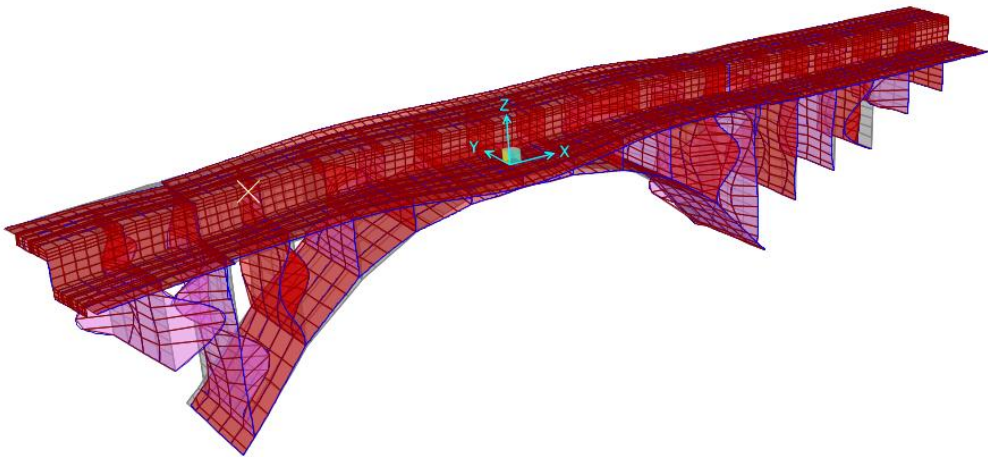
Modo	T [sec]	UX (%)	UY (%)	UZ (%)	Sum UX	Sum UY	Sum UZ
42	0.2151	11.252	0.090	0.000	51.880	52.164	0.903
Modo	T [sec]	RX (%)	RY (%)	RZ (%)	Sum RX	Sum RY	Sum RZ
42	0.2151	0.592	4.476	0.049	10.632	14.779	24.597

Modo 50: T= 0.1749 sec, UY= 9.268%, RZ= 10.24%



Modo	T [sec]	UX (%)	UY (%)	UZ (%)	Sum UX	Sum UY	Sum UZ
50	0.1749	0.116	9.268	0.474	58.933	64.828	2.332
Modo	T [sec]	RX (%)	RY (%)	RZ (%)	Sum RX	Sum RY	Sum RZ
50	0.1749	4.39	0.038	10.237	18.162	20.938	40.805

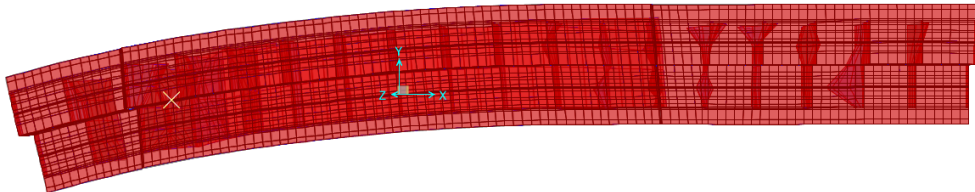
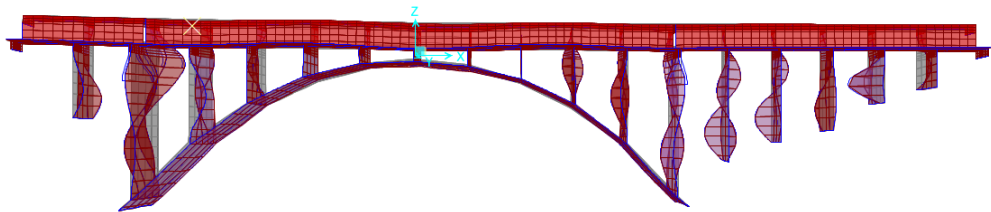
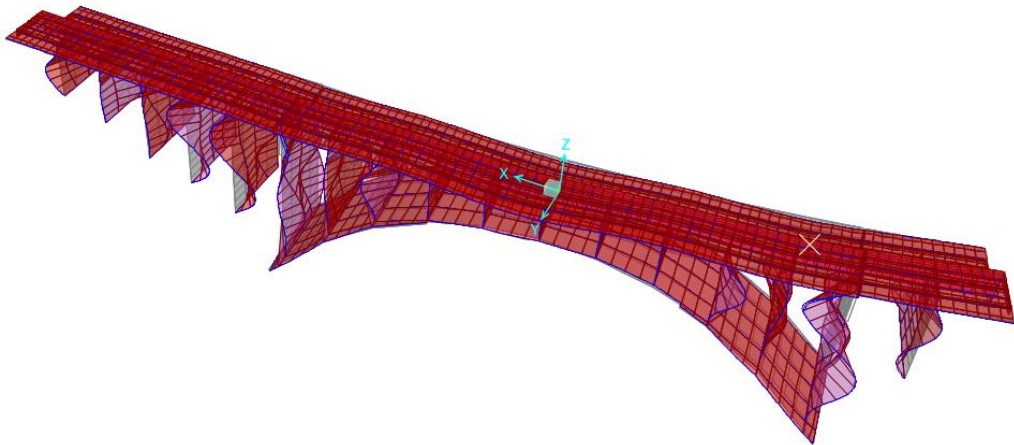
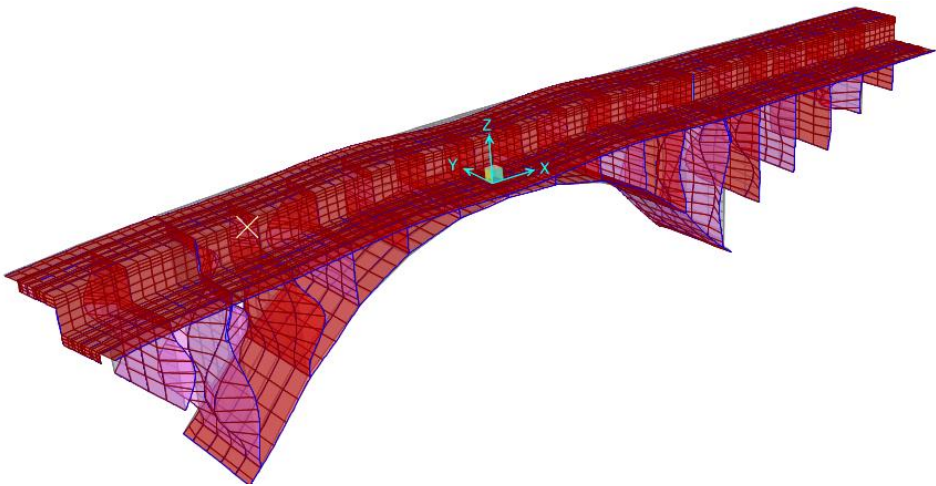
Modo 51: T= 0.1723 sec, UZ= 46.65%, RY= 5.378%



Modo	T [sec]	UX (%)	UY (%)	UZ (%)	Sum UX	Sum UY	Sum UZ
51	0.1723	0.00	0.683	46.651	58.933	65.511	48.983
Modo	T [sec]	RX (%)	RY (%)	RZ (%)	Sum RX	Sum RY	Sum RZ
51	0.1723	0.803	5.378	0.10	18.965	26.316	40.905



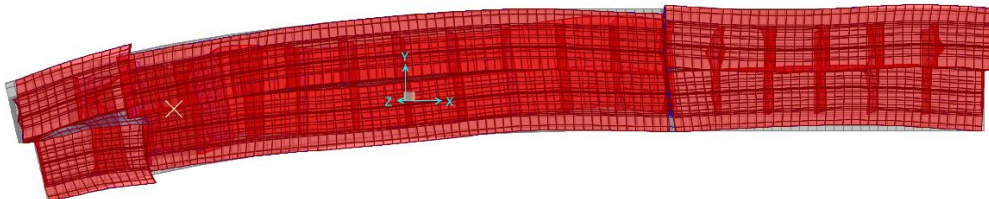
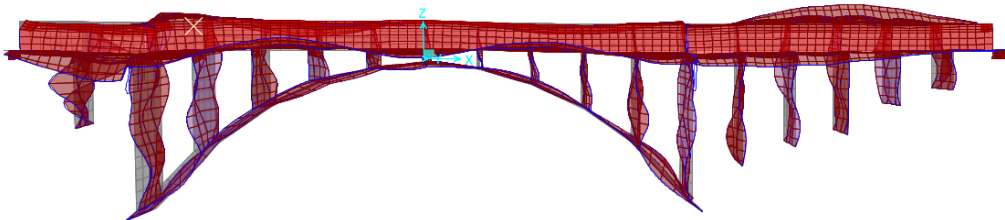
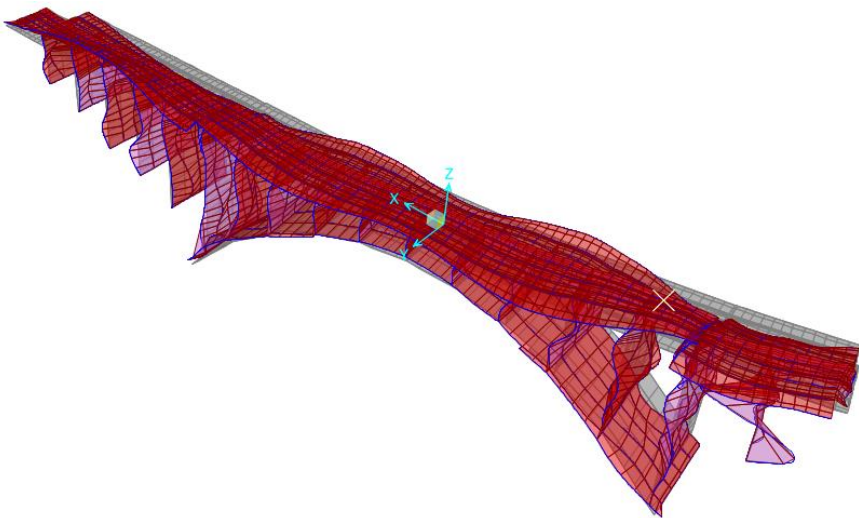
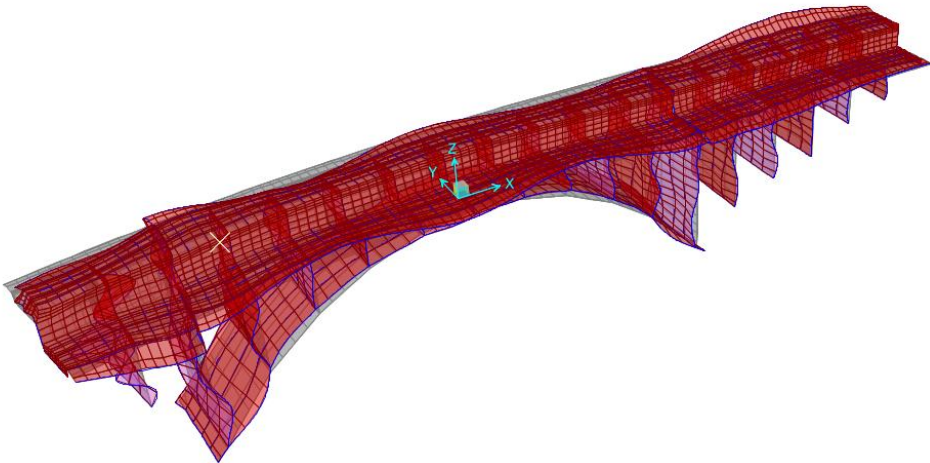
Modo 54: T= 0.1617 sec, UY= 6.62%, RX= 10.65%



Modo	T [sec]	UX (%)	UY (%)	UZ (%)	Sum UX	Sum UY	Sum UZ
54	0.1617	0.023	6.618	4.671	59.354	72.159	53.727
Modo	T [sec]	RX (%)	RY (%)	RZ (%)	Sum RX	Sum RY	Sum RZ
54	0.1617	10.65	0.734	0.187	29.65	27.065	41.72

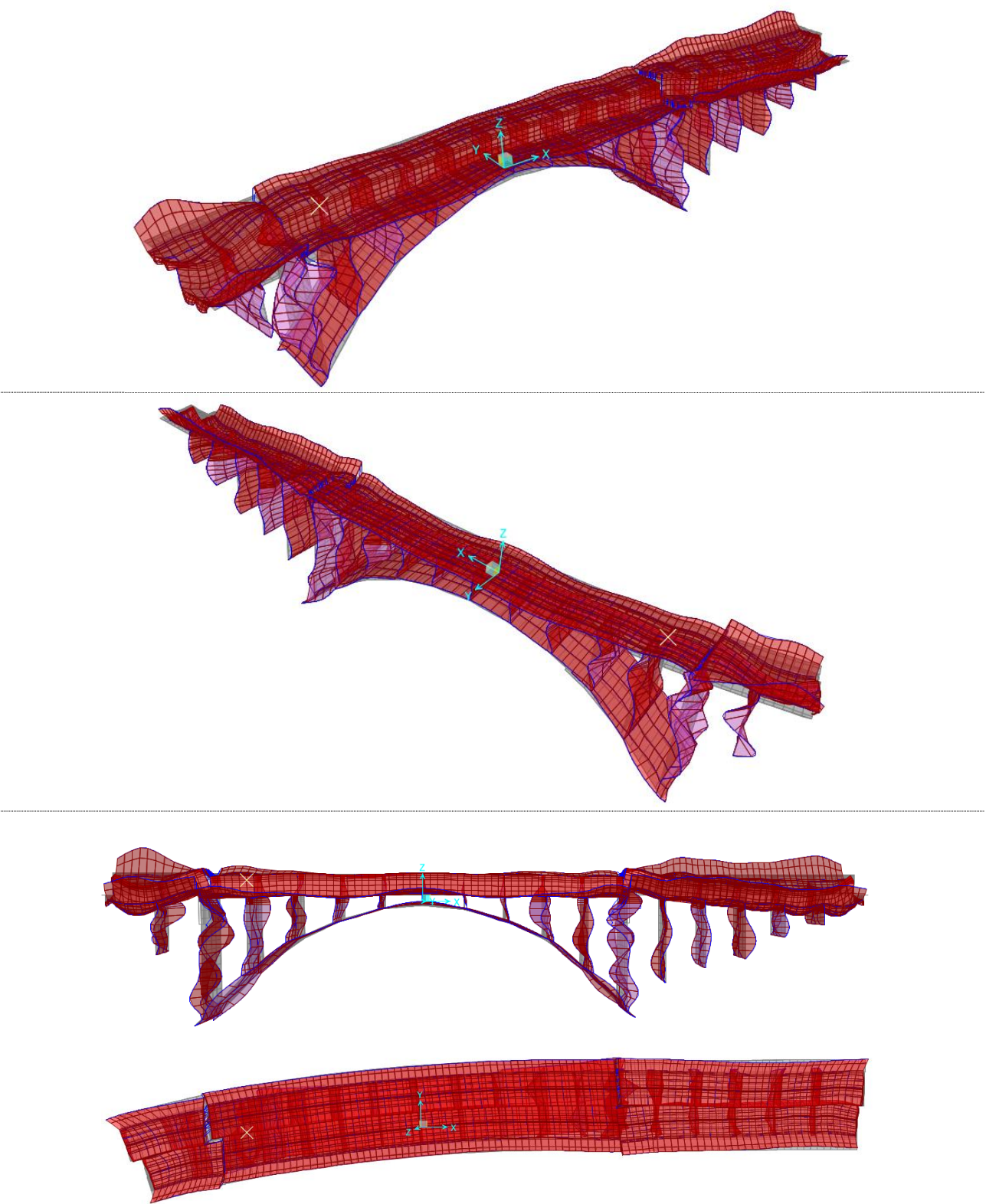


Modo 65: T= 0.1003 sec, UX= 15.77%



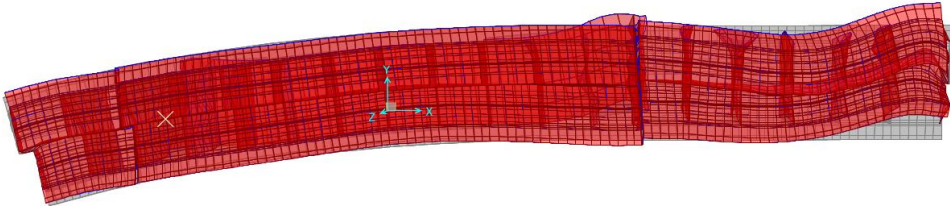
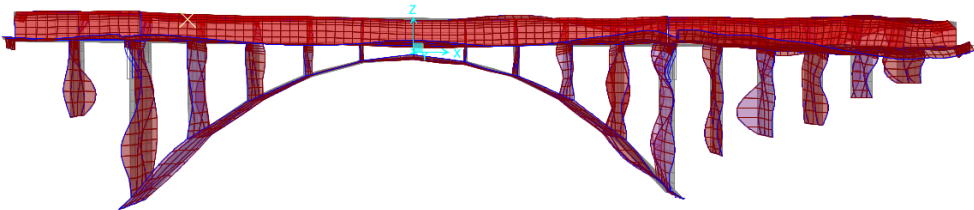
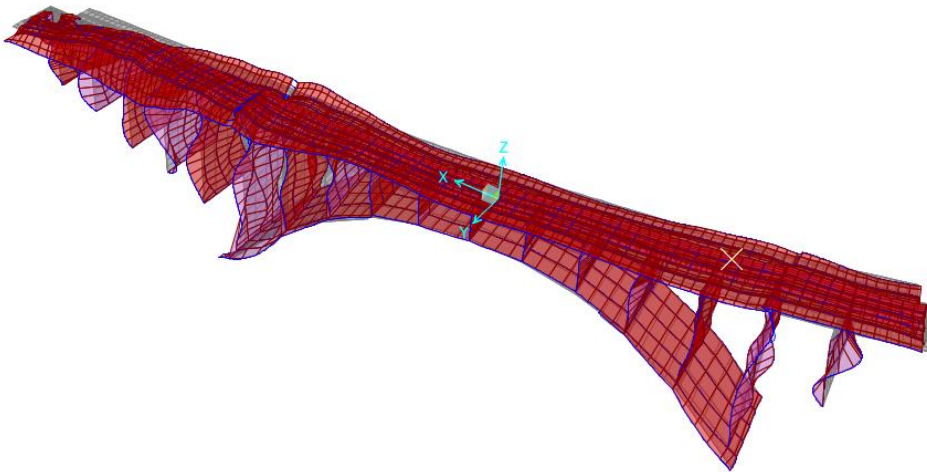
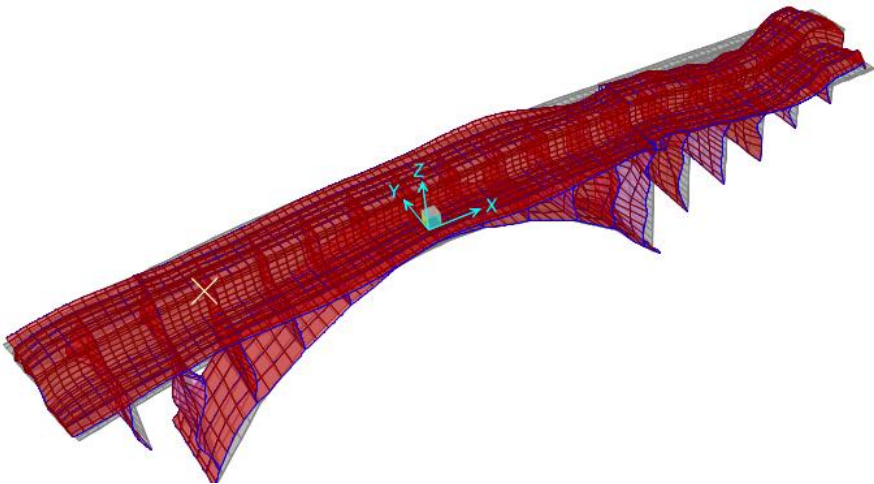
Modo	T [sec]	UX (%)	UY (%)	UZ (%)	Sum UX	Sum UY	Sum UZ
65	0.1003	15.765	0.010	0.074	79.241	73.062	61.196
Modo	T [sec]	RX (%)	RY (%)	RZ (%)	Sum RX	Sum RY	Sum RZ
65	0.1003	0.028	0.17	0.69	34.129	29.64	46.314

Modo 68: T= 0.0783 sec, RZ= 7.72%



odo	T [sec]	UX (%)	UY (%)	UZ (%)	Sum UX	Sum UY	Sum UZ
68	0.0783	0.014	4.416	0.410	79.615	78.785	63.016
Modo	T [sec]	RX (%)	RY (%)	RZ (%)	Sum RX	Sum RY	Sum RZ
68	0.0783	1.14	0.469	7.724	36.304	30.712	58.376

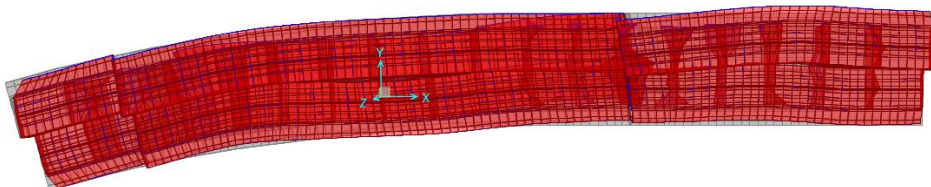
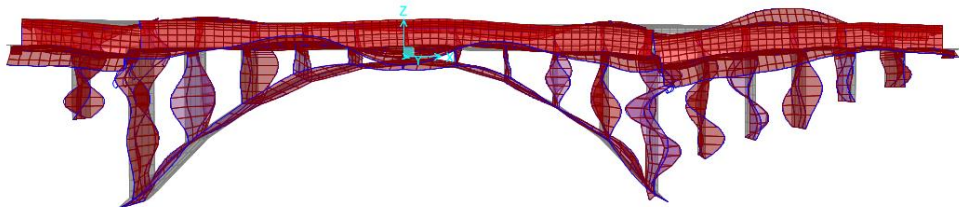
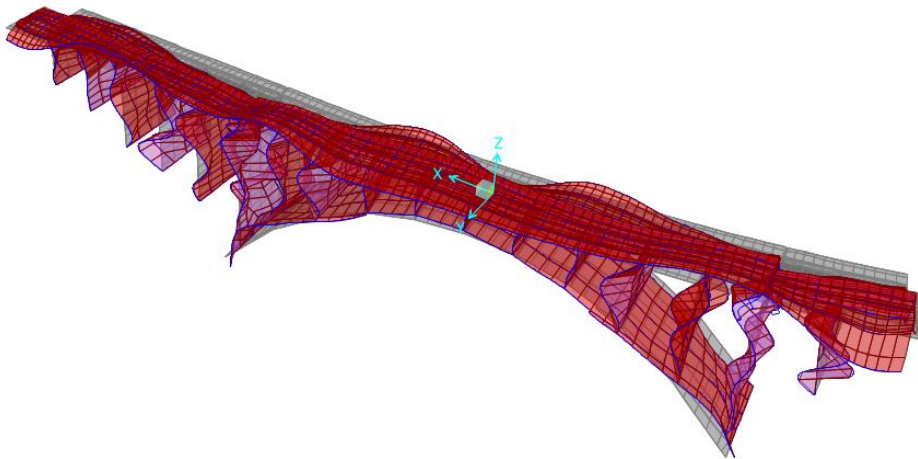
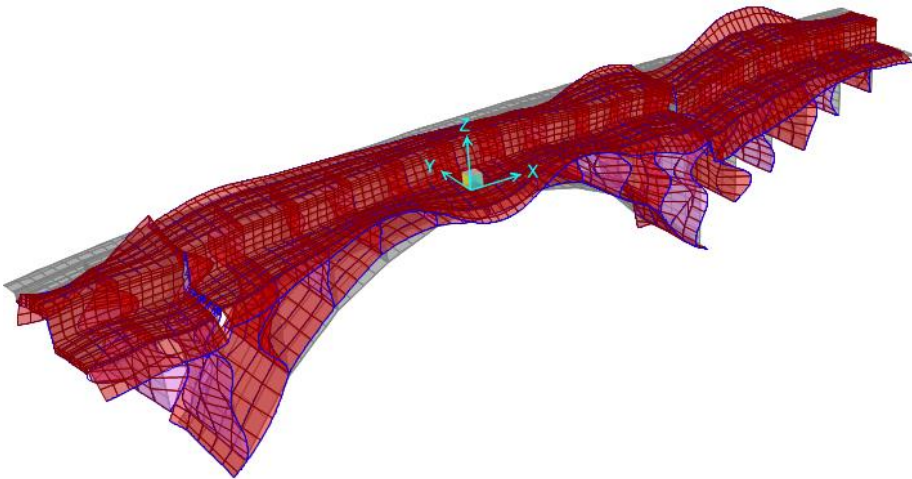
**Modo 70: T= 0.0656sec, RX= 14.45%**



Modo	T [sec]	UX (%)	UY (%)	UZ (%)	Sum UX	Sum UY	Sum UZ
70	0.0656	0.195	2.213	1.854	83.276	81.239	64.870
Modo	T [sec]	RX (%)	RY (%)	RZ (%)	Sum RX	Sum RY	Sum RZ
70	0.0656	14.452	1.504	0.583	50.762	32.783	60.874

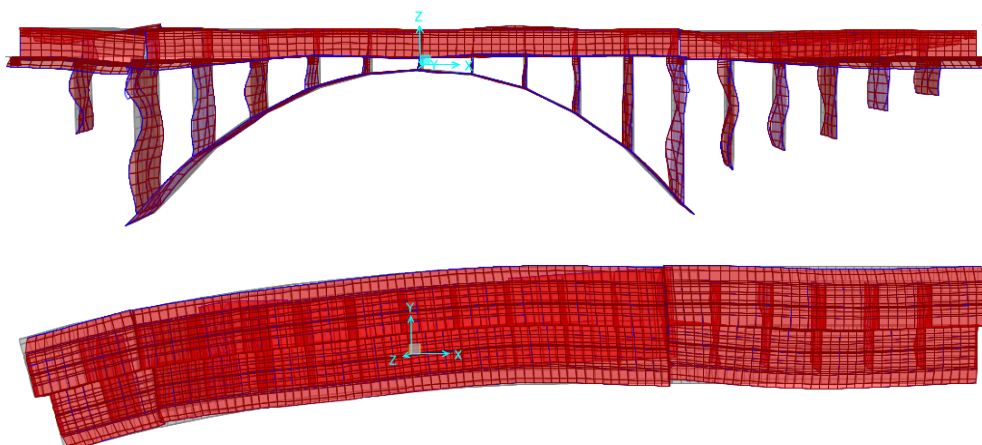
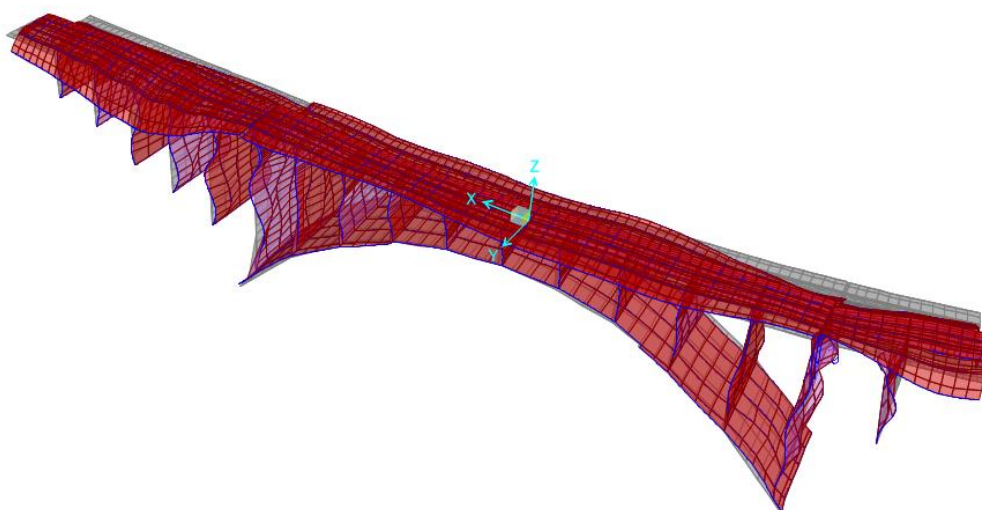
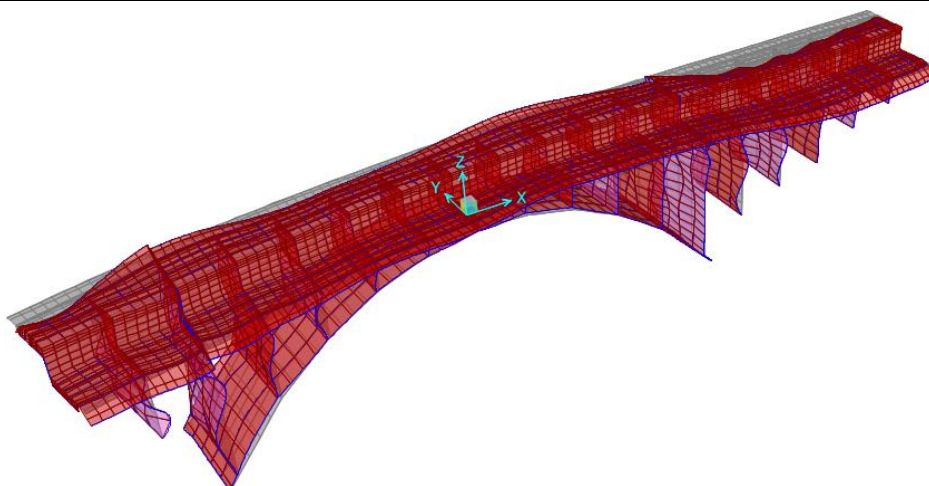


Modo 72: T= 0.0587sec, UZ= 7.21%, RZ= 5.07%



Modo	T [sec]	UX (%)	UY (%)	UZ (%)	Sum UX	Sum UY	Sum UZ
72	0.0587	0.636	0.625	7.209	84.092	84.595	74.239
Modo	T [sec]	RX (%)	RY (%)	RZ (%)	Sum RX	Sum RY	Sum RZ
72	0.0587	0.692	1.282	5.067	53.755	34.085	66.663

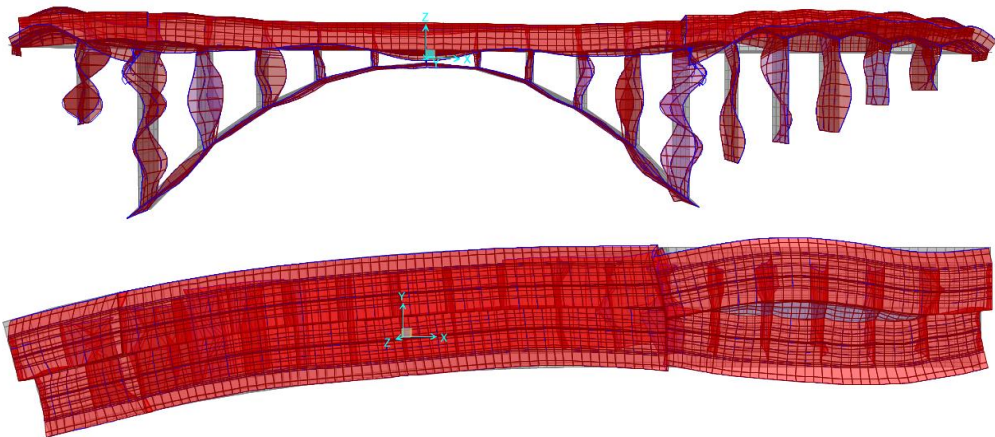
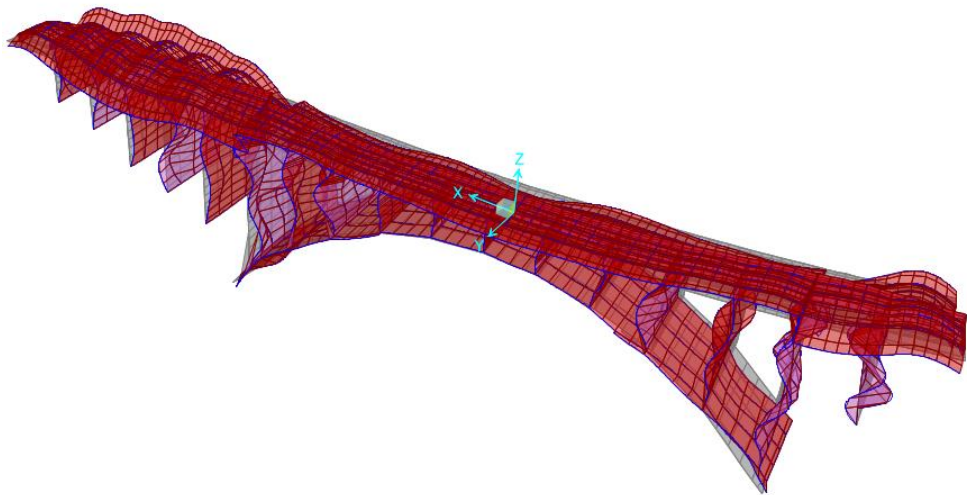
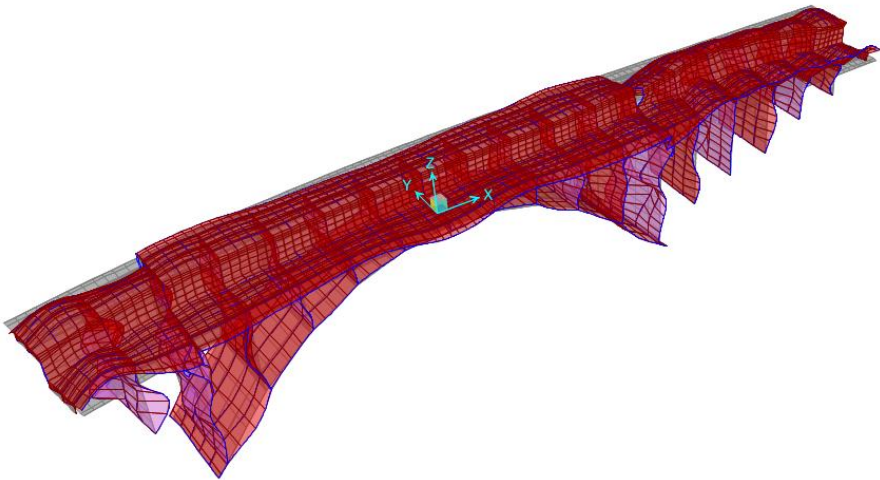
**Modo 73: T= 0.0514sec, UX= 9.47%**



<b>Modo</b>	<b>T [sec]</b>	<b>UX (%)</b>	<b>UY (%)</b>	<b>UZ (%)</b>	<b>Sum UX</b>	<b>Sum UY</b>	<b>Sum UZ</b>
73	0.0514	9.468	0.020	0.354	93.560	84.615	74.593
<b>Modo</b>	<b>T [sec]</b>	<b>RX (%)</b>	<b>RY (%)</b>	<b>RZ (%)</b>	<b>Sum RX</b>	<b>Sum RY</b>	<b>Sum RZ</b>
73	0.0514	0.341	1.694	1.026	54.096	35.778	67.689

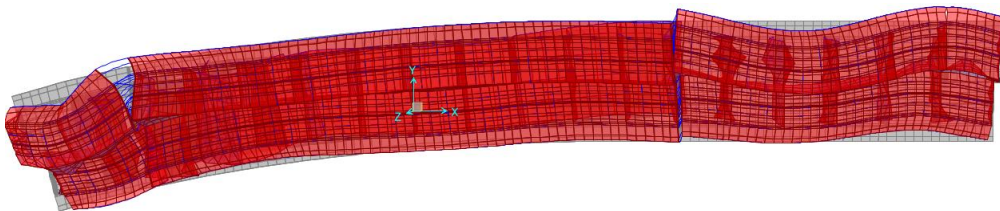
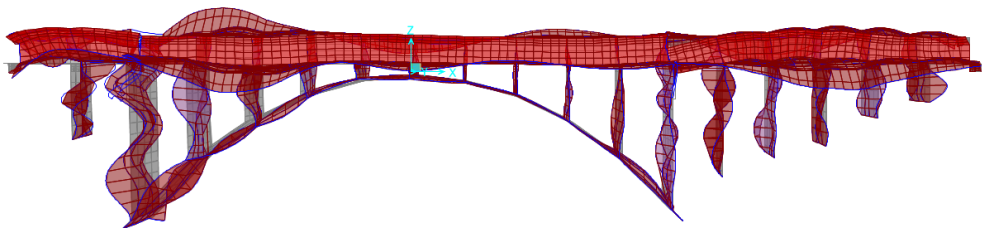
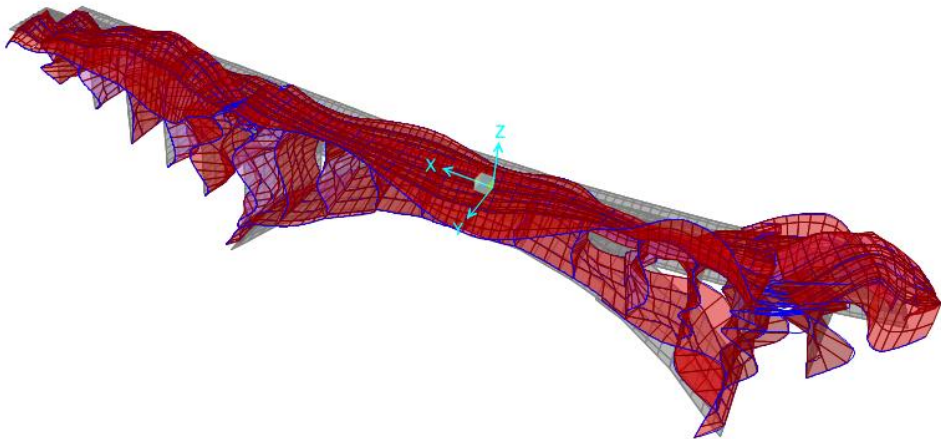
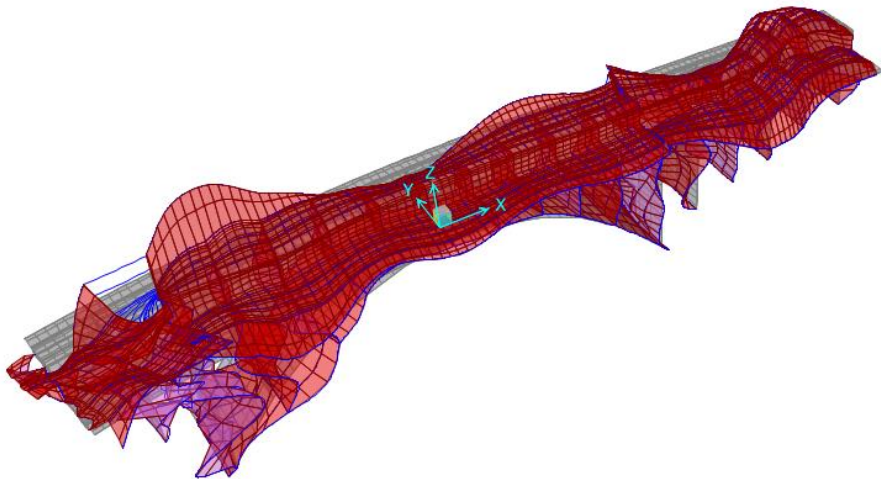


Modo 74: T= 0.0436sec, UZ= 12.22%, RY= 5.498%



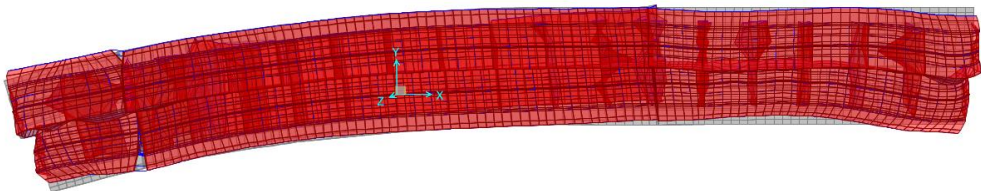
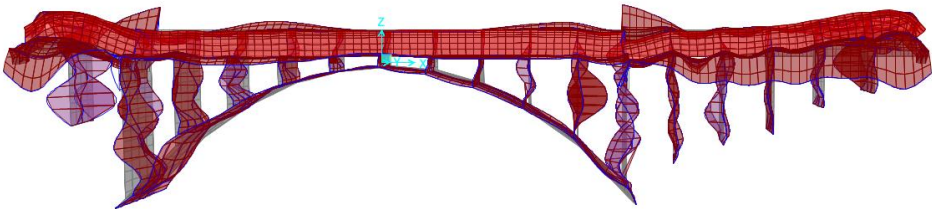
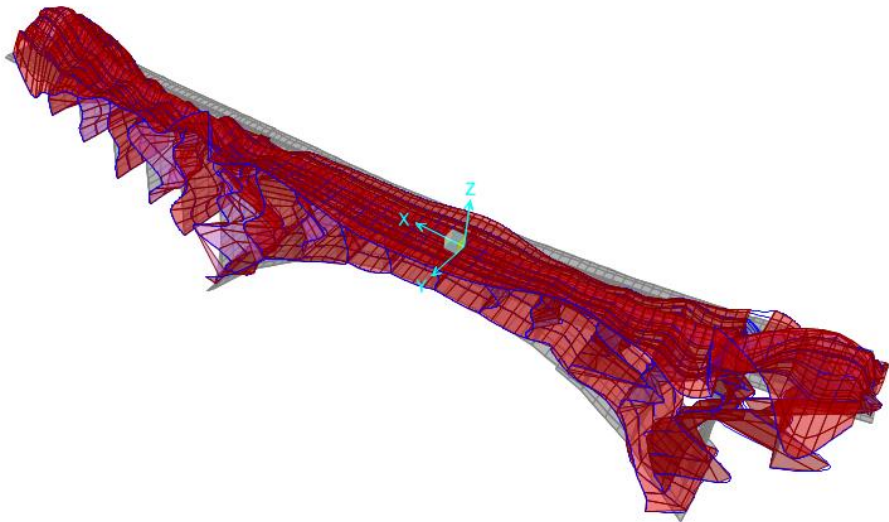
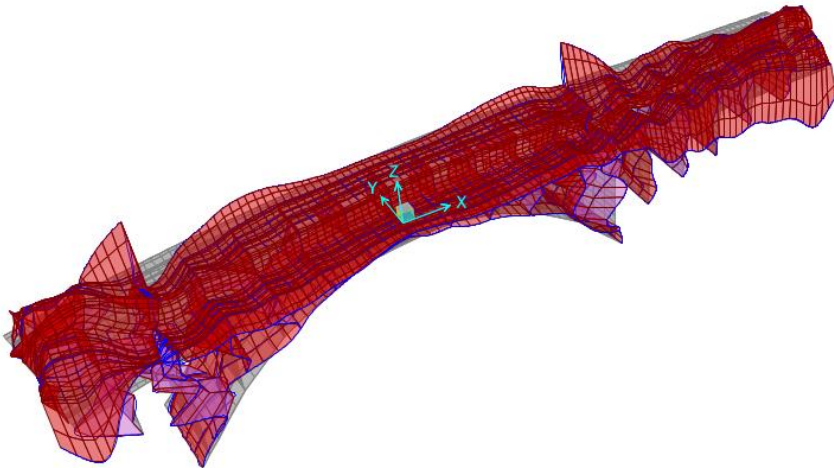
Modo	T [sec]	UX (%)	UY (%)	UZ (%)	Sum UX	Sum UY	Sum UZ
74	0.0436	0.004	1.183	12.222	93.564	85.798	855.798
Modo	T [sec]	RX (%)	RY (%)	RZ (%)	Sum RX	Sum RY	Sum RZ
74	0.0436	0.88	5.498	2.559	54.976	41.276	70.248

Modo 76: T= 0.0375sec, RZ= 10.85%



Modo	T [sec]	UX (%)	UY (%)	UZ (%)	Sum UX	Sum UY	Sum UZ
76	0.0375	0.001	0.208	0.565	93.987	90.462	89.015
Modo	T [sec]	RX (%)	RY (%)	RZ (%)	Sum RX	Sum RY	Sum RZ
76	0.0375	1.865	1.087	0.42	56.841	42.363	70.669

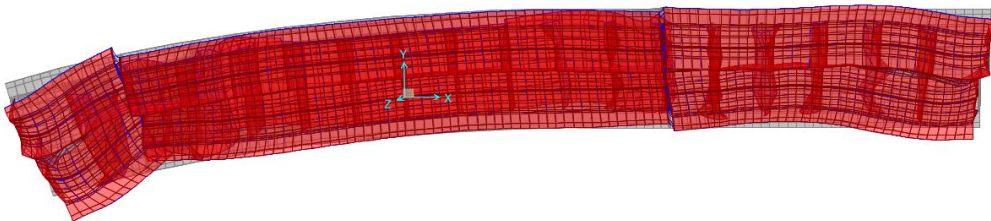
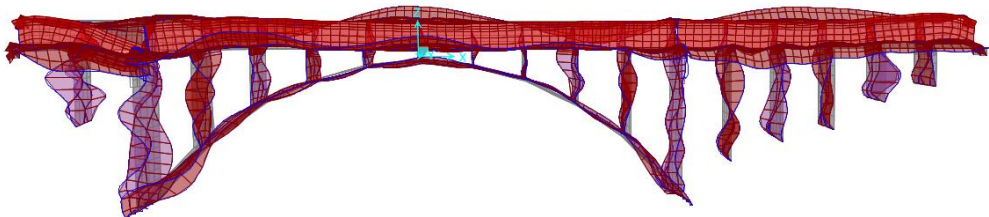
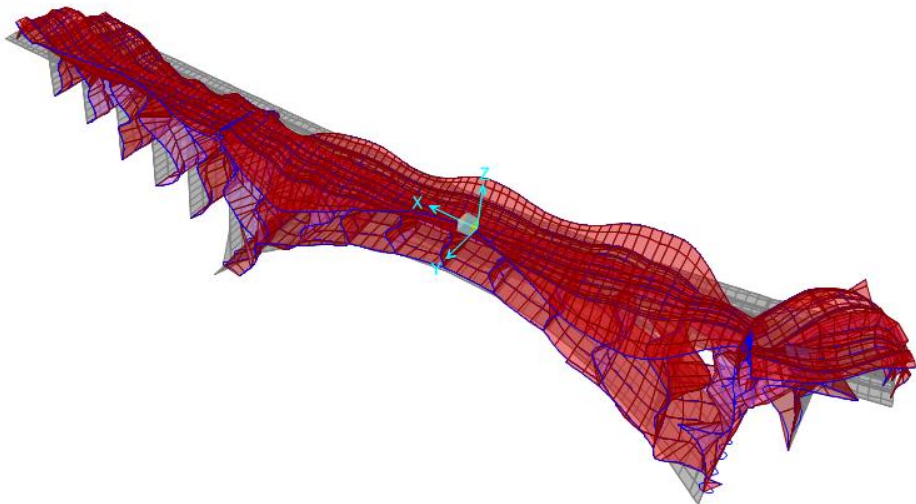
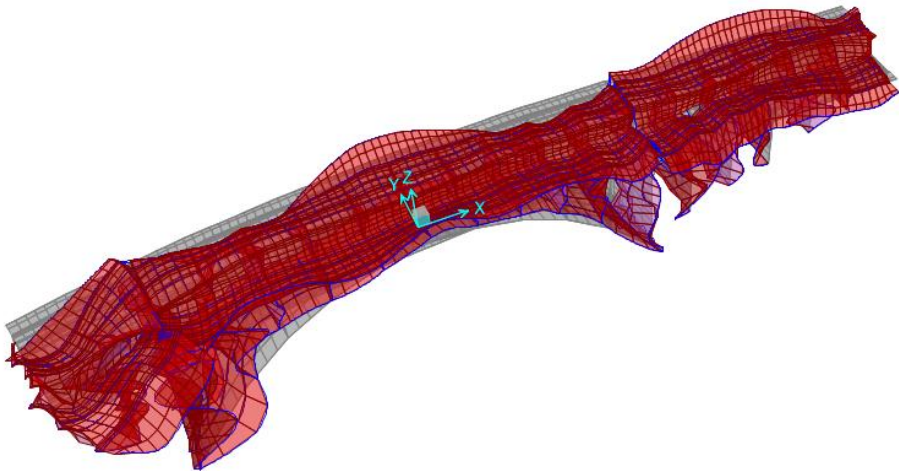
Modo 78: T= 0.0244sec, UZ= 5.564%



Modo	T [sec]	UX (%)	UY (%)	UZ (%)	Sum UX	Sum UY	Sum UZ
78	0.0244	0.048	0.032	5.564	97.970	91.490	95.422
Modo	T [sec]	RX (%)	RY (%)	RZ (%)	Sum RX	Sum RY	Sum RZ
78	0.0244	2.568	1.359	0.68	60.548	45.676	85.40



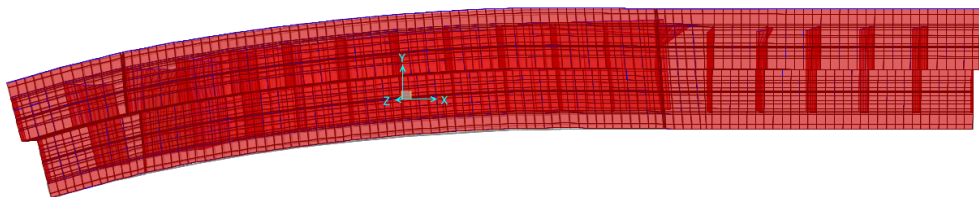
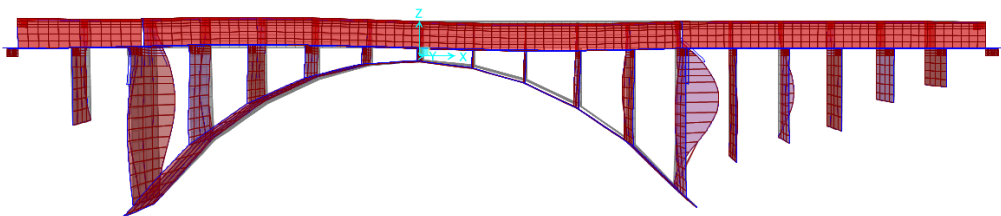
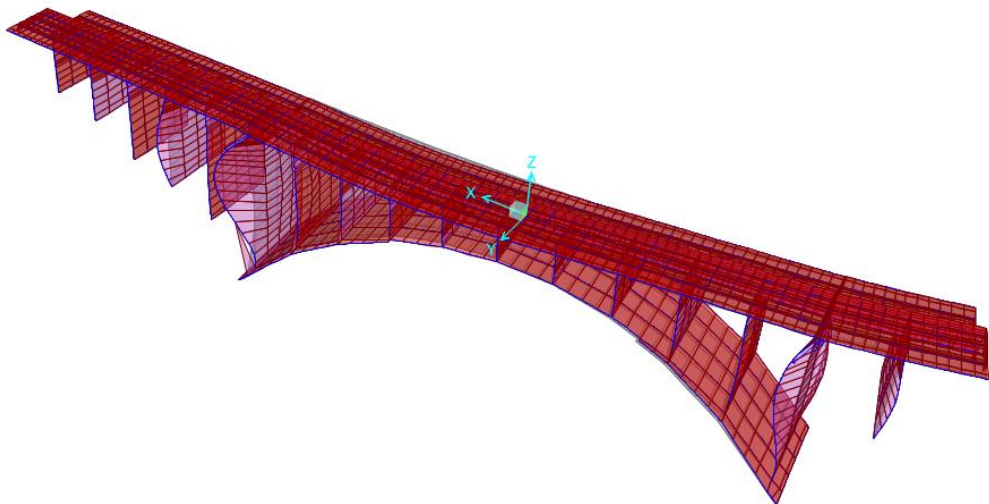
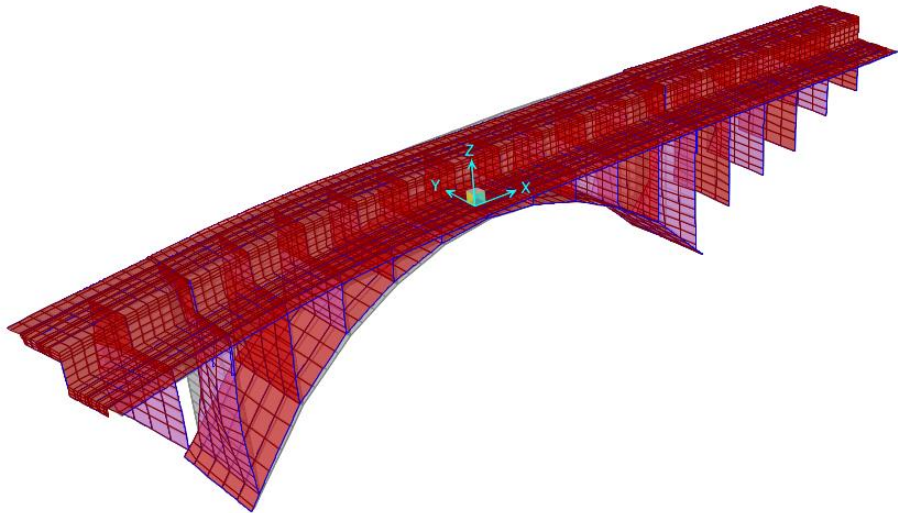
Modo 79: T= 0.0227sec, UY= 5.303%



Modo	T [sec]	UX (%)	UY (%)	UZ (%)	Sum UX	Sum UY	Sum UZ
79	0.0227	0.037	5.303	0.288	98.008	96.793	95.710
Modo	T [sec]	RX (%)	RY (%)	RZ (%)	Sum RX	Sum RY	Sum RZ
79	0.0227	0.138	0.002	10.62	60.68	45.67	96.02

(3.1) Single – deformable- deck model with fixed joints

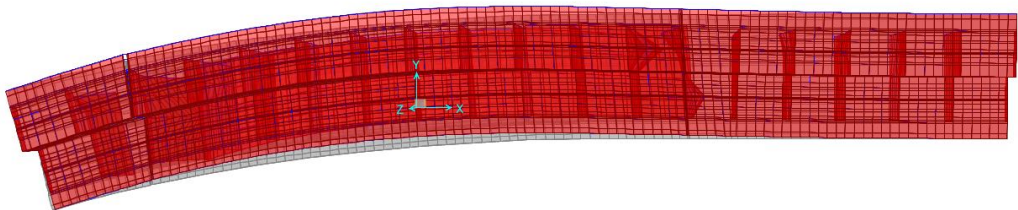
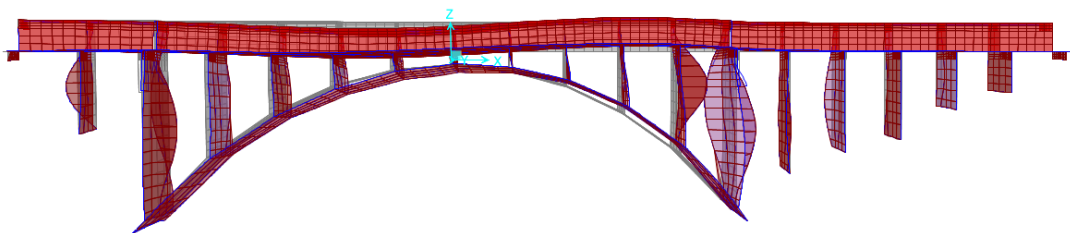
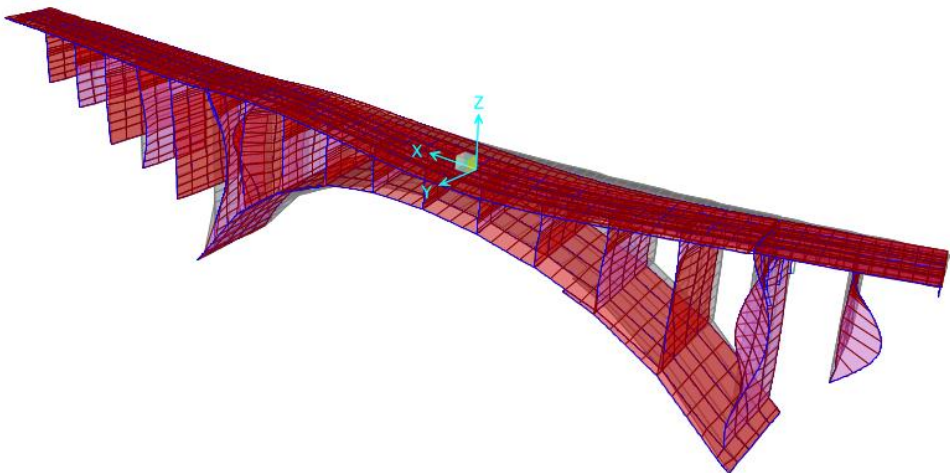
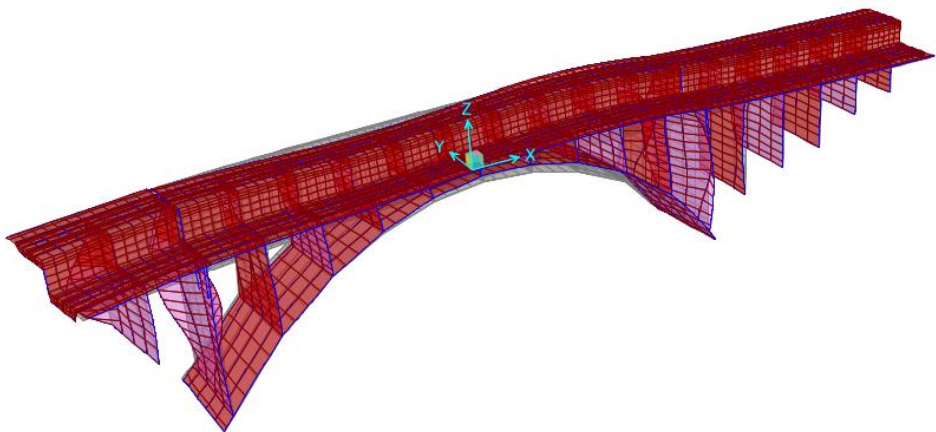
Modo 13: T= 0.3942 sec, UX= 5.508%, RX= 4.741%



Modo	T [sec]	UX (%)	UY (%)	UZ (%)	Sum UX	Sum UY	Sum UZ
13	0.3942	5.508	9.525	0.110	19.488	12.502	0.214
Modo	T [sec]	RX (%)	RY (%)	RZ (%)	Sum RX	Sum RY	Sum RZ
13	0.3942	4.741	4.093	0.883	7.752	10.111	1.054

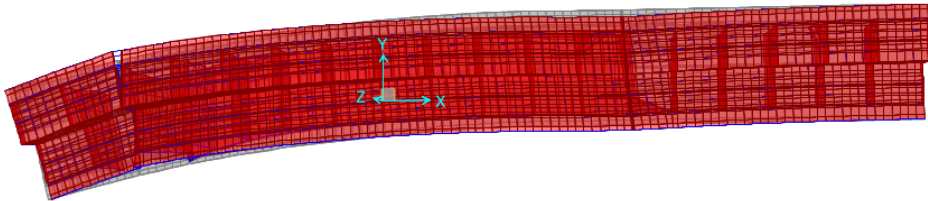
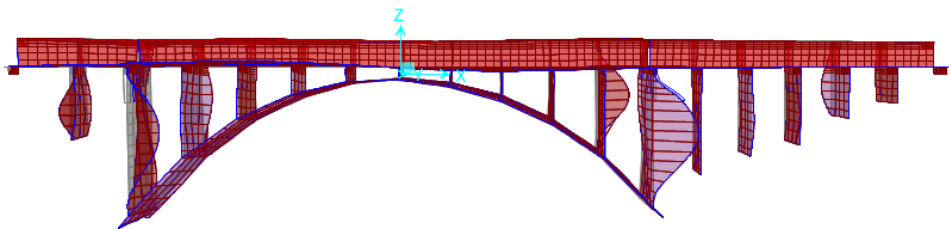
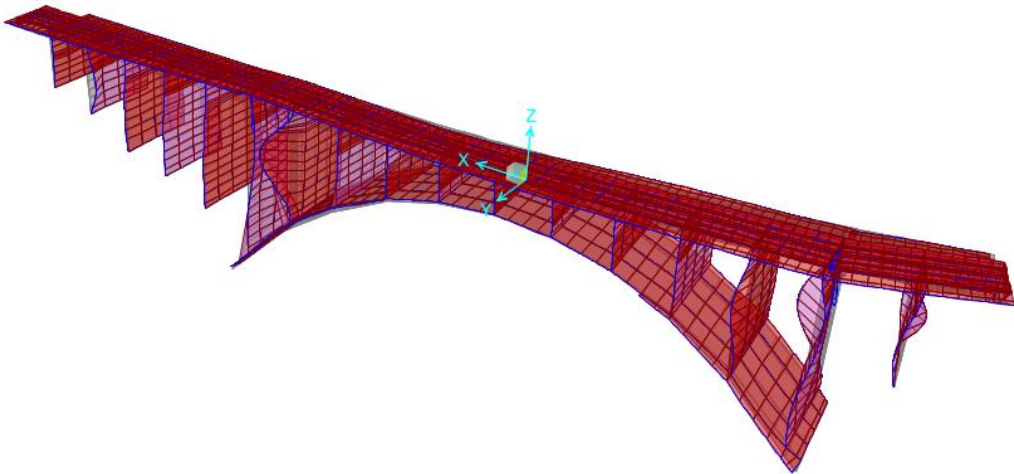
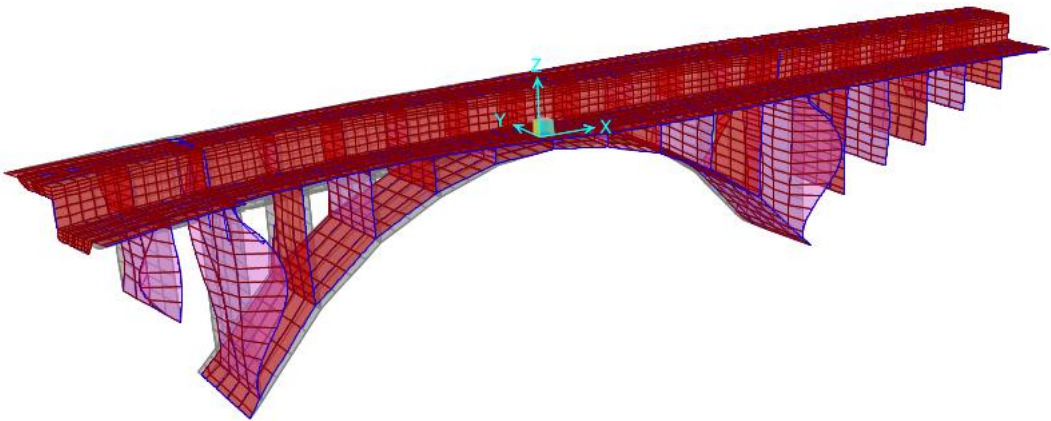


Modo 14: T= 0..3729 sec, UY= 41.41%



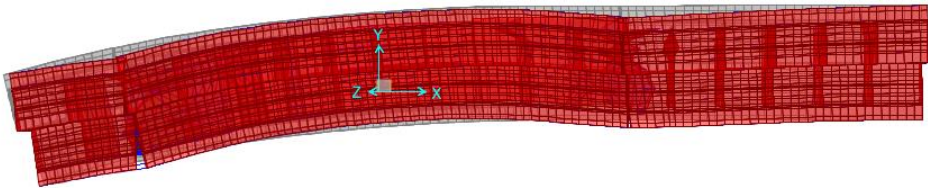
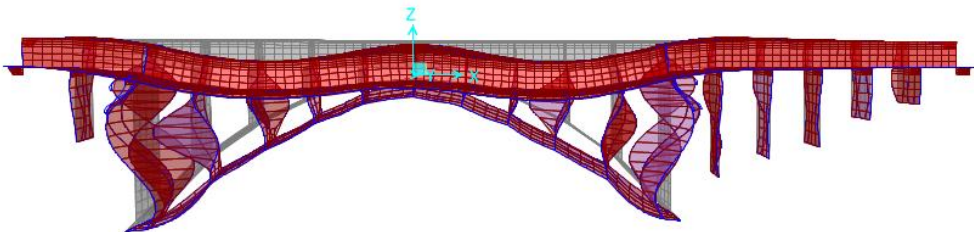
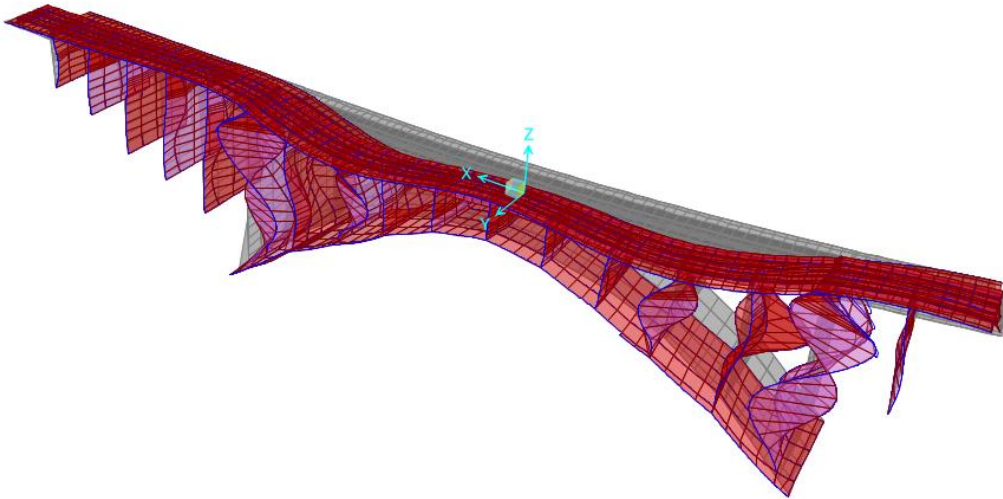
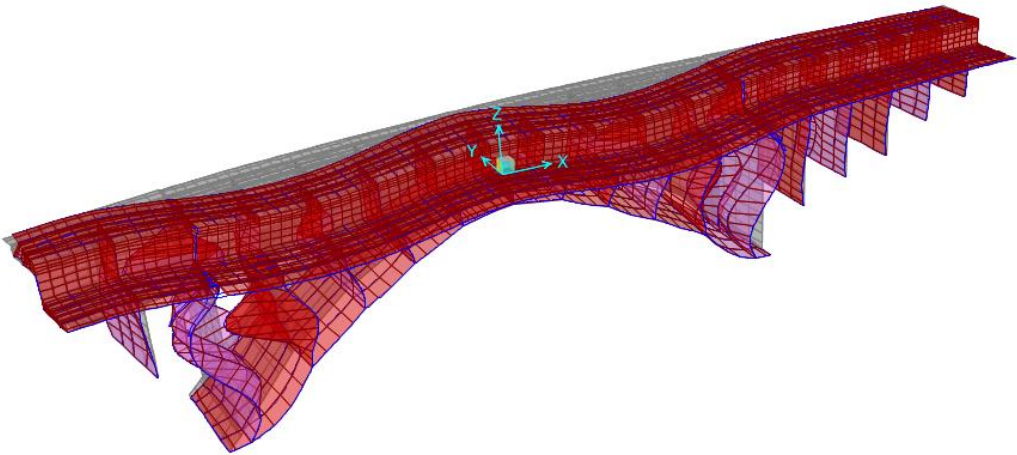
Modo	T [sec]	UX (%)	UY (%)	UZ (%)	Sum UX	Sum UY	Sum UZ
14	0.3729	1.041	41.41	0.35	20.529	53.916	0.563
Modo	T [sec]	RX (%)	RY (%)	RZ (%)	Sum RX	Sum RY	Sum RZ
14	0.3729	3.896	4.119	4.158	11.648	14.234	5.259

Modo 33: T= 0.2520 sec, RZ= 22.67%



Modo	T [sec]	UX (%)	UY (%)	UZ (%)	Sum UX	Sum UY	Sum UZ
33	0.2520	0.168	0.643	0.018	23.314	60.413	1.008
Modo	T [sec]	RX (%)	RY (%)	RZ (%)	Sum RX	Sum RY	Sum RZ
33	0.2520	0.110	0.018	22.670	12.307	14.991	35.282

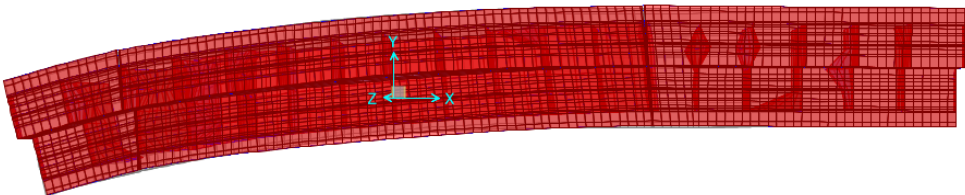
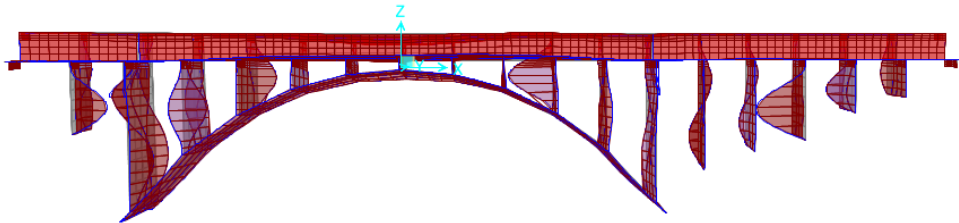
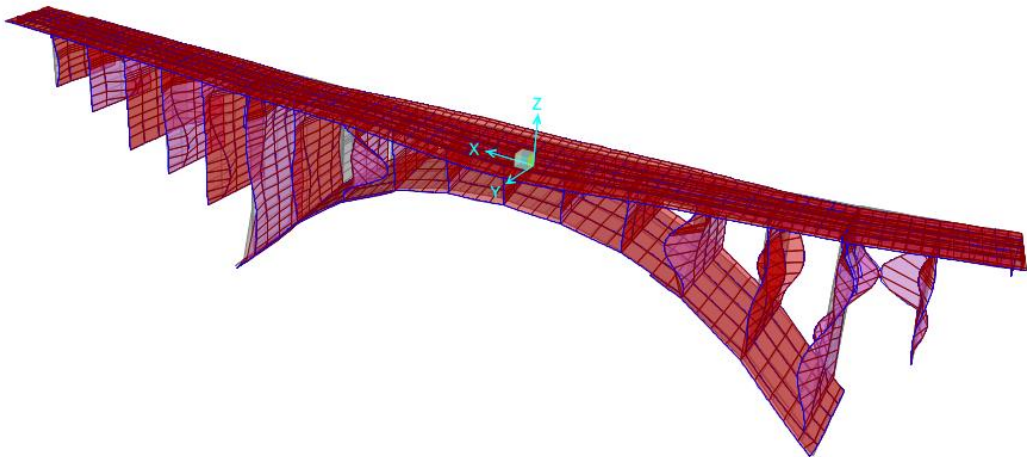
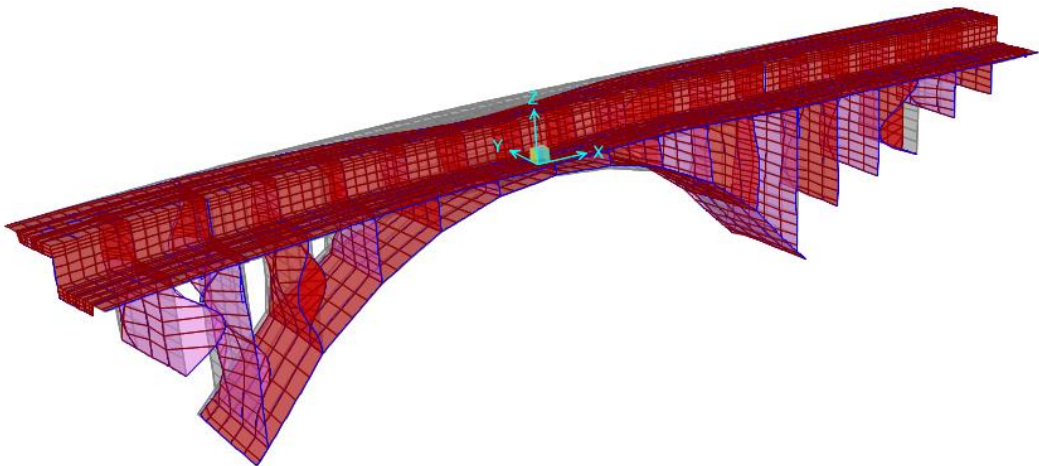
**Modo 49: T= 0.1717 sec, UZ= 46.956%**



Modo	T [sec]	UX (%)	UY (%)	UZ (%)	Sum UX	Sum UY	Sum UZ
49	0.1717	0.131	0.384	46.956	28.514	61.007	48.925
Modo	T [sec]	RX (%)	RY (%)	RZ (%)	Sum RX	Sum RY	Sum RZ
49	0.1717	2.304	4.676	0.287	15.239	24.625	37.405

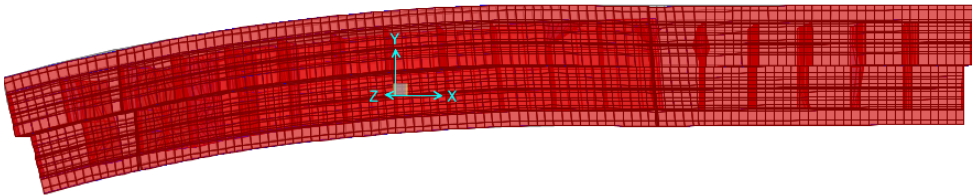
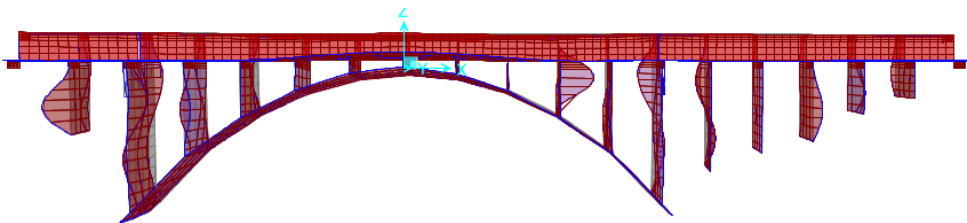
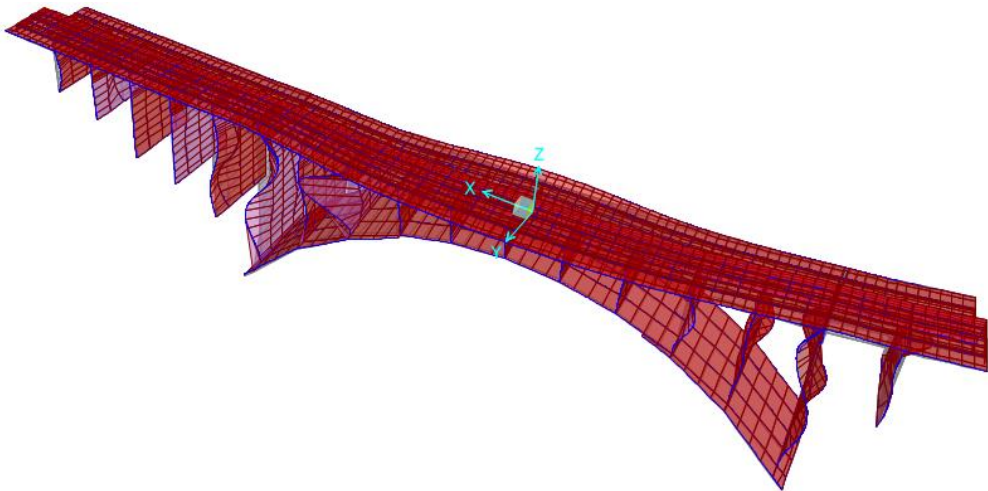
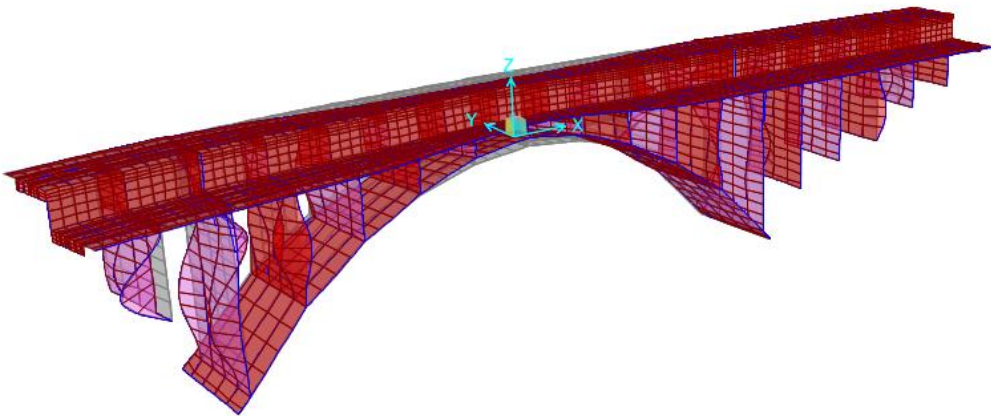


Modo 52: T= 0.1612 sec, RX= 10.229%



Modo	T [sec]	UX (%)	UY (%)	UZ (%)	Sum UX	Sum UY	Sum UZ
52	0.1612	0.604	1.388	2.991	30.022	62.451	52.372
Modo	T [sec]	RX (%)	RY (%)	RZ (%)	Sum RX	Sum RY	Sum RZ
52	0.1612	10.229	0.482	1.120	27.083	25.368	38.840

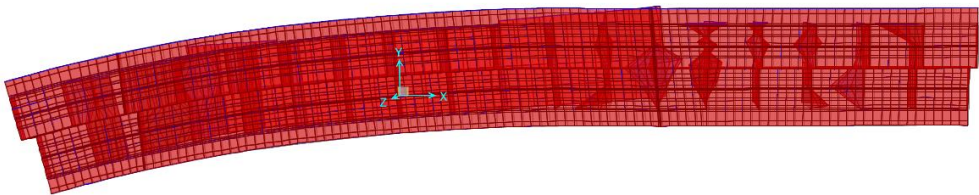
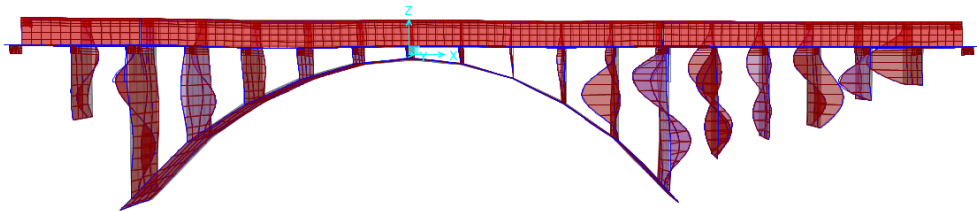
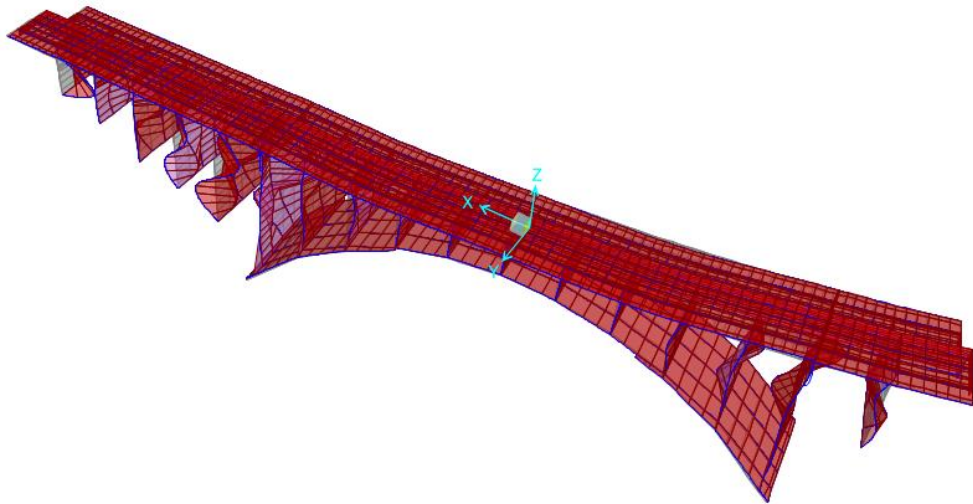
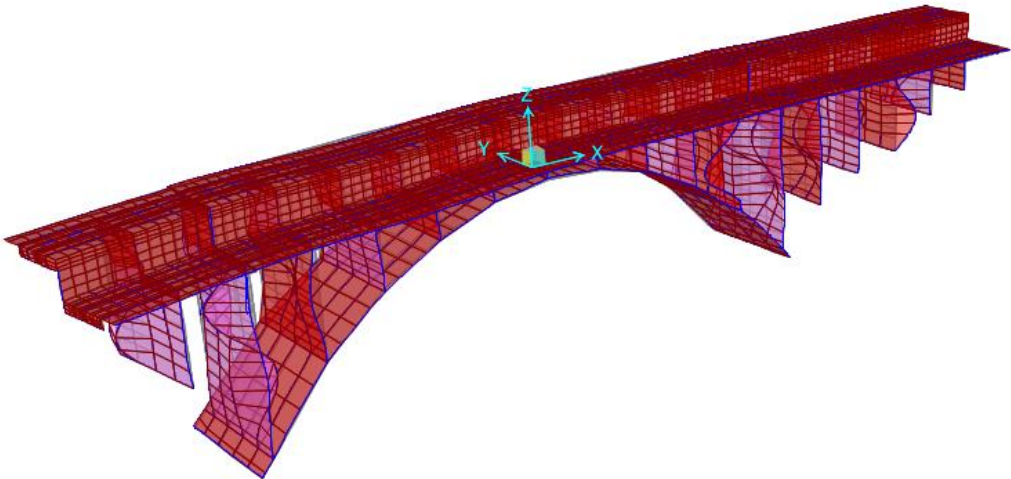
Modo 53: T= 0.1568 sec, UY= 4.417%, RX= 4.963%



Modo	T [sec]	UX (%)	UY (%)	UZ (%)	Sum UX	Sum UY	Sum UZ
53	0.1568	0.505	4.417	0.237	30.527	66.868	52.609
Modo	T [sec]	RX (%)	RY (%)	RZ (%)	Sum RX	Sum RY	Sum RZ
53	0.1568	4.963	0.059	0.011	32.045	25.427	38.851

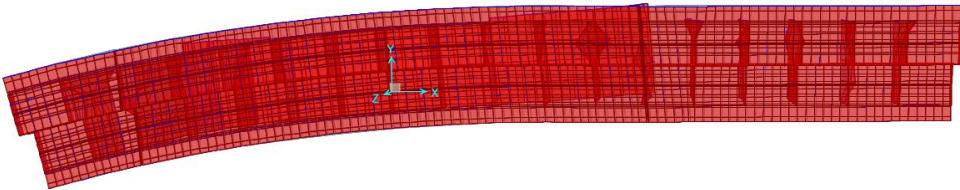
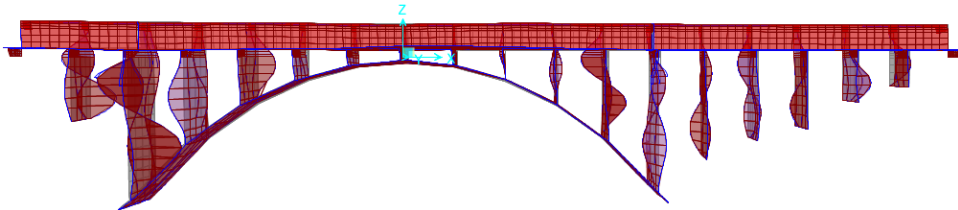
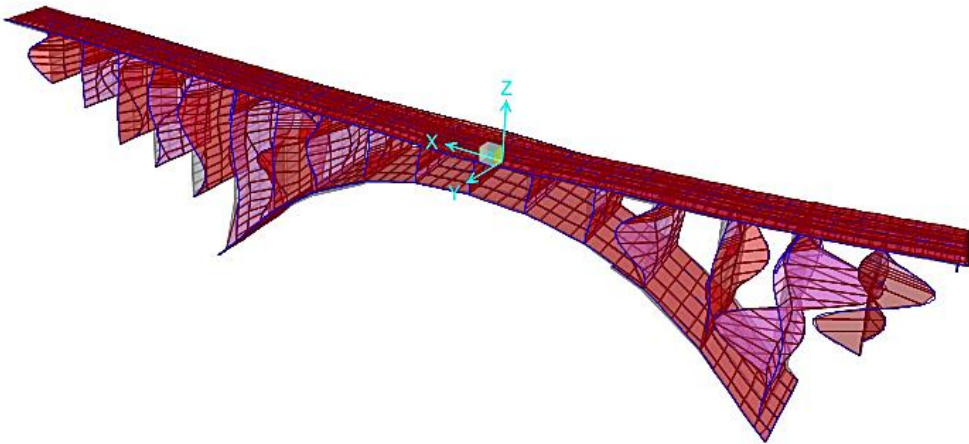
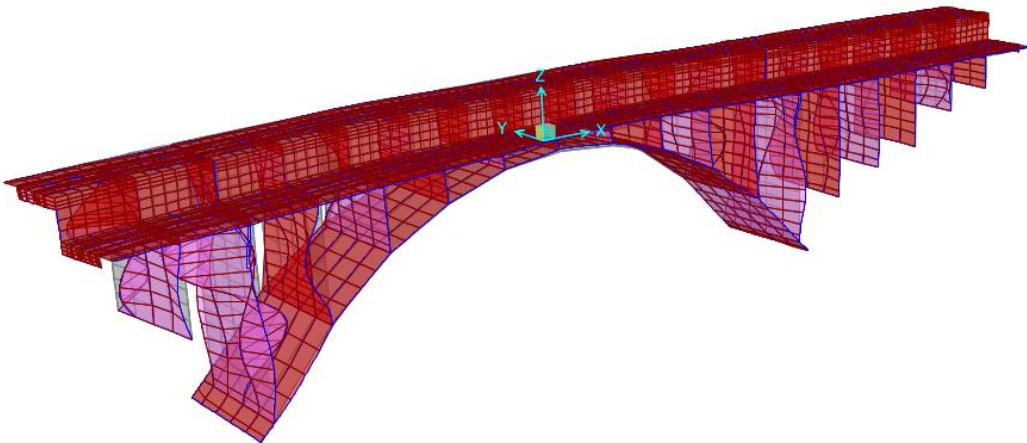


Modo 57: T= 0.1428 sec, UX= 11.93%



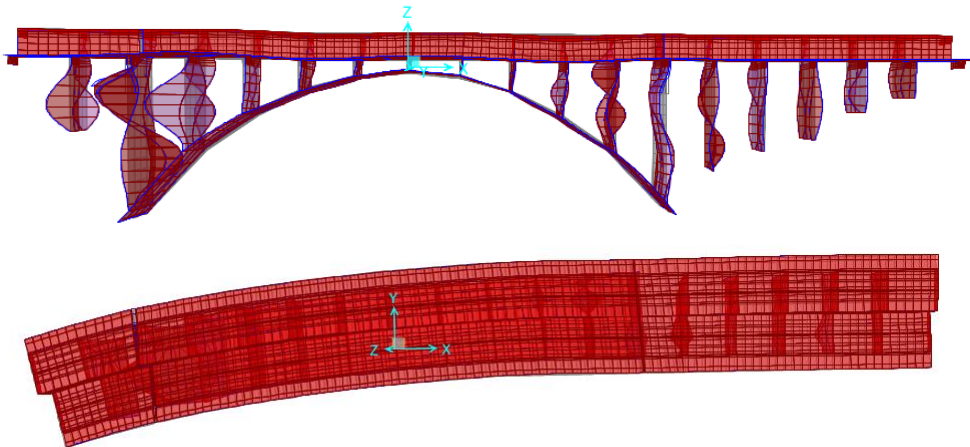
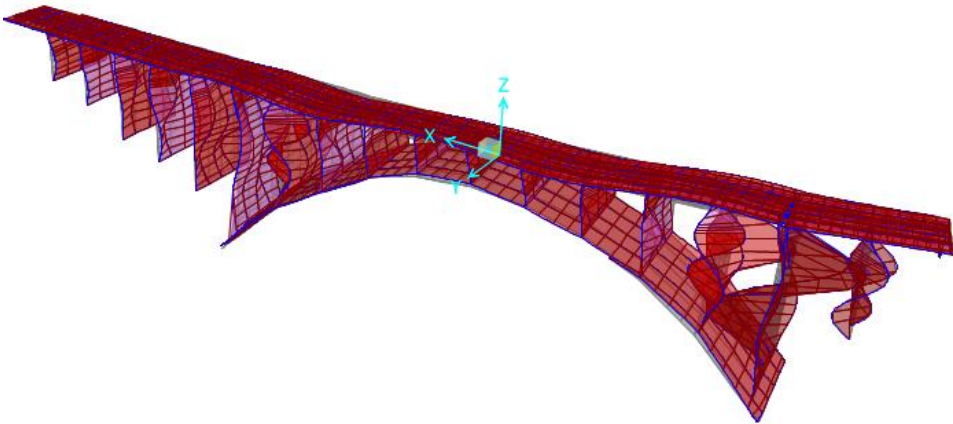
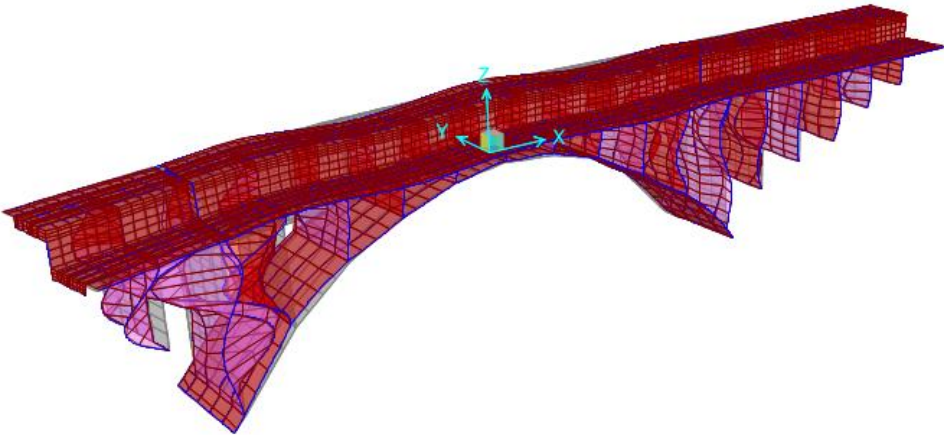
Modo	T [sec]	UX (%)	UY (%)	UZ (%)	Sum UX	Sum UY	Sum UZ
57	0.1428	11.936	0.218	0.007	45.260	70.645	57.893
Modo	T [sec]	RX (%)	RY (%)	RZ (%)	Sum RX	Sum RY	Sum RZ
57	0.1428	0.151	0.443	0.009	32.477	27.496	39.838

**Modo 58: T= 0.1336sec, UX= 14.61%**



Modo	T [sec]	UX (%)	UY (%)	UZ (%)	Sum UX	Sum UY	Sum UZ
58	0.1336	14.661	0.807	0.163	59.922	71.452	58.056
Modo	T [sec]	RX (%)	RY (%)	RZ (%)	Sum RX	Sum RY	Sum RZ
58	0.1336	0.839	1.101	0.025	33.315	28.597	39.863

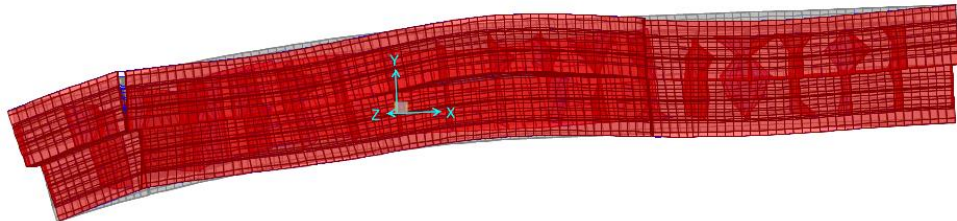
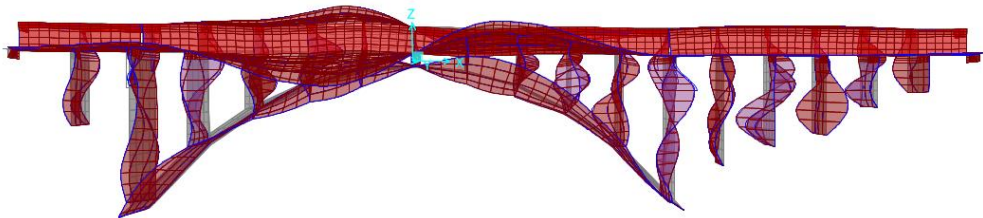
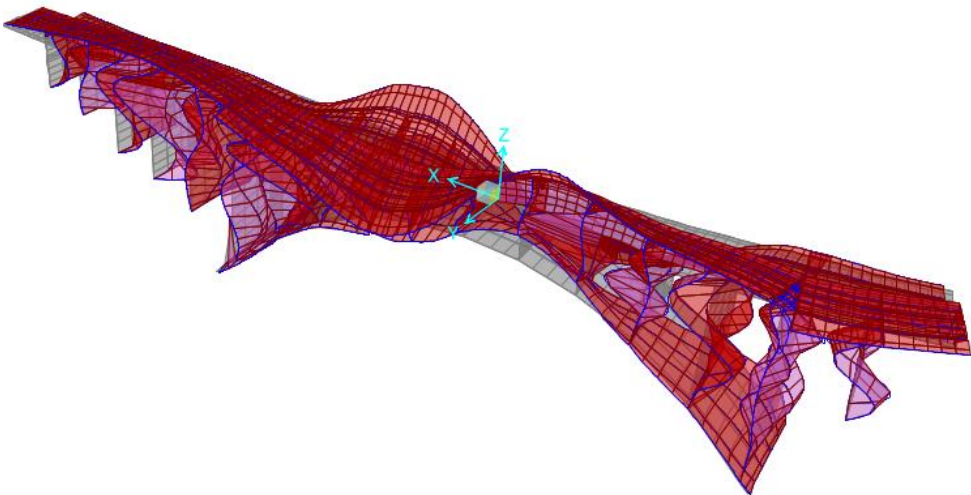
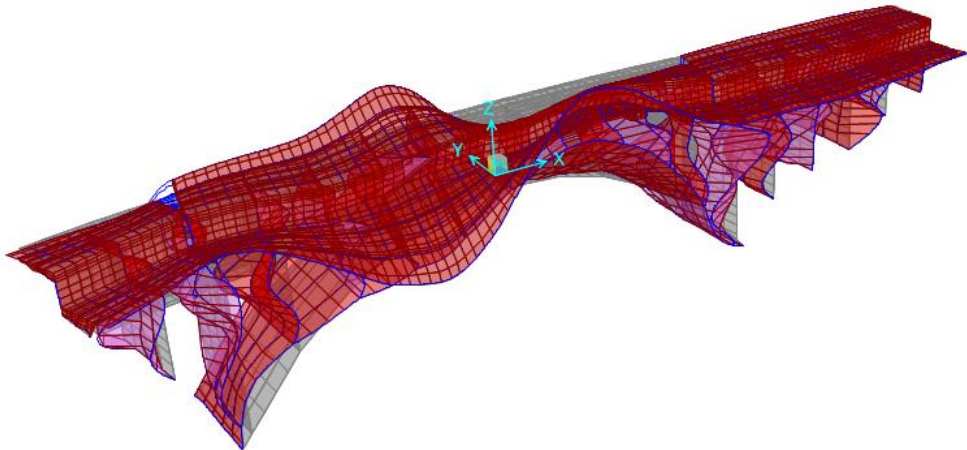
Modo 60: T= 0.1277 sec, UX= 16.83%



Modo	T [sec]	UX (%)	UY (%)	UZ (%)	Sum UX	Sum UY	Sum UZ
60	0.1277	16.831	0.478	0.228	80.674	72.017	58.745
Modo	T [sec]	RX (%)	RY (%)	RZ (%)	Sum RX	Sum RY	Sum RZ
60	0.1277	0.525	1.021	0.001	34.041	30.386	39.984



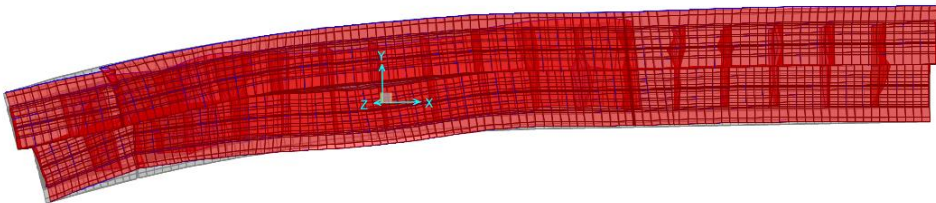
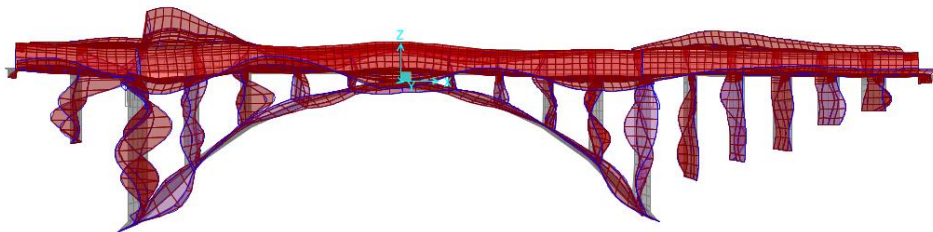
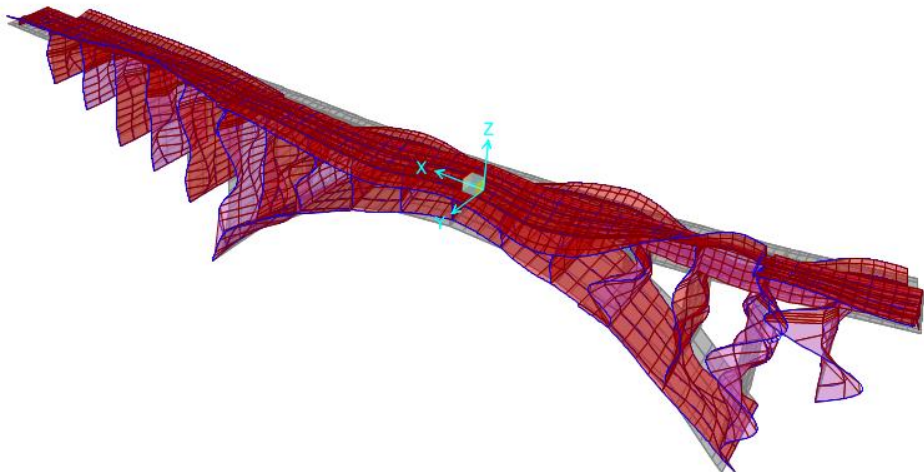
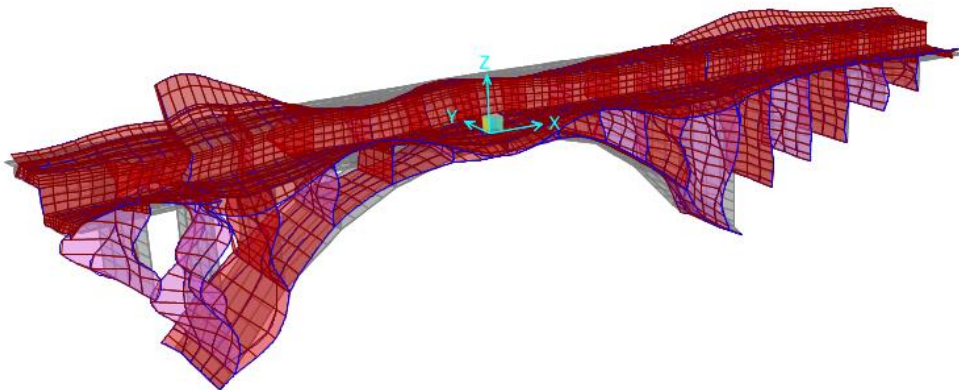
**Modo 62: T= 0.1038 sec, RZ= 7.65%**



Modo	T [sec]	UX (%)	UY (%)	UZ (%)	Sum UX	Sum UY	Sum UZ
62	0.1038	0.033	0.558	0.035	81.121	72.655	60.743
Modo	T [sec]	RX (%)	RY (%)	RZ (%)	Sum RX	Sum RY	Sum RZ
62	0.1038	0.185	0.040	7.648	34.565	30.875	47.633

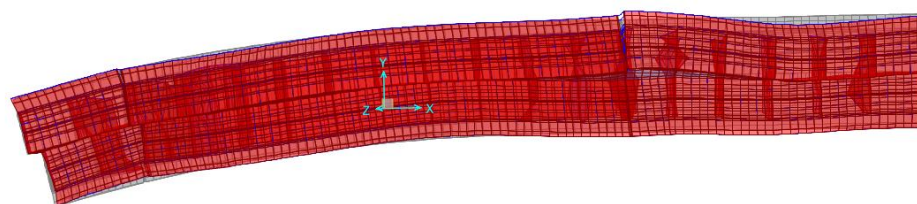
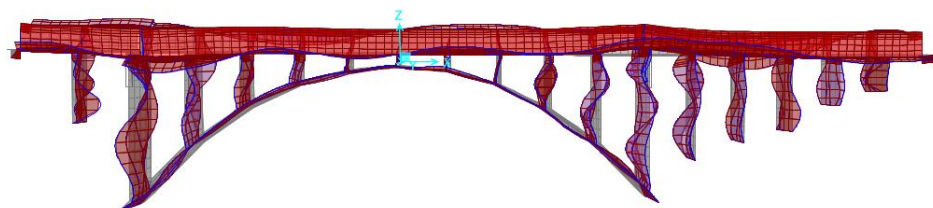
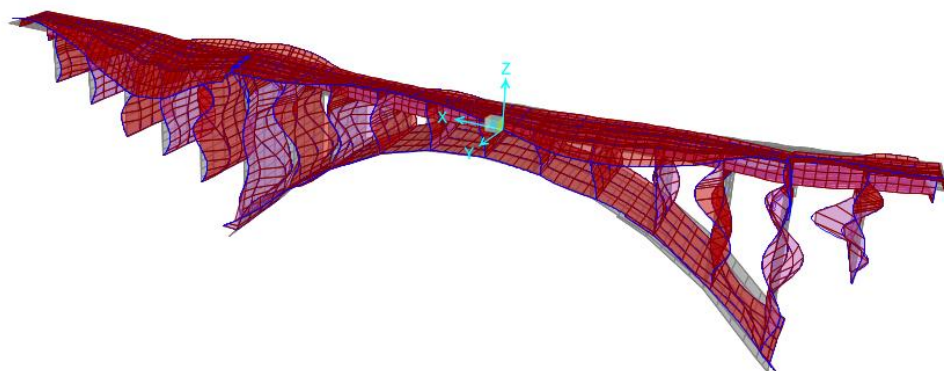
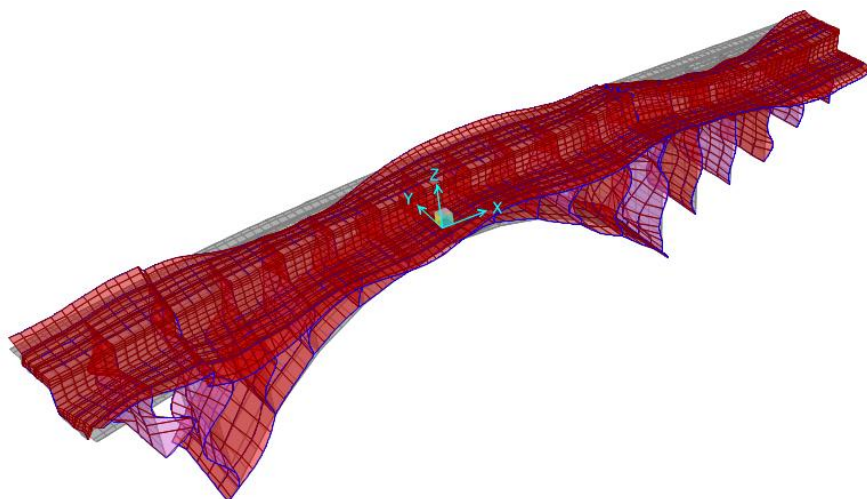


**Modo 70: T= 0.0638 sec, RX= 9.03%**



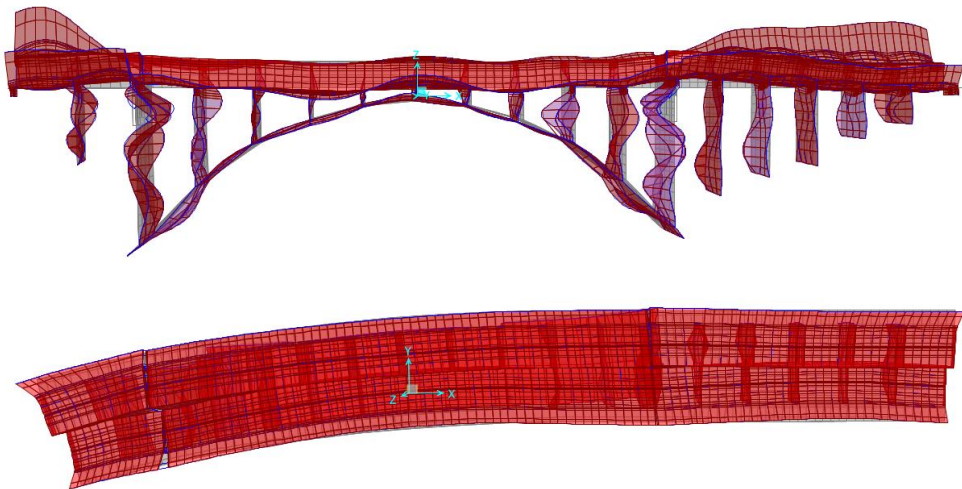
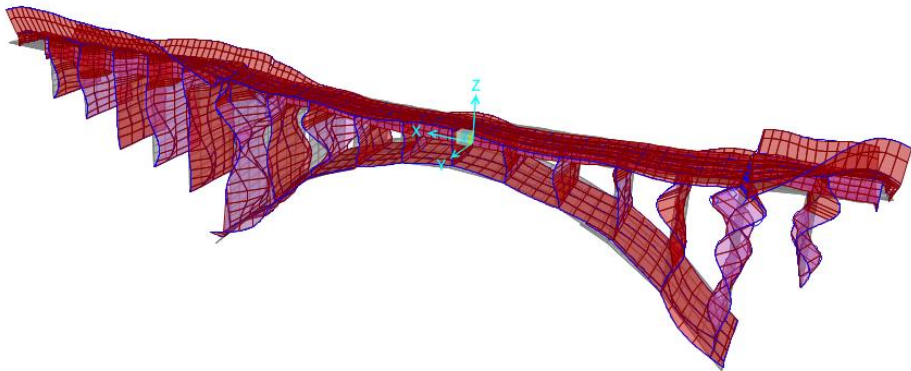
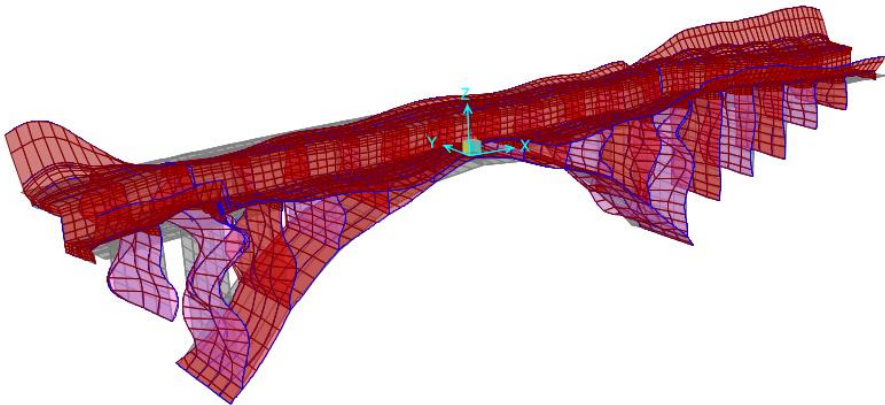
Modo	T [sec]	UX (%)	UY (%)	UZ (%)	Sum UX	Sum UY	Sum UZ
70	0.0638	0.145	3.964	0.728	85.877	83.347	64.160
Modo	T [sec]	RX (%)	RY (%)	RZ (%)	Sum RX	Sum RY	Sum RZ
70	0.0638	9.031	0.598	0.169	50.846	33.368	59.725

**Modo 71: T= 0.0596 sec, RZ= 5.651%**



Modo	T [sec]	UX (%)	UY (%)	UZ (%)	Sum UX	Sum UY	Sum UZ
71	0.0596	0.657	0.967	0.300	86.535	84.314	64.460
Modo	T [sec]	RX (%)	RY (%)	RZ (%)	Sum RX	Sum RY	Sum RZ
71	0.0596	0.043	0.002	5.651	50.889	33.369	65.376

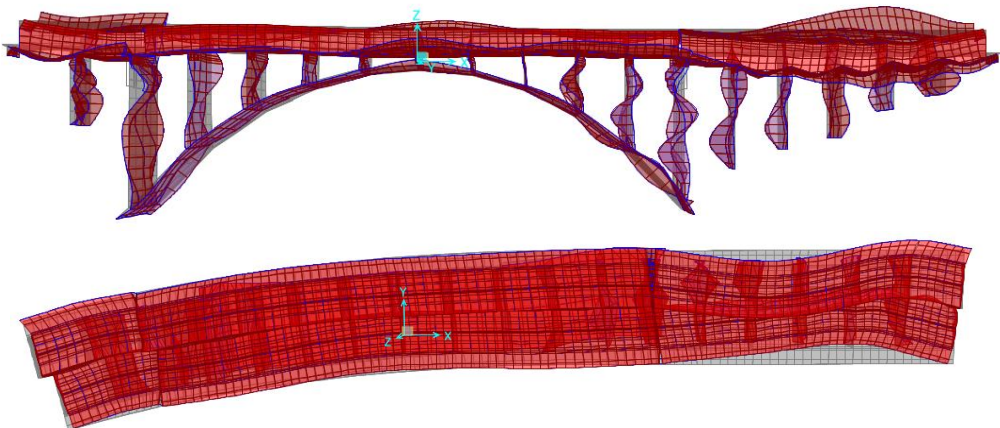
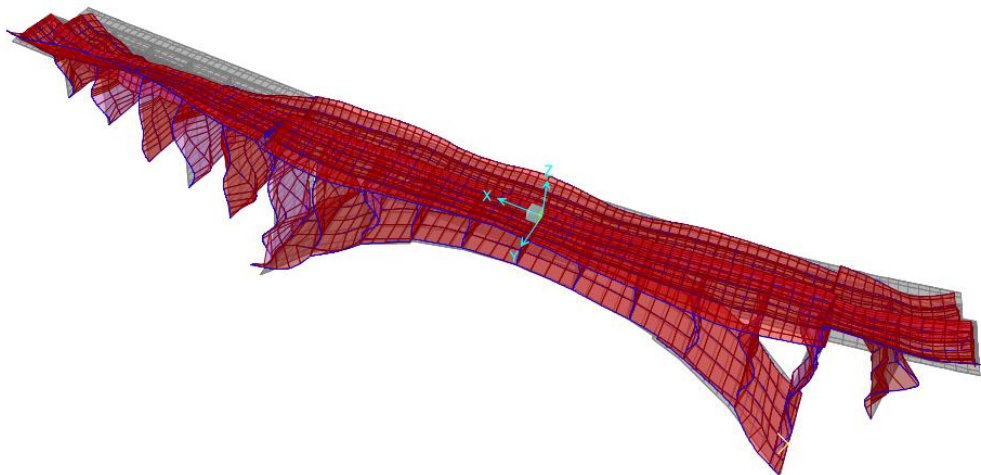
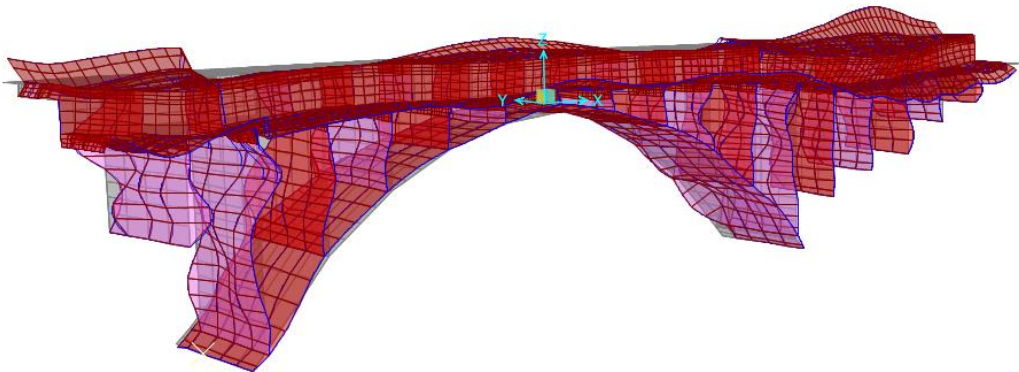
**Modo 72: T= 0.0585 sec, UZ= 10.31%**



Modo	T [sec]	UX (%)	UY (%)	UZ (%)	Sum UX	Sum UY	Sum UZ
72	0.0585	0.110	0.013	10.311	86.645	84.326	74.771
Modo	T [sec]	RX (%)	RY (%)	RZ (%)	Sum RX	Sum RY	Sum RZ
72	0.0585	0.416	3.864	0.783	51.305	37.233	66.159



**Modo 74: T= 0.0436 sec, UZ= 8.067%**



Modo	T [sec]	UX (%)	UY (%)	UZ (%)	Sum UX	Sum UY	Sum UZ
74	0.0436	0.210	3.143	8.067	94.213	87.490	82.938
Modo	T [sec]	RX (%)	RY (%)	RZ (%)	Sum RX	Sum RY	Sum RZ
74	00436	1.226	2.777	2.790	53.357	40.667	69.857